Service Profile-Aware Control Plane:

A Multi-Instance Fixed Point Approximation within a Multi-Granularity VPN Loss Networks Perspective

By
Wesam Alanqar
B.S.E.E., UAE University, UAE, 1997
M.S.E.E., University of Missouri-Columbia, 1999

Submitted to the Department of Electrical Engineering and Computer Science and the Faculty of the Graduate School of the University of Kansas in partial fulfillment of the requirements for the degree of Doctor of Philosophy

Chairman

David W. Petr

Tyrone Duncan

Committee Members

April 25, 2005

Date Dissertation Defended

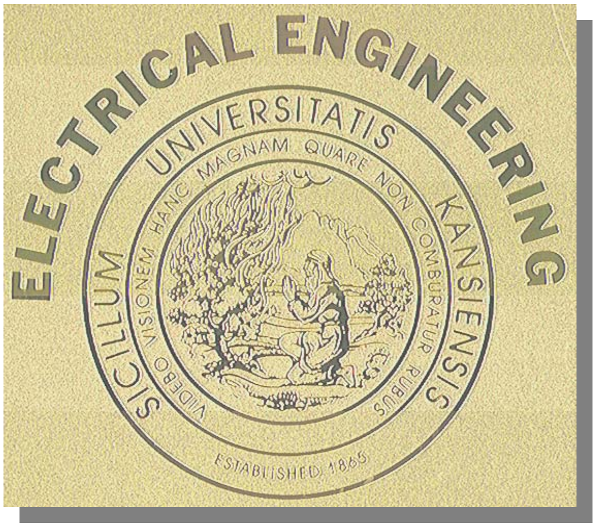
ELECTRICAL ENGINEERING
SICILLUM UNIVERSITATIS KANSIENSIS
VIDEBO VISIONEM HANC MAGNAM QUARE NON COMBURATUR RUBUS
ESTABLISHED 1865

ABSTRACT

The need to establish network connections in a service profile-aware fashion is becoming increasingly important due to the variety of candidate wired and wireless client networks with Quality of Service (QoS) networking infrastructures for some of emerging services like VoIP/Multimedia for wireless networks and Ethernet for wired networks. The control plane optimization of network connections will have to take into account a number of service profile parameters and network constraints to efficiently utilize network resources. In a networking scenario where a multi-service operation in common network infrastructure is assumed, efficient algorithms and protocols for service profile-differentiation and dynamic allocation of network resources will play a key role. To fulfill this need, a new Service Profile-Aware (SPA) control plane model is required to play a vital role in future converged wired and wireless networks in integrating service profile layer, control plane layer, and switching infrastructure layer.

Up until now, the criteria for network infrastructure operation via the existing Internet Engineering Task Force (IETF) and International Telecommunications Union (ITU) control plane models do not consider the service profile layer when establishing network connections. This work proposes the novel concept of a SPA control plane model that demonstrates its superiority over existing control plane models in multiple aspects including full realization of the multi-granularity network resources, and its complete consideration for services' architectures and their associated service profile feature set. Detailed comparison between the three control plane models were considered from multiple dimensions including traffic management schemes, components-level interaction between (service profile, control plane, network infrastructure) layers, and network infrastructure realization from both horizontal "network domains" and vertical "resource granularity and network partitions" perspective. Multiple service models were analyzed based on their service profile parameters from both an architectural and mathematical perspective. Detailed mathematical analysis of the three control plane models was performed based on a multi-instance Fixed Point Approximation (FPA) within a multi-granularity Virtual Private Network (VPN) loss networks. The performance analysis of the SPA new traffic management schemes found a significant increase in service allowed load while maintaining lower service blocking probability and network utilization over IETF and ITU control plane models.

ACKNOWLEDGMENTS

This dissertation could not have been completed without the support and inspiration of many people. I would like to acknowledge the contributions of, and thank, the following: My academic and dissertation advisor, Dr. Victor Frost for his vision for this project and his guidance and persistence in insisting on high quality results. His timely suggestions and feedback helped me immensely in my work. The trust that he put in my technical capabilities has been a strong support and encouragement during the hard times I faced while completing my residency requirement and working on the dissertation.

I am grateful to my parents, Ibrahim Alanqar and Laila Qaradaya, for all their prayers and for giving me the gifts of life and education. I couldn’t have reached what I have achieved in life without their sacrifices. I can never forget they instilled in me values of conviction, persistence, and hard work.

My wife and friend, Haya Qadi Al-Tamimi, for her sacrifice, encouragement and support of my efforts throughout my four years of study. Her walk with God, support, sacrifice, encouragement, and love for me has been a source of constant strength. I can never thank her enough for her patience and understanding on those days during this undertaking where my approach to family needs and life in general was less than optimum. My two sons, Loay and Qusay, for living their first few years without their father being available for them.

My twin sister, Taghreed, for her love that will continue growing in my heart for the rest of my life. My two sisters, Amal and Areej, for their true love. My brothers, Wael and Waleed, for their love and continuous encouragement.

Above all, to God for giving me the strength and confidence to realize my goals.

TABLE OF CONTENTS

LIST OF FIGURES

LIST OF TABLES

1 Introduction

1.1 Problem statement

The architectures and functional operation of the control plane components for existing IETF and ITU control plane models do not consider the service profile layer parameters. In addition, the IETF control plane components do not consider a full realization of the network resources multi-granularity representation. This component-level separation between the service profile layer, control plane layer, and network infrastructure layer leads to a lack of harmony between service demands' detailed parameters and network infrastructure detailed resources representation. This lack of harmony would lead to inefficient utilization of network resources especially under operation scenarios requiring dynamic allocation of network resources for differentiated services. Achieving this harmony will lead to a higher optimization of network resources supporting differentiated services under dynamic network operations.

Through the use of service profile layer parameters and network infrastructure multi-granularity resources representation, the architectures and functional operation of the SPA control plane components provide significant harmony between the network infrastructure resources and service profile parameters. The SPA control plane components were architected to utilize both the service profile layer parameters (service flow connectivity, load partitioning flexibility, and service demand granularity), and network infrastructure detailed resource representation parameter in its allocation of network resources supporting differentiated services requests. Therefore, the problem is to develop a new control plane model that provides this harmony and then demonstrate its superiority over existing control plane models.

1.2 Problem motivation/significance

There are multiple aspects that differentiate this work from previous control plane research efforts. First, this research proposes a new SPA control plane model with a detailed description of its architectural and functional operation and then analytically shows its superiority over existing IETF and ITU control plane models. Second, the current control plane models are service architectures agnostic. This is the first time that services were characterized by multiple architectures based on service profile features set including service flow connectivity, load partitioning flexibility, and service demand granularity. Third, this is the first time that the performance of both the IETF and the ITU control plane models were analyzed while considering the proposed SPA control plane model in a common framework. The comparison between the three control plane models was carried from three perspectives including transport network granularity realization, operational level, and component-level interaction between the transport layer, control plane layer, and the service profile layer.

1.3 Research approach

Detailed architectural and operational comparison of the IETF, ITU, and the proposed SPA control plane models was performed (see sections 4-6). Performance analysis of the three control plane models was carried using Fixed Point Approximation analytical models. The advantages of the SPA control plane over IETF/ITU models were analyzed using service request blocking probability, permissible “non-blocked” load, and transport resources utilization performance metrics. Detailed description of the performance metrics and their relevant mathematical formulations for each control plane model is provided in section 9.3.

The analysis was divided into four phases, the first phase focused on defining the architectures of the multiple configured VPN service proposed models, the second phase focused on defining the architectures and functional operation of the control plane components for the three control plane models, the third phase focused on defining the mathematical models for the three control plane models traffic management schemes, the fourth phase used Fixed Point Approximation (FPA) analytical model to compute the performance metrics for the traffic management schemes of the three control plane models.

1.4 Research hypotheses

The hypotheses of this research were:

1. Since the SPA control plane model has a full knowledge of both the services architectures/profile features set and the transport network granularity levels, the SPA would provide a better match between service architectures/profile features set and the transport network granularity levels; this will lead to a lower blocking, a higher

permissible “non-blocked” load, and a lower transport network utilization compared to both the IETF and the ITU control plane models. It is expected that the benefit of the SPA control plane will be highly dependent on the profile of the service request features set (service flow connectivity, load partitioning flexibility, and service demand granularity).

2. Since the routing component in the IETF control plane model has a coarse representation of a multi-granularity transport network, whereas the ITU/SPA routing has a granular representation of transport granularity levels, the following hypotheses are also considered:
   - The IETF control plane model produces higher transport utilization and a higher blocking probability than the ITU/SPA control plane models. This is also dependent on the service request features set profile (service flow connectivity, load partitioning flexibility, and service demand granularity).
   - IETF path computation element has less path options to compute. In ITU/SPA, since routing component accurately represents transport granularity levels, path computation has more path options to compute than IETF path computation element. Thus, using IETF control plane model would lead to higher transport utilization and higher blocking than using the ITU or SPA control plane models. This is also dependent on profile of service features set (service flow connectivity, load partitioning flexibility, and service demand granularity).

1.5 Research objectives

The main objective of this research is to prove that the SPA control plane model provides lower blocking probability, higher permissible “non-blocked” load, and lower transport network utilization compared to both the IETF and ITU control plane models. Thus, the proposed SPA control plane model provides a new architecture for control plane deployments. To achieve this objective, the following tasks were carried:

1. Develop detailed architectures for the service configuration models from the following three perspectives:
   a. Service flow connectivity
   b. Load partitioning flexibility
   c. Service demand granularity

2. Develop architectures for the three control plane models (IETF, ITU, SPA) from the following three perspectives:
    a. Transport network granularity realization
    b. Component-level
    c. Operational-level
3. Develop detailed mathematical models for the service configuration models to compute the applied input load on each of the topology links based on the service flow connectivity.
4. Modifying Fixed Point Approximation (FPA) to develop detailed mathematical models for the three control plane models to compute the following performance metrics[1]:
    a. Service blocking probability for both network-wide and per source-destination pair
    b. Permissible "non-blocked" load for both network-wide and per source-destination pair
    c. Occupancy probability "Utilization" for both network-wide and per source-destination pair
5. Demonstrate the superiority of the SPA control plane model using the results of the performance analysis.

1.6 Overview

The Dissertation is organized as follows: section 2 provides an overview of related previous research and standardization activities. Section 3 provides a detailed architectural analysis of the configured VPN service models applied to the three control plane models. Section 4 provides a detailed architectural analysis of the three control plane models from traffic management schemes perspective. Section 5 provides a control plane technology overview and a detailed architectural analysis of the three control plane models from transport network realization perspective. Section 6 provides the component-level interaction between service profile layer, control plane layer, and network infrastructure layer for the three control plane models. Section 7 covers he analysis methodology. Section 8 provides detailed mathematical

[1] Detailed description of the performance metrics and their relevant mathematical formulations for each control plane model is provided in section 9.3.

analysis for the three control plane models. Section 9 covers analysis framework and performance evaluation metrics. Section 10 covers the computational cost of the traffic management schemes of each control plane model. Section 11 covers the mathematical models validation and computation accuracy. Section 12 provides a summary of results analysis for a seven-node topology. Section 13 provides a detailed analysis of SPA control plane components impact. Section 14 provides conclusions. Section 15 provides recommendations for future work. Section 16 provides references. Appendix-A provides list of acronyms. Appendix-B provides pseudo-code generic algorithms for the FPA of the IETF, ITU, and SPA control plane models. Appendix-C provides detailed results for the four-node topology. Appendix-D provides detailed results for the seven-node topology with two alternate routing. Appendix-E provides detailed results for the seven-node topology with three alternate routing.

2 Background- Previous Research and Standardization Efforts

Telecommunications networks are usually segmented in a three-tier hierarchy: access, metropolitan, and long haul. Long-haul/backbone networks span global distance and provide large tributary connectivity between regional and metro domains. On the other end of the hierarchy are access networks, providing connectivity to a plethora of customers within close proximity. Straddled in the middle are metropolitan (metro) networks interconnecting access and long-haul networks. Transport networks today are based on SONET digital hierarchy ring architectures. Namely, smaller tributary rings, for example, OC-3 (155 Mb/s) or OC-12 (622 Mb/s), aggregate traffic onto larger core rings at higher bit rates, for example OC-48 (2.5 Gb/s). Overall, SONET has been very successful in delivering the fast wave of end-user connectivity, namely voice.

Various emerging trends have greatly affected legacy SONET systems suitability for future applications. The first trend is the growth in Internet applications, residential Internet has produced sustained data traffic growth, with close to half of the households in North America now having Internet connectivity [74]. Meanwhile, penetration rates are also growing significantly in Europe and Asia [75]. One the corporate side, many businesses are heavily utilizing existing Internet applications and busy developing new possibilities. For example, Internet teleconferencing is commonplace and web hosting/mirroring and e-commerce are growing rapidly. Other, more distance possibilities such as telemedicine and remote sensing are also being studied. Apart from application/bandwidth growth, the number of simultaneous peered sessions is also increasing rapidly, further accelerating volumes [76]. Also, many studies indicate that Internet traffic exhibits highly bursty, asymmetric behaviors [77] and overall customer demands can be more difficult to predict as compared to legacy voice [78,76].

The second aspect is the growth in virtual Line/LAN services with varying bit-rate requirements. These offerings are particularly attractive for enterprise clients wanting to build Layer 1 VPNs (L1-VPNs) [26] to interconnect multiple locations via a full variety of data interfaces/protocols (e.g., Gigabit Ethernet, SONET, frame relay, ATM, etc.).The lower-cost native Ethernet interfaces is a key factor in the emerging metro market [7] (i.e., over 80% of enterprise traffic originates in Ethernet form [6]. Overall, “LAN-like” service may become subsets of more generalized virtual private networks (Layer-1 VPN) services [8,9]. Unlike legacy leased-line services, virtual-line services will provide genuine transparency, enabling customers to manage their own networks [6,8,10,11].

Pure capacity expansion will hardly suffice, as operators need intelligent “network level” provisioning capabilities to support a full range of client protocols and applications. Specifically, network infrastructures must efficiently allocate capacity resources and at the same time provide very selective handling in order to enable competitive Service Level Agreement (SLA) differentiation. Service differentiation can be achieved in many facets, such as turn-up speed, channel quality, priority, protection levels/speed, etc [12]. Overall, it has been argued that transparency and rapid, intelligent service creation capabilities are even more important than raw capacity and equipment consolidation [8,13]. Additionally, given the plethora of competing vendors, standards-based interoperable network control and management will become more important as operators gradually induct differing gears.

In light of the above legacy SONET systems shortcomings, vendors and service providers have sought to “enhance” SONET paradigms to better suit data traffic needs [6-14]. Although these proposals have appeared under different names, e.g., “data-aware SONET” [17], herein the term Next-Generation SONET (NGS) was selected. Overall, all these solutions share two main features, namely efficient data tributary mapping and integrated higher layer (two/three) protocol functionalities. SONET mapping of smaller packet interfaces (10,100 Mb/s Ethernet) is usually done in “coarse” STS-1 increments and the resultant bit-rate in-congruencies usually yield large amounts of stranded bandwidth [14] (e.g., 10 Mb/s Ethernet allocated at full STS-1, 80% unused capacity).

NGS set of recommendations includes the development of ITU-T Link Capacity Adjustment Scheme (LCAS) [20] recommendation, approved in 2001 which defines a transport network capability that allows for “hitlessly” increasing/decreasing the number of “trails” (e.g., STS-1 circuits) assigned to a connection. Moreover, each circuit trail can be diversely router to improve resiliency and failed trails can be removed together. Overall, LCAS defines a very powerful new capability for exploiting virtual concatenation techniques and improving capacity utilization. ITU-T G.707 [21] recommendation, approved in 2001, defines the virtual concatenation mechanism. Virtual concatenation is a mechanism that provides flexible and effective use of SONET/SDH payload. Virtual concatenation breaks the limitation incurred by the legacy SONET hierarchy rigidity via the definition of pay-loads with flexible bandwidth. It “virtually” concatenates several payloads to provide a payload with flexible bandwidth, appropriate for data service accommodation.

Both the IETF and ITU standardization organizations had completely two opposite approaches in standardizing optical control plane architectures and its supporting protocols. The IETF approach was focused on extending MPLS-based protocols that were designed for data networks to support the transport networks without taking into considerations the NGS architectures. On the other hand, the ITU approach was focused initially on building generic control plane architectures that are based on NSG architectures and then proposed protocol-specific implementations of the generic control plane architectures using both GMPLS and PNNI; this indicates that the IETF control plane model architectures were not optimized to utilize NGS capabilities. ITU-T started the development of control plane architectures by focusing on developing a set of NGS recommendations first and then developed generic control plane architectures that were optimized to utilize NGS capabilities.

ITU-T G.8080 [15] recommendation, approved in 2001, defines the architecture for the Automatic Switched Optical Network (ASON) that was developed within the context of NGS capabilities. This recommendation provides canonical architecture for Call and Connection operations and lays foundation for more detailed ITU-T control plane recommendations. ITU-T G.7713 [17] recommendation, approved in 2001, addresses intra- and inter-control domain signaling. This recommendation provides protocol neutral specifications support for User Network Interface (UNI), Interior-Network-Network Interface (I-NNI), and Exterior-Network-Network-Interface (E-NNI). Also, this recommendation functionally specifies control plane architecture per transport network granularity level basis, allowing for implementation of single control plane for multiple transport network granularity levels.

ITU-T G.7715 [19] recommendation, approved in 2002, provides the architecture and requirements for routing in ASON, it covers aspects of ASON routing architectures, ASON routing requirements, routing attributes, routing messages, routing message distribution topology, and path selection. ITU-T G.7715.1 [24] recommendation, approved in 2003, provides the generic ASON routing architecture and requirements for Link State protocols. This recommendation provides architecture and requirements for a link state realization of ITU-T G.7715 and ITU-T G.8080. In addition, this recommendation provides details on routing information flow and communications between routing hierarchical levels. ITU-T G.7714 [18] recommendation, approved in 2001, covers ASON generalized automatic discovery techniques including aspects of neighbor/adjacency and service discoveries (i.e., transport network granularity level adjacencies discovery and service capability exchange).

IETF Generalized Multi-Protocol Label Switching (GMPLS) architecture [34] provides the generic architecture of the optical control plane from an IETF perspective. GMPLS architecture represents a strong push to increase vertical control plane integration (data and optical) by extending/reusing existing data networking concepts/protocols. The overall aim is to replace the features of multiple protocol layers in traditional multilayered models (e.g., separate addressing schemes, SONET/SDH protection, ATM traffic engineering) with a more unified solution. There are several major required components for dynamic channel provisioning and advanced SLA management optical networks, namely setup signaling, resource discovery, and constraint-based routing. GMPLS implements all of these requirements by extending MPLS signaling [35] and resource discovery protocols [38] and defining multiple link-specific abstractions of the original MPLS label-swapping paradigm (i.e., “implicit labels” for time-slots, wavelengths, and fibers). These definitions can be further coupled with hierarchical label-stacking schemes to exploit scalability (e.g., packet labels into TDM circuit labels into lambda labels). In particular, this ubiquity makes GMPLS an ideal control framework for multi-service network platform. First, optical channel setup signaling is accomplished by extensions to MPLS signaling protocols, namely RSVP-TE (RSVP Traffic Engineering) [37] and CR-LDP (Constraint-Routing Label Distribution Protocols) [36]. Here, the Explicit-Routing (ER) capability is used to indicate the channel route and reserve resources. Meanwhile, actual route computation is done via constrained routing/path computation. Finally, route computation requires network topological/resource information, and is propagated via extensions to pertinent routing protocols, namely open-shortest path first (OSPF) [39].

Multiple research efforts focused on the analysis of GMPLS control plane routing and signaling performance in a single domain environment, some of the research efforts are provided in [1-5]. The analysis of GMPLS routing and signaling performance concluded with multiple disadvantages of the GMPLS control plane solution, this can be attributed to the lack of consideration of NGS during the development of GMPLS protocols. GMPLS performance issues led to the need to establish formal communications and liaison with ITU-T to help in modifying GMPLS protocols to support NGS capabilities. Since 2003, both the IETF and ITU-T standardization organizations established formal communications and liaisons between the two organizations to collaborate in defining GMPLS protocols extensions to support ASON generic architectures and NGS capabilities.

This collaboration led to the development of multiple ITU-T recommendations providing protocol specific implementation of ASON signaling and routing protocols as specified in both ITU-T G.7713.2 [22] recommendation that defines ASON distributed call and connection management signaling mechanism using GMPLS RSVP-TE and ITU-T G.7713.3 [23] recommendation that defines ASON distributed call and connection management signaling mechanism using GMPLS CR-LDP. In addition to the signaling extensions, a routing core team was established between IETF and ITU experts to build the requirements

[43] for GMPLS routing for ASON based on ITU-T G.7715.1. Figure 2-1 provides the current mapping between ITU-T control plane generic architectures and IETF control plane specific protocols.

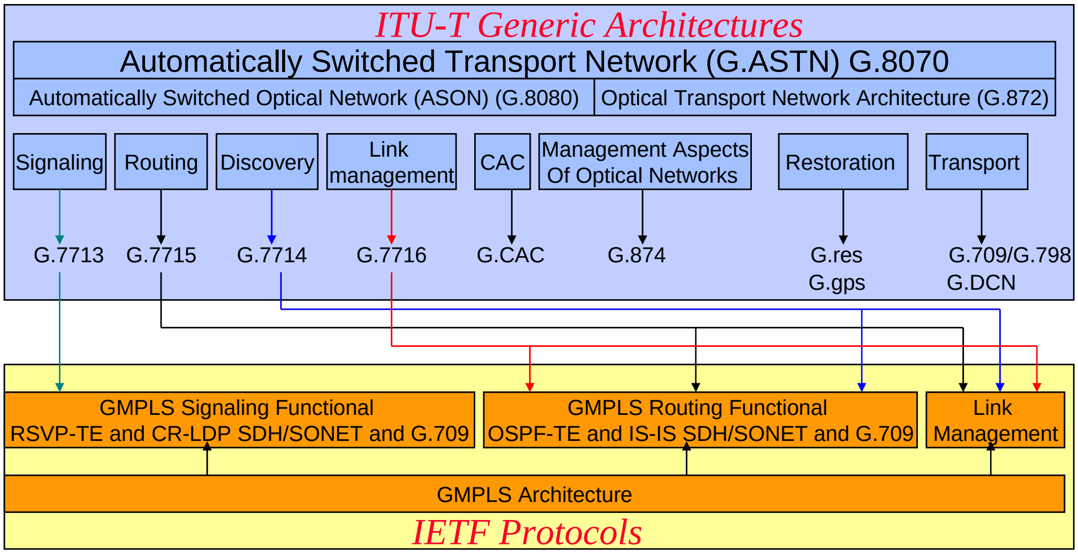
ITU-T Generic Architectures
Automatically Switched Transport Network (G.ASTN) G.8070
Automatically Switched Optical Network (ASON) (G.8080)
Optical Transport Network Architecture (G.872)
Signaling
Routing
Discovery
Link management
CAC
Management Aspects Of Optical Networks
Restoration
Transport
G.7713
G.7715
G.7714
G.7716
G.CAC
G.874
G.res
G.gps
G.709/G.798
G.DCN
GMPLS Signaling Functional
RSVP-TE and CR-LDP SDH/SONET and G.709
GMPLS Routing Functional
OSPF-TE and IS-IS SDH/SONET and G.709
Link Management
GMPLS Architecture
IETF Protocols

Figure 2-1: Mapping ITU-T Generic Control Plane Architectures Recommendations to IETF Control Plane Protocols

Despite the IETF and ITU-T standardization organizations collaboration, the architectures and functional operation of the control plane components for existing IETF and ITU control plane models lack the service profile layer parameters consideration. This component-level separation between the service profile layer, control plane layer, and network infrastructure layer led to the lack of harmony between service demands' detailed parameters and network infrastructure detailed resources representation. This lack of harmony would lead to inefficient utilization of network resources especially under operation scenarios requiring dynamic allocation of network resources for differentiated services.

The provided survey gave guidance in identifying the drawbacks of both IETF and ITU control plane architectures which was the starting point in developing the proposed SPA control plane model. Through the accurate realization of both service profile layer parameters and network infrastructure multi-granularity detailed resources representation, the architectures and functional operation of the proposed SPA control plane components provide significant harmony between the network infrastructure resources and service profile parameters. This research is focused on studying the impact of the architectural and functional operation of the IETF, ITU, and SPA control plane models components on the performance of a range of proposed configured VPN service models while considering a multi-granularity transport network infrastructure.

3 Configured VPN Service Models- Service Profile Parameters

The SPA control plane model uses the service profile layer parameters as input to its traffic management schemes; this section defines the parameters of the service profile layer and the different service models architectures that can be defined based on the service profile layer parameters. Nine service models architectures are defined in this section, the service models are considered configured VPN service models because the service arrivals belong to different customers that use common physical network resources, the set of service arrivals belonging to the same customer must be able access a certain partition of the physical network resources, a VPN, without competing with service arrivals from other customers.

Each customer's VPN is constructed by reserving resources from the physical network links to connect the customer's end nodes; the reserved resources on any link for a certain customer are reserved solely for the service arrivals of that customer. The physical network resources are partitioned into multiple partitions with one partition for each configured customer; this means that the physical network topology is partitioned logically into multiple VPNs for the configured customers. This section defines the detailed architectures for the VPN service configuration models from the perspective of the following service profile parameters that are used by the SPA control plane model components:

1. *Service flow connectivity:* is a service profile layer parameter that defines the level of service requests meshing between source-destination pairs. This parameter can be configured as "fully-meshed", "semi-meshed", or "point-to-point".

2. *Load partitioning flexibility:* is a service profile layer parameter that defines if the load of the configured VPN service request can be partitioned between a dedicated network resources partition and a shared network resources partition. This parameter can be configured as "enabled" or "disabled". The "enabled" configuration means that the

service request load can be partitioned. The “disabled” configuration means that the service request load can not be partitioned.

3. <u>*Service demand granularity*</u>: is a service profile layer parameter that defines if the actual bandwidth requirement b_k^A, e.g., 2 STS-1, of a service request flow can be split into multiple flows each with a granular bandwidth requirement b_k^G, e.g., STS-1,. This parameter can be configured as “actual” or “granular”. The “actual” configuration means that the actual service request flow can not be split into multiple service request flows. The “granular” configuration means that the actual service request flow can be split into multiple service request flows. The relationship between actual and granular bandwidth requirements flows is illustrated in Figure 3-1.

4. <u>*Configured VPN service identification number:*</u> is a service profile layer parameter that identifies the VPN service that the service request belongs to.

Each service request will be characterized by the following parameters (service demand granularity, load partitioning flexibility, service flow connectivity, and configured VPN service identification number). The reason for considering the service request a "VPN" is that it SHOULD only use the allowed resources partition allocated to it based on the "configured VPN service identification number" parameter in the service profile layer.

For a given physical link, each of its dedicated resources partitions is labelled with a "configured VPN service identification number" that allows the service arrivals belonging to a VPN with the same "configured VPN service identification number" to access the dedicated resources partition. The shared sources partition is labelled with multiple "configured VPN service identification numbers" indicating that the shared resources partition can be accessed by any service arrivals with "configured VPN service identification number" that map to one of the multiple "configured VPN service identification numbers" included in the shared resources partition.

The IETF model does not consider the "configured VPN service identification number" parameter as it multiplexes all the service requests from multiple customers on the same physical resources. The ITU model uses the "configured VPN service identification number" parameter by applying the set of service arrivals belonging to a specific customer to the corresponding dedicated resources partition. The Service-Oriented-Shared model uses the "configured VPN service identification number" parameter to split the load between the dedicated and shared network resources partitions.

3.1 Definitions and notation[2]

1. C_j: The physical capacity or bandwidth of link *j*, in units of bandwidth, circuits, or trunks. $C_j = (\sum_{vD} C_j^{vD}) + C_j^S$
2. Dedicated Resource Partition C_j^{vD} : The dedicated capacity on link *j* for configured VPN service *v*. The dedicated arrival rate λ_{rk}^{vD} from the configured VPN service's VPN arrival rate λ_{rk}^{v} is applied to C_j^{vD} resources without allowing an arrival rate from other configured VPN services to use C_j^{vD} resources.
3. Shared Resources Partition C_j^S : The shared capacity on link *j*. The shared arrival rate λ_{rk}^{vS} from multiple configured VPN services is applied to C_j^S
4. VPN Resources C_j^v : The VPN capacity on link *j* used by configured VPN service *v*. $C_j^v = C_j^{vD} + C_j^S$
5. λ_{rk}^{v} : The arrival rate of class *k* calls between node pair *r* for configured VPN service *v*. The configured VPN service arrival rate λ_{rk}^{v} can be partitioned into two rates; a dedicated rate λ_{rk}^{vD} that can be applied to a dedicated resources partition C_j^{vD}, and shared rate λ_{rk}^{vS} that can be applied to a shared resources partition C_j^S. $\lambda_{rk}^{v} = \lambda_{rk}^{vD} + \lambda_{rk}^{vS}$
6. λ_{rk}^{vD} : The dedicated arrival rate. The portion of λ_{rk}^{v} which is applied to the dedicated resources partition C_j^{vD} of the link capacity C_j. The dedicated rate applied to the dedicated resources partition does not share its resources with any arrival rates from other configured VPN services.

[2] The listed notation will be in used in section 6.1 to derive the mathematical models for the service models.

7. λ_{rk}^{vS} : The shared arrival rate. The portion of λ_{rk}^{v} which is applied to the shared resources partition C_j^S of the link capacity C_j. The service's shared rate applied to the shared resources partition share its resources with other configured VPN services' shared rates.

8. b_k^C : The coarse bandwidth requirement of class *k* service request, in units of bandwidth, circuits, or trunks. b_k^C represents the transport network maximum level of multiplexing.

9. b_k^G : The granular, sub-rate, bandwidth requirement of b_k^C , in units of bandwidth, circuits, or trunks. b_k^G represents the transport network minimum level of inverse multiplexing.

10. b_k^A **:** The actual bandwidth requirement of class k, in units of bandwidth, circuits, or trunks. Figure 3-1 illustrates the relationship between b_k^A , b_k^C , and b_k^G . For example, a class k with actual bandwidth requirement b_k^A of 2 STS-1, has a coarse bandwidth requirement b_k^C of 3 STS-1 and a granular bandwidth requirement b_k^G of 1 STS-1.

11. Point-to-Point Flow: The service request takes place over a network between a single sender and a single receiver.

12. Semi-Meshed Flow: The service request takes place between a source and a select group of destinations.

13. Fully-Meshed Flow: The service request takes place between a source and all the reachable destinations by the source node.

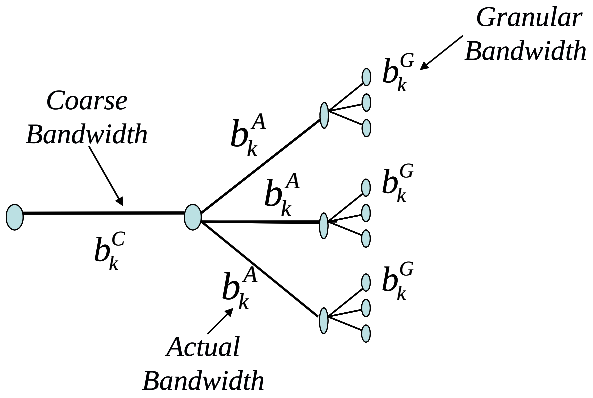

Figure 3-1: Coarse, Actual, Granular Bandwidth Relationship

3.2 Configured VPN service models

Figure 3-2 provides a graphical view of the different configured VPN service models based on the listed service profile features set as provided in section 3.1. Based on the three service's profile features (service flow connectivity, load partitioning, service demand granularity), multiple service configurations are introduced in Table 3-1. The following sub-sections will provide a detailed architectural view of each of the listed configured VPN service models as provided in Table 3-1.

Configured VPN Services Models	Service Flow Connectivity	Load Partitioning Flexibility	Service Demand Granularity
Point Dedicated Actual(PDA)	Point-to-Point	Disabled	Actual
Point Shared Actual (PSA)	Point-to-Point	Enabled	Actual
Point Shared Granular (PSG)	Point-to-Point	Enabled	Granular
Semi-meshed Dedicated Actual (SDA)	Semi-meshed	Disabled	Actual
Semi-mesh Shared Actual (SSA)	Semi-meshed	Enabled	Actual
Semi-meshed Shared Granular (SSG)	Semi-meshed	Enabled	Granular
Fully-meshed Dedicated Actual (FDA)	Fully-meshed	Disabled	Actual
Fully-mesh Shared Actual (FSA)	Fully-meshed	Enabled	Actual
Fully-meshed Shared Granular (FSG)	Fully-meshed	Enabled	Granular

Table 3-1: Configured VPN Service Models

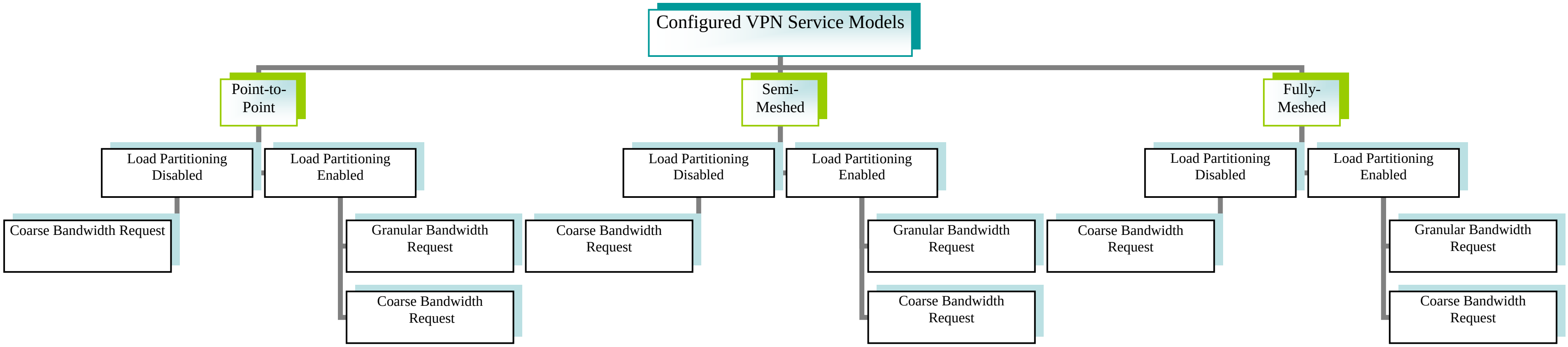
Configured VPN Service Models
Point-to-Point
Semi-Meshed
Fully-Meshed
Load Partitioning Disabled
Load Partitioning Enabled
Coarse Bandwidth Request
Granular Bandwidth Request
Coarse Bandwidth Request
Load Partitioning Disabled
Load Partitioning Enabled
Coarse Bandwidth Request
Granular Bandwidth Request
Coarse Bandwidth Request
Load Partitioning Disabled
Load Partitioning Enabled
Coarse Bandwidth Request
Granular Bandwidth Request
Coarse Bandwidth Request

Figure 3-2: Configured VPN Service Models

3.2.1 Point Dedicated Actual (PDA)

Figure 3-3 illustrates the Point Dedicated Actual (PDA) configured VPN service model; the *point-to-point* nature of the service flow connectivity feature indicates that the configured VPN service arrival rate λ_{rk}^{v} generated from a source node is destined to only one destination node. The *dedicated* nature of load partitioning nature indicates that the VPN service arrival rate λ_{rk}^{v} is applied to the total physical capacity C_j for all the links part of the source-destination pair r. The *actual* nature of the service demand granularity level indicates that the actual service demand b_k^A between a source-destination pair can not be split into sub rates b_k^G .

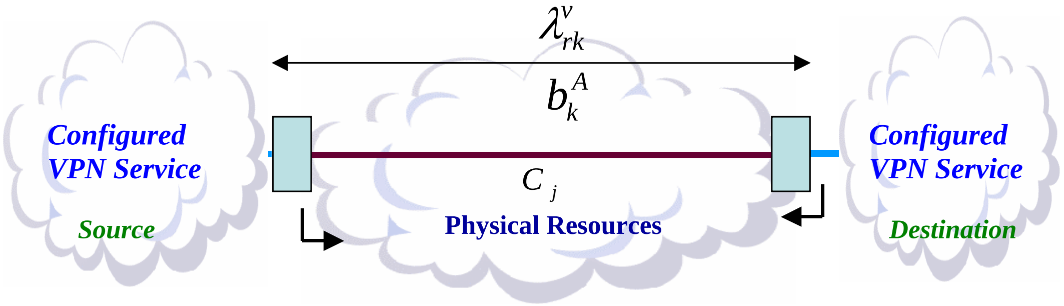

Figure 3-3: PDA Service Configuration

3.2.2 Point Shared Actual (PSA) and Point Shared Granular (PSG)

Figure 3-4 illustrates the Point Shared Actual (PSA) and the Point Shared Granular (PSG) configured VPN service models; the *point-to-point* nature of the service flow connectivity feature indicates that the configured VPN service arrival rate λ_{rk}^{v} generated from a source node is destined to only one destination node. The *shared* nature of load indicates that the VPN service arrival rate λ_{rk}^{v} can be split into λ_{rk}^{vD} and λ_{rk}^{vS} across C_j^{vD} and C_j^{S} resources partitions respectively. The *actual* nature of the service demand granularity level indicates that a service request flow with actual bandwidth requirement b_k^A between a source-destination pair can not be split into multiple service request flows each with granular bandwidth requirement b_k^G . In PSG, a service request flow with actual bandwidth requirement b_k^A between a source-destination pair can be split into multiple flows each with granular bandwidth requirement b_k^G.

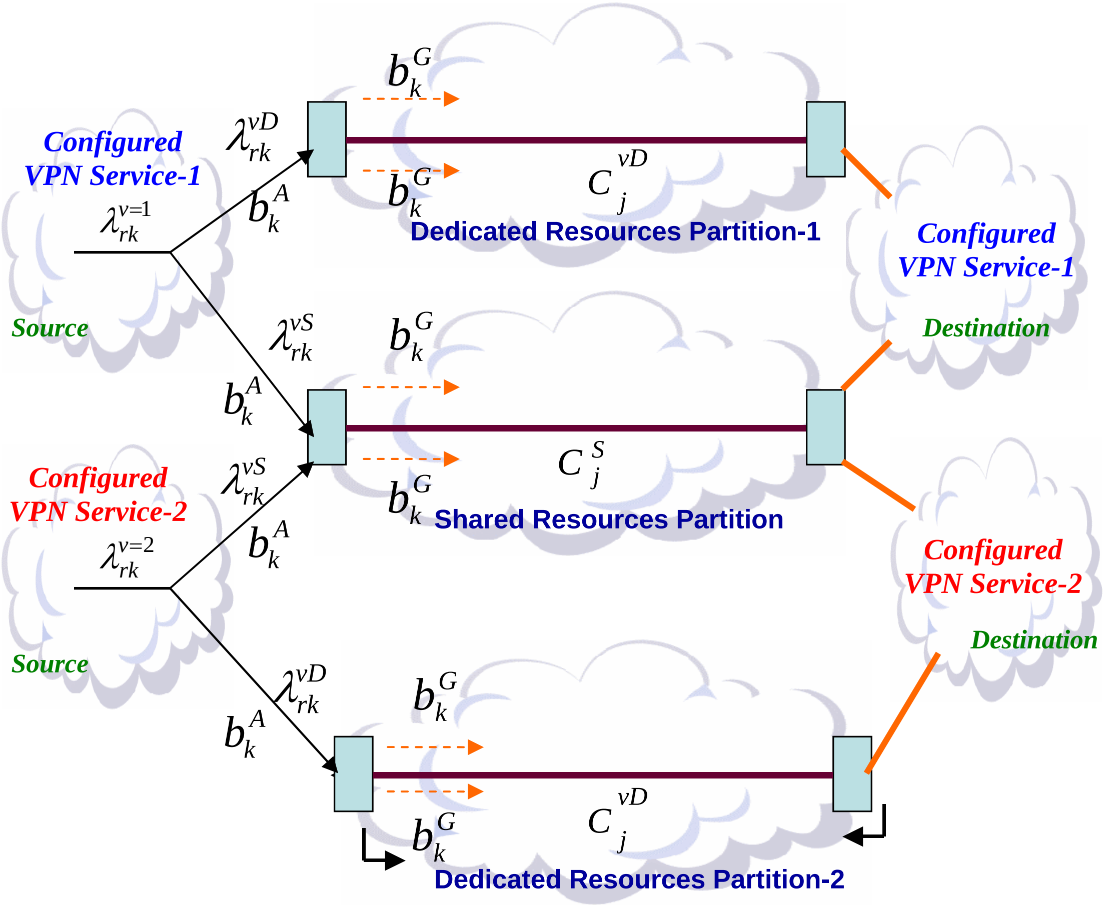

Figure 3-4: PSA and PSG Service Configurations

3.2.3 Semi-meshed Dedicated Actual (SDA)

Figure 3-5 illustrates the Semi-meshed Dedicated Actual (SDA) configured VPN service model; the *Semi-meshed* nature of the service flow connectivity feature indicates that the configured VPN service arrival rate λ_{rk}^v generated from a source node is destined to selected destination nodes. The *dedicated* nature of load indicates that the VPN service arrival rate λ_{rk}^v is applied to the total physical capacity C_j for all the links part of the source-destination pair r. The *actual* nature of the service demand granularity level indicates that the service request flow with actual bandwidth requirement b_k^A between a source-destination pair can not be split into multiple service request flows each with granular bandwidth requirement b_k^G.

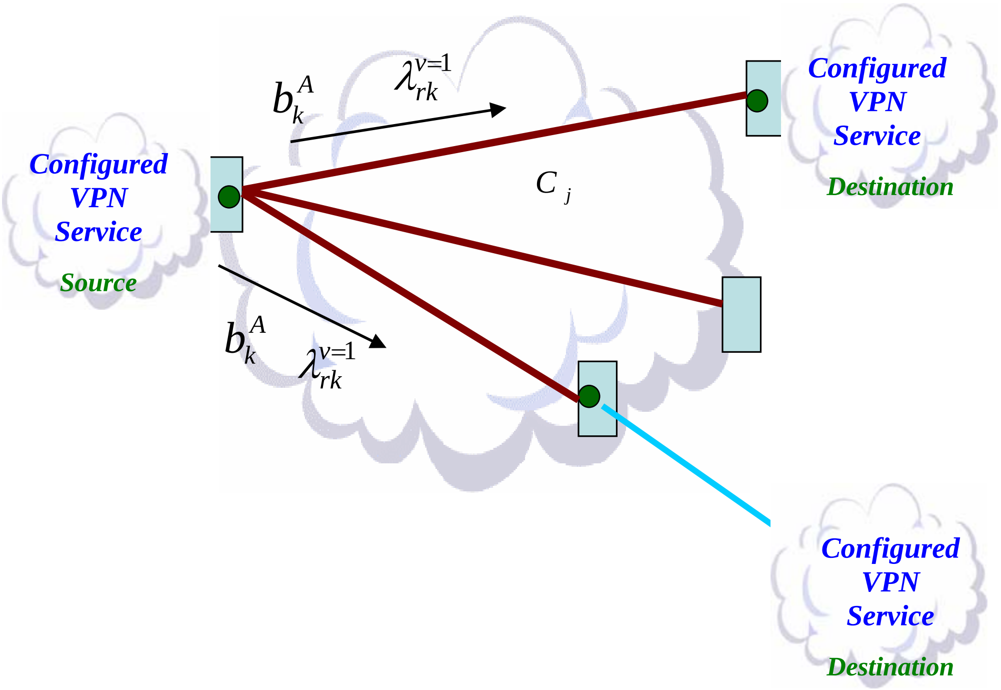

Figure 3-5: SDA Service Configuration

3.2.4 Semi-meshed Shared Actual (SSA) and Semi-meshed Shared Granular (SSG)

Figure 3-6 illustrates the Semi-meshed Shared Actual (SSA) and the Semi-meshed Shared Granular (SSG) configured VPN service models, the *semi-meshed* nature of the service flow connectivity feature indicates that the configured VPN service arrival rate λ_{rk}^v generated from a source node is destined to multiple selected destination nodes. The shared nature of load partitioning nature indicates that the VPN service arrival rate λ_{rk}^v can be split into λ_{rk}^{vD} and λ_{rk}^{vS} across C_j^{vD} and C_j^S resources partitions respectively. The *actual* nature of the service demand granularity level indicates that a service request flow with actual bandwidth requirement b_k^A between a source-destination pair can not be split into multiple service request flows each with granular bandwidth requirement b_k^G. In SSG, a service request flow with actual bandwidth requirement b_k^A between a source-destination pair can be split into multiple flows each with granular bandwidth requirement b_k^G .

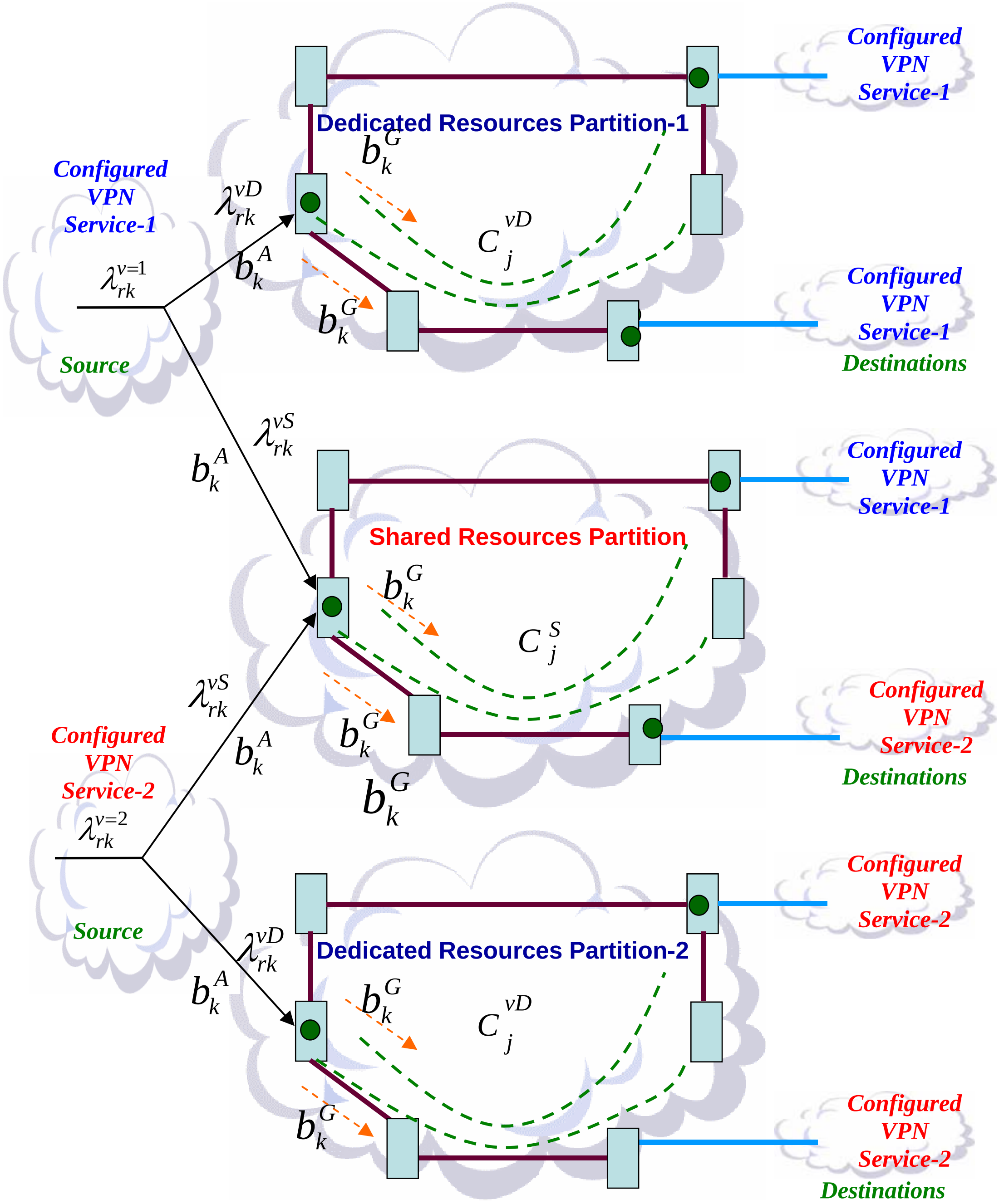

Figure 3-6: SSA and SSG Service Configurations

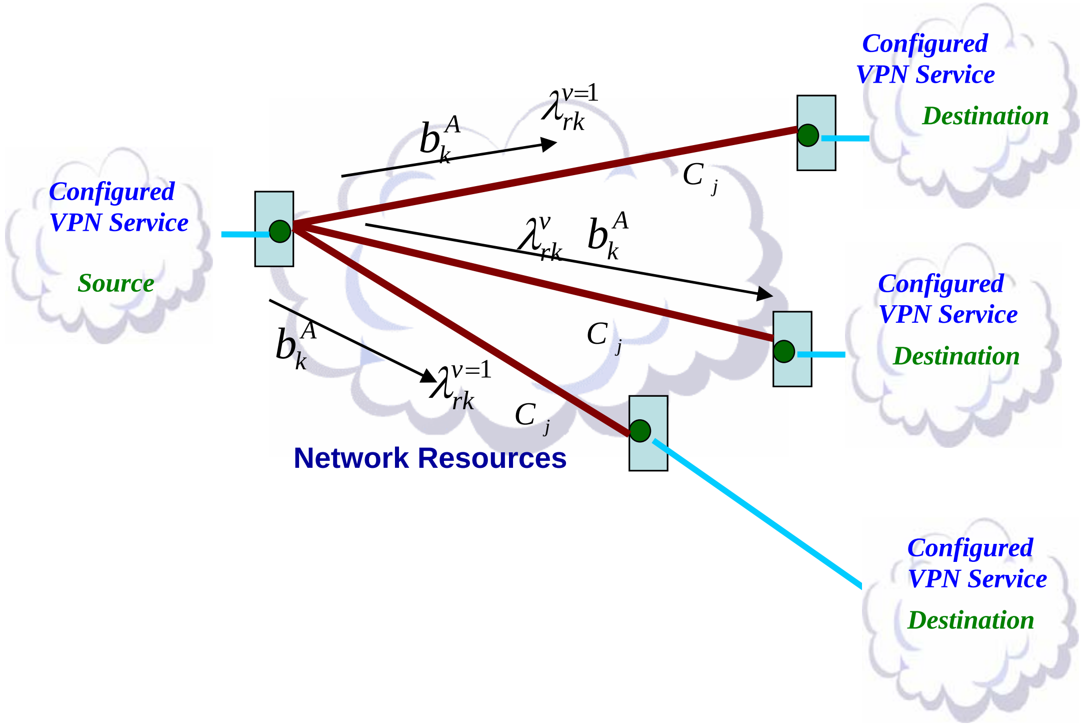

Figure 3-7: FDA Service Configuration

3.2.5 Fully-meshed Dedicated Actual (FDA)

Figure 3-7 illustrates the Fully-meshed Dedicated Actual (FDA) configured VPN service model, the fully-meshed nature of the service flow connectivity feature indicates that the configured VPN service arrival rate λ_{rk}^{v} generated from a source node is destined to all reachable destination nodes. The dedicated nature of load partitioning nature indicates that the VPN service arrival rate λ_{rk}^{v} is applied to the total physical capacity C_j for all the links part of the source-destination pair r. The actual nature of the service demand granularity level indicates that the service request flow with actual bandwidth requirement b_k^A between a source-destination pair can not be split into multiple service request flows each with granular bandwidth requirement b_k^G .

3.2.6 Fully-meshed Shared Actual (FSA) and Fully-meshed Shared Granular (FSG)

Figure 3-8 illustrates the Fully-meshed Shared Actual (FSA) and the Fully-meshed Shared Granular (FSG) configured VPN service models; the *fully-meshed* nature of the service flow connectivity feature indicates that the configured VPN service arrival rate λ_{rk}^{v} generated from a source node is destined to all reachable destination nodes. The *shared* nature of load partitioning nature indicates that the VPN service arrival rate λ_{rk}^{v} can be split into λ_{rk}^{vD} and λ_{rk}^{vS} across C_{j}^{vD} and C_{j}^{S} resources partitions respectively. The *actual* nature of the service demand granularity level indicates that a service request flow with actual bandwidth requirement b_{k}^{A} between a source-destination pair can not be split into multiple service request flows each with granular bandwidth requirement b_{k}^{G}. In FSG, a service request flow with actual bandwidth requirement b_{k}^{A} between a source-destination pair can be split into multiple flows each with granular bandwidth requirement b_{k}^{G}.

The FSG VPN service configuration model is the service model analyzed in this research for the following reasons:

1. The fully-mesh service flow connectivity would indicate a higher network-wide input load compared to the semi-meshed and point-to-point service flow connectivity; this would allow the performance of the three control plane models to be evaluated under realistic high input loads.
2. The Shared load partitioning would allow the Load Partitioning Function of the SPA control plane to be evaluated
3. The Granular service demand would allow the Inverse Multiplexing Function of the SPA control plane model to be evaluated.

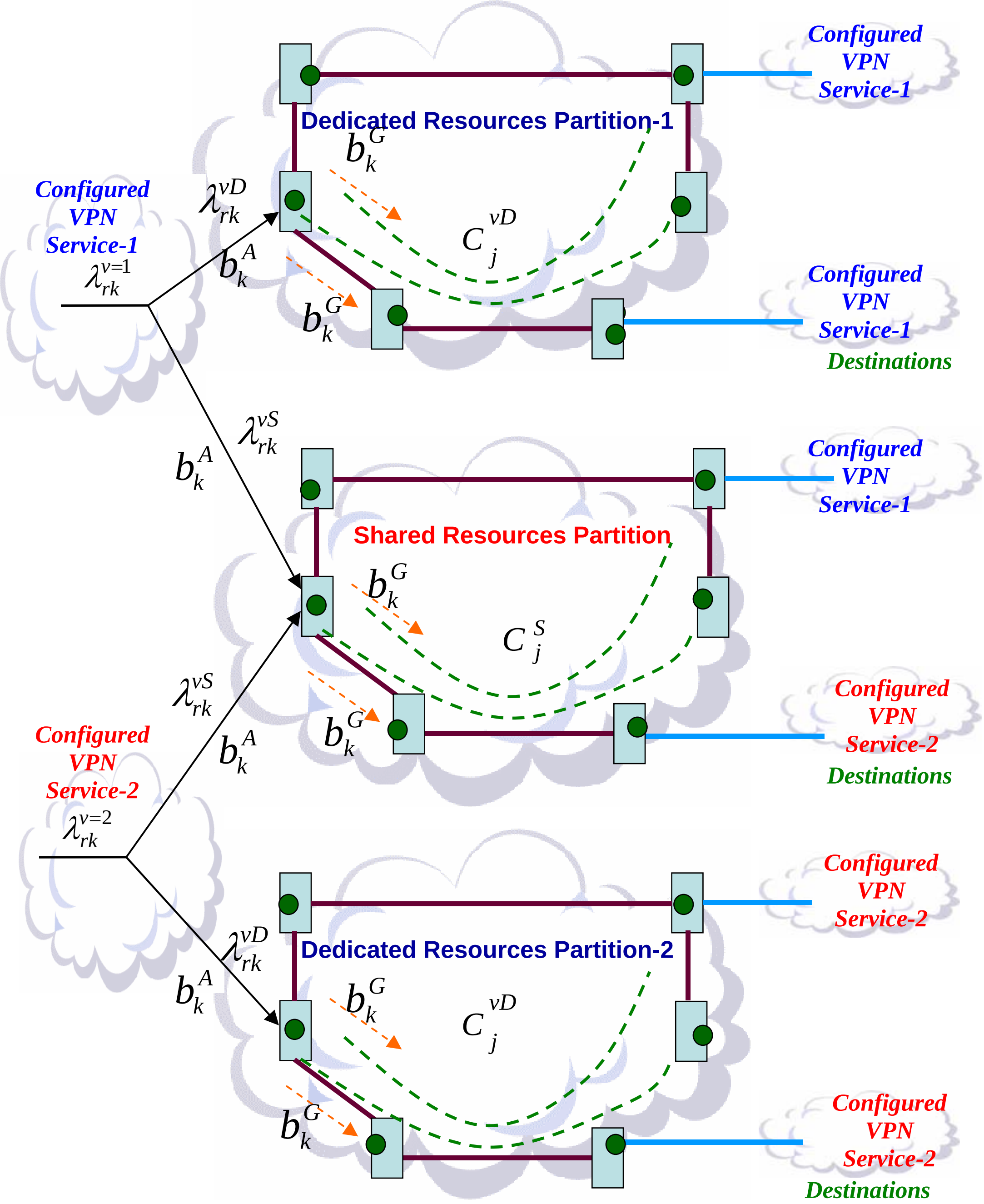

Figure 3-8: FSA and FSG Service Configurations

4 Control Plane Models- Traffic Management Schemes

This section describes the traffic management schemes of IETF, ITU, and SPA control plane models from the following control plane traffic management capabilities (details in section 4.2):

1. Routing update triggers
2. Network routing granularity
3. Load Partitioning Function (LPF)
4. Inverse Multiplexing Function (IMF)

4.1 Control plane components overview

This section provides a summary of the control plane components and operation. The control plane enables the automation of transport network connections setup and teardown; this will facilitate end-to-end connection setup. The purpose of the control plane is to:

1. Facilitate the fast and efficient configuration of transport layer connections.
2. Re-configure and modify connections that support existing configured services.
3. Perform a rapid restoration function. The control plane can automatically restore failed connections to backup connections and prevent any violation of customers' service level agreement.
4. Reduce operational costs via more accurate inventory and topology information, resource optimization through self-aware network, automated processes that eliminate manual steps.

The control plane performs those operations that can be automated. These include automatic connection setup "signaling", resource/topology auto-discovery, routing, and the connection admission control (CAC) function. The control plane interfaces with the transport plane to perform these tasks. The control plane takes service setup requests, these requests are put through a policy server to ensure that the client is allowed to make the request (i.e., CAC, check bandwidth, destination, etc.). Next, the control plane computes a path, signals the destination, and enables cross-connects in the transport network to reach the destination through multiple connections establishment across the multiple switching elements.

The control plane is the collection of control plane components that are used to manipulate transport plane network resources in order to provide the functionality of setting up, maintaining, and releasing connections. The control plane architecture is described in terms of components that represent abstract entities. Generically, every component has a set of interfaces to support a collection of operations that specify a provided or used service of that component. Figure 4-1 shows the functional block diagram of the control plane according to ITU-T recommendation G.8080 [15] mainly highlighting the functional flow among the different components. Following are brief description of each component:

- *NetCallC:* Network call "service request" controller component accepts (after verifying user rights and resource policy) and processes incoming call requests from a client network, processes and generates service termination requests towards a client network, and validates service parameters.
- *Connection Control (CC):* is responsible for the establishment, termination, and modifications of connections' parameters for existing network connections. Connection control is responsible for coordinating among the link resource manager, routing controller, and both peer and subordinate connection controllers. The overall control of a connection is performed by the protocol undertaking the set-up and release procedures associated with a connection and the maintenance of the state of the connection.
- *Connection Admission Control (CAC):* Connection admission control is essentially a process that determines if there are sufficient resources to admit a connection (or re-negotiates resources during a service request). This is usually performed on a link-by-link basis, based on local conditions and policy. For a simple circuit switched network this may simply devolve to whether there are free resources available. In contrast, for packet switched networks such as ATM, where there are multiple quality of service parameters, connection admission control needs to ensure that admission of new connections is compatible with existing quality of service agreements for existing connections. Connection admission control may refuse the connection request.
- *Traffic policy (TP):* provides the function of implementing the set of rules applied to a system. It is responsible for checking that the incoming user connection is sending traffic according to the parameters.

- *Link Resource Manager (LRM):* provides information about the allocation and de-allocation of link connections, providing topology and status information status.
- Neighbor Discovery: provides the function of collecting information about the topology of the neighboring nodes in addition to the connectivity and capability of the links connecting the network element to other network elements.
- *Protocol Controller (PC):* provides the function of mapping the parameters of the abstract interfaces of the control components into messages that are carried by a protocol to support interconnection via an interface. Protocol Controllers are a sub class of Policy Ports, and provide all the functions associated with those components. In particular, they report protocol violations to their monitoring ports. They may also perform the role of multiplexing several abstract interfaces into a single protocol instance. The details of an individual protocol controller are in the realm of protocol design.
- *Routing Controller (RC):* responds to requests from connection controller for path information needed to set up connections and respond to requests for topology information for network management purposes. Three approaches to dynamic path control can be identified: hierarchical, source routing, and step-by-step routing. Hierarchical routing is based on decomposition of a layer network into a hierarchy of sub-networks, each having its own dynamic connection control. A node contains a routing controller, connection controller, and link resource managers for a single level in a sub-network hierarchy. In the case of source routing, in which the route of the connection is determined at a source node, a federation of distributed connection controllers and routing controllers' implements the connection control process. A step-by-step routing differs from the previous case in a reduction of routing information that each routing controller provides information only about the next step. In this case, the operator cannot know the route of the paths before executing of the path setup command, but they can easily establish new paths due to avoidance of complicated path configurations.

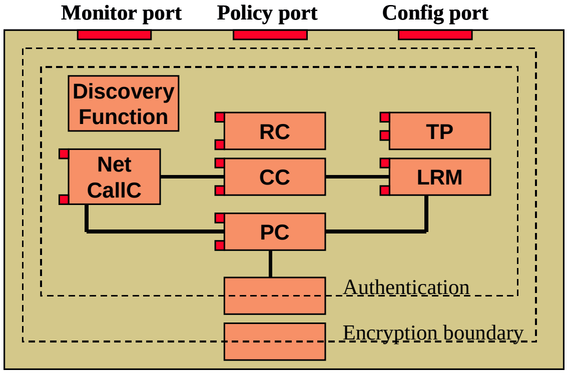

Figure 4-1: Control Plane Components

4.2 Traffic management capabilities definitions

This section provides detailed description of the different traffic management capabilities for the IETF, ITU, and SPA control plane models. The traffic management capabilities include the different traffic handling mechanisms that are implemented in the control plane components including routing component, Load Partitioning Function (LPF), and Inverse Multiplexing Function (IMF). Nine traffic management schemes are defined based on the traffic management mechanism configured for each control plane component. The detailed description of the nine traffic management schemes is provided in section 4.3. The following describes the configuration details for each traffic management capability:

1. *Static routing:* a routing mechanism where routes' routing probabilities for each source-destination pair are *not* prioritized based on the traffic occupancy state of all the links for each possible route between a source-destination pair. Instead, the routing options between a source-destination pair are statically prioritized. Two versions exist of static routing. The first version is Direct Routing (DR) where the direct link "minimum number of hops" between a source-destination pair is given a routing probability of one. The second version is Split Routing (SR) where the routing probability of each route between a source-destination pair is configured manually with the total probability of all the routes between a source-destination pair equals one.
2. *State-dependent routing:* a routing mechanism where the routing probabilities for each source-destination pair are determined based on the traffic occupancy state of all the links for each possible route between a source-destination pair.

3. <u>*Network routing granularity:*</u> The network granularity level (b_k^A, b_k^C, b_k^G) used to construct the routing tables.
4. <u>*Load Partitioning Function (LPF):*</u> a control plane capability to partition the configured VPN service arrival load λ_{rk}^{v} into two partitions; a dedicated load λ_{rk}^{vD} applied to the dedicated resources partition and a shared load λ_{rk}^{vS} applied to the shared resources partition. The rate partitioning handling capability has two options; Static Partitioning (SS) and Network Engineering.
    a. *Static Sharing (SS):* a control plane capability that statically partitions the configured VPN service arrival load into two partitions between the dedicated and shared resources partitions. One load partition, dedicated load, based on the capacity ratio of the dedicated resources partition to the VPN resources partition (sum of dedicated and shared resources), and another load partition, shared load, based on the capacity ratio of the shared resources to the VPN resources partition.
    b. *Network Engineering (NE):* a control plane capability that dynamically partition the configured VPN service arrival load between the dedicated and shared resources partitions based on the blocking probability of the dedicated resources partition. Here a two-round process is used to find the load partition ratio. In round-1, the configured VPN service total load is applied to the dedicated resources partition and a blocking probability is generated. In round-2, the load is applied again to the dedicated resources partition in proportion to the unblocked load and to the shared resources partition in proportion to the blocked load.
5. <u>*Inverse Multiplexing Function (IMF):*</u> a control plane capability that allows for multiplexing and inverse multiplexing of traffic bandwidth. IMF function is used at the source and destination nodes of a service request when inverse multiplexing and multiplexing of traffic bandwidth is required to increase network bandwidth efficiency.
    a. *Multiplexing:* Multiplexing is sending multiple signals or streams of information on a carrier at the same time in the form of a single, complex signal and then recovering the separate signals at the receiving end.
    b. *Inverse Multiplexing (IM):* Inverse multiplexing speeds up data transmission by dividing a service request with actual bandwidth requirement b_k^A into multiple

concurrent granular streams or flows with bandwidth requirement b_k^G that are transmitted at the same time across separate channels and are then reconstructed at the other end back into the original data stream.

4.3 Control plane models and associated traffic management capabilities

Based on the three control plane traffic management capabilities (Routing, LPF, IMF), multiple control plane models are defined (see table 4-1 and Figure 4-2).

Control Plane Model	**Routing Component**	**Load Partitioning Function (LPF)**	**Inverse Multiplexing Function (IMF)**
IETF-DR	Static- Direct	Disabled	Disabled
IETF-SR	Static- Split	Disabled	Disabled
ITU-DR	Static- Direct	Disabled	Disabled
ITU-SR	Static- Split	Disabled	Disabled
SPA-Dedicated	State-Dependent	Disabled	Disabled
SPA-Shared W/O (NE,IM)	State-Dependent	Enabled (SS)	Disabled
SPA- Shared (W/ NE, W/O IM)	State-Dependent	Enabled (NE)	Disabled
SPA- Shared (W/O NE, W/ IM)	State-Dependent	Enabled (SS)	Enabled
SPA- Shared W/ (NE,IM)	State-Dependent	Enabled (NE)	Enabled

Table 4-1: Control Plane Models and Associated Traffic Management Schemes

Figure 4-2 provides a graphical view of the different control plane models based on the above listed control plane capabilities. As illustrated in Table 4-1, The SPA control plane model can operate under five traffic management schemes. It is important to note that the SPA control plane model adds three additional capabilities on top of the IETF and ITU control plane models capabilities; the SPA routing component is state-dependent, the LPF is enabled with two possible configuration options (SS,NE), and the IMF with two configuration options (enabled, disabled). This research compares each of these control plane models in a common framework. Each of the control plane models listed in Table 4-1 will be discussed in details in sections 44.4, 4.5, and 4.6.

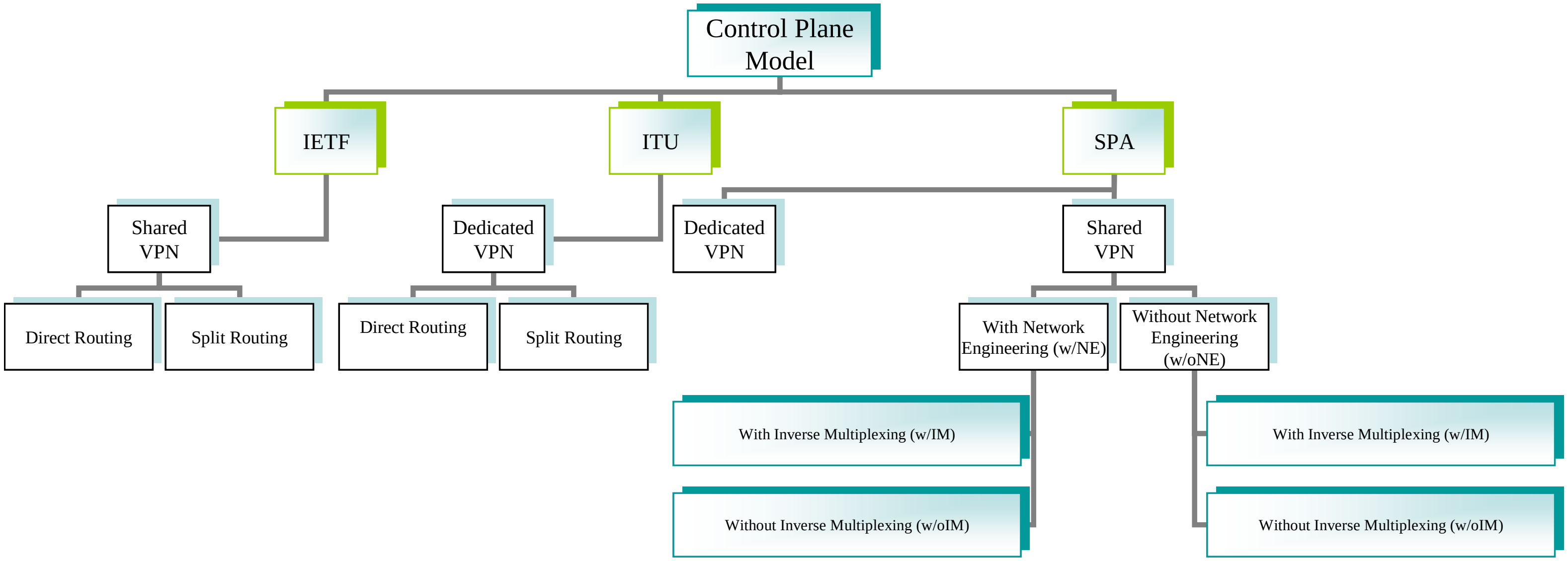
Control Plane Model
IETF
ITU
SPA
Shared VPN
Dedicated VPN
Dedicated VPN
Shared VPN
Direct Routing
Split Routing
Direct Routing
Split Routing
With Network Engineering (w/NE)
Without Network Engineering (w/oNE)
With Inverse Multiplexing (w/IM)
Without Inverse Multiplexing (w/oIM)
With Inverse Multiplexing (w/IM)
Without Inverse Multiplexing (w/oIM)

Figure 4-2: Control Plane Models Based on Traffic Management Schemes

4.4 IETF control plane model

As listed in Table 4-1, the IETF control plane model has the following traffic management capabilities:

1. *Disabled LPF:* The IETF control plane model does have the Load Partitioning Function (LPF) implemented; thus all the load from multiple configured VPN services are multiplexed on the same physical topology. This is illustrated in Figure 4-3 where arrival load from both configured VPN service-1 and configured VPN service-2 are multiplexed into the same physical resources. As will be mention in section 5.3, this is considered Complete Sharing (CS) from a transport network perspective.

2. *Static Routing:* As illustrated in Figure 4-3, the IETF control plane model routes traffic between a source-destination pair not based on the traffic occupancy state of the network.

3. *Disabled IMF:* The IETF control plane model does not implement the IMF on the arriving service flow so bandwidth requirement b_k^A is not split it into multiple flows each with granular bandwidth b_k^G. On the contrary, the IETF control plane model consumes b_k^C coarse resources from the transport network; this is due to the coarse realization of the transport network by the IETF routing component. For example, a service request with actual bandwidth requirement b_k^A = 2STS-1 will consume b_k^G = 3STS-1 from the transport network resources.

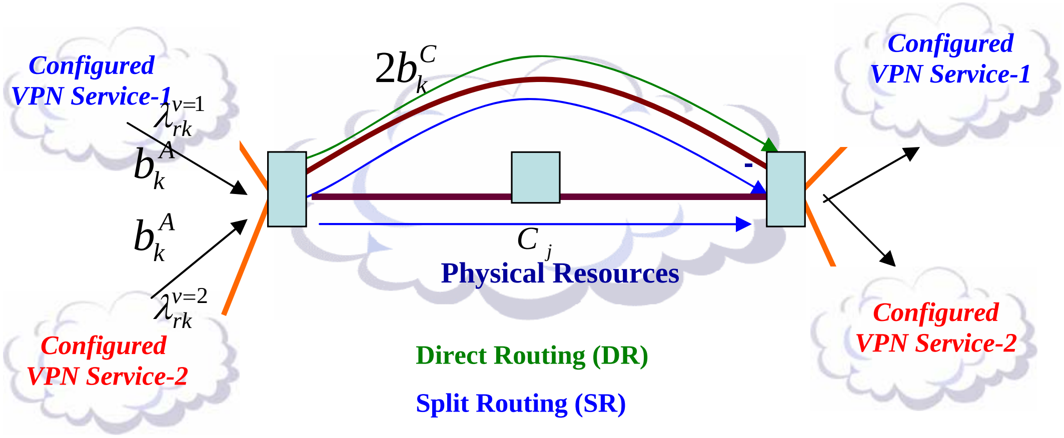

Figure 4-3: Traffic Management of IETF Control Plane Model

4.5 ITU control plane model

As listed in Table 4-1, the ITU control plane model has the following traffic management capabilities:

1. *Enabled LPF:* The ITU control plane model has the Load Partitioning Function (LPF) implemented; thus the load from multiple configured VPN services is partitioned into multiple transport network partitions, and no traffic multiplexing between different configured VPN services is allowed. This is illustrated in Figure 4-4 where load from configured VPN service-1 and configured VPN service-2 is directed to dedicated resources partition-1 and dedicated resource partition-2 respectively. As will be mention in section 5.3, this is considered Complete Partitioning (CP) from a transport network perspective.
2. *Static Routing:* Similar to the IETF control plane model; the static routing is implemented in each transport network partition.
3. *Disabled IMF:* The ITU control plane model does not implement the IMF on the arriving service request.

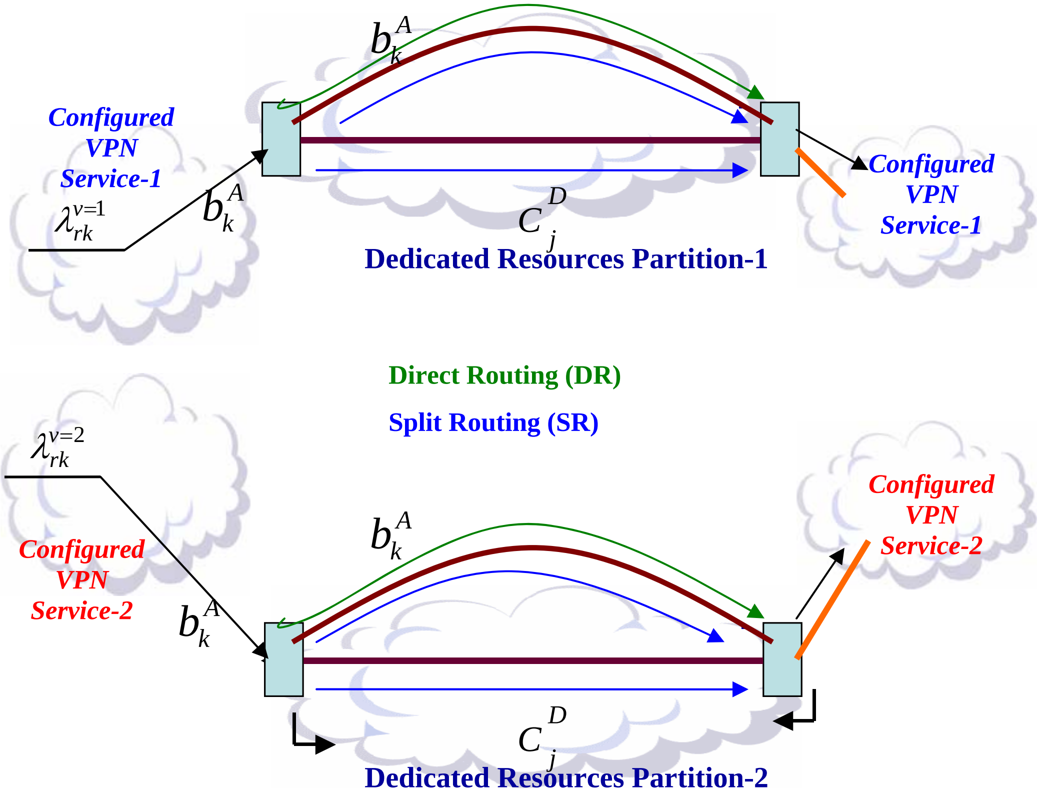

Figure 4-4: Traffic Management of ITU Control Plane Model

4.6 SPA-Dedicated control plane model

As listed in Table 4-1, the SPA-Dedicated control plane model has the exact traffic management capabilities like the ITU model except state-dependent routing instead of static routing.

4.7 SPA-Shared control plane model

As listed in Table 4-1, the SPA Shared control plane model has the following traffic management capabilities:

1. *Enabled LPF:* The SPA control plane shared control plane model has the Load Partitioning Function (LPF) implemented; thus the load from multiple configured VPN services is partitioned into multiple resources partitions, LPF can be configured as Static Partitioning (SS) or Network Engineering (NE). The SPA Shared control plane model implementation of the LPF is different from the ITU or SPA-Dedicated control plane

models. In the ITU or SPA-Dedicated control plane models, *the entire* arriving load from a configured VPN service-1 is applied to dedicated resources partition-1. Similarly, *the entire* load from a configured VPN service-2 is applied to dedicated resources partition-2. In the SPA Shared control plane model, the load from a configured VPN service-1 is partitioned into dedicated load applied to dedicated resources-1 partition, and a shared load applied to shared resources partition. Similarly, the arriving load from a configured VPN service-2 is partitioned into dedicated load applied to dedicated resources-2 partition, and a shared load applied to shared resources partition. This is illustrated in Figure 4-5 . As will be mention in section 5.3, this is considered Virtual Partitioning (VP) from a transport network perspective. In summary, VP divides the network resources into a dedicated resources partition *(D)* and a shared resources partition *(S).* A dedicated load from a configured VPN service-1 is applied to the dedicated resources partition-1; hence no multiplexing of arriving loads from different configured VPN services is allowed on the dedicated resources partition-1. Arriving load from different configured VPN services can share the shared resources partition; hence multiplexing of arriving loads from different configured VPN services is allowed on the shared resources partition.

2. *State-dependent Routing:* performed in all the dedicated resources partitions in addition to the shared resources partition.

3. *Enabled IMF:* The SPA shared control plane model implements the Inverse Multiplex (IM) where the arriving service request flow with actual bandwidth requirement b_k^A is split into multiple flows each with granular bandwidth requirement b_k^G .

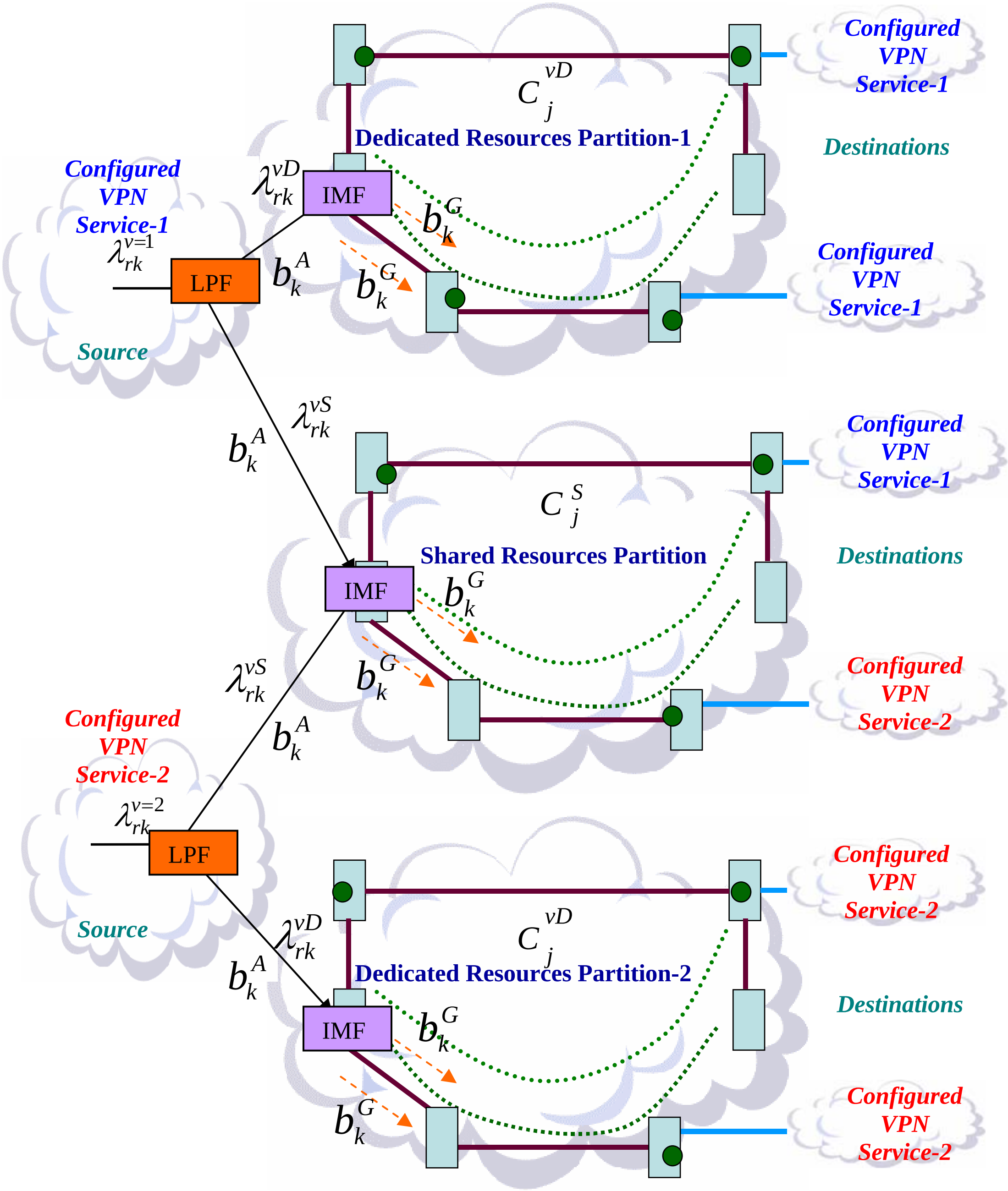

Figure 4-5: Traffic Management of SPA Shared Control Plane Model

5 Control Plane Models– Transport Network Realization

This section compares the three control plane models from a transport network architecture realization perspective. The transport network can be viewed from both horizontal and vertical perspective. Horizontally, the transport network can be divided into network domains. One dimension of the vertical view is dividing the transport network into multi-granularity levels, each granularity level with actual bandwidth rate b_k^A. The sub-rate at a specific transport network granularity level is multiplexed into the upper transport network granularity level. The other dimension of the vertical view is dividing the physical transport network resources into network resources partitions or Virtual Private Networks (VPNs). The IETF, ITU, and SPA control plane model do not differ in their realization of a multi-domain transport network but differ in their realization of a multi-granularity transport network. The multi-domain view was described to provide a full view, from the three control planes perspective, of the multi-domain multi-granularity transport network.

5.1 Horizontal view: multi-domain realization

The following concepts need to be described to understand the architectural differences for the three control plane models realizations of the transport network architecture and more specifically the multi-granularity aspect of the transport network.

1. *Sub-network:* The physical transport network can be divided into sub-networks based on different technologies or ownership of network domains. A physical topology can be divided into multiple sub-networks “domains” to simplify and scale routing protocols. Parent sub-networks can be further divided into child sub-networks. A sub-network can be partitioned into smaller sub-networks. Sub-networks are defined to be completely contained within higher level sub-networks. Figure 5-1 illustrates sub-network partitioning.
2. *Sub-network point (SNP):* A control plane representation of a transport network resource. Each transport network granularity level is represented by a group of SNPs. The group of SNPs are connected to each other by Sub-Network Connections (SNCs) in the same topological view of the transport network granularity level. When the network resource represented by a certain SNP is allocated to a service request, the status of the relevant

SNP is changed to "busy", otherwise when the resource is available for a service request, the status of the relevant SNP remains "idle".

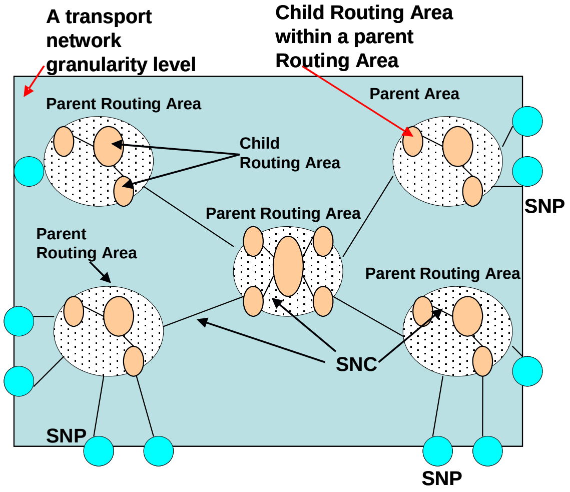

Figure 5-1: Control Plane Routing Areas Realization of Transport Network Partitioning into Sub-Networks

3. *Sub-network connection (SNC):* A sub-network connection is a dynamic relation between two (or more in the case of broadcast connections) Sub-network points (SNPs) at the boundary of the same sub-network. For example, two adjacent sub-networks can be connected by an SNC.

4. *Sub-network point pool (SNPP):* A control plane representation of a set of sub-network points that are grouped together for the purposes of routing. An SNP pool can represent a collection of SNPs within the same sub-network "horizontal-view" or represent a collection of SNPs across multiple granularity levels "vertical-view".

5. *Routing Area (RA):* A control plane representation of a transport network sub-network. Each transport network sub-network is represented by a routing area. RAs are hierarchically contained: a higher level (parent) RA contains lower level (child) RAs that in turn MAY also contain RAs, etc. Thus, RAs contain RAs that recursively define successive hierarchical RA levels. If a parent sub-network is divided into child sub-networks, the parent RA is divided into child routing areas, each child transport sub-

network is represented by a control plane child routing area. The group of routing areas at different routing levels represents a hierarchal routing architecture[3].

6. *Routing Level (RL):* In a multi-level hierarchy of RAs, it is necessary to distinguish between routing at different levels of the RA hierarchy. Two routing areas at the same level of the routing hierarchy but belong to two different parent routing areas can not directly exchange routing topology between them as routing topology exchange has to be carried via their parent routing areas in a routing level above the child routing areas level. Routing information can be exchanged across adjacent levels of the RA hierarchy i.e. parent level and child level, where child level represents the RAs contained by parent level.[4]

5.2 Vertical view: multi-granularity realization

The multi-granularity realization has two dimensions; the first dimension is the transport network multi-granularity aspect, e.g., an STS-12 carry 12STS-1, the second dimension is the demand multi-granularity aspect, e.g., a service request flow with actual bandwidth requirement b_k^A=2STS-1 can be split into two flows each with granular bandwidth requirement b_k^G =1STS1.

5.2.1 IETF control plane model

From a demand granularity perspective, the Inverse Multiplexing Function (IMF) in the IETF control plane model is disabled. Hence, IETF control plane model will not consider the demand granularity level feature of the service profile in its service request routing or path computation. As illustrated in Figure 5-2, the service request flow with actual bandwidth requirement b_k^A is not split into multiple flows each with granular bandwidth

[3] It is important to note that a single transport network granularity level can be represented by a hierarchal routing architecture.

[4] There is no implied relationship between multi-granularity transport networks and multi-level routing. The group of Routing Controllers (RCs) providing routing update for a sub network can be architected as flat or hierarchal routing architecture

requirements b_k^G , instead b_k^A service request is considered a service request with coarse bandwidth requirements b_k^C , because the routing and path computation components in the IETF control plane model have a coarse representation of transport network granularity. In other words, IETF routing and path computation components are not architected to optimize mapping between the granularity level of service demands and the available granularity levels of transport network. As a result, transport network resources will not be efficiently utilized due to mismatch between the granularity level of the service demand and the granularity level of the transport network.

Figure 5-2 illustrates the IETF control plane realization of the granularity levels of the transport network. It can be observed that the IETF control plane model represents a multi-granularity transport network by one SNP; this indicates the coarse representation of the transport network granularity levels. From an IETF control plane model perspective, the multi-granularity transport network is one physical layer. This leads that a service request with granular demand requirement will be mapped to a coarse granularity level in the transport network. This is illustrated in Figure 5-2 where the service request with actual bandwidth requirement b_k^A= 2 STS-1 is mapped to the transport network resources as a service request with coarse bandwidth requirement b_k^C = 3 STS-1.

5.2.2 ITU control plane model

From a demand granularity perspective, the Inverse Multiplexing Function (IMF) in the ITU control plane model is disabled. Hence, ITU control plane model will not consider the demand granularity level feature, of the service profile, in its service demand routing or path computation. As illustrated in Figure 5-3, the service request flow with actual bandwidth requirement b_k^A is not split into multiple flows each with granular bandwidth requirements b_k^G ; instead b_k^A service request is considered a service request with actual bandwidth requirements b_k^A . The reason for that is since the routing and path computation components in the ITU control plane model have a granular representation of transport network granularity levels.

In other words, ITU routing and path computation components are architected to optimize mapping between the granularity level of service demands and the available granularity levels of transport network. As a result, transport network resources will be more efficiently utilized than the IETF control plane model due to match between the granularity level of the service request and the granularity level of the transport network. Figure 5-3 illustrates the ITU control plane realization of the granularity levels of the transport network. It can be observed that the ITU control plane model represents a multi-granularity transport network by multiple SNPs, one SNP for each granularity level of the transport network, this indicates the granular representation of the transport network granularity levels. This leads that a service request with a certain granularity demand requirement will be mapped to the most optimum granularity level in the transport network. This is illustrated in Figure 5-3 where the service request with actual bandwidth requirement b_k^A = 2 STS-1 is mapped to the transport network resources as a service request with actual bandwidth requirement b_k^A = 2 STS-1.

5.2.3 SPA control plane model

Similar to the ITU control plane model, the SPA-Dedicated control plane model has the same granular representation of the transport network granularity level and the demand granularity level. The SPA-Shared differs from the SPA-Dedicated since the IMF can be enabled which further splits a service request flow with actual bandwidth requirement b_k^A into multiple flows each with granular bandwidth requirements b_k^G as illustrated in Figure 5-4.

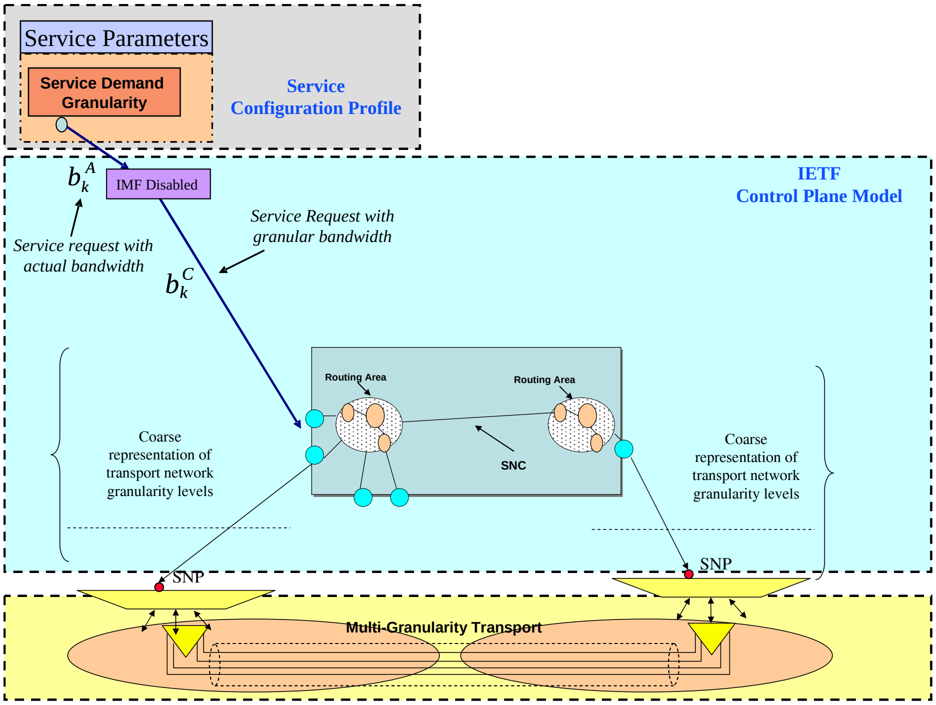
Service Parameters
Service Demand Granularity
Service Configuration Profile
b_k^A
IMF Disabled
IETF Control Plane Model
Service request with actual bandwidth
Service Request with granular bandwidth
b_k^C
Routing Area
Routing Area
SNC
Coarse representation of transport network granularity levels
Coarse representation of transport network granularity levels
SNP
SNP
Multi-Granularity Transport

Figure 5-2: IETF Control Plane Model Realization of Transport Network Granularity Levels

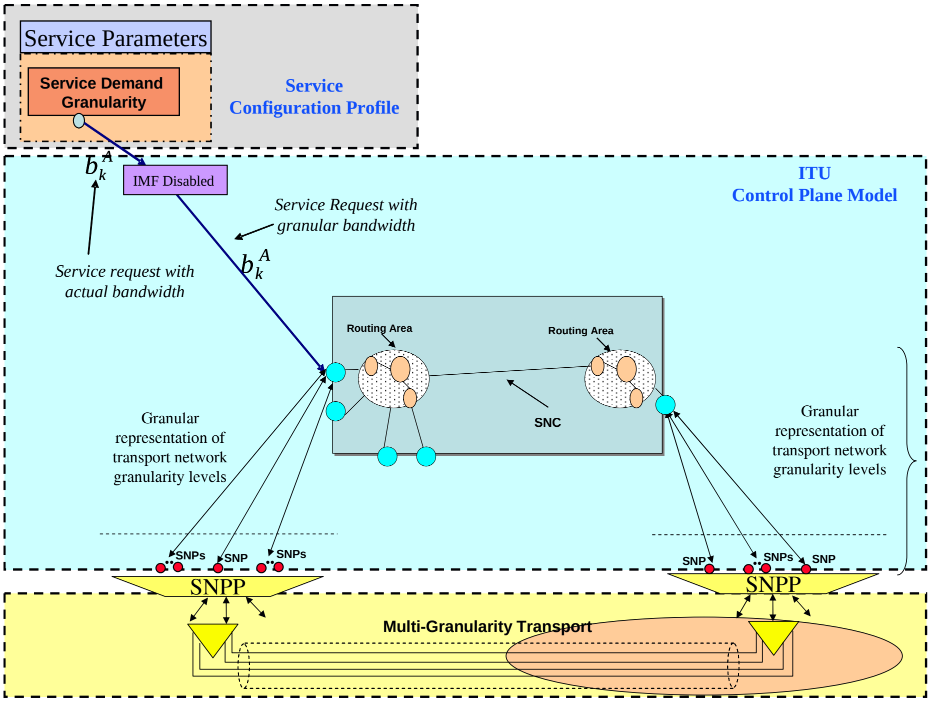
Service Parameters
Service Demand Granularity
Service Configuration Profile
b_k^A
IMF Disabled
ITU Control Plane Model
Service request with actual bandwidth
Service Request with granular bandwidth
b_k^A
Routing Area
Routing Area
SNC
Granular representation of transport network granularity levels
Granular representation of transport network granularity levels
SNPs
SNP
SNPs
SNP
SNPs
SNP
SNPP
SNPP
Multi-Granularity Transport

Figure 5-3: ITU and SPA-Dedicated Control Plane Models Realization of Transport Network Granularity Levels

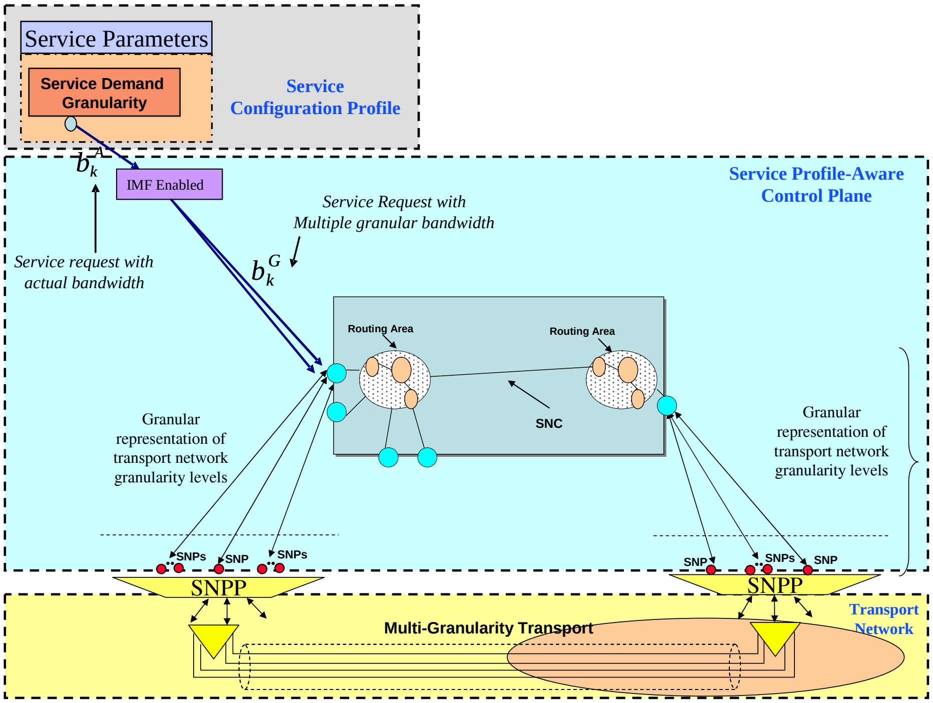
Service Parameters
Service Demand Granularity
Service Configuration Profile
b_k^A
IMF Enabled
Service Profile-Aware Control Plane
Service Request with Multiple granular bandwidth
b_k^G
Service request with actual bandwidth
Routing Area
Routing Area
SNC
Granular representation of transport network granularity levels
Granular representation of transport network granularity levels
SNPs
SNP
SNPs
SNP
SNPs
SNP
SNPP
SNPP
Multi-Granularity Transport
Transport Network

Figure 5-4: SPA-Shared Control Plane Models Realization of Transport Network Granularity Levels

5.3 Vertical view: resources partitioning

The concept of resource partitioning and reservation has been extensively studied [44-54]. Many of these were focused on different resources partitioning and reservation methods to maintain the SLA requirements, lower blocking probability, of some services. One of the concepts introduced was Complete Sharing (CS) where the network resources are completely shared among all configured VPN services; this represents the extreme form of unrestricted sharing. Complete Partitioning (CP) was another concept that was analyzed which provides complete isolation of the traffic between different configured services accessing the same network resources; this represents the other side of extreme form of restricted sharing. Virtual Partitioning (VP) was an intermediate paradigm for disciplined sharing; this paradigm assigns a dedicated and shared network resources partition to each configured VPN service. Dividing the physical resources into multiple partitions is realized by the control plane using the Control Plane Instance (CPI)[5] concept. Each CPI includes the following:

1. *Routing Database (RDB):* Contains the local topology and resources within each network partition. The Routing Information Database (RDB) is a repository for the local topology within, network topology, reachability, and other routing information that is updated as part of the routing information exchange. The RDB may contain routing information for more than one routing area. Each control plane instance has a RDB that includes the network topology controlled by the control plane instance.

2. *Collection of Routing Controllers (RCs)*[6]*:* Exchange topology information within the network partition. The RCs can be divided into multiple Routing Areas (RAs) within the same Routing Level (RL). The RCs can be grouped in a flat routing architecture, one routing level, or a hierarchal routing architecture, multiple routing levels. In this research, the RCs are assumed to be grouped in a flat routing architecture. The hierarchal routing architecture is proposed to be analyzed in the future work beyond the scope of this research.

1. *Link Resource Manager (LRM):* Supplies all the relevant connection resource information to the Routing Controller. It informs the RC about any state changes of the connection resources it controls.

[5] The Control Plane Instance (CPI) is another definition that can be used to define a group of Routing Areas within the same Routing Level. In the case of IETF control plane model, one control plane instance will be used to provide resource updates and capacity allocation across the N-transport network partitions. In the case of ITU control plane model, *N* control plane instances will be used to provide resource updates and capacity allocation across the *N*-transport network partitions. The SPA-Shared control plane model is similar to the ITU control plane model as it has *N* control plane instances but with LPF across the *N* control plane instances.

[6] The RC functions include exchanging routing information with peer RCs and replying to a route query (path selection) by operating on the Routing Database (RDB).

5.3.1 IETF control plane model

The IETF control plane model does not partition its physical topology RDB into multiple RDB partitions based on transport network partitioning; thus, the resources at different network partitions of the transport network are represented by one RDB. In other words, the IETF control plane model supports the Complete Sharing (CS) concept. The IETF control plane model represents the *N*-partitions of the transport network by one Control Plane Instance (CPI). Figure 5-5 illustrates the IETF single control plane instance controlling three transport network partitions.

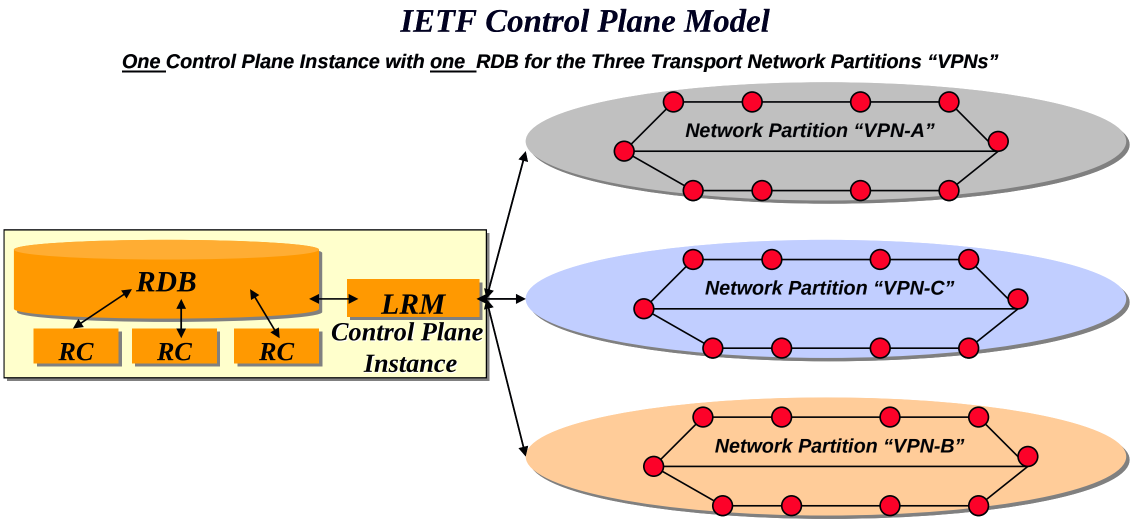
IETF Control Plane Model
One Control Plane Instance with one RDB for the Three Transport Network Partitions "VPNs"
Network Partition "VPN-A"
RDB
LRM
RC
RC
RC
Control Plane Instance
Network Partition "VPN-C"
Network Partition "VPN-B"

Figure 5-5: Instance Realization of Transport Network Partitions for the IETF Control Plane

5.3.2 ITU control plane model

The ITU control plane model partitions its physical topology RDB into multiple RDB partitions based on transport network partitioning; thus the resources of each network partitions of the transport network is represented by a separate RDB. In other words, the ITU control plane model supports the Complete Partitioning (CP) concept. The ITU control plane model represents the *N*-partitions of the transport network by *N* Control Plane Instances (CPIs). Figure 5-6 illustrates ITU three control plane instances controlling three network resources partitions. It is important to note that ITU control plane instances do not exchange routing information across CPIs by linking the Link Resource Management (LRM) components of the control plane instances; thus not allowing customer traffic to be re-routed from one network resources partition to another network resources partition based on the configured policy. The network resources within each network partition, controlled by a control plane instance, are not shared with other network resources partitions. In other words, the control plane instances in the ITU model are *independent* in their traffic management scheme of each network resources partition. This would imply that ITU control plane model has no Load Partitioning Function (LPF) implemented to coordinate load sharing by the control plane instances across network resources partitions.

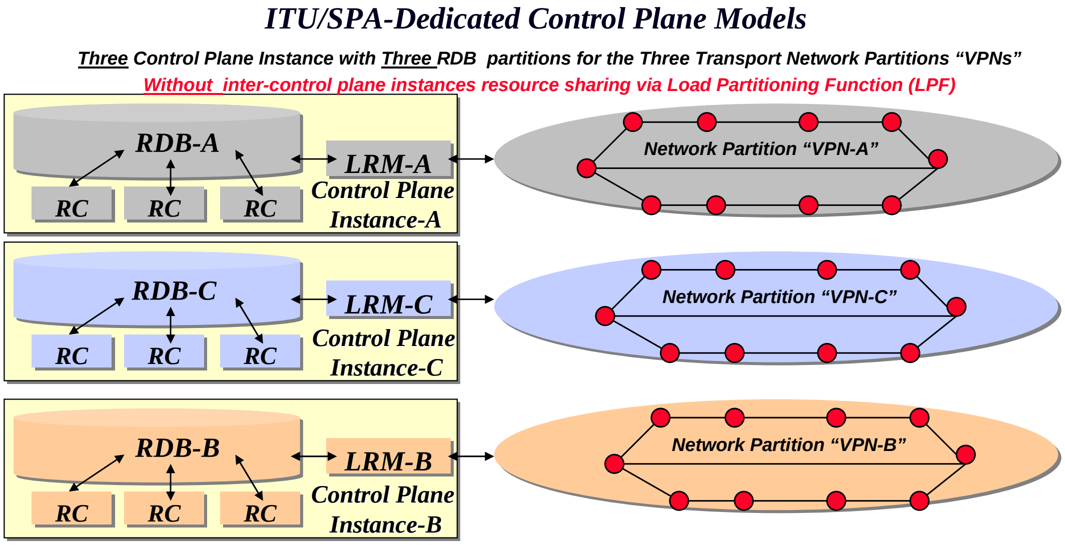
ITU/SPA-Dedicated Control Plane Models
Three Control Plane Instance with Three RDB partitions for the Three Transport Network Partitions "VPNs"
Without inter-control plane instances resource sharing via Load Partitioning Function (LPF)
RDB-A
RC
RC
RC
LRM-A
Control Plane
Instance-A
Network Partition "VPN-A"
RDB-C
RC
RC
RC
LRM-C
Control Plane
Instance-C
Network Partition "VPN-C"
RDB-B
RC
RC
RC
LRM-B
Control Plane
Instance-B
Network Partition "VPN-B"

Figure 5-6: Instance Realization of Transport Network Partitions for ITU/SPA-Dedicated Control Plane Models

5.3.3 SPA control plane model

The SPA control plane model has two versions; dedicated and shared. The SPA-Dedicated control plane model implements the Complete Partitioning (CP) concept in its realization of transport network resources partitions. The difference between the ITU and the SPA-Dedicated control plane models is that the later implements state-dependent routing instead of the static routing implemented by the ITU control plane model. The SPA-Shared control plane model supports the Virtual Partitioning (VP) concept by allowing traffic exchange across network resources partitions. This is enabled in the SPA-Shared control plane model by linking the Link Resource Management (LRM) components of the control plane instances via the Load Partitioning Function (LPF). Similar to the ITU control plane model, the SPA-

Shared control plane model represents the *N*-partitions of the transport network by *N*-Control Plane Instances *(CPIs)*. Figure 5-7 illustrates the SPA-Shared three control plane instances controlling three network resources partitions with LPF, linking the Link Resource Management (LRM) component of each control plane instance, which allows traffic exchange across network resources partitions.

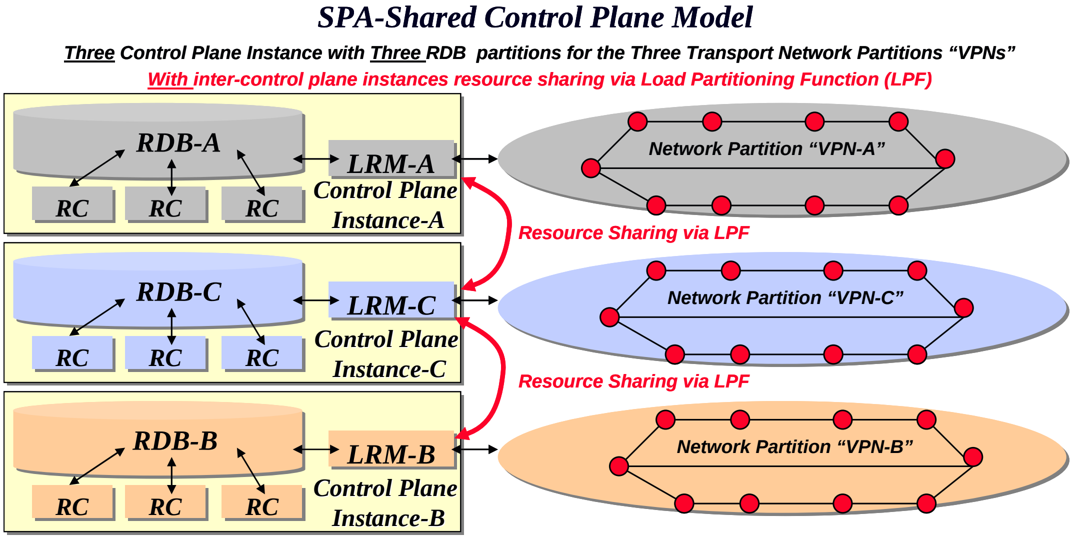
SPA-Shared Control Plane Model
Three Control Plane Instance with Three RDB partitions for the Three Transport Network Partitions "VPNs"
With inter-control plane instances resource sharing via Load Partitioning Function (LPF)
RDB-A
RC
RC
RC
LRM-A
Control Plane Instance-A
Network Partition "VPN-A"
Resource Sharing via LPF
RDB-C
RC
RC
RC
LRM-C
Control Plane Instance-C
Network Partition "VPN-C"
Resource Sharing via LPF
RDB-B
RC
RC
RC
LRM-B
Control Plane Instance-B
Network Partition "VPN-B"

Figure 5-7: Instance Realization of Transport Network Partitions for the SPA-Shared Control Plane

6 Control Plane Models- Component-Level Interaction

This section is focused on the component-level interaction between the control plane components with both the service configuration profile components and the transport network components. In analyzing the components operational flow for each of the three control plane models, we need to include the impact of both the service configuration profile layer and the transport network layer. As mentioned earlier, the service configuration profile layer includes the following parameters:

1. Load partitioning flexibility (disabled vs. enabled)
2. Service demand granularity (granular vs. coarse)
3. Service flow connectivity (point-to-point, semi-meshed, fully-meshed)

4. Configured VPN service identification number *(v)*

The transport network provides parameters that are related to the transport network including:

1. Transport network granularity level (granular vs. coarse)

2. Transport topology occupancy state (per link)

6.1 IETF control plane model

The following service configuration profile parameters are considered in IETF control plane model when a service request is handled:

1. Service demand granularity

2. Service flow connectivity

As illustrated in Figure 6-1, the following is the IETF control plane model components operational flow sequence:

Component Interaction: Control Plane Models & Service Configuration Profile:

1. Based on a service request initiation, the "service flow connectivity" parameter from the service configuration profile layer is sent to the "path computation" component in the IETF control plane layer, the "service demand granularity" parameter from the service configuration profile layer is sent the Inverse Multiplexing Function (IMF) in the IETF control plane layer.

2. Since IMF is disabled, the service request flow with actual bandwidth requirement b_k^A is not split into multiple flows each with granular bandwidth requirement b_k^G. Instead b_k^A service request is considered a service request with coarse bandwidth requirement b_k^C.

3. The "path computation" component analyzes the service flow to determine the source-destination pair and the appropriate routing controllers to be contacted to determine the appropriate route for the service request.

4. The "path computation" component sends a route query request to the "static routing" component in the control plane layer.

Component Interaction: Control Plane Models & Transport Network :

5. Since the routing component in the IETF control plane model has a coarse realization of the transport network multi-granularity levels, the transport network coarse-granularity level is provided to the “static routing” component.

6. The “static routing” component provides the topology routing options to the “path computation” component without considering the transport topology traffic occupancy state for each of the topology links.

7. The “path computation” component computes a route based on:

    a. Service flow connectivity

    b. Service demand coarse bandwidth requirement b_k^C

    c. Transport network coarse granularity level.

8. A connection setup is initiated.

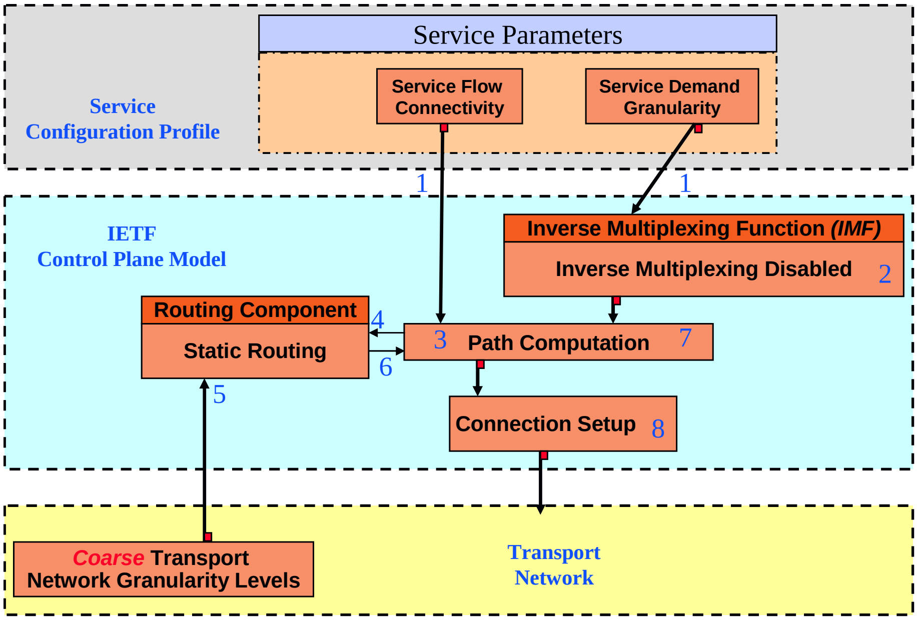
Service Parameters
Service Flow Connectivity
Service Demand Granularity
Service Configuration Profile
1
1
IETF Control Plane Model
Inverse Multiplexing Function (IMF)
Inverse Multiplexing Disabled
2
Routing Component
Static Routing
4
6
3
Path Computation
7
5
Connection Setup
8
Coarse Transport Network Granularity Levels
Transport Network

Figure 6-1: IETF Control Plane Components Operational Flow Sequence

6.2 ITU control plane model

The following service configuration profile parameters are considered in ITU control plane model when a service request is handled:

1. Service demand granularity
2. Service flow connectivity
3. Configured VPN service identification number *(v)*

As illustrated in Figure 6-2, the following is the ITU control plane model components operational flow sequence:

<u>Component Interaction: Control Plane Models & Service Configuration Profile:</u>

1. Based on a service request initiation, the "service flow connectivity", "service demand granularity" and "configured VPN service identification number" parameters from the service configuration profile layer are sent to the "control plane instance selection" component in the ITU control plane layer.
2. Based on the "configured VPN service identification number" parameter, the "control plane instance selection" component decides which control plane instance is responsible for handling the arriving service request.
3. Since IMF is disabled for all Control Plane Instances *(CPIs)*, the service request flow with actual bandwidth requirement b_k^A is not split into multiple flows each with granular bandwidth requirements b_k^G , instead b_k^A service request is considered a service request with actual bandwidth requirement b_k^A . The reason for that is provided in section 5.2.2.
4. The "path computation" component for the selected control plane instance analyzes the service flow to determine the source-destination pair and the appropriate routing controllers to be contacted to determine the appropriate route for the service request.
5. The "path computation" component sends a route query request to the "static routing" component in the control plane layer.

Component Interaction: Control Plane Models & Transport Network :

6. Since the ITU control plane model has a granular realization of the transport network multi-granularity levels, the transport network fine-granularity levels are provided to the "static routing" component.

7. The "static routing" component provides the topology routing options to the "path computation" component without considering the transport topology traffic occupancy state for each of the topology links.

8. The "path computation" component computes a route based on:

   a. Service flow connectivity

   b. Service demand actual bandwidth requirement b_k^A

   c. Transport network fine "detailed" granularity level.

9. A connection setup is initiated.

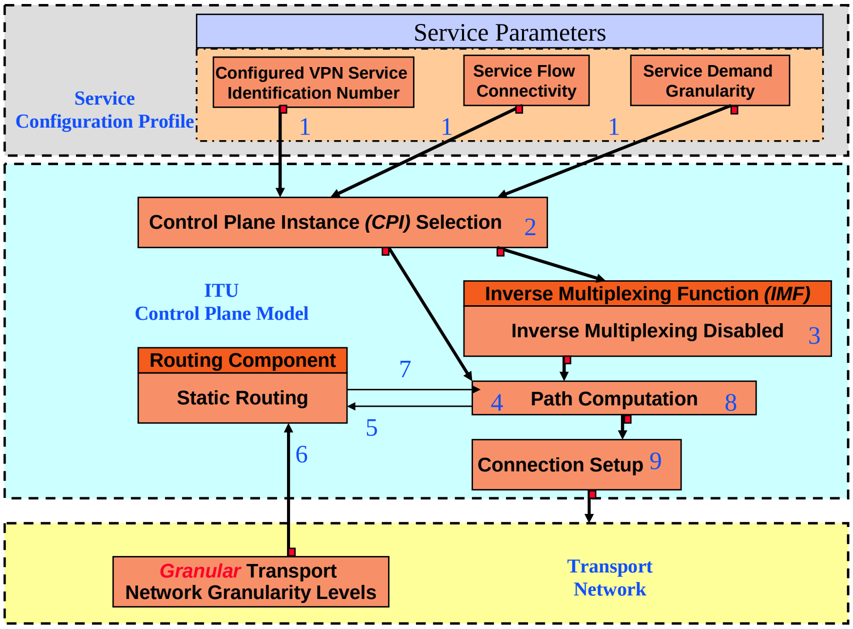
Service Parameters
Service Configuration Profile
Configured VPN Service Identification Number
Service Flow Connectivity
Service Demand Granularity
1
1
1
Control Plane Instance (CPI) Selection
2
ITU Control Plane Model
Inverse Multiplexing Function (IMF)
Inverse Multiplexing Disabled
3
Routing Component
Static Routing
7
5
4
Path Computation
8
6
Connection Setup
9
Granular Transport Network Granularity Levels
Transport Network

Figure 6-2: ITU Control Plane Components Operational Flow Sequence

6.3 SPA control plane model

The SPA-Dedicated control plane model has the same sequence like the ITU control plane model expect step (6) since the routing component in the SPA-Dedicated implements state-dependent routing instead of fixed routing. The following service configuration profile parameters are considered in SPA-Shared control plane model when a service request is handled:

1. Load partitioning flexibility
2. Service demand granularity
3. Service flow connectivity
4. Configured VPN service identification number *(v)*

As illustrated in Figure 6-4, the following is the SPA-Shared control plane model components operational flow sequence:

Component Interaction: Control Plane Models & Service Configuration Profile:

1. Based on a service request initiation, the "service flow connectivity", "service demand granularity", "load partitioning flexibility" and "configured VPN service identification number" parameters from the service configuration profile layer are sent to the "control plane instance selection" component in the SPA-Shared control plane layer.
2. Based on the "configured VPN service identification number" parameter, the "control plane instance selection" component decides which control plane instance is responsible for handling the arriving service request.
3. If the service load partitioning is permissible by the arrival service request, the service arrival rate is partitioned between the dedicated and shared resources partitions using the following two options:
    a. Static Sharing (SS): statically partition the configured VPN service arrival load into two partitions. A dedication load based on the capacity ratio of the dedicated resources partition to the VPN resources partition (sum of dedicated and shared resources), and a shared load based on the capacity ratio of the shared resources partition to the VPN resources partition. This option is called "without Network Engineering"

b. Network Engineering (NE) enabled: dynamically partition the arrival load between the dedicated and shared resources partitions of a configured VPN service based on the blocking probability of the dedicated resources partition. In round-1, the configured VPN service total load is applied to the dedicated resources and a blocking probability is generated. In round-2, the unblocked load is applied again to the dedicated resources partition and the blocked load is applied to the shared resources partition.

4. If the service demand granularity is provided by service request, the control plane Inverse Multiplexing Function will split each service request with actual bandwidth requirement b_k^A into multiple flows each with granular bandwidth requirement b_k^G .

5. The "path computation" component for the selected control plane instance analyzes the service flow to determine the source-destination pair and the appropriate routing controllers to be contacted to determine the appropriate route for the service request.

6. The "path computation" component sends a route query request to the "state-dependent routing" component in the control plane layer.

<u>Component Interaction: Control Plane Models & Transport Network :</u>

7. Since the SPA control plane model has granular realization of the transport network multi-granularity levels, the transport network fine-granularity levels are provided to the "state-dependent routing" component. In addition, the "state-dependent routing" component captures the transport topology traffic occupancy state for each of the topology links.

8. The "state-dependent routing" component provides the topology routing options to the "path computation" component while considering both the transport topology traffic occupancy state for each of the topology links and the transport network fine granularity levels.

9. The "path computation" component computes a route based on:

   a. Service flow connectivity

   b. Service demand actual bandwidth requirement b_k^A

c. Arrival load partitioning flexibility

d. Transport network fine granularity levels.

e. Transport network occupancy state per topology link

10. A connection setup is initiated.

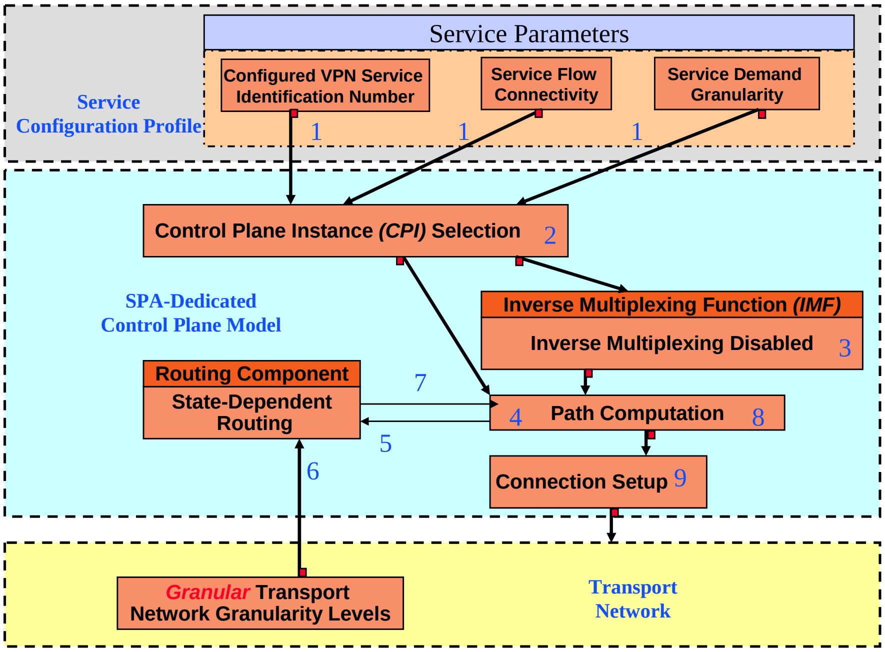
Service Parameters
Service Configuration Profile
Configured VPN Service Identification Number
Service Flow Connectivity
Service Demand Granularity
1
1
1
Control Plane Instance (CPI) Selection
2
SPA-Dedicated Control Plane Model
Inverse Multiplexing Function (IMF)
Inverse Multiplexing Disabled
3
Routing Component
State-Dependent Routing
7
4
Path Computation
8
5
6
Connection Setup
9
Granular Transport Network Granularity Levels
Transport Network

Figure 6-3: SPA-Dedicated Control Plane Components Operational Flow Sequence

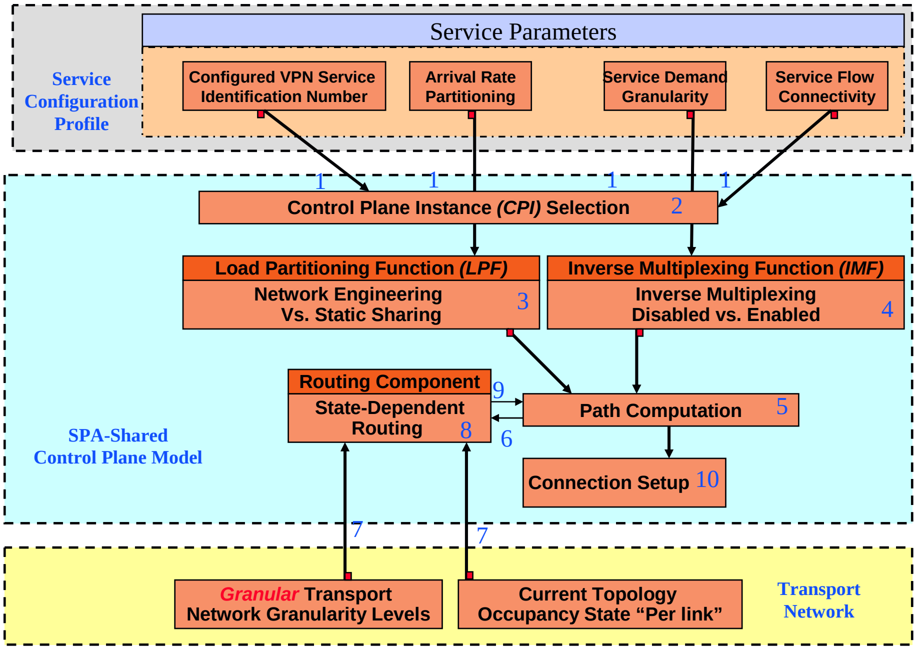
Service Parameters
Service Configuration Profile
Configured VPN Service Identification Number
Arrival Rate Partitioning
Service Demand Granularity
Service Flow Connectivity
1
1
1
1
Control Plane Instance (CPI) Selection
2
Load Partitioning Function (LPF)
Network Engineering Vs. Static Sharing
3
Inverse Multiplexing Function (IMF)
Inverse Multiplexing Disabled vs. Enabled
4
Routing Component
State-Dependent Routing
8
9
6
Path Computation
5
Connection Setup
10
SPA-Shared Control Plane Model
7
7
Granular Transport Network Granularity Levels
Current Topology Occupancy State "Per link"
Transport Network

Figure 6-4: SPA-Shared Control Plane Components Operational Flow Sequence

7 Analysis Methodology – Fixed Point Approximation

This section provides the analysis methodology used to provide a common quantitative framework for studying the performance of the IETF, ITU, and SPA control plane models. Fixed Point Approximation (FPA) concept was used to compute the following parameters where the last three were used as performance metrics:

1. Link's reduced load λ_{jk}
2. Link's occupancy probability $p_j(n)$ and link's blocking probability a_{jk}
3. Routing probability for each possible route q_{rk}^{m}
4. Network-wide blocking probability B_k
5. Network-wide average permissible load $\hat{\lambda}_k$
6. Network-wide utilization U

Detailed description of the performance metrics and their relevant mathematical formulations for each control plane model is provided in section 9.3.

The analytical models need to provide a mathematical representation for:

1. Connection Admission Control (CAC) for service requests with multi-rate bandwidth requirements in a multi-granularity transport network. The mathematical models have to provide three versions addressing the IETF, ITU, and SPA control plane realization of multi-granularity service request and multi-granularity transport network.
2. A routing mechanism for multi-rate multi-hop loss networks
3. Traffic management schemes, capacity assignment/allocation, in presence of the control plane Load Partitioning Function (LPF) and Inverse Multiplexing Function (IMF)

For the rest of our discussion we will use the terms *calls* and *service requests* interchangeably. In a loss network traffic arrives in the form of calls, each requiring a fixed amount of bandwidth on every link along a path/route chosen between the source and destination nodes. Upon a service request arrival, if the network has a route with the required bandwidth available on its entire links, the service request is admitted and set up, and it will hold the requested bandwidth for the entire duration of the service request; otherwise the service request is rejected or blocked. Upon the departure of a service request, the occupied bandwidth is released from all the links on the route. State-dependent routing [68] is a commonly studied routing policy, under which a service request is assigned to a certain route based on the state of the network, e.g., link congestion level.

Kelly in [59] provided an analytical framework for a multiple links and multiple classes of calls with different arrival rates and different bandwidth requirement. When static or fixed routing is associated with each source-destination node pair, a loss network can be modeled as a multi-dimensional Markov process, with the dimension of the state space being the product of the number of routes allowed in the network and the number of service request classes. This can be explained since the number of calls of each class on each route uniquely defines the state of the network. This Markov process possesses a product form which simplifies the computation of the solution. In the case of alternative routing, each source-destination node pair is allowed more than one route. This leads to a situation that can no longer be represented in product form. Kelly in [59] defined equilibrium state probabilities that can be derived by writing out the entire set of detailed balance equations and solving them. This approach however, is not practical in dealing with large networks with a large number of routes and integrated services with potentially a large number of service classes, since the computational complexity is both exponential in the number of routes and exponential in the number of service classes. This leads to the need for fast computational techniques that provide accurate estimates.

Blocking probabilities in a loss network, and the *reduced load approximation* (also known as the *fixed point method*) proposed for computing blocking probabilities have been studied extensively. As discussed in [63]–[66], the reduced load approximation is based on the following two assumptions:

1. *Link independence assumption.* Under this assumption, blocking is regarded as to occur independently from link-to-link. This assumption allows us to compute the blocking probability at each link separately.
2. *Poisson assumption.* Under this assumption, calls arrive at a link as a Poisson process and the corresponding arrival rate is the original external offered rate thinned by blocking on other links, thus known as the *reduced load*. Consider the case of a single class of calls with fixed/static routing. Using Erlang's formula, the blocking probability of each link can be expressed by the offered service request arrival rate and the blocking probabilities of other links. This leads to a set of nonlinear fixed point equations with the link blocking probabilities as the unknown variables. Solving these equations gives us the approximation on the blocking probability of each link. Recent work on using reduced load approximation for fixed routing can be found in [60], [61], [66], and [67].

The analytical methods developed here are based on *Liu* and *Baras* [68] which proposed a mathematical model to compute the blocking probability of a multi-rate multi-hop loss networks with state-dependent routing. We will assume the same assumptions used in [68] as follows:

1. *All links are assumed to be undirected.* For traffic between two nodes, we will not differentiate the source from the destination. Consequently a feasible route set is associated with a pair of nodes, regardless of the ordering. This assumption is adopted only for the simplicity of notation and our discussion. Our models can be applied to directional link scenarios in a straightforward manner.

2. *Calls arrive at the network as a Poisson process* and the total offered load to an individual link is also a Poisson process with rate thinned by blocking on other links.
3. *Blocking occurs independently from link to link*, determined by their respective arrival rates. That is, even though the conditions of successive links along a route are dependent (so is the blocking on these links), we will nevertheless treat them as being independent. This assumption becomes more reasonable as traffic gets heavier.
4. *We will assume that given stationary inputs*, certain random quantities of interest have well-defined averages. These include the number of on-going calls on a link of each class, the average service request holding time, and the reduced load on a link. With these averages we can further assume that there is a stationary probability of choosing a particular route under the state-dependent routing scheme. Thus, the key is to find these probabilities so that the state-dependent routing can be approximated with a stationary, non-state-dependent routing algorithm with the derived probabilities of route selection.

7.1 Notation

The Fixed Point Approximation mechanism uses the notation specified in sections 3.1 and 4.1 to describe the configuration VPN service models and the control plane models respectively. In addition, the following notation is used:

1. N : The set of nodes in the network. We will use N to denote both the set and the total number of nodes in a network topology.
2. J : The set of links in the network. Again, we will use J to denote both the set and the total number of links in the network.
3. K : The total number of service request classes. Each class k has a bandwidth requirement denoted by b_k , and a mean service request holding time denoted by μ_k . $K = [k1, k2,....., K]$
4. R : Both the set and the total number of node pairs in the network. Since we ignore the ordering of a pair. $R = \frac{N(N-1)}{2}$
5. M_r : The set of routes allowed between node pair r . We will also use M_r to denote the total number of routes between node pair r

6. r_m: The m^{th} route of the source-destination node pair r. Here, $m = 1,2,.....,M_r$. r_m defines a set of links.

7. B_{rk} : The blocking probability of a class *k* service request between node pair *r*

8. B_{rk}^{D}: The blocking probability of a class *k* service request between node pair *r* for dedicated network resources partition *D.*

9. B_{rk}^{vD} : The blocking probability of a class *k* service request between node pair *r* for dedicated network resources partition *D* of configured VPN service- *v*. This blocking probability is obtained during round-1 of FPA when Network Engineering is enabled for the SPA-Shared control plane model.

10. B_{rk}^{S} : The blocking probability of a class *k* service request between node pair *r* for shared network resources partition *S.*

11. B_{rk}^{v} : The blocking probability of a class *k* service request between node pair *r* for VPN network resource partition *v.*

12. B_k : The network-wide blocking probability of a class *k* service request.

13. B_k^{v} : The network-wide blocking probability of a class *k* service request for VPN network resource partition *v.*

14. a_{jk} : The probability that link *j* is in a state of admitting class *k* calls, or the admissibility probability of link *j.*

15. a_{jk}^{D} : The probability that dedicated network resources partition *D* in link *j* is in a state of admitting class *k* calls, or the admissibility probability of link's resources partition D in link *j.*

16. a_{jk}^{S} : The probability that shared network resources partition *S* in link *j* is in a state of admitting class *k* calls, or the admissibility probability of link's resource partition S in link *j.*

17. a_{jk}^{vD} : The probability that dedicated resources for configured VPN service *v* in link *j* is in a state of admitting class *k* calls, or the admissibility probability of link's resources partition *D* for configured VPN service *v* in link *j.*

18. a_{jk}^{v}: The probability that VPN network resources partition *v* in link *j* is in a state of admitting class *k* calls, or the admissibility probability of link's resources partition *v* in link *j*. This is the admissibility of both the dedicated resources partition a_{jk}^{vD} and the shared resources partition a_{jk}^{S}.

19. $p_j(n)$: The stationary occupancy probability of link *j*, i.e., the probability that exactly n circuits/trunks are being used on link *j*.

20. p_j^D: The stationary occupancy probability of dedicated resources partition *D* for link *j*, i.e., the probability that exactly n circuits/trunks are being used on network resource partition *D* for link *j*.

21. $p_j^{vD}(n)$: The stationary occupancy probability of dedicated resources partition *D* for configured VPN service-*v* for link *j*, i.e., the probability that exactly *n* circuits/trunks are being used on dedicated resources partition *D of* configured VPN service-*v* for link *j*.

22. $p_j^S(n)$: The stationary occupancy probability of shared resources partition *S* for link *j*, i.e., the probability that exactly n circuits/trunks are being used on network resource partition *S* for link *j*.

23. q_{rk}^{m}: The probability that the m^{th} route is chosen for a class *k* service request between node pair *r*.

24. q_{rk}^{mD}: The probability that the m^{th} route is chosen for a class *k* service request between node pair *r* in network resources partition *D*.

25. q_{rk}^{mS}: The probability that the m^{th} route is chosen for a class *k* service request between node pair *r* in shared network resources partition *S*.

26. $A_n^D(r_m)$: The event that all links in network resources partition *D* on route r_m have at least *n* free circuits/trunks.

27. $A_{n+1}^D(r_m)$: The event that all links in network resources partition *D* on route r_m have at least *n+1* free circuits/trunks.

28. $A_n^D(r_k - r_m)$: The event that all links belonging to route r_k and not route r_m in network resources partition *D* have at least *n* free circuits/trunks.

29. $\overline{A}_n^D(r_k - r_m)$: The event that at least one of the links belonging to route r_k and not route r_m in network resources partition *D* has less than *n* free circuits/trunks.

30. $A_{n+1}^D(r_k - r_m)$: The event that all links belonging to route r_k and not route r_m in network resources partition *D* have at least *n+1* free circuits/trunks.

31. $\overline{A}_{n+1}^D(r_k - r_m)$: The event that at least one of the links belonging to route r_k and not route r_m in network resources partition *D* has less than *n+1* free circuits/trunks.

32. $\tilde{A}_n^D(r_m)$: The event that all links in shared network partition *D* on route r_m have at least *n* free trunks/circuits and at least one link on route r_m has exactly *n* free trunks/circuits.

33. $A_{n+1}^S(r_m)$: The event that all links in shared network resources partition *S* on route r_m have at least *n+1* free circuits/trunks.

34. $A_n^S(r_k - r_m)$: The event that all links belonging to route r_k and not route r_m in shared network resources partition *S* have at least *n* free circuits/trunks.

35. $\overline{A}_n^S(r_k - r_m)$: The event that at least one of the links belonging to route r_k and not route r_m in shared network resources partition *S* has less than *n* free circuits/trunks.

36. $A_{n+1}^S(r_k - r_m)$: The event that all links belonging to route r_k and not route r_m in shared network resources partition *S* have at least *n+1* free circuits/trunks.

37. $\overline{A}_{n+1}^S(r_k - r_m)$: The event that at least one of the links belonging to route r_k and not route r_m in shared network resources partition *S* has less than *n+1* free circuits/trunks.

38. $\tilde{A}_n^S(r_m)$: The event that all links in shared network resources partition *S* on route r_m have at least *n* free trunks/circuits and at least one link on route r_m has exactly *n* free trunks/circuits.

39. $\lambda_{jk}^{r_m}$: The reduced load on link j contributed by traffic class *k* on route r_m and thinned by blocking probability on other links.

40. $\lambda_{jk}^{D_{r_m}}$: The reduced load on dedicated resources partition *D* in link *j* contributed by traffic class *k* on route r_m and thinned by blocking probability on other network partitions from other links.

41. ${}^{NE}\lambda_{jk}^{D_{r_m}}$: The reduced load on dedicated resources partition *D* in link *j* contributed by traffic class *k* on route r_m and thinned by blocking probability on other network partitions from other links. This reduced load results from configuring the Load Partitioning Function (LPF) to perform Network Engineering (NE) traffic management.

42. $\lambda_{jk}^{S_{r_m}}$: The reduced load on shared resources partition *S* in link *j* contributed by traffic class *k* on route r_m and thinned by blocking probability on other network partitions from other links.

43. ${}^{NE}\lambda_{jk}^{S_{r_m}}$: The reduced load on shared resources partition *S* in link *j* contributed by traffic class *k* on route r_m and thinned by blocking probability on other network partitions from other links. This reduced load results from configuring the Load Partitioning Function (LPF) to perform Network Engineering (NE) traffic management.

44. $\tilde{\lambda}_{rk}^{S}$: sum of all the shared loads applied to the shared network resources partition C_j^S

45. ${}^{NE}\tilde{\lambda}_{rk}^{S}$: sum of all the shared loads applied to the shared network resources partition C_j^S .This reduced load results from configuring the Load Partitioning Function (LPF) to perform Network Engineering (NE) traffic management.

46. λ_{jk}^{D} : The aggregated load of class *k* on dedicated network resources partition *D* for link *j* from the load generated at all the source-destination pairs *r*.

47. ${}^{NE}\lambda_{jk}^{D}$: The aggregated load of class *k* on dedicated network resources partition *D* for link *j* from the load generated at all the source-destination pairs *r*. This reduced load results from configuring the Load Partitioning Function (LPF) to perform Network Engineering (NE) traffic management.

48. λ_{jk}^{S} : The aggregated load of class *k* on shared network resources partition *S* for link *j* from the load generated at all the source-destination pair *r*.

49. ${}^{NE}\lambda_{jk}^{S}$: The aggregated load of class *k* on shared network resources partition *S* for link *j* from the load generated at all the source-destination pair *r*. This reduced load results from configuring the Load Partitioning Function (LPF) to perform Network Engineering (NE) traffic management.

50. n_j : The number of "in-progress" calls in the link *j*. $n_j = 1,2,.....,C_j$.

51. n_j^D : The number of "in-progress" calls in the network resource partition *D* for link *j*.

52. n_{jk}^D : The number of "in-progress" class-k calls in the dedicated resourced partition *D.*

53. n_{jk}^{vD} : The number of "in-progress" class-k calls in the dedicated resources partition *D* of VPN *v*.

54. n_{jk}^S : The number of "in-progress" class-k calls in the shared resources partition *S.*

55. $\hat{\lambda}_{rk}$: Source-destination pair *r* permissible "non-blocked" load for class *k* service request arrivals.

56. $\hat{\lambda}_{rk}^D$: Source-destination pair *r* permissible "non-blocked" load for class *k* service request arrivals on network resource partition *D.*

57. $\hat{\lambda}_k$: Network-wide permissible "non-blocked" load for class *k* service request arrivals.

58. $\hat{\lambda}_k^D$: Network-wide permissible "non-blocked" load for class *k* service request arrivals on network resource partition *D.*

59. U_j : Link *j* utilization.

60. U_j^D : Network resource partition *D* in Link *j* utilization.

61. U : Network-wide utilization.

7.2 Fixed Point Approximation (FPA) framework

This section provides the FPA common framework that will be specialized for each control plane model. The detailed fixed point approximation mathematical formulas for each control plane model are provided in section 8. The main objective of the Fixed Point Approximation is to compute the source-destination pair *r* route blocking probability B_{rk} for class *k*. In order to compute B_{rk}, we need to use the first point approximation to compute λ_{jk}, a_{jk}, $p_j(n)$ and q_{rk}^m. We will use the same analysis done by *Liu* and *Baras* in [68] to compute the above variables. The FPA steps are as follows:

- *Step-1 Calculating link's reduced load* λ_{jk}. Recall that $\lambda_{jk}^{r_m}$ is the reduced load on link *j* contributed by traffic class *k* on route r_m and thinned by blocking probability on other links. Note that we first take a portion of the total offered load λ_{rk} that is routed on r_m with probability q_{rk}^m, and then multiple it with the probability that this portion is admitted by all links other than link *j*. We fix the link admissibility probability a_{jk} and the route probability q_{rk}^m. Once a_{jk} and q_{rk}^m are calculated, then λ_{jk}, reduced load on link *j* based on service class *k,* can be computed.
- Step-2: Calculating link's occupancy probability $p_j(n)$ and link's admissibility probability a_{jk}. We fix λ_{jk} to get the link occupancy probability $p_j(n)$ and a_{jk}. The CAC mechanism for each control plane model is used to deny or grant network resources to a service request bandwidth requirements.
- Step-3: Calculating routing probability for each possible route q_{rk}^m. Once the occupancy probability is calculated, q_{rk}^m can be calculated.
- Step-4: Compute network-wide blocking probability B_k for class *k*
- Step-5: Compute the network-wide average permissible load $\hat{\lambda}_k$ for class *k*
- Step-6: Compute network-wide utilization U
- By repeated substitution, the equilibrium fixed point can be solved for all the set of unknowns.

Figure 7-1 illustrates the interaction of the set of unknowns during FPA computation. Figure 7-2 illustrates the modeling framework by showing the network topology parameters and the service parameters as input to the Fixed Point Approximation mechanism. When the FPA variables converge, the per-route blocking probability is computed. The contribution of this work was to specialize this common FPA for each control plane model to compute the compute λ_{jk} , a_{jk} , $p_j(n)$ and q_{rk}^m .

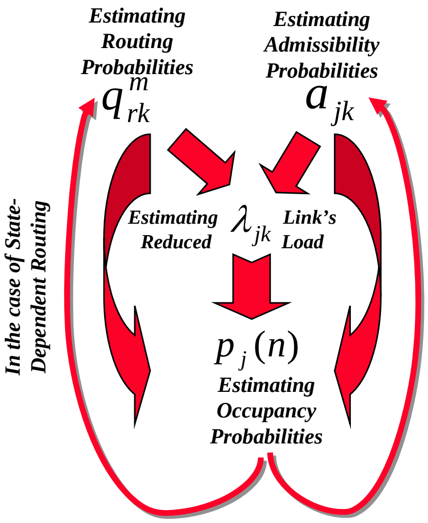
Estimating Routing Probabilities
q_{rk}^m
Estimating Admissibility Probabilities
a_{jk}
Estimating Reduced
λ_{jk}
Link's Load
$p_j(n)$
Estimating Occupancy Probabilities
In the case of State-Dependent Routing

Figure 7-1: Fixed Point Approximation (FPA) Computation Steps

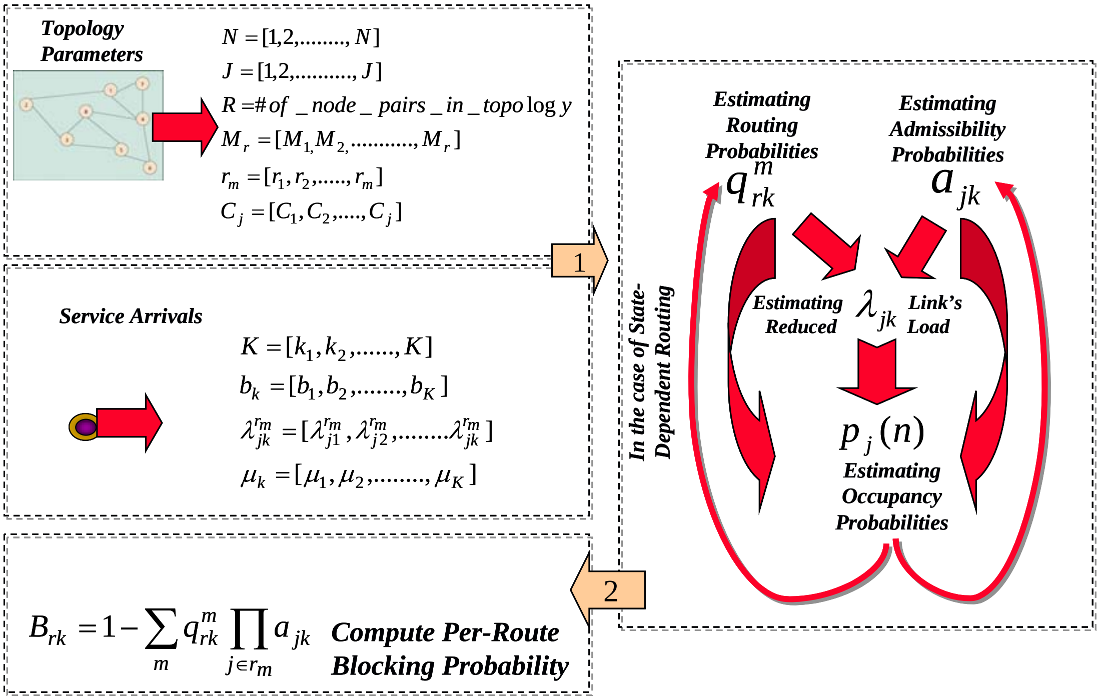
Topology Parameters
$N = [1,2,........, N]$
$J = [1,2,.........., J]$
$R = \# of\_node\_pairs\_in\_topology$
$M_r = [M_{1,} M_{2,} ...., M_r]$
$r_m = [r_1, r_2,....., r_m]$
$C_j = [C_1, C_2,...., C_j]$
1
Service Arrivals
$K = [k_1, k_2,......, K]$
$b_k = [b_1, b_2,......., b_K]$
$\lambda_{jk}^{r_m} = [\lambda_{j1}^{r_m}, \lambda_{j2}^{r_m},........\lambda_{jk}^{r_m}]$
$\mu_k = [\mu_1, \mu_2,........, \mu_K]$
2
$B_{rk} = 1 - \sum_m q_{rk}^m \prod_{j \in r_m} a_{jk}$
Compute Per-Route Blocking Probability
Estimating Routing Probabilities
q_{rk}^m
Estimating Admissibility Probabilities
a_{jk}
Estimating Reduced
λ_{jk}
Link's Load
$p_j(n)$
Estimating Occupancy Probabilities
In the case of State-Dependent Routing

Figure 7-2: FPA Framework

7.2.1 IETF control plane model

As described in section 5.3.1, the IETF control plane model represents the *N*-network resources partitions of the transport network by one Control Plane Instance (CPI). This leads to a one Fixed Point Approximation (FPA) instance required to compute λ^{v}_{jk} , a_{jk} and $p_j(n)$ on the physical resources level. As describes in section 5.3.1, the IETF control plane model has one RDB providing routing options for the multiple network partitions within the physical network topology. From a FPA perspective, the FPA statically sets the routing probability for each possible route between a source-destination pair *r*. Thus, no q^{m}_{rk} is computed based on the link(s) occupancy probabilities between the source –destination pair *r*. Figure 7-3 illustrates the IETF control plane model single FPA instance for multiple network resource partitions. It should be noted that there is no arrow from the occupancy probability $p_j(n)$ computation step and the routing probability q^{m}_{rk} computation step; which indicates that the routing probability q^{m}_{rk} for each source-destination pair is set statically.

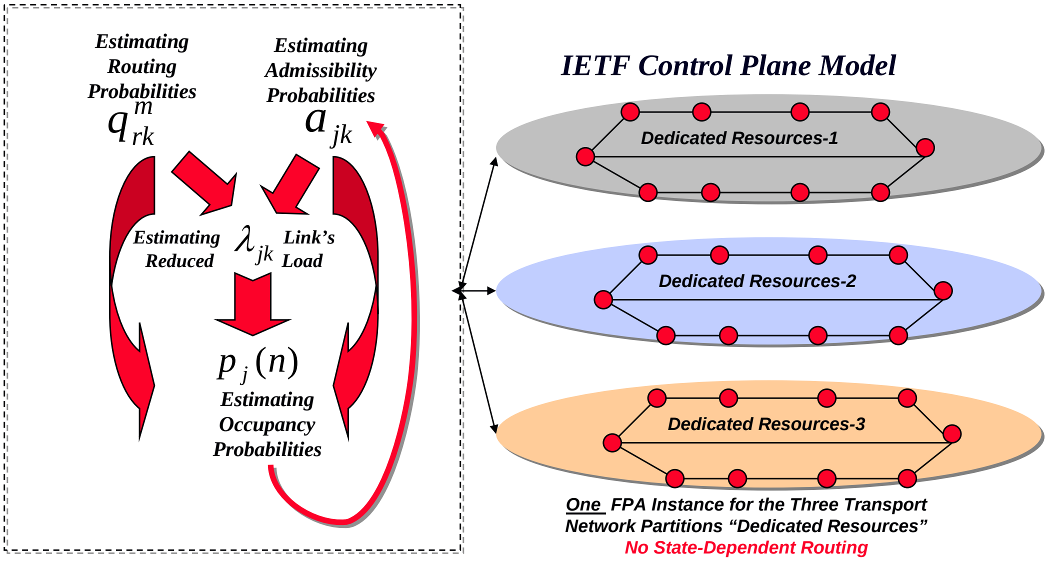
Estimating Routing Probabilities
q^{m}_{rk}
Estimating Admissibility Probabilities
a_{jk}
Estimating Reduced
λ_{jk}
Link's Load
$p_j(n)$
Estimating Occupancy Probabilities
IETF Control Plane Model
Dedicated Resources-1
Dedicated Resources-2
Dedicated Resources-3
One FPA Instance for the Three Transport Network Partitions "Dedicated Resources"
No State-Dependent Routing

Figure 7-3: IETF single FPA Instance for Three Transport Network Partitions

7.2.2 ITU control plane model

As described in section 5.3.2, the ITU control plane model represents the *N*-network resources partitions of the transport network by *N*-Control Plane Instances (CPIs). This leads to *N*-Fixed Point Approximation (FPA) instances required to compute λ_{jk}^{D}, a_{jk}^{D}, $p_{j}^{D}(n)$ on each network resources partition. As describes in section 5.3.2, the ITU control plane model has *N*- RDB providing routing options for the *N*-network resources partitions within the physical network topology. Similar to the IETF control plane model and from a FPA instance perspective, each of the *N* FPA instances statically sets the routing probability for each possible route between a source-destination pair *r*. Thus, no q_{rk}^{mD} is computed based on the link(s) occupancy probabilities between the source –destination pair *r* within the transport resources partition controlled by the FPA instance.

Figure 7-4 illustrates the ITU control plane model three FPA instances for the three network resource partitions. Similar to the IETF control plane model, it should be noted that, for each FPA instance, there is no arrow from the occupancy probability $p_{j}^{D}(n)$ computation step and the routing probability q_{rk}^{mD} computation step; which indicates that the routing probability q_{rk}^{mD} for each source-destination pair is set statically. The Complete Partitioning (CP) from a physical resources perspective is reflected on the *N*-FPA instances as it should be noted from Figure 7-4 that there is no interaction between the FPA instances; this indicates that no Load Partitioning Function (LPF) is implemented.

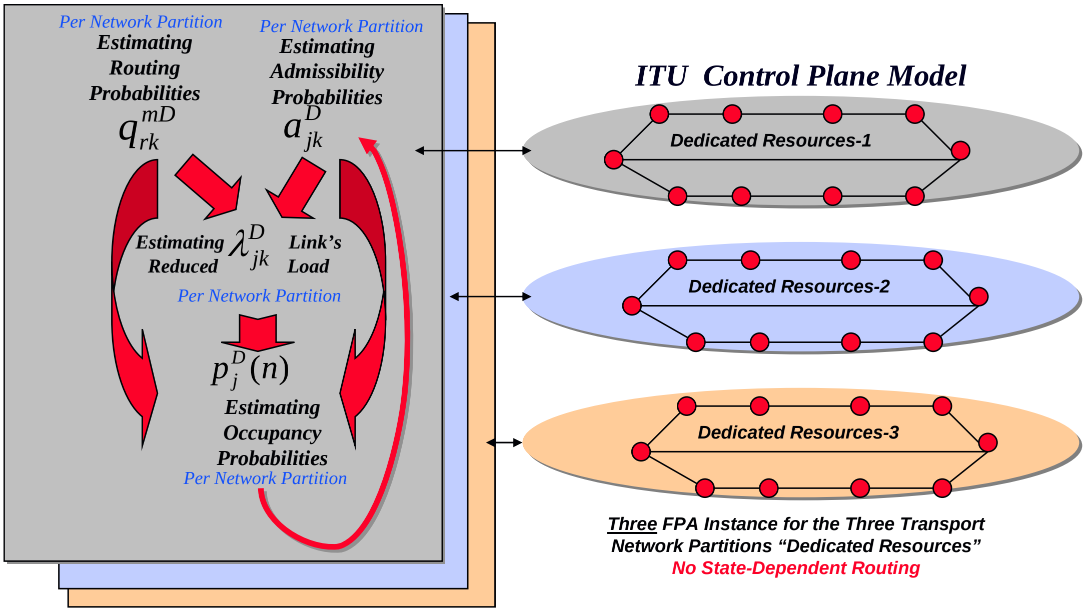
Per Network Partition
Estimating Routing Probabilities
q_{rk}^{mD}
Per Network Partition
Estimating Admissibility Probabilities
a_{jk}^{D}
Estimating Reduced λ_{jk}^{D} Link's Load
Per Network Partition
$p_j^D(n)$
Estimating Occupancy Probabilities
Per Network Partition
ITU Control Plane Model
Dedicated Resources-1
Dedicated Resources-2
Dedicated Resources-3
Three FPA Instance for the Three Transport Network Partitions "Dedicated Resources"
No State-Dependent Routing

Figure 7-4: ITU Three FPA Instances for Three Transport Network Partitions

7.2.3 SPA control plane model

Similar to the ITU control plane mode, the SPA-Dedicated control plane model represents the N-network resources partitions of the transport network by N-Control Plane Instances (CPIs). This leads to N-Fixed Point Approximation (FPA) instances required to compute λ_{jk}^{D}, a_{jk}^{D}, $p_j^D(n)$ and q_{rk}^{mD} on each network resources partition. A difference from the ITU control plane model, each of the N FPA instances, in the SPA-Dedicated control plane model, dynamically computes the routing probability for each possible route between a source-destination pair r. Thus, q_{rk}^{mD} is computed based on the link(s) occupancy probabilities between the source –destination pair r within the transport resources partition controlled by each FPA instance. Figure 7-5 illustrates the SPA-Dedicated control plane model three FPA instances for the three network resource partitions. To enable the state-dependent routing, it should be noted that, for each FPA instance, there is an arrow from the occupancy probability $p_j^D(n)$ computation step and the routing probability q_{rk}^{mD} computation step; which indicates that the routing probability q_{rk}^{mD} or each source-destination pair is computed dynamically based on the links' occupancy probabilities within each network resources partition.

The SPA-Shared control plane mode is similar to the SPA-Dedicated control plane model in its state-dependent routing and N-CPIs for the N-network resources partitions, but differs in allowing load sharing between the FPA instances via the Load Partitioning Function (LPF). Figure 7-6 illustrates the SPA-Shared control plane model three FPA instances for the three network resource partitions. It should be noted that the three FPA instances are inter-connected by a Load Partitioning Function (LPF) to allow the arrival load allocation on different network resources partitions based on the defined policy by the (LPF).

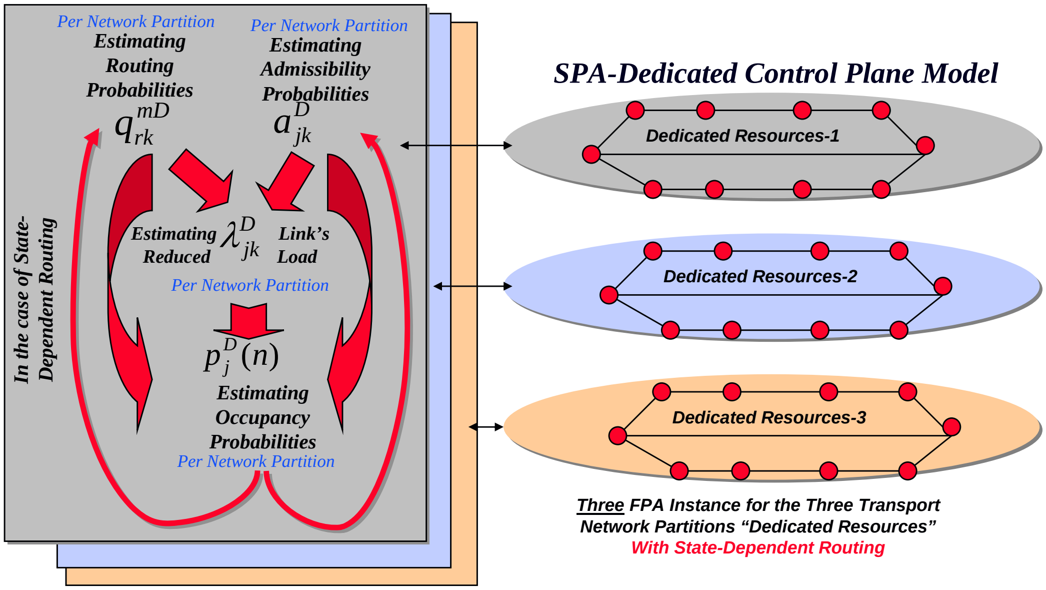
Per Network Partition
Estimating Routing Probabilities
q_{rk}^{mD}
Per Network Partition
Estimating Admissibility Probabilities
a_{jk}^{D}
Estimating Reduced
λ_{jk}^{D}
Link's Load
Per Network Partition
$p_j^D(n)$
Estimating Occupancy Probabilities
Per Network Partition
In the case of State-Dependent Routing
SPA-Dedicated Control Plane Model
Dedicated Resources-1
Dedicated Resources-2
Dedicated Resources-3
Three FPA Instance for the Three Transport Network Partitions "Dedicated Resources"
With State-Dependent Routing

Figure 7-5: SPA-Dedicated Three FPA Instances for Three Transport Network Partitions

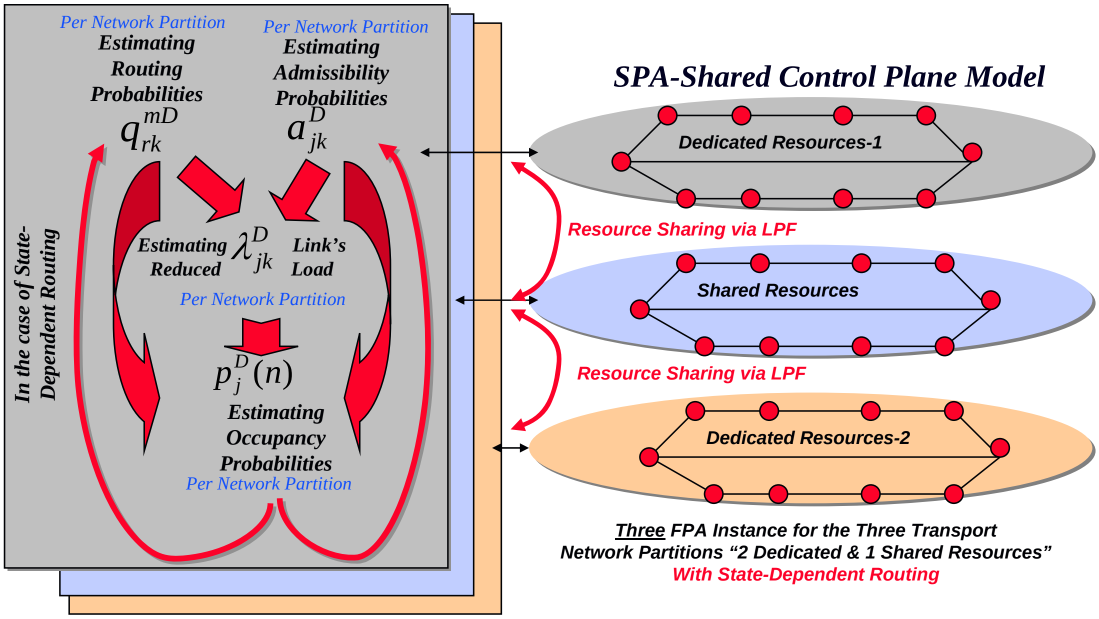
Per Network Partition
Estimating Routing Probabilities
q_{rk}^{mD}
Per Network Partition
Estimating Admissibility Probabilities
a_{jk}^{D}
Estimating Reduced
λ_{jk}^{D}
Link's Load
Per Network Partition
$p_j^D(n)$
Estimating Occupancy Probabilities
Per Network Partition
In the case of State-Dependent Routing
SPA-Shared Control Plane Model
Dedicated Resources-1
Resource Sharing via LPF
Shared Resources
Resource Sharing via LPF
Dedicated Resources-2
Three FPA Instance for the Three Transport Network Partitions "2 Dedicated & 1 Shared Resources"
With State-Dependent Routing

Figure 7-6: SPA-Shared Three FPA Instances for Three Transport Network Partitions

8 Mathematical Formulation of Control Plane Models for Traffic Management Schemes

This section presents the detailed Fixed Point Approximation mathematical models developed for the traffic management schemes of the IETF, ITU, SPA-Dedicated, and SPA-Shared control plane models. As described in section 7.2, the main objective of the Fixed Point Approximation is to compute the source-destination pair route r blocking probability B_{rk}. In order to compute B_{rk}, we need to use the FPA to compute λ_{jk}, a_{jk}, $p_j(n)$ and q_{rk}^m. The FPA steps are as follows:

- Step-1: Connection Admission Control (CAC) for multi-rate service requests
- Step-2: Calculating link's reduced load λ_{jk}.
- Step-3: Calculating link's occupancy probability $p_j(n)$ and link's admissibility probability a_{jk}.

- Step-4: Calculating routing probability for each possible route q_{rk}^{m}.[7]
- Step-5: Compute network-wide blocking probability B_k for class *k*
- Step-6: Compute network-wide average permissible load $\hat{\lambda}_k$ for class *k*
- Step-7: Compute network-wide utilization U

We will first present the base method as provided in [68] and then specialize for each traffic management scheme of the three control plane models.

8.1 Step-1 CAC for multi-rate service requests

8.1.1 Base method

The problem of fair and efficient resource sharing has a long history. Foschini, Gopinath and Hayes [44] consider admission control policies which induce product-form equilibrium distributions, and show that a threshold policy is optimal. Gopal and Stern [45] use Markov Decision Theory to determine threshold policies that maximize the link utilization. Kraimeche and Schwartz [46] consider a class of restricted-access policies which aim to reduce blocking probabilities. The recent important work on Link Sharing by Floyd and Jacobson [47] has motivations in common with this work, except that the framework here is that of calls and loss models. The work of Ash et. al. [48] on class-of-routing is also aimed at balancing fairness and efficiency. Borst and Mitra [49] develop computational algorithms for analyzing heterogeneous traffic classes in virtual partitioning network architectures. A key assumption in our analytic approximation is link independence, which is common to FPAs for loss networks. Excellent sources of information on FPAs are Kelly [50] and Ross [51]. Recent applications of virtual partitioning to admission control and buffer management are reported in [52] and [53], respectively.

Finding the equilibrium distribution for the individual granularity levels is nontrivial in the presence of multi-rate traffic. Various approximations have been suggested for single links with multi-rate traffic, some of which can be modified to apply here. Kaufman [54] and

[7] Calculating routing probability for IETF and ITU control plane models are not carried since both control plane models support static routing rather than state-dependent routing.

Roberts [55] developed an exact recursion for the multi-rate case when there are no admission controls. Roberts [56] and Bean [57] give approximations for links with trunk reservation. Borst and Mitra [153] compare these approaches for virtual partitioning, as well as considering two-dimensional approximations.

For Liu and Baras in [68], a service request with bandwidth requirement b_k for class *k* is admitted to a link *j* with capacity C_j if the total consumed resources by all classes *k* is less than C_j as provided in the equation below:

$b_k \le C_j - \sum_{i \in K} b_i n_i$; where n_i is the number of existing connections of class *i.*

8.1.2 IETF control plane model

Since the IETF control plane model routing component has a coarse representation of the *M*-granularity transport network as described in section 5.2.1, the IETF routing component advertises the traffic occupancy of the c<u>*oarse*</u>, e.g., STS-3, granularity level of the transport link without granular view of the traffic occupancy of the <u>*fine*</u>*, e.g.,* STS-1, granularity level. As discussed in section 5.2.1, the Inverse Multiplexing Function (IMF) in the IETF control plane model is disabled. Hence, IETF control plane model will not consider the service request granularity level feature, of the service profile, in its CAC mechanism. A service request with actual bandwidth requirements b_k^A *=2 STS-1* that arrives at a link will consume b_k^C *=3 STS-1* resources from the physical link capacity C_j. A service request *(*b_k^A*)* will be accepted if the following condition apply:

$b_k^A \le C_j - \sum_{k \in K} b_k^C n_j^k$ …………….. (1)

Where n_j^K is the number of “in-progress” class-k calls in the link *j*. It should be noted that the IETF CAC mechanism permits a service request based on the coarse bandwidth requirement b_k^C of the arriving service request rather than actual bandwidth requirements b_k^A. This leads to higher link utilization, under low input loads, due to the mismatch between service request bandwidth requirements and link's granularity levels.

8.1.3 ITU and SPA-Dedicated control plane model

Since the ITU control plane model routing component has a granular representation of the transport network granularity levels as described in section 5.2.2, the ITU routing component advertises the traffic occupancy of the *fine*, for example STS-1, granularity level of the transport link. As discussed in section 5.2.2, the Inverse Multiplexing Function (IMF) in the ITU control plane model is disabled. Hence, ITU control plane model will not consider the service request granularity level feature, of the service profile, in its service request routing or path computation. The service request flow with actual bandwidth requirement b_k^A *=2 STS-1* is not split into multiple flows each with granular bandwidth requirements b_k^G *=1 STS-1*, instead b_k^A service request is considered a service request with actual bandwidth requirement b_k^A [8]. A service request *(* b_k^A *)* will be accepted if the following condition apply:

$$b_k^A \leq C_j^D - \sum_{k \in K} b_k^A n_{jk}^D \quad \ldots\ldots\ldots\ldots\ldots.. (2)$$

Where n_{jk}^D is the number of "in-progress" class-k calls in the in dedicated resources partition *D*. It should be noted that the ITU CAC mechanism permits a service request based on its actual bandwidth requirement *(* b_k^A *)* of the arriving service request rather than coarse bandwidth requirements (b_k^C *)*. This leads to lower link utilization due to the match between service request bandwidth requirements and link's granularity levels.

[8] The reason for that is since the routing and path computation components in the ITU control plane model have a granular representation of transport network granularity levels. In other words, ITU routing and path computation components are architected to optimize mapping between the granularity level of service demands and the available granularity levels of transport network. As a result, transport network resources will more efficiently utilized than the IETF control plane model due to match between the granularity level of the service demand and the granularity level of the transport network.

The SPA-Dedicated control plane model has the exact CAC like the ITU control plane model except utilizing state-dependent routing in its routing component.

8.1.4 SPA-Shared control plane model

The SPA-Shared control plane model *differs* from both the ITU and SPA-Dedicated control plane models since it can enable the IMF and further divide the service request flow with actual bandwidth requirement $b_k^A = 2STS$ into multiple flows each with granular service requests $b_k^G = 1STS$. A service request (b_k^A) will be accepted on the dedicated resources partition D if the following condition applies:

$$b_k^G \leq C_j^{vD} - \sum_{k \in K} b_k^G n_{jk}^{vD} \quad \text{…………….. (3)}$$

A service request (b_k^A) will be accepted on the shared resources partition S if the following condition applies:

$$b_k^G \leq C_j^{vS} - \sum_{k \in K} b_k^G n_{jk}^{vS} \quad \text{…………….. (4)}$$

8.2 Step-2: Calculating link’s reduced load

8.2.1 Base method

Liu and Baras in [68] introduced a method to compute the reduced load on link j due to class k by each source-destination pair r that passes through link j. Recall that $\lambda_{jk}^{r_m}$ is the reduced load on link j contributed by traffic class k on route r_m and thinned by blocking probability on other links. It is given by the reduced load approximation as:

$$\lambda_{jk}^{r_m} = \lambda_{rk} q_{rk}^m I[j \in r_m] \prod_{i \in r_m, i \neq j} a_{ik} \quad \text{…………….. (5)}$$

where I is the indicator function. Note that we first take a portion of the total offered load λ_{rk} that is routed on r_m with probability q_{rk}^m, and then multiple it with the probability that this portion is admitted by all links other than link *j*. The aggregated load of class *k* on link *j* from the load generated at all the source-destination pairs *r* is:

$$\lambda_{jk} = \sum_{r \in R} \sum_{r_m \in M_r} \lambda_{jk}^{r_m} \text{ …………….. (6)}$$

8.2.2 IETF control plane model

In the IETF control plane model, the total offered load λ_{rk}^{v} for each configured VPN service *v* is applied to link *j*, this indicated the Complete Sharing (CS) concept introduced above. Equation (5) can be modified by replacing λ_{rk} by λ_{rk}^{v} as shown in equation (7), equation (6) used to compute the aggregate, reduced, load due to all source-destination pair *r* remains the same.

$$\lambda_{jk}^{r_m} = \lambda_{rk}^{v} q_{rk}^{m} I[j \in r_m] \prod_{i \in r_m, i \neq j} a_{ik} \text{ …………….. (7)}$$

8.2.3 ITU and SPA-Dedicated control plane models

In the ITU control plane model, the total offered load λ_{rk}^{v} for each configured VPN service *v* is applied to its dedicated resources partition *D*; this indicated the Complete Partitioning (CP) concept introduced above. In the ITU control plane model, the reduced load is computed for each network resources partition *D* as shown in equation (8)

$$\lambda_{jk}^{D_{rm}} = \lambda_{rk}^{D} q_{rk}^{mD} I[j \in r_m] \prod_{i \in r_m, i \neq j} a_{ik}^{D} \text{ …………….. (8)}$$

The aggregated load of class *k* on network resources partition *D* for link *j* from the load generated at all the source-destination pairs *r* is:

$$\lambda_{jk}^{D} = \sum_{r \in R} \sum_{r_m \in M_r} \lambda_{jk}^{D_{r_m}} \text{ …………….. (8)}$$

8.2.4 SPA-Shared with static load partitioning (without NE)

Traffic partitioning without Network Engineering “w/oNE” is when the Load Partitioning Function (LPF) is configured to partition the configured VPN service *v* total arrival load λ_{rk}^{v} between the dedicated resources C_j^{vD} and the shared resources C_j^{S} based on the resources ratios between dedicated and shared resources partitions[9] as given below:

$$\lambda_{rk}^{vD} = \lambda_{rk}^{v} . \frac{C_j^{vD}}{C_j^{vD} + C_j^{S}} \text{ …………….. (9)}$$

$$\lambda_{rk}^{vS} = \lambda_{rk}^{v} . \frac{C_j^{vS}}{C_j^{vD} + C_j^{S}} \text{ …………….. (10)}$$

The dedicated load λ_{rk}^{vD} from configured VPN service-*v* is then used to generate per-link *j* load as given below based on the dedicated resources routing and admissibility probabilities

$$\lambda_{jk}^{D_{r_m}} = \lambda_{rk}^{vD} q_{rk}^{mD} I[j \in r_m] \prod_{i \in r_m, i \neq j} a_{ik}^{D} \text{ …………….. (11)}$$

The aggregated load of class *k* on network resources partition *D* for link *j* from the load generated at all the source-destination pairs is the same as equation (8). Each of the configured VPN services-*v* apply their shared load λ_{rk}^{vS} on the shared resources *S*; thus the total shared load from all configured VPN services on the shared resources partition is the sum of all the shared loads as given below:

$$\tilde{\lambda}_{rk}^{S} = \sum_{\forall v} \lambda_{rk}^{vS} \text{ …………….. (12)}$$

The total shared load $\tilde{\lambda}_{rk}^{S}$ is then used to generate per-link *j* load as given below based on the shared resources routing and admissibility probabilities

$$\lambda_{jk}^{S_{r_m}} = \tilde{\lambda}_{rk}^{S} q_{rk}^{Sm} I[j \in r_m] \prod_{i \in r_m, i \neq j} a_{ik}^{S} \text{ …………….. (13)}$$

The aggregated load of class *k* on network shared resources partition *S* for link *j* from the load generated at all the source-destination pairs *r* is provided in equation (14).

$$\lambda_{jk}^{S} = \sum_{r \in R} \sum_{r_m \in M_r} \lambda_{jk}^{S_{r_m}} \text{ …………….. (14)}$$

[9] This partitioning configuration is considered Static Splitting (SS). Other load partitioning configuration is considered when LPF is configured as Network Engineering (NE) to perform dynamic load partitioning

8.2.5 SPA-Shared with dynamic load partitioning (with NE)

Traffic partitioning with Network Engineering “w/NE” is when the Load Partitioning Function (LPF) is configured to partition the configured VPN service *v* total arrival load λ_{rk}^{v} between the dedicated resources C_{j}^{vD} and the shared resources C_{j}^{S} based on the dedicated resources pair blocking probability B_{rk}^{vD} . FPA is carried in two rounds on the dedicated resources partitions and one round on the shared resources partition. In round-1, the configured VPN service-*v* total arrival load λ_{rk}^{v} is applied to the dedicate resource partition C_{j}^{vD} as given below:

$${}^{NE}\lambda_{jk}^{D_{r_m}} = \lambda_{rk}^{v} q_{rk}^{mD} I[\, j \in r_m] \prod_{i \in r_m, i \neq j} a_{ik}^{D} \ \text{…………….. (14)}$$

The aggregated load of class *k* on network resources partition *D* for link *j* from the load generated at all the source-destination pairs *r* is the same as equation (8) but with replacing λ_{jk}^{D} and $\lambda_{jk}^{D_{r_m}}$ by ${}^{NE}\lambda_{jk}^{D}$ and ${}^{NE}\lambda_{jk}^{D_{r_m}}$ respectively. When round-1 of the FPA on dedicated resources partitions is complete, the pair blocking probability B_{rk}^{vD} is used to generate the configured VPN service-*v* shared load ${}^{NE}\lambda_{rk}^{vS}$ which is the configured VPN service *v* total load multiplied by the dedicated resources partition blocking probability.

$${}^{NE}\lambda_{rk}^{vS} = \lambda_{rk}^{v} . B_{rk}^{vD} \ \text{…………….. (15)}$$

The blocking probability B_{rk}^{vD} is the complement of the admissibility probability of a class *k* service request between node pair *r* for dedicated network resources partition *D* of configured VPN service- *v*. for a source-destination pair *r*. The pair admissibility probability is the sum of the admissibility probability of each route $m \in r_m$ multiplied by the routing probability q_{rk}^{m} . The route admissibility probability is the product of the admissibility probability of all the links $j \in r_m$.

$$B_{rk}^{vD} = 1 - \sum_{m} q_{rk}^{mD} \prod_{j \in r_m} a_{jk}^{vD} \ \text{…………….. (16)}$$

The reduced load on the shared resources is computed using the same equations as provided in (12-14) but with replacing the terms $\tilde{\lambda}_{rk}^{S}, \lambda_{jk}^{S_{r_m}}$, and λ_{jk}^{S} by the terms ${}^{NE}\lambda_{jk}^{S}, {}^{NE}\lambda_{jk}^{S_{r_m}}$, and ${}^{NE}\tilde{\lambda}_{rk}^{S}$ respectively. In round-2, the non-blocked load from round-1 is applied again to each dedicate resource partition C_j^{vD} as given in equation (17) below:

$${}^{NE}\lambda_{rk}^{vD} = \lambda_{rk}^{v}.(1-B_{rk}^{D}) \text{ …………….. (17)}$$

The reduced load on the dedicated resources partition *D* is computed using the same equation as provided in (14)

8.3 Step-3: Calculating link’s occupancy probability and admissibility probability

8.3.1 Base method

In [69] Kaufman gave a simple one-dimensional recursion for calculating the link’s occupancy probabilities.

$$np_j(n) = \sum_{K} b_k \frac{\lambda_{jk}}{\mu_k} p_j(n-b_k) \text{ …………….. (18)}$$

The total number of in-progress calls in link *j* is the sum of weighted sum of all the in-progress classes from all classes $n = \sum_{b_k \in K, n_k \in C_j} b_k^C n_k$. Note that $p_j(n) = 0$ if $n < 0$ and $\sum_{n=0}^{C_j} p_j(n) = 1$. The link’s admissibility probability of link *j* for class *k* is the sum of the occupancy probability of all the states from $n \in [0, C_j - b_k]$ as given in equation (20) below:

$$a_{jk} = \sum_{n=0}^{C_j - b_k} p_j(n) \text{ …………….. (20)}$$

8.3.2 IETF control plane model

In the IETF control plane model, the link’s occupancy probability $p_j(n)$ is based on the coarse bandwidth requirement b_k^C of class *k* rather than the actual bandwidth requirement b_k^A of class *k*. The link’s occupancy probability in given in equation (21)

$$np_j(n) = \sum_K b_k^C \frac{\lambda_{jk}}{\mu_k} p_j(n - b_k^C) \text{ ……………. (21)}$$

The link’s admissibility probability of link *j* for class *k* is given in equation (22) below:

$$a_{jk} = \sum_{n=0}^{C_j - b_k^C} p_j(n) \text{ ……………. (22)}$$

It should be observed that the IETF link’s occupancy and admissibility probabilities are calculated based on the coarse bandwidth requirements b_k^C of class *k*. This is compliant with the IETF CAC mechanism described in section 8.1.2. Another enforcement of IETF–CAC is the total number of in-progress calls n; which is based on class *k* coarse demand b_k^C.

8.3.3 ITU and SPA-Dedicated control plane model

Similar to the link’s reduced load where the reduced load is computed for each network resources partition *D*; in the link admissibility probability, each network resources partition *D* has its separate occupancy probability $p_j^D(n)$ and admissibility probability a_{jk}^D.

$$np_j^D(n) = \sum_K b_k^A \frac{\lambda_{jk}^D}{\mu_k} p_j^D(n - b_k^A) \text{ ……………. (23)}$$

The link’s admissibility probability of link *j* for class *k* is given in equation (24) below:

$$a_{jk}^D = \sum_{n=0}^{C_j^D - b_k^A} p_j^D(n) \text{ ……………. (24)}$$

It should be observed that the ITU link’s occupancy and admissibility probabilities are calculated based on the actual bandwidth requirements b_k^A of class *k*. This is compliant with the ITU CAC mechanism described in sections 8.1.1, 8.3.3, and 8.1.3 respectively. Another enforcement of ITU–CAC is the total number of in-progress calls n^D in network resources partition *D*; which is based on class *k* actual demand b_k^A. The link’s admissibility probability for a class *k* is the weighted average of a_{jk}^D multiplied by C_j^D as indicated in equation (25).

$$a_{jk} = \frac{\sum_{\forall D} a_{jk}^D * C_j^D}{C_j} \text{ ……………. (25)}$$

8.3.4 SPA-Shared- Static load partitioning and disabled inverse multiplexing (without NE, without IM)

This case is when the Load Partitioning Function (LPF) is configured to static load sharing "without Network Engineering" and the Inverse Multiplexing Function (IMF) is configured to "disabled". The dedicated load λ_{jk}^{vD} and shared load λ_{jk}^{vS} from configured VPN service-*v* is the load computed in section 8.2.4. Since IMF is disabled, no inverse multiplexing of the service request flow with actual bandwidth requirement b_k^A into multiple flows each with granular bandwidth requirement b_k^G is performed. Thus, it should be observed that the link's occupancy probability $p_j^{vD}(n)$ and $p_j^S(n)$ is based on the actual bandwidth requirement b_k^A of class *k* rather than the granular bandwidth requirement b_k^G of class *k* as given in equations (26, 27).

$$np_j^{vD}(n) = \sum_K b_k^A \frac{\lambda_{jk}^{vD}}{\mu_k} p_j^{vD}(n - b_k^A) \text{ …………….. (26)}$$

$$np_j^S(n) = \sum_K b_k^A \frac{\lambda_{jk}^S}{\mu_k} p_j^S(n - b_k^A) \text{ …………….. (27)}$$

The admissibility probability at the dedicated resources partitions *D* and shared resources partition *S* is given in equations (28) and (29) respectively.

$$a_{jk}^{vD} = \sum_{n=0}^{C_j^{vD} - b_k^A} p_j^{vD}(n) \text{ …………….. (28)}$$

$$a_{jk}^S = \sum_{n=0}^{C_j^S - b_k^A} p_j^S(n) \text{ …………….. (29)}$$

The configured VPN service-*v* link's admissibility probability for a class *k* is the weighted average of a_{jk}^{vD} and a_{jk}^S multiplied by C_j^{vD} and C_j^S respectively as indicated below:

$$a_{jk}^v = \frac{a_{jk}^{vD}.C_j^{vD} + a_{jk}^S.C_j^S}{C_j^{vD} + C_j^S} \text{ …………….. (30)}$$

The physical resources link's admissibility probability for a class *k* is the weighted average of all a_{jk}^{vD} and a_{jk}^S multiplied by C_j^{vD} and C_j^S respectively as indicated below:

$$a_{jk} = \frac{(\sum_{\forall D} a_{jk}^{vD}.C_j^{vD}) + a_{jk}^{S}.C_j^{S}}{C_j} \text{ …………….. (31)}$$

8.3.5 SPA-Shared- Dynamic load partitioning and disabled inverse multiplexing (with NE, without IM)

This case is when the Load Partitioning Function (LPF) is configured to dynamic load sharing “with Network Engineering” and the Inverse Multiplexing Function (IMF) is configured to “disabled”. The dedicated load λ_{jk}^{vD} and shared load λ_{jk}^{S} from configured VPN service-*v* is the load computed in section 8.2.5. Since IMF is disabled, no inverse multiplexing of the service request flow with actual bandwidth requirement b_k^A into multiple flows each with granular bandwidth requirement b_k^G is performed. Equations (26-31) are used but while using dedicated load λ_{jk}^{vD} and shared load λ_{jk}^{S} from configured VPN service-*v* as computed in section 8.2.5.

8.3.6 SPA-Shared- Static load partitioning and enabled inverse multiplexing (without NE, with IM)

This case is when the Load Partitioning Function (LPF) is configured to static load sharing “without Network Engineering” and the Inverse Multiplexing Function (IMF) is configured to “enabled”. The dedicated load λ_{jk}^{vD} and shared load λ_{jk}^{S} from configured VPN service-*v* is the load computed in section 8.2.4. Since IMF is enabled, inverse multiplexing of the service request flow with actual bandwidth requirement b_k^A into multiple flows each with granular bandwidth requirement b_k^G is performed. Thus, it should be observed that the link’s occupancy probability $p_j^{vD}(n)$ and $p_j^{S}(n)$ is based on the granular bandwidth requirement b_k^G of class *k* rather than the actual bandwidth requirement b_k^A of class *k* as given in equations (26, 27). Also, it should be observed that an additional term (*i)* is multiplied by the Erlang load $b_k^G \frac{\lambda_{jk}^{vD}}{\mu_k}$ to maintain the same Erlang load before and after inverse multiplexing operation where $b_k^A = ib_k^G$.

$$np_j^{vD}(n) = \sum_K b_k^G \frac{\lambda_{jk}^{vD} i}{\mu_k} p_j^{vD}(n - b_k^G) \text{ …………….. (32)}$$

$$np_j^{S}(n) = \sum_K b_k^G \frac{\lambda_{jk}^{S} i}{\mu_k} p_j^{S}(n - b_k^G) \text{ …………….. (33)}$$

The admissibility probability at the dedicated resources partitions *D* and shared resources partition *S* is the same like equations (28) and (29) respectively but with replacing b_k^A by b_k^G .

8.3.7 SPA-Shared- Dynamic load partitioning and enabled inverse multiplexing (with NE, with IM)

This case is when the Load Partitioning Function (LPF) is configured to dynamic load partitioning "with Network Engineering" and the Inverse Multiplexing Function (IMF) is configured to "enabled". The dedicated load λ_{jk}^{vD} and shared load λ_{jk}^{S} from configured VPN service-*v* is the load computed in section 8.2.5. Since IMF is enabled, inverse multiplexing of the service request flow with actual bandwidth requirement b_k^A into multiple flows each with granular bandwidth requirement b_k^G is performed. Equations (26-31) are used but while using dedicated load λ_{jk}^{vD} and shared load λ_{jk}^{S} as computed in section 8.2.5 and with replacing b_k^A by b_k^G .

8.4 Step-4: Calculating routing probability for each possible route

8.4.1 Base method

Liu and Baras in [68] introduced a mathematical model to compute the routing probability based on the occupancy probability computed in step-3. The following equations describe the mathematical equations used by the FPA routing component to calculate the routing probability q_{rk}^{mD}

$$\Pr[A_n^D(r_m)] = \prod_{j\in(r_m)} \sum_{k=0}^{C_j^D - n} P_j^D(k) \text{ …………….. (34)}$$

$$\Pr[A_{n+1}^D(r_m)] = \prod_{j\in(r_m)} \sum_{k=0}^{C_j^D - n+1} P_j^D(k) \text{ …………….. (35)}$$

$$\Pr[A_n^D(r_k - r_m)] = \prod_{j\in(r_k - r_m)} \sum_{k=0}^{C_j^D - n} P_j^D(k) \text{ .... (36)}$$

$$\Pr[\overline{A}_n^D(r_k - r_m)] = 1 - \prod_{j\in(r_k - r_m)} \sum_{k=0}^{C_j^D - n} P_j^D(k) \text{ .... (37)}$$

$$\Pr[A_{n+1}^D(r_k - r_m)] = \prod_{j\in(r_k - r_m)} \sum_{k=0}^{C_j^D - n+1} P_j^D(k) \text{ .... (38)}$$

$$\Pr[\overline{A}_{n+1}^D(r_k - r_m)] = 1 - \prod_{j\in(r_k - r_m)} \sum_{k=0}^{C_j^D - n+1} P_j^D(k) \text{ .... (39)}$$

$$\Pr[\widetilde{A}_n^D(r_m)] = \Pr[A_n^D(r_m)] - \Pr[A_{n+1}^D(r_m)] \text{ .... (40)}$$

The routing probability q_{rk}^{mD} that a service request of class k is routed on route r_m is the probability that all routes prior to the m^{th} route on the ascending ordered route list $\prod_{k=1}^{k=m-1} \Pr[\overline{A}_n^D(r_k - r_m)]$, based on number of hops between source-destination pair *r*, have less free bandwidth, and that all routes following the m^{th} route in the same list $\prod_{k=m+1}^{k=M_r} \Pr[\overline{A}_{n+1}^D(r_k - r_m)]$ have at most the same amount of free bandwidth. It should be observed that the summation upper bound is $C_{\min}(r_m)$ to prevent the second probability to be zero when n is bigger than $C_{\min}(r_m)$

$$q_{rk}^{mD} = \sum_{n=0}^{C_{\min}(r_m)} \prod_{k=1}^{k=m-1} \Pr[\overline{A}_n^D(r_k - r_m)]. \prod_{k=m+1}^{k=M_r} \Pr[\overline{A}_{n+1}^D(r_k - r_m)]. \Pr[\widetilde{A}_n^D(r_m)] \text{ .... (41)}$$

8.4.2 IETF control plane model

The IETF control plane model does not implement state-dependent routing as indicated in sections 6.1 and 7.2.1; thus the routing probability q_{rk}^{mD} is static and does not depend on the occupancy state of the network topology links. The routing probability is configured manually to be either Direct Routing (DR) or Split Routing (SR).

8.4.3 ITU control plane model

Similar to the IETF control plane model, the ITU control plane model does not implement state-dependent routing; thus the routing probability q_{rk}^{mD} is static and does not depend on the occupancy state of the network topology links. For each network resources partition *D*, the routing probability is configured manually to be either Direct Routing (DR) or Split Routing (SR).

8.4.4 SPA-Dedicated control plane model

As described in sections 6.3 and 7.2.3, the SPA-Dedicated control plane model supports state-dependent routing. A state-dependent routing capability by the control plane routing component indicates that the routing probability q_{rk}^{mD} is computed based on the occupancy state of all the links belonging to route r_m, this was indicated in Figure 7-5 where the routing probability q_{rk}^{mD} is computed based on the occupancy probability $p_j^D(n)$ for each FPA iteration. Equations (34-41) are used to compute the routing probability q_{rk}^{mD}.

8.4.5 SPA-Shared control plane model

As described in sections 6.3 and 7.2.3, the SPA-Shared control plane model supports state-dependent routing on both the dedicated and shared resources partitions, this was indicated in Figure 7-6 where the routing probabilities for the dedicated resources partition q_{rk}^{mvD} and the shared resources partition q_{rk}^{mS} is computed based on the occupancy probability $p_j^D(n)$ and $p_j^S(n)$ respectively for each FPA iteration. Equations (42,43) describe the final mathematical equation used by the FPA routing component to calculate the routing probability q_{rk}^{mvD} and q_{rk}^{mS}.

$$q_{rk}^{mvD} = \sum_{n=0}^{C_{\min}(r_m)} \prod_{k=1}^{k=m-1} \Pr[\overline{A}_n^{vD}(r_k - r_m)]. \prod_{k=m+1}^{k=M_r} \Pr[\overline{A}_{n+1}^{vD}(r_k - r_m)].\Pr[\widetilde{A}_n^{vD}(r_m)] \ldots\ldots\ldots\ldots\ldots.. (42)$$

$$q_{rk}^{mS} = \sum_{n=0}^{C_{\min}(r_m)} \prod_{k=1}^{k=m-1} \Pr[\overline{A}_n^{S}(r_k - r_m)]. \prod_{k=m+1}^{k=M_r} \Pr[\overline{A}_{n+1}^{S}(r_k - r_m)].\Pr[\widetilde{A}_n^{S}(r_m)] \ldots\ldots\ldots\ldots\ldots.. (43)$$

8.5 Step-5: Compute network-wide blocking probability

8.5.1 Base Methods

Based on the assumption carried by Liu and Baras in [68] to compute the route blocking probability, the pair r blocking probability for class k is:

$$B_{rk} = 1 - \sum_{m} q_{rk}^{m} \prod_{j \in r_m} a_{jk} \text{ …………….. (44)}$$

Where $\sum_{m} q_{rk}^{m} = 1$. If the service request cannot be admitted, it is considered blocked.

8.5.2 IETF control plane model

Since the IETF control plane model implements the Complete Sharing (CS) concept, the blocking probability is computed on the physical resources capacity level only; thus the blocking probability B_{rk} depends on the physical link admissibility probably a_{jk} and routing probability q_{rk}^{m}. The IETF control plane model uses equation (44). The network-wide blocking probability B_k for class k is the average of the per-pair r blocking probability for $r \in R$ as provided in equation (45)

$B_k = \underset{r \in R}{AVR}[B_{rk}]$ …………….. (45) ; where *AVR* is the average function

8.5.3 ITU and SPA-Dedicated control plane models

Since the ITU and SPA-Dedicated control plane models implements the Complete Partitioning (CP) concept, the blocking probability is computed on each dedicated resources partition. Similar to the link's reduced load, occupancy probability, and admissibility probability where the reduced load is computed for each network resources partition *D*; the pair blocking probability on the dedicated network resources partition *D* for class *k* is provided in equation (46).

$$B_{rk}^{D} = 1 - \sum_{m} q_{rk}^{Dm} \prod_{j \in r_m} a_{jk}^{D} \text{ …………….. (46)}$$

The network-wide blocking probability B_k^D on dedicated resources partition *D* for class *k* is the average of the per-pair *r* blocking probability for $r \in R$ as provided in equation (47)

$$B_k^D = \underset{r\in R}{AVR}[B_{rk}^D] \text{ ……………. (47)}$$

The pair *r* blocking probability from a link perspective is the weighted average of B_{rk}^D multiplied by C_j^D. The network-wide blocking probability B_k for class *k* is the average of the pair *r* blocking probability for $r \in R$

$$B_{rk} = \frac{\sum_{\forall D} B_{rk}^D * C_j^D}{C_j} \text{ ……………. (48)}$$

$$B_k = \underset{r\in R}{AVR}[B_{rk}] \text{ ……………. (49)}$$

8.5.4 SPA-Shared control plane models

Since the SPA-Shared control plane model implements the Virtual Partitioning (VP) concept, the blocking probability is computed on each dedicated resources partition *D* and the shared resources partition *S*. The pair r blocking probability on the dedicated network resources partition *D* for class *k* is provided in equation (46). The pair blocking probability on the shared network resources partition *S* for class *k* is provided in equation (50).

$$B_{rk}^S = 1 - \sum_m q_{rk}^{mS} \prod_{j\in r_m} a_{jk}^S \text{ ……………. (50)}$$

The pair *r* blocking probability from a VPN resources partition, dedicated and shared resources for a configured VPN service *v*, perspective is the weighted average of B_{rk}^D multiplied by C_j^D and B_{rk}^S multiplied by C_j^S, and the network-wide blocking probability B_k^v for class *k* is the average of the pair *r* blocking probability for $r \in R$

$$B_{rk}^v = \frac{B_{rk}^D * C_j^D + B_{rk}^S * C_j^S}{C_j^D + C_j^S} \text{ ……………. (51)}$$

$$B_k^v = \underset{r\in R}{AVR}[B_{rk}^v] \text{ ……………. (52)}$$

The pair *r* blocking probability from a link perspective is the weighted average of B_{rk}^D multiplied by C_j^D for all dedicated resources and B_{rk}^S multiplied by C_j^S, and the network-wide blocking probability B_k for class *k* is the average of the pair *r* blocking probability for $r \in R$ as:

$$B_{rk} = \frac{(\sum_{\forall D} B_{rk}^{D} * C_{j}^{D}) + B_{rk}^{S} * C_{j}^{S}}{C_{j}} \text{ …………….. (53)}$$

$$B_{k} = \underset{r \in R}{AVR}[B_{rk}] \text{ …………….. (54)}$$

8.6 Step-6: Compute network-wide average permissible load

8.6.1 IETF control plane model

Since the IETF control plane model implements the Complete Sharing (CS) concept, the permissible load $\hat{\lambda}_{k}$ is computed on the physical resources only. The pair *r* permissible load is the sum of the permissible load on each route $m \in r_{m}$. Each route *m* permissible load is the minimum permissible load on all the links $j \in r_{m}$ multiplied by the routing probability q_{rk}^{m} on route r_{m}, and the network-wide average permissible load $\hat{\lambda}_{k}$ is the average of the per-pair permissible load $\hat{\lambda}_{rk}$ for $\forall r \in R$ as:

$$\hat{\lambda}_{rk} = \sum_{m=1}^{M_{r}} q_{rk}^{m} \underset{j \in r_{m}}{MIN}(\lambda_{jk}) \text{ …………….. (55)}$$

$$\hat{\lambda}_{k} = \underset{r \in R}{Avr}[\hat{\lambda}_{rk}] \text{ …………….. (56)}$$

8.6.2 ITU and SPA-Dedicated control plane models

Since the ITU and SPA-Dedicated control plane models implements the Complete Partitioning (CP) concept, the permissible load is computed on both the dedicated resources partitions and the physical resources levels. As provided in equation (58), the network-wide average permissible load $\hat{\lambda}_{k}^{D}$ on the dedicated resource partition *D* is the average of the per-pair permissible load $\hat{\lambda}_{rk}^{D}$ for $\forall r \in R$.

$$\hat{\lambda}_{rk}^{D} = \sum_{m=1}^{M_{r}} q_{rk}^{mD} \underset{j \in r_{m}}{MIN}(\lambda_{jk}^{D}) \text{ …………….. (57)}$$

$$\hat{\lambda}_{k}^{D} = \underset{r \in R}{Avr}[\hat{\lambda}_{rk}^{D}] \text{ …………….. (58)}$$

The per-pair *r* permissible load for class *k* from a link perspective is the weighted average of $\hat{\lambda}_{rk}^{D}$ multiplied by C_j^D as:

$$\hat{\lambda}_{rk} = \frac{(\sum_{\forall D} \hat{\lambda}_{rk}^{D} * C_j^D)}{C_j} \text{……………..} (59)$$

8.6.3 SPA-Shared control plane models

Since the SPA-Shared control plane model implements the Virtual Partitioning (VP) concept, the permissible load is computed on the dedicated resources partitions, shared resources partition, VPN partition, and the physical resources levels. The permissible load on the dedicated resources partition is computed using equations (57-58).The network-wide average permissible load on the shared resources $\hat{\lambda}_{k}^{S}$ is computed in a similar manner to the dedicated resources partition as:.

$$\hat{\lambda}_{rk}^{S} = \sum_{m=1}^{M_r} q_{rk}^{mS} \underset{j \in r_m}{MIN}(\lambda_{jk}^{S}) \text{……………..} (60)$$

$$\hat{\lambda}_{k}^{S} = \underset{r \in R}{Avr}[\hat{\lambda}_{rk}^{S}] \text{……………..} (61)$$

The pair *r* permissible load for class *k* from a VPN perspective is the weighted average of $\hat{\lambda}_{rk}^{D}$ multiplied by C_j^D and $\hat{\lambda}_{rk}^{S}$ multiplied by C_j^S. $\hat{\lambda}_{rk}^{v} = \frac{\hat{\lambda}_{rk}^{D} * C_j^D + \hat{\lambda}_{rk}^{S} * C_j^S}{C_j^D + C_j^S}$ …………….. (62)

The pair *r* permissible load for class *k* from a link perspective is the weighted average of $\hat{\lambda}_{rk}^{D}$ multiplied by C_j^D and the $\hat{\lambda}_{rk}^{S}$ multiplied by C_j^S.

$$\hat{\lambda}_{rk} = \frac{(\sum_{\forall D} \hat{\lambda}_{rk}^{D} * C_j^D) + \hat{\lambda}_{rk}^{S} * C_j^S}{C_j} \text{……………..} (63)$$

8.7 Step-7: Compute network-wide utilization

8.7.1 IETF control plane model

Since the IETF control plane model implements the Complete Sharing (CS) concept, the link's utilization is computed on the physical resources only. As provided in equation (64), the per link's utilization is the sum of the link *j* occupancy probability $p_j(n)$ where $n > 0$.

$$U_j = \frac{\sum_{n=0}^{C_j} np_j(n)}{C_j} \text{ .... (64)}$$

The network-wide utilization U is the average of the per link's utilization.

$$U = \underset{j \in J}{Avr}[U_j] \text{ .... (65)}$$

8.7.2 ITU and SPA-Dedicated control plane models

Since the ITU and SPA-Dedicated control plane models implements the Complete Partitioning (CP) concept, the utilization is computed on both the dedicated resources partition and the physical resources levels. The per link's utilization on a dedicated network resource partition *D*

$$U_j^D = \frac{\sum_{n=0}^{C_j^D} np_j^D(n)}{C_j^D} \text{ .... (66)}$$

The link's utilization is the weighted average of U_j^D multiplied by C_j^D

$$U_j = \frac{(\sum_{\forall D} U_j^D * C_j^D)}{C_j} \text{ .... (67)}$$

The network-wide utilization U is provided in equation (65)

8.7.3 SPA-Shared control plane models

Since the SPA-Shared control plane model implements the Virtual Partitioning (VP) concept, the utilization is computed on the dedicated resources partitions, shared resources partition, VPN partition, and the physical resources levels. The utilization on the dedicated resources partition is computed using equations (66-67). The network-wide average utilization on the shared resources is computed in a similar manner to the dedicated resources partition as:

$$U_j^S = \frac{\sum_{n=0}^{C_j^S} np_j^S(n)}{C_j^S} \text{ …………….. (68)}$$

The utilization U_j^v on the VPN resources partition *v* level, dedicated and shared resources, is the weighted average of U_j^D multiplied by C_j^D and U_j^S multiplied by C_j^S as:

$$U_j^v = \frac{U_j^D * C_j^D + U_j^S * C_j^S}{C_j^D + C_j^S} \text{ …………….. (69)}$$

The link’s utilization is the weighted average of U_j^D multiplied by C_j^D for all dedicated resources and U_j^S multiplied by C_j^S as:

$$U_j = \frac{(\sum_{\forall D} U_j^D * C_j^D) + U_j^S * C_j^S}{C_j} \text{ …………….. (70)}$$

The network-wide utilization U is provided in equation (65)

9 Scenarios and Performance Evaluation

This section describes the specific scenarios used to study the performance of the IETF, ITU, and SPA control plane models. This section also provides detailed view of the network topologies analyzed, modeling environment, performance metrics, and parameters settings for both the control plane models and the configured VPN service models.

9.1 Network topology analyzed

Two topologies were used to compare the performance of the IETF, ITU, and SPA control plane models, a 4-node topology as illustrated in Figure 9-1 and 7-node topology as illustrated in Figure 9-3. The 4-node topology was used as a modelling prototype to ensure that the control plane components and their associated functionalities are performed according to the mathematical models as expected. The 7-node topology was used to study the relative performance of the IETF, ITU, SPA control plane models. The following transport network parameters are considered in the modeling analysis:

1. The physical resources capacity C_j of each link j is 24 STS-1
2. In the IETF control plane model, service requests from different configured VPN service models are applied “multiplexed” to the 24 STS-1.
3. In the ITU control plane model, the 24 STS-1 are divided into two network resources partition C_j^D, each with 12 STS-1 resources.
4. The SPA-Dedicated control plane model uses the same transport network configuration like the ITU control plane model.
5. The SPA-Shared control plane model partitions the 24 STS-1 into three network resources partitions; two dedicated resources partitions C_j^{vD} and one shared resources partition C_j^S. Four sharing levels are considered as follows:
    a. STS-1 sharing: C_j^{vD} =11 STS-1, C_j^S =2 STS-1
    b. STS-2 sharing: C_j^{vD} =10 STS-1, C_j^S =4 STS-1
    c. STS-3 sharing: C_j^{vD} =9 STS-1, C_j^S =6 STS-1
    d. STS-4 sharing: C_j^{vD} =8 STS-1, C_j^S =8 STS-1

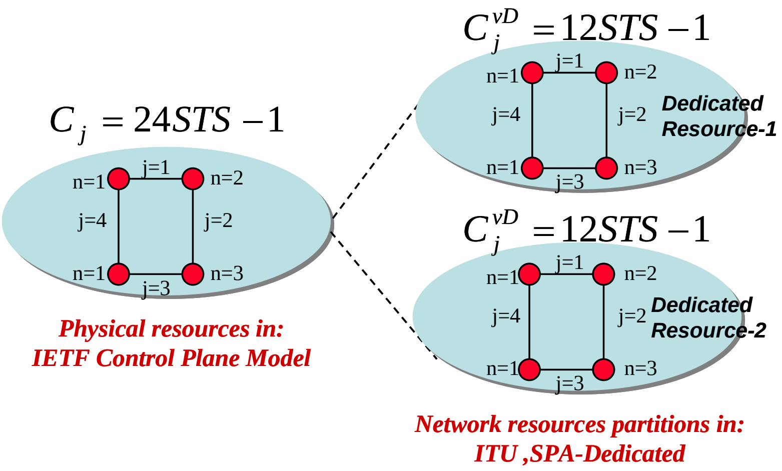

Figure 9-1: Modeled ITU, SPA-Dedicated Network Partitions Compared to IETF Physical Resources “4-node topology”

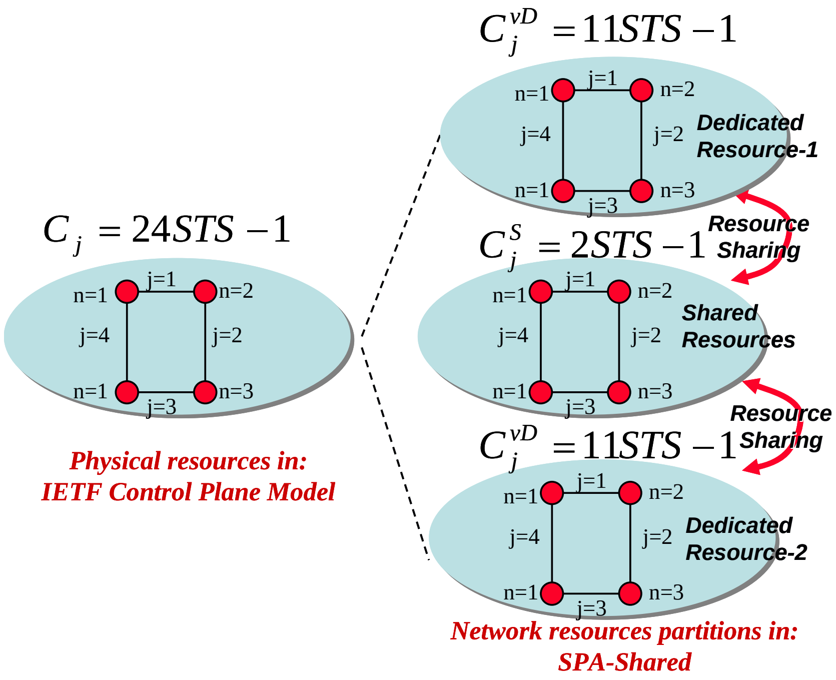

Figure 9-2: Modeled SPA-Shared Network Partitions Compared to IETF Physical Resources "4-node topology"- 1STS-1 Sharing Scenario

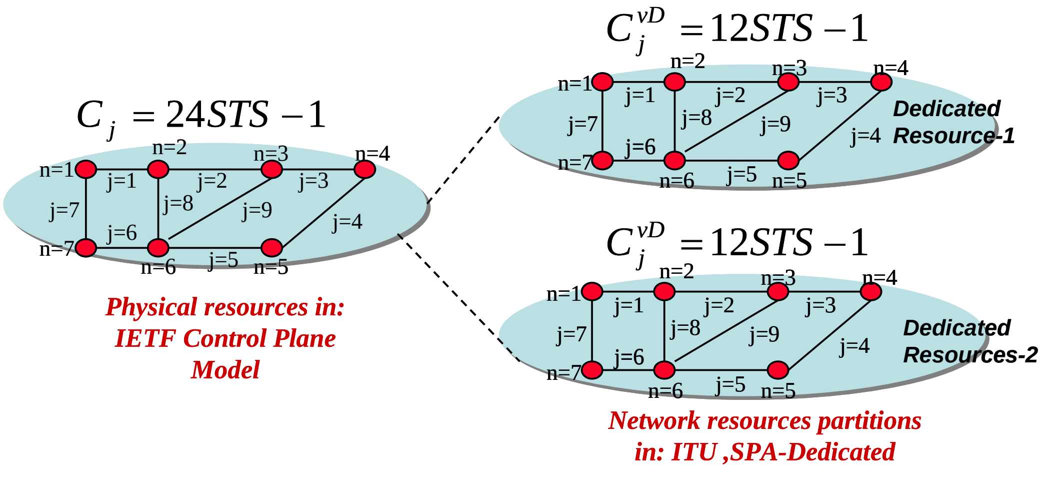

Figure 9-3: Modeled ITU, SPA-Dedicated Network Partitions Compared to IETF Physical Resources "7-node topology"

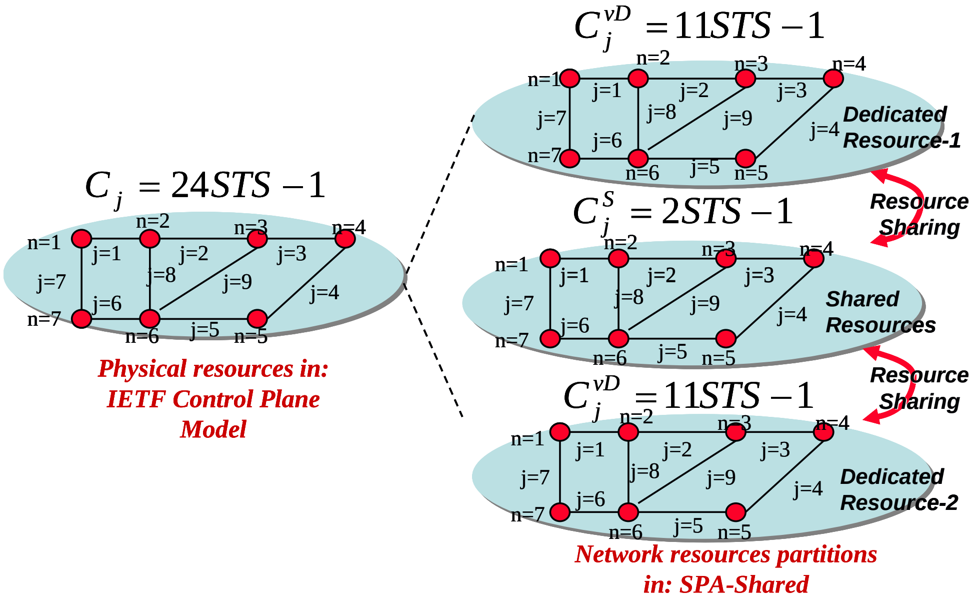

Figure 9-4: Modeled SPA-Shared Network Partitions Compared to IETF Physical Resources "7-node topology"- 1 STS-1 Sharing Scenario

Figure 9-5 provides a numerical example of the FPA parameters for the 4-node topology. For the 4-node topology, the following parameters are specified:

1. *N=4* for the 4-node topology
2. *J=4* for the four links of the 4-node topology
3. $M_r = 3$ to indicate that each source node is connected to three destination node.
4. r_m is a matrix that lists the possible source-destination pairs.
5. $C_j = 24, \; \forall j \in J$ to indicate the physical resources capacity for all links to be 24 STS-1

In addition to the network topology parameters, additional parameters are specified for the configured VPN service model analyzed as follows:

1. $k = 2$ to indicate a service request with actual bandwidth requirement b_k^A=2 STS-1.
2. $\lambda_{jk}^{r_m} = [\lambda_{jk}^{r_m} = 10 -> 30 Erlang]$ to indicate an input load ranging from [10-30] Erlangs.
3. $\mu_k = 1$ to indicate an average service duration time to be 1 with exponential service time.

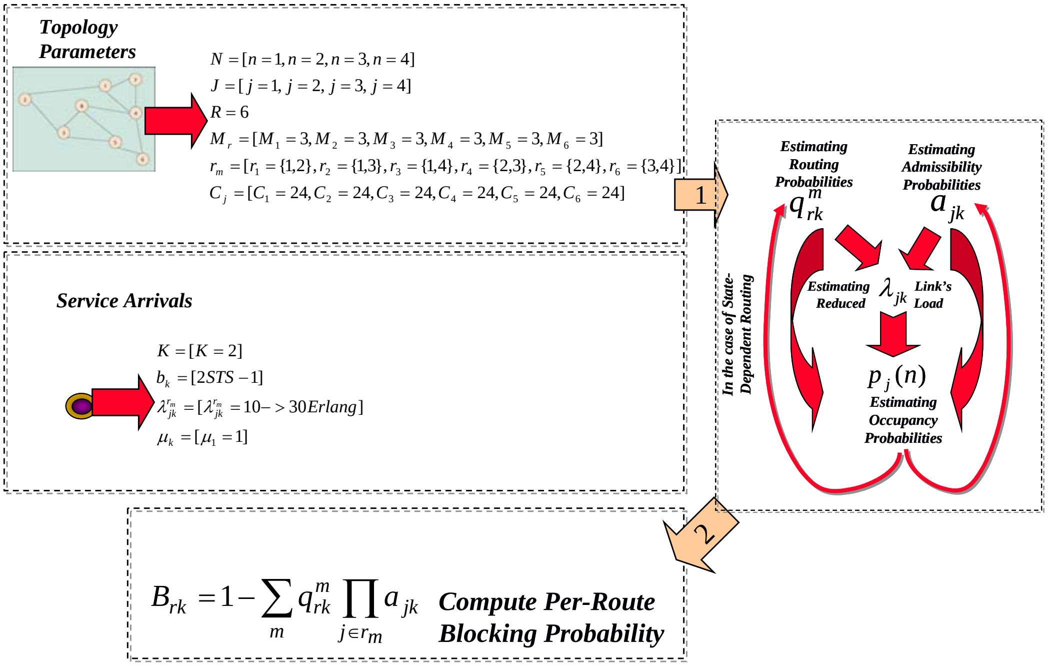
Topology Parameters
$N=[n=1,n=2,n=3,n=4]$
$J=[j=1,j=2,j=3,j=4]$
$R=6$
$M_r=[M_1=3,M_2=3,M_3=3,M_4=3,M_5=3,M_6=3]$
$r_m=[r_1=\{1,2\},r_2=\{1,3\},r_3=\{1,4\},r_4=\{2,3\},r_5=\{2,4\},r_6=\{3,4\}]$
$C_j=[C_1=24,C_2=24,C_3=24,C_4=24,C_5=24,C_6=24]$
1
Estimating Routing Probabilities
q^m_{rk}
Estimating Admissibility Probabilities
a_{jk}
Estimating Reduced
λ_{jk}
Link's Load
$p_j(n)$
Estimating Occupancy Probabilities
In the case of State-Dependent Routing
Service Arrivals
$K=[K=2]$
$b_k=[2STS-1]$
$\lambda^{r_m}_{jk}=[\lambda^{r_m}_{jk}=10->30Erlang]$
$\mu_k=[\mu_1=1]$
2
$B_{rk}=1-\sum_m q^m_{rk}\prod_{j\in r_m} a_{jk}$
Compute Per-Route Blocking Probability

Figure 9-5: Modeled SPA-Shared Network Partitions Compared to IETF Physical Resources "7-node topology"- 1 STS-1 Sharing Scenario

9.2 Modeling parameters

This section provides details on the modelling parameters used for the input loads, control plane components configuration options, and configured VPN service models.

9.2.1 Parameters specifics of input load

This section provides details on the modelling parameters used for the input load. One input class was evaluated with the following parameters: $k=2$, $b_k^A=2$ STS-1, $\mu_k=1$unit time, $\lambda_{rk}=4$ calls/unit time. Range of input load for 4-node topology is 10 to 30 Erlangs. Range of input load for 7-node topology is 30 to 70 Erlangs.

9.2.2 Parameters specifics of control plane components

The following components parameters in the three control plane models are used to evaluate the control plane performance under different traffic management schemes:

1. *Control Plane Instance (CPI) Selection: CPI* is used to allow the partitioning of the incoming load into transport resources partitions based on the configured VPN service identified number parameter from the service configuration profile layer

2. *Routing Computation components:* Two parameters are specified:

   1.1. *Routing probability:* In static routing, the routing probability is configured to Direct Routing (DR) or Split Routing (SR) independent of the network links occupancy probability. In state-dependent routing, the FPA mechanism is used to provide the routing component with the link's traffic occupancy probability for all the network topology links within each network resources partition. The links occupancy probabilities are used to compute the state-dependent routing probabilities.

   1.2. *Routing granularity level:* The routing component can be set to build routing tables based on transport network *coarse* granularity level or *fine* granularity level. The coarse granularity level is set to be STS-3; the fine granularity level is set to be STS-1.

2. *Load Partitioning Function (LPF):* Allows the load partitioning of the arriving service requests between dedicated and shared network resources partitions. Two configuration options are available:

   2.1. *Static Partitioning "without network engineering w/o(NE)":* In this configuration scenario, LPF is configured to statically partition the configured VPN service arriving load between the dedicated and shared resources based on the resource ratios between dedicated and shared resources

   2.2. *Dynamic Partitioning "with network engineering w/(NE)":* In this configuration scenario, LPF is configured to dynamically partition the configured VPN service arriving load between the dedicated and shared resources based on the blocking probability on the dedicated resources partition.

3. *Inverse Multiplexing Function (IMF)*: Allows inverse multiplexing of the arriving service requests flow with actual bandwidth b_k^A into multiple flows each with granular bandwidth requirement b_k^G . Two configuration options are available:

   3.1. *Without Inverse Multiplexing "w/o(IM)":* IMF is disabled

3.2. *With Inverse Multiplexing "w/(IM)":* IMF is enabled.

Table 9-1 illustrates the control plane components configuration for the IETF, ITU, and SPA control plane models, the tick symbol indicate that this configuration option is enabled for the corresponding control plane model. For example, the tick symbol for the static routing probability in both the IETF and ITU control plane models indicated that the routing probability is configured statically.

9.2.3 Parameters specifics of configured VPN service models considered

The service configuration profile layer parameters are configured as follows:

1. *Configured VPN service identification number* parameter is configured to enabled mode indicating that the incoming service requests are labelled with different VPN service identification numbers to differentiate service arrivals ownerships
2. *Service demand granularity* parameter is configured as 1-STS-1 granular
3. *Service flow connectivity* parameter is configured as fully-meshed.

9.3 Performance metrics

A key objective is to compute the following performance metrics:

1. Average network-wide blocking probability B_k: the network-wide average probability over all network links that service requests of class *k* is denied access to network resources; $B_k = 0.3$ indicates that 30% of the service arrival of class K, on a network-wide basis, is blocked and denied access to network resources.
2. Average per source-destination pair r permissible "non-blocked" load $\hat{\lambda}_{rk}$: the average offered load over all network links that service requests of class *k* is allowed.
3. Average network-wide resource utilization U: the network-wide average traffic occupancy percentage over all network' links; $U = 50\%$ for a network with 24 STS-1 capacity for each link indicates that, on a network-wide average, 12 STS-1 per link are occupied with service request traffic.

Table 9-2 lists the performance metrics computed for each control plane model with their relevant mathematical formulation provided in section 8, the numbers in parenthesis indicate the mathematical formulas' number provided in section 8. As illustrated in Table 9-2, since the IETF control plane model supports the Complete Sharing (CS) concept, the IETF control plane model computes the above performance metrics on the link *(L)* resources level only. Since both the ITU and SPA-Dedicated control plane models support the Complete Partitioning (CP) concept, the ITU and SPA-Dedicated control plane models compute the above performance metrics on the dedicated resources partition *(D)* and link *(L)* levels. Since the SPA-Shared control plane model supports the Virtual Partitioning (VP) concept, the SPA-Shared computes the above performance metrics on the dedicated resources partitions *(D)*, shared resources partition (*S)*, VPN resources partition *(V)*, and link *(L)* levels.

	Routing Probability		**Routing Granularity**		**Control Plane Instance (CPI) Selection**	**Load Partitioning Function (LPF) enabled**		**Inverse Multiplexing Function (IMF) enabled**	
Component Configuration	Static	State-Dependent	Coarse	Granular		w/oNE	w/NE	w/oIM	w/IM
IETF	✓		✓						
ITU	✓			✓	✓				
SPA-Dedicated		✓		✓	✓				
SPA-w/o(NE,IM)		✓		✓	✓	✓		✓	
SPA-w/NE,w/oIM		✓		✓	✓		✓	✓	
SPA-w/oNE,w/IM		✓		✓	✓	✓			✓
SPA-w/(NE,IM)		✓		✓	✓		✓		✓

Table 9-1: Control Planes Components Configuration Options

Performance Metric	*Blocking probability*				*Permissible load*				*Utilization*			
Network Partition Level	D	S	V	L	D	S	V	L	D	S	V	L
IETF Relevant Equations				✓				✓				✓
				(44-45)				(55-56)				(64-65)
ITU Relevant Equations	✓			✓	✓			✓	✓			✓
	(46-47)			(48-49)	(57-58)			(59)	(66)			(67)
SPA-Dedicated Relevant Equations	✓			✓	✓			✓	✓			✓
	(46-47)			(48-49)	(57-58)			(59)	(66)			(67)
SPA-Shared Relevant Equations	✓	✓	✓	✓	✓	✓	✓	✓	✓	✓	✓	✓
	(46-47)	(50)	(51-52)	(53-54)	(57-58)	(60-61)	(62)	(63)	(66)	(68)	(69)	(70)

Table 9-2: Performance Metrics for the Three Control Plane Models

9.4 Modeling environment

The numerical evaluation of the analytical models was implemented in a combination of Mathematica^{TM}, Microsoft Excel^{TM}, and Visual Basic^{TM}. As illustrated in Figure 9-5, multiple Excel spreadsheets were used to compute both the reduced load approximation λ_{jk}^{vD} for each link *j* and class *k* within each network resources partition *D*, and the routing probability q_{rk}^{mD} for each route *m* for source-destination pair *r* and class *k*. Mathematica^{TM} was used to compute the occupancy probability $p_j(n)$ for each link *j* in the network topology. Visual Basic^{TM} was used to program the Fixed Point Approximation module used to compute the blocking probability B_{rk}^{D} for each pair *r*, class k within network resources partition *D*, and the permissible load $\hat{\lambda}_k^D$ for each class *k* within network resources partition *D*. It is important to mention the scaling issues faced with both Mathematica^{TM} and Excel^{TM}. Mathematica^{TM} was not able compute the occupancy probability when the number of resources *(n)* within a resources partition is greater than 12 and the applied classes (*k)* are greater than 2. When *n=12* and *k=2*, the occupancy probability $p_j(n)$ output equations provided by Mathematica^{TM} were 120 pages in length. Multiple recursive substitutions were carried to shorten the Mathematica^{TM} output equations to be able to fit the Visual Basic^{TM} arrays limited length.

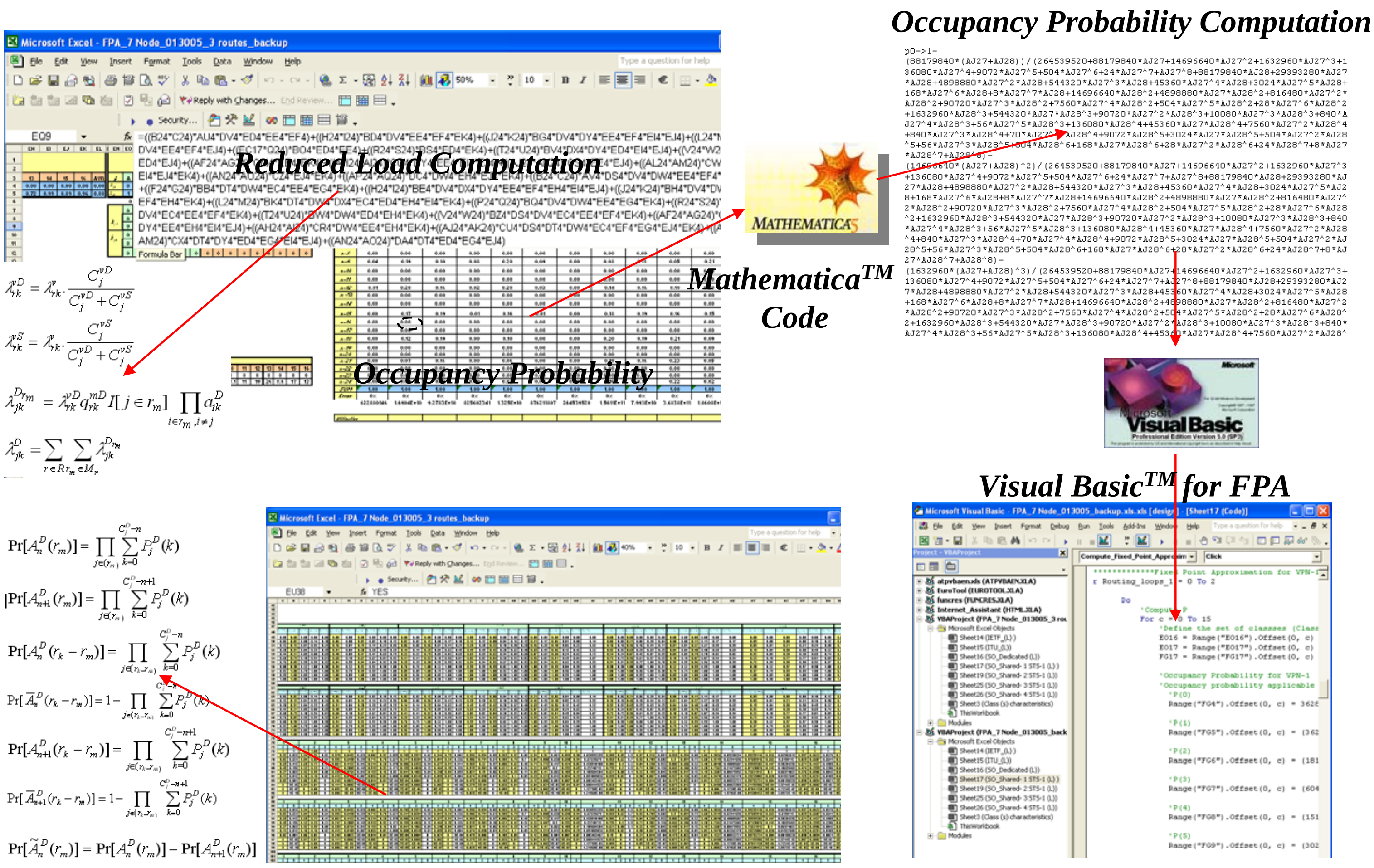
Occupancy Probability Computation
Reduced Load Computation
Occupancy Probability
Mathematica^{TM} Code
MATHEMATICA 5
Visual Basic^{TM} for FPA
Microsoft Excel - FPA_7 Node_013005_3 routes_backup
File Edit View Insert Format Tools Data Window Help
Type a question for help
Reply with Changes... End Review...
Security...
EQ9
Formula Bar
EU38
YES
Microsoft
Visual Basic
Professional Edition Version 5.0 (SP3)
Microsoft Visual Basic - FPA_7 Node_013005_backup.xls.xls [design] - [Sheet17 (Code)]
File Edit View Insert Format Debug Run Tools Add-Ins Window Help
Project - VBAProject
Compute_Fixed_Point_Approxim
Click
atpvbaen.xls (ATPVBAEN.XLA)
EuroTool (EUROTOOL.XLA)
funcres (FUNCRES.XLA)
Internet_Assistant (HTML.XLA)
VBAProject (FPA_7 Node_013005_3 rou
Microsoft Excel Objects
Sheet14 (IETF_(L))
Sheet15 (ITU_(L))
Sheet16 (SO_Dedicated (L))
Sheet17 (SO_Shared- 1 STS-1 (L))
Sheet19 (SO_Shared- 2 STS-1 (L))
Sheet25 (SO_Shared- 3 STS-1 (L))
Sheet26 (SO_Shared- 4 STS-1 (L))
Sheet3 (Class (s) characteristics)
ThisWorkbook
Modules
VBAProject (FPA_7 Node_013005_back

```
=((B24*C24)*AU4*DV4*ED4*EE4*EF4)+((H24*I24)*BD4*DV4*EE4*EF4*EK4)+((J24*K24)*BG4*DV4*DY4*EE4*EF4*EI4*EJ4)+((L24*M
DV4*EE4*EF4*EJ4)+((EC17*Q24)*BO4*ED4*EE4)+((R24*S24)*BS4*ED4*EK4)+((T24*U24)*BV4*DX4*DY4*ED4*EI4*EJ4)+((V24*W2
ED4*EJ4)+((AF24*AG [illegible] E4*EJ4)+((AL24*AM24)*CW
EI4*EJ4*EK4)+((AN24*AO24)*CZ4*EJ4*EK4)+((AP24*AQ24)*DC4*DW4*EH4*E [illegible] EK4)+((B24*C24)*AV4*DS4*DV4*DW4*EE4*EF4*
+((F24*G24)*BB4*DT4*DW4*EC4*EE4*EG4*EK4)+((H24*I24)*BE4*DV4*DX4*DY4*EE4*EF4*EH4*EI4*EJ4)+((J24*K24)*BH4*DV4*DW
EF4*EH4*EK4)+((L24*M24)*BK4*DT4*DW4*DX4*EC4*ED4*EH4*EI4*EK4)+((P24*Q24)*BQ4*DV4*DW4*EE4*EG4*EK4)+((R24*S24)*
DV4*EC4*EE4*EF4*EK4)+((T24*U24)*BW4*DW4*ED4*EH4*EK4)+((V24*W24)*BZ4*DS4*DV4*EC4*EE4*EF4*EK4)+((AF24*AG24)*C
DY4*EE4*EH4*EI4*EJ4)+((AH24*AI24)*CR4*DW4*EE4*EH4*EK4)+((AJ24*AK24)*CU4*DS4*DT4*DW4*EC4*EF4*EG4*EJ4*EK4)+((A
AM24)*CX4*DT4*DY4*ED4*EG4*EI4*EJ4)+((AN24*AO24)*DA4*DT4*ED4*EG4*EJ4)
```

$$\lambda_{rk}^{vD} = \lambda_{rk}^{v} \cdot \frac{C_j^{vD}}{C_j^{vD} + C_j^{vS}}$$

$$\lambda_{rk}^{vS} = \lambda_{rk}^{v} \cdot \frac{C_j^{vS}}{C_j^{vD} + C_j^{vS}}$$

$$\lambda_{jk}^{D_{r_m}} = \lambda_{rk}^{vD} q_{rk}^{mD} I[j \in r_m] \prod_{i \in r_m, i \neq j} a_{ik}^{D}$$

$$\lambda_{jk}^{D} = \sum_{r \in R} \sum_{r_m \in M_r} \lambda_{jk}^{D_{r_m}}$$

```
p0->1-
(88179840*(AJ27+AJ28))/(264539520+88179840*AJ27+14696640*AJ27^2+1632960*AJ27^3+1
36080*AJ27^4+9072*AJ27^5+504*AJ27^6+24*AJ27^7+AJ27^8+88179840*AJ28+29393280*AJ27
*AJ28+4898880*AJ27^2*AJ28+544320*AJ27^3*AJ28+45360*AJ27^4*AJ28+3024*AJ27^5*AJ28+
168*AJ27^6*AJ28+8*AJ27^7*AJ28+14696640*AJ28^2+4898880*AJ27*AJ28^2+816480*AJ27^2*
AJ28^2+90720*AJ27^3*AJ28^2+7560*AJ27^4*AJ28^2+504*AJ27^5*AJ28^2+28*AJ27^6*AJ28^2
+1632960*AJ28^3+544320*AJ27*AJ28^3+90720*AJ27^2*AJ28^3+10080*AJ27^3*AJ28^3+840*A
J27^4*AJ28^3+56*AJ27^5*AJ28^3+136080*AJ28^4+45360*AJ27*AJ28^4+7560*AJ27^2*AJ28^4
+840*AJ27^3*AJ28^4+70*AJ27^4*AJ28^4+9072*AJ28^5+3024*AJ27*AJ28^5+504*AJ27^2*AJ28
^5+56*AJ27^3*AJ28^5+504*AJ28^6+168*AJ27*AJ28^6+28*AJ27^2*AJ28^6+24*AJ28^7+8*AJ27
*AJ28^7+AJ28^8)-
(14696640*(AJ27+AJ28)^2)/(264539520+88179840*AJ27+14696640*AJ27^2+1632960*AJ27^3
+136080*AJ27^4+9072*AJ27^5+504*AJ27^6+24*AJ27^7+AJ27^8+88179840*AJ28+29393280*AJ
27*AJ28+4898880*AJ27^2*AJ28+544320*AJ27^3*AJ28+45360*AJ27^4*AJ28+3024*AJ27^5*AJ2
8+168*AJ27^6*AJ28+8*AJ27^7*AJ28+14696640*AJ28^2+4898880*AJ27*AJ28^2+816480*AJ27^
2*AJ28^2+90720*AJ27^3*AJ28^2+7560*AJ27^4*AJ28^2+504*AJ27^5*AJ28^2+28*AJ27^6*AJ28
^2+1632960*AJ28^3+544320*AJ27*AJ28^3+90720*AJ27^2*AJ28^3+10080*AJ27^3*AJ28^3+840
*AJ27^4*AJ28^3+56*AJ27^5*AJ28^3+136080*AJ28^4+45360*AJ27*AJ28^4+7560*AJ27^2*AJ28
^4+840*AJ27^3*AJ28^4+70*AJ27^4*AJ28^4+9072*AJ28^5+3024*AJ27*AJ28^5+504*AJ27^2*AJ
28^5+56*AJ27^3*AJ28^5+504*AJ28^6+168*AJ27*AJ28^6+28*AJ27^2*AJ28^6+24*AJ28^7+8*AJ
27*AJ28^7+AJ28^8)-
(1632960*(AJ27+AJ28)^3)/(264539520+88179840*AJ27+14696640*AJ27^2+1632960*AJ27^3+
136080*AJ27^4+9072*AJ27^5+504*AJ27^6+24*AJ27^7+AJ27^8+88179840*AJ28+29393280*AJ2
7*AJ28+4898880*AJ27^2*AJ28+544320*AJ27^3*AJ28+45360*AJ27^4*AJ28+3024*AJ27^5*AJ28
+168*AJ27^6*AJ28+8*AJ27^7*AJ28+14696640*AJ28^2+4898880*AJ27*AJ28^2+816480*AJ27^2
*AJ28^2+90720*AJ27^3*AJ28^2+7560*AJ27^4*AJ28^2+504*AJ27^5*AJ28^2+28*AJ27^6*AJ28^
2+1632960*AJ28^3+544320*AJ27*AJ28^3+90720*AJ27^2*AJ28^3+10080*AJ27^3*AJ28^3+840*
AJ27^4*AJ28^3+56*AJ27^5*AJ28^3+136080*AJ28^4+45360*AJ27*AJ28^4+7560*AJ27^2*AJ28^
```

$$\mathbf{Pr}[A_n^D(r_m)] = \prod_{j \in (r_m)} \sum_{k=0}^{C_j^D - n} P_j^D(k)$$

$$\mathbf{Pr}[A_{n+1}^D(r_m)] = \prod_{j \in (r_m)} \sum_{k=0}^{C_j^D - n+1} P_j^D(k)$$

$$\mathbf{Pr}[A_n^D(r_k - r_m)] = \prod_{j \in (r_k - r_m)} \sum_{k=0}^{C_j^D - n} P_j^D(k)$$

$$\Pr[\overline{A}_n^D(r_k - r_m)] = 1 - \prod_{j \in (r_k - r_m)} \sum_{k=0}^{C_j^D - n} P_j^D(k)$$

$$\mathbf{Pr}[A_{n+1}^D(r_k - r_m)] = \prod_{j \in (r_k - r_m)} \sum_{k=0}^{C_j^D - n+1} P_j^D(k)$$

$$\Pr[\overline{A}_{n+1}^D(r_k - r_m)] = 1 - \prod_{j \in (r_k - r_m)} \sum_{k=0}^{C_j^D - n+1} P_j^D(k)$$

$$\mathbf{Pr}[\widetilde{A}_n^D(r_m)] = \mathbf{Pr}[A_n^D(r_m)] - \mathbf{Pr}[A_{n+1}^D(r_m)]$$

```
*************Fixed Point Approximation for VPN-I
r Routing_loops_1 = 0 To 2

      Do
          'Compute P
          For c = 0 To 15
              'Define the set of classses (Class
              E016 = Range("E016").Offset(0, c)
              E017 = Range("E017").Offset(0, c)
              FG17 = Range("FG17").Offset(0, c)

              'Occupancy Probability for VPN-1
              'Occupancy probability applicable
                'P(0)
                Range("FG4").Offset(0, c) = 3626

                'P(1)
                Range("FG5").Offset(0, c) = (362

                'P(2)
                Range("FG6").Offset(0, c) = (181

                'P(3)
                Range("FG7").Offset(0, c) = (604

                'P(4)
                Range("FG8").Offset(0, c) = (151

                'P(5)
                Range("FG9").Offset(0, c) = (302
```

Figure 9-6: Modeling Environment

10 Computational Cost of the Traffic Management Schemes

This section provides details on the computation cost of the traffic management schemes for the three control plane models; the computation cost is analyzed from both FPA and implementation perspectives.

10.1 Computed cost of FPA

This section provides details on the computation cost for the three control plane models based on the FPA steps for both the base model and different traffic management schemes for the three control plane models. The computation cost of the FPA depends on the iterations required to compute the set of unknowns, the following discussion covers the computational cost for each iteration of the FPA.

10.1.1 Base model

The first computation step involves *O(J . K)* operations of (2) where *J* is the number of links and *K* is the number of service request classes, each of which has *O(R . M)* operations of (1), where *R* is the number of node pairs and *M* is the average number of routes each node pair has. The cost of (1) is also linear in the average length in hops of a route, denoted by *H*.

$$\lambda_{jk}^{r_m} = \lambda_{rk} q_{rk}^{m} I[j \in r_m] \prod_{i \in r_m, i \neq j} a_{ik} \text{ ……………... (1)}$$

$$\lambda_{jk} = \sum_{r \in R} \sum_{r_m \in M_r} \lambda_{jk}^{r_m} \text{ ……………... (2)}$$

The second computation step as provided in (3) involves operations of either the Kaufman recursion [69] or the one-dimensional approximation by Gibbens and Zachary [72,73], they both have a cost of *O(C . K)* where *C* is the physical link capacity.

$$np_j(n) = \sum_{K} b_k \frac{\lambda_{jk}}{\mu_k} p_j(n - b_k) \text{ ……………... (3)}$$

The third computation step to compute a single q_{rk}^{mD} as provided in (5) involves *O(R . M)* operations. The cost of a single q_{rk}^{mD} is based on the cost of evaluating $A_n(r_m)$ as provided in

(4), the cost of evaluating $A_n(r_m)$ for a route r_m involves *O(H)* operations (multiplications). As provided in (5), each route on the route list is evaluated for every value $n \in C$, which gives *O(M .C)* such operations. This results in a total computation cost of *O(M . C . H)* operations for each pair *r* and *O(R . M . C . H)* operations for all source-destination pairs.

$$\Pr[A_n^D(r_m)] = \prod_{j \in (r_m)} \sum_{k=0}^{C_j^D - n} P_j^D(k) \ldots\ldots\ldots\ldots\ldots\ldots (4)$$

$$q_{rk}^{mD} = \sum_{n=0}^{C_{\min}(r_m)} \prod_{k=1}^{k=m-1} \Pr[\overline{A}_n^D(r_k - r_m)] . \prod_{k=m+1}^{k=M_r} \Pr[\overline{A}_{n+1}^D(r_k - r_m)] . \Pr[\widetilde{A}_n^D(r_m)] \ldots\ldots\ldots\ldots\ldots\ldots (5)$$

10.1.2 IETF control plane model

Since the IETF control plane model does not support state-dependent routing but rather fixed routing, the IETF control plane model has the same exact computation cost as the base model for the first two computations steps, the base model third computation step is not considered in the IETF control plane model as the routing probability for any route is assigned rather than computed.

10.1.3 ITU control plane model

Similar to the IETF control plane model, the ITU control plane model does not support state-dependent routing but rather fixed routing. Hence, the ITU control plane model has the same computation cost as the IETF control plane model for each control plane instance. As provided earlier, the ITU control plane model supports the Complete Partitioning (CP) concept and hence there is a FPA instance for each network partition (*D).* Each FPA instance will have the first two computations steps as provided in the base model.

From a computation cost perspective, to take into consideration the possible *D* FPA instances, each computation cost in the first two steps as provided in the base model will be multiplied by *D* factor. The first computation step involves *O(J . K. D)* operations of (2), each of which has *O(R . M. D)* operations of (1). The second computation step as provided in (3) involves *O(C . K)* operations. It is important to note that the second computation step is not multiplied by the *D* factor since each FPA instance will involve *O(C/D . K)* operations; thus the computation cost for all the *D* FPA instances is *O(C . K)* operations.

10.1.4 SPA-Dedicated control plane model

As provided earlier, SPA-Dedicated control plane model supports state-dependent routing. Hence, the SPA-Dedicated control plane model has the same computation cost as the base control plane model for each control plane instance. As provided earlier, the SPA-Dedicated control plane model supports the Complete Partitioning (CP) concept and hence there is a FPA instance for each network partition (*D)*. Each FPA instance will have the three computations steps as provided in the base model.

From a computation cost perspective, the first two computation steps are exactly like the ITU control plane model. The third computation step to compute a single q_{rk}^{mD} as provided in (5) involves *O(R. . M . D)* operations. The cost of evaluating $A_n(r_m)$ for a route r_m involves *O(H . D)* operations (multiplications) [10]. As provided in (5), each route on the route list is evaluated for every value $n \in D$, which gives *O(M .C/D)* such operations. This results in a total computation cost of *O(M . C . H)* operations[11] for each pair *r* and *O(R . M . C . H)* operations for all source-destination pairs.

10.1.5 SPA-Shared control plane model

The SPA-Shared control plane model has the same computation cost like the SPA-Dedicated for the three computation steps. One important aspect to consider is that the parameter *D* used to define the number of network resources partitions need to include the total number of network resources partitions including dedicated and shared partitions.

10.2 Implementation cost

This section provides details on the expected control plane messages' overhead of the traffic management schemes for the three control plane models. In our analysis of the control plane messages' overhead we will use the IETF control plane model as a reference model. The analysis of the messages' overhead is based on analyzing the impact of the following control

[10] The *D* factor was included to count for the number of network partitions *D*.

[11] It is important to note that the third computation step is not multiplied by the D factor since each FPA instance will involve O(M .C/D) operations for each pair *r*; thus the computation cost for all the *D* FPA instances is O(M . C . H) operations for each pair *r*.

plane traffic management capabilities on control plane routing and signaling messages' overhead:

1. Routing update triggers: static routing vs. state-dependent routing
2. Network routing granularity: coarse vs. fine routing granularity
3. Load handling capability: Complete Sharing (CS) in IETF, Complete Partitioning (CP) in ITU and SPA-Dedicated, and Virtual Partitioning (VP) in SPA-Shared. In SPA-Shared, the load can be divided statically "Static Sharing (SS)" vs. dynamically "Network Engineering (NE)" via LPF.
4. Demand inverse multiplexing via (IMF): enabled vs. disabled inverse multiplexing

10.2.1 IETF control plane model

The following is an analysis of the IETF traffic management configurations impact on routing messages overhead:

- The static routing configuration will eliminate the need to adjust the routing probabilities of the routes stored in the Routing Database (RDB). This elimination of routing probability modification will reduce the CPU time required to update the RDB with the routing topology status of the network, the only CPU time required to update the RDB is for updating the RDB with the coarse routing granularity of the network topology rather than an additional CPU time to adjust the routing probabilities of the stored routes based on the occupancy state of the network.
- From a control plane perspective, each transport network granularity level is represented by a collection of Routing Controllers (RCs) that collect the routing topology at that transport network granularity level and store it in the corresponding RDB of that transport network granularity level. Thus, each transport network granularity level supported by the control plane will generate its own volume of routing messages to capture the routing topology state at that transport network granularity level. For example, the coarse routing granularity at the STS-3 transport network granularity level will reduce the volume of routing messages by third compared to the fine routing granularity, at the STS-1 transport network granularity level, carried by both the ITU and SPA control plane models. This reduction of

routing messages volume will lead to reduction in bandwidth requirements on either an in-band or out of-band channel to carry the routing messages between the RCs and the RDB, and a reduction of RDB memory needs. The RDB memory needed in the IETF control plane model will be one third of the memory needs requirements in both the ITU and SPA control plane models.

- Due to the IETF Complete Sharing (CS) of load arriving from *N* configured VPN services, the routing messages updates via a single control plane instance will be used to provide routing topology updates to the *N* configured VPN services. Both the LFP and IMF are disabled in the IETF control plane model; thus no affect on routing message volume and signaling messages volume is expected.

10.2.2 ITU control plane model

The following is an analysis of the ITU traffic management configurations impact on routing messages overhead:

- Static routing configuration will have the same impact on CPU time as provided in section 10.2.1 on the IETF control plane messages analysis.
- Since each transport network granularity level supported by the control plane will require its own volume of routing messages to capture the routing topology state at that transport network granularity level. For example, the fine routing granularity at the STS-1 transport network granularity level will multiply the volume of routing messages updates by 3 compared to STS-3 coarse routing granularity. This increase of routing messages volume will lead to increase in bandwidth requirements on either an in-band or out of-band channel to carry the routing messages between the RCs and the RDB, and an increase of RDB memory needs. The RDB memory needs in the ITU control plane model will be three times the memory needs requirements in the IETF control plane model.
- Due to ITU Complete Partitioning (CP) of load arriving from *N* configured VPN services, the routing messages volume via the *N* control plane instances will be *N* times the routing messages volume of the IETF single control plane instance. This increase of routing messages volume will lead to the same impact on in-band or out-of band channel bandwidth requirements and RDB memory requirements similar to

the fine routing granularity impact. Both the LFP and IMF are disabled in the ITU control plane model; thus no affect on routing message volume is expected.

10.2.3 SPA-Dedicated control plane model

The following is an analysis of the SPA-Dedicated traffic management configurations impact on routing messages overhead:

- State-dependent routing configuration will require the need to adjust the routing probabilities of the routes stored in the RDB, the routing probability modification will increase the CPU time required to update the RDB with the routing topology status of the network. In addition to the CPU time required to update the RDB with the routing topology fine granularity level, additional CPU time is required to update the routing probabilities of the routes stored in the RDB based on the occupancy state of the network.

- The fine routing granularity, e.g., STS-1 transport network granularity level, will have the same affect on routing messages volume and the same implications on in-band/out-of band bandwidth requirements and RDB memory as provided in the ITU control plane model.

- The Complete Partitioning (CP) of load arriving from *N* configured VPN services will have the same affect on routing messages volume and the same implications on in-band/out-of band bandwidth requirements and RDB memory as provided in the ITU control plane model. Both the LFP and IMF are disabled in the SPA-Dedicated control plane model; thus no affect on routing message volume is expected.

10.2.4 SPA-Shared control plane model

The following is an analysis of the SPA-Shared traffic management configurations impact on routing messages overhead:

- State-dependent routing configuration will have the same impact CPU time as provided in the SPA-Dedicated control plane model.

- The fine routing granularity, e.g., STS-1 transport network granularity level, will have the same affect on routing messages volume and the same implications on in-band/out-of band bandwidth requirements and RDB memory as provided in the ITU/SPA-Dedicated control plane model.

- The Virtual Partitioning (VP) of load arriving from *N* configured VPN services will have an increase in routing messages volume and an increase in in-band/out-of band bandwidth requirements and RDB memory over IETF/ITU/SPA-Dedicated control plane models. The reason for the routing messages volume increase is due to the addition of the shared resources partition which will have its own volume of routing messages beyond the routing messages volume on the dedicated resources partitions.

The following is an analysis of the SPA-Shared traffic management configuration on signaling messages overhead:

- The Virtual Partitioning (VP) of load arriving from *N* configured VPN services will introduce additional signaling messages between the control plane instances controlling the dedicated and shared resources partitions. The additional signaling messages will be used to partition the load across the dedicated and shared resources partitions. It is important to mention that when LPF is configured as NE, the volume of signaling messages between the dedicated and shared resources partitions will increase over LPF when configured as (SS), this is due to the dynamic load partitioning across the dedicated and shared resources partitions based on the blocking probability state at the dedicated resources partitions.
- When inverse multiplexing is enabled to divide the service demand with actual bandwidth requirements b_k^A into N flows each with granular bandwidth requirements b_k^G , the signaling messages volume will increase by *N* compared to when inverse multiplexing is disabled.

Table 10-1 summarizes the traffic management schemes impact on control plane messages. The numbers in Table 10-1 assume a transport network coarse granularity level of 3 STS-1, transport network fine granularity level of 1 STS-1, IMF that splits the actual service request demand of 2 STS-1 into two granular service demands each with 1 STS-1 demand, and *N=3* network resources partitions.

	Control Plane Messages Impact on Single Control Plane Instance (CPI)				**Number of Network Partitions (N=3)**
Traffic Management Scheme Capability	Impact on Additional CPU Time to Update Routing Probability	Impact on Routing Messages Volume	Impact on Signaling Messages Volume		Impact on Signaling and Routing Messages Volume
	Routing Update Triggers	Routing Granularity Level	Load Partitioning	Inverse Multiplexing	
IETF	No impact	1/3 of ITU and SPA	NA	NA	NA
ITU	No impact	3 times of IETF	NA	NA	N times single CPI messages
SPA-Dedicated	Increased	3 times of IETF	NA	NA	N times single CPI messages
SPA-Shared	Increased	3 times of IETF	Increased between control plane instances	2 times when IMF enabled compared to IMF disabled	N times single CPI messages

Table 10-1: Traffic Management Schemes Impact on Control Plane Messages

11 Discussion of Model Validation and Accuracy

Section 11.1 is focused on the mathematical models validation, section 11.2 is focused on the mathematical models computation accuracy and sanity checks carried, and section 11.3 is focused on the performance results trends.

11.1 Discussion of model validation

11.1.1 Fixed point uniqueness

While it can be shown the existence of a fixed point under the proposed fixed point approximation by applying Brouwer's fixed point theorem [59], the uniqueness of this fixed point need to be further analyzed. The possibility of bi-stability or multiple fixed points has been analyzed in previous literature and was mainly focused on the impact of alternate routing and connection admission control via trunk reservation factors on bi-stability or multiple fixed points scenario, we will address the uniqueness of the fixed point approximation for the IETF, ITU, and SPA control plane models using the same two factors [59-72].

11.1.1.1 Alternate routing impact

Two alternate routing schemes were used for the three control plane models. In both the IETF and ITU control plane model, fixed alternate routing was used where the routing probability of routing traffic on a certain route for any source-destination pair is assigned statically without consideration for the occupancy state of the links on that route, two options were used in assigning the routing probability under fixed alternate routing; Direct Routing (DR) and Split Routing (SR). In DR, the traffic between any source-destination pair is routed on the direct route only with the least number of hops. In SR, the traffic between any source-destination pair is split evenly across the possible routes between the source-destination pair.

In the SPA control plane model, state-dependent routing was used where the routing probability of routing traffic on a certain route for any source-destination pair is assigned dynamically based on the occupancy state of the links on that route. The state-dependent routing used is based on the least loaded routing (LLR) scheme. In LLR scheme, a service request is first tried on the direct route, if there is one. If it cannot be setup along the direct route, then the non-direct route is chosen. LLR chooses the route that has the maximum units of end-to-end free bandwidth (also called the residual bandwidth) among all routes. In the state-dependent routing, each source-destination node pair is allowed a list of feasible routes, ordered in increasing length, i.e., number of hops. A service request is then routed on the one that has the largest amount of end-to-end residual bandwidth. In the state-dependent routing, we will not require that the direct link always be selected with priority over all other routes, but rather that it is selected if it has the maximum residual bandwidth.

Regarding the uniqueness of fixed point approximation under fixed routing, Kelly in [59] and others in [60, 61, 64, 66, 67, 71] proved that blocking probability estimates of a network have a unique solution under any of the following two modeling framework conditions:

1. When the link capacities and load are increased together, keeping the routing probabilities fixed.
2. When the number of links and routes are increased while the link load is kept constant.

In both the IETF and ITU fixed routing, the second modeling framework condition was considered. Under the 4-node and 7-node topologies with both two and three alternate routing, the number of links and routes were increased while the link load is kept the same. In other words, the same range of load was applied to the two network topologies which resulted in similar performance of the IETF and ITU direct and split routing when compared to the SPA control plane model.

Regarding the uniqueness of fixed point approximation under state-dependent routing which is based on dynamic alternate routing scheme, it has been pointed out in [59] that under dynamic alternative routing there may be more than one fixed point. This may be associated with multiple stable states for the network. For example, in networks with random alternative routing the system can oscillate between a low blocking state where calls are accepted readily over the direct route with minimum number of hops, and a high blocking state where calls are accepted over the alternate route with larger number of hops than the direct route. This is due to the fact that calls admitted to the alternate route use more network resources and may force more calls to be routed through their alternate route instead of their direct route. Thus, the network may enter a bi-stable region where there are two equilibrium points, one stable and one unstable.

As described in [68], there is a correlation between the existence of multiple fixed points or bi-stability case and the possibility of oscillations at the final values of the FPA. As described in section 8.4, the FPA with state-dependent routing for the SPA control plane model is based on the base model as provided in [68]. In [68], no oscillations were observed on the FPA final values for the two topologies analyzed as illustrated in Figure 11-1. In our analysis, no oscillations were observed in the 4-node and 7-node topologies analyzed using state-dependent routing; which eliminates the possibility of a bi-stability or multiple fixed point case for the SPA control plane model. For each FPA, it was observed that there was no oscillations scenario in the final values where there were multiple fixed points for a low probability state and a high probability state. Instead, it was observed that each FPA with state-dependent routing had a single fixed point that converged with a higher routing probability for the direct route over the possible alternate routes due to the way the direct route and possible alternate routes were selected.

As indicated earlier for the SPA state-dependent routing, each source-destination node pair is allowed a list of feasible routes, ordered in increasing length, i.e., number of hops. Recall the mathematical equation used to compute the routing probability as follows:

$$q_{rk}^{mD} = \sum_{n=0}^{C_{\min}(r_m)} \prod_{k=1}^{k=m-1} \Pr[\overline{A}_n^D(r_k - r_m)]. \prod_{k=m+1}^{k=M_r} \Pr[\overline{A}_{n+1}^D(r_k - r_m)].\Pr[\widetilde{A}_n^D(r_m)] \ldots\ldots\ldots\ldots\ldots.. (1)$$

Also, recall the occupancy events as follows:

$$\Pr[\overline{A}_n^D(r_k - r_m)] = 1 - \prod_{j \in (r_{k-} r_m)} \sum_{k=0}^{C_j^D - n} P_j^D(k) \ldots\ldots\ldots\ldots\ldots.. (2)$$

$$\Pr[\overline{A}_{n+1}^D(r_k - r_m)] = 1 - \prod_{j \in (r_{k-} r_m)} \sum_{k=0}^{C_j^D - n+1} P_j^D(k) \ldots\ldots\ldots\ldots\ldots.. (3)$$

It is observed from equations (2, 3) that the larger the number of hops (*j)* for a route *(r)*, the smaller the probabilities of events $\overline{A}_n^D(r_k - r_m)$ and $\overline{A}_{n+1}^D(r_k - r_m)$ and thus the smaller the routing probability q_{rk}^{mD} . The routing probability q_{rk}^{mD} for the direct route will be much greater than the routing probability for route-2 and route-3 due to the smaller number of links (*j)*. In the 4-node topology, for each source-destination pair, there was a direct route of one hop and an alternate route of two hops. As indicated in Table 10-1 for the 7-node topology, route-1 which is the direct route between any source-destination pair has an average number of hops over all the source-destination pairs of 1.76 hops while route-2 and route-3 has an average number of hops over all the source-destination pairs of 2.8 and 4 hops respectively.

Also, it was argued in [63] that if the ratio between hop numbers of any two alternative routes is sufficiently large (e.g., greater than 0.5), then the network resources used by routing a service request on different alternative routes do not significantly vary, and thus the blocking probability will increase more smoothly with the increase in traffic without going into a bi-stable region. In all our numerical experiments, our fixed point algorithms did not have a bi-stability case due to the fact that the ratio between hop numbers of any two alternative routes is sufficiently large. In the 4-node topology, for each source-destination pair, there was a direct route of one hop and an alternate hop of two hops; thus the ratio between hop numbers for the direct and alternate routes is 0.5. In the 7-node topology with 2-alternate routing case, the ratio between hop numbers of any two alternate routes is 0.88 average and 0.5 minimum. In the 7-node topology with 3-alternate routing case, the ratio between hop numbers of any two alternate routes is 0.7 average and 0.4 minimum.

Gibbens and Kelly in [70] analyzed a symmetric fully connected network with *N* nodes and every pair of nodes is connected by a link of capacity *C*, giving a total of *K=N(N-1)/2* links with *r* alternate routes. Gibbens and Kelly analyzed a network with parameters *N=11, C=120, and r=5* as the load *v* varies. It was observed that the high blocking state for alternate routes is a lot less stable than the low blocking state for smaller values of *v* but becomes more stable as *v* increases until finally there is one stable point. In addition, Gibbens and Kelly analytically proved that the low blocking state using the direct route become more stable very rapidly as the link capacity and number of links increase. **x =** (x_o, x_1,…..,x_c) is a range of possible fixed points of the network. Diffusion approximation was used to calculate the time taken for the process to move from one fixed point to another fixed point, *$T(x_1;x_2)$* is the first time that the diffusion hits x_2 given that it starts at x_2, and $f(x_1;x_2)=E[T(x_1;x_2)]$. So if $x_1<x_2$ are two possible fixed points, then stability from $f(x_1;x_2)$ can be assessed. Gibbens and Kelly found that for some A_1 and A_2 constants that:

$$\frac{e^{A_1CK}}{CK} \leq f(x_1;x_2) \leq \frac{e^{A_2CK}}{CK}$$

The above equation shows that the high blocking probability state using any of the alternate routes becomes stable rapidly with increased number of links but more unstable as the link capacity increases. The number of links of the topologies analyzed increased when the analysis covered a 7-node topology with 9 links in addition to the 4-node topology with 4 links. In addition, the links' capacities increased when SPA-shared control plane model was used as the VPN resource partition increased in number of trunks from 13 to 16 trunks when the sharing ratio between dedicated and shared resources was increased from 1 to 4 trunks respectively.

Despite that the topologies analyzed in our problem are smaller than the topology analyzed in [70], it is important to note that all the network topologies analyzed in previous literature to study the bi-stability scenario were focused on a symmetric fully connected network where the existence of a bi-stability scenario has a higher probability than the 7-node topology analyzed. The reason for that is since each alternate route for a source-destination pair in the fully connected network has 2 hops where the direct route has one hop, this would lead that any possible two fixed points will be close in value and won't be with a low probability state for the direct route and a high probability state for the alternate route. That is why trunk reservation on the alternate route is used to increase the blocking probability on the alternate route and hence increase the blocking probability distinction between the direct and alternate route, such distinction would lead to a faster convergence of the two fixed points to a single fixed point. In the 7-node topology, there was a clear difference in the number of routes between the direct and alternate routes which lead to a clear distinction in the blocking probabilities between possible routes and hence between any possible fixed points.

As indicated in Table 10-1 for the 7-node topology, route-1 which is the direct route between any source-destination pair has an average number of hops over all the source-destination pairs of 1.76 hops while route-2 and route-3 has an average number of hops over all the source-destination pairs of 2.8 and 4 hops respectively. This distinction in the number of hops between different routes for each source-destination pair would lead to a faster convergence of any possible fixed points to a single fixed point.

11.1.1.2 Connection admission control via trunk reservation

This section describes the impact of CAC with trunk reservation for alternate routes to avoid bi-stability or multiple fixed points' scenario. The CAC mechanism used in the three control plane models did not use trunk reservation; thus this section is provided for completeness of analyzing the fixed point uniqueness rather than validating the existence of single fixed point for the three control plane models, the validation of the fixed point uniqueness for the three control plane models is provided in section 11.1.1.1

The dynamic alternate routing used in the state-dependent routing is based on the maximum residual bandwidth routing scheme, this scheme tries to avoid bottlenecks on a route. However, since a route is chosen only based on the amount of free bandwidth, we may be forced to take a longer or even the longest route in the feasible route set, using more network resources. This may in turn force service requests arriving later to also be routed on their longer/longest routes, which leads to increased loss/blocking probability in a network. Therefore, using some form of admission control along with this routing scheme is a valid choice when traffic is heavy. If the trunk reservation is used on the alternate route, the direct route of every source-destination pair is given a higher priority, and all routes other than the direct route will require an extra bandwidth "number of trunks" to be reserved on their links when admitting a call. This trunk reservation scheme with CAC would increase the possibility of unique fixed point that converges at the low probability state using the direct route path.

11.1.2 Accuracy of mathematical models assumptions

As mentioned in section 8, the mathematical models of the IETF, ITU, and SPA control plane models were extensions carried on the mathematical models in [68] as a base method. In analyzing the accuracy of the mathematical models developed for the three control plane models, we will first discuss the assumptions made and the mathematical models accuracy analysis carried in [68], then we will discuss how the modeling parameters and network topologies analyzed in our problem followed the same guidance carried in the base method regarding the assumptions and network topologies analyzed. The mathematical models in [68] were based on three main assumptions:

1. *Link independence assumption.* Under this assumption, blocking is regarded as to occur independently from link to link. This assumption allows in computing the blocking probability at each link separately.

2. *Poisson assumption.* Under this assumption, service arrivals arrive at a link as Poisson process and the corresponding arriving load is the original external offered load thinned by blocking on the other links, thus known as the *reduced load.*

3. *Stationary input assumption.* Under this assumption, certain time varying quantities of interest have well-defined averages. These include the number of on-going service requests on a link of each class, the average service request holding time, and he reduced load on the link.

The accuracy of the mathematical models assumptions provided in [68] were validated by comparing the analytical results of the FPA with the results of the Discrete Event Simulation (DES) for the two topologies illustrated in Figure 10-1. One observation provided in [68] based on the FPA and DES comparison is that the above assumptions were more accurate when the network is better connected, routes are diverse and as the input load becomes heavier. In addition to that, the accuracy heavily relies on the structure of the network topology. Recall the mathematical equation used to compute the routing probability as follows:

$$q_{rk}^{mD} = \sum_{n=0}^{C_{\min}(r_m)} \prod_{k=1}^{k=m-1} \Pr[\overline{A}_n^D(r_k - r_m)].\prod_{k=m+1}^{k=M_r} \Pr[\overline{A}_{n+1}^D(r_k - r_m)].\Pr[\tilde{A}_n^D(r_m)]$$

The approximation of the routing probability would be accurate in a network when routes between each source-destination node pair share one or more common links but are disjoint elsewhere; thus $\overline{A}_n^D(r_k - r_m) \approx \overline{A}_n^D(r_k)$ and $\overline{A}_{n+1}^D(r_k - r_m) \approx \overline{A}_{n+1}^D(r_k - r_m)$. This assumption on link-disjoint between routes for a source-destination pair node would only be valid for a network topology with minimal overlapping between routes. The routing computation in the

FPA used largely ignores the dependence between routes. Therefore, if we consider the case where a network has mostly disjoint routes/paths and a second case where a network has many routes sharing links, the algorithm will in general produce better approximation in the first case. If routes are not all disjoint but the majority of routes between a given node pair share the same set of links and are otherwise disjoint, then the approximation error may also be reduced.

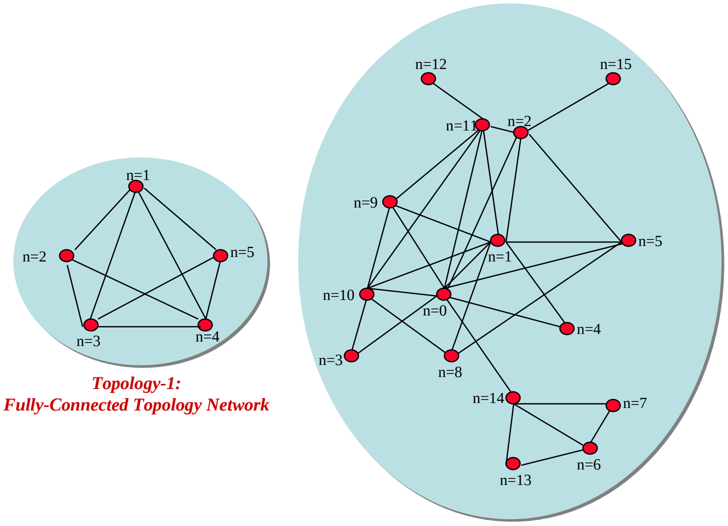

Topology-1:
Fully-Connected Topology Network

Topology-2:
Random Topology Network

Figure 11-1: Network Topologies Analyzed in Base Method

The following observations were made for the fully-connected topology considered in [68] illustrated in Figure 11-1:

1. When the input load is very light and the blocking probability is (far) below 1%, the FPA did not generate accurate results when compared to the DES, overestimates of relative errors were around +300%.

2. The accuracy of the FPA improves as the input load increases, and as the blocking probability increases. Under heavier input load, the average percentage error, over all the source-destination pairs, between the FPA and the DES for service request with bandwidth requirement b_k^A = 3 STS-1 is 1.01%, and for service request with bandwidth requirement b_k^A = 2 STS-1 is 2.83%.

3. This accuracy of the FPA compared to DES was expected since in the fully-connected network there is no route overlapping. The improvement in accuracy while increasing input load is due to the fact that as input load becomes heavier, assumptions 1 and 2 become more accurate.

For the random topology, selected node pairs and classes were used to compare the FPA and DES. The following observations were pointed in [68] for the random topology illustrated in Figure 11-1:

1. The accuracy of the FPA improves as the input load increases, and as the blocking probability increases. Under heavier input load, the absolute percentage error, over selected source-destination pairs, between the FPA and the DES for service request with bandwidth requirement b_k^A = 3 STS-1 is 1.32%, and for service request with bandwidth requirement b_k^A = 2 STS-1 is 2.51%.

2. The accuracy of the FPA despite obvious route overlapping, this is since the random topology consists of three distinct groups of nodes. As illustrated in Figure 11-1, the first group of links consists of nodes 0-5 and 8-9, note that this group of nodes are very well connected among themselves. The second group consists of nodes 12 and 15, which are attached to the first group via a single link. Thus, all traffic between either of the two nodes and the rest of the network will share a single link. Similarly the third group, which consists of nodes 6-7 and 13-14, it is also attached to the first group via a single link. As a result, most of the node pairs have routes that either do not overlap significantly and/or share common links that are likely to be the common bottleneck links. These properties have made the assumptions underlying the FPA more accurate.

The modeling parameters and network topologies analyzed in our problem followed the same guidance carried in the base method [68] regarding the assumptions and network topologies analyzed as follows:

1. Higher input loads were considered to make the first and second assumption provided above more accurate. The higher input loads resulted in blocking probabilities ranging from 5-25% for the 4-node topology and 5-40% for the 7-node topology. In [68], it was validated that under higher input loads resulting blocking probabilities, FPA algorithm average percentage error compared to DES is below 5%.

2. Minimal route overlapping was considered for the 4-node and 7-node topologies analyzed; this increased the routing probability approximation accuracy as discussed above. In the 4-node topology, the 2 possible alternate routes between any source-destination pair with no overlapping links between the two routes. In the 7-node topology, the links selected for the 2-alternate routing and 3-alternate routing between each source-destination pair are listed in Table 11-1. It can be observed from Table 11-1 that in the 2-alternate routing case, route-1 and route-2 have completely distinct links, whereas in the 3-alternate routing case, the three routes (1, 2, 3) have minimal link overlapping between them. This will increase the accuracy of the routing probability approximation as validated in the two topologies analyzed in [68].

Since the systems analyzed here using FPA have the properties that have previously been shown to produce a unique solution with adequate accuracy a direct comparison between the FPA and DES is not required here. Further since we are primarily concerned with ratio of performance between the different control plane architectures, and not the absolute values of the performance metrics, we do not expect the issues of uniqueness and accuracy to have an impact on the conclusions of the analysis.

Source-Destination Nodes	Route-1	Route-2	Route-3
{A,B}	8	9,10,11	10,11,12,16
{A,C}	8,9	10,11	8,12,16
{A,D}	11	8,9,10	8,10,12,16
{A,E}	8,12	10,11,16	10,11,13,14,15
{A,F}	8,12,13	10,11,14,15	10,11,13,16
{A,G}	10,11,15	8,12,13,14	8,9,13,14,16
{B,C}	9	8,10,11	12,13,14,15
{B,D}	9,10	8,11	10,12,16
{B,E}	12	9,16	8,10,11,16
{B,F}	12,13	9,14,15	9,13,16
{B,G}	9,15	12,13,14	8,10,11,15
{C,D}	10	8,9,11	11,12,16
{C,E}	16	9,12	13,14,15
{C,F}	13,16	14,15	9,12,13
{C,G}	15	14,16	9,12,13,14
{D,E}	10,16	8,11,12	10,13,14,15
{D,F}	8,11,12,13	10,14,15	10,13,16
{D,G}	10,15	1,8,12,13,14	8,11,12,15,16
{E,F}	13	14,15,16	9,12,14,15
{E,G}	13,14	15,16	9,12,15
{F,G}	14	13,15,16	9,12,15

Table 11-1: Routes of the 7-Node Topology

11.2 Discussion of model accuracy

11.2.1 Occupancy probabilities computation

As provided in section 8.3 focused on Calculating the link's occupancy and admissibility probabilities, the summation of occupancy probabilities of link *j* for all the states $n \in [0, C_j]$ has to equal 1 as provided in the following mathematical constraint: $\sum_{n=0}^{C_j} p_j(n) = 1$. As mentioned in section 9, Mathematica^{TM} tool was used to compute the occupancy probability $p_j(n)$ for each link *j* in the network topology, the Mathematica^{TM} code that was written for each control plane model took into consideration the occupancy probability mathematical constraint.

As provided in section 9.1, the ITU and SPA-Dedicated control plane models partition the 24 STS-1 physical resources into two dedicated network resources partitions with 12 STS-1 per dedicated network resources partition, whereas the SPA-Shared control plane model partitions the 24 STS-1 physical resources into three network resources partitions according to the sharing ratio between dedicated and shared network resources partitions. The following is the Mathematica^{TM} code written for the dedicated network resources partition with 1 STS-1 sharing for SPA-Shared:

Dedicated Network Resources Partition Occupancy Probabilities Equations:

```
eqns = {
p1 ==a*p0,
p2 == a/2p1+b/2p0,
p3 == a/3p2+b/3p1,
p4 == a/4p3+b/4p2,
p5 == a/5p4+b/5p3,
p6 == a/6p5+b/6p4,
p7 == a/7p6+b/7p5,
p8 == a/8p7+b/8p6,
p9 == a/9p8+b/9p7,
p10 == a/10p9+b/10p8,
p11 == a/11p10+b/11p9,
p0 == 1 - p1 - p2 - p3 - p4 - p5 - p6-p7-p8-p9-p10-p11}
```

As the list of equations indicate, for 1 STS-1 sharing between the dedicated and shared network resources partitions, the dedicated network resources partition will have 11 STS-1 resources ($C_j^D = 11$) and 12 states (n=12). The terms a and b indicate the two classes arrivals with 1 STS-1 and 2 STS-1 bandwidth requirements respectively, and p ranging from 0 to 11 indicating the occupancy probabilities for the 12 states (n=12). The last equation indicating the occupancy probability when none of the link j resources is occupied, *(p0)* is written to fulfil the occupancy probability constraint discussed above. It is observed from the last equation that the summation of occupancy probabilities of link j for all the states $n \in [0, C_j^D]$ is equal to 1 as provided in the constraint: $\sum_{n=0}^{C_j^D} p_j(n) = 1$. When the output of the of the occupancy probabilities equations was used in the FPA algorithm, validating that the summation of occupancy probabilities of link j for all the states $n \in [0, C_j^D]$ is equal to 1 was carried after each FPA convergence, the percentage of error was 0%.

Note that we do not independently calculate p0-p11 and then check to see if they add to 1; instead, we force that by calculating p1…p11 and then find p0 = 1-sum(p1..p11); which will always converge to 1. So this sanity check does not check the accuracy of the occupancy probability equations solution provided by Mathematic^{TM}, rather it provides a check that the occupancy probability computation phase of the FPA mechanism provided accurate estimates that help in FPA convergence. If the occupancy probability computation phase provides in-accurate estimates, the FPA will oscillate and will not converge. In [68] that was used as a base model for problem, it was pointed out that the FPA fast convergence depends heavily on the accurate computation of the required values. In [68], the FPA algorithm managed to converge via heavy dampening techniques where during the iteration newly computed values are heavily weighted by their old values to prevent drastic changes from happening and hence allowing for the possibility of oscillations at the final values of the FPA. As discussed in section 11.1.1.1, no oscillations scenario was observed at the final values of the FPA which indicated the accurate computation of the occupancy probabilities.

11.2.2 Routing probabilities computation

The accuracy of the routing probability computation was validated by two methods. The first method is based on the accuracy of the occupancy probability, as provided in section 8.4 focused on Calculating the routing probability q_{rk}^{mD}, the routing probability computation is based on the computed occupancy probability as provided in equations (34-41). If we consider equations (37, 39, 40, 41), the state probabilities $\Pr[\overline{A}_n^D(r_k - r_m)]$, $\Pr[\overline{A}_n^D(r_k - r_m)]$, , and $\Pr[\widetilde{A}_n^D(r_m)]$ are all based on the occupancy probability $P_j^D(k)$, since the accuracy of the occupancy computation was validated as provided in section 11.2.1, the first method of validating the accuracy of the routing probability computation was carried. The second method of validation is based on the routing probability constraint that the summation of the routing probability q_{rk}^{mD} for all the routes between a source-destination pair r has to equal 1 as given in: $\sum_{r_m \in M_r} q_{rk}^{mD} = 1$. After each FPA convergence, the routing probability constraint was validated. Percentage error was in the range below 3%, for the 7-node topology and 0% for the 4-node topology.

The reason for a percentage error higher than zero for the 7-node topology is due to the limitations of the routing probabilities computation base algorithm for larger network topology. The mathematical formulation used in [68] to compute the state-dependent routing probability q_{rk}^{m} for each route r_m lacks the accuracy needed when computing routing probability for a network topology with higher level of meshing among routes. Recall the mathematical equation used to compute the routing probability as follows:

$$q_{rk}^{mD} = \sum_{n=0}^{C_{\min}(r_m)} \prod_{k=1}^{k=m-1} \Pr[\overline{A}_n^D(r_k - r_m)] . \prod_{k=m+1}^{k=M_r} \Pr[\overline{A}_{n+1}^D(r_k - r_m)] . \Pr[\widetilde{A}_n^D(r_m)]$$

The approximation of the routing probability would be accurate in a network when routes between each source-destination node pair share one or more common links but are disjoint elsewhere; thus $\overline{A}_n^D(r_k - r_m) \approx \overline{A}_n^D(r_k)$ and $\overline{A}_{n+1}^D(r_k - r_m) \approx \overline{A}_{n+1}^D(r_k - r_m)$. This assumption on link-disjoint between routes for a source-destination pair node would only be valid for a network topology with minimal or no overlapping between routes as in the 4-node topology case.

11.2.3 LPF and IMF traffic management operations

When the performance of the SPA-shared control plane model was evaluated, a sanity check was implemented to check the accuracy of the LPF and IMF traffic management operations. The sanity check of the LPF operation made sure that the summation of the load applied to the dedicated network resources partitions and the shared network resources partition is equal to the total input load, this was verified in both the load partitioning without NE and with NE. In the case of load partitioning without NE, LPF is configured to partition the configured VPN service v total arrival load λ_{rk}^{v} between the dedicated resources C_j^{vD} and the shared resources C_j^{S} based on the resources ratios between dedicated and shared resources partitions as given in equations (9,10), it can be concluded that the summation of λ_{rk}^{vD} and λ_{rk}^{vS} will equals λ_{rk}^{v}. In the case of load partitioning with NE, FPA is carried in two rounds on the dedicated resources partitions and one round on the shared resources partition to make sure that the summation of λ_{rk}^{vD} and λ_{rk}^{vS} will equal λ_{rk}^{v}. In round-1, the configured VPN service-*v* total arrival load λ_{rk}^{v} is applied to the dedicate resource partition C_{j}^{vD} as given in equation (14). When round-1 of the FPA on dedicated resources partitions is complete, the pair blocking probability B_{rk}^{vD} is used to generate the configured VPN service-*v* shared load ${}^{NE}\lambda_{rk}^{vS}$ as provided in equation (15). In round-2, the non-blocked load from round-1 is applied again to each dedicate resource partition C_{j}^{vD} as given in equation (17). The sanity check of the IMF operation made sure that the input load before an inverse multiplexing operation is equal to the input load after the inverse multiplexing operation. As provided in equations (32, 33), it should be observed that an additional term *(i)* is multiplied by the Erlang load $b_{k}^{G}\dfrac{\lambda_{jk}^{vD}}{\mu_{k}}$ to maintain the same Erlang input load before and after inverse multiplexing operation where $b_{k}^{A} = ib_{k}^{G}$.

11.3 Discussion of trends in system performance

11.3.1 Analysis of operational space for network topologies and services

It is important to mention the following before any generalization of the performance results is carried to predict a possible performance trend of each control plane model:

1. Limited topologies size: the 4-node and 7-node topologies analyzed were limited in both number of nodes and nodes' connectivity (not fully meshed). The main objective of this research is to prove the SPA control plane model superiority compared to both the IETF and ITU control plane models rather than analyzing the impact of the network topology size on the performance and control plane messages scalability of the three control plane models.
2. Network topologies specific routing attributes: the network topologies analyzed and the routing options for each network topology were carefully selected to enforce minimal or no link overlapping between possible routes for each source-destination pair, the 4-node

topology had no link overlapping between routes for each source-destination pair whereas the 7-node topology had minimal link overlapping between routes for each source-destination pair. The minimal link overlapping constraint between routes was enforced to increase the computation accuracy of the routing probability using the FPA mechanism as provided in section 11.1.2.

3. Limited classes considered: two classes were considered; class-A with actual bandwidth requirement b_k^A =1-STS-1 and class-B with actual bandwidth requirement b_k^A =2-STS-1. One of the objectives of this research is to study the impact of the SPA IMF inverse multiplexing capability on the performance of SPA control plane model when compared to the IETF and ITU control plane models. To analyze the IMF impact, we need to run the model using a service class with actual bandwidth requirement of 2-STS-1 or higher, this will allow the IMF to split "inverse-multiplex" the service's single flow with actual bandwidth requirements b_k^A into multiple flows each with granular bandwidth requirement b_k^G . Thus, running the model with class-B service arrivals will be sufficient to analyze the IMF impact.
4. Call-Oriented model: the model used is a call-oriented model. In call-oriented model, network resources are assigned to a service request from the source to the destination nodes before the start of the transfer, thus creating a "circuit". The resources remain dedicated to the circuit during the entire transfer and the entire message follows the same path. In the packet-oriented model, the message is broken into packet, each of which can take a different route to the destination where the packets are recompiled into the original message.
5. Flexible Service Level Agreement (SLA) for the analyzed FSG service configuration model: the performance analysis was carried on a single service configuration with specific service profile parameters as indicated in section 3.2.6. The FSG configured VPN service model allows the input load to be partitioned across dedicated and shared resources partitions in addition to allowing a granular portion b_k^G of its actual service demand b_k^A to be accepted if no available resource are available to accept the actual service demand.

The FSG with its service profile parameters is considered a service with flexible SLA that does not dictates its input load and demand from being partitioned and thus accepting the possibility of receiving a lower SLA than its optimum SLA. Other defined service models in section 3.2 do not have the same flexible SLA like the FSG configured service model. The FSG flexibility in partitioning its load between the dedicated and shared resources partitions will give the SPA control plane model an advantage over the IETF and ITU control plane models due to the Load Partitioning Function (LPF) of the SPA control plane model affect on improving the SPA control plane performance. In addition, the FSG flexibility in partitioning its actual demand into granular demands will give the SPA control plane model an advantage over the IETF and ITU control plane models due to the Inverse Multiplexing Function (IMF) of the SPA control plane model affect on improving the FPA control plane performance.

Thus, under the specific operational space for the network topologies and flexible service SLA specific above, a performance trend of the IETF, ITU, and SPA control plane model can be provided.

11.3.2 7-node topology case study

The 7-node topology with its 2-alternate and 3-alternate routing cases were used to draw a conclusion on the performance comparison of the nine traffic management schemes of the IETF, ITU, and SPA control plane models.

In analyzing the results trend, the IETF-DR traffic management scheme was considered as a reference model; thus the IETF-DR traffic management scheme was given a rank of zero and the rest of the eight traffic management schemes were ranked accordingly in ascending order based on the performance metric evaluated. For any performance metric, a traffic management scheme with a negative rank indicates that this traffic management scheme performs worse than the IETF-DR traffic management scheme, whereas a traffic management scheme with a positive rank indicates that this traffic management scheme performs better than the IETF-DR traffic management scheme.

For the blocking probability performance metric, a traffic management scheme with a lower blocking probability than the IETF-DR is given a positive number in the blocking probability reduction rank, whereas a traffic management scheme with a higher blocking probability than the IETF-DR is given a negative number in the blocking probability reduction rank. Table 11-2 illustrates the eight traffic management schemes rank in blocking probability compared to the IETF-DR traffic management schemes. A consistent trend was observed for the 2-alternate routing and 3-alternate routing case with the following observations:

1. Both the IETF-SR and ITU-SR traffic management schemes lead to higher blocking probability, lower reduction in blocking probability, compared to the IETF-DR with IETF-SR providing the highest blocking probability.
2. SPA-Dedicated traffic management scheme does not provide any reduction in blocking probability compared to the IETF-DR traffic management scheme, but provides lower blocking probability, higher reduction in blocking probability, compared to IETF-SR and ITU-SR traffic management schemes.
3. The SPA two traffic management schemes with enabled inverse multiplexing lead to the lowest blocking probability, the highest reduction in blocking probability, compared to the rest of the traffic management schemes.

For the permissible load performance metric, a traffic management scheme with a lower permissible load than the IETF-DR is given a negative number in the permissible load increase rank, whereas a traffic management scheme with a higher permissible load than the IETF-DR is given a positive number in the permissible load rank. Table 11-3 illustrates the eight traffic management schemes rank in permissible load compared to the IETF-DR traffic management schemes. A consistent trend was concluded for the 2-alternate routing and 3-alternate routing case with the following observations:

1. The SPA-Shared control plane model with disabled inverse multiplexing leads to a reduction in permissible load compared to the IETF-DR traffic management scheme.
2. IETF-SR and ITU-DR traffic management schemes do not provide increase or decrease in permissible load compared to the IETF-DR traffic management scheme.
3. The SPA two traffic management schemes with enabled inverse multiplexing lead to the highest increase in permissible load compared to the rest of the traffic management schemes.

For the utilization performance metric, a traffic management scheme with a lower utilization than the IETF-DR is given a positive number in the utilization reduction rank, whereas a traffic management scheme with a higher utilization than the IETF-DR is given a negative number in the utilization rank. Table 11-4 illustrates the eight traffic management schemes rank in utilization compared to the IETF-DR traffic management schemes. A consistent trend was concluded for the 2-alternate routing and 3-alternate routing case with the following observations:

1. IETF-SR traffic management scheme provides the highest utilization, lowest reduction in utilization, compared to the IETF-DR traffic management scheme.

2. For both the IETF and ITU control plane models, direct routing leads to higher reduction in utilization compared to split routing.

3. All the traffic management schemes of the SPA control plane model provide a reduction in utilization compared to the IETF and ITU control plane models under both direct and split routing.

Traffic Management Scheme	7-Node Topology “2-Alternate Routing”	7-Node Topology “2-Alternate Routing”
IETF-SR	-4	-4
ITU-DR	1	1
ITU-SR	-3	-3
SPA-Dedicated	0	0
SPA-w/o(NE,IM)	-2	-2
SPA-w/NE,w/oIM	-1	-1
SPA-w/oNE,w/IM	2	2
SPA-w/(NE,IM)	3	3

Table 11-2: Traffic Management Schemes Rank in Blocking Probability Reduction (IETF-DR as Reference Model)

Traffic Management Scheme	7-Node Topology “2-Alternate Routing”	7-Node Topology “2-Alternate Routing”
IETF-SR	0	0
ITU-DR	0	0
ITU-SR	2	2
SPA-Dedicated	1	1
SPA-w/o(NE,IM)	-1	-1
SPA-w/NE,w/oIM	-2	-2
SPA-w/oNE,w/IM	4	4
SPA-w/(NE,IM)	3	3

Table 11-3: Traffic Management Schemes Rank in Permissible Load Increase (IETF-DR as Reference Model)

Traffic Management Scheme	7-Node Topology “2-Alternate Routing”	7-Node Topology “2-Alternate Routing”
IETF-SR	-1	-1
ITU-DR	6	6
ITU-SR	2	2
SPA-Dedicated	4	4
SPA-w/o(NE,IM)	5	5
SPA-w/NE,w/oIM	7	7
SPA-w/oNE,w/IM	3	3
SPA-w/(NE,IM)	1	1

Table 11-4: Traffic Management Schemes Rank in Utilization Reduction (IETF-DR as Reference Model)

12 Summary of System Performance

This section provides a summary of the performance analysis results for the 7-node topology. The framework of the performance comparison between the different traffic management schemes is as follows:

1. Rank the nine traffic management schemes based on the operational complexity (more parameters to set including enabling state-dependent routing, load partitioning, and inverse multiplexing). The following is the rank based on ascending level of operational complexity: IETF-DR, IETF-SR, ITU-DR, ITU-SR, SPA-Dedicated, SPA-w/o(NE,IM), SPA-w/oNE,w/IM, SPA-w/NE,w/oIM, SPA-w/(NE,IM).
2. Use IETF-DR as a reference model to compare the rest of the eight traffic management schemes.

3. Define three performance metrics (blocking probability, permissible load, and utilization). For each performance metric, compare the rest eight traffic management schemes to IETF-DR traffic management scheme. For each plot, the eight traffic management schemes are plotted (x-axis) against the IETF-DR as a reference model.

The following performance metrics from a physical resources perspective were studied:

1. Network-Wide blocking probability
2. Network-Wide permissible “non-blocked” load
3. Network-Wide utilization

12.1 Average network-wide blocking probability

Table 12-1, Figure 12-1, and Figure 12-2 compare the blocking probability reduction among the nine traffic management schemes while considering the IETF-DR as a reference model. For Table 12-1, Figure 12-1, and Figure 12-2, it is important to mention that a negative number for a blocking probability reduction is an increase in blocking probability over IETF-DR control plane model. The performance analysis found the following:

1. While considering the IETF-DR as a reference control plane model, all the traffic management schemes of the SPA control plane provide a higher reduction in blocking probability compared to the IETF-SR and ITU-(DR,SR) control plane models. The blocking probability reduction is 0-131% and 39-122% respectively; depending on the SPA traffic management scheme, SPA number of alternate routes, and the IETF/ITU static routing configuration (direct routing vs. split routing).

2. When IMF is disabled in the SPA control plane model, IETF-DR traffic management scheme produces less blocking probability than the SPA control plane model. On the contrary, when IMF is enabled, the SPA control plane model leads to a reduction in blocking probability compared to IETF-DR; the reduction in blocking probability is 22-48% depending on the SPA traffic management scheme and the number of alternate routes. The highest reduction in blocking probability occur for “w/(NE,IM)” SPA traffic management scheme where LPF is configured to Network Engineering (with NE) and IMF function is configured to enabled Inverse Multiplexing (with IM); a reduction of 43-80% of blocking probability depending on the number of alternate routes.

3. The SPA-Dedicated control plane model does not provide a reduction in blocking probability compared to IETF-DR as reference model, but provides a 5-10% reduction in blocking probability compared to SPA-Shared with static load partitioning.

Network Topology	Control Plane Model	Reduction in Blocking Probability	
		Reduction %	Relevant Figure
7-Node “2-aternateRoutes”	IETF-DR	0	Figure 13-1
	IETF-SR	-83	
	ITU-DR	9	
	ITU-SR	-74	
	SPA-Dedicated	0	
	SPA-w/o(NE,IM)	-13	Figure 13-2
	SPA-w/NE,w/oIM	-9	Figure 13-3
	SPA-w/oNE,w/IM	22	Figure 13-4
	SPA-w/(NE,IM)	48	Figure 13-5
7-Node “3-aternateRoutes”	IETF-DR	0	Figure 13-15
	IETF-SR	-43	
	ITU-DR	9	
	ITU-SR	-35	
	SPA-Dedicated	0	
	SPA-w/o(NE,IM)	-9	Figure 13-16
	SPA-w/NE,w/oIM	-5	Figure 13-17
	SPA-w/oNE,w/IM	26	Figure 13-18
	SPA-w/(NE,IM)	43	Figure 13-19

Table 12-1: Blocking Probability Reduction (IETF-DR as Reference Model)- 7-node topology

12.2 Average per source-destination pair permissible load

Table 12-2, Figure 12-3, and Figure 12-4 compare the permissible load increase among the nine traffic management schemes while considering the IETF-DR as reference model. For Table 12-2, Figure 12-3, and Figure 12-4, it is important to mention that a percentage increase in permissible load that is negative is a decrease in permissible load over IETF-DR reference model. The performance analysis found the following:

1. While considering the IETF-DR as a reference control plane model, all the traffic management schemes of the SPA control plane, except when IMF is disabled, provide a higher increase in permissible load compared to the IETF-SR and ITU-(DR,SR) control plane models. The increase in permissible load is 120-134% and 110-120% respectively;

depending on the SPA traffic management scheme, SPA number of alternate routes, and the IETF/ITU static routing configuration (direct routing vs. split routing).

2. The highest increase in permissible load occurs for SPA-"w/oNE,w/IM" traffic management scheme where LPF is configured to static load partitioning (without NE) and IMF function is configured to enabled Inverse Multiplexing (with IM). The increase in permissible load is 120-134% compared to IETF-DR control plane model; depending on the number of alternate routes.

3. While enabling IM, performing load partitioning statically "without Network Engineering" or dynamically "with Network Engineering" does not provide a significant impact on the percentage gain in permissible load.

4. While disabling IM and regardless of static or dynamic load partitioning for SPA-Shared control plane model, the SPA control plane model provides less permissible load than IETF-DR control plane model.

Network Topology	Control Plane Model	Increase in Permissible Load	
		Increase %	Relevant Figure
7-Node "2-aternateRoutes"	IETF-DR	0	Figure 13-6
	IETF-SR	0	
	ITU-DR	0	
	ITU-SR	4	
	SPA-Dedicated	3	
	SPA-w/o(NE,IM)	-2	Figure 13-7
	SPA-w/NE,w/oIM	-11	Figure 13-8
	SPA-w/oNE,w/IM	134	Figure 13-9
	SPA-w/(NE,IM)	127	Figure 13-10
7-Node "3-aternateRoutes"	IETF-DR	0	Figure 13-20
	IETF-SR	0	
	ITU-DR	0	
	ITU-SR	1	
	SPA-Dedicated	2	
	SPA-w/o(NE,IM)	-1	Figure 13-21
	SPA-w/NE,w/oIM	-11	Figure 13-22
	SPA-w/oNE,w/IM	120	Figure 13-23
	SPA-w/(NE,IM)	111	Figure 13-24

Table 12-2: Permissible Load Increase (IETF-DR as Reference Model) - 7-node topology

12.3 Average network-wide resource utilization

Table 12-3, Figure 12-5, and Figure 12-6 compare the utilization reduction among the nine traffic management schemes while considering the IETF-DR as reference model. For Table 12-3, Figure 12-5, and Figure 12-6, it is important to mention that a percentage reduction in utilization that is negative is an increase in utilization over IETF-DR reference model. The performance analysis found the following:

1. Compared to IETF-DR, all the traffic management schemes of the SPA control plane model provide a reduction in utilization; the reduction in utilization is 7-31% depending on the SPA traffic management scheme and number of alternate routes.
2. Compared to IETF-DR, the lowest reduction in utilization occur for "w/(NE,IM)" and "w/oNE,w/IM" SPA traffic management schemes when IMF is configured to enabled Inverse Multiplexing (with IM) and regardless of LPF configuration as static or dynamic partitioning; a reduction of 7-25% in utilization over the IETF-DR control plane model depending on the number of alternate routes.

Network Topology	Control Plane Model	Reduction in Utilization	
		Increase %	Relevant Figure
7-Node "2-aternateRoutes"	IETF-DR	0	Figure 13-11
	IETF-SR	-21	
	ITU-DR	25	
	ITU-SR	7	
	SPA-Dedicated	23	
	SPA-w/o(NE,IM)	25	
	SPA-w/NE,w/oIM	30	Figure 13-12
	SPA-w/oNE,w/IM	10	Figure 13-13
	SPA-w/(NE,IM)	7	Figure 13-14
7-Node "3-aternateRoutes"	IETF-DR	0	Figure 13-25
	IETF-SR	-16	
	ITU-DR	27	
	ITU-SR	13	
	SPA-Dedicated	20	
	SPA-w/o(NE,IM)	27	
	SPA-w/NE,w/oIM	31	Figure 13-26
	SPA-w/oNE,w/IM	25	Figure 13-27
	SPA-w/(NE,IM)	14	Figure 13-28

Table 12-3: Utilization Reduction (IETF-DR as Reference Model) - 7-node topology

While considering the operational space of the network topologies and the service analyzed as provided in section 11.3.1, the SPA control plane demonstrates its superiority over IETF and ITU control plane models as follows:

1. All the traffic management schemes of the SPA control plane provide a higher reduction in blocking probability compared to the IETF-SR and ITU-SR control plane models. The SPA control plane model provides a higher reduction in blocking probability over ITU-DR when IMF is enabled to allow inverse multiplexing.
2. All the traffic management schemes of the SPA control plane, except when IMF is disabled, provide a higher increase in permissible load compared to the IETF-SR and ITU-(DR,SR) control plane models.
3. All the traffic management schemes of the SPA control plane provide a higher reduction in utilization compared to the IETF-(DR, SR) and ITU-(DR,SR) traffic management schemes.

The consistent performance analysis results carried on the 7-node topologies for both two and three alternate routes validated the hypotheses of this work and indicated a common trend of the superiority of the SPA control plane model over the IETF and ITU control plane models under specific operational space as provided in section 11.3.1; this consistent performance for the 7-node topology for both two and three alternate routes can be used to generalize the superiority of the SPA control plane model over both IETF and ITU control plane models under specific operational space as provided in section 11.3.1.

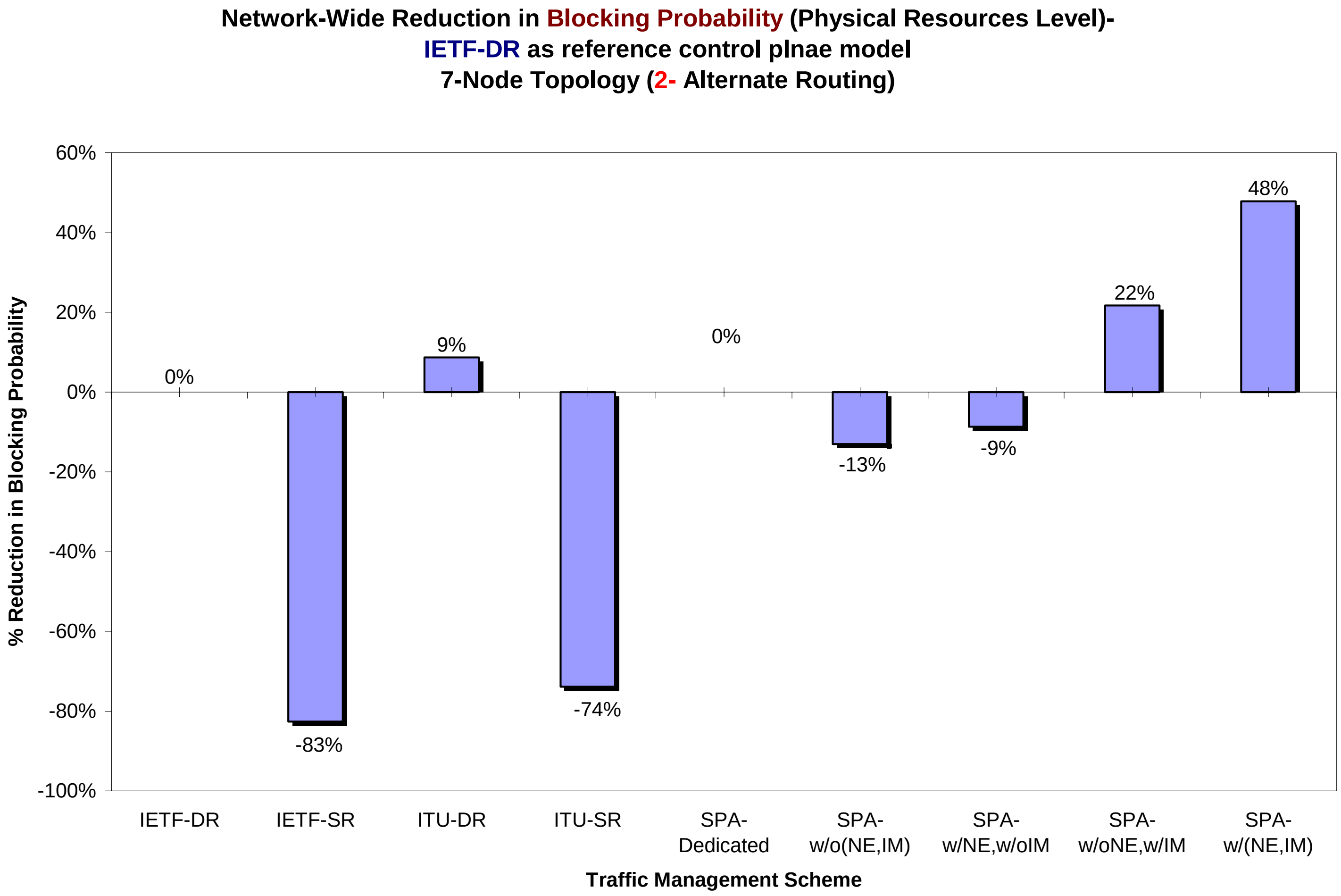

Figure 12-1: Network-Wide Blocking Probability Percentage Reduction (IETF-DR as Reference Model)- 7-node with 2-Alternate Routing

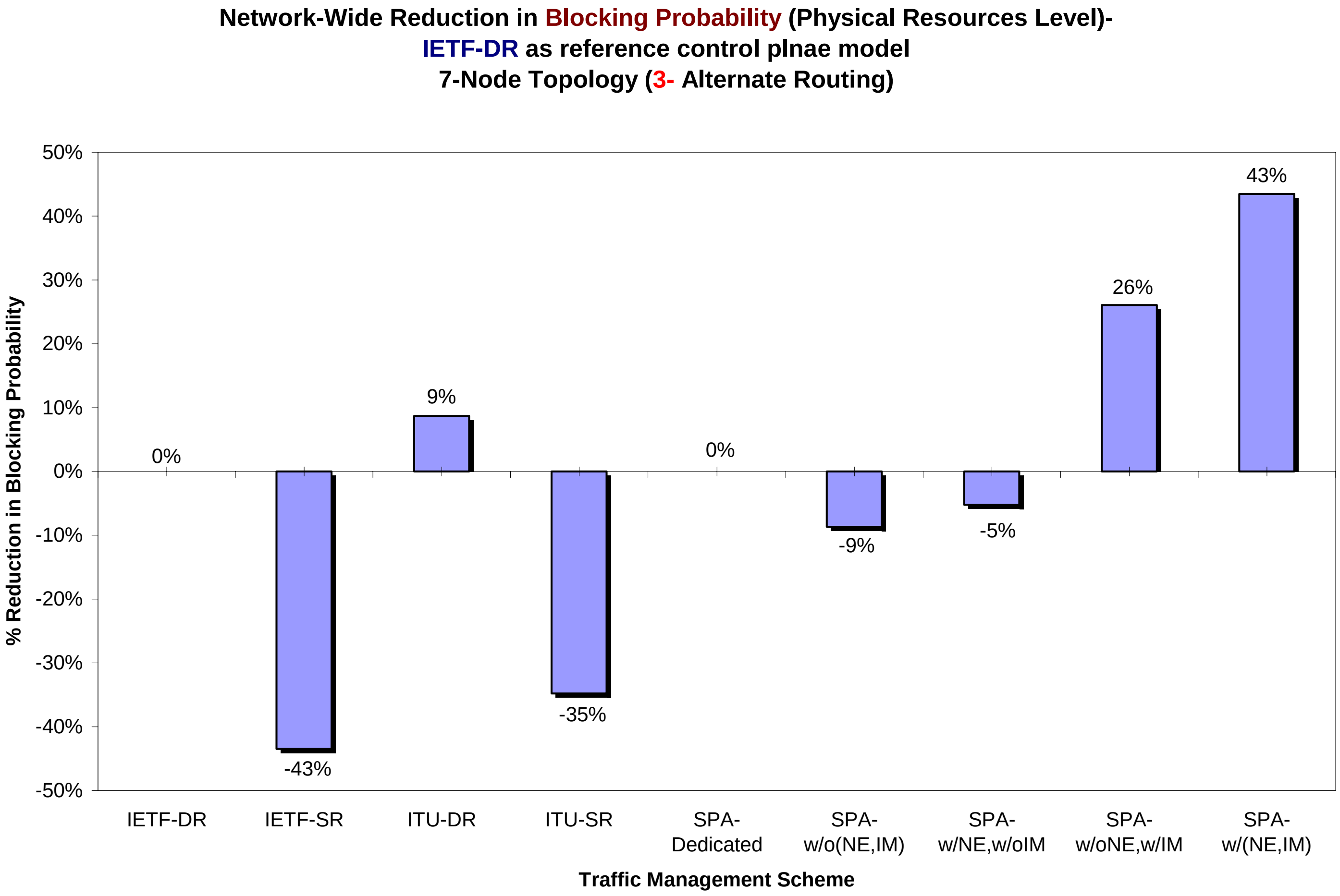

Figure 12-2: Network-Wide Blocking Probability Percentage Reduction (IETF-DR as Reference Model)- 7-node with 3-Alternate Routing

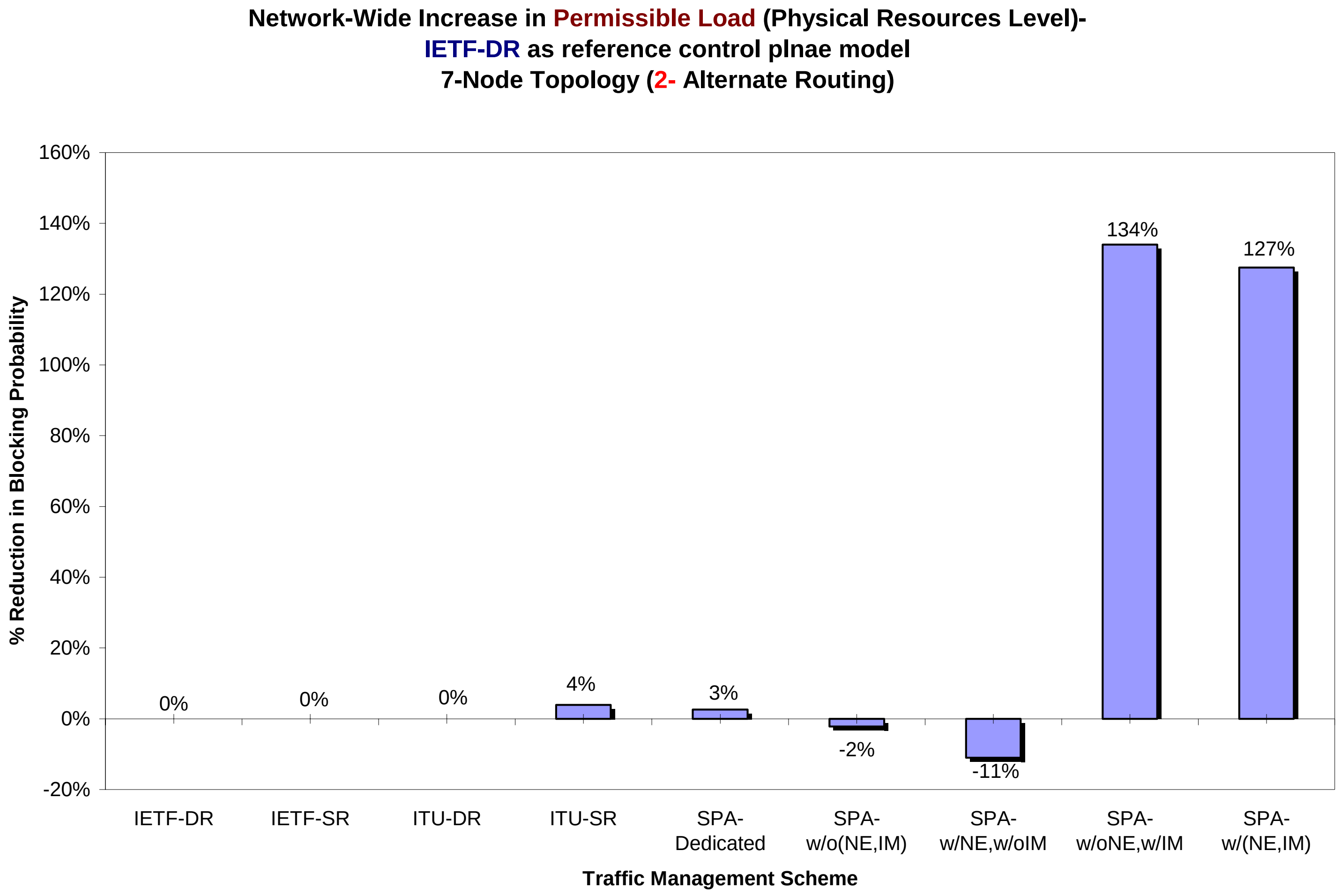

Figure 12-3: Network-Wide Permissible Load Percentage Difference (IETF-DR as Reference Model) - 7-node with 2-Alternate Routing

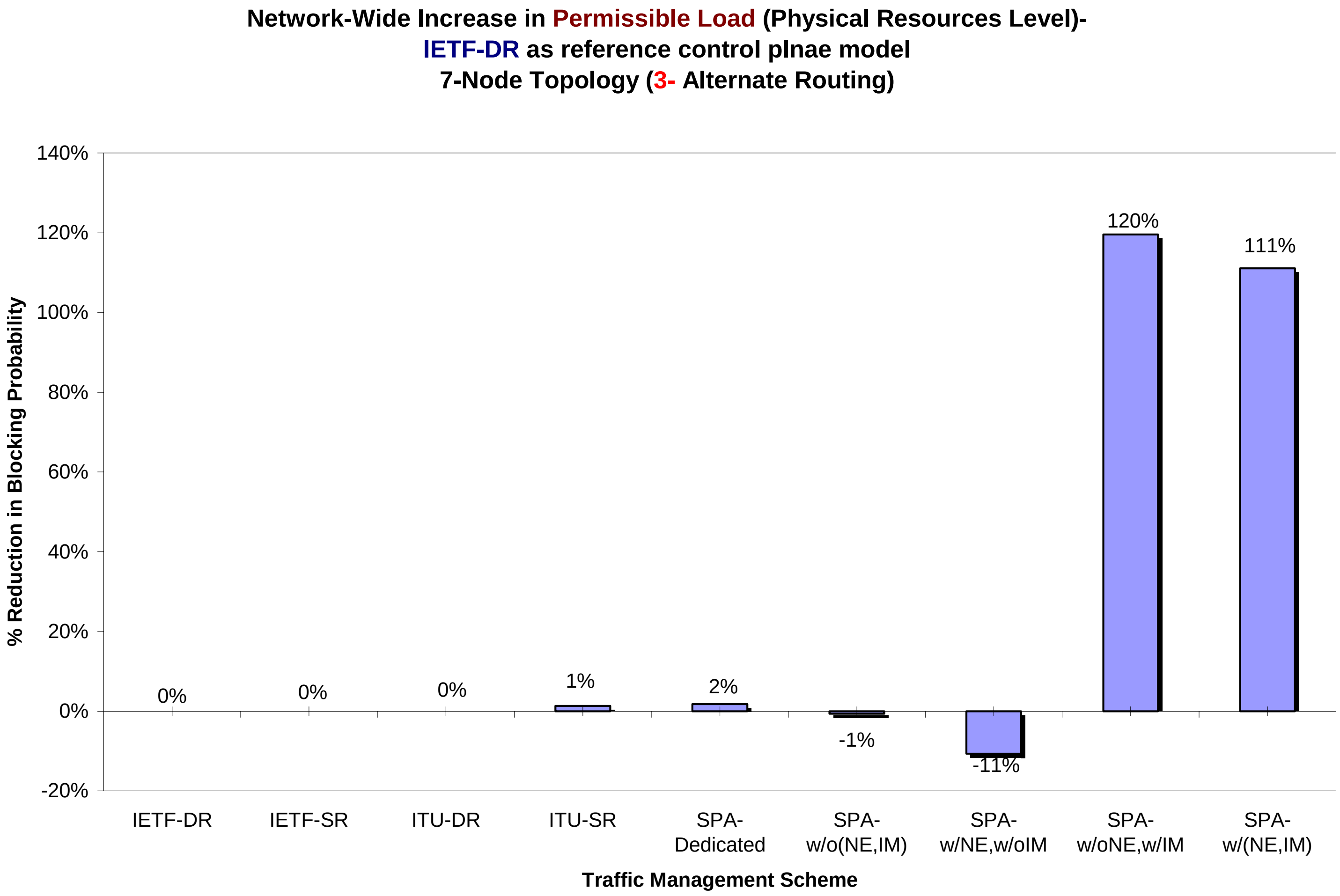

Figure 12-4: Network-Wide Permissible Load Percentage Difference (IETF-DR as Reference Model) - 7-node with 3-Alternate Routing

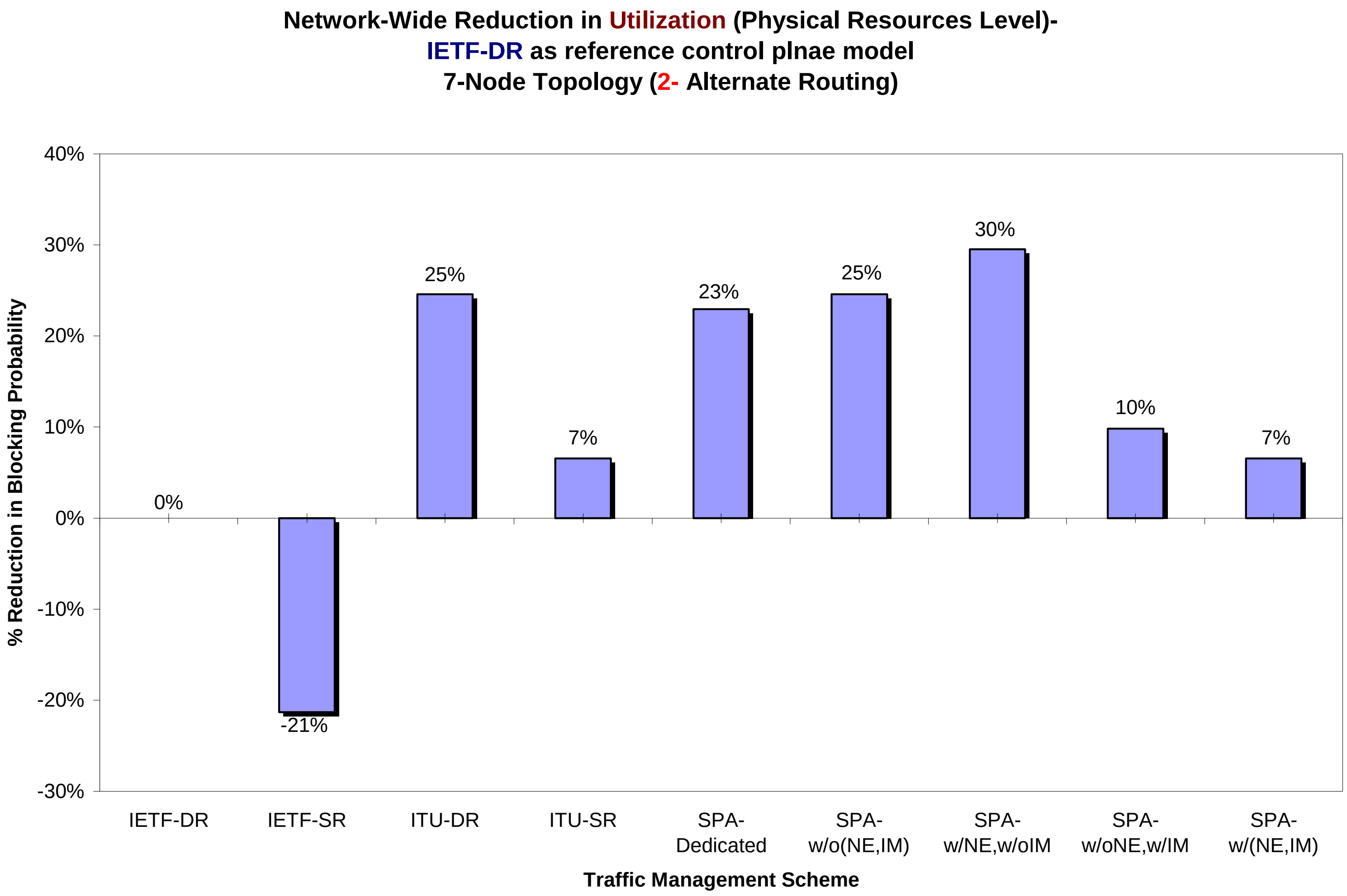

Figure 12-5: Network-Wide Utilization Percentage Reduction (IETF-DR as Reference Model) - 7-node with 2-Alternate Routing

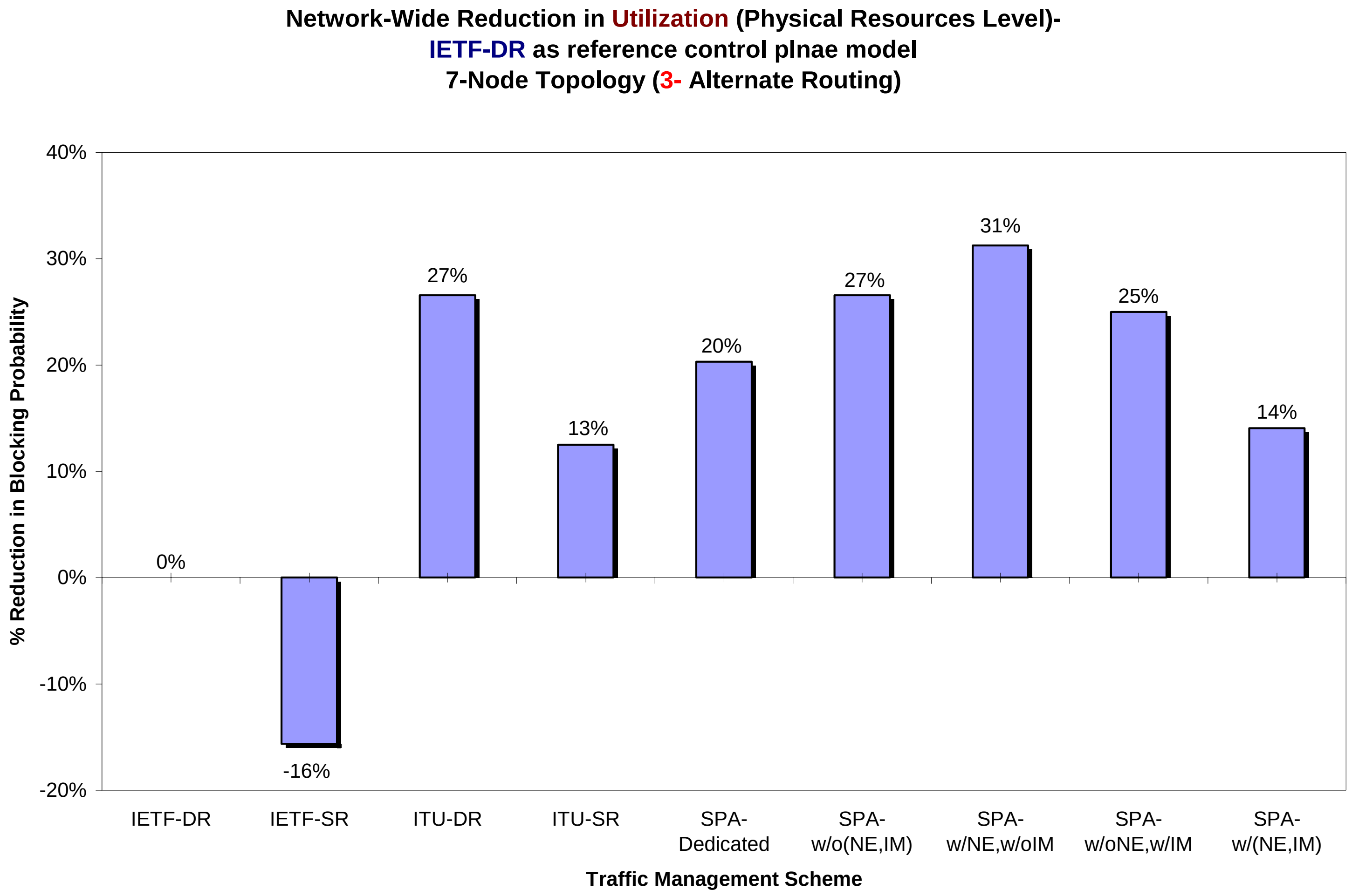

Figure 12-6: Network-Wide Utilization Percentage Reduction (IETF-DR as Reference Model) - 7-node with 3-Alternate Routing

13 Discussion of the Impact of SPA Functionality on System Performance

This section provides detailed analysis of the impact of the five traffic management schemes of the SPA control plane model on blocking probability, permissible load, and utilization. The five SPA traffic management schemes are as follows:

1. State-dependent routing traffic management scheme when the routing component is enabled to perform state-dependent routing.
2. “w/o(NE,IM) traffic management scheme is when configuring LPF to partition the input load statically (without Network Engineering “w/oNE”) and configuring IMF to disabled Inverse Multiplexing (without Inverse Multiplexing “w/oIM”) across dedicated and shared resources.
3. “w/NE,w/oIM” traffic management scheme is when configuring LPF to partition the input load dynamically (with Network Engineering “w/NE”) and configuring IMF to disabled Inverse Multiplexing (without Inverse Multiplexing “w/oIM”) across dedicated and shared resources.
4. “w/oNE,w/IM” traffic management scheme is when configuring LPF to partition the input load statically (without Network Engineering “w/oNE”) and configuring IMF to enabled Inverse Multiplexing (with Inverse Multiplexing “w/IM”) across dedicated and shared resources.
5. “w/(NE,IM) traffic management scheme is when configuring LPF to partition the input load dynamically (with Network Engineering “w/NE”) and configuring IMF to enabled Inverse Multiplexing (with Inverse Multiplexing “w/IM”) across dedicated and shared resources.

13.1 State-Dependent routing impact on blocking probability

As illustrated in Figure 13-1 and Figure 13-15, the state-dependent routing in the SPA control plane leads to higher reduction in physical resources blocking probability compared to IETF and ITU static routing. This is related to the state-dependent nature of the SPA routing component; which would distribute the input load across all the identified routes between a source-destination pair based on the traffic occupancy of each identified route between a source-destination pair. In both DR and SR, the input traffic between a source-destination pair is applied to routes regardless of their traffic occupancy state. This would lead to higher blocking probability and hence lower permissible load if the traffic is applied to routes with higher occupancy state.

13.2 State-Dependent routing impact on permissible load

As illustrated in Figure 13-6 and Figure 13-20, the state-dependent routing in the SPA control plane leads to comparable physical resources permissible load to IETF and ITU control plane models.

13.3 State-Dependent routing impact on utilization

As illustrated in Figure 13-11 and Figure 13-25, the state-dependent routing in the SPA control plane leads to higher reduction in physical resources utilization compared to IETF-(DR) and ITU-(DR,SR) control plane models. This is related to the state-dependent nature of the SPA routing component; which would distribute the input traffic load across all the identified routes between a source-destination pair based on the traffic occupancy of each identified route between a source-destination pair, this would lead that the network-wide occupancy and hence the utilization is less under the same input load. In both IETF and ITU control plane models, the input load between a source-destination pair is applied to routes regardless of their traffic occupancy state; this would lead to higher utilization if the load is applied to routes with higher occupancy state.

13.4 w/o(NE,IM) traffic management scheme impact on blocking probability

As illustrated in Figure 13-2 and Figure 13-16, this traffic management scheme leads to higher reduction in physical resources blocking probability compared to IETF-SR and ITU-SR control plane models but lower reduction in physical resources blocking probability compared to IETF-DR and ITU-DR control plane models. It is important to note that the reduction in blocking probability using the “w/o(NE,IM)” traffic management scheme is lower than that achieved by Dedicated traffic management scheme of the SPA control plane model. This is expected since static load partitioning partitions the load across the dedicated and shared resources partitions without considering the occupancy state on both partitions. Thus, a higher load could be applied to network resource partition with higher occupancy state which will lead to a higher blocking probability on the physical resources-level. No direct affect of increasing sharing ratio on blocking probability was observed for the 7-node topology.

13.5 w/o(NE,IM) traffic management scheme impact on permissible load

As illustrated in Figure 13-7 and Figure 21, this traffic management scheme leads to reduction in physical resources permissible load compared to IETF-SR and ITU-(DR,SR) control plane models. It is important to note that this traffic management scheme provides a higher permissible load on the VPN resources level compared to the ITU-SR and ITU-(DR,SR) control plane models as illustrated in Figure 20-23 for the 7-node topology with two alternate routing, and Figure 21-23 for the 7-node topology with three alternate routing. The reduction in physical resources permissible load compared to IETF-SR and ITU-(DR,SR) control plane models can be explained be analyzing the permissible load on the dedicated and shared resources partitions by the “w/o(NE,IM)” traffic management scheme. The “w/o(NE,IM)” traffic management scheme leads to lowest permissible load on the dedicated resources partitions compared to other SPA traffic management schemes; this is due to the static load partitioning and disabled inverse multiplexing features. This is illustrated in the permissible load plots on the dedicated resources as provided in Appendix-C, D, and E for the two topologies. Taking into consideration the weighted average formula used to compute the physical resources permissible load, it is observed that the dedicated resources partition permissible load has a higher load than the shared resources partition permissible load; thus the weighted average permissible load on the physical resources will be lowest among the SPA traffic management schemes. No direct affect of increasing sharing ratio on permissible load was observed.

13.6 w/o(NE,IM) traffic management scheme impact on utilization

As illustrated in Figure 13-11 and Figure 13-25, this traffic management scheme leads to higher reduction in physical resources utilization over IETF-(DR,SR) and ITU-SR control plane models. It is important to note that the reduction in utilization using the “w/o(NE,IM) traffic management scheme is higher than that achieved by Dedicated traffic management scheme. This is expected since each configured VPN service will have higher resources, than

IETF and ITU control plane models, by combining dedicated and shared network resources partitions used by each configured VPN service.

13.7 (w/NE,w/oIM) traffic management scheme impact on blocking probability

As illustrated in Figure 13-3 and Figure 13-17, this traffic management scheme leads to higher reduction in physical resources blocking probability compared to IETF-SR and ITU-SR control plane models but lower reduction in physical resources blocking probability compared to IETF-DR and ITU-DR control plane models. It is important to note that the reduction in blocking probability using the "w/NE,w/oIM" traffic management scheme is higher than that achieved by "w/o(NE,IM)" traffic management scheme. The *"w/NE,w/oIM"* traffic management scheme higher reduction in blocking probability than "w/o(NE,IM)" traffic management scheme is due to the dynamic allocation of input load between dedicated and shared resources based on dedicated resources blocking probability rather than splitting the input load statically across dedicated and shared resources based on sharing ratio between dedicated and shared resources. There is no direct relation between increasing the sharing ratio and the physical resources blocking probability for the 7-node topology.

13.8 (w/NE,w/oIM) traffic management scheme impact on permissible load

As illustrated in Figure 13-8 and Figure 13-22, this traffic management scheme leads to reduction in physical resources permissible load compared to IETF-SR and ITU-(DR,SR) control plane models. This can be explained by analyzing the permissible load on the dedicated and shared resources partitions, this is illustrated in the permissible load plots on the dedicated resources as provided in Appendix-C, D, and E for the two topologies. The "w/NE,w/oIM" traffic management scheme led to lowest permissible load on the dedicated resources partition and second from lowest on shared resources partition compared to other SPA traffic management schemes.

Increasing sharing ratio lowers the permissible load on both the 3-alternate and 3-alternate routing for the 7-node topologies.

13.9 (w/NE,w/oIM) traffic management scheme impact on utilization

As illustrated in Figure 13-2 and Figure 13-26, this traffic management scheme leads to higher reduction in physical resources blocking probability compared to IETF-(DR,SR) and

ITU-(DR,SR) control plane models. This traffic management scheme leads to the highest reduction in physical resources utilization. It is important to note that the reduction in utilization using the “w/NE,w/oIM” traffic management scheme is higher than that achieved by Dedicated and “w/o(NE,IM)” traffic management schemes. This is expected due to the dynamic allocation of traffic between dedicated and shared resources based on dedicated resources blocking probability rather than splitting the input load statically across dedicated and shared resources based on sharing ratio between dedicated and shared resources.

13.10 (w/oNE,w/IM) traffic management scheme impact on blocking probability

As illustrated in Figure 13-4 and Figure 13-18, this traffic management scheme leads to higher reduction in physical resources blocking probability compared to IETF-SR and ITU-(DR,SR) control plane models. It is important to note that the reduction in blocking probability using the “w/oNE,w/IM” traffic management scheme is higher than Dedicated, “w/o(NE,IM)”, and “w/NE,w/oIM” traffic management schemes. The reason for a higher reduction in blocking probability when IM is enabled is due to the fact that the incoming service request flows between a source-destination pair with an actual bandwidth requirements b_k^A are split “inverse-multiplexed” into multiple flows each with granular bandwidth requirement b_k^G , each granular flow is routed independently across the available routes, this leads to lower blocking probability due to the highly probability to grant resources to service with granular bandwidth requirements than coarse bandwidth requirements.

13.11 (w/oNE,w/IM) traffic management scheme impact on permissible load

As illustrated in Figure 13-9 and Figure 13-23, this traffic management scheme leads to an increase permissible load over IETF-SR and ITU-(DR,SR) control plane models. This can be explained due to the lower blocking probability when IM is enabled.

13.12 (w/oNE,w/IM) traffic management scheme impact on utilization

As illustrated in Figure 13-13 and Figure 13-27, this traffic management scheme leads to a reduction in physical resources utilization over IETF-(DR,SR) and ITU-SR control plane models. It is important to note that the reduction in utilization using the “w/oNE,w/IM” traffic management scheme is less than that achieved by Dedicated, “w/o(NE,IM)”, and "w/NE,w/oIM" traffic management schemes. The reason for a higher utilization and hence lower utilization reduction over IETF and ITU control plane models when IM is enabled is due to the same reason provided in section 13.10.

13.13 w/(NE,IM) traffic management scheme impact on blocking probability

As illustrated in Figure 13-5 and Figure 13-19, this traffic management scheme leads to a higher reduction in physical resources blocking probability compared to IETF-SR and ITU-(DR,SR) control plane models. It is important to note that the reduction in blocking probability using the "w/(NE,IM)" traffic management scheme is the highest compared to all other SPA traffic management schemes, this is due to the dynamic allocation of traffic between dedicated and shared resources, based on the traffic occupancy state, in addition to enabling Inverse Multiplexing (IM).

13.14 w/(NE,IM) traffic management scheme impact on permissible load

As illustrated in Figure 13-10 and Figure 13-24, this traffic management scheme leads to an increase in permissible load over IETF-SR and ITU-(DR,SR) control plane models. It is important to note that the increase in permissible load using the "w/(NE,IM)" traffic management scheme is less than that achieved by "w/oNE,w/IM" traffic management scheme. This can be explained by analyzing the permissible load on the dedicated and shared resources partitions for both the "w/oNE,w/IM" and "w/(NE,IM)" traffic management schemes. As illustrated in Figure 18-14 and Figure 19-14 for the 7-node topology with 2-alternate routing and 3-alternate routing respectively, the permissible load is higher in the "w/(NE,IM)" traffic management scheme than the "w/oNE,w/IM" traffic management scheme on the dedicated resources partition, but lower in the "w/(NE,IM)" traffic management scheme than the "w/oNE,w/IM" on the shared resources partition. Using the weighted average permissible load on the physical resources level, the "w/oNE,w/IM" traffic management scheme provides higher permissible load than the "w/(NE,IM)" traffic management scheme. Increasing sharing ratio leads to lower permissible load on the physical resource level for both 2-alternate and 3-alternate routing for the 7-node topology. This is due to the higher blocking probability on the physical resources level with increasing the sharing ratio.

13.15 w/(NE,IM) traffic management scheme impact on utilization

As illustrated in Figure 13-14 and Figure 13-28, this traffic management scheme leads to a reduction in physical resources utilization compared to IETF-(DR,SR) and ITU-SR but lower reduction in physical resources utilization compared to ITU-DR control plane model. It is important to note that the reduction in utilization using the “w/(NE,/IM)” traffic management scheme is less than that achieved by Dedicated, “w/o(NE,IM)”, “w/NE,w/oIM”, and “w/oNE,w/IM” traffic management schemes. The reason for a higher utilization and hence lower utilization reduction over ITU control plane model is due to enabled dynamic load partitioning and inverse multiplexing which will lead to lowest blocking probability and hence highest utilization among the SPA traffic management schemes.

13.16 Generalizing the performance analysis results

13.16.1 SPA superiority trend based on 4-node and 7-node topologies

In section 11.3, it was proved that both 2-alternate and 3-alternate routing cases for the 7-node topology gave the same consistent trends for the SPA superiority under specific operational space as provided in section 11.3.1. In this section, we compare the SPA superiority trend for both the 4-node and 7-node topologies under the same specific operational space as provided in section 11.3.1. The following consistent trends were observed for the blocking probability performance metric:

1. In the 4-node topology, all the five SPA traffic management schemes provide a lower blocking probability than IETF-DR, IETF-SR, ITU-DR, and ITU-SR.
2. In the 7-node topology and for both 2 and 3 alternate routing, all the five SPA traffic management schemes provide a lower blocking probability than IETF-SR and ITU-SR. When IMF is enabled in SPA control plane model to allow inverse multiplexing, the two related SPA traffic management schemes provide a lower blocking probability than IETF-DR and ITU-DR.

The following consistent trends were observed for the permissible load performance metric:

1. In the 4-node topology, all the five SPA traffic management schemes provide a comparable permissible load to IETF-DR and ITU-DR. When IMF is enabled to allow inverse multiplexing, the two related SPA traffic management schemes provide a higher permissible load than IETF-SR and ITU-SR.
2. In the 7-node topology and for both 2 and 3 alternate routing, the same trend in point 3 was concluded.

The following consistent trends were observed for the utilization performance metric:

1. In the 4-node topology, when IMF is disabled for SPA control plane model, the two related SPA traffic management schemes provide lower utilization than IETF and ITU models for both direct and split routing. When IMF is enabled for the SPA control plane model, the two related SPA traffic management schemes provide higher utilization than IETF and ITU models except IETF-SR control plane model. SPA-Dedicated control plane model provides lower utilization than IETF and ITU models except ITU-DR.
2. In the 7-node topology and for both 2 and 3 alternate routing, the same trend in point 5 was concluded.

13.16.2 SPA superiority trend justification based on the performance impact of the SPA control plane model components

In this section, we justify the SPA superiority trend for other possible topologies than the 4-node and 7-node topologies that were analyzed in this research, the trend is justified based on the expected consistent impact of the SPA control plane components on the blocking probability, permissible load, and utilization performance metrics under specific operational space as provided in section 11.3.1. As provided below, the SPA control plane components that were analyzed to justify the SPA control plane model superiority trend are the state-dependent routing, LPF, and IMF.

1. State-dependent routing component impact on SPA superiority trend:
   - *Blocking probability impact:* the state-dependent routing in the SPA control plane will lead to higher reduction in physical resources blocking probability compared to IETF and ITU static routing. This is related to the state-dependent nature of the SPA routing component; which would distribute the input load across all the identified

routes between a source-destination pair based on the traffic occupancy of each identified route between a source-destination pair. In IETF and ITU direct and split routing, the input load between a source-destination pair is applied to routes regardless of their traffic occupancy state; this would lead to higher blocking probability if the traffic is applied to routes with higher occupancy state.

- *Permissible load impact:* the state-dependent routing in the SPA control plane will lead to comparable or slightly higher physical resources permissible load than the IETF and ITU control plane models; this is related to the higher blocking probability reduction by the SPA state-dependent routing component than IETF and ITU static routing component.
- *Utilization impact:* the state-dependent routing in the SPA control plane will lead to higher reduction in physical resources utilization compared to IETF-SR and ITU-SR control plane models, but lower reduction in utilization, higher utilization, compared to ITU-DR control plane model. This is related to the state-dependent nature of the SPA routing component; which would distribute the input load across all the identified routes between a source-destination pair based on the traffic occupancy of each identified route between a source-destination pair, this would lead that the network-wide occupancy and hence the utilization is less under the same input load. In both IETF and ITU control plane models, the input load between a source-destination pair is applied to routes regardless of their traffic occupancy state; this would lead to higher utilization if the load is applied to routes with higher occupancy state.

2. Inverse Multiplexing Function (IMF) impact on SPA superiority trend:

- *Blocking probability impact:* Enabling inverse multiplexing will lead to higher reduction in blocking probability compared to IETF and ITU control plane models under both direct and split routing. The reason for a higher reduction in blocking probability when inverse multiplexing is enabled is due to the fact that the incoming service request flows between a source-destination pair with an actual bandwidth requirements b_k^A are split “inverse-multiplexed” into multiple flows each with granular bandwidth requirement b_k^G , each granular flow is routed independently across the available routes, this leads to lower blocking probability due to the highly probability to grant resources to service with granular bandwidth requirements than coarse bandwidth requirements.

- *Permissible load impact:* Enabling inverse multiplexing will lead to higher permissible load compared to IETF and ITU control plane models under both direct and split routing. This can be explained due to the lower blocking probability when inverse multiplexing is enabled.

- *Utilization impact:* Similar to the other SPA traffic management schemes, enabling inverse multiplexing leads to a reduction in utilization compared to the IETF-(DR, SR) and ITU-SR traffic management schemes. It is important to note that enabling inverse multiplexing will lead to a lower reduction in utilization compared to the other SPA-Shared control plane model with disabled inverse multiplexing. The reason for a higher utilization and hence lower utilization reduction compared to IETF and ITU control plane models when inverse multiplexing is enabled is due to the same reason provided for the blocking probability reduction when inverse multiplexing is enabled.

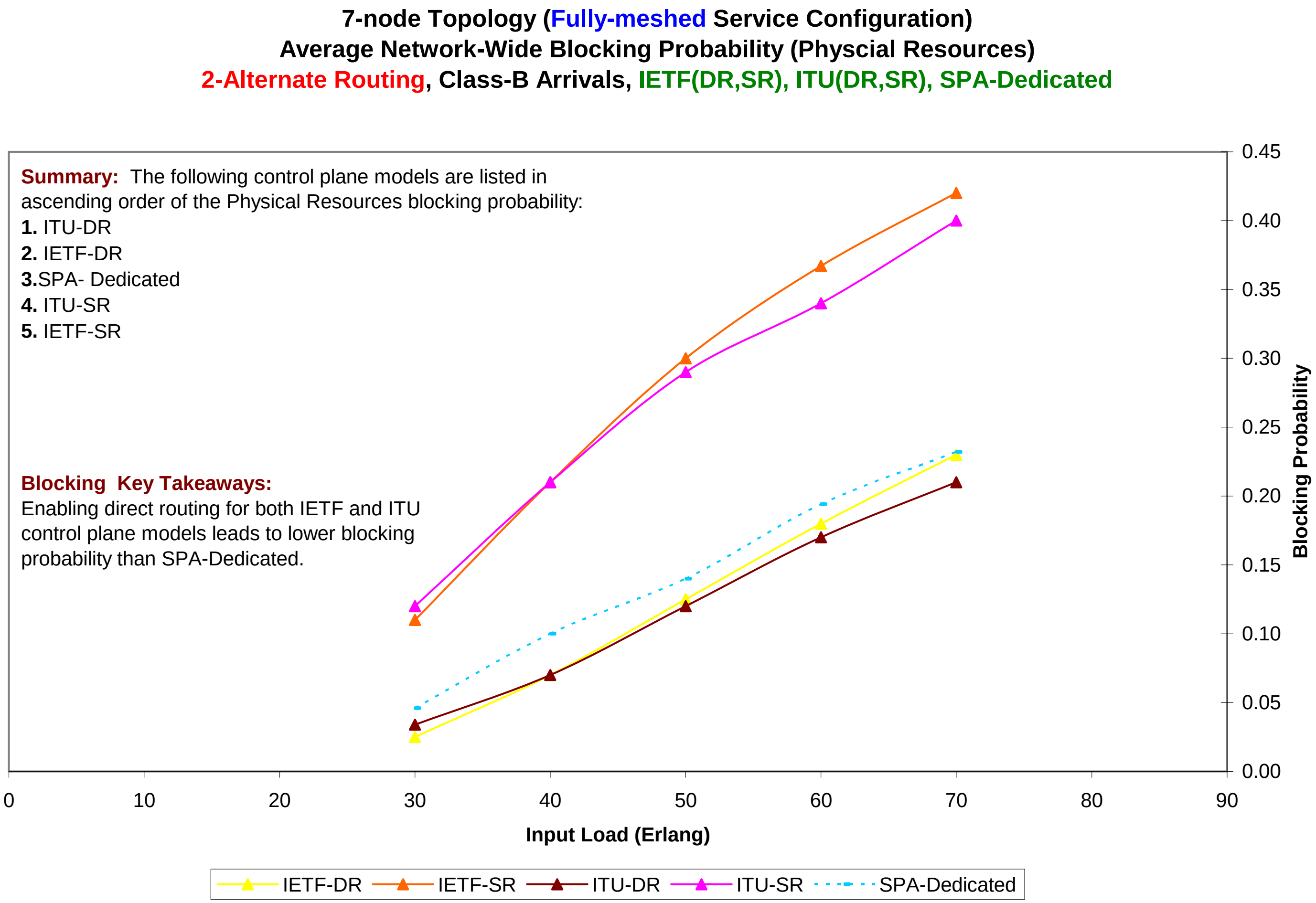

Summary: The following control plane models are listed in ascending order of the Physical Resources blocking probability:

1. ITU-DR
2. IETF-DR
3.SPA- Dedicated
4. ITU-SR
5. IETF-SR

Blocking Key Takeaways:
Enabling direct routing for both IETF and ITU control plane models leads to lower blocking probability than SPA-Dedicated.

Figure 13-1: Average Network-Wide Blocking Probability (Physical Resources)-7 Node-2 Alternate Route- IETF (DR, SR), ITU (DR, SR), SPA-Dedicated

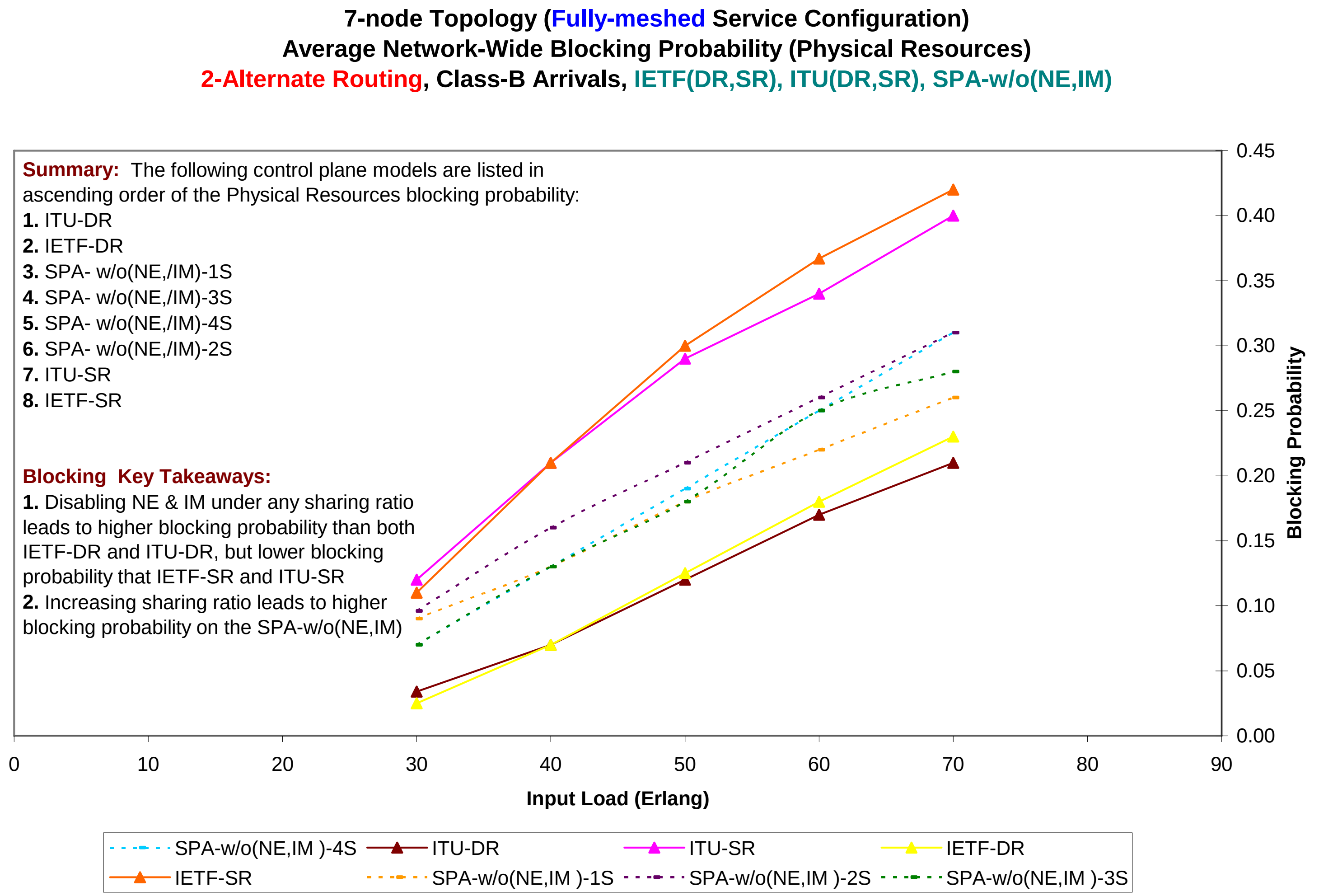
7-node Topology (Fully-meshed Service Configuration)
Average Network-Wide Blocking Probability (Physical Resources)
2-Alternate Routing, Class-B Arrivals, IETF(DR,SR), ITU(DR,SR), SPA-w/o(NE,IM)

Summary: The following control plane models are listed in ascending order of the Physical Resources blocking probability:

1. ITU-DR
2. IETF-DR
3. SPA- w/o(NE,/IM)-1S
4. SPA- w/o(NE,/IM)-3S
5. SPA- w/o(NE,/IM)-4S
6. SPA- w/o(NE,/IM)-2S
7. ITU-SR
8. IETF-SR

Blocking Key Takeaways:

1. Disabling NE & IM under any sharing ratio leads to higher blocking probability than both IETF-DR and ITU-DR, but lower blocking probability that IETF-SR and ITU-SR
2. Increasing sharing ratio leads to higher blocking probability on the SPA-w/o(NE,IM)

Figure 13-2: Average Network-Wide Blocking Probability (Physical Resources)-7 Node –2 Alternate Route- IETF(DR,SR), ITU(DR,SR), SPA-w/o(NE,IM)

7-node Topology (Fully-meshed Service Configuration)
Average Network-Wide Blocking Probability (Physical Resources)
2-Alternate Routing, Class-B Arrivals, IETF(DR,SR), ITU(DR,SR), SPA-(w/NE,w/oIM)

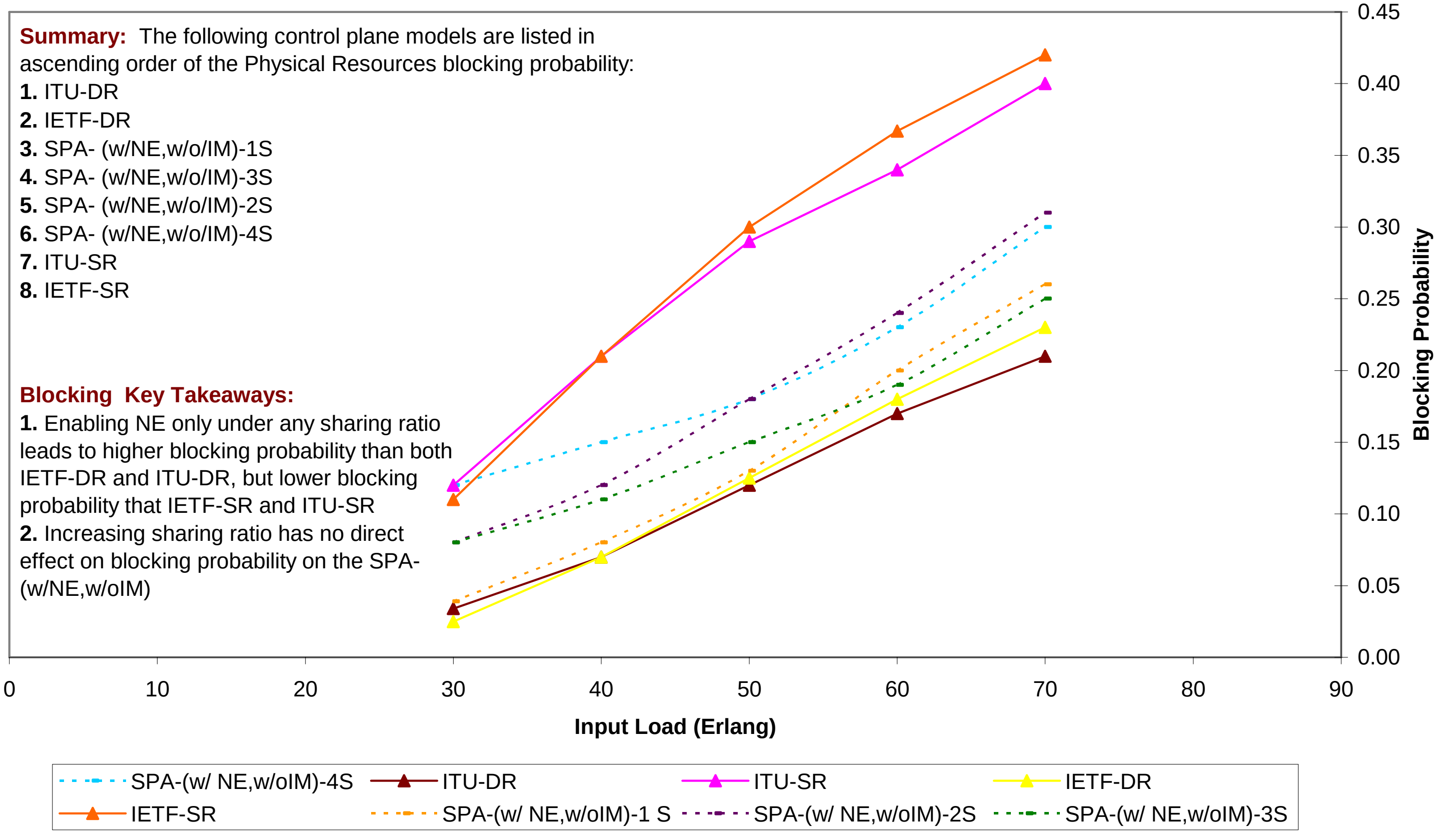

Summary: The following control plane models are listed in ascending order of the Physical Resources blocking probability:

1. ITU-DR
2. IETF-DR
3. SPA- (w/NE,w/o/IM)-1S
4. SPA- (w/NE,w/o/IM)-3S
5. SPA- (w/NE,w/o/IM)-2S
6. SPA- (w/NE,w/o/IM)-4S
7. ITU-SR
8. IETF-SR

Blocking Key Takeaways:

1. Enabling NE only under any sharing ratio leads to higher blocking probability than both IETF-DR and ITU-DR, but lower blocking probability that IETF-SR and ITU-SR
2. Increasing sharing ratio has no direct effect on blocking probability on the SPA-(w/NE,w/oIM)

Figure 13-3: Average Network-Wide Blocking Probability (Physical Resources)-7 Node – 2 Alternate Route-IETF(DR,SR), ITU(DR,SR), SPA-(w/NE,w/oIM)

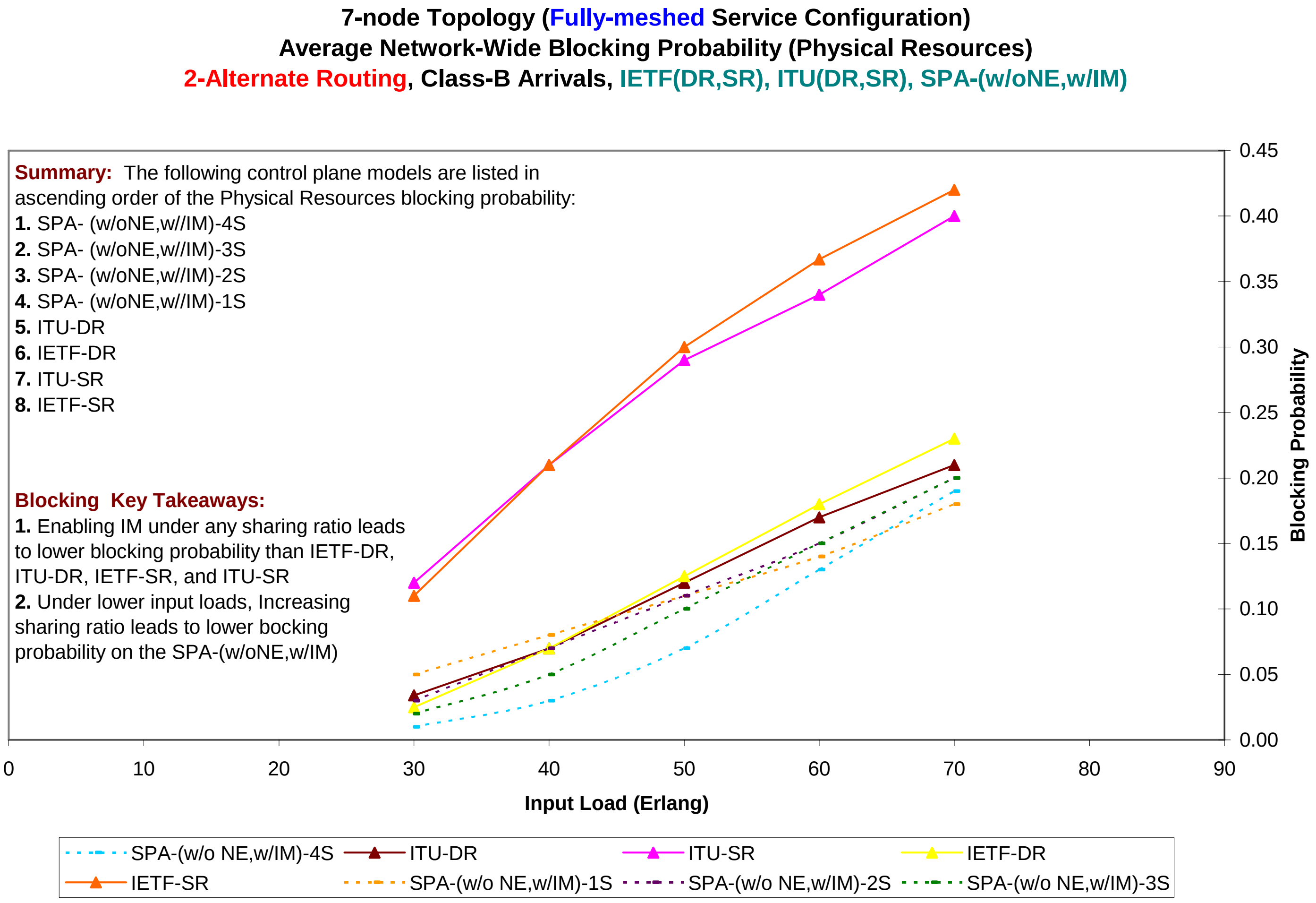

Figure 13-4: Average Network-Wide Blocking Probability (Physical Resources)-7 Node – 2 Alternate Route-IETF(DR,SR), ITU(DR,SR), SPA-(w/oNE,w/IM)

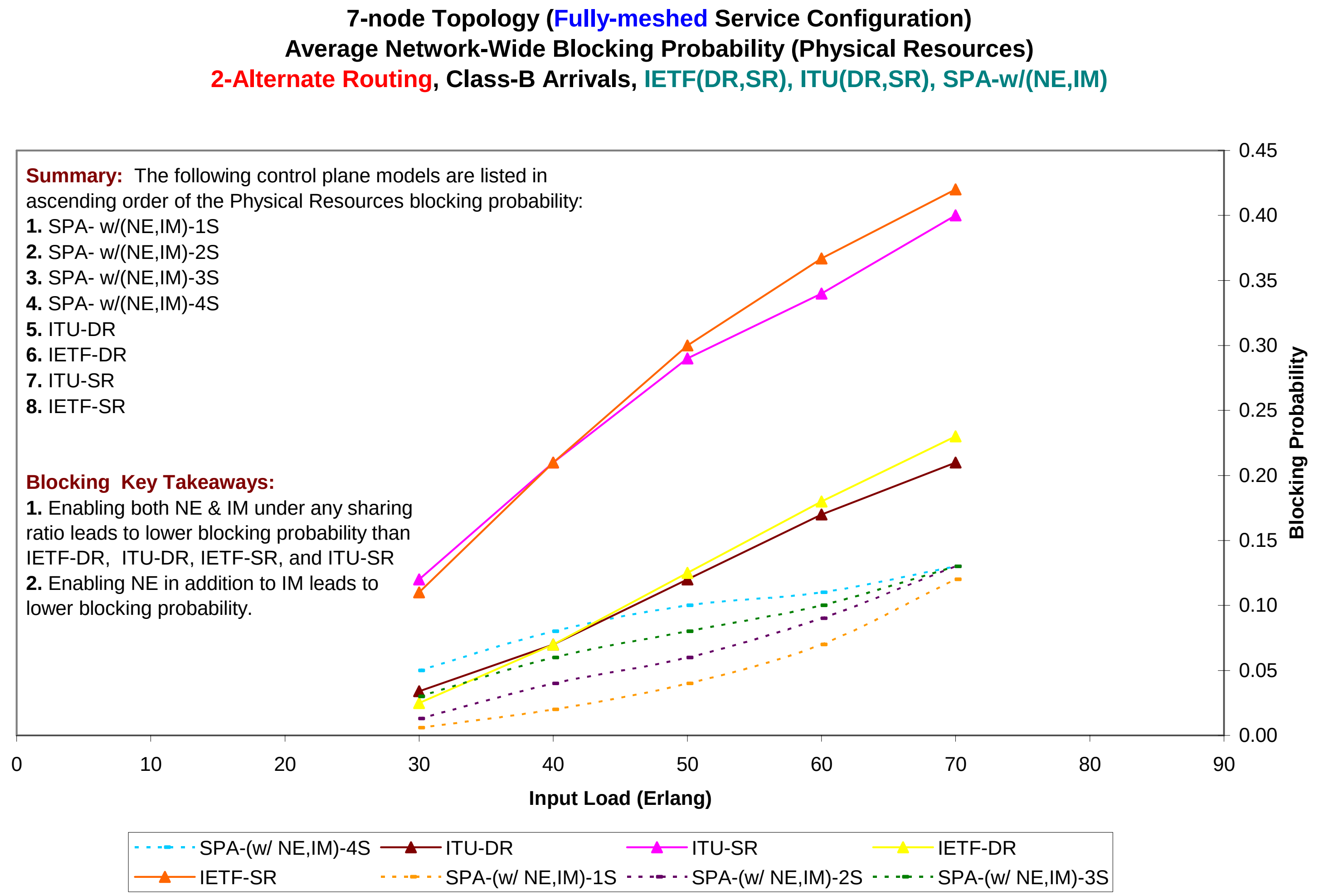

7-node Topology (Fully-meshed Service Configuration)
Average Network-Wide Blocking Probability (Physical Resources)
2-Alternate Routing, Class-B Arrivals, IETF(DR,SR), ITU(DR,SR), SPA-w/(NE,IM)

Summary: The following control plane models are listed in ascending order of the Physical Resources blocking probability:

1. SPA- w/(NE,IM)-1S
2. SPA- w/(NE,IM)-2S
3. SPA- w/(NE,IM)-3S
4. SPA- w/(NE,IM)-4S
5. ITU-DR
6. IETF-DR
7. ITU-SR
8. IETF-SR

Blocking Key Takeaways:

1. Enabling both NE & IM under any sharing ratio leads to lower blocking probability than IETF-DR, ITU-DR, IETF-SR, and ITU-SR
2. Enabling NE in addition to IM leads to lower blocking probability.

Figure 13-5: Average Network-Wide Blocking Probability (Physical Resources)-7 Node – 2 Alternate Route-IETF(DR,SR), ITU(DR,SR), SPA-w/(NE,IM)

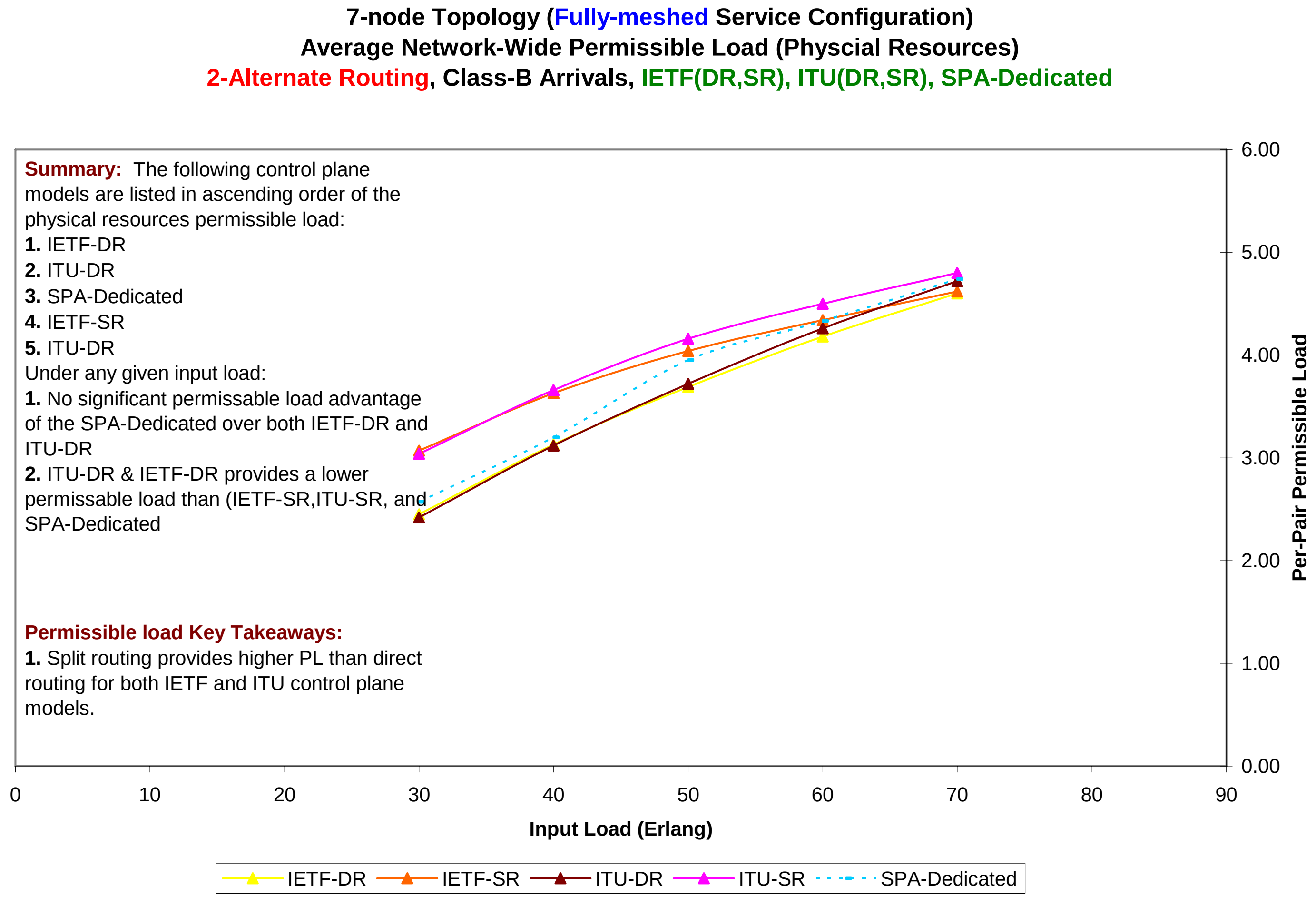

7-node Topology (Fully-meshed Service Configuration)
Average Network-Wide Permissible Load (Physcial Resources)
2-Alternate Routing, Class-B Arrivals, IETF(DR,SR), ITU(DR,SR), SPA-Dedicated

Summary: The following control plane models are listed in ascending order of the physical resources permissible load:

1. IETF-DR
2. ITU-DR
3. SPA-Dedicated
4. IETF-SR
5. ITU-DR

Under any given input load:

1. No significant permissable load advantage of the SPA-Dedicated over both IETF-DR and ITU-DR
2. ITU-DR & IETF-DR provides a lower permissable load than (IETF-SR,ITU-SR, and SPA-Dedicated

Permissible load Key Takeaways:

1. Split routing provides higher PL than direct routing for both IETF and ITU control plane models.

Figure 13-6: Average Network-Wide Permissible Load (Physical Resources)-7 Node –2 Alternate Route- IETF(DR,SR), ITU(DR,SR), SPA-Dedicated

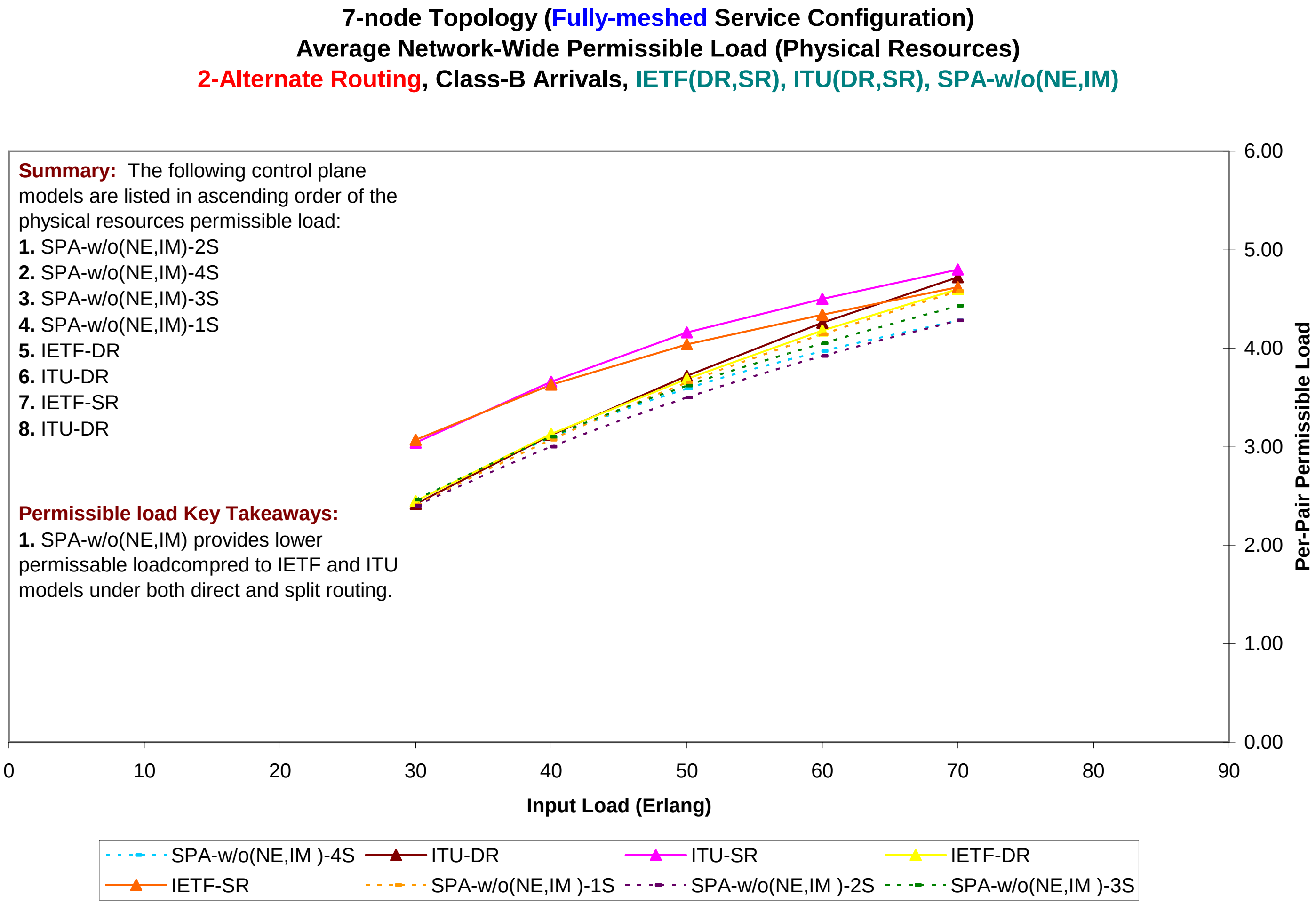

Summary: The following control plane models are listed in ascending order of the physical resources permissible load:

1. SPA-w/o(NE,IM)-2S
2. SPA-w/o(NE,IM)-4S
3. SPA-w/o(NE,IM)-3S
4. SPA-w/o(NE,IM)-1S
5. IETF-DR
6. ITU-DR
7. IETF-SR
8. ITU-DR

Permissible load Key Takeaways:

1. SPA-w/o(NE,IM) provides lower permissable loadcompred to IETF and ITU models under both direct and split routing.

Figure 13-7: Average Network-Wide Permissible Load (Physical Resources)-7 Node –2 Alternate Route- IETF(DR,SR), ITU(DR,SR), SPA-w/o(NE,IM)

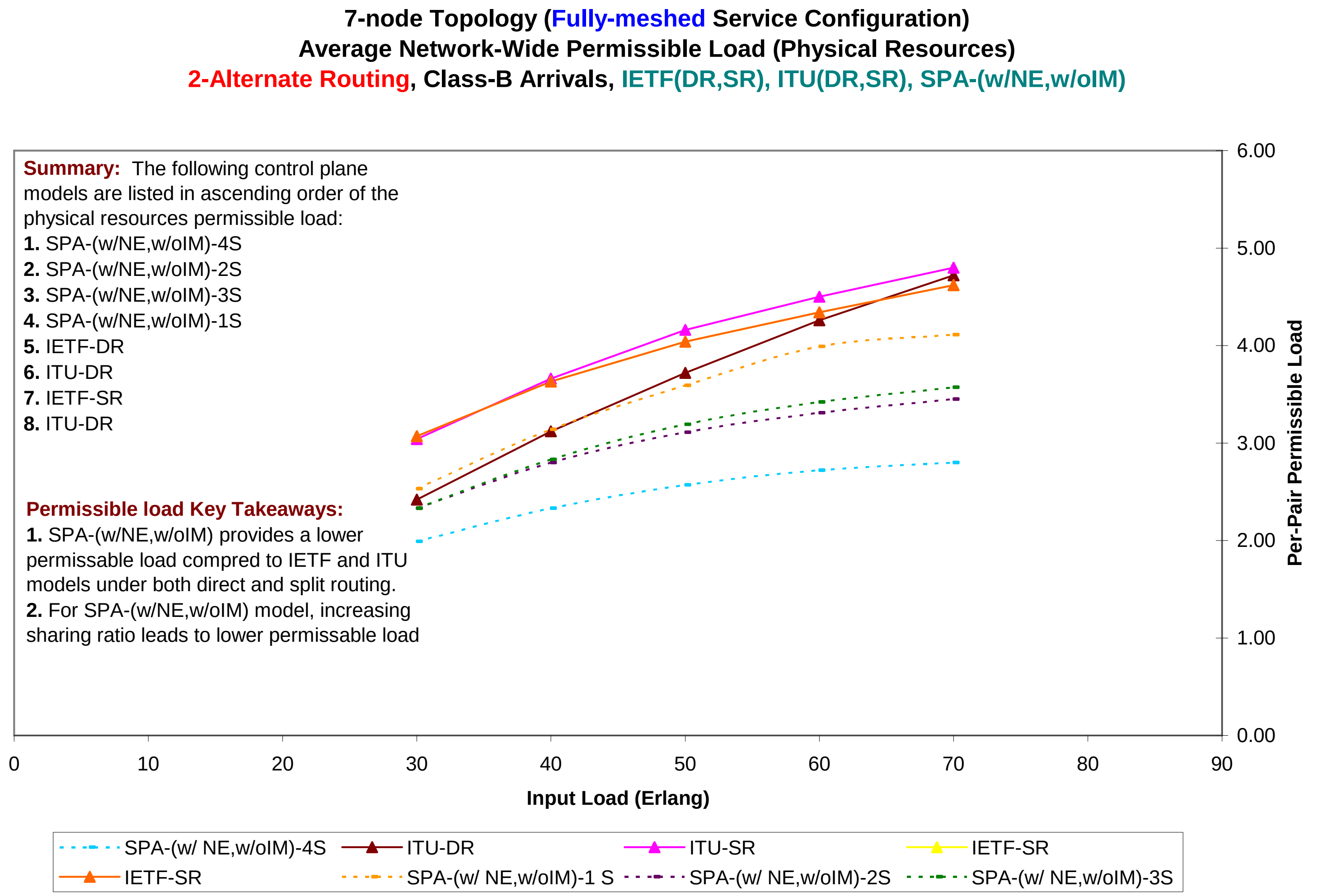

7-node Topology (Fully-meshed Service Configuration)
Average Network-Wide Permissible Load (Physical Resources)
2-Alternate Routing, Class-B Arrivals, IETF(DR,SR), ITU(DR,SR), SPA-(w/NE,w/oIM)

Summary: The following control plane models are listed in ascending order of the physical resources permissible load:
1. SPA-(w/NE,w/oIM)-4S
2. SPA-(w/NE,w/oIM)-2S
3. SPA-(w/NE,w/oIM)-3S
4. SPA-(w/NE,w/oIM)-1S
5. IETF-DR
6. ITU-DR
7. IETF-SR
8. ITU-DR

Permissible load Key Takeaways:
1. SPA-(w/NE,w/oIM) provides a lower permissable load compred to IETF and ITU models under both direct and split routing.
2. For SPA-(w/NE,w/oIM) model, increasing sharing ratio leads to lower permissable load

Figure 13-8: Average Network-Wide Permissible Load (Physical Resources)-7 Node – 2 Alternate Route- IETF(DR,SR), ITU(DR,SR), SPA-(w/NE,w/oIM)

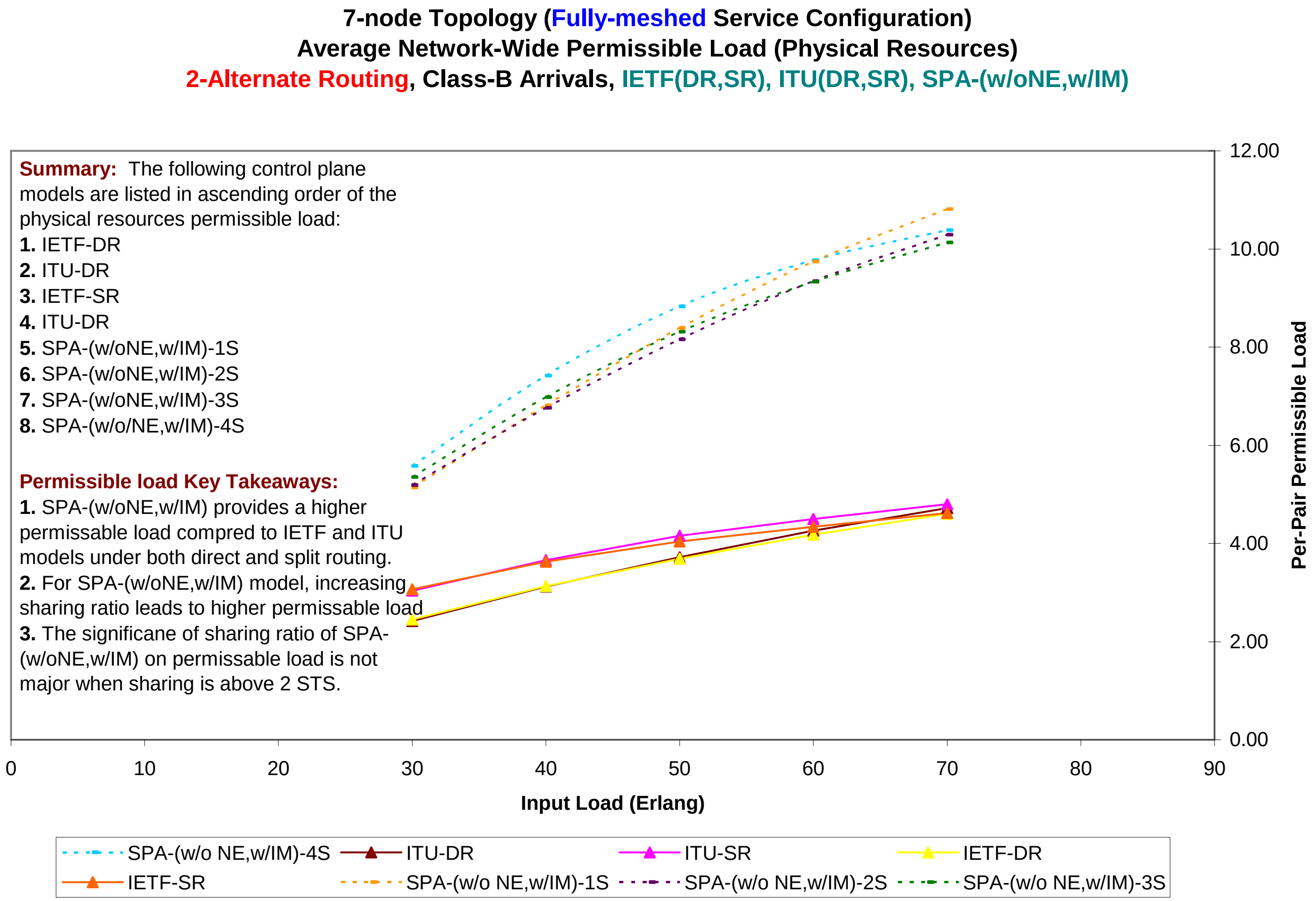

7-node Topology (Fully-meshed Service Configuration)
Average Network-Wide Permissible Load (Physical Resources)
2-Alternate Routing, Class-B Arrivals, IETF(DR,SR), ITU(DR,SR), SPA-(w/oNE,w/IM)

Summary: The following control plane models are listed in ascending order of the physical resources permissible load:

1. IETF-DR
2. ITU-DR
3. IETF-SR
4. ITU-DR
5. SPA-(w/oNE,w/IM)-1S
6. SPA-(w/oNE,w/IM)-2S
7. SPA-(w/oNE,w/IM)-3S
8. SPA-(w/o/NE,w/IM)-4S

Permissible load Key Takeaways:

1. SPA-(w/oNE,w/IM) provides a higher permissable load compred to IETF and ITU models under both direct and split routing.
2. For SPA-(w/oNE,w/IM) model, increasing sharing ratio leads to higher permissable load
3. The significane of sharing ratio of SPA-(w/oNE,w/IM) on permissable load is not major when sharing is above 2 STS.

Figure 13-9: Average Network-Wide Permissible Load (Physical Resources)-7 Node – 2 Alternate Route- IETF(DR,SR), ITU(DR,SR), SPA-(w/oNE,w/IM)

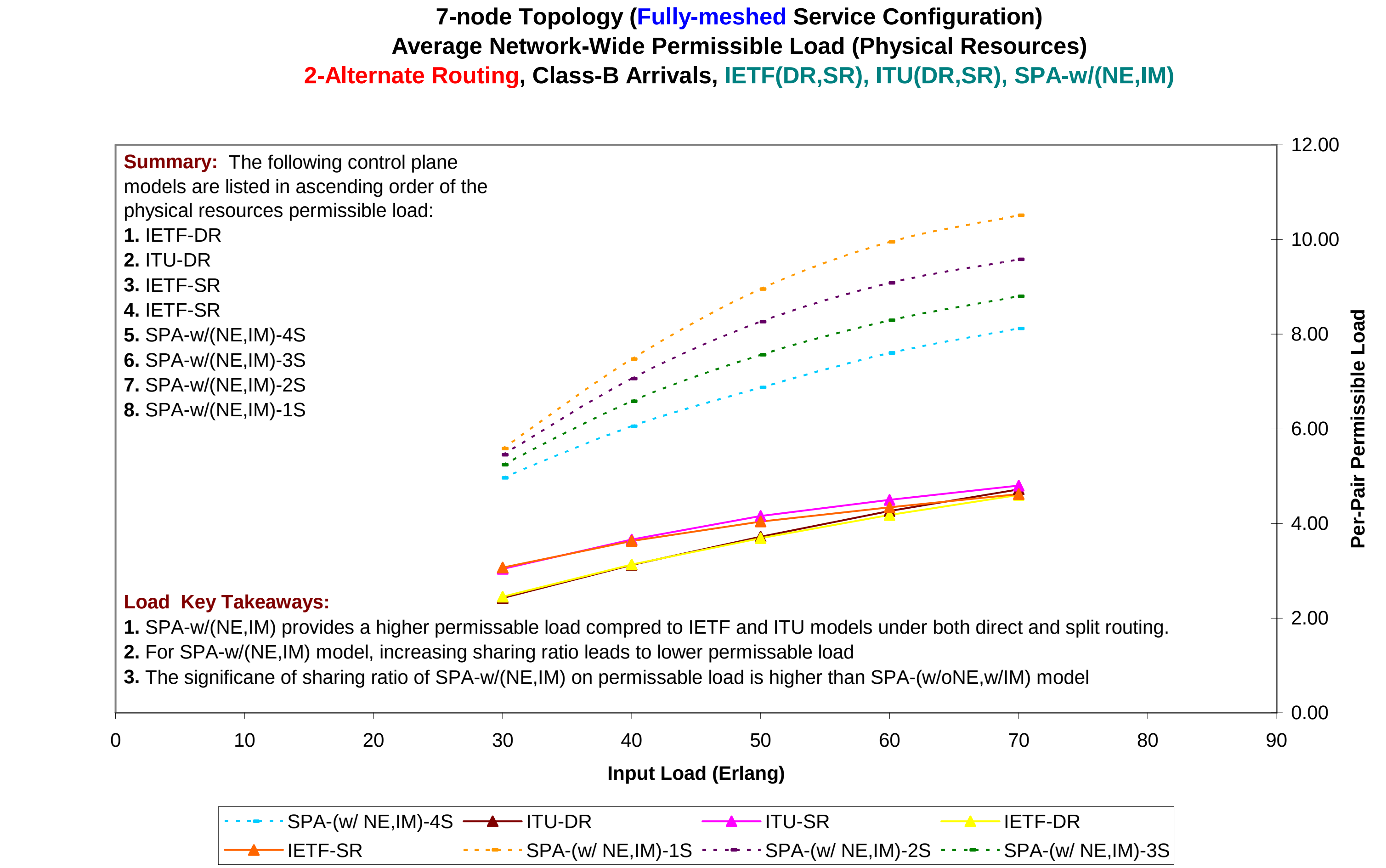

Summary: The following control plane models are listed in ascending order of the physical resources permissible load:

1. IETF-DR
2. ITU-DR
3. IETF-SR
4. IETF-SR
5. SPA-w/(NE,IM)-4S
6. SPA-w/(NE,IM)-3S
7. SPA-w/(NE,IM)-2S
8. SPA-w/(NE,IM)-1S

Load Key Takeaways:

1. SPA-w/(NE,IM) provides a higher permissable load compred to IETF and ITU models under both direct and split routing.
2. For SPA-w/(NE,IM) model, increasing sharing ratio leads to lower permissable load
3. The significane of sharing ratio of SPA-w/(NE,IM) on permissable load is higher than SPA-(w/oNE,w/IM) model

Figure 13-10: Average Network-Wide Permissible Load (Physical Resources)-7 Node –2 Alternate Route- IETF(DR,SR), ITU(DR,SR), SPA-w/(NE,IM)

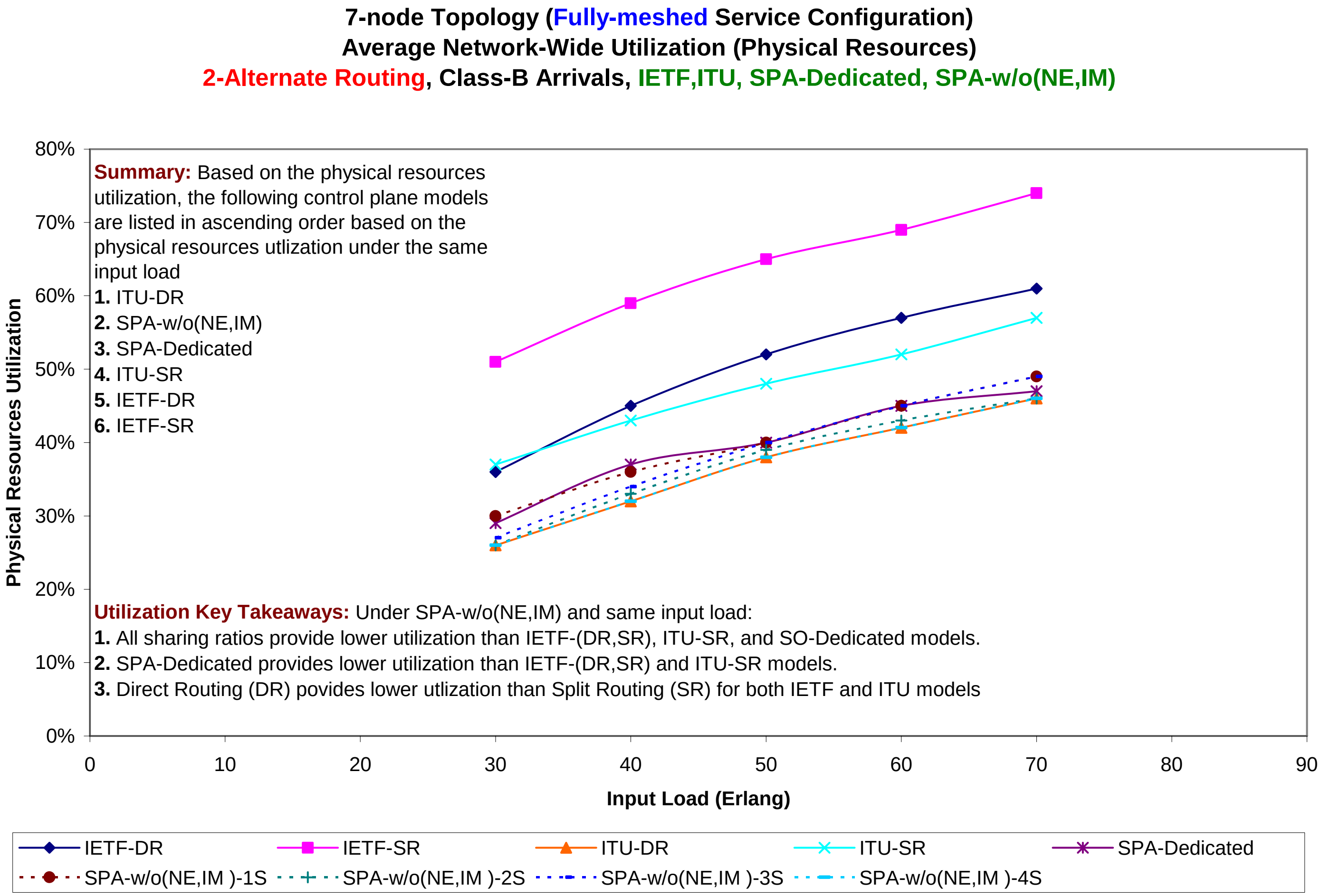

Figure 13-11: Average Network-Wide Utilization (Physical Resources)-7 Node –2 Alternate Route- IETF,ITU, SPA-Dedicated, SPA-w/o(NE,IM)

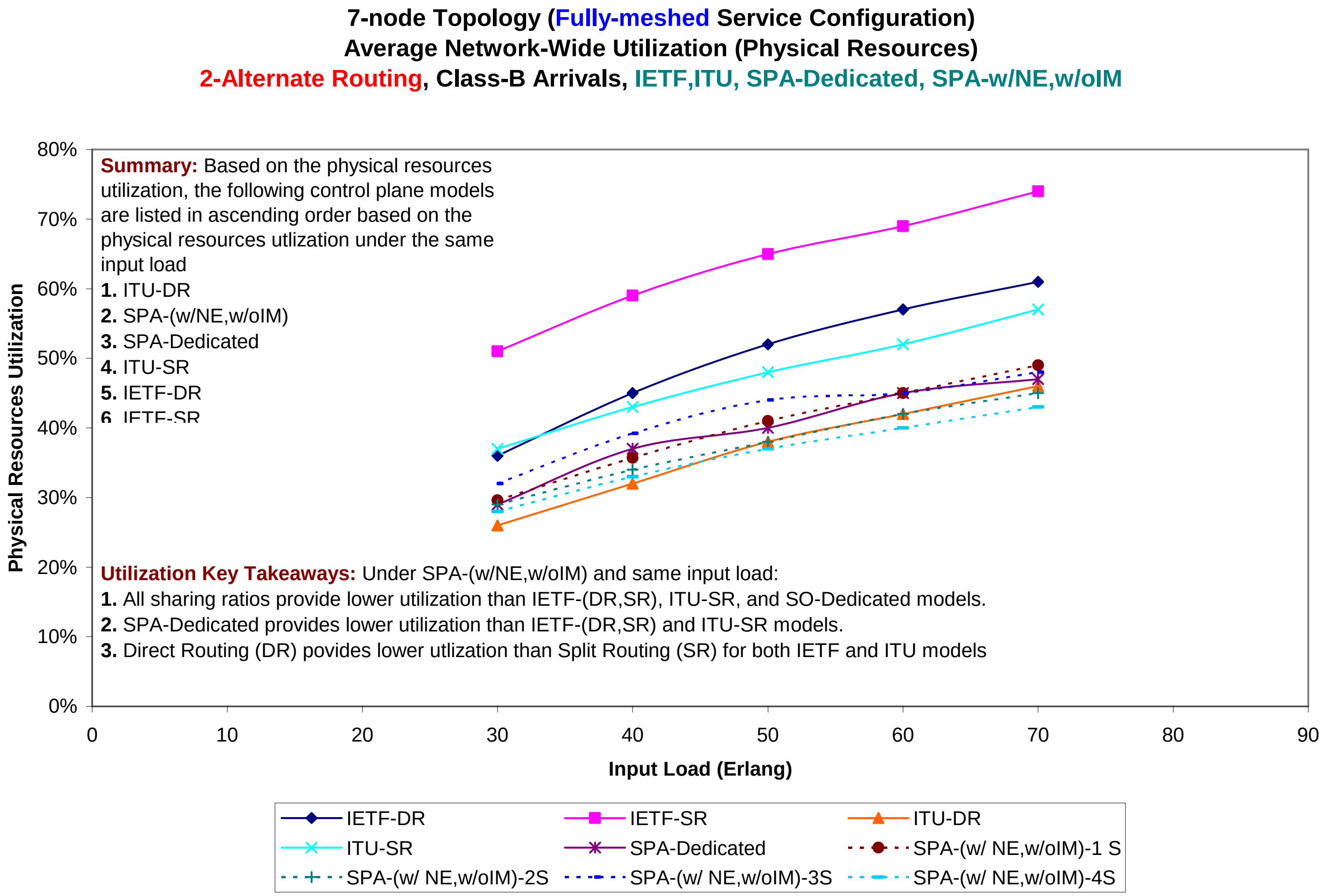

Summary: Based on the physical resources utilization, the following control plane models are listed in ascending order based on the physical resources utlization under the same input load

1. ITU-DR
2. SPA-(w/NE,w/oIM)
3. SPA-Dedicated
4. ITU-SR
5. IETF-DR
6. IETF-SR

Utilization Key Takeaways: Under SPA-(w/NE,w/oIM) and same input load:
1. All sharing ratios provide lower utilization than IETF-(DR,SR), ITU-SR, and SO-Dedicated models.
2. SPA-Dedicated provides lower utilization than IETF-(DR,SR) and ITU-SR models.
3. Direct Routing (DR) povides lower utlization than Split Routing (SR) for both IETF and ITU models

Figure 13-12: Average Network-Wide Utilization (Physical Resources)-7 Node –2 Alternate Route- IETF,ITU, SPA-Dedicated, SPA-w/NE,w/oIM

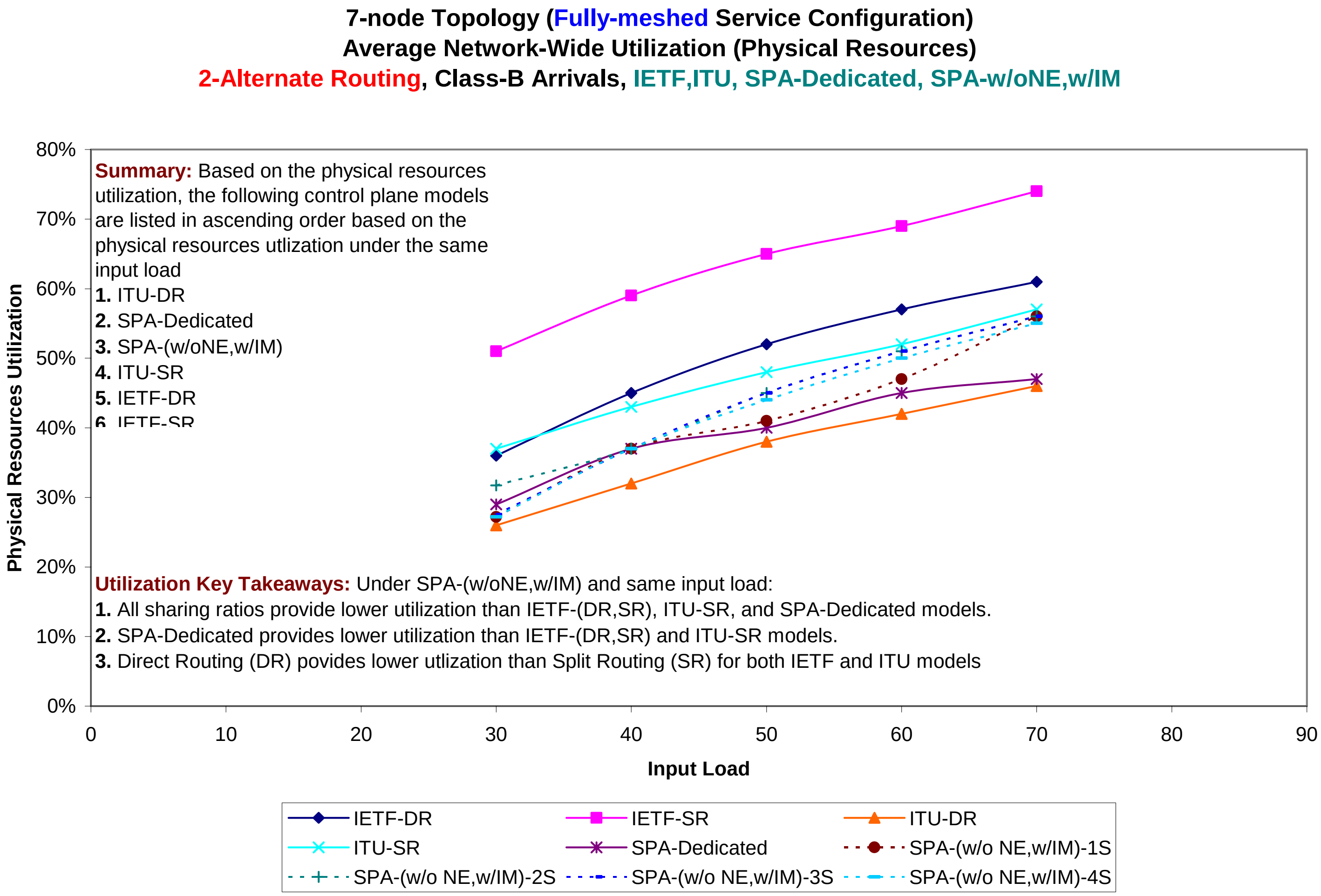

Summary: Based on the physical resources utilization, the following control plane models are listed in ascending order based on the physical resources utlization under the same input load

1. ITU-DR
2. SPA-Dedicated
3. SPA-(w/oNE,w/IM)
4. ITU-SR
5. IETF-DR
6. IETF-SR

Utilization Key Takeaways: Under SPA-(w/oNE,w/IM) and same input load:

1. All sharing ratios provide lower utilization than IETF-(DR,SR), ITU-SR, and SPA-Dedicated models.
2. SPA-Dedicated provides lower utilization than IETF-(DR,SR) and ITU-SR models.
3. Direct Routing (DR) povides lower utlization than Split Routing (SR) for both IETF and ITU models

Figure 13-13: Average Network-Wide Utilization (Physical Resources)-7 Node –2 Alternate Route- IETF,ITU, SPA-Dedicated, SPA-w/oNE,w/IM

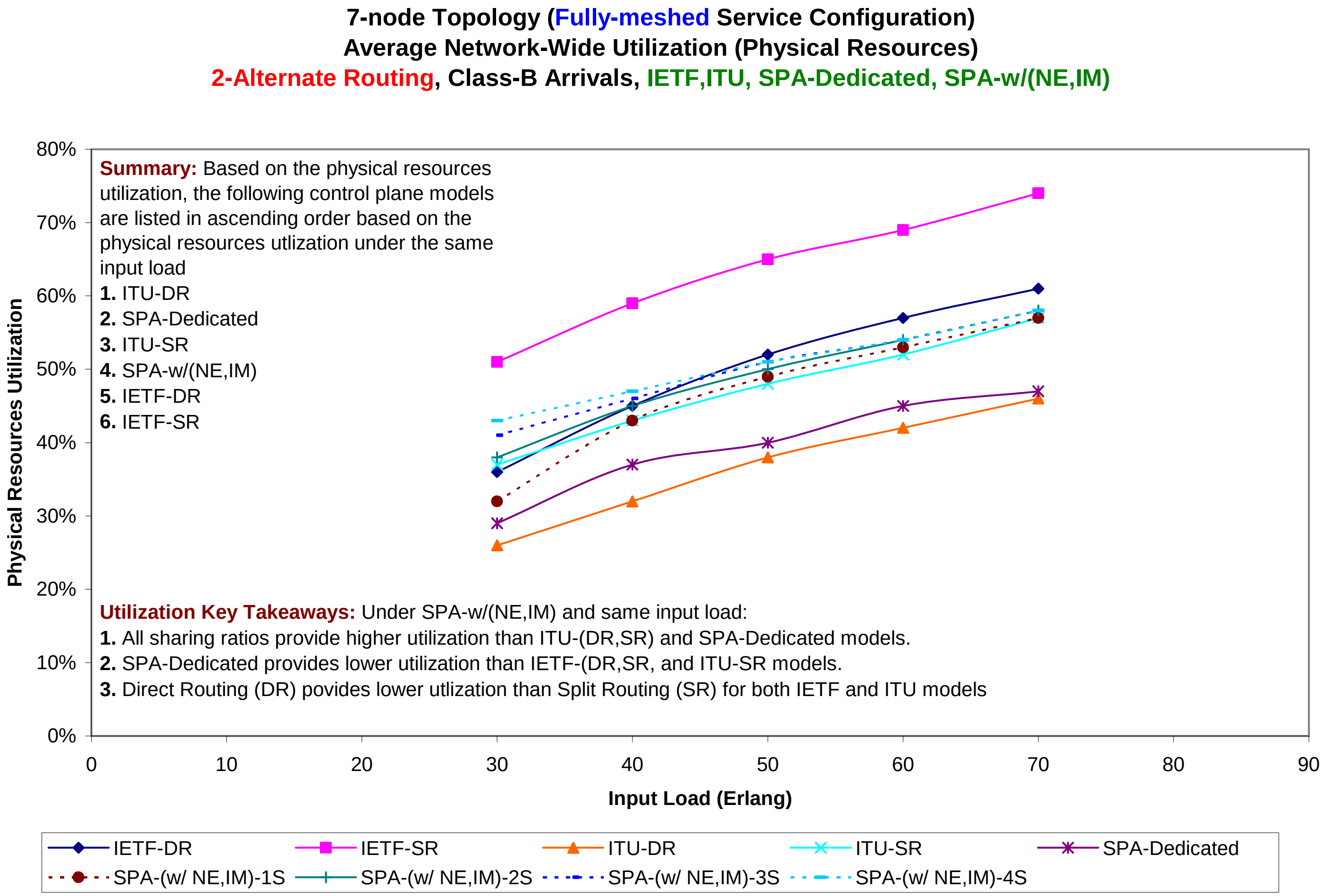
7-node Topology (Fully-meshed Service Configuration)
Average Network-Wide Utilization (Physical Resources)
2-Alternate Routing, Class-B Arrivals, IETF,ITU, SPA-Dedicated, SPA-w/(NE,IM)

Summary: Based on the physical resources utilization, the following control plane models are listed in ascending order based on the physical resources utlization under the same input load

1. ITU-DR
2. SPA-Dedicated
3. ITU-SR
4. SPA-w/(NE,IM)
5. IETF-DR
6. IETF-SR

Utilization Key Takeaways: Under SPA-w/(NE,IM) and same input load:

1. All sharing ratios provide higher utilization than ITU-(DR,SR) and SPA-Dedicated models.
2. SPA-Dedicated provides lower utilization than IETF-(DR,SR, and ITU-SR models.
3. Direct Routing (DR) povides lower utlization than Split Routing (SR) for both IETF and ITU models

Figure 13-14: Average Network-Wide Utilization (Physical Resources)-7 Node – 2 Alternate Route-IETF,ITU, SPA-Dedicated, SPA-w/(NE,IM)

7-node Topology (Fully-meshed Service Configuration)
Average Network-Wide Blocking Probability (Physcial Resources)
3-Alternate Routing, Class-B Arrivals, IETF(DR,SR), ITU(DR,SR), SPA-Dedicated

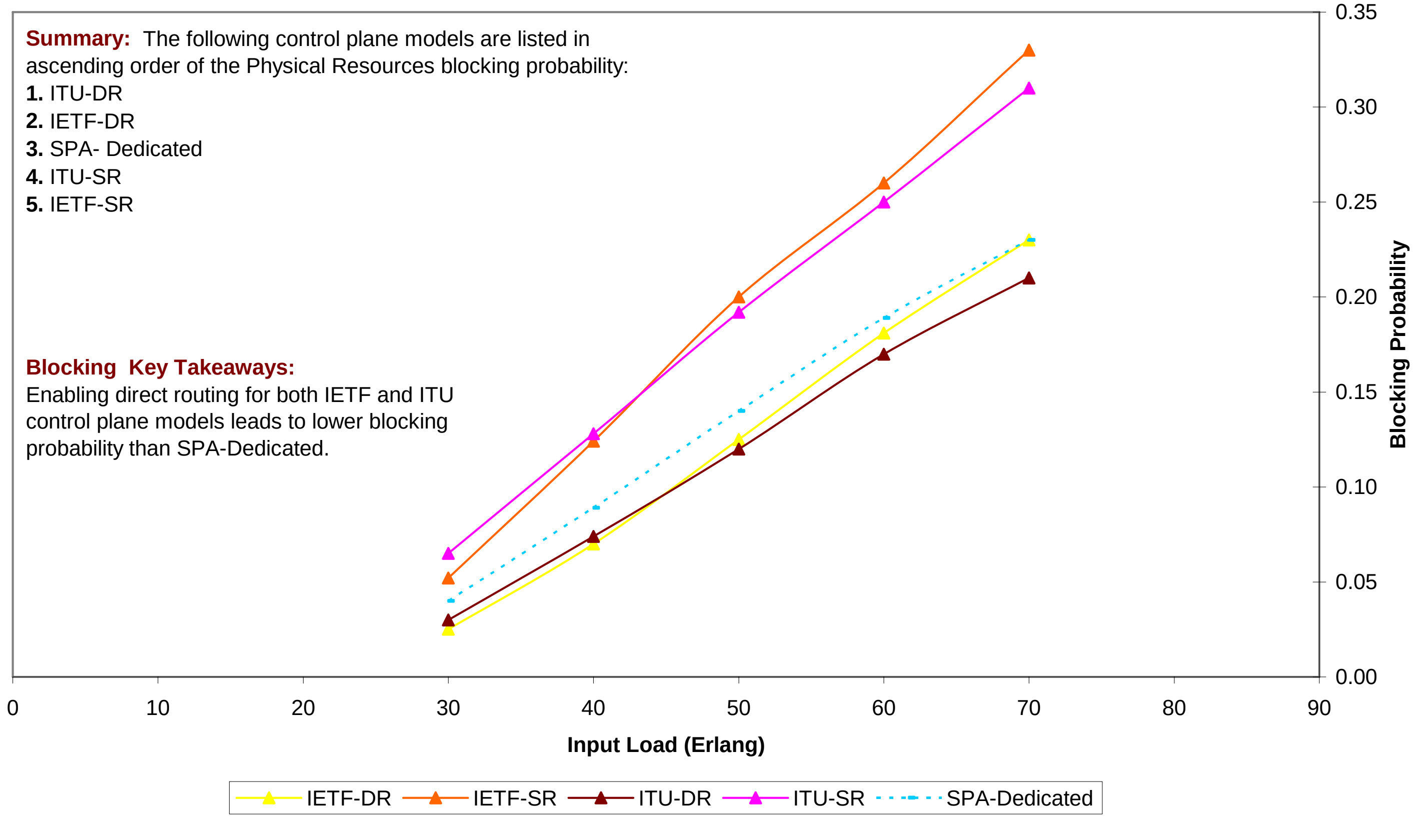

Summary: The following control plane models are listed in ascending order of the Physical Resources blocking probability:

1. ITU-DR
2. IETF-DR
3. SPA- Dedicated
4. ITU-SR
5. IETF-SR

Blocking Key Takeaways:
Enabling direct routing for both IETF and ITU control plane models leads to lower blocking probability than SPA-Dedicated.

Figure 13-15: Average Network-Wide Blocking Probability (Physical Resources)-7 Node-3 Alternate Route- IETF (DR, SR), ITU (DR, SR), SPA-Dedicated

7-node Topology (Fully-meshed Service Configuration)
Average Network-Wide Blocking Probability (Physical Resources)
3-Alternate Routing, Class-B Arrivals, IETF(DR,SR), ITU(DR,SR), SPA-w/o(NE,IM)

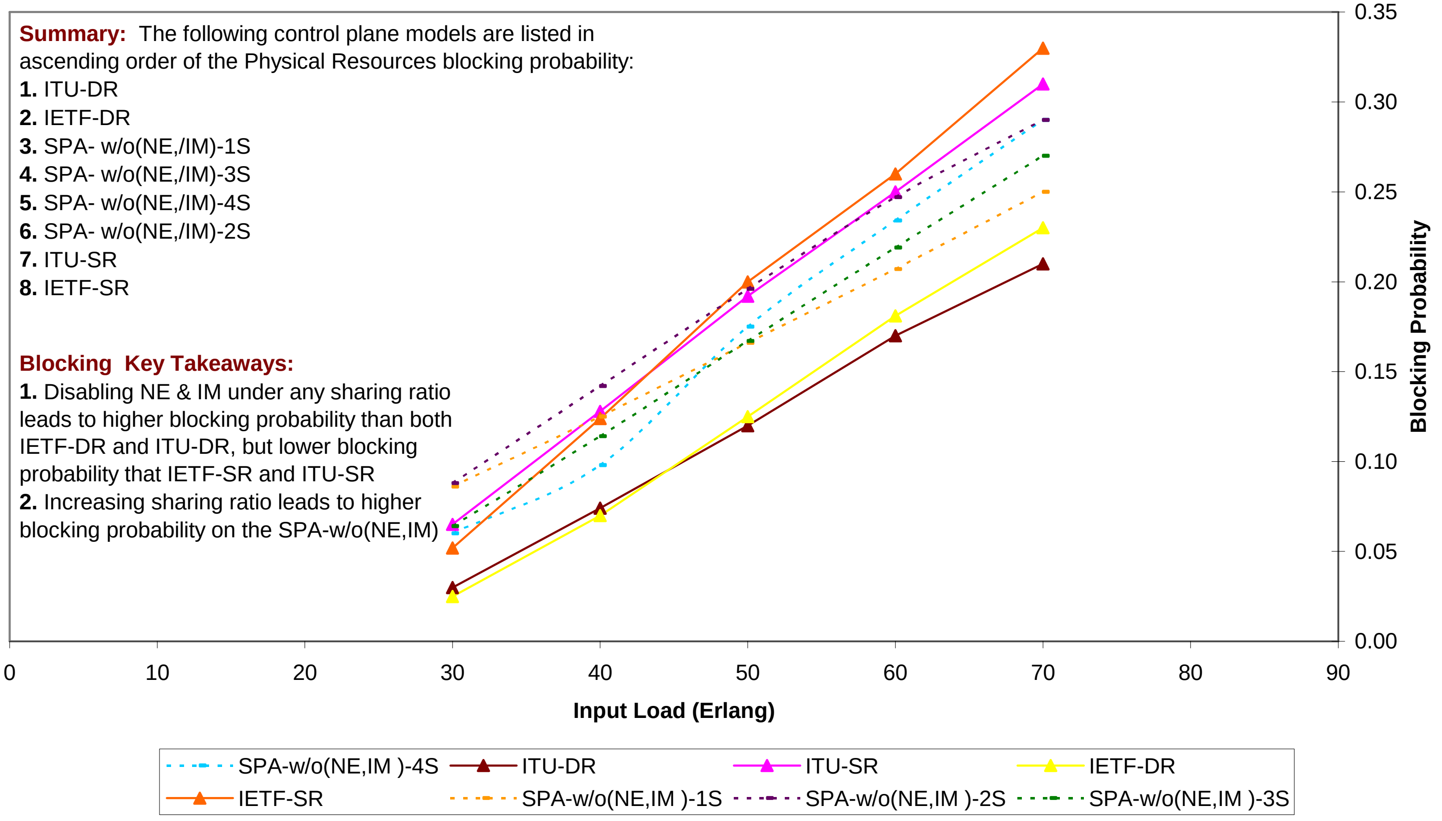

Summary: The following control plane models are listed in ascending order of the Physical Resources blocking probability:

1. ITU-DR
2. IETF-DR
3. SPA- w/o(NE,/IM)-1S
4. SPA- w/o(NE,/IM)-3S
5. SPA- w/o(NE,/IM)-4S
6. SPA- w/o(NE,/IM)-2S
7. ITU-SR
8. IETF-SR

Blocking Key Takeaways:

1. Disabling NE & IM under any sharing ratio leads to higher blocking probability than both IETF-DR and ITU-DR, but lower blocking probability that IETF-SR and ITU-SR

2. Increasing sharing ratio leads to higher blocking probability on the SPA-w/o(NE,IM)

Figure 13-16: Average Network-Wide Blocking Probability (Physical Resources)-7 Node –3 Alternate Route- IETF(DR,SR), ITU(DR,SR), SPA-w/o(NE,IM)

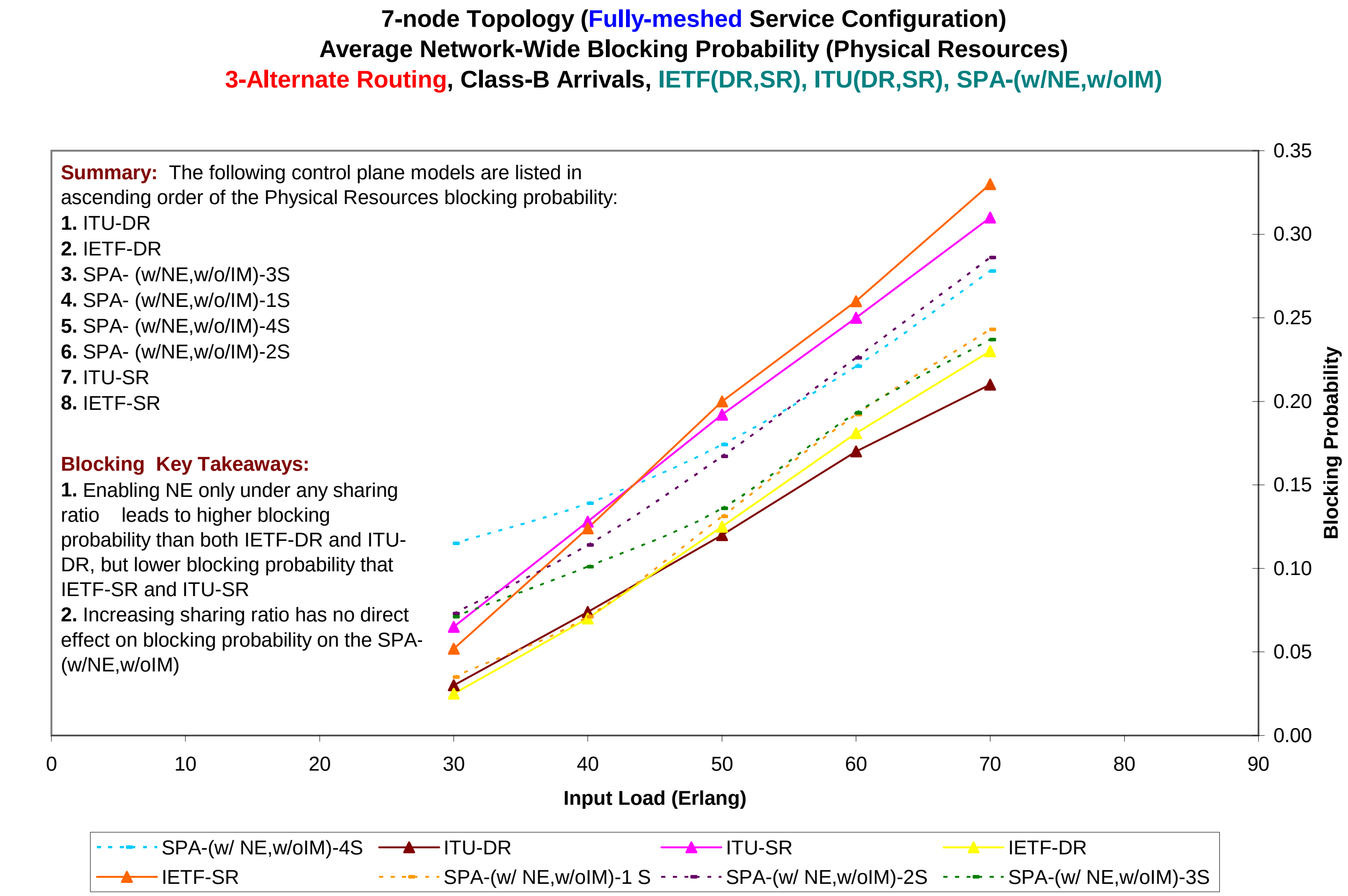

Summary: The following control plane models are listed in ascending order of the Physical Resources blocking probability:

1. ITU-DR
2. IETF-DR
3. SPA- (w/NE,w/o/IM)-3S
4. SPA- (w/NE,w/o/IM)-1S
5. SPA- (w/NE,w/o/IM)-4S
6. SPA- (w/NE,w/o/IM)-2S
7. ITU-SR
8. IETF-SR

Blocking Key Takeaways:

1. Enabling NE only under any sharing ratio leads to higher blocking probability than both IETF-DR and ITU-DR, but lower blocking probability that IETF-SR and ITU-SR

2. Increasing sharing ratio has no direct effect on blocking probability on the SPA-(w/NE,w/oIM)

Figure 13-17: Average Network-Wide Blocking Probability (Physical Resources)-7 Node – 3 Alternate Route-IETF(DR,SR), ITU(DR,SR), SPA-(w/NE,w/oIM)

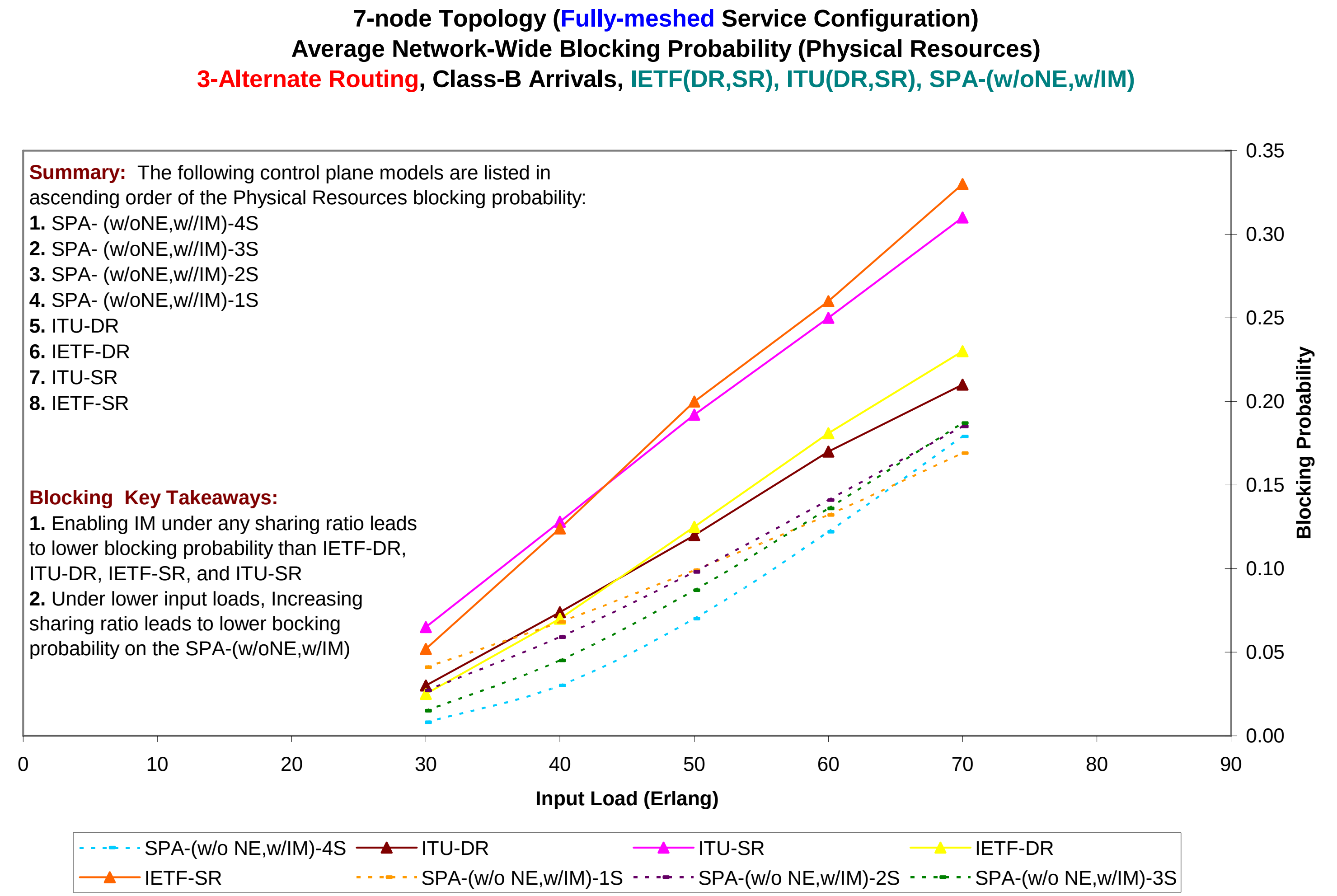

7-node Topology (Fully-meshed Service Configuration)
Average Network-Wide Blocking Probability (Physical Resources)
3-Alternate Routing, Class-B Arrivals, IETF(DR,SR), ITU(DR,SR), SPA-(w/oNE,w/IM)

Summary: The following control plane models are listed in ascending order of the Physical Resources blocking probability:

1. SPA- (w/oNE,w//IM)-4S
2. SPA- (w/oNE,w//IM)-3S
3. SPA- (w/oNE,w//IM)-2S
4. SPA- (w/oNE,w//IM)-1S
5. ITU-DR
6. IETF-DR
7. ITU-SR
8. IETF-SR

Blocking Key Takeaways:

1. Enabling IM under any sharing ratio leads to lower blocking probability than IETF-DR, ITU-DR, IETF-SR, and ITU-SR
2. Under lower input loads, Increasing sharing ratio leads to lower bocking probability on the SPA-(w/oNE,w/IM)

Figure 13-18: Average Network-Wide Blocking Probability (Physical Resources)-7 Node – 3 Alternate Route-IETF(DR,SR), ITU(DR,SR), SPA-(w/oNE,w/IM)

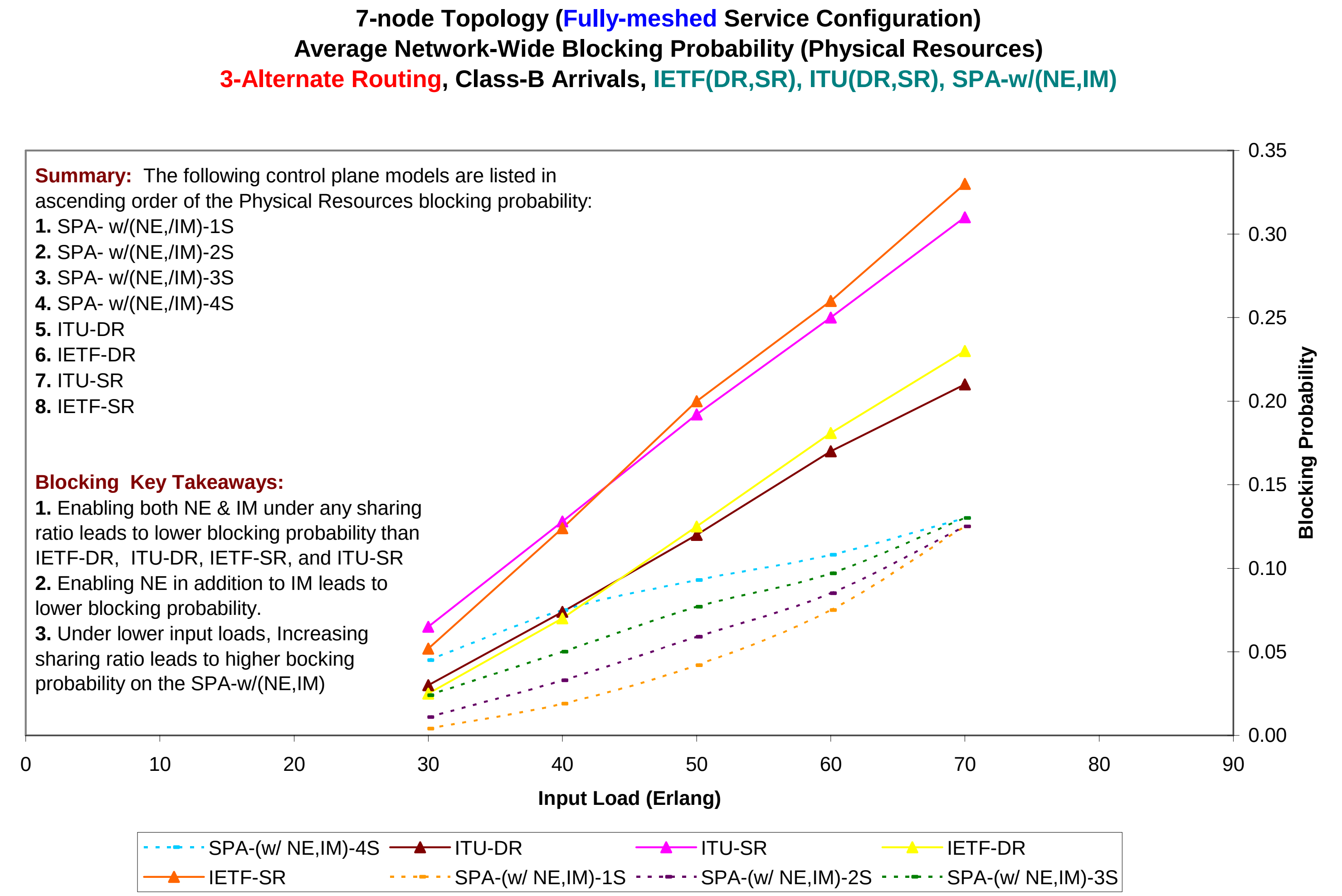

7-node Topology (Fully-meshed Service Configuration)
Average Network-Wide Blocking Probability (Physical Resources)
3-Alternate Routing, Class-B Arrivals, IETF(DR,SR), ITU(DR,SR), SPA-w/(NE,IM)

Summary: The following control plane models are listed in ascending order of the Physical Resources blocking probability:

1. SPA- w/(NE,/IM)-1S
2. SPA- w/(NE,/IM)-2S
3. SPA- w/(NE,/IM)-3S
4. SPA- w/(NE,/IM)-4S
5. ITU-DR
6. IETF-DR
7. ITU-SR
8. IETF-SR

Blocking Key Takeaways:

1. Enabling both NE & IM under any sharing ratio leads to lower blocking probability than IETF-DR, ITU-DR, IETF-SR, and ITU-SR
2. Enabling NE in addition to IM leads to lower blocking probability.
3. Under lower input loads, Increasing sharing ratio leads to higher bocking probability on the SPA-w/(NE,IM)

Figure 13-19: Average Network-Wide Blocking Probability (Physical Resources)-7 Node – 3 Alternate Route-IETF(DR,SR), ITU(DR,SR), SPA-w/(NE,IM)

7-node Topology (Fully-meshed Service Configuration)
Average Network-Wide Permissible Load (Physcial Resources)
3-Alternate Routing, Class-B Arrivals, IETF(DR,SR), ITU(DR,SR), SPA-Dedicated

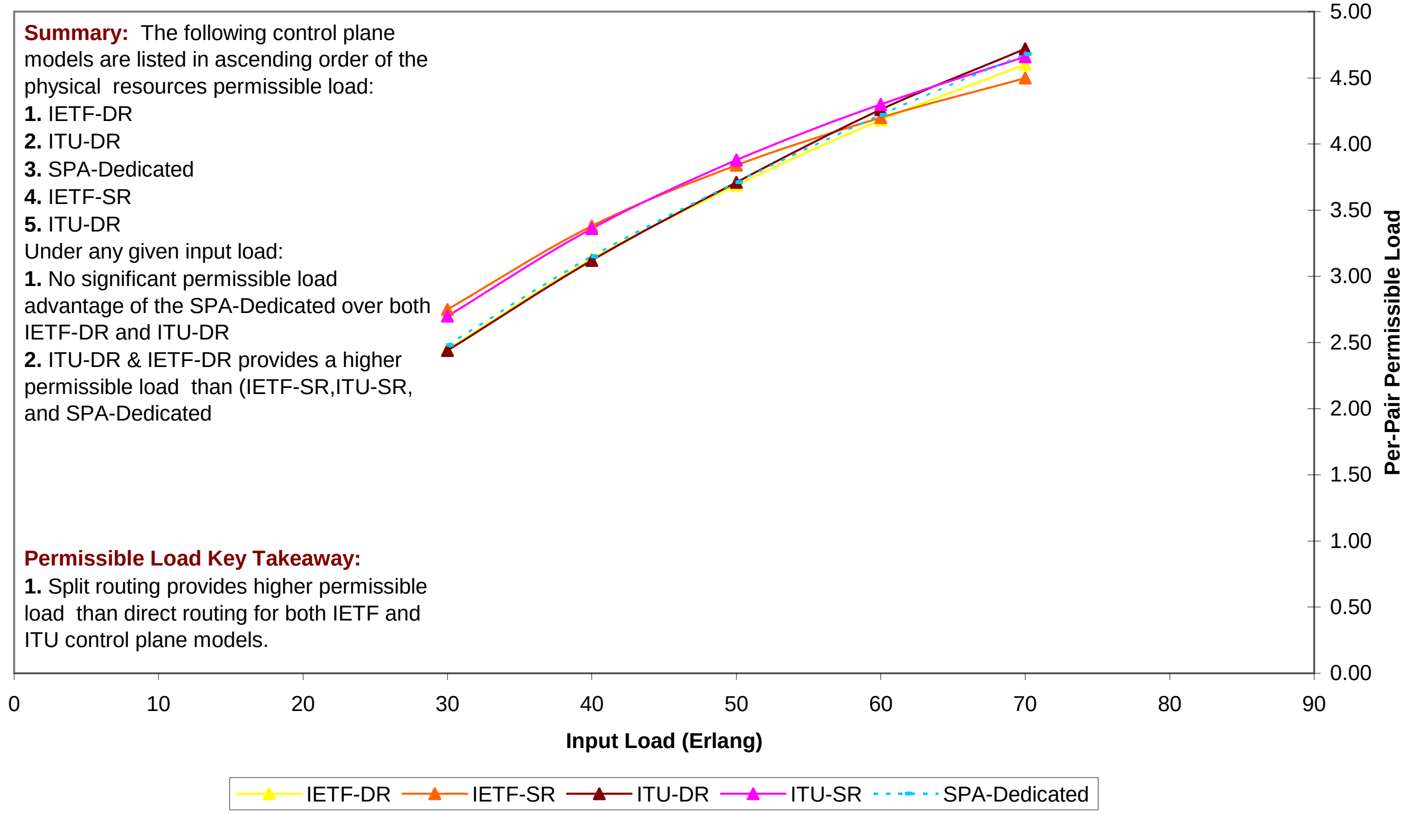

Summary: The following control plane models are listed in ascending order of the physical resources permissible load:
1. IETF-DR
2. ITU-DR
3. SPA-Dedicated
4. IETF-SR
5. ITU-DR
Under any given input load:
1. No significant permissible load advantage of the SPA-Dedicated over both IETF-DR and ITU-DR
2. ITU-DR & IETF-DR provides a higher permissible load than (IETF-SR,ITU-SR, and SPA-Dedicated

Permissible Load Key Takeaway:
1. Split routing provides higher permissible load than direct routing for both IETF and ITU control plane models.

Figure 13-20: Average Network-Wide Permissible Load (Physical Resources)-7 Node –3 Alternate Route- IETF(DR,SR), ITU(DR,SR), SPA-Dedicated

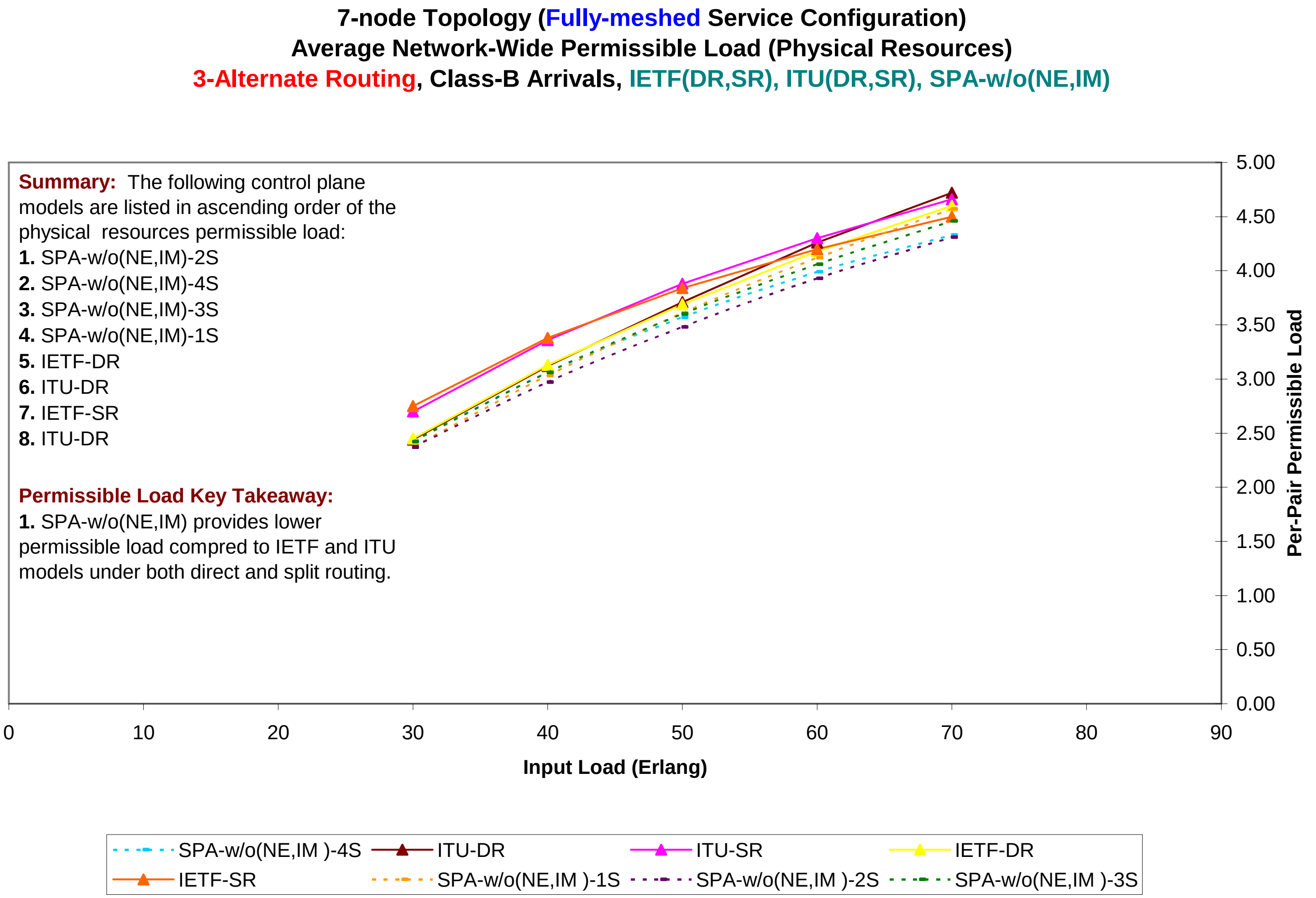

7-node Topology (Fully-meshed Service Configuration)
Average Network-Wide Permissible Load (Physical Resources)
3-Alternate Routing, Class-B Arrivals, IETF(DR,SR), ITU(DR,SR), SPA-w/o(NE,IM)

Summary: The following control plane models are listed in ascending order of the physical resources permissible load:

1. SPA-w/o(NE,IM)-2S
2. SPA-w/o(NE,IM)-4S
3. SPA-w/o(NE,IM)-3S
4. SPA-w/o(NE,IM)-1S
5. IETF-DR
6. ITU-DR
7. IETF-SR
8. ITU-DR

Permissible Load Key Takeaway:

1. SPA-w/o(NE,IM) provides lower permissible load compred to IETF and ITU models under both direct and split routing.

Figure 13-21: Average Network-Wide Permissible Load (Physical Resources)-7 Node –3 Alternate Route- IETF(DR,SR), ITU(DR,SR), SPA-w/o(NE,IM)

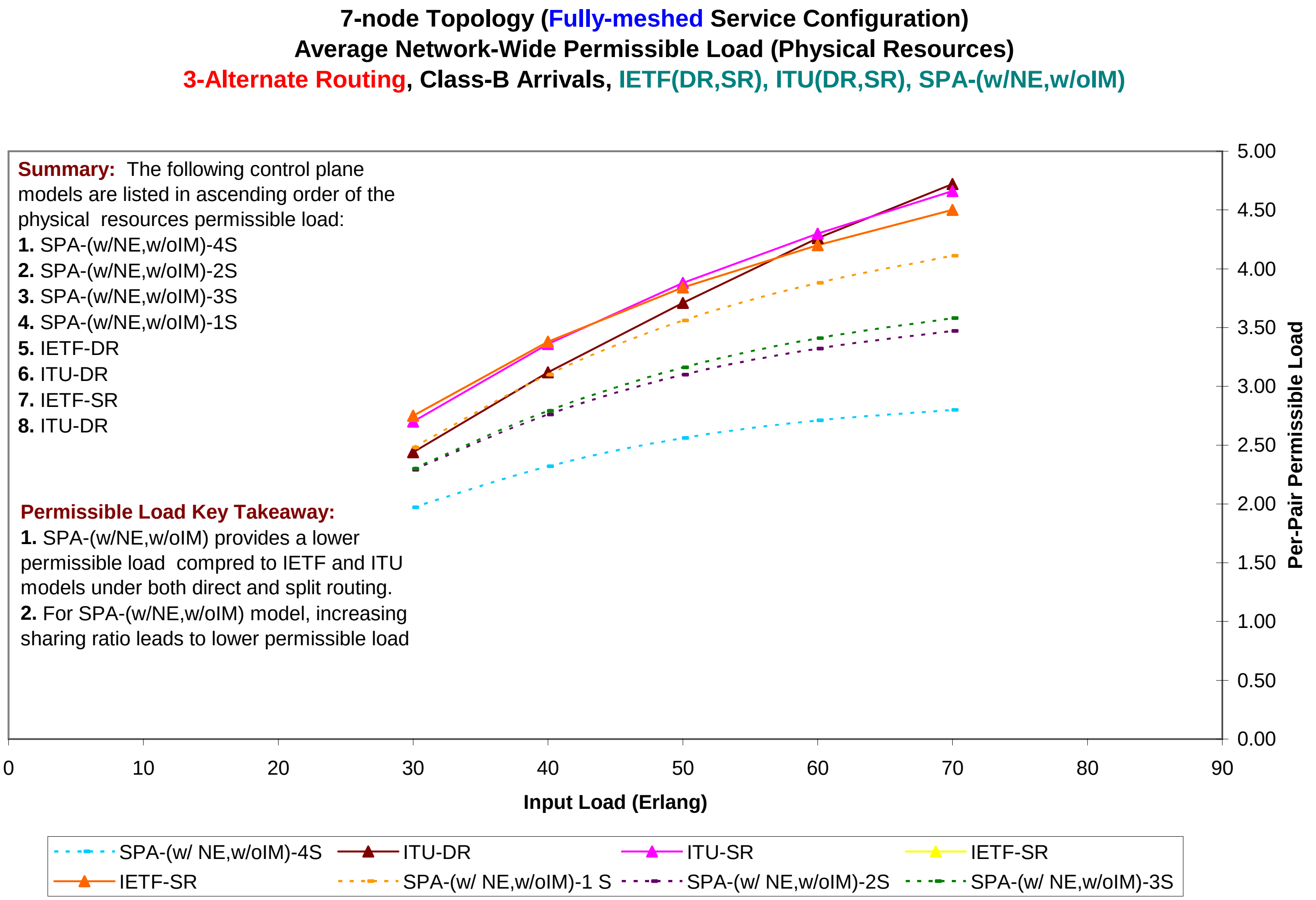

7-node Topology (Fully-meshed Service Configuration)
Average Network-Wide Permissible Load (Physical Resources)
3-Alternate Routing, Class-B Arrivals, IETF(DR,SR), ITU(DR,SR), SPA-(w/NE,w/oIM)

Summary: The following control plane models are listed in ascending order of the physical resources permissible load:

1. SPA-(w/NE,w/oIM)-4S
2. SPA-(w/NE,w/oIM)-2S
3. SPA-(w/NE,w/oIM)-3S
4. SPA-(w/NE,w/oIM)-1S
5. IETF-DR
6. ITU-DR
7. IETF-SR
8. ITU-DR

Permissible Load Key Takeaway:
1. SPA-(w/NE,w/oIM) provides a lower permissible load compred to IETF and ITU models under both direct and split routing.
2. For SPA-(w/NE,w/oIM) model, increasing sharing ratio leads to lower permissible load

Figure 13-22: Average Network-Wide Permissible Load (Physical Resources)-7 Node – 3 Alternate Route- IETF(DR,SR), ITU(DR,SR), SPA-(w/NE,w/oIM)

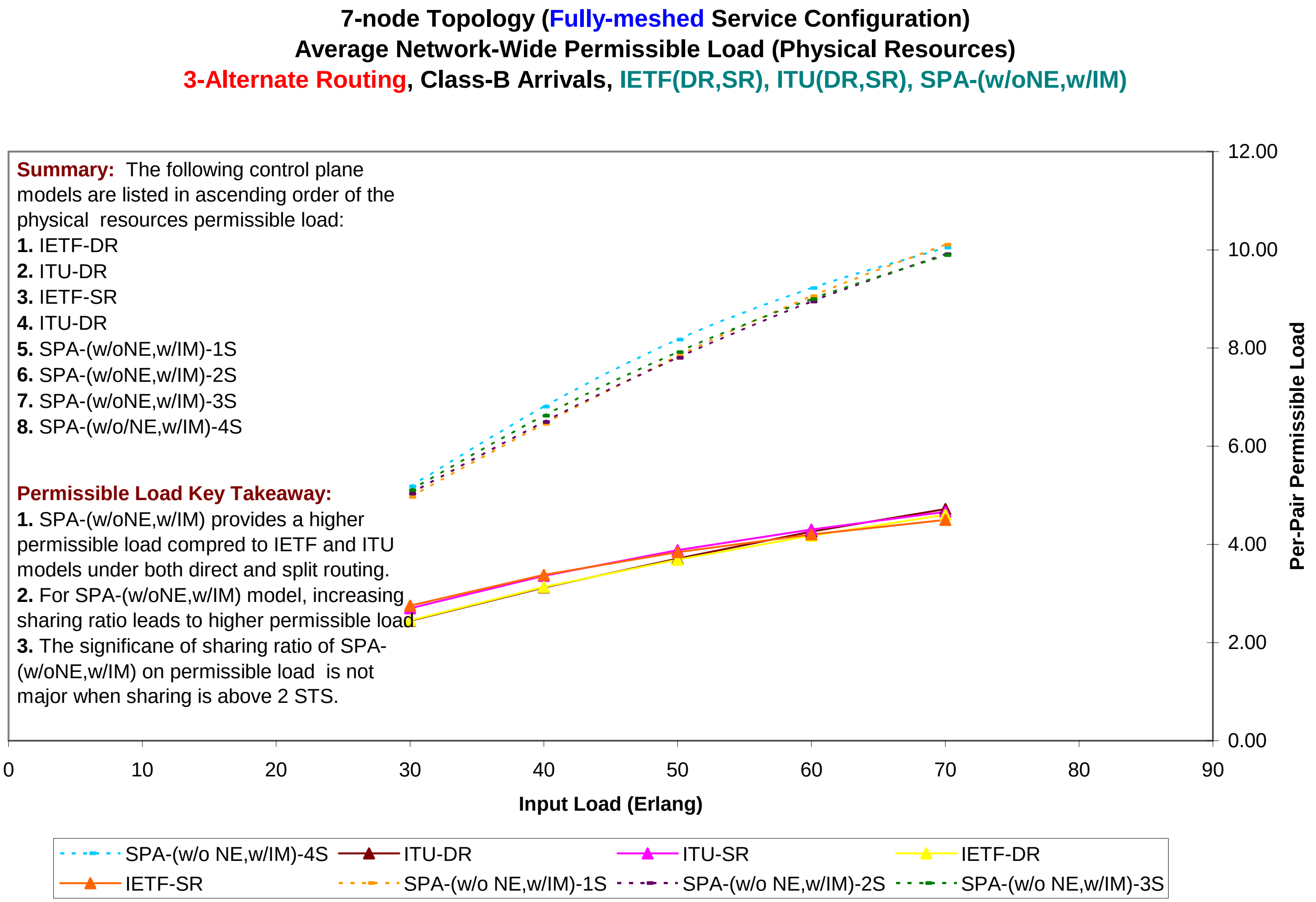

7-node Topology (Fully-meshed Service Configuration)
Average Network-Wide Permissible Load (Physical Resources)
3-Alternate Routing, Class-B Arrivals, IETF(DR,SR), ITU(DR,SR), SPA-(w/oNE,w/IM)

Summary: The following control plane models are listed in ascending order of the physical resources permissible load:
1. IETF-DR
2. ITU-DR
3. IETF-SR
4. ITU-DR
5. SPA-(w/oNE,w/IM)-1S
6. SPA-(w/oNE,w/IM)-2S
7. SPA-(w/oNE,w/IM)-3S
8. SPA-(w/o/NE,w/IM)-4S

Permissible Load Key Takeaway:
1. SPA-(w/oNE,w/IM) provides a higher permissible load compred to IETF and ITU models under both direct and split routing.
2. For SPA-(w/oNE,w/IM) model, increasing sharing ratio leads to higher permissible load
3. The significane of sharing ratio of SPA-(w/oNE,w/IM) on permissible load is not major when sharing is above 2 STS.

Figure 13-23: Average Network-Wide Permissible Load (Physical Resources)-7 Node – 3 Alternate Route- IETF(DR,SR), ITU(DR,SR), SPA-(w/oNE,w/IM)

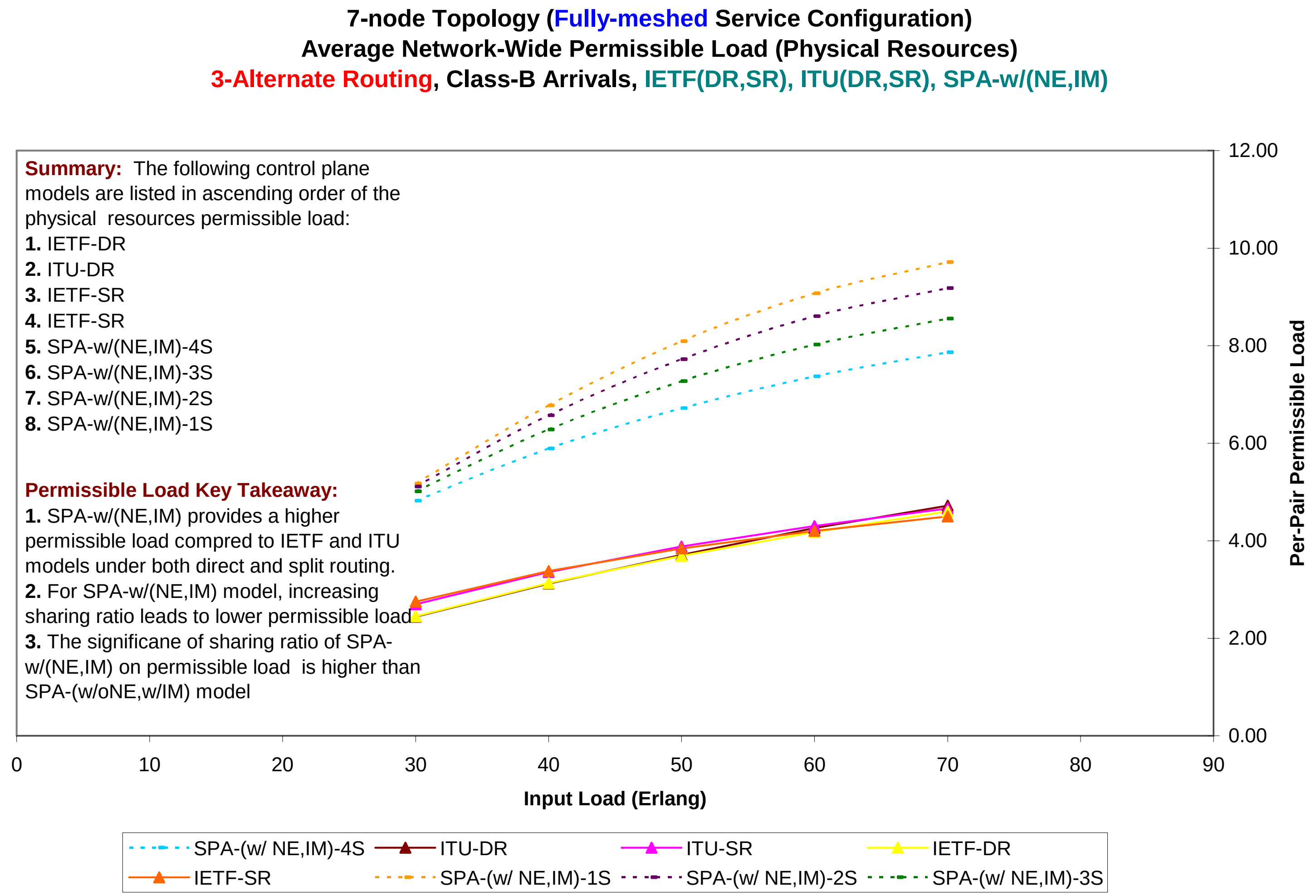

Summary: The following control plane models are listed in ascending order of the physical resources permissible load:

1. IETF-DR
2. ITU-DR
3. IETF-SR
4. IETF-SR
5. SPA-w/(NE,IM)-4S
6. SPA-w/(NE,IM)-3S
7. SPA-w/(NE,IM)-2S
8. SPA-w/(NE,IM)-1S

Permissible Load Key Takeaway:

1. SPA-w/(NE,IM) provides a higher permissible load compred to IETF and ITU models under both direct and split routing.
2. For SPA-w/(NE,IM) model, increasing sharing ratio leads to lower permissible load
3. The significane of sharing ratio of SPA-w/(NE,IM) on permissible load is higher than SPA-(w/oNE,w/IM) model

Figure 13-24: Average Network-Wide Permissible Load (Physical Resources)-7 Node –3 Alternate Route- IETF(DR,SR), ITU(DR,SR), SPA-w/(NE,IM)

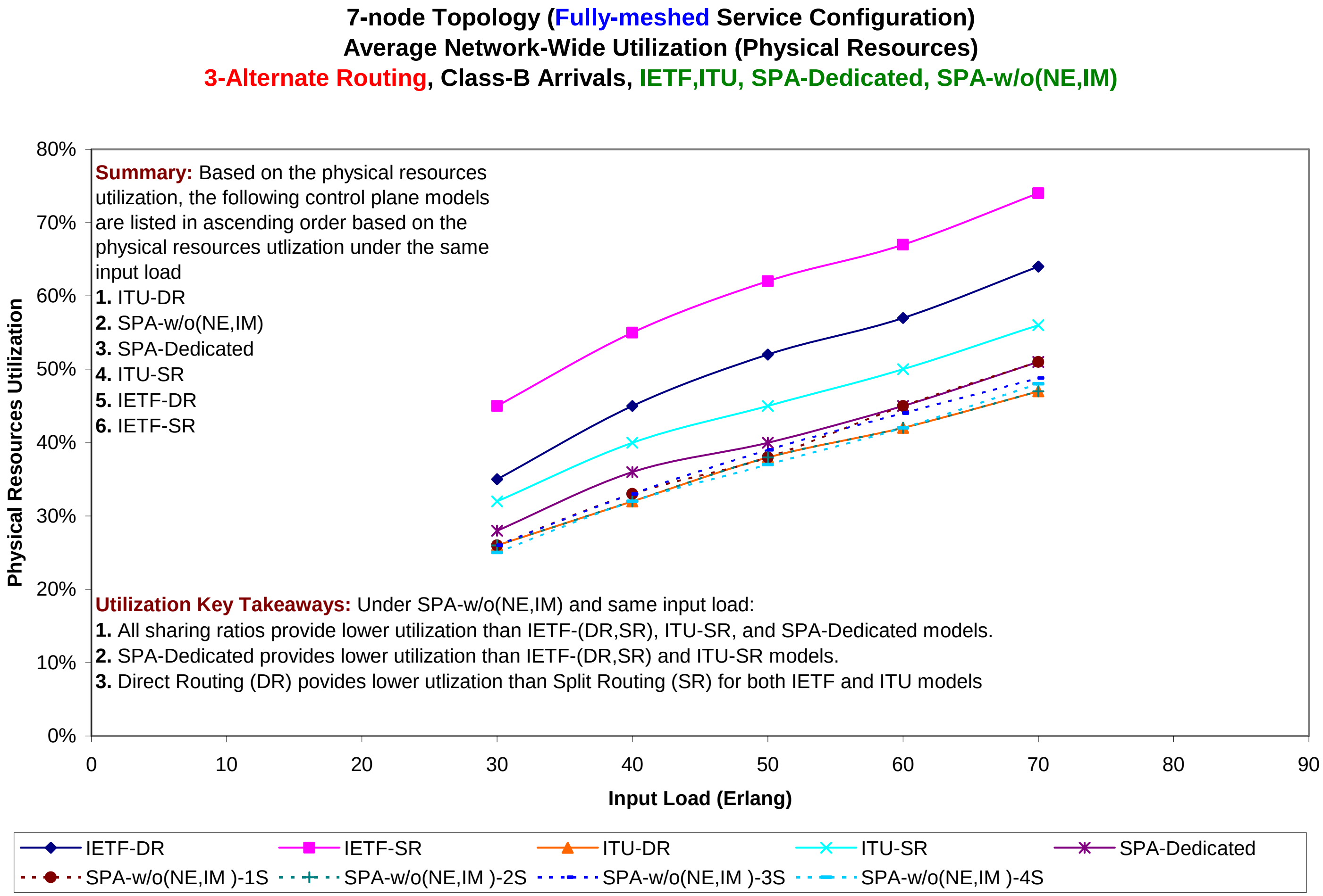

7-node Topology (Fully-meshed Service Configuration)
Average Network-Wide Utilization (Physical Resources)
3-Alternate Routing, Class-B Arrivals, IETF,ITU, SPA-Dedicated, SPA-w/o(NE,IM)

Summary: Based on the physical resources utilization, the following control plane models are listed in ascending order based on the physical resources utlization under the same input load

1. ITU-DR
2. SPA-w/o(NE,IM)
3. SPA-Dedicated
4. ITU-SR
5. IETF-DR
6. IETF-SR

Utilization Key Takeaways: Under SPA-w/o(NE,IM) and same input load:

1. All sharing ratios provide lower utilization than IETF-(DR,SR), ITU-SR, and SPA-Dedicated models.
2. SPA-Dedicated provides lower utilization than IETF-(DR,SR) and ITU-SR models.
3. Direct Routing (DR) povides lower utlization than Split Routing (SR) for both IETF and ITU models

Figure 13-25: Average Network-Wide Utilization (Physical Resources)-7 Node –3 Alternate Route- IETF,ITU, SPA-Dedicated, SPA-w/o(NE,IM)

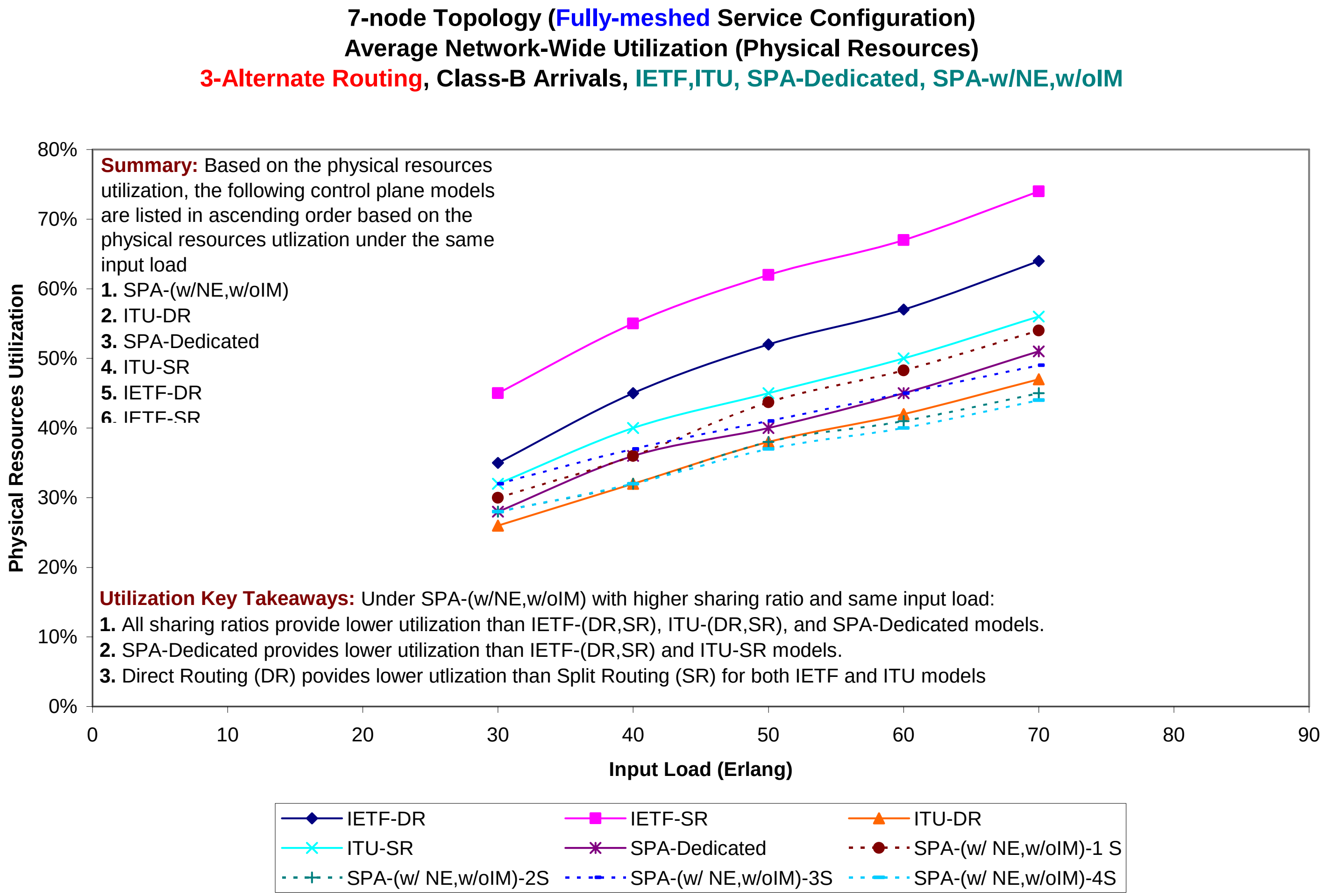

7-node Topology (Fully-meshed Service Configuration)
Average Network-Wide Utilization (Physical Resources)
3-Alternate Routing, Class-B Arrivals, IETF,ITU, SPA-Dedicated, SPA-w/NE,w/oIM

Summary: Based on the physical resources utilization, the following control plane models are listed in ascending order based on the physical resources utlization under the same input load

1. SPA-(w/NE,w/oIM)
2. ITU-DR
3. SPA-Dedicated
4. ITU-SR
5. IETF-DR
6. IETF-SR

Utilization Key Takeaways: Under SPA-(w/NE,w/oIM) with higher sharing ratio and same input load:

1. All sharing ratios provide lower utilization than IETF-(DR,SR), ITU-(DR,SR), and SPA-Dedicated models.
2. SPA-Dedicated provides lower utilization than IETF-(DR,SR) and ITU-SR models.
3. Direct Routing (DR) povides lower utlization than Split Routing (SR) for both IETF and ITU models

Figure 13-26: Average Network-Wide Utilization (Physical Resources)-7 Node –3 Alternate Route- IETF,ITU, SPA-Dedicated, SPA-w/NE,w/oIM

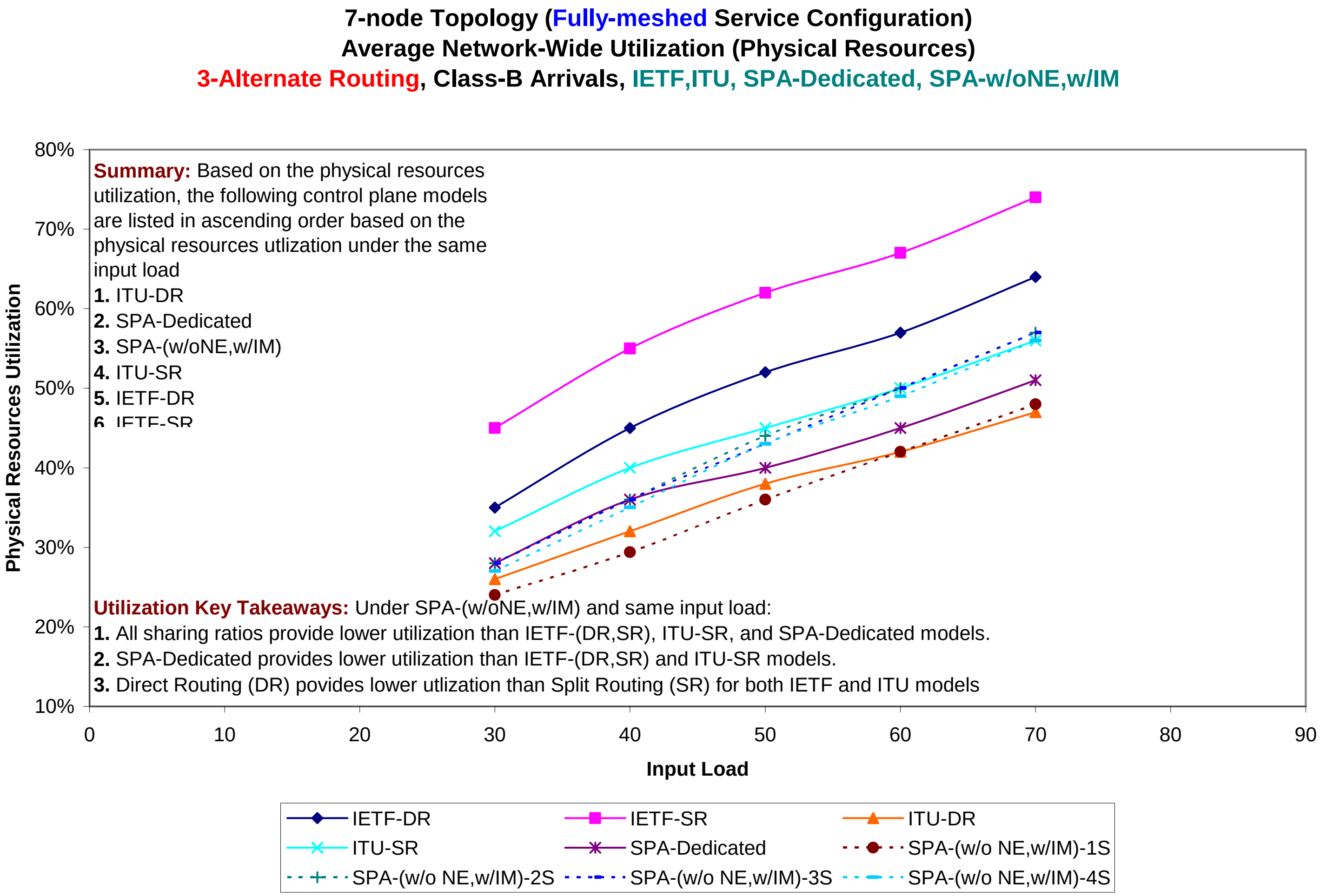

7-node Topology (Fully-meshed Service Configuration)
Average Network-Wide Utilization (Physical Resources)
3-Alternate Routing, Class-B Arrivals, IETF,ITU, SPA-Dedicated, SPA-w/oNE,w/IM

Summary: Based on the physical resources utilization, the following control plane models are listed in ascending order based on the physical resources utlization under the same input load

1. ITU-DR
2. SPA-Dedicated
3. SPA-(w/oNE,w/IM)
4. ITU-SR
5. IETF-DR
6. IETF-SR

Utilization Key Takeaways: Under SPA-(w/oNE,w/IM) and same input load:
1. All sharing ratios provide lower utilization than IETF-(DR,SR), ITU-SR, and SPA-Dedicated models.
2. SPA-Dedicated provides lower utilization than IETF-(DR,SR) and ITU-SR models.
3. Direct Routing (DR) povides lower utlization than Split Routing (SR) for both IETF and ITU models

Figure 13-27: Average Network-Wide Utilization (Physical Resources)-7 Node –3 Alternate Route- IETF,ITU, SPA-Dedicated, SPA-w/oNE,w/IM

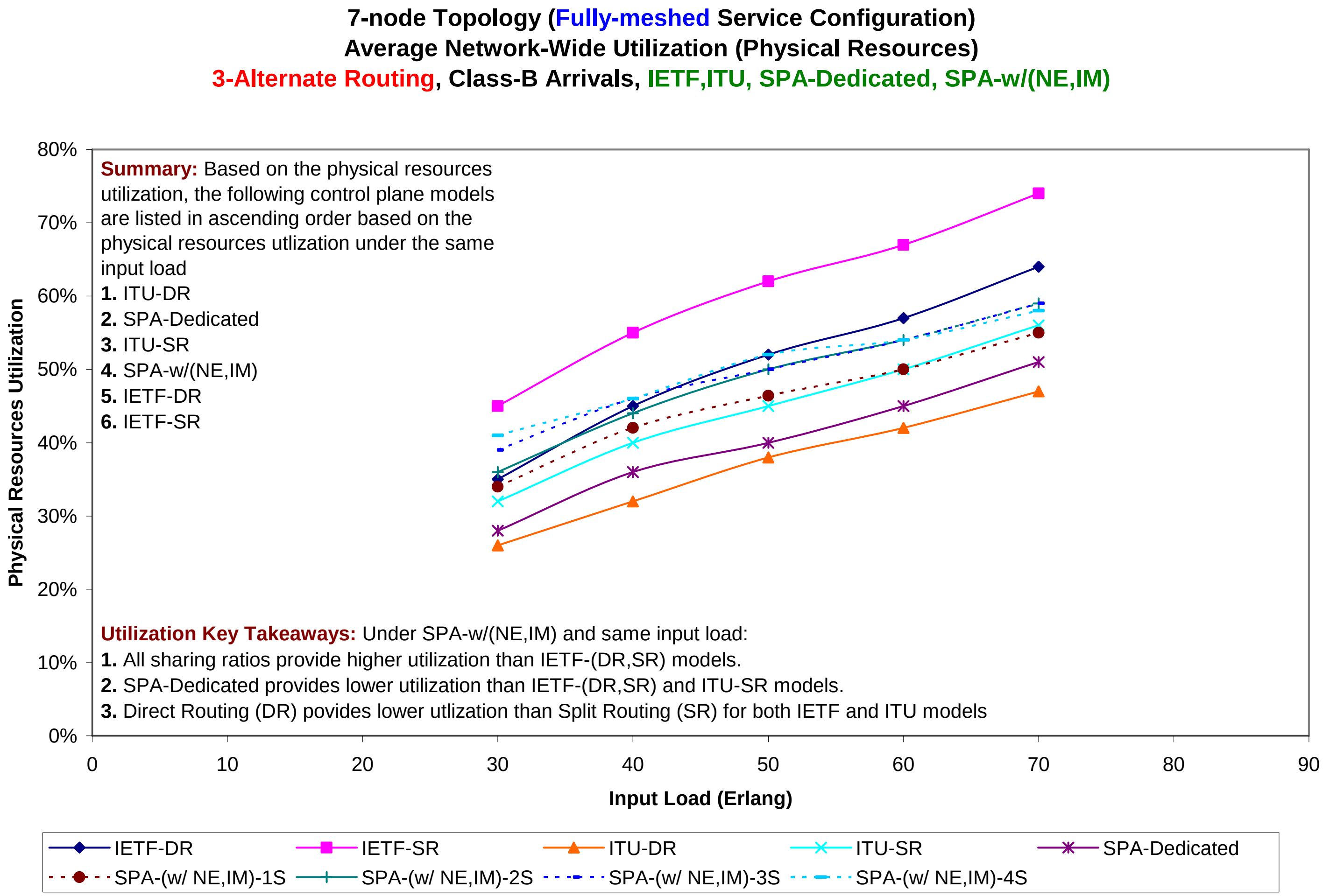

7-node Topology (Fully-meshed Service Configuration)
Average Network-Wide Utilization (Physical Resources)
3-Alternate Routing, Class-B Arrivals, IETF,ITU, SPA-Dedicated, SPA-w/(NE,IM)

Summary: Based on the physical resources utilization, the following control plane models are listed in ascending order based on the physical resources utlization under the same input load

1. ITU-DR
2. SPA-Dedicated
3. ITU-SR
4. SPA-w/(NE,IM)
5. IETF-DR
6. IETF-SR

Utilization Key Takeaways: Under SPA-w/(NE,IM) and same input load:

1. All sharing ratios provide higher utilization than IETF-(DR,SR) models.
2. SPA-Dedicated provides lower utilization than IETF-(DR,SR) and ITU-SR models.
3. Direct Routing (DR) povides lower utlization than Split Routing (SR) for both IETF and ITU models

Figure 13-28: Average Network-Wide Utilization (Physical Resources)-7 Node – 3 Alternate Route-IETF,ITU, SPA-Dedicated, SPA-w/(NE,IM)

14 Conclusions

The performance analysis of the proposed Service Profile-Aware control plane model proved its superiority compared to the IETF and ITU control plane models under specific operational space as provided in section 11.3.1. Through its accurate realization of both service profile layer parameters and network infrastructure multi-granularity detailed resources representation, the architectures and functional operation of the Service-Profile Aware control plane components provide significant harmony between the network infrastructure resources and service profile parameters. This harmony resulted in the SPA control plane model superiority, under specific operational space as provided in section 11.3.1, in the following aspects while considering the IETF-DR as a reference control plane model:

1. All the traffic management schemes of the SPA control plane provide a higher reduction in blocking probability compared to the IETF-SR and ITU-(DR,SR) control plane models. The increase in blocking probability reduction is 0-131% and 39-122% respectively; depending on the SPA traffic management scheme, SPA number of alternate routes, and the IETF/ITU static routing configuration (direct routing vs. split routing).

2. All the traffic management schemes of the SPA control plane, except when IMF is disabled, provide a higher increase in permissible load compared to the IETF-SR and ITU-(DR,SR) control plane models. The increase in permissible load is 120-134% and 110-120% respectively; depending on the SPA traffic management scheme, SPA number of alternate routes, and the IETF/ITU static routing configuration (direct routing vs. split routing).

3. All the traffic management schemes of the SPA control plane provide a higher reduction in utilization compared to the IETF-(DR,SR) and ITU-(DR,SR) traffic management schemes; the increase in utilization reduction is 7-31% depending on the SPA traffic management scheme, and SPA number of alternate routes.

It was observed that since the architectures and functional operation of the control plane components for existing IETF and ITU control plane models lack the service profile layer parameters consideration, this led to a lack of harmony between the service profile layer, control plane layer, and network infrastructure layer. This lack of harmony led to inefficient utilization of network resources especially under operation scenarios requiring dynamic allocation of network resources for differentiated services.

Clearly the need to establish network connections in a service profile-aware fashion is beneficial and will become increasingly important for future wired and wireless client networks. The architectures and functional operation of future control plane models will have to take into account a number of service profile parameters and network constraints to efficiently utilize network resources, this will play a key role under a networking scenario where a multi-service operation in common network infrastructure is assumed. Under such scenario, efficient algorithms and protocols for service profile-differentiation and dynamic allocation of network resources by the control plane is a must.

15 Next Steps - Future Related Work

The most potential next step related to this dissertation is analyzing the advantages of the SPA traffic management schemes over IETF and ITU control plane models for multi-domain network topologies. Two possible approaches for multi-domain analysis are possible; a mathematical and simulation approach.

Regarding the mathematical approach, a new routing architecture needs to be proposed to overcome the limitations of the routing probability approximation as used in [68]. As described in the dissertation, the routing component in the SPA control plane model is state-dependent in its computation of the routing probability for each identified route in the network topology. The mathematical formulation used in [68] to compute the state-dependent routing probability q_{rk}^{m} for each route r_m lacks the accuracy needed when computing routing probability under large network topologies with higher level of meshing among routes. Recall the mathematical equation used to compute the routing probability as follows:

$$q_{rk}^{mD} = \sum_{n=0}^{C_{\min}(r_m)} \prod_{k=1}^{k=m-1} \Pr[\overline{A}_n^D(r_k - r_m)].\prod_{k=m+1}^{k=M_r} \Pr[\overline{A}_{n+1}^D(r_k - r_m)].\Pr[\widetilde{A}_n^D(r_m)]$$

The approximation of the routing probability would be accurate in a network when routes between each source-destination node pair share one or more common links but are disjoint elsewhere; thus $\overline{A}_n^D(r_k - r_m) \approx \overline{A}_n^D(r_k)$ and $\overline{A}_{n+1}^D(r_k - r_m) \approx \overline{A}_{n+1}^D(r_k - r_m)$. This assumption on link-disjoint between routes for a source-destination pair node would limit the flexibility of selecting link-disjoint routes under a large network topology especially for non-meshed network topologies.

The current routing architecture assumed in the SPA control plane model is a flat routing architecture; a hierarchal routing architecture is a proposed alternative to overcome the link-disjoint route limitation. The hierarchal routing architecture by the control plane is another logical representation of the network infrastructure layer compared to the flat routing architecture. In other words, the same infrastructure layer topology can be represented logically by two different flat vs. hierarchal routing architectures. As described in details in section 5.1 on horizontal view of the network topology from a multi-domain realization, the large network topology can be segmented into sub-networks or network domains. From a routing architecture perspective, network topology segmenting into sub-networks results into routing architecture segmenting in Routing Areas (RAs). A hierarchal routing architecture can be used to connect multiple routing areas in a hierarchical architecture.

A routing architecture is a logical representation of the transport network, the routing architecture can be flat or hierarchal based on the scale of the transport network, geographic and administrative constraints, or technological boundaries. Thus, the decision to implement a hierarchal vs. flat routing architecture for a control plane instance is not based on the transport topology granularity levels controlled by the control plane instance. For an *N* control plane instances, we can have *N* control plane routing architecture instances, each one of the routing architecture instances can be hierarchically or flat represented.

Building on the Control Plane Instance (CPI) concept described in section 5 for the three control plane models; from a hierarchal routing architecture perspective, a control plane instance can be described as a collection of Routing Areas (RAs) and Routing Levels (RLs), in the case of hierarchical routing architecture. Figure 15-1 illustrates two transport network subnetworks represented by two routing areas; the boundaries of the routing areas are connected by a connection link. A physical network topology can be recursively partitioned into subnetworks. Partitioning in the transport plane leads to multiplicity of routing areas in the control plane. Recursive partitioning principles leads to hierarchical organization of routing areas into multiple levels. Routing Areas follow the organization of subnetworks. The internal topology of a sub-network is completely opaque to the outside. For routing purposes, the sub-network may appear as a node (reachability only), or may be transformed to appear as some set of nodes and links, in which case the sub-network is not visible as a distinct entity. Methods of transforming sub-network structure to improve routing performance will likely depend on sub-network topology.

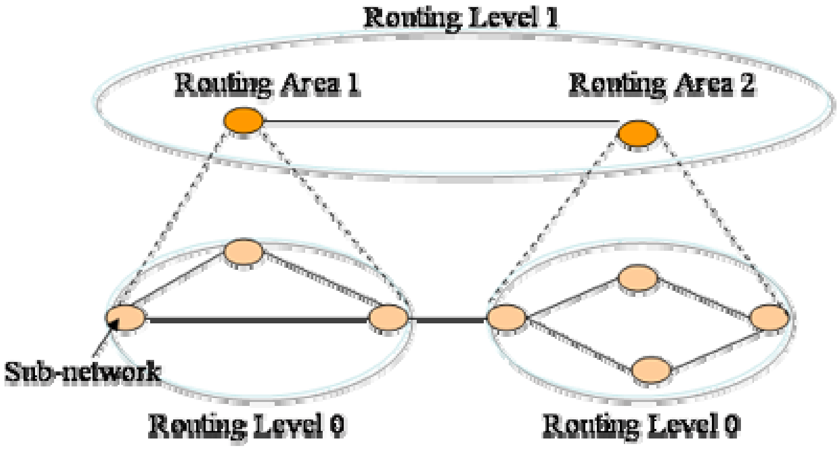

Figure 15-1: Hierarchical Routing Architecture

15.1 IETF control plane model

As described in sections 5.35.3.1 and 6.1, the IETF control plane model represents the transport network multiple partitions by one control plane instance. Figure 15-2 illustrates the IETF control plane representation of transport network multiple partitions.

IETF Control Plane Model

One Control Plane Instance with one **Hierarchal Routing Instance** *for the Three Transport Network Partitions*

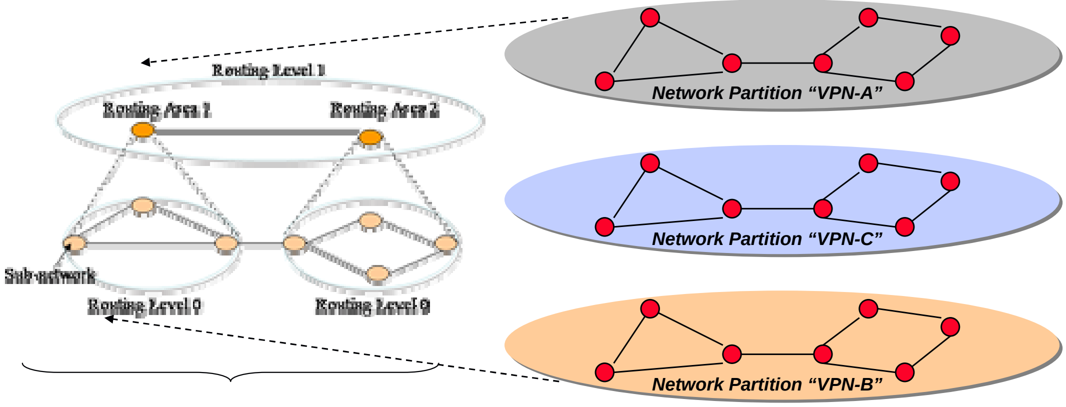

Figure 15-2: IETF Control Plane Representation for Multi-Domain Network Architecture

15.2 ITU control plane model

As described in sections 5.3.2 and6.2, the ITU and SPA-Dedicated control plane models represents the transport network multiple partitions by multiple control plane instances. Figure 15-3 illustrates the two models representation of transport network multiple partitions. Each control plane instance is a group of RAs that can be represented by a hierarchal routing architecture. It is important to note that both models routing and capacity allocation decisions made by the multiple control plane instances are not correlated. In other words, the multiple control plane instances function independently of each other and hence no topology exchange across the parallel control plane instances takes place; thus no Load Partitioning Function (LPF) is implemented.

15.3 SPA control plane model

The SPA-Dedicated control plane model builds on the ITU control plane model but with state-dependent routing for each control plane instance with its hierarchal routing architecture. In the SPA-Shared control plane model, a LPF is implemented between the control plane instances as illustrated in Figure 15-4.

ITU/SPA-Dedicated Control Plane Models

Three* Control Plane Instance with *Three* Hierarchal Routing Instances *for the Three Transport Network Partitions

***No* inter-control plane instances resource sharing via Load Partitioning Function (LPF)**

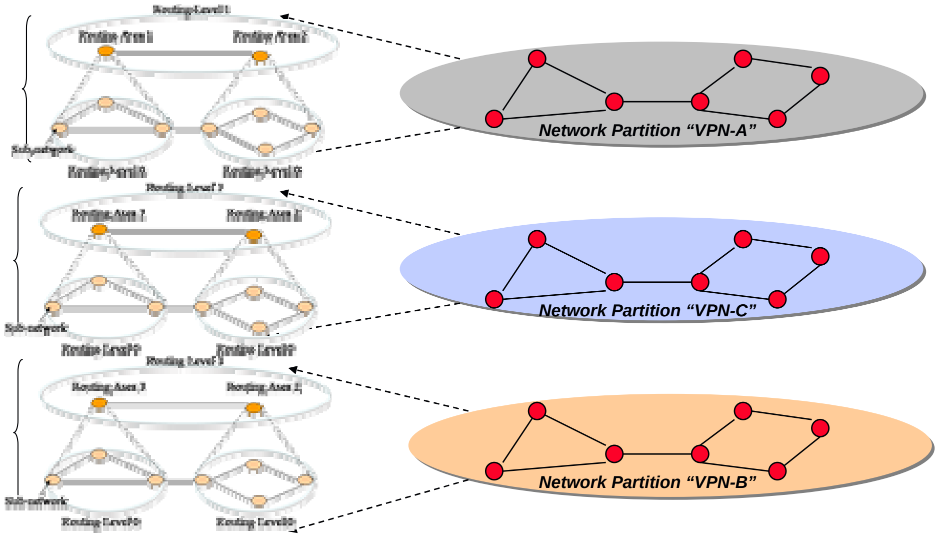
Sub-network
Network Partition “VPN-A”
Sub-network
Network Partition “VPN-C”
Sub-network
Network Partition “VPN-B”

Figure 15-3: ITU & SPA-Dedicated Control Plane Models Representation for Multi-Domain Network Architecture

SPA-Shared Control Plane Model

Three ***Control Plane Instance with*** ***Three*** **Hierarchal Routing Instances** ***for the Three Transport Network Partitions***

With inter-control plane instances resource sharing via Load Partitioning Function (LPF)

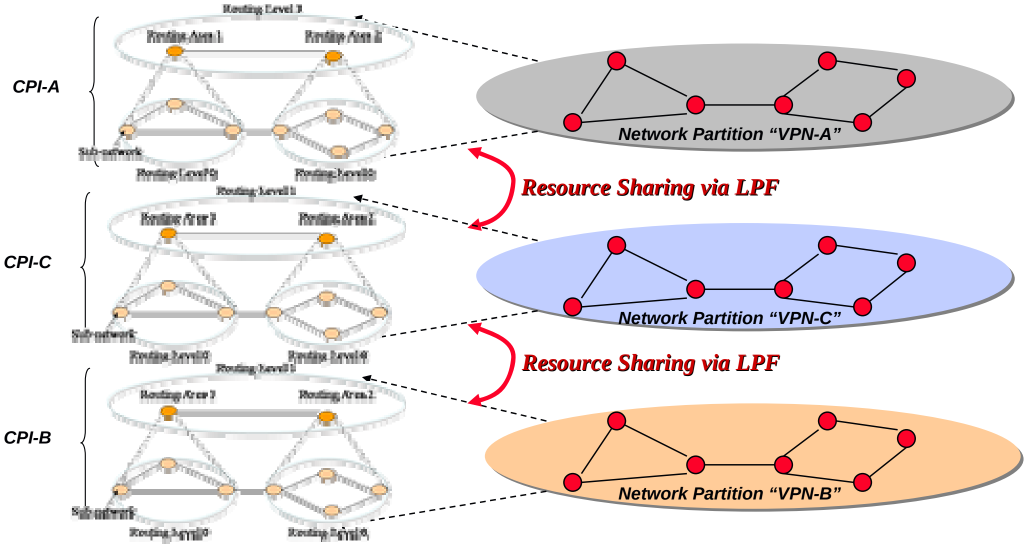

Figure 15-4: SPA-Shared Control Plane Representation of Multi-Domain Network Architecture

16 References

16.1 Journals & papers

16.1.1 Single-Domain control plane function analysis

[1] Jong-Moon Chung; Khan, H.K.; Hooi Miin Soo; Reyes, J.S.; Cho, G.Y.; Analysis of GMPLS architectures, MWSCAS-2002. The 2002 45th Midwest Symposium on topologies and algorithms, Volume: 3 , 4-7 Aug. 2002 , Page(s): III-284 -III-287 vol.3

[2] Pin-Han Ho; Mouftah, H.T.; Path selection with tunnel allocation in the optical Internet based on generalized MPLS architecture, ICC 2002. IEEE International Conference on Communications, 2002 , Volume: 5 , 28 April-2 May 2002, Page(s): 2697 -2701 vol.5

[3] Jong-Moon Chung; Hooi Miin Soo; Jitter analysis of homogeneous traffic in differentiated services networks, IEEE Communications Letters, Volume: 7 Issue: 3 , March 2003, Page(s): 130 -132

[4] Ozugur, T.; Verchere, D; Congestion control mechanism using LSP differentiation for label-switched optical burst networks, IP Operations and Management, 2002 IEEE Workshop on , 2002 Page(s): 31 -36

[5] Tomic, S.; Jukan, A.; GMPLS-based exchange points: architecture and functionality, . Workshop on High Performance Switching and Routing, 2003, June 24-27, 2003, Page(s): 245 -249

16.1.2 Next-Generation SONET

[6] M. Simcoe, A layered Architecture for Metro optical Networks, National Fiber Optic Engineers Conference (NFOEC) 2000, Denver, CO, August 2000

[7] F. Moore, Extending the LAN to the Transport Network, National Fiber Optic Engineers Conference (NFOEC) 2000, Denver, CO, August 2000

[8] Optical Edge Networks: Market Opportunities for Integrated Optical Network Solutions in Metro Networks, Pioneer Consulting Report, July 2000

[9] B. Rajagopapaln, et al., IP over Optical Networks: Architectural Aspects, IEEE Communications Magazine, Vol. 39, No. 1, January 2001, pp. 144-150

[10] S. Wilkinson, Metropolitan Area Transport Requirements, National Fiber Optic Engineers Conference (NFOEC) 2000, Denver, CO, August 2000

[11] L. Castellon, T., Rado, The Future of SONET, National Fiver Optic Engineers Conference (NFOEC), Denver, CO, August 2000

[12] N. Golmi, T. Ndousse, D. Su, A Differentiated Optical Services Model for WDM Networks, IEEE Communications Magazine, Vol. 38, No. 2, February 2000, pp. 68-73.

[13] Metro Optical Networks: Metro DWDM and the New Public Network", Pioneer Consulting Report, 1999

[14] G. A. Young, Planning SONET Architecture for Improved Capacity Utilization, National Fiber optic Engineers Conference (NFOEC) 1998, Orlando, FL, September 1998.

16.2 Standards recommendations

16.2.1 ITU-T optical control building blocks generic architecture

[15] ITU-T Rec. G.8080/Y.1304, Architecture for the Automatic Switched Optical Network (ASON)

[16] ITU-T G.8080/Y.1304 Incorporating Amendment.

[17] ITU-T Rec. G.7713/Y.1704, Distributed call and connection management

[18] ITU-T Rec. G.7714/Y.1705, Generalized automatic discovery techniques

[19] ITU-T Rec. G.7715, Architecture and Requirements for routing the ASON

[20] ITU-T Rec. G.7042/Y.1305, Link capacity adjustment scheme (LCAS) for virtual concatenated signals.

[21] ITU-T Rec. G.707, Virtual Concatenation

16.2.2 ITU-T protocol specific implementations

[22] ITU-T Rec. G.7713.2, ASON distributed call and connection management signaling mechanism using GMPLS RSVP-TE

[23] ITU-T Rec. G.7713.3, ASON distributed call and connection management signaling mechanism using GMPLS CR-LDP

[24] ITU-T Rec. G.7715.1, ASON routing architecture and requirements for links state protocols

[25] ITU-T Rec. G.7714.1, Protocol for automatic discovery in SDH and OTN networks.

[26] Framework for Layer 1 Virtual Private Networks, draft-takeda-l1vpn-framework-03

16.2.3 ITU-T optical transport standards

[27] ITU-T Rec. G.872, “Architecture of Optical Transport Networks” (OTN)

[28] ITU-T Rec. G.8070/Y.1301, Requirements for Automatic Switched Transport Networks (ASTN)

[29] ITU-T Rec. G.7714, Generalized Automatic Discovery Techniques

[30] ITU-T Rec. G.7712/Y.1703, Data Communications Network

[31] ITU-T Rec. G.798, “Characteristics of Optical Transport Network (OTN) Hierarchy Equipment functional Blocks”

[32] ITU-T Rec. G.874, “Management Aspects of the Optical Transport Network Element”

[33] ITU-T Rec. G.693, “Optical Interfaces for Intra-Office Systems”

16.2.4 IETF GMPLS building blocks specific protocols

[34] IETF RFC 3945- Generalized Multi-Protocol Label Switching Architecture

[35] IETF RFC 3471, Generalized Multi-Protocol Label Switching (GMPLS) Signaling Functional Description.

[36] IETF RFC 3472, Generalized Multi-Protocol Label Switching (GMPLS) Signaling Constraint-based Routed Label Distribution Protocol (CR-LDP) Extensions.

[37] IETF RFC 3473, Generalized Multi-Protocol Label Switching (GMPLS) Signaling Resource ReserVation Protocol-Traffic Engineering (RSVP-TE) Extensions

[38] IETF draft-Routing Extensions in Support of Generalized MPLS, draft-ietf-ccamp-gmpls-routing-09

[39] IETF OSPF Extensions in Support of Generalized MPLS, draft-ietf-ccamp-ospf-gmpls-extensions-11, October 2003

[40] IETF draft, Generalized MPLS Signaling Extensions for G.709 Optical Transport Networks Control, draft-ietf-ccamp-gmpls-g709-09

[41] IETF draft, Framework for GMPLS-based Control of SDH/SONET Networks, draft-ietf-ccamp-sdhsonet-control-02

[42] G.Berstein, E. Mannie, V.Sharma, Framework for MPLS-based Control of Optical SDH/SONET Networks, IETF Draft, Draft-bms-optical-sdhsonet-mpls-contro-frmwrk-00, November 2000

[43] IETF Requirements for Generalized MPLS (GMPLS) Usage and Extensions for Automatically Switched Optical Network (ASON), draft-ietf-ccamp-gmpls-ason-reqts-05, October 2004

16.3 Traffic allocation and resource partitioning schemes

[44] FOSCHINI, G.J., GOPINATH, B. AND HAYES, J.F. (1981) Optimum allocation of servers to two types of competing customers. IEEE Trans. Comm. COM-29, 1051-1055.

[45] GOPAL, 1.S. AND STERN, T.E. (1983) optimal call blocking policies in an integrated services environment. Proceedings of the Conference on Information Sciences and Systems, Johns Hopkins University, 383-388.

[46] KRAIMECHE, B. AND SCHWARTZ, M. (1984) Traffic access control strategies in integrated digital networks. Proceedings of Infocom '84, 230-235.

[47] FLOYD, S. AND JACOBSON, V. (1995) Link-sharing and resource management models for packet networks. IEEE/ACM Trans. Networking 3(4), 365-386.

[48] ASH, G.R., CHEN, J.S., FREY, A.E. AND HUANG, B.D. (1991) Real-time network routing in an integrated network. Proceedings of the International Teletraffic Congress (ITC-13), Copenhagen.

[49] BORST, S. AND MITRA, D. (1997) Virtual partitioning for resource sharing by state-dependent priorities: analysis, approximations, and performance for heterogeneous traffic. In Teletraffic Contributions for the Information Age, Proc. ITC-15, ed. V. Ramaswami and P. E. Wirth, Elsevier, 1457-1468.

[50] KELLY, F.P. (1991) Loss networks. Ann. Appl. Prob. 1, 319378.

[51] MITRA, D., REIMAN, M. 1. AND WANG, J. (1997) Robust admission control for heterogeneous ATM systems with both cell and call QoS requirements, In Teletraffic Contributions for the Information Age, Proc. ITC-15, ed. V. Ramaswami and P. E. Wirth, Elsevier, 1421-1432.

[52] KUMARAN, K. AND MITRA, D. (1997) Performance and fluid simulations of a novel shared buffer management system. Submitted to INFO COM 98.

[53] MITRA, D. AND ZIEDINS, 1. (1997) Hierarchical virtual partitioning: Algorithms for virtual private networking. Bell Labs Tech. J. 2(2), 68-81.

[54] KAUFMAN, J.S. (1981) Blocking in a shared resource environment. IEEE Trans. Commun. 29, 1471-1481.

[55] ROBERTS, J. W. (1981) A service system with heterogeneous service requirements. In: Performance of Data Communications Systems and their Applications. (ed. G. Pujolle) North-Holland, Amsterdam. 423-431.

[56] ROBERTS, J.W. (1983) Teletraffic models for the Telecom 1 integrated services network. In: Proc. ITC-l 0, session 1.1. Ross, K. (1995) Multirate Loss Models for Broadband Telecommunications Networks. Springer.

[57] BEAN, N.G., GIBBENS, R.G. AND ZACHARY, S. (1995) Asymptotic analysis of single resource loss systems in heavy traffic, with applications to integrated networks. Adv. Appl. Prob. 27, 273-292.

[58] BORST, S. AND MITRA, D. (1997) Virtual partitioning for resource sharing by state-dependent priorities: analysis, approximations, and performance for heterogeneous traffic. In Teletraffic Contributions for the Information Age, Proc. ITC-15, ed. V. Ramaswami and P. E. Wirth, Elsevier, 1457-1468.

16.4 Fixed point approximation for multi-rate loss networks

[59] KELLY, F.P. (1991) Loss networks. Ann. Appl. Prob. 1, 319-378.

[60] “Blocking probabilities in large circuit switched networks,” Adv. Applied. Probabilities, vol. 18, pp. 473–505, 1986.

[61] S. Chung and K. W. Ross, “Reduced load approximations for multirate loss networks,” IEEE Trans. Commun., vol. 41, pp. 1222–1231, Aug. 1993.

[62] D. Mitra, R. Gibbens, and B. D. Huang, “State-dependent routing on symmetric loss networks with trunk reservations I,” IEEE Trans. Commun., vol. 41, pp. 400–411, Feb. 1993.

[63] A. G. Greenberg and R. Srikant, “Computational techniques for accurate performance evaluation of multirate, multihop communication networks,” IEEE/ACM Trans. Networking, vol. 5, pp. 266–277, Feb. 1997.

[64] W. Whitt, “Blocking when service is required from several facilities simultaneously,” AT&T Tech. J., vol. 64, no. 8, pp. 1807–1857, 1985.

[65] A. Girard and M. A. Bell, “Blocking evaluation for networks with residual capacity adaptive routing,” IEEE Trans. Commun., vol. 37, pp.1372–1380, Dec. 1989.

[66] P. J. Hunt, “Implied costs in loss networks,” Adv. Applied. Probabilities, vol.21, pp. 661–680, 1989.

[67] F. P. Kelly, “Routing and capacity allocation in networks with trunk reservation,” Math. Oper. Res., vol. 15, pp. 771–793, 1990.

[68] Mingyan Liu, John S. Baras, " Fixed Point Approximation for Multirate Multihop Loss Networks With State-Dependent Routing ", IEEE/ACM Transactions on Networking, no. 2, March 2004

[69] J. S. Kaufman, “Blocking in a shared resource environment,” IEEE Trans. Commun., vol. 29, pp. 1474–1481, Aug. 1981.

[70] Gibbens, R.J., Hunt, P.J. and Kelly, F.P. (1990) Bi-stability in communications networks, Oxford University Press, Oxford, 113-127

[71] I. Ziedins and F. Kelly. Limit theorems for loss networks with diverse routing. Adv. Applied Probabilities. 21, 804–830, 1989.

[72] N. G. Bean, R. J. Gibbens, and S. Zachary, “The performance of single resource loss systems in multiservice networks,” in The Fundamental Role of Teletraffic in the Evolutionof Telecommunications Networks, Proceedings of the 14th International Teletraffic Congress ITC 14, J. Labetoulle and J. W. Roberts, Eds. New York: Elsevier Science B.V., June 1994, vol. 1a, Teletraffic Science and Engineering, pp. 13–21.

[73] N. B. Bean, R. J. Gibbens, and S. Zachary, “Asymptotic analysis of single resource loss systems in heavy traffic, with applications to integrated networks,” Adv. Appl. Probabil., pp. 273–292, Mar. 1995.

16.5 Optical networking market analysis

[74] R. Boncek, et al., “Fiber and Systems for Metropolitan Optical Networks,” National Fiber Optic Engineers Conference (NFOEC), Orlando, FL, September 1998

[75] Optical Edge Networks: Market Opportunities for Integrated Optical Network Solutions in Metro Networks,” Poineer Consulting Report, July 2000

[76] B. S. Arnuad, “Current Optical Network Designs May Be Flawed,”, Optical Networks Magazine, Vol. 2, No. 2, March/April 2000, pp. 21-28

[77] B. St. Arnuad, “Overview of Latest Development in Optical Internets,” Optical Networks Magazine, Vol. 1, No. 4, October 2000, pp. 51-54

[78] P.V. Hatton, F. Cheston, “WDM Deployment in the Local Exchange Networks,” IEEE Communications Magazine, Vol. 36, No. 2, February 1998, pp. 56-61

17 Appendix-A: List of Acronyms

Term	Description
CAC	Connection Admission Control
CC	Connection Controller
CP	Complete Partitioning
CPI	Control Plane Instance
CS	Complete Sharing
DR	Direct Routing
FDA	Fully-meshed Dedicated Actual
FPA	Fixed Point Approximation
FSA	Fully-mesh Shared Actual
FSG	Fully-meshed Shared Granular
IETF	Internet Engineering Task Force
IM	Inverse Multiplexing
IMF	Inverse Multiplexing Function
ITU	International Telecommunications Union
LPF	Load Partitioning Function
LRM	Link Resource Manager
NE	Network Engineering
PC	Protocol Controller
PDA	Point Dedicated Actual
PSA	Point Shared Actual
PSG	Point Shared Granular
QoS	Quality of Service
RA	Routing Area
RC	Routing Controller
RDB	Routing Database
RL	Routing Level
SDA	Semi-meshed Dedicated Actual
SNC	Sub-Network Connection
SNP	Sub-Network Point

SNPP	Sub-Network Point Pool
SONET	Synchronous Optical Network
SPA	Service Profile-Aware
SR	Split Routing
SS	Static Sharing
SSA	Semi-meshed Shared Actual
SSG	Semi-meshed Shared Granular
TP	Traffic Policy
VP	Virtual Partitioning
VPN	Virtual Private Network

18 Appendix-B: Pseudo-Code generic algorithms

18.1 IETF control plane model

Define Topology Parameters:

- *N=Set of Nodes*
- *J=Set of Links*
- *R= Total number of node pair*
- *M_r= Set of routes allowed between source-destination pair r.*
- *R_m= m^{th} route of the source-destination pair r*
- *C_j= Links j capacity (number of resource units)*

Define Arriving Services Parameters:

- *K= Classes of service requests*
- *J=Bandwidth demands of service requests*
- *λ_{rk} = Arriving rate of class k on source-destination pair r*
- *μ_k = Service rate of class k*

Initialize: *link admissibility probability* a_{jk} for all topology links

If IETF Direct Routing Selected:

Set: *Routing probability q_{rk}^{m} of direct path for each source-destination pair=1*

If IETF Split Routing Selected:

Set: *Routing probability q_{rk}^{m} of each path for each source-destination pair=1/Number of possible paths between source-destination pair*

Start Fixed Point Approximation (FPA) Mechanism

Compute: *(Per link j, Per class k) arriving rate $\lambda_{jk}^{r_m}$ based routing probability q_{rk}^{m}*

Compute: *(Per link j, Per class k) arriving rate λ_{jk} based on all possible r_m*

Perform: *IETF-CAC Mechanism based on initial* a_{jk} and λ_{jk}

Compute: *Occupancy probability* $p_j(n)$ *for each link j*

Compute: *New* a_{jk} based on $p_j(n)$ *for each link j*

Loop FPA until a_{jk} converges

18.2 ITU control plane model

Define Topology Parameters Per Network Resources Partition:

- *N=Set of Nodes*
- *J=Set of Links*
- *R= Total number of node pair*
- *M_r= Set of routes allowed between source-destination pair r.*
- *R_m= m^{th} route of the source-destination pair r*
- C_j^D *= Links j capacity (number of resource units)**Per Network Resources Partition***

Define Arriving Services Parameters:

- *K= Classes of service requests*
- *J=Bandwidth demands of service requests*
- λ_{rk}^D *Arrival rate of class k calls between node pair r **for configured VPN service v.***
- μ_k *= Service rate of class k*

Initialize: *link admissibility probability* a_{jk}^D for all topology links

If ITU Direct Routing Selected:

Set: *Routing probability* q_{rk}^{mD} *of direct path for each source-destination pair=1*

"Per Network Resources Partition"

If ITU Split Routing Selected:

Set: *Routing probability* q_{rk}^{mD} *of each path for each source-destination pair=1/Number of possible paths between source-destination pair*

"Per Network Resources Partition"

Per Control Plane Instance "FPA Instance":

Start Fixed Point Approximation (FPA) Mechanism

Compute: *(Per link j, Per class k) arriving rate* $\lambda_{jk}^{D_{r_m}}$ *based routing probability* q_{rk}^{mD}

Compute: *(Per link j, Per class k) arriving rate* λ_{jk}^{D} *based on all possible* r_m

Perform: *ITU-CAC Mechanism based on initial* a_{jk}^{D} and λ_{jk}^{D}

Compute: *Occupancy probability* $p_j^D(n)$ *for each link j*

Compute: *New* a_{jk}^{D} based on $p_j^D(n)$ *for each link j*

Loop FPA until a_{jk}^{D} converges

18.3 SPA-Dedicated control plane model

Define Topology Parameters Per Network Resources Partition:

- *N=Set of Nodes*
- *J=Set of Links*
- *R= Total number of node pair*
- *M_r= Set of routes allowed between source-destination pair r.*
- *R_m= m^{th} route of the source-destination pair r*
- C_j^D = *Links j capacity (number of resource units)**Per Network Resources Partition***

Define Arriving Services Parameters:

- *K= Classes of service requests*
- *J=Bandwidth demands of service requests*
- λ_{rk}^{D} *Arrival rate of class k calls between node pair r* ***for configured VPN service v.***
- μ_k = *Service rate of class k*

Initialize: *link admissibility probability* a_{jk}^{D} *and* q_{rk}^{mD} for all topology links

Per Control Plane Instance "FPA Instance":

Start Fixed Point Approximation (FPA) Mechanism

Compute: *(Per link j, Per class k) arriving rate* $\lambda_{jk}^{D_{r_m}}$ *based routing probability* q_{rk}^{mD}

Compute: *(Per link j, Per class k) arriving rate* λ_{jk}^{D} *based on all possible* r_m

Perform: *ITU-CAC Mechanism based on initial* a_{jk}^{D} and λ_{jk}^{D}

Compute: *Occupancy probability* $p_j^D(n)$ *for each link j*

Compute: *New* a_{jk}^{D} based on $p_j^D(n)$ *for each link j*

Compute: *New* q_{rk}^{mD} *based on new* $p_j^D(n)$

Loop FPA until a_{jk}^{D} *and* $p_j^D(n)$ *converges*

18.4 SPA-Shared control plane model

Define Topology Parameters Per Network Resources Partition:

- *N=Set of Nodes*
- *J=Set of Links*
- *R= Total number of node pair*
- *M_r= Set of routes allowed between source-destination pair r.*
- *R_m= m^{th} route of the source-destination pair r*
- C_j^D = *Links j capacity (number of resource units)**Per Network Resources Partition***

Define Arriving Services Parameters:

- *K= Classes of service requests*
- *J=Bandwidth demands of service requests*
- λ_{rk}^{v} *Arrival rate of class k calls between node pair r **for configured VPN service v.***
- μ_k *= Service rate of class k*

Initialize: *link admissibility probability* a_{jk}^{D} *and* q_{rk}^{mD} for all topology links

Round1: Per Control Plane Instance "FPA Instance" of the dedicated resources:

Set: Load Partitioning Function (LPF) policy (Static vs. NE)

Set: Inverse Multiplexing Function (IMF) policy (actual b_k^A ***vs. granular*** b_k^G ***)***

Start Fixed Point Approximation (FPA) Mechanism

```
            Compute: (Per link j, Per class k) arriving rate $\lambda_{jk}^{D_{r_m}}$ based routing probability $q_{rk}^{mD}$
            Compute: (Per link j, Per class k) arriving rate $\lambda_{jk}^{D}$ based on all possible $r_m$
            Perform: SPA-Shared-CAC Mechanism based on initial $a_{jk}^{D}$ and $\lambda_{jk}^{D}$
            Compute: Occupancy probability $p_j^D(n)$ for each link j
            Compute: New $a_{jk}^{D}$ based on $p_j^D(n)$ for each link j
            Compute: New $q_{rk}^{mD}$ based on new $p_j^D(n)$
        Loop FPA until $a_{jk}^{D}$ and $p_j^D(n)$ converges

Round2: Per Control Plane Instance “FPA Instance” of the dedicated resources:
    Start Fixed Point Approximation (FPA) Mechanism
            Compute: (Per link j, Per class k) arriving rate $\lambda_{jk}^{D_{r_m}}$ based routing probability $B_{rk}^{D}$
            Compute: (Per link j, Per class k) arriving rate $\lambda_{jk}^{D_{r_m}}$ based routing probability $q_{rk}^{mD}$
            Compute: (Per link j, Per class k) arriving rate $\lambda_{jk}^{D}$ based on all possible $r_m$
            Perform: SPA-Shared-CAC Mechanism based on initial $a_{jk}^{D}$ and $\lambda_{jk}^{D}$
            Compute: Occupancy probability $p_j^D(n)$ for each link j
            Compute: New $a_{jk}^{D}$ based on $p_j^D(n)$ for each link j
            Compute: New $q_{rk}^{mD}$ based on new $p_j^D(n)$
        Loop FPA until $a_{jk}^{D}$ and $p_j^D(n)$ converges
```

```
Start Fixed Point Approximation (FPA) Mechanism for Shared Resources

        Compute: (Per link j, Per class k) arriving rate $\lambda_{jk}^{D_{r_m}}$ based routing probability $q_{rk}^{mD}$

        Compute: (Per link j, Per class k) arriving rate $\lambda_{jk}^{D}$ based on all possible $r_m$

        Perform: SPA-Shared-CAC Mechanism based on initial $a_{jk}^{D}$ and $\lambda_{jk}^{D}$

        Compute: Occupancy probability $p_j^D(n)$ for each link j

        Compute: New $a_{jk}^{D}$ based on $p_j^D(n)$ for each link j

        Compute: New $q_{rk}^{mD}$ based on new $p_j^D(n)$

    Loop FPA until $a_{jk}^{D}$ and $p_j^D(n)$ converges
```

19 Appendix-C: Detailed Modeling Results- 4-Node Topology

19.1 Blocking probability

19.1.1 Dedicated resources

This section provides detailed performance analysis of the network-wide blocking probability on the dedicated network resources partition for the 4-node topology. The configured VPN service evaluated is the Fully-meshed Shared Granular (FSF) with the following service profile layer parameters:

a. Service flow connectivity: configured as “fully-meshed”.

b. Service demand granularity: configured as “granular” with 1 STS-1 granularity level.

c. Load partitioning flexibility: configured as “enabled”.

One input class was evaluated with the following parameters: $k = 2$, $b_k^A = 2$ STS-1, $\mu_k = 1$unit time, $\lambda_{rk} = 4$ calls/unit time. Range of input load for 4-node topology is 10 to 30 Erlangs. The five traffic management schemes of the SPA control plane model are evaluated as provided in Table 9-1. Four sharing levels are considered as follows:

a. STS-1 sharing: C_j^{vD} =11 STS-1, C_j^S =2 STS-1

b. STS-2 sharing: C_j^{vD} =10 STS-1, C_j^S =4 STS-1

c. STS-3 sharing: C_j^{vD} =9 STS-1, C_j^S =6 STS-1

d. STS-4 sharing: C_j^{vD} =8 STS-1, C_j^S =8 STS-1

4-node Topology (Fully-meshed Service Configuration)
Average Network-Wide Blocking Probability (Dedicated Resources)
2-Alternate Routing, Class-B Arrivals, STS-1 Sharing

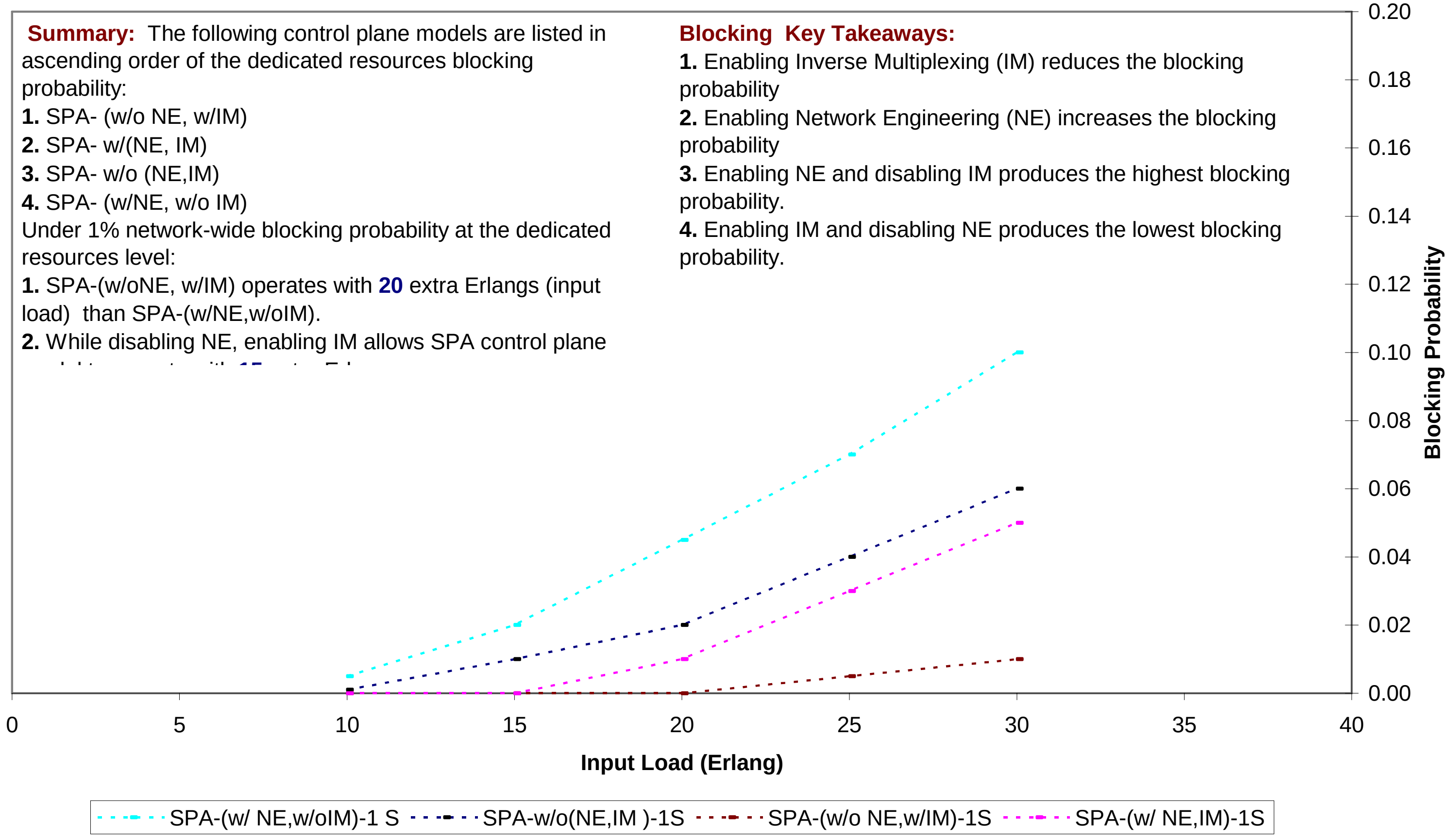

Summary: The following control plane models are listed in ascending order of the dedicated resources blocking probability:

1. SPA- (w/o NE, w/IM)
2. SPA- w/(NE, IM)
3. SPA- w/o (NE,IM)
4. SPA- (w/NE, w/o IM)

Under 1% network-wide blocking probability at the dedicated resources level:

1. SPA-(w/oNE, w/IM) operates with **20** extra Erlangs (input load) than SPA-(w/NE,w/oIM).
2. While disabling NE, enabling IM allows SPA control plane

Blocking Key Takeaways:

1. Enabling Inverse Multiplexing (IM) reduces the blocking probability
2. Enabling Network Engineering (NE) increases the blocking probability
3. Enabling NE and disabling IM produces the highest blocking probability.
4. Enabling IM and disabling NE produces the lowest blocking probability.

Figure 19-1: Average Network-Wide Blocking Probability (Dedicated Resources)-4 Node – 2 Alternate Route-STS-1 Sharing

4-node Topology (Fully-meshed Service Configuration)
Average Network-Wide Blocking Probability (Dedicated Resources)
2-Alternate Routing, Class-B Arrivals, STS-2 Sharing

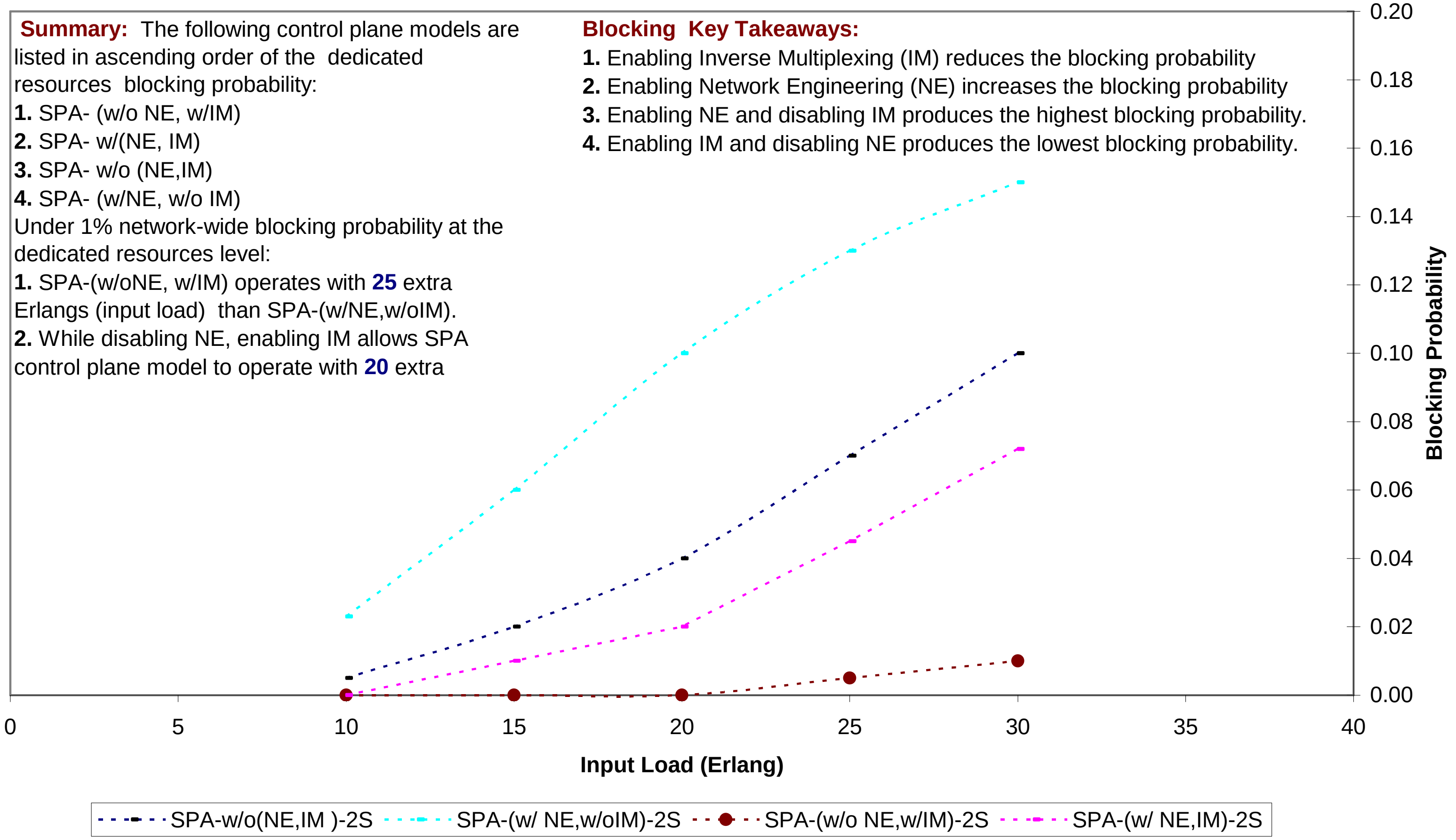

Summary: The following control plane models are listed in ascending order of the dedicated resources blocking probability:
1. SPA- (w/o NE, w/IM)
2. SPA- w/(NE, IM)
3. SPA- w/o (NE,IM)
4. SPA- (w/NE, w/o IM)
Under 1% network-wide blocking probability at the dedicated resources level:
1. SPA-(w/oNE, w/IM) operates with **25** extra Erlangs (input load) than SPA-(w/NE,w/oIM).
2. While disabling NE, enabling IM allows SPA control plane model to operate with **20** extra

Blocking Key Takeaways:
1. Enabling Inverse Multiplexing (IM) reduces the blocking probability
2. Enabling Network Engineering (NE) increases the blocking probability
3. Enabling NE and disabling IM produces the highest blocking probability.
4. Enabling IM and disabling NE produces the lowest blocking probability.

Figure 19-2: Average Network-Wide Blocking Probability (Dedicated Resources)-4 Node – 2 Alternate Route-STS-2 Sharing

4-node Topology (Fully-meshed Service Configuration)
Average Network-Wide Blocking Probability (Dedicated Resources)
2-Alternate Routing, Class-B Arrivals, STS-3 Sharing

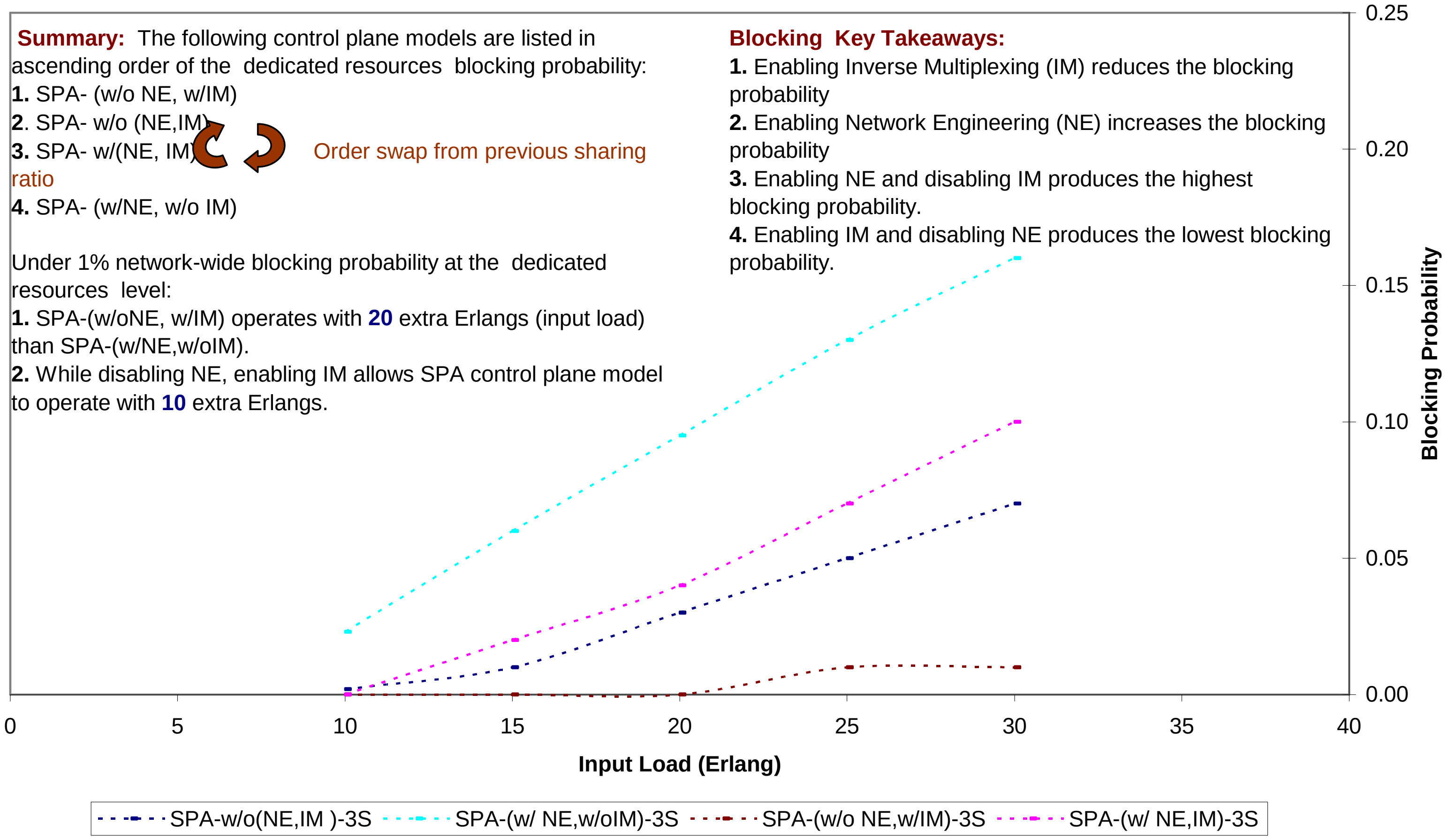

Summary: The following control plane models are listed in ascending order of the dedicated resources blocking probability:

1. SPA- (w/o NE, w/IM)
2. SPA- w/o (NE,IM)
3. SPA- w/(NE, IM) ↻ ↷ Order swap from previous sharing ratio
4. SPA- (w/NE, w/o IM)

Under 1% network-wide blocking probability at the dedicated resources level:

1. SPA-(w/oNE, w/IM) operates with **20** extra Erlangs (input load) than SPA-(w/NE,w/oIM).
2. While disabling NE, enabling IM allows SPA control plane model to operate with **10** extra Erlangs.

Blocking Key Takeaways:

1. Enabling Inverse Multiplexing (IM) reduces the blocking probability
2. Enabling Network Engineering (NE) increases the blocking probability
3. Enabling NE and disabling IM produces the highest blocking probability.
4. Enabling IM and disabling NE produces the lowest blocking probability.

Figure 19-3: Average Network-Wide Blocking Probability (Dedicated Resources)-4 Node – 2 Alternate Route-STS-3 Sharing

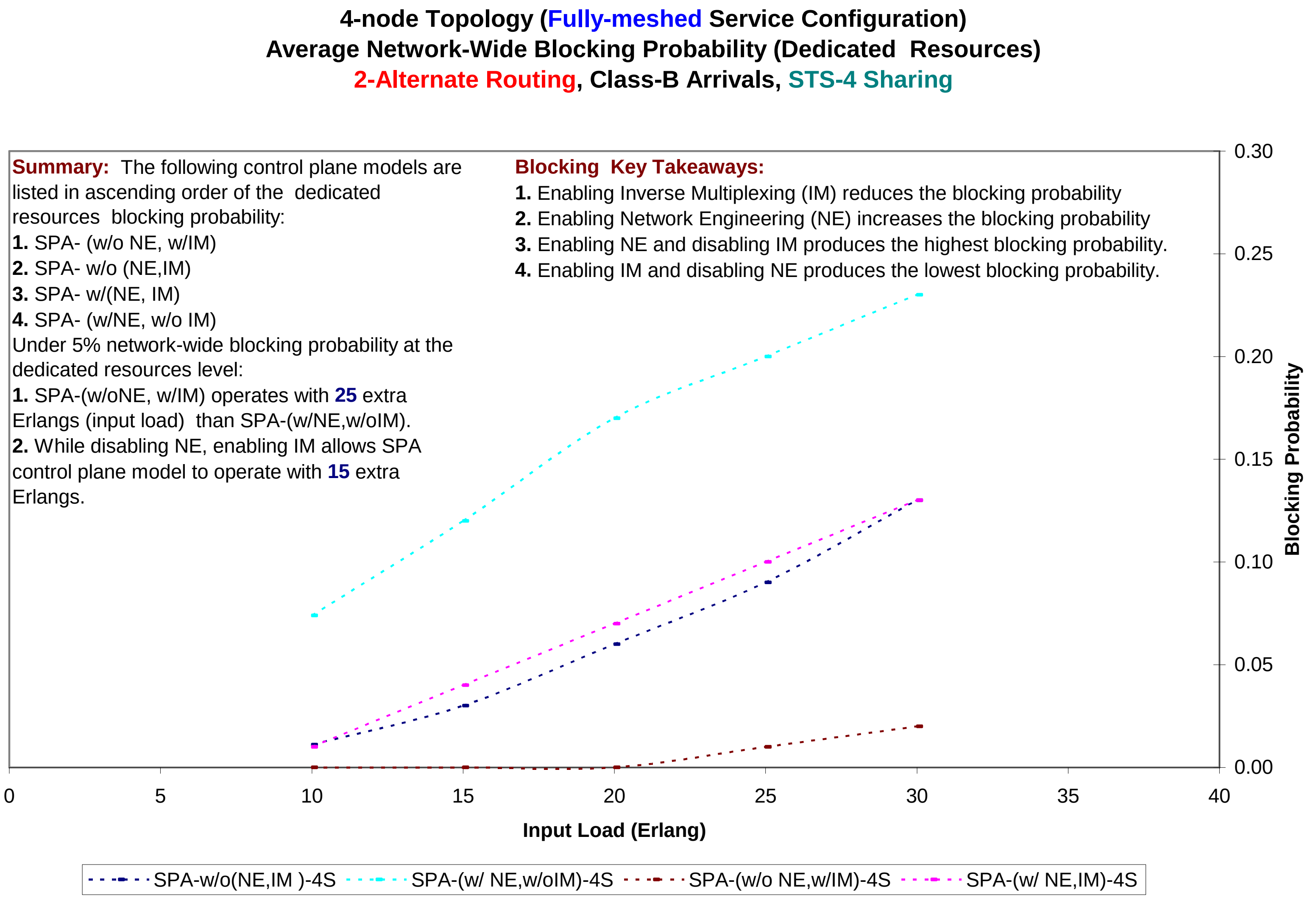

4-node Topology (Fully-meshed Service Configuration)
Average Network-Wide Blocking Probability (Dedicated Resources)
2-Alternate Routing, Class-B Arrivals, STS-4 Sharing

Summary: The following control plane models are listed in ascending order of the dedicated resources blocking probability:

1. SPA- (w/o NE, w/IM)

2. SPA- w/o (NE,IM)

3. SPA- w/(NE, IM)

4. SPA- (w/NE, w/o IM)

Under 5% network-wide blocking probability at the dedicated resources level:

1. SPA-(w/oNE, w/IM) operates with **25** extra Erlangs (input load) than SPA-(w/NE,w/oIM).

2. While disabling NE, enabling IM allows SPA control plane model to operate with **15** extra Erlangs.

Blocking Key Takeaways:

1. Enabling Inverse Multiplexing (IM) reduces the blocking probability

2. Enabling Network Engineering (NE) increases the blocking probability

3. Enabling NE and disabling IM produces the highest blocking probability.

4. Enabling IM and disabling NE produces the lowest blocking probability.

Figure 19-4: Average Network-Wide Blocking Probability (Dedicated Resources)-4 Node – 2 Alternate Route-STS-4 Sharing

19.1.2 Shared resources

This section provides detailed performance analysis of the network-wide blocking probability on the shared network resources partition for the 4-node topology. The configured VPN service evaluated is the Fully-meshed Shared Granular (FSF) with the following service profile layer parameters:

a. Service flow connectivity: configured as "fully-meshed".

b. Service demand granularity: configured as "granular" with 1 STS-1 granularity level.

c. Load partitioning flexibility: configured as "enabled".

One input class was evaluated with the following parameters: $k = 2$, $b_k^A = 2$ STS-1, $\mu_k = 1$unit time, $\lambda_{rk} = 4$ calls/unit time. Range of input load for 4-node topology is 10 to 30 Erlangs. The five traffic management schemes of the SPA control plane model are evaluated as provided in Table 9-1. Four sharing levels are considered as follows:

a. STS-1 sharing: C_j^{vD} =11 STS-1, C_j^S =2 STS-1

b. STS-2 sharing: C_j^{vD} =10 STS-1, C_j^S =4 STS-1

c. STS-3 sharing: C_j^{vD} =9 STS-1, C_j^S =6 STS-1

d. STS-4 sharing: C_j^{vD} =8 STS-1, C_j^S =8 STS-1

4-node Topology (Fully-meshed Service Configuration)
Average Network-Wide Blocking Probability (Shared Resources)
2-Alternate Routing, Class-B Arrivals, STS-1 Sharing

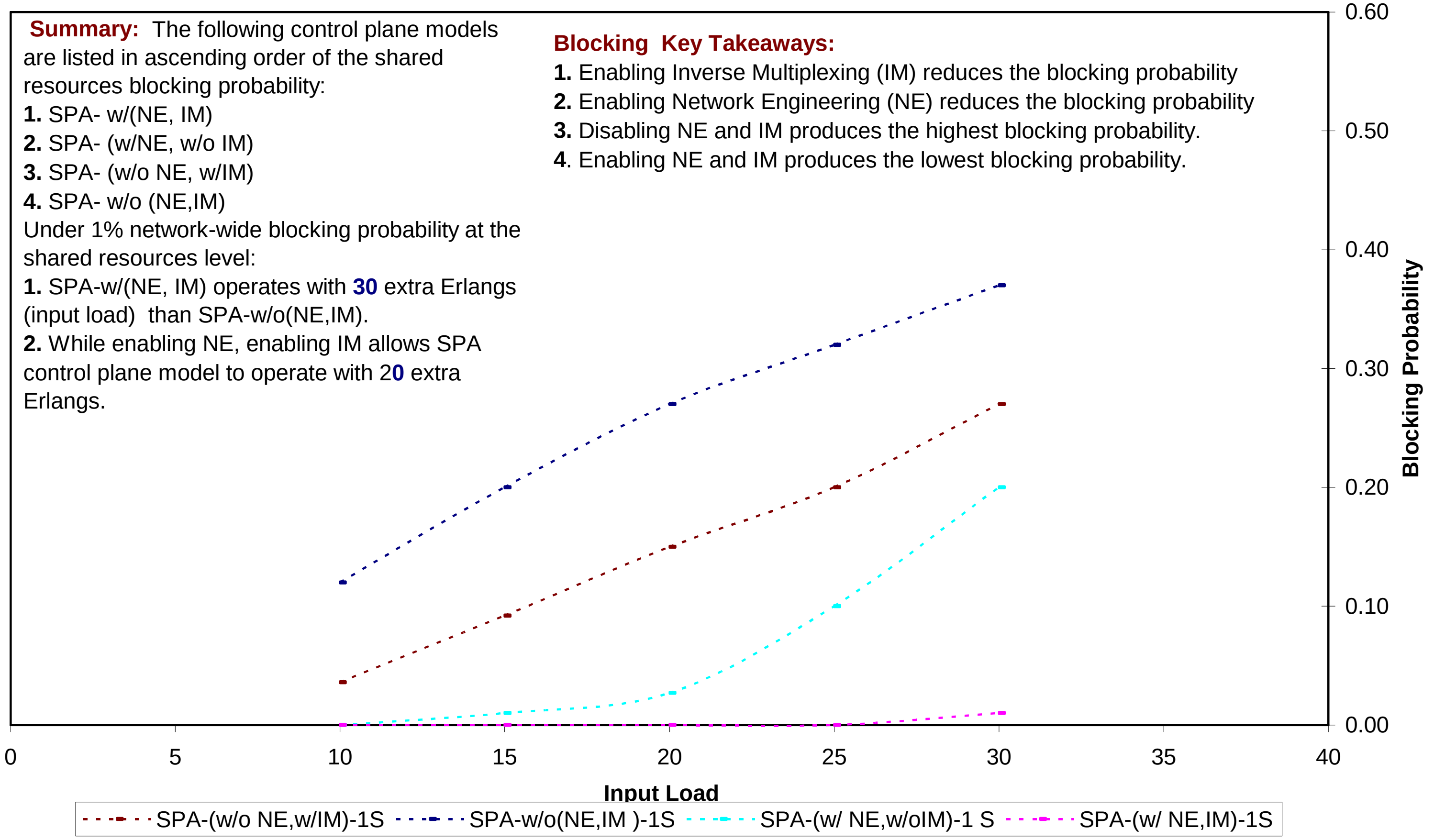

Summary: The following control plane models are listed in ascending order of the shared resources blocking probability:
1. SPA- w/(NE, IM)
2. SPA- (w/NE, w/o IM)
3. SPA- (w/o NE, w/IM)
4. SPA- w/o (NE,IM)
Under 1% network-wide blocking probability at the shared resources level:
1. SPA-w/(NE, IM) operates with **30** extra Erlangs (input load) than SPA-w/o(NE,IM).
2. While enabling NE, enabling IM allows SPA control plane model to operate with 2**0** extra Erlangs.

Blocking Key Takeaways:
1. Enabling Inverse Multiplexing (IM) reduces the blocking probability
2. Enabling Network Engineering (NE) reduces the blocking probability
3. Disabling NE and IM produces the highest blocking probability.
4. Enabling NE and IM produces the lowest blocking probability.

Figure 19-5: Average Network-Wide Blocking Probability (Shared Resources)-4 Node – 2 Alternate Route-STS-1 Sharing

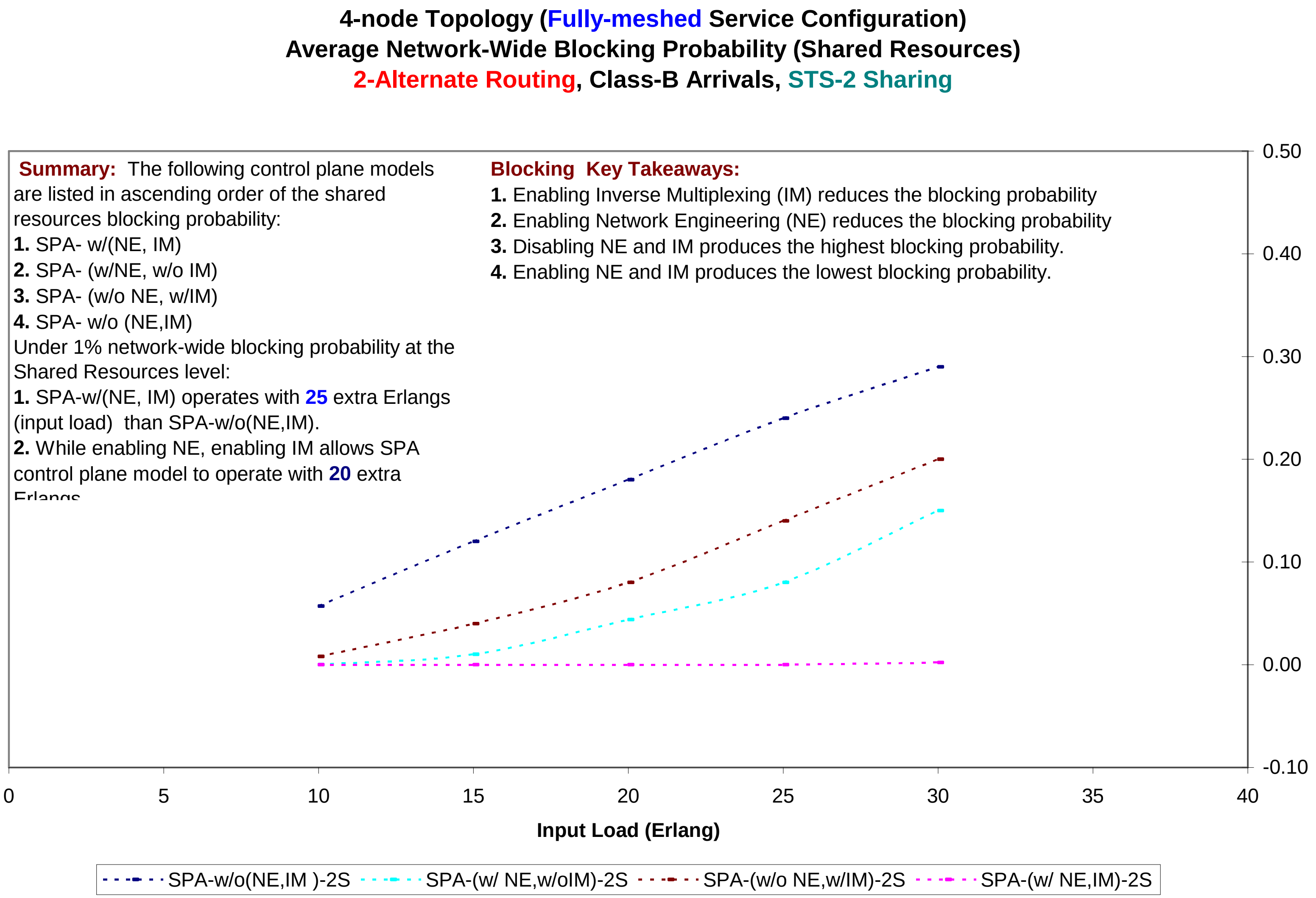

Summary: The following control plane models are listed in ascending order of the shared resources blocking probability:

1. SPA- w/(NE, IM)
2. SPA- (w/NE, w/o IM)
3. SPA- (w/o NE, w/IM)
4. SPA- w/o (NE,IM)

Under 1% network-wide blocking probability at the Shared Resources level:

1. SPA-w/(NE, IM) operates with **25** extra Erlangs (input load) than SPA-w/o(NE,IM).
2. While enabling NE, enabling IM allows SPA control plane model to operate with **20** extra Erlangs

Blocking Key Takeaways:

1. Enabling Inverse Multiplexing (IM) reduces the blocking probability
2. Enabling Network Engineering (NE) reduces the blocking probability
3. Disabling NE and IM produces the highest blocking probability.
4. Enabling NE and IM produces the lowest blocking probability.

Figure 19-6: Average Network-Wide Blocking Probability (Shared Resources)-4 Node – 2 Alternate Route-STS-2 Sharing

4-node Topology (Fully-meshed Service Configuration)
Average Network-Wide Blocking Probability (Shared Resources)
2-Alternate Routing, Class-B Arrivals, STS-3 Sharing

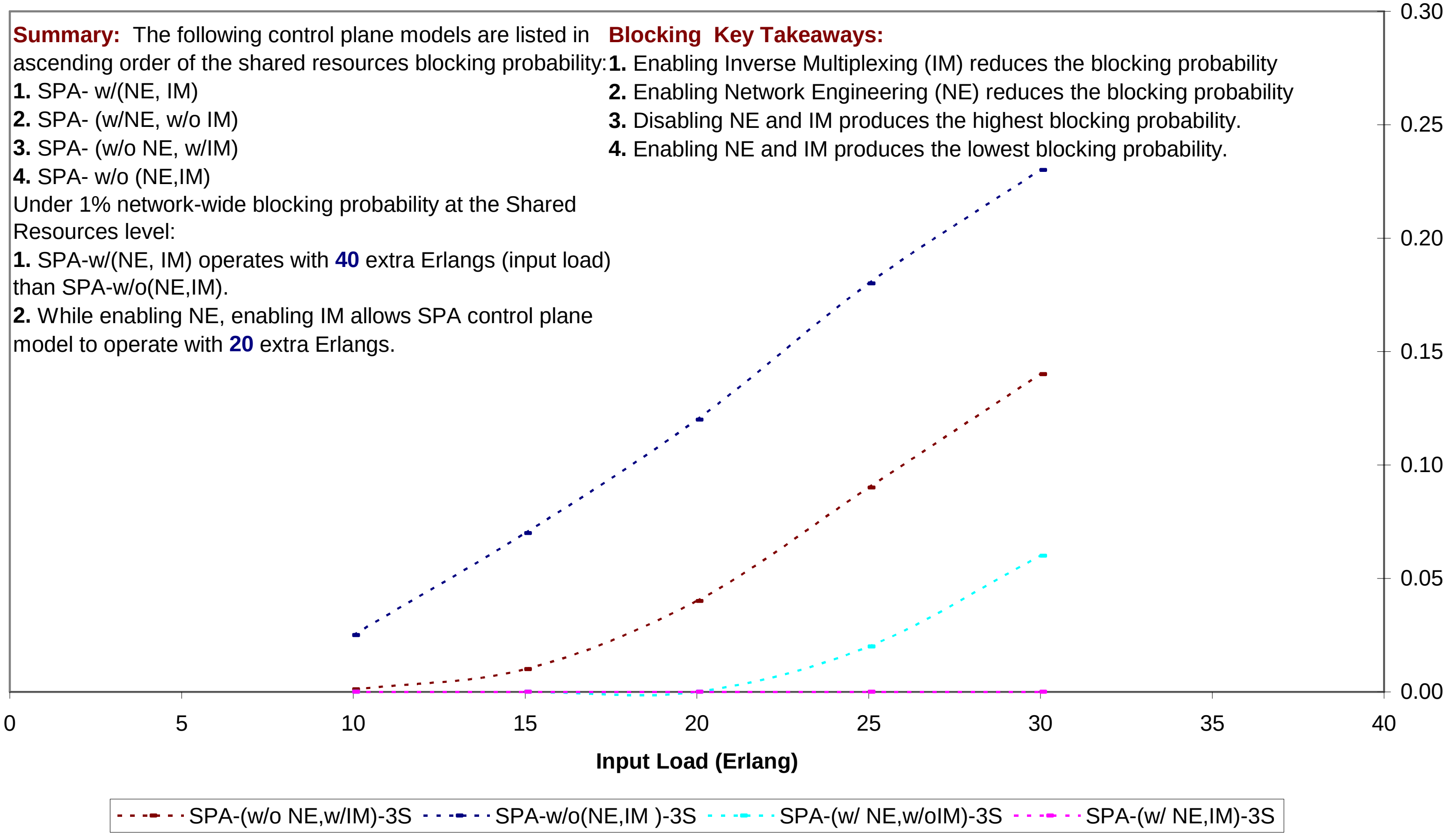

Summary: The following control plane models are listed in ascending order of the shared resources blocking probability:

1. SPA- w/(NE, IM)
2. SPA- (w/NE, w/o IM)
3. SPA- (w/o NE, w/IM)
4. SPA- w/o (NE,IM)

Under 1% network-wide blocking probability at the Shared Resources level:

1. SPA-w/(NE, IM) operates with **40** extra Erlangs (input load) than SPA-w/o(NE,IM).

2. While enabling NE, enabling IM allows SPA control plane model to operate with **20** extra Erlangs.

Blocking Key Takeaways:

1. Enabling Inverse Multiplexing (IM) reduces the blocking probability
2. Enabling Network Engineering (NE) reduces the blocking probability
3. Disabling NE and IM produces the highest blocking probability.
4. Enabling NE and IM produces the lowest blocking probability.

Figure 19-7: Average Network-Wide Blocking Probability (Shared Resources)-4 Node – 2 Alternate Route-STS-3 Sharing

4-node Topology (Fully-meshed Service Configuration)
Average Network-Wide Blocking Probability (Shared Resources)
2-Alternate Routing, Class-B Arrivals, STS-4 Sharing

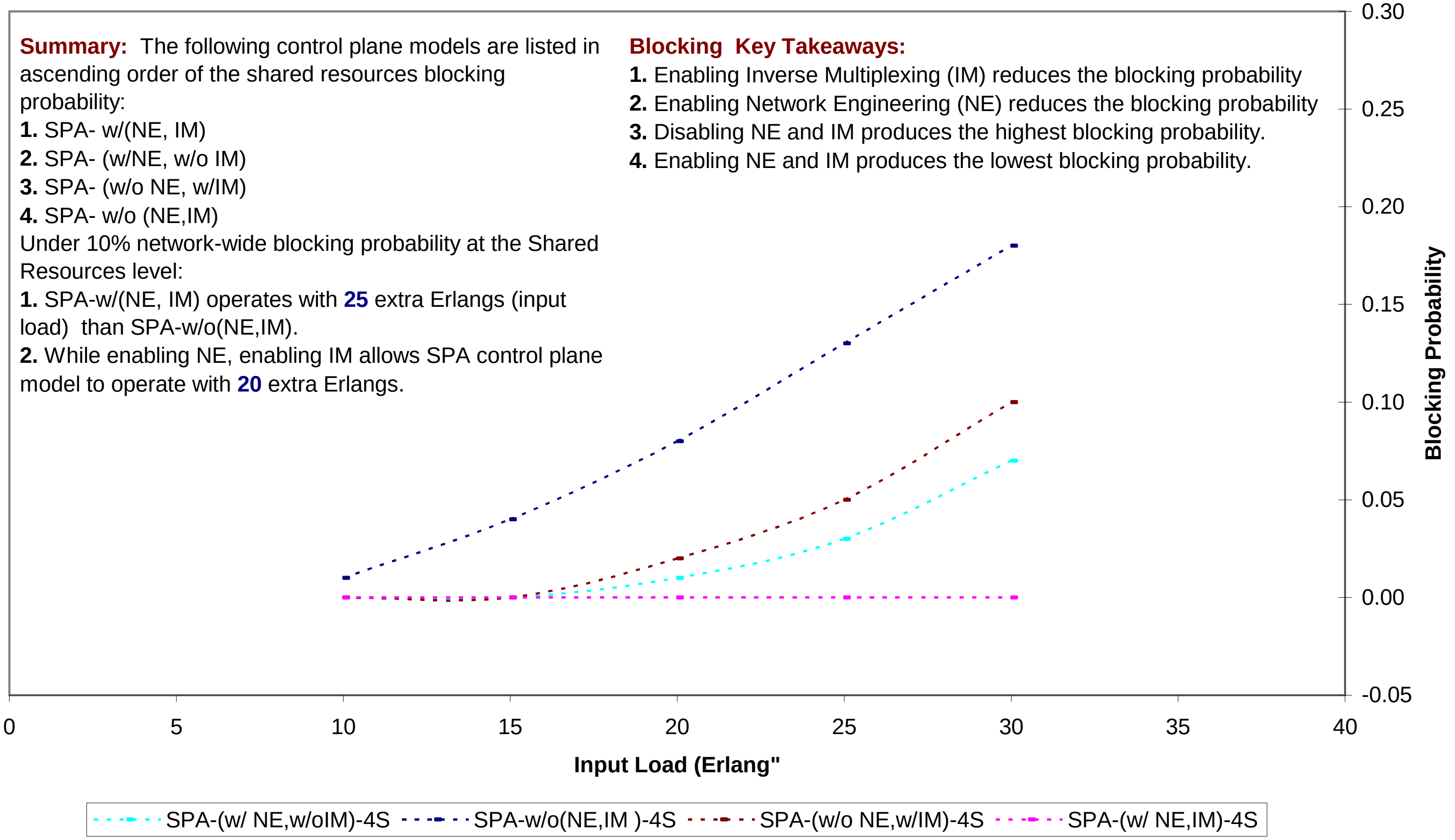

Summary: The following control plane models are listed in ascending order of the shared resources blocking probability:
1. SPA- w/(NE, IM)
2. SPA- (w/NE, w/o IM)
3. SPA- (w/o NE, w/IM)
4. SPA- w/o (NE,IM)
Under 10% network-wide blocking probability at the Shared Resources level:
1. SPA-w/(NE, IM) operates with **25** extra Erlangs (input load) than SPA-w/o(NE,IM).
2. While enabling NE, enabling IM allows SPA control plane model to operate with **20** extra Erlangs.

Blocking Key Takeaways:
1. Enabling Inverse Multiplexing (IM) reduces the blocking probability
2. Enabling Network Engineering (NE) reduces the blocking probability
3. Disabling NE and IM produces the highest blocking probability.
4. Enabling NE and IM produces the lowest blocking probability.

Figure 19-8: Average Network-Wide Blocking Probability (Shared Resources)-4 Node – 2 Alternate Route-STS-4 Sharing

19.1.3 VPN resources

This section provides detailed performance analysis of the network-wide blocking probability on the VPN network resources partition for the 4-node topology. The configured VPN service evaluated is the Fully-meshed Shared Granular (FSF) with the following service profile layer parameters:

a. Service flow connectivity: configured as “fully-meshed”.

b. Service demand granularity: configured as “granular” with 1 STS-1 granularity level.

c. Load partitioning flexibility: configured as “enabled”.

One input class was evaluated with the following parameters: $k = 2$, $b_k^A = 2$ STS-1, $\mu_k = 1$unit time, $\lambda_{rk} = 4$ calls/unit time. Range of input load for 4-node topology is 10 to 30 Erlangs. The five traffic management schemes of the SPA control plane model are evaluated as provided in Table 9-1. Four sharing levels are considered as follows:

a. STS-1 sharing: C_j^{vD} =11 STS-1, C_j^S =2 STS-1

b. STS-2 sharing: C_j^{vD} =10 STS-1, C_j^S =4 STS-1

c. STS-3 sharing: C_j^{vD} =9 STS-1, C_j^S =6 STS-1

d. STS-4 sharing: C_j^{vD} =8 STS-1, C_j^S =8 STS-1

4-node Topology (Fully-meshed Service Configuration)
Average Network-Wide Blocking Probability (VPN Resources)
2-Alternate Routing, Class-B Arrivals, ITU(DR,SR), SPA-Dedicated

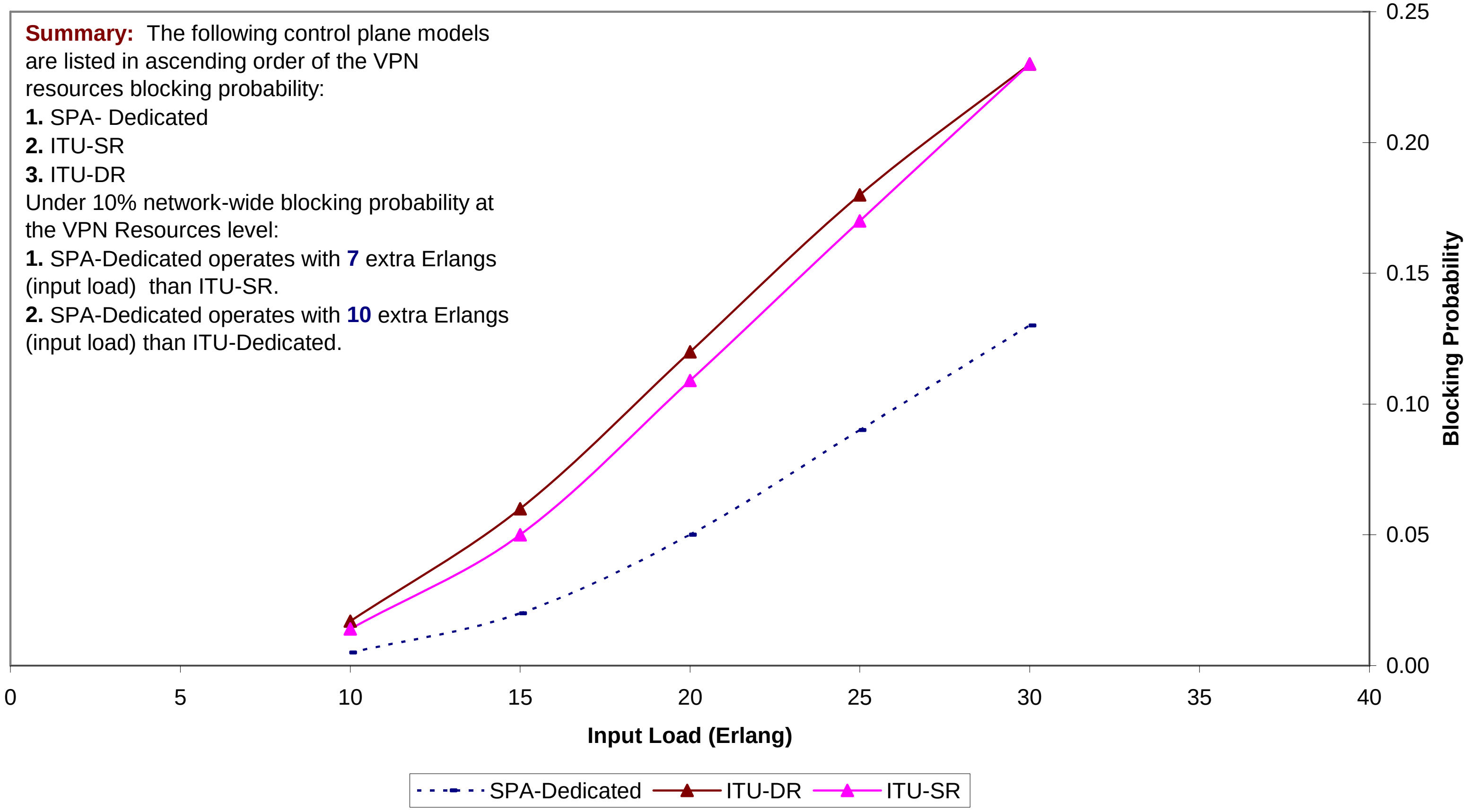

Summary: The following control plane models are listed in ascending order of the VPN resources blocking probability:

1. SPA- Dedicated
2. ITU-SR
3. ITU-DR

Under 10% network-wide blocking probability at the VPN Resources level:

1. SPA-Dedicated operates with **7** extra Erlangs (input load) than ITU-SR.
2. SPA-Dedicated operates with **10** extra Erlangs (input load) than ITU-Dedicated.

Figure 19-9: Average Network-Wide Blocking Probability (VPN Resources)-4 Node – 2 Alternate Route-ITU (DR,SR), SPA-Dedicated

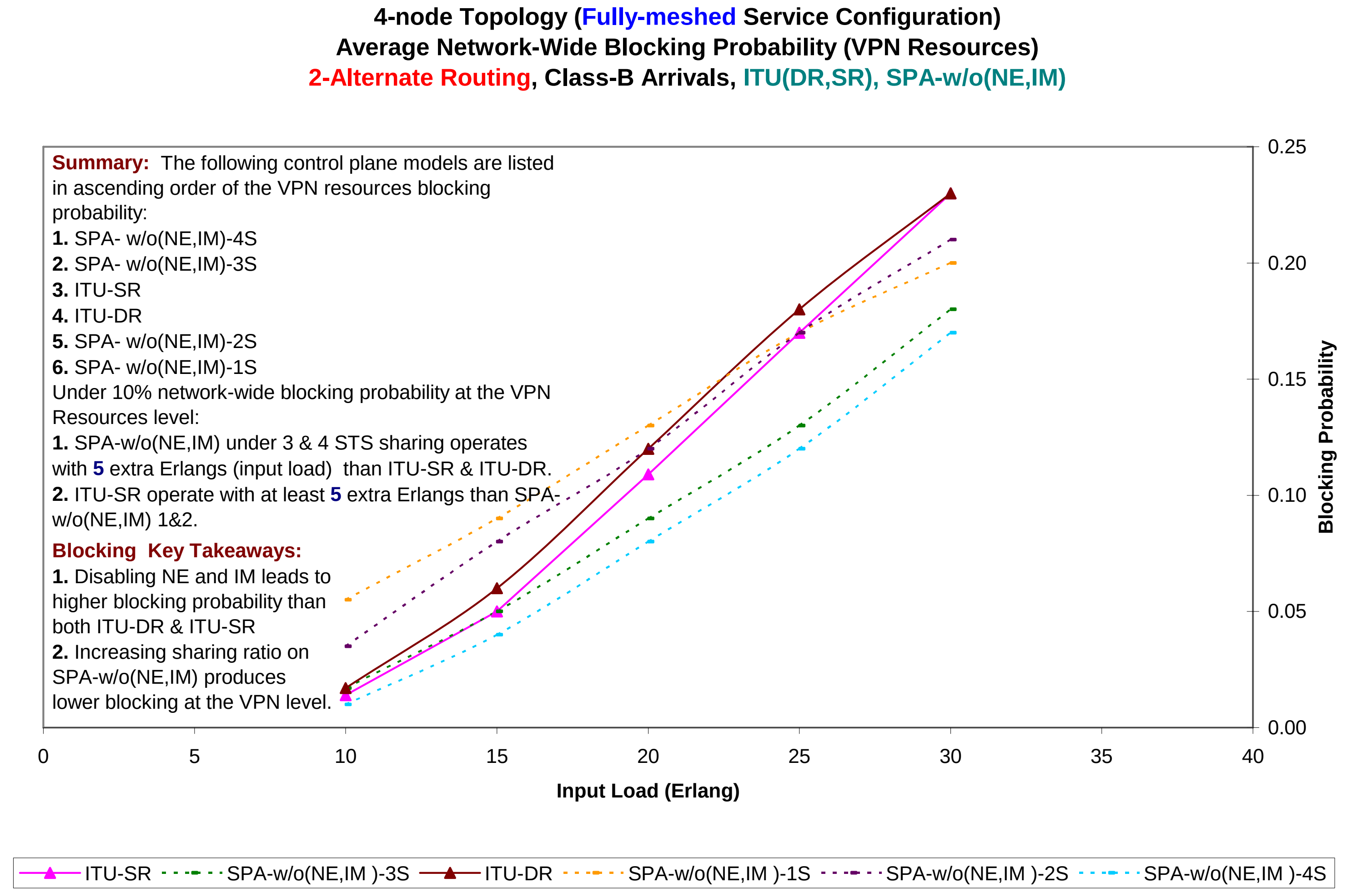

4-node Topology (Fully-meshed Service Configuration)
Average Network-Wide Blocking Probability (VPN Resources)
2-Alternate Routing, Class-B Arrivals, ITU(DR,SR), SPA-w/o(NE,IM)

Summary: The following control plane models are listed in ascending order of the VPN resources blocking probability:

1. SPA- w/o(NE,IM)-4S
2. SPA- w/o(NE,IM)-3S
3. ITU-SR
4. ITU-DR
5. SPA- w/o(NE,IM)-2S
6. SPA- w/o(NE,IM)-1S

Under 10% network-wide blocking probability at the VPN Resources level:

1. SPA-w/o(NE,IM) under 3 & 4 STS sharing operates with **5** extra Erlangs (input load) than ITU-SR & ITU-DR.
2. ITU-SR operate with at least **5** extra Erlangs than SPA-w/o(NE,IM) 1&2.

Blocking Key Takeaways:

1. Disabling NE and IM leads to higher blocking probability than both ITU-DR & ITU-SR
2. Increasing sharing ratio on SPA-w/o(NE,IM) produces lower blocking at the VPN level.

Figure 19-10: Average Network-Wide Blocking Probability (VPN Resources)-4 Node – 2 Alternate Route- ITU (DR,SR), SPA-w/o(NE,IM)

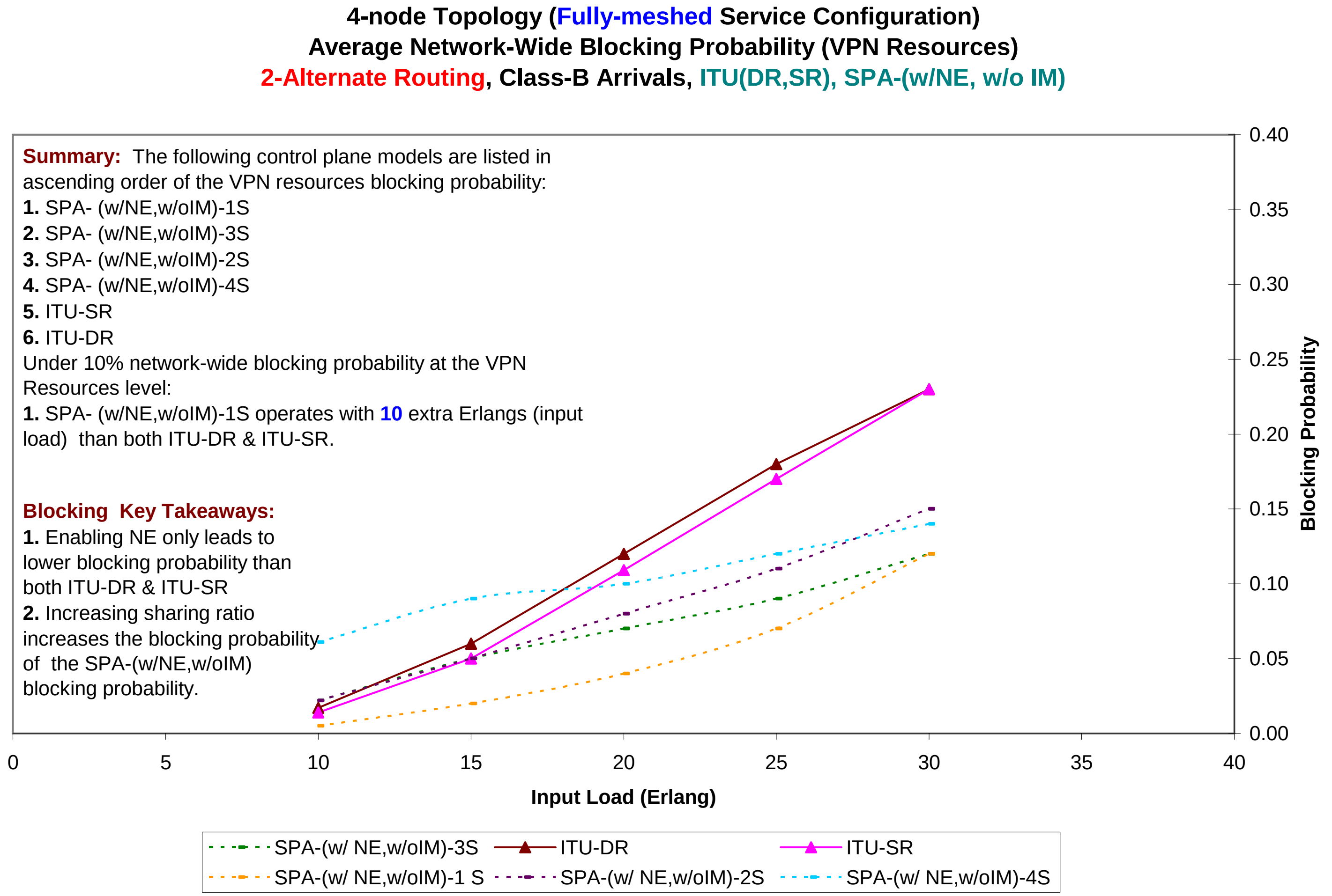

Summary: The following control plane models are listed in ascending order of the VPN resources blocking probability:

1. SPA- (w/NE,w/oIM)-1S
2. SPA- (w/NE,w/oIM)-3S
3. SPA- (w/NE,w/oIM)-2S
4. SPA- (w/NE,w/oIM)-4S
5. ITU-SR
6. ITU-DR

Under 10% network-wide blocking probability at the VPN Resources level:

1. SPA- (w/NE,w/oIM)-1S operates with **10** extra Erlangs (input load) than both ITU-DR & ITU-SR.

Blocking Key Takeaways:

1. Enabling NE only leads to lower blocking probability than both ITU-DR & ITU-SR
2. Increasing sharing ratio increases the blocking probability of the SPA-(w/NE,w/oIM) blocking probability.

Figure 19-11: Average Network-Wide Blocking Probability (VPN Resources)-4 Node – 2 Alternate Route-- ITU (DR,SR), SPA-w/NE,w/oIM

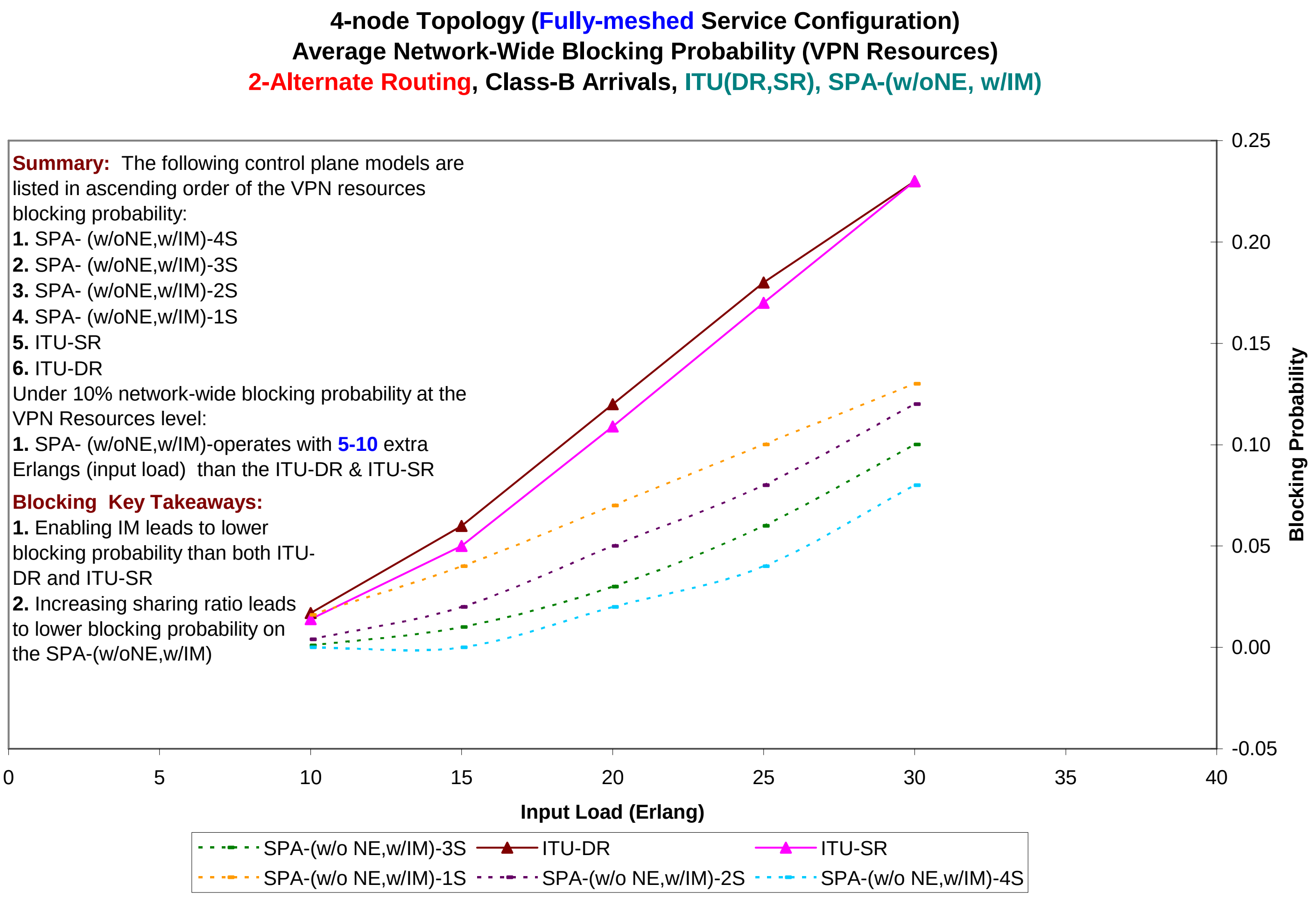

4-node Topology (Fully-meshed Service Configuration)
Average Network-Wide Blocking Probability (VPN Resources)
2-Alternate Routing, Class-B Arrivals, ITU(DR,SR), SPA-(w/oNE, w/IM)

Summary: The following control plane models are listed in ascending order of the VPN resources blocking probability:

1. SPA- (w/oNE,w/IM)-4S
2. SPA- (w/oNE,w/IM)-3S
3. SPA- (w/oNE,w/IM)-2S
4. SPA- (w/oNE,w/IM)-1S
5. ITU-SR
6. ITU-DR

Under 10% network-wide blocking probability at the VPN Resources level:

1. SPA- (w/oNE,w/IM)-operates with 5-10 extra Erlangs (input load) than the ITU-DR & ITU-SR

Blocking Key Takeaways:

1. Enabling IM leads to lower blocking probability than both ITU-DR and ITU-SR

2. Increasing sharing ratio leads to lower blocking probability on the SPA-(w/oNE,w/IM)

Figure 19-12: Average Network-Wide Blocking Probability (VPN Resources)-4 Node – 2 Alternate Route-- ITU (DR,SR), SPA-w/oNE,w/IM

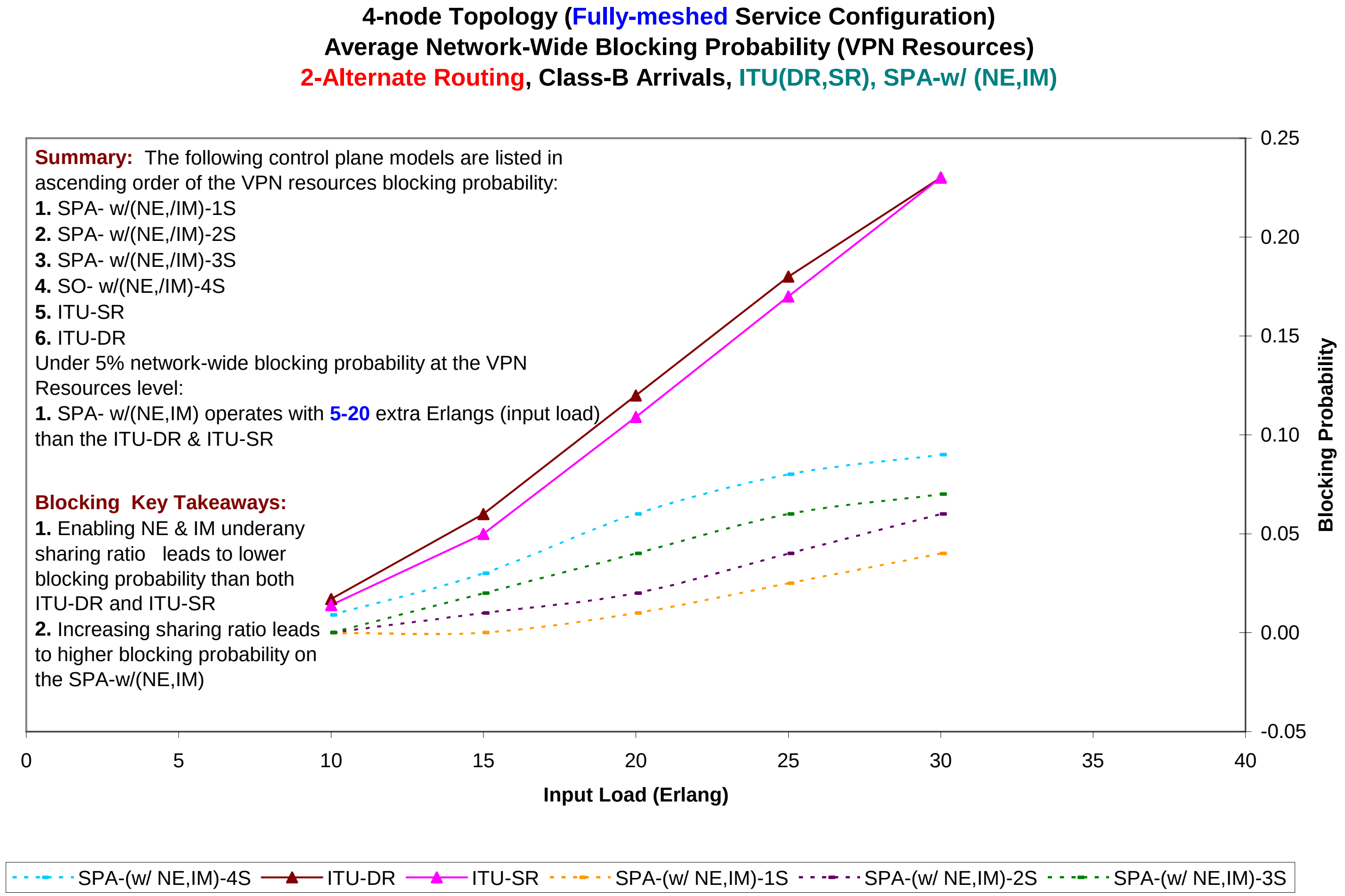

4-node Topology (Fully-meshed Service Configuration)
Average Network-Wide Blocking Probability (VPN Resources)
2-Alternate Routing, Class-B Arrivals, ITU(DR,SR), SPA-w/ (NE,IM)

Summary: The following control plane models are listed in ascending order of the VPN resources blocking probability:

1. SPA- w/(NE,/IM)-1S
2. SPA- w/(NE,/IM)-2S
3. SPA- w/(NE,/IM)-3S
4. SO- w/(NE,/IM)-4S
5. ITU-SR
6. ITU-DR

Under 5% network-wide blocking probability at the VPN Resources level:

1. SPA- w/(NE,IM) operates with 5-20 extra Erlangs (input load) than the ITU-DR & ITU-SR

Blocking Key Takeaways:

1. Enabling NE & IM underany sharing ratio leads to lower blocking probability than both ITU-DR and ITU-SR
2. Increasing sharing ratio leads to higher blocking probability on the SPA-w/(NE,IM)

Figure 19-13: Average Network-Wide Blocking Probability (VPN Resources)-4 Node – 2 Alternate Route-- ITU (DR,SR), SPA-w/(NE,IM)

19.1.4 Physical resources

This section provides detailed performance analysis of the network-wide blocking probability on the physical resource level for the 4-node topology. The configured VPN service evaluated is the Fully-meshed Shared Granular (FSF) with the following service profile layer parameters:

a. Service flow connectivity: configured as “fully-meshed”.

b. Service demand granularity: configured as “granular” with 1 STS-1 granularity level.

c. Load partitioning flexibility: configured as “enabled”.

One input class was evaluated with the following parameters: $k = 2$, $b_k^A = 2$ STS-1, $\mu_k = 1$unit time, $\lambda_{rk} = 4$ calls/unit time. Range of input load for 4-node topology is 10 to 30 Erlangs. The five traffic management schemes of the SPA control plane model are evaluated as provided in Table 9-1.

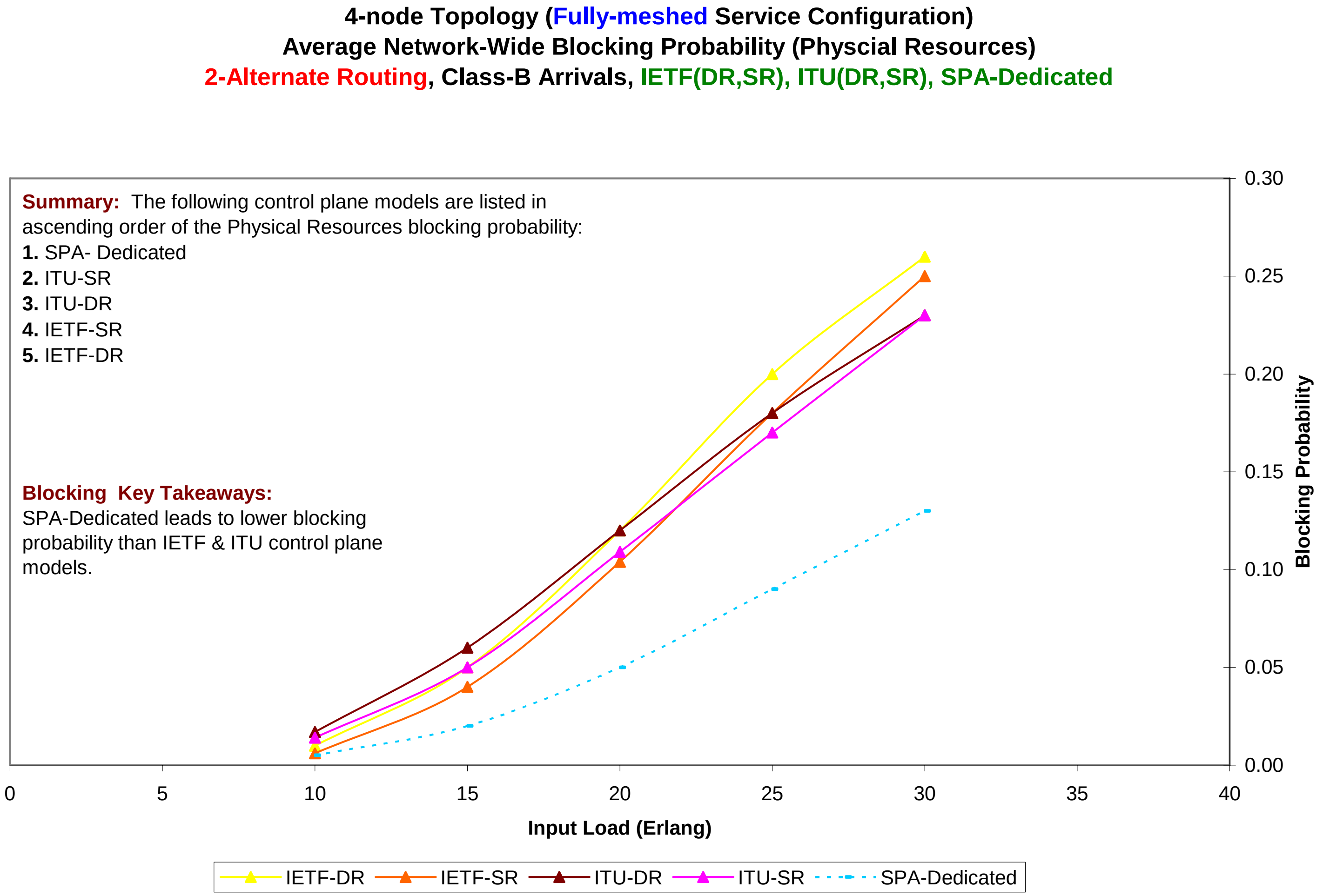

4-node Topology (Fully-meshed Service Configuration)
Average Network-Wide Blocking Probability (Physcial Resources)
2-Alternate Routing, Class-B Arrivals, IETF(DR,SR), ITU(DR,SR), SPA-Dedicated

Summary: The following control plane models are listed in ascending order of the Physical Resources blocking probability:

1. SPA- Dedicated
2. ITU-SR
3. ITU-DR
4. IETF-SR
5. IETF-DR

Blocking Key Takeaways:
SPA-Dedicated leads to lower blocking probability than IETF & ITU control plane models.

Figure 19-14: Average Network-Wide Blocking Probability (Physical Resources)-4 Node- IETF (DR, SR), ITU (DR, SR), SPA-Dedicated

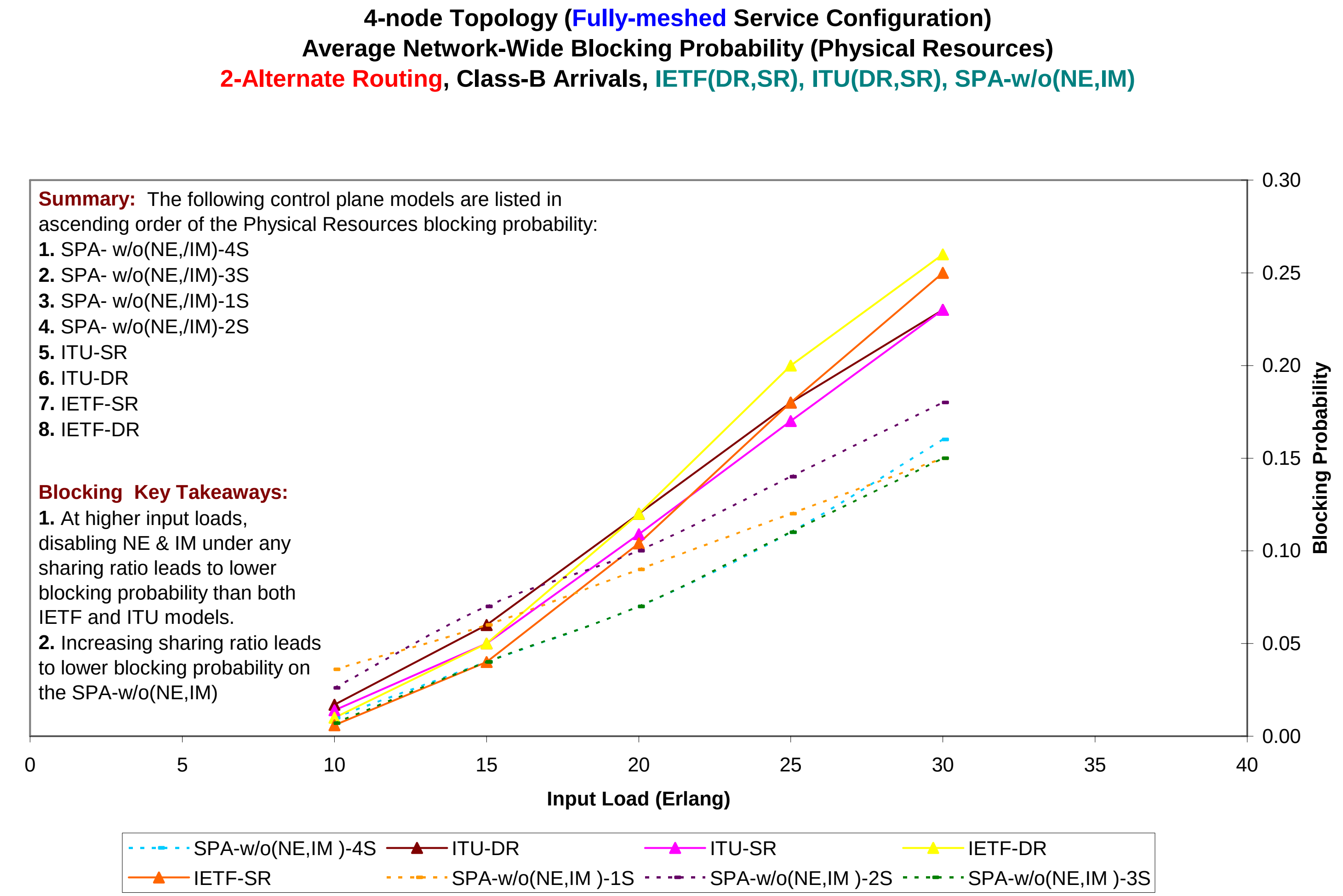

4-node Topology (Fully-meshed Service Configuration)
Average Network-Wide Blocking Probability (Physical Resources)
2-Alternate Routing, Class-B Arrivals, IETF(DR,SR), ITU(DR,SR), SPA-w/o(NE,IM)

Summary: The following control plane models are listed in ascending order of the Physical Resources blocking probability:

1. SPA- w/o(NE,/IM)-4S
2. SPA- w/o(NE,/IM)-3S
3. SPA- w/o(NE,/IM)-1S
4. SPA- w/o(NE,/IM)-2S
5. ITU-SR
6. ITU-DR
7. IETF-SR
8. IETF-DR

Blocking Key Takeaways:

1. At higher input loads, disabling NE & IM under any sharing ratio leads to lower blocking probability than both IETF and ITU models.

2. Increasing sharing ratio leads to lower blocking probability on the SPA-w/o(NE,IM)

Figure 19-15: Average Network-Wide Blocking Probability (Physical Resources)-4 Node – IETF(DR,SR), ITU(DR,SR), SPA-w/o(NE,IM)

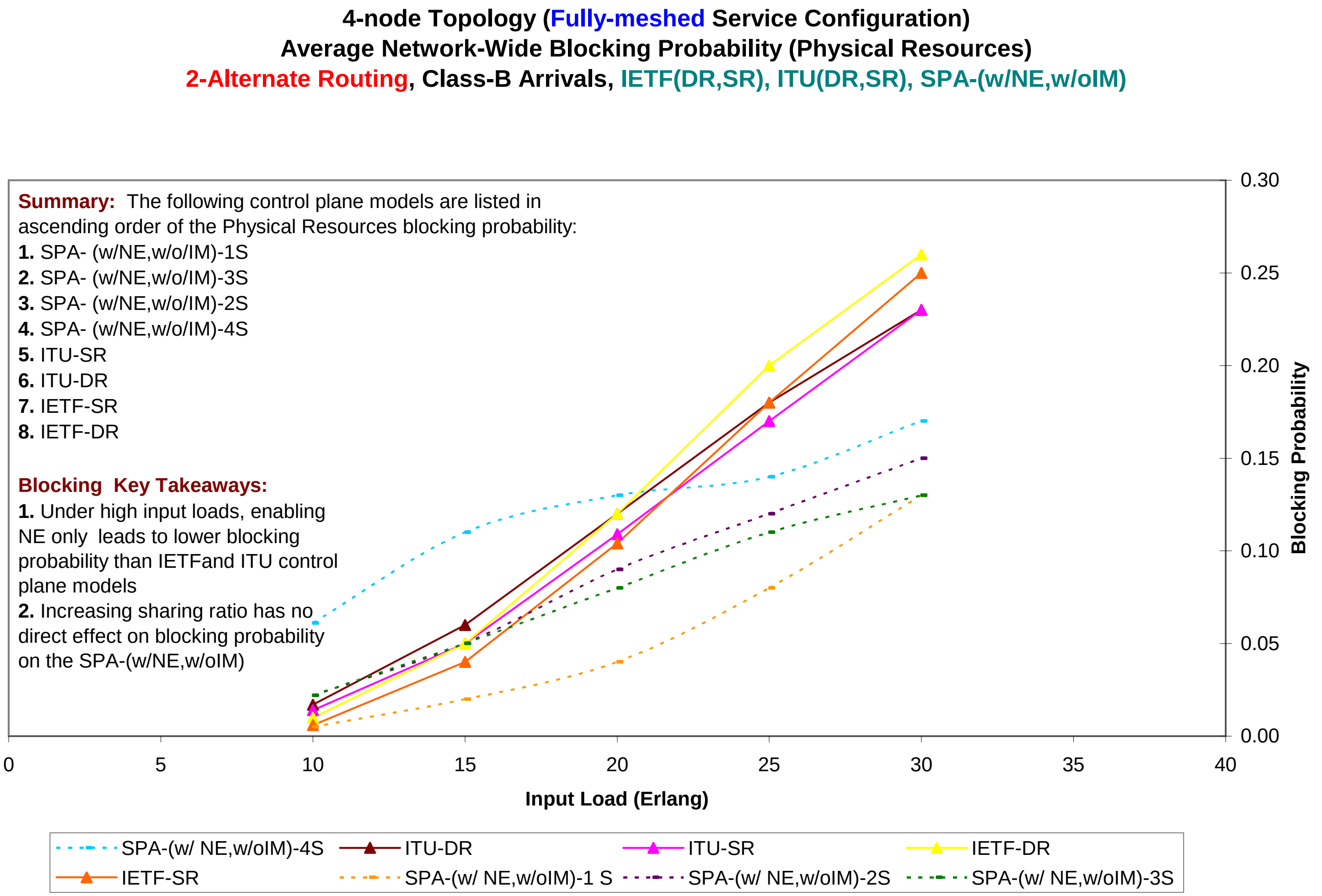

4-node Topology (Fully-meshed Service Configuration)
Average Network-Wide Blocking Probability (Physical Resources)
2-Alternate Routing, Class-B Arrivals, IETF(DR,SR), ITU(DR,SR), SPA-(w/NE,w/oIM)

Summary: The following control plane models are listed in ascending order of the Physical Resources blocking probability:

1. SPA- (w/NE,w/o/IM)-1S
2. SPA- (w/NE,w/o/IM)-3S
3. SPA- (w/NE,w/o/IM)-2S
4. SPA- (w/NE,w/o/IM)-4S
5. ITU-SR
6. ITU-DR
7. IETF-SR
8. IETF-DR

Blocking Key Takeaways:

1. Under high input loads, enabling NE only leads to lower blocking probability than IETFand ITU control plane models
2. Increasing sharing ratio has no direct effect on blocking probability on the SPA-(w/NE,w/oIM)

Figure 19-16: Average Network-Wide Blocking Probability (Physical Resources)-4 Node – IETF(DR,SR), ITU(DR,SR), SPA-(w/NE,w/oIM)

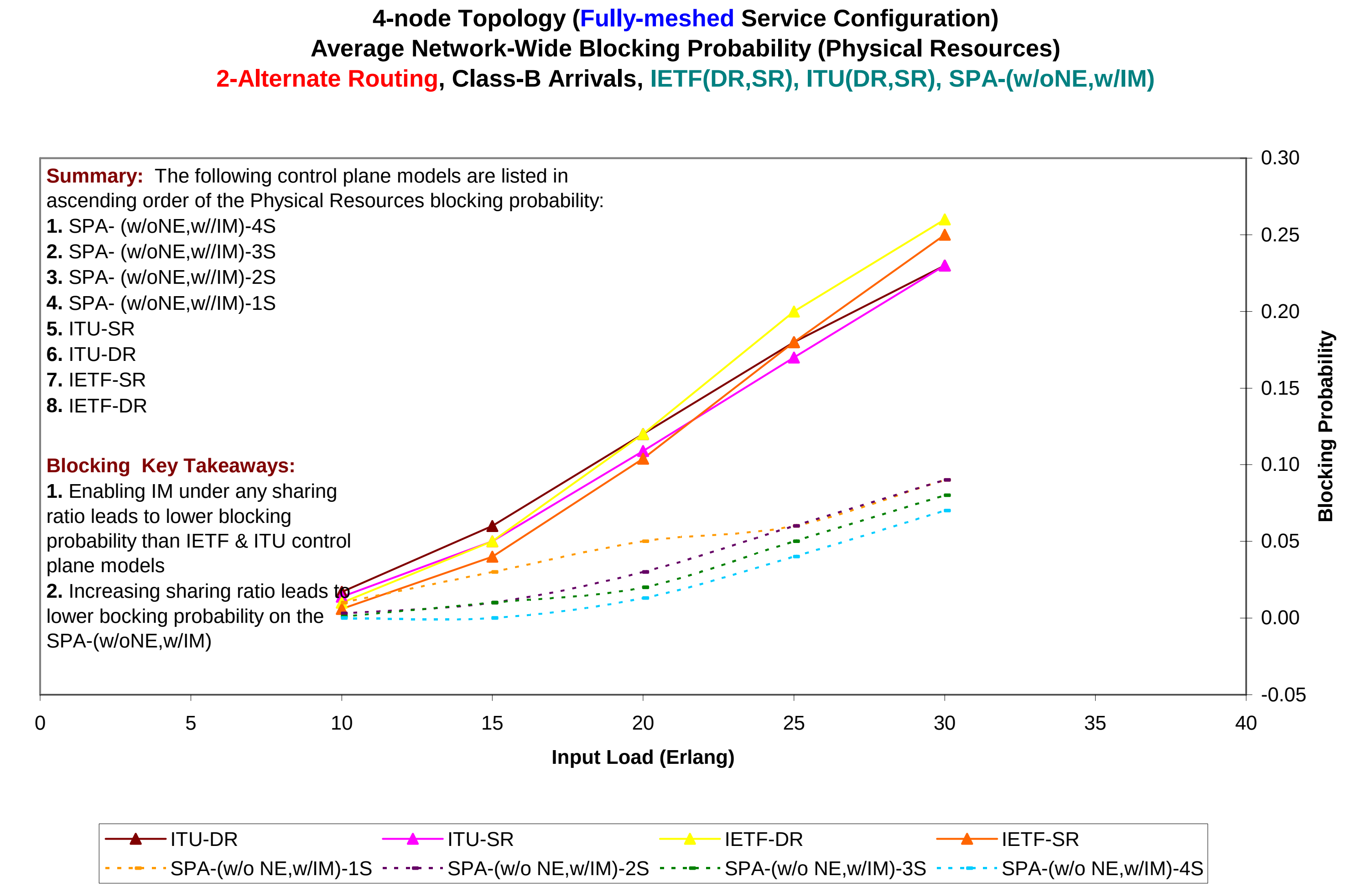

Figure 19-17: Average Network-Wide Blocking Probability (Physical Resources)-4 Node – IETF(DR,SR), ITU(DR,SR), SPA-(w/oNE,w/IM)

4-node Topology (Fully-meshed Service Configuration)
Average Network-Wide Blocking Probability (Physical Resources)
2-Alternate Routing, Class-B Arrivals, IETF(DR,SR), ITU(DR,SR), SPA-w/(NE,IM)

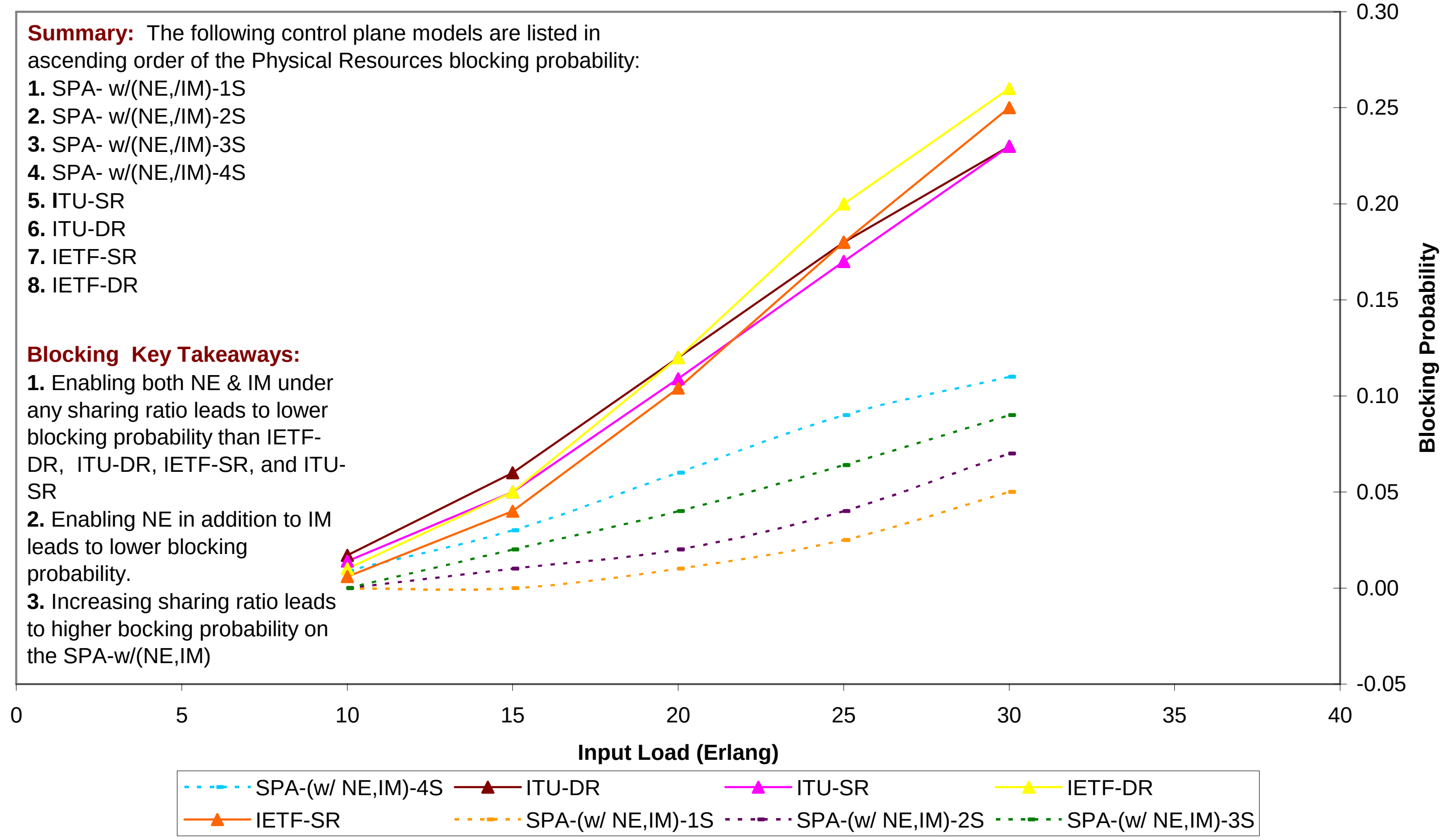

Summary: The following control plane models are listed in ascending order of the Physical Resources blocking probability:
1. SPA- w/(NE,/IM)-1S
2. SPA- w/(NE,/IM)-2S
3. SPA- w/(NE,/IM)-3S
4. SPA- w/(NE,/IM)-4S
5. ITU-SR
6. ITU-DR
7. IETF-SR
8. IETF-DR

Blocking Key Takeaways:
1. Enabling both NE & IM under any sharing ratio leads to lower blocking probability than IETF-DR, ITU-DR, IETF-SR, and ITU-SR
2. Enabling NE in addition to IM leads to lower blocking probability.
3. Increasing sharing ratio leads to higher bocking probability on the SPA-w/(NE,IM)

Figure 19-18: Average Network-Wide Blocking Probability (Physical Resources)-4 Node – IETF(DR,SR), ITU(DR,SR), SPA-w/(NE,IM)

19.2 Permissible load

19.2.1 Dedicated resources

This section provides detailed performance analysis of network-wide permissible load on the dedicated network resources partition for the 4-node topology. The configured VPN service evaluated is the Fully-meshed Shared Granular (FSF) with the following service profile layer parameters:

a. Service flow connectivity: configured as “fully-meshed”.

b. Service demand granularity: configured as “granular” with 1 STS-1 granularity level.

c. Load partitioning flexibility: configured as “enabled”.

One input class was evaluated with the following parameters: $k = 2$, $b_k^A = 2$ STS-1, $\mu_k = 1$unit time, $\lambda_{rk} = 4$ calls/unit time. Range of input load for 4-node topology is 10 to 30 Erlangs. The five traffic management schemes of the SPA control plane model are evaluated as provided in Table 9-1. Four sharing levels are considered as follows:

a. STS-1 sharing: C_j^{vD} =11 STS-1, C_j^S =2 STS-1

b. STS-2 sharing: C_j^{vD} =10 STS-1, C_j^S =4 STS-1

c. STS-3 sharing: C_j^{vD} =9 STS-1, C_j^S =6 STS-1

d. STS-4 sharing: C_j^{vD} =8 STS-1, C_j^S =8 STS-1

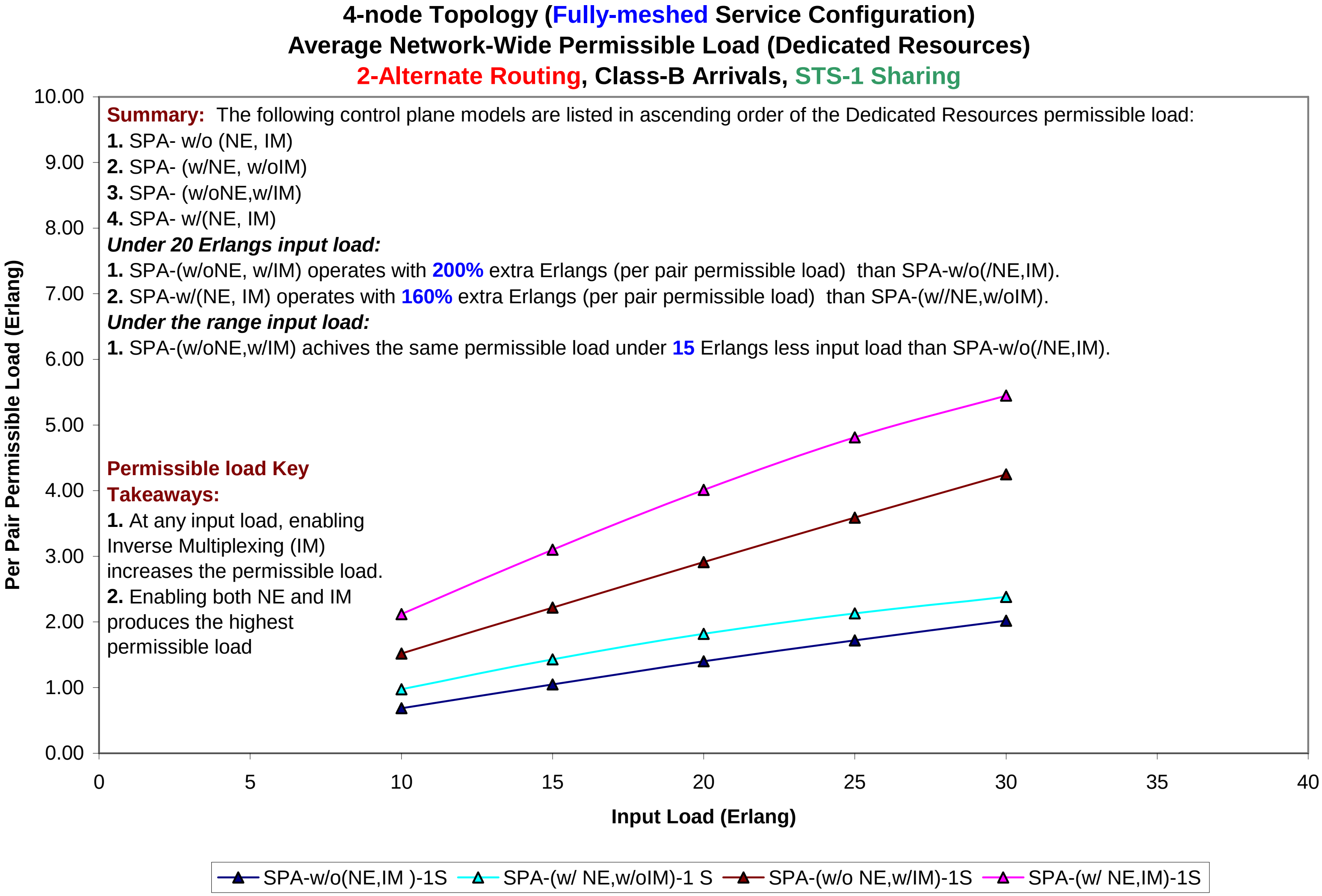

4-node Topology (Fully-meshed Service Configuration)
Average Network-Wide Permissible Load (Dedicated Resources)
2-Alternate Routing, Class-B Arrivals, STS-1 Sharing

Summary: The following control plane models are listed in ascending order of the Dedicated Resources permissible load:

1. SPA- w/o (NE, IM)
2. SPA- (w/NE, w/oIM)
3. SPA- (w/oNE,w/IM)
4. SPA- w/(NE, IM)

Under 20 Erlangs input load:

1. SPA-(w/oNE, w/IM) operates with **200%** extra Erlangs (per pair permissible load) than SPA-w/o(/NE,IM).
2. SPA-w/(NE, IM) operates with **160%** extra Erlangs (per pair permissible load) than SPA-(w//NE,w/oIM).

Under the range input load:

1. SPA-(w/oNE,w/IM) achives the same permissible load under **15** Erlangs less input load than SPA-w/o(/NE,IM).

Permissible load Key Takeaways:

1. At any input load, enabling Inverse Multiplexing (IM) increases the permissible load.
2. Enabling both NE and IM produces the highest permissible load

Figure 19-19: Average Network-Wide Permissible Load (Dedicated Resources)-4 Node – 2 Alternate Route-STS-1 Sharing

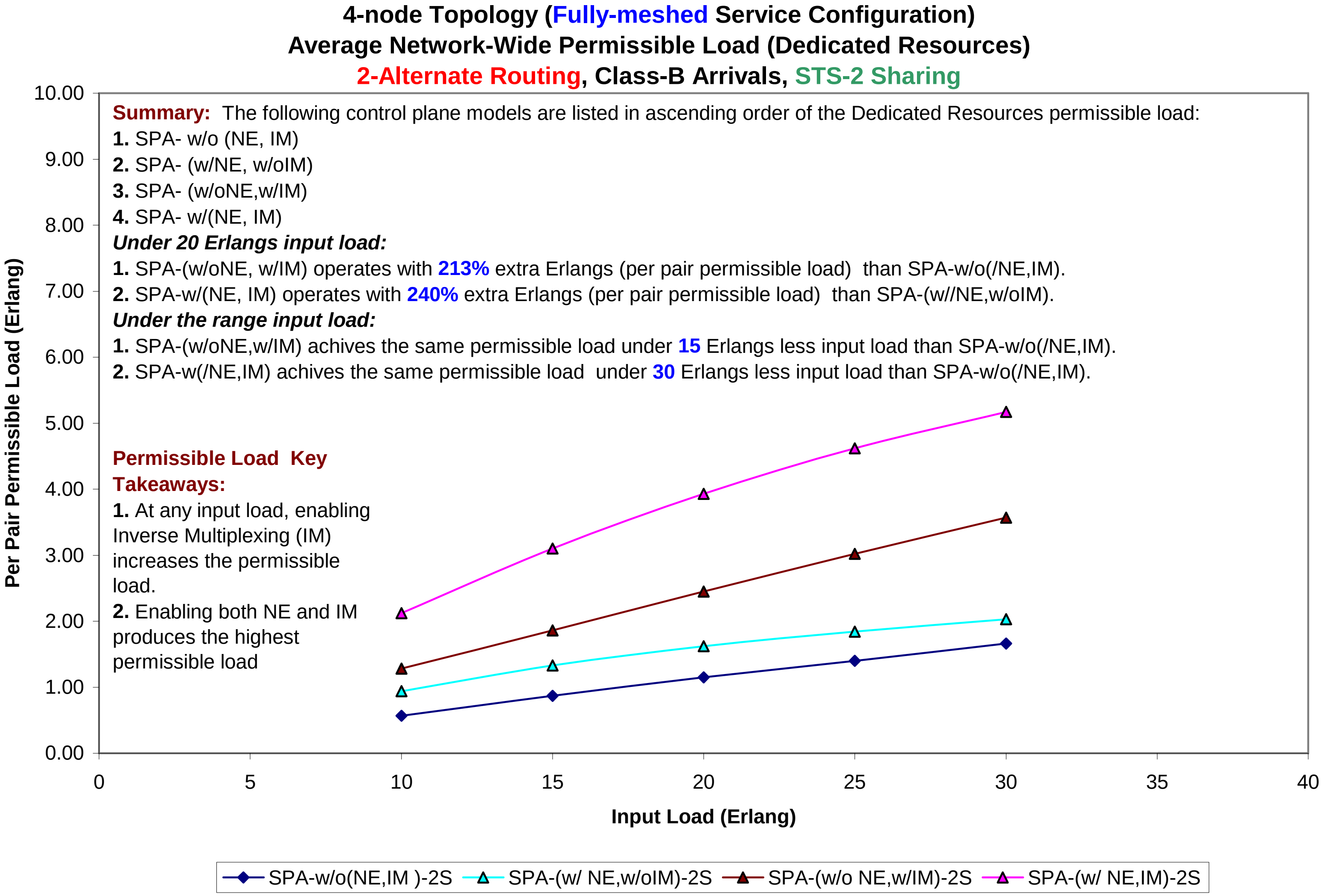

4-node Topology (Fully-meshed Service Configuration)
Average Network-Wide Permissible Load (Dedicated Resources)
2-Alternate Routing, Class-B Arrivals, STS-2 Sharing

Summary: The following control plane models are listed in ascending order of the Dedicated Resources permissible load:

1. SPA- w/o (NE, IM)
2. SPA- (w/NE, w/oIM)
3. SPA- (w/oNE,w/IM)
4. SPA- w/(NE, IM)

Under 20 Erlangs input load:

1. SPA-(w/oNE, w/IM) operates with **213%** extra Erlangs (per pair permissible load) than SPA-w/o(/NE,IM).
2. SPA-w/(NE, IM) operates with **240%** extra Erlangs (per pair permissible load) than SPA-(w//NE,w/oIM).

Under the range input load:

1. SPA-(w/oNE,w/IM) achives the same permissible load under **15** Erlangs less input load than SPA-w/o(/NE,IM).
2. SPA-w(/NE,IM) achives the same permissible load under **30** Erlangs less input load than SPA-w/o(/NE,IM).

Permissible Load Key Takeaways:

1. At any input load, enabling Inverse Multiplexing (IM) increases the permissible load.
2. Enabling both NE and IM produces the highest permissible load

Figure 19-20: Average Network-Wide Permissible Load (Dedicated Resources)-4 Node – 2 Alternate Route-STS-2 Sharing

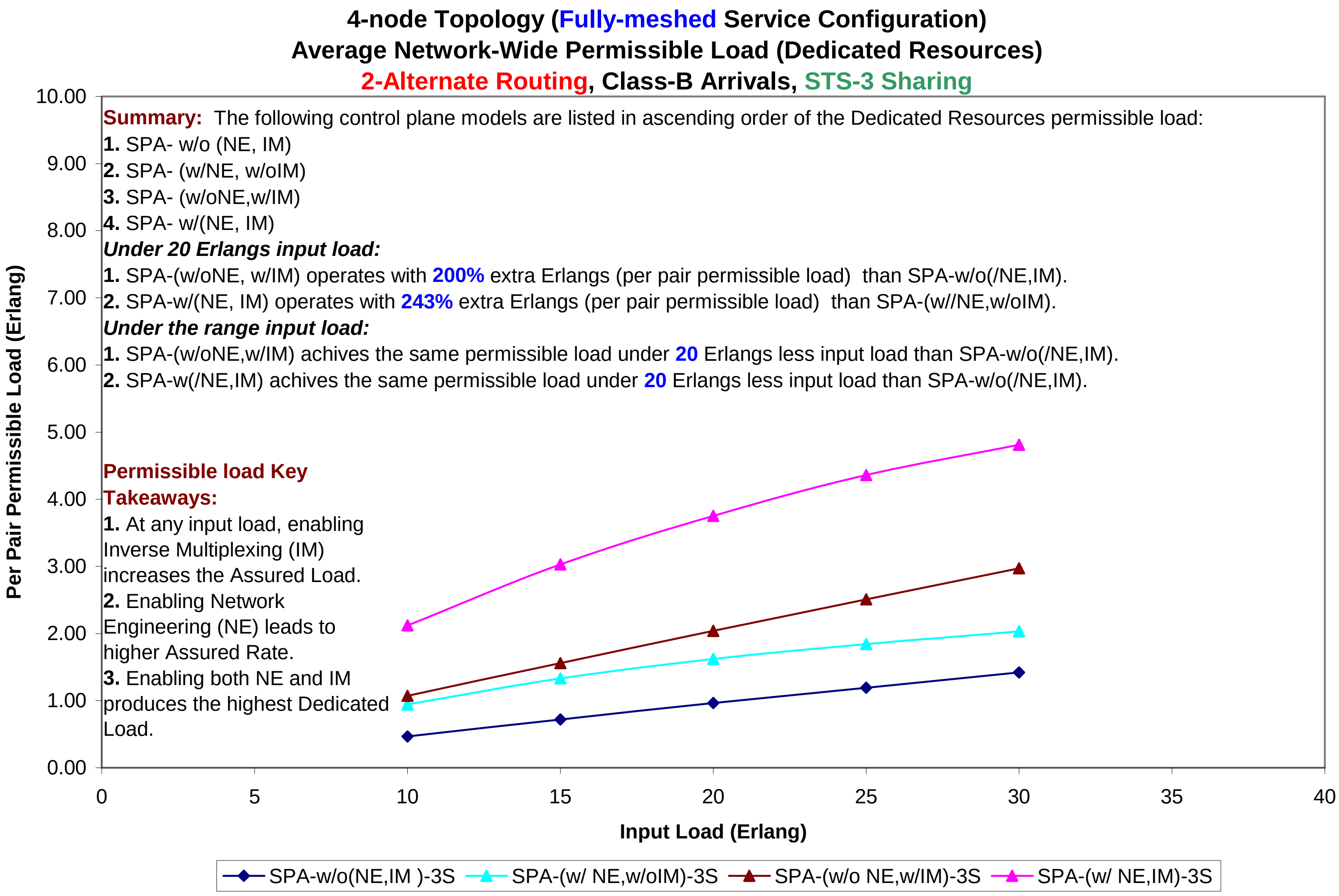

4-node Topology (Fully-meshed Service Configuration)
Average Network-Wide Permissible Load (Dedicated Resources)
2-Alternate Routing, Class-B Arrivals, STS-3 Sharing

Summary: The following control plane models are listed in ascending order of the Dedicated Resources permissible load:
1. SPA- w/o (NE, IM)
2. SPA- (w/NE, w/oIM)
3. SPA- (w/oNE,w/IM)
4. SPA- w/(NE, IM)

Under 20 Erlangs input load:
1. SPA-(w/oNE, w/IM) operates with **200%** extra Erlangs (per pair permissible load) than SPA-w/o(/NE,IM).
2. SPA-w/(NE, IM) operates with **243%** extra Erlangs (per pair permissible load) than SPA-(w//NE,w/oIM).

Under the range input load:
1. SPA-(w/oNE,w/IM) achives the same permissible load under **20** Erlangs less input load than SPA-w/o(/NE,IM).
2. SPA-w(/NE,IM) achives the same permissible load under **20** Erlangs less input load than SPA-w/o(/NE,IM).

Permissible load Key Takeaways:
1. At any input load, enabling Inverse Multiplexing (IM) increases the Assured Load.
2. Enabling Network Engineering (NE) leads to higher Assured Rate.
3. Enabling both NE and IM produces the highest Dedicated Load.

Figure 19-21: Average Network-Wide Permissible Load (Dedicated Resources)-4 Node – 2 Alternate Route-STS-3 Sharing

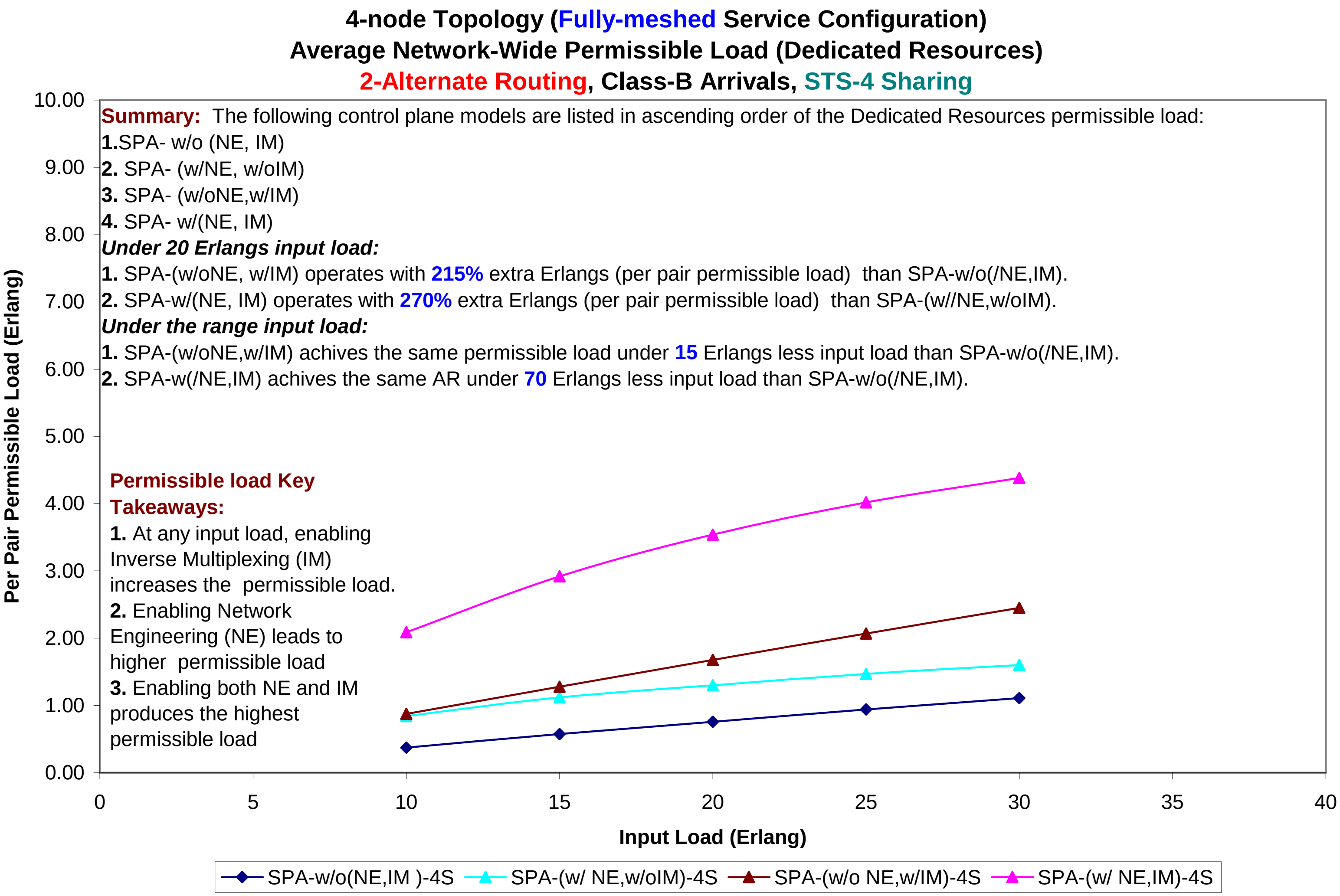

Summary: The following control plane models are listed in ascending order of the Dedicated Resources permissible load:

1.SPA- w/o (NE, IM)
2. SPA- (w/NE, w/oIM)
3. SPA- (w/oNE,w/IM)
4. SPA- w/(NE, IM)

Under 20 Erlangs input load:

1. SPA-(w/oNE, w/IM) operates with **215%** extra Erlangs (per pair permissible load) than SPA-w/o(/NE,IM).
2. SPA-w/(NE, IM) operates with **270%** extra Erlangs (per pair permissible load) than SPA-(w//NE,w/oIM).

Under the range input load:

1. SPA-(w/oNE,w/IM) achives the same permissible load under **15** Erlangs less input load than SPA-w/o(/NE,IM).
2. SPA-w(/NE,IM) achives the same AR under **70** Erlangs less input load than SPA-w/o(/NE,IM).

Permissible load Key Takeaways:

1. At any input load, enabling Inverse Multiplexing (IM) increases the permissible load.
2. Enabling Network Engineering (NE) leads to higher permissible load
3. Enabling both NE and IM produces the highest permissible load

Figure 19-22: Average Network-Wide Permissible Load (Dedicated Resources)-4 Node – 2 Alternate Route-STS-4 Sharing

19.2.2 Shared resources

This section provides detailed performance analysis of the network-wide permissible load on the shared network resources partition for the 4-node topology. The configured VPN service evaluated is the Fully-meshed Shared Granular (FSF) with the following service profile layer parameters:

a. Service flow connectivity: configured as "fully-meshed".

b. Service demand granularity: configured as "granular" with 1 STS-1 granularity level.

c. Load partitioning flexibility: configured as "enabled".

One input class was evaluated with the following parameters: $k = 2$, $b_k^A = 2$ STS-1, $\mu_k = 1$unit time, $\lambda_{rk} = 4$ calls/unit time. Range of input load for 4-node topology is 10 to 30 Erlangs. The five traffic management schemes of the SPA control plane model are evaluated as provided in Table 9-1. Four sharing levels are considered as follows:

a. STS-1 sharing: C_j^{vD}=11 STS-1, C_j^S=2 STS-1

b. STS-2 sharing: C_j^{vD}=10 STS-1, C_j^S=4 STS-1

c. STS-3 sharing: C_j^{vD}=9 STS-1, C_j^S=6 STS-1

d. STS-4 sharing: C_j^{vD}=8 STS-1, C_j^S=8 STS-1

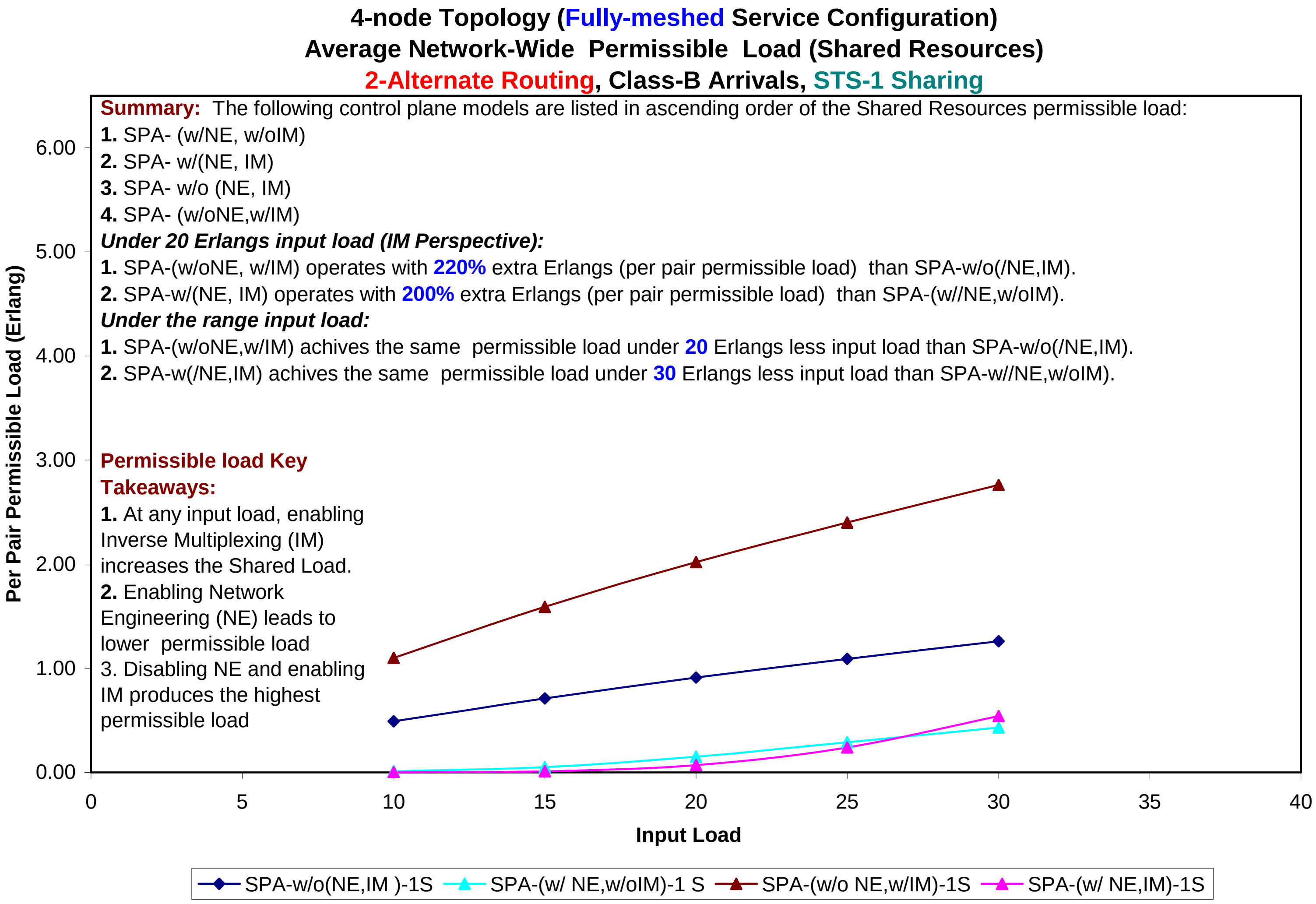

4-node Topology (Fully-meshed Service Configuration)
Average Network-Wide Permissible Load (Shared Resources)
2-Alternate Routing, Class-B Arrivals, STS-1 Sharing

Summary: The following control plane models are listed in ascending order of the Shared Resources permissible load:

1. SPA- (w/NE, w/oIM)
2. SPA- w/(NE, IM)
3. SPA- w/o (NE, IM)
4. SPA- (w/oNE,w/IM)

Under 20 Erlangs input load (IM Perspective):

1. SPA-(w/oNE, w/IM) operates with **220%** extra Erlangs (per pair permissible load) than SPA-w/o(/NE,IM).
2. SPA-w/(NE, IM) operates with **200%** extra Erlangs (per pair permissible load) than SPA-(w//NE,w/oIM).

Under the range input load:

1. SPA-(w/oNE,w/IM) achives the same permissible load under **20** Erlangs less input load than SPA-w/o(/NE,IM).
2. SPA-w(/NE,IM) achives the same permissible load under **30** Erlangs less input load than SPA-w//NE,w/oIM).

Permissible load Key Takeaways:

1. At any input load, enabling Inverse Multiplexing (IM) increases the Shared Load.
2. Enabling Network Engineering (NE) leads to lower permissible load
3. Disabling NE and enabling IM produces the highest permissible load

Figure 19-23: Average Network-Wide Permissible Load (Shared Resources)-4 Node – 2 Alternate Route-STS-1 Sharing

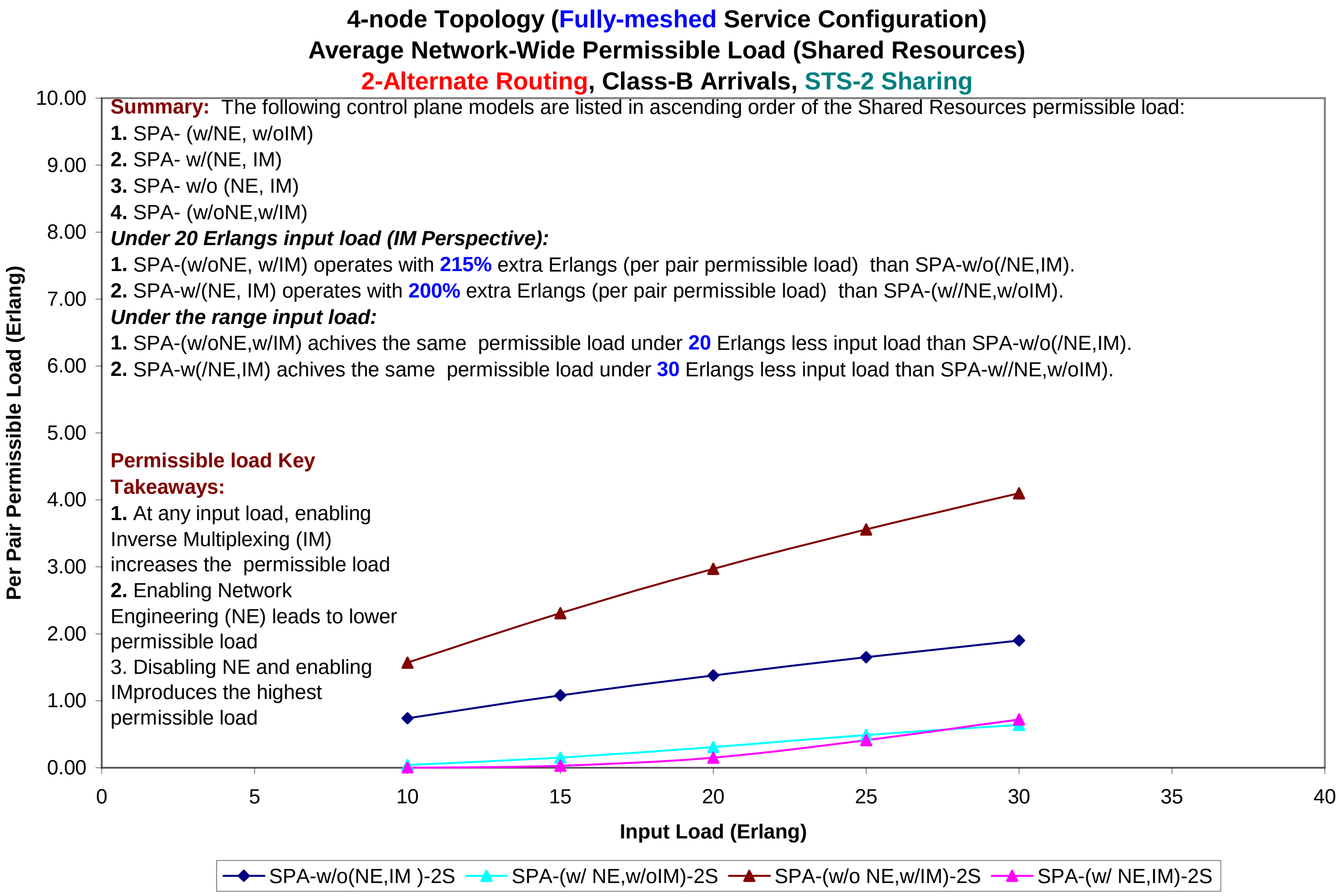

Summary: The following control plane models are listed in ascending order of the Shared Resources permissible load:

1. SPA- (w/NE, w/oIM)
2. SPA- w/(NE, IM)
3. SPA- w/o (NE, IM)
4. SPA- (w/oNE,w/IM)

Under 20 Erlangs input load (IM Perspective):

1. SPA-(w/oNE, w/IM) operates with **215%** extra Erlangs (per pair permissible load) than SPA-w/o(/NE,IM).
2. SPA-w/(NE, IM) operates with **200%** extra Erlangs (per pair permissible load) than SPA-(w//NE,w/oIM).

Under the range input load:

1. SPA-(w/oNE,w/IM) achives the same permissible load under **20** Erlangs less input load than SPA-w/o(/NE,IM).
2. SPA-w(/NE,IM) achives the same permissible load under **30** Erlangs less input load than SPA-w//NE,w/oIM).

Permissible load Key Takeaways:

1. At any input load, enabling Inverse Multiplexing (IM) increases the permissible load
2. Enabling Network Engineering (NE) leads to lower permissible load
3. Disabling NE and enabling IMproduces the highest permissible load

Figure 19-24: Average Network-Wide Permissible Load (Shared Resources)-4 Node – 2 Alternate Route-STS-2 Sharing

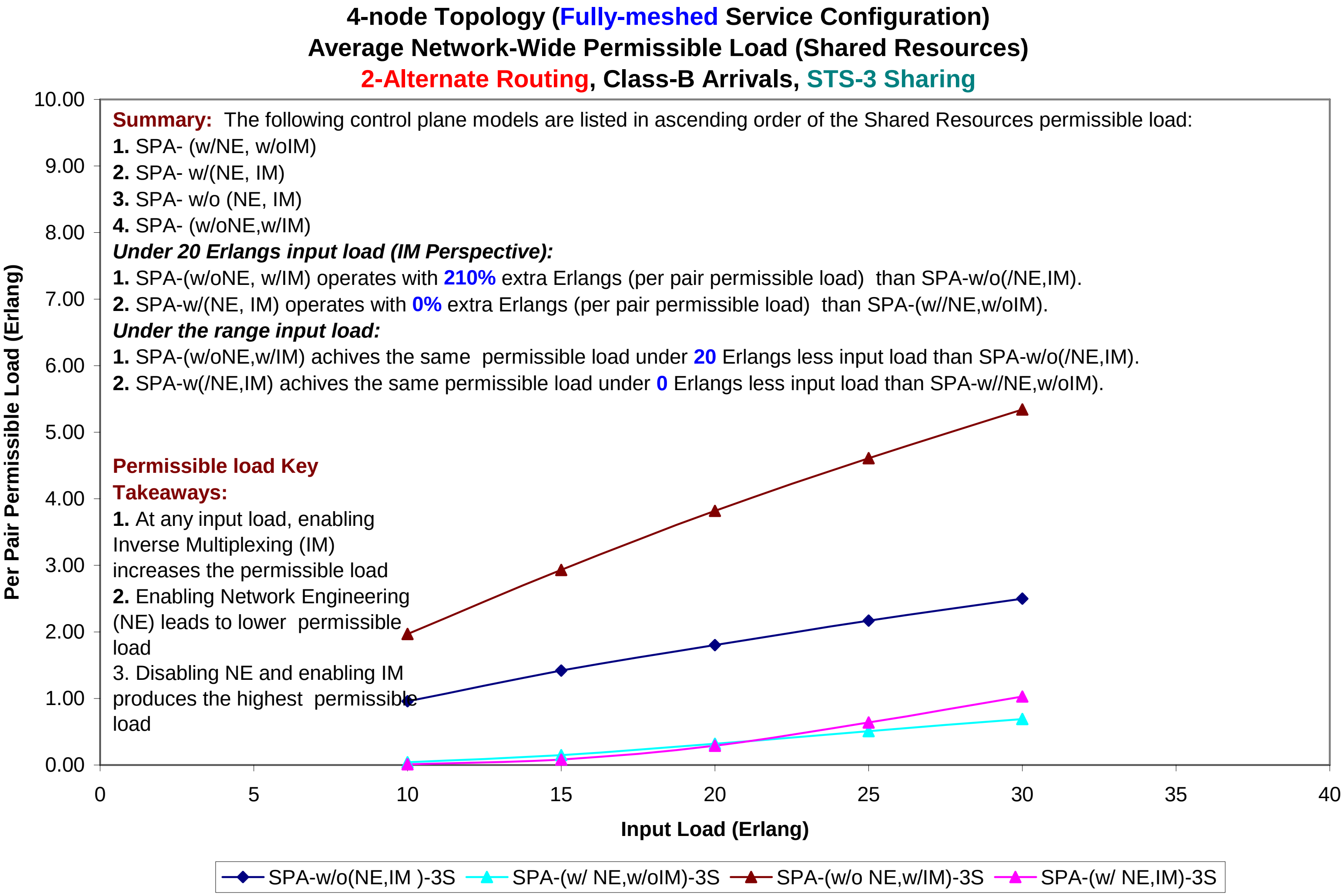

Summary: The following control plane models are listed in ascending order of the Shared Resources permissible load:

1. SPA- (w/NE, w/oIM)
2. SPA- w/(NE, IM)
3. SPA- w/o (NE, IM)
4. SPA- (w/oNE,w/IM)

Under 20 Erlangs input load (IM Perspective):

1. SPA-(w/oNE, w/IM) operates with **210%** extra Erlangs (per pair permissible load) than SPA-w/o(/NE,IM).
2. SPA-w/(NE, IM) operates with **0%** extra Erlangs (per pair permissible load) than SPA-(w//NE,w/oIM).

Under the range input load:

1. SPA-(w/oNE,w/IM) achives the same permissible load under **20** Erlangs less input load than SPA-w/o(/NE,IM).
2. SPA-w(/NE,IM) achives the same permissible load under **0** Erlangs less input load than SPA-w//NE,w/oIM).

Permissible load Key Takeaways:

1. At any input load, enabling Inverse Multiplexing (IM) increases the permissible load
2. Enabling Network Engineering (NE) leads to lower permissible load
3. Disabling NE and enabling IM produces the highest permissible load

Figure 19-25: Average Network-Wide Permissible Load (Shared Resources)-4 Node – 2 Alternate Route-STS-3 Sharing

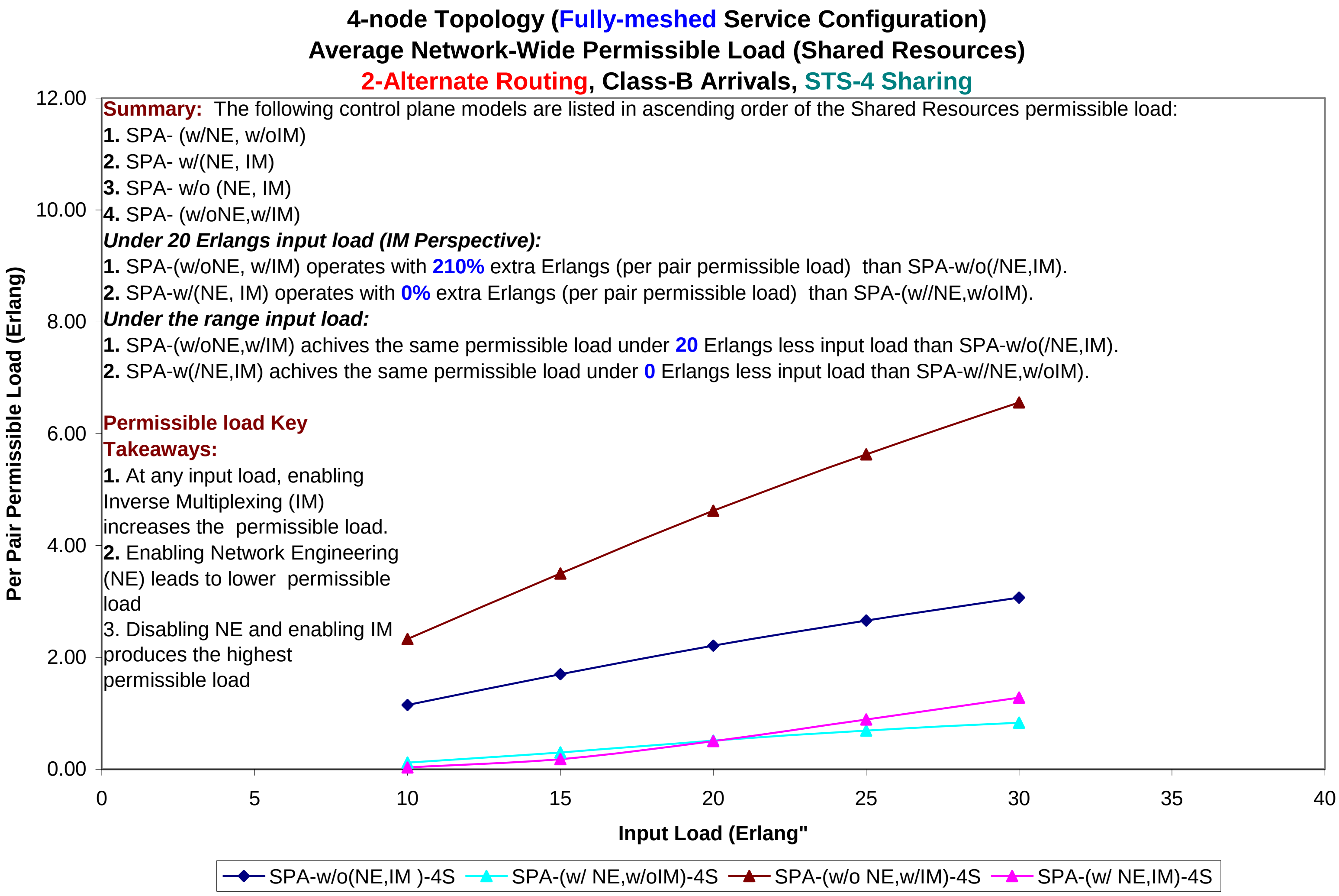

Summary: The following control plane models are listed in ascending order of the Shared Resources permissible load:

1. SPA- (w/NE, w/oIM)
2. SPA- w/(NE, IM)
3. SPA- w/o (NE, IM)
4. SPA- (w/oNE,w/IM)

Under 20 Erlangs input load (IM Perspective):

1. SPA-(w/oNE, w/IM) operates with **210%** extra Erlangs (per pair permissible load) than SPA-w/o(/NE,IM).
2. SPA-w/(NE, IM) operates with **0%** extra Erlangs (per pair permissible load) than SPA-(w//NE,w/oIM).

Under the range input load:

1. SPA-(w/oNE,w/IM) achives the same permissible load under **20** Erlangs less input load than SPA-w/o(/NE,IM).
2. SPA-w(/NE,IM) achives the same permissible load under **0** Erlangs less input load than SPA-w//NE,w/oIM).

Permissible load Key Takeaways:

1. At any input load, enabling Inverse Multiplexing (IM) increases the permissible load.
2. Enabling Network Engineering (NE) leads to lower permissible load
3. Disabling NE and enabling IM produces the highest permissible load

Figure 19-26: Average Network-Wide Permissible Load (Shared Resources)-4 Node – 2 Alternate Route-STS-4 Sharing

19.2.3 VPN resources

This section provides detailed performance analysis of the network-wide permissible load on the VPN network resources partition for the 4-node topology. The configured VPN service evaluated is the Fully-meshed Shared Granular (FSF) with the following service profile layer parameters:

a. Service flow connectivity: configured as “fully-meshed”.

b. Service demand granularity: configured as “granular” with 1 STS-1 granularity level.

c. Load partitioning flexibility: configured as “enabled”.

One input class was evaluated with the following parameters: $k = 2$, $b_k^A = 2$ STS-1, $\mu_k = 1$unit time, $\lambda_{rk} = 4$ calls/unit time. Range of input load for 4-node topology is 10 to 30 Erlangs. The five traffic management schemes of the SPA control plane model are evaluated as provided in Table 9-1. Four sharing levels are considered as follows:

a. STS-1 sharing: C_j^{vD} =11 STS-1, C_j^S =2 STS-1

b. STS-2 sharing: C_j^{vD} =10 STS-1, C_j^S =4 STS-1

c. STS-3 sharing: C_j^{vD} =9 STS-1, C_j^S =6 STS-1

d. STS-4 sharing: C_j^{vD} =8 STS-1, C_j^S =8 STS-1

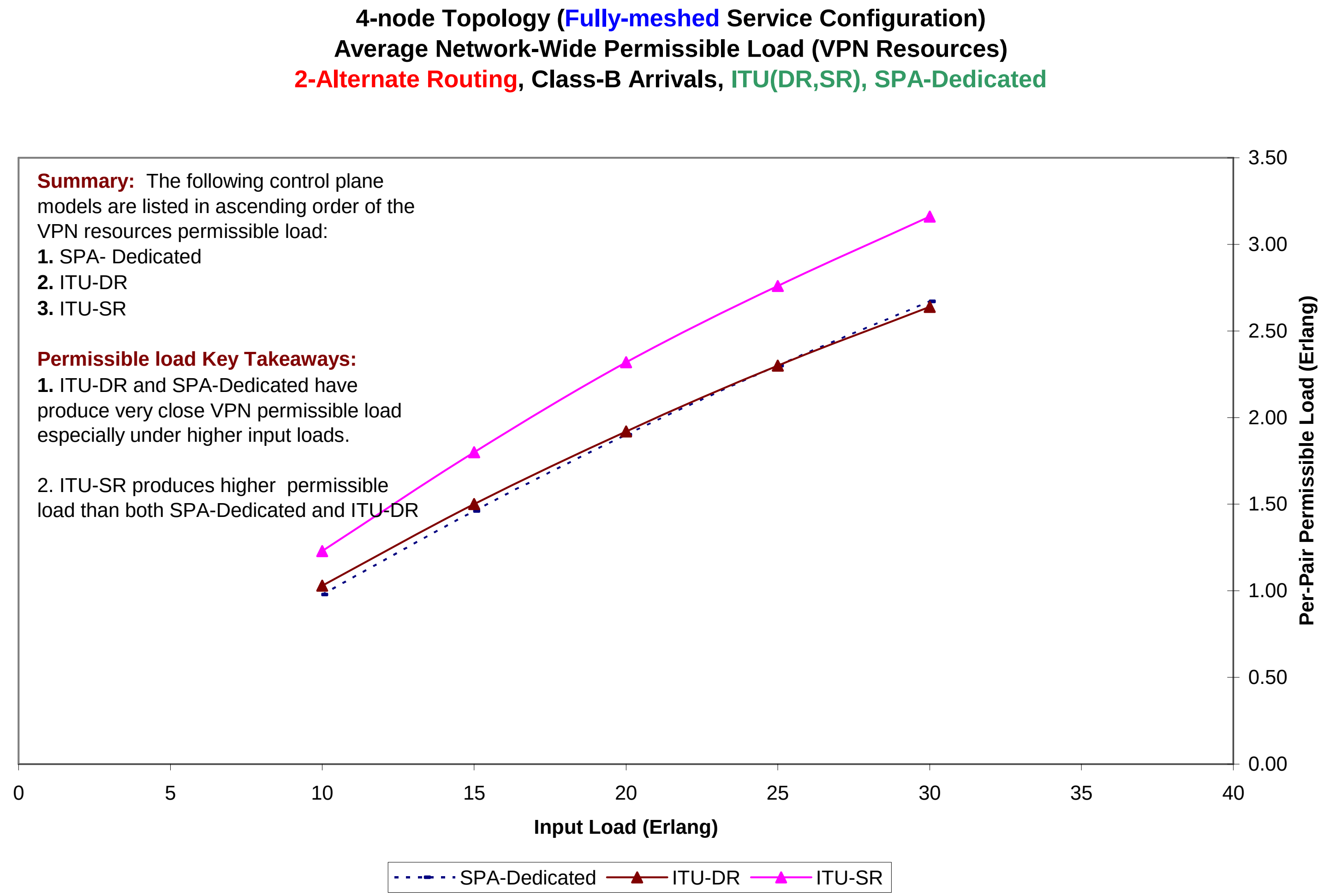

4-node Topology (Fully-meshed Service Configuration)
Average Network-Wide Permissible Load (VPN Resources)
2-Alternate Routing, Class-B Arrivals, ITU(DR,SR), SPA-Dedicated

Summary: The following control plane models are listed in ascending order of the VPN resources permissible load:
1. SPA- Dedicated
2. ITU-DR
3. ITU-SR

Permissible load Key Takeaways:
1. ITU-DR and SPA-Dedicated have produce very close VPN permissible load especially under higher input loads.

2. ITU-SR produces higher permissible load than both SPA-Dedicated and ITU-DR

Figure 19-27: Average Network-Wide Permissible Load (VPN Resources)-4 Node – 2 Alternate Route-ITU(DR,SR),SPA-Dedicated

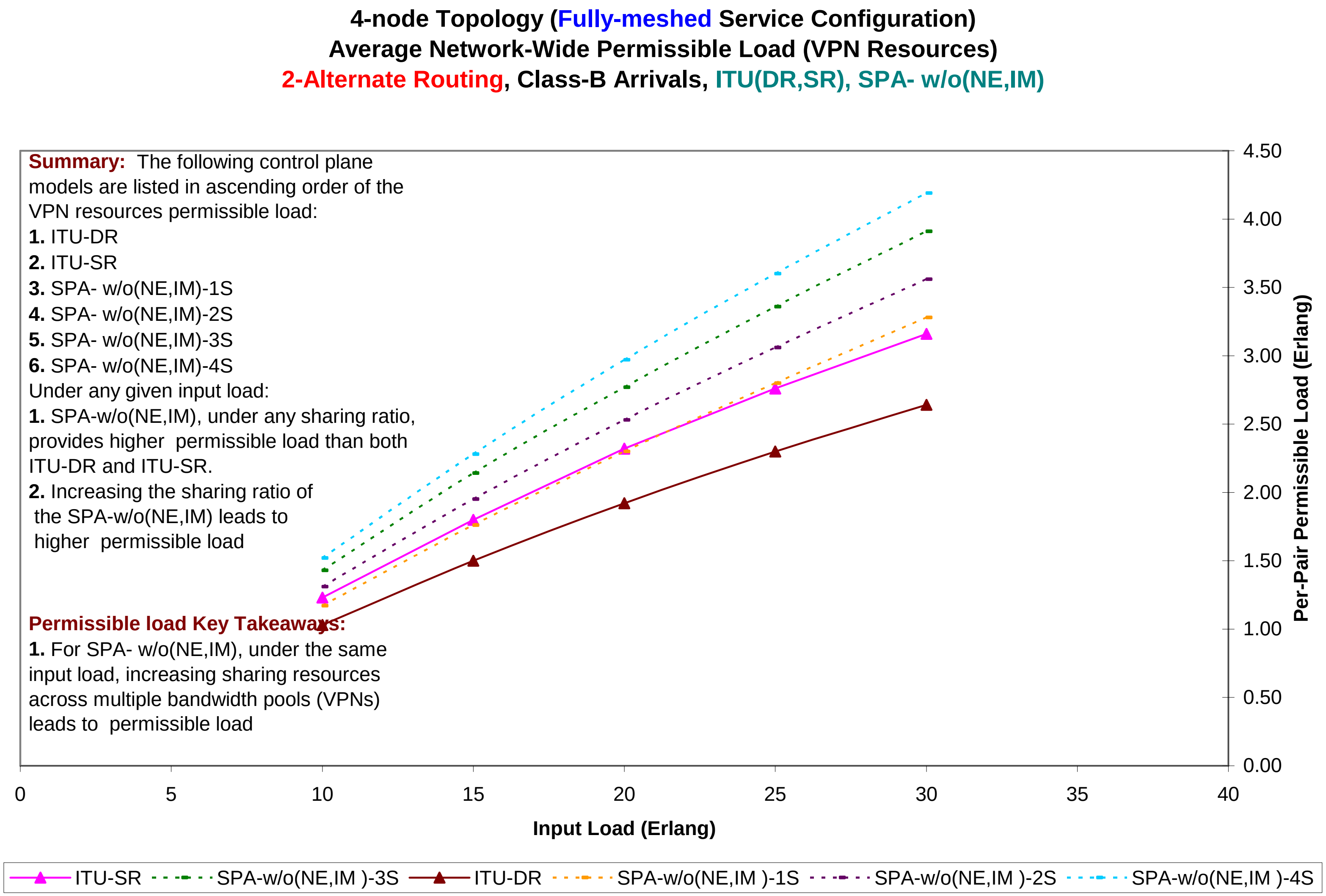

4-node Topology (Fully-meshed Service Configuration)
Average Network-Wide Permissible Load (VPN Resources)
2-Alternate Routing, Class-B Arrivals, ITU(DR,SR), SPA- w/o(NE,IM)

Summary: The following control plane models are listed in ascending order of the VPN resources permissible load:

1. ITU-DR
2. ITU-SR
3. SPA- w/o(NE,IM)-1S
4. SPA- w/o(NE,IM)-2S
5. SPA- w/o(NE,IM)-3S
6. SPA- w/o(NE,IM)-4S

Under any given input load:
1. SPA-w/o(NE,IM), under any sharing ratio, provides higher permissible load than both ITU-DR and ITU-SR.
2. Increasing the sharing ratio of the SPA-w/o(NE,IM) leads to higher permissible load

Permissible load Key Takeaways:
1. For SPA- w/o(NE,IM), under the same input load, increasing sharing resources across multiple bandwidth pools (VPNs) leads to permissible load

Figure 19-28: Average Network-Wide Permissible Load (VPN Resources)-4 Node – 2 Alternate Route-ITU(DR,SR),SPA-w/o(NE,IM)

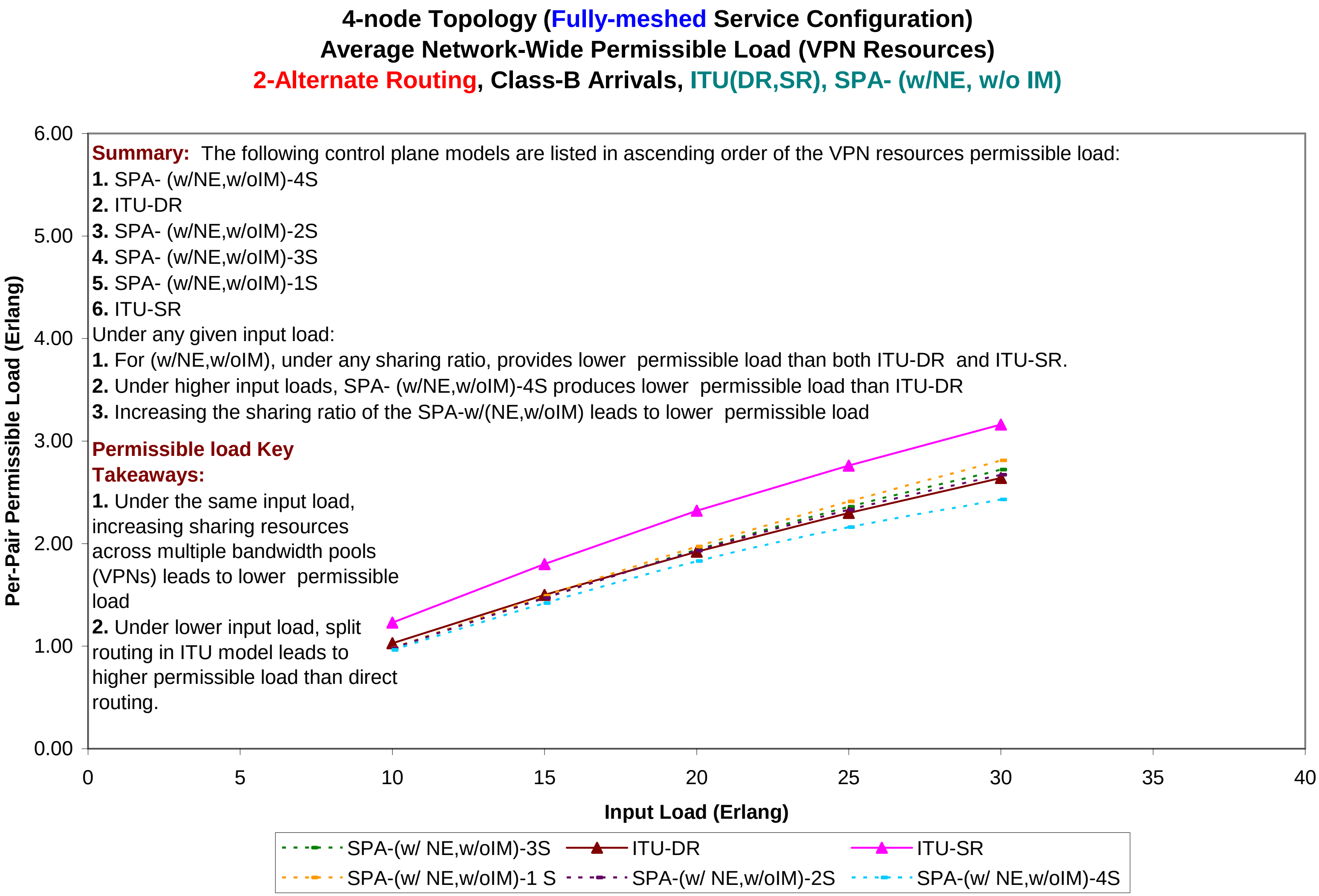

4-node Topology (Fully-meshed Service Configuration)
Average Network-Wide Permissible Load (VPN Resources)
2-Alternate Routing, Class-B Arrivals, ITU(DR,SR), SPA- (w/NE, w/o IM)

Summary: The following control plane models are listed in ascending order of the VPN resources permissible load:

1. SPA- (w/NE,w/oIM)-4S
2. ITU-DR
3. SPA- (w/NE,w/oIM)-2S
4. SPA- (w/NE,w/oIM)-3S
5. SPA- (w/NE,w/oIM)-1S
6. ITU-SR

Under any given input load:

1. For (w/NE,w/oIM), under any sharing ratio, provides lower permissible load than both ITU-DR and ITU-SR.
2. Under higher input loads, SPA- (w/NE,w/oIM)-4S produces lower permissible load than ITU-DR
3. Increasing the sharing ratio of the SPA-w/(NE,w/oIM) leads to lower permissible load

Permissible load Key Takeaways:

1. Under the same input load, increasing sharing resources across multiple bandwidth pools (VPNs) leads to lower permissible load
2. Under lower input load, split routing in ITU model leads to higher permissible load than direct routing.

Figure 19-29: Average Network-Wide Permissible Load (VPN Resources)-4 Node – 2 Alternate Route-ITU(DR,SR),SPA-w/NE,w/oIM

4-node Topology (Fully-meshed Service Configuration)
Average Network-Wide Permissible Load (VPN Resources)
2-Alternate Routing, Class-B Arrivals, ITU(DR,SR), SPA- (w/oNE, w/IM)

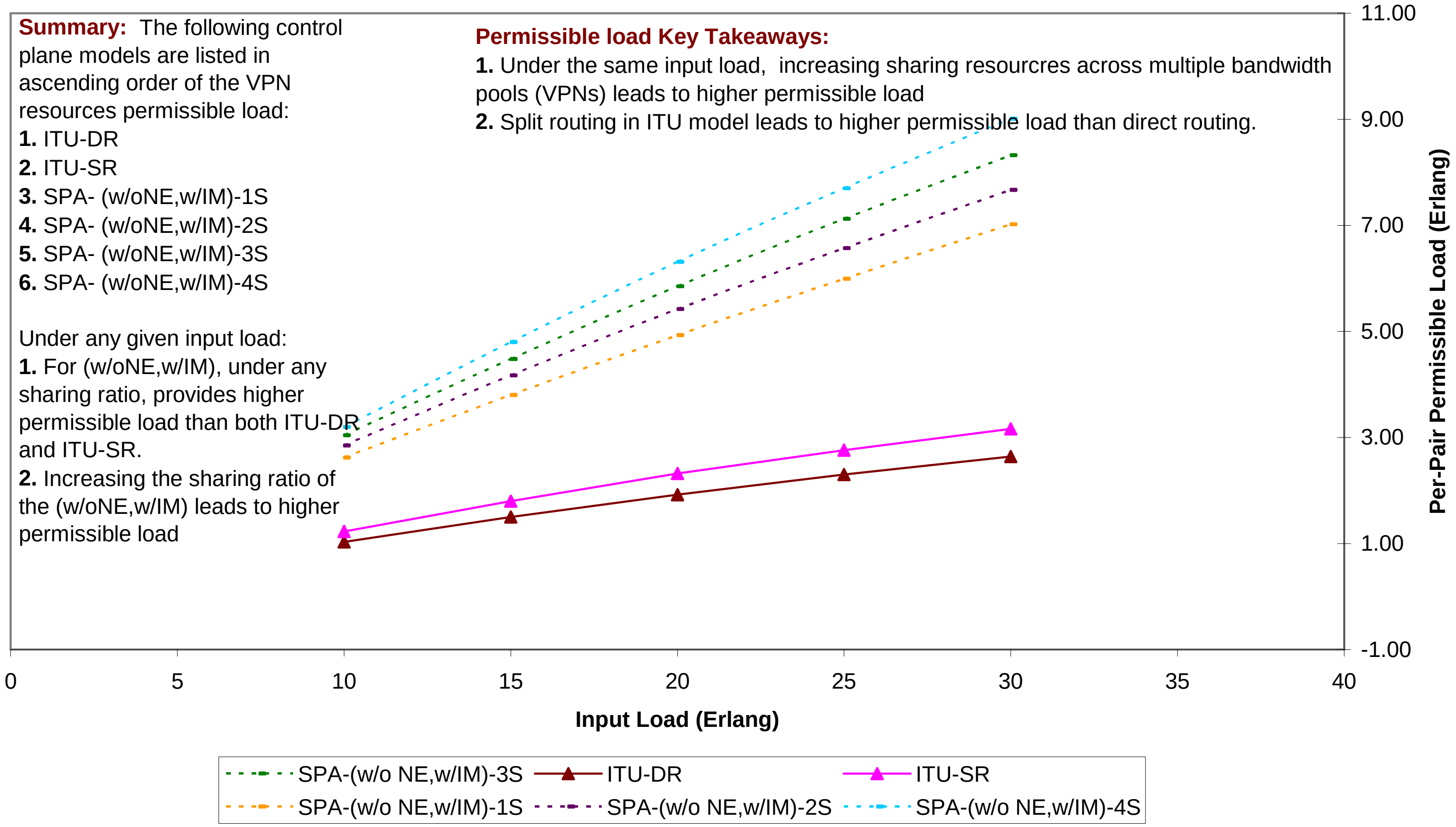

Summary: The following control plane models are listed in ascending order of the VPN resources permissible load:

1. ITU-DR
2. ITU-SR
3. SPA- (w/oNE,w/IM)-1S
4. SPA- (w/oNE,w/IM)-2S
5. SPA- (w/oNE,w/IM)-3S
6. SPA- (w/oNE,w/IM)-4S

Under any given input load:
1. For (w/oNE,w/IM), under any sharing ratio, provides higher permissible load than both ITU-DR and ITU-SR.
2. Increasing the sharing ratio of the (w/oNE,w/IM) leads to higher permissible load

Permissible load Key Takeaways:
1. Under the same input load, increasing sharing resourcres across multiple bandwidth pools (VPNs) leads to higher permissible load
2. Split routing in ITU model leads to higher permissible load than direct routing.

Figure 19-30: Average Network-Wide Permissible Load (VPN Resources)-4 Node – 2 Alternate Route--ITU(DR,SR),SPA-w/oNE,w/IM

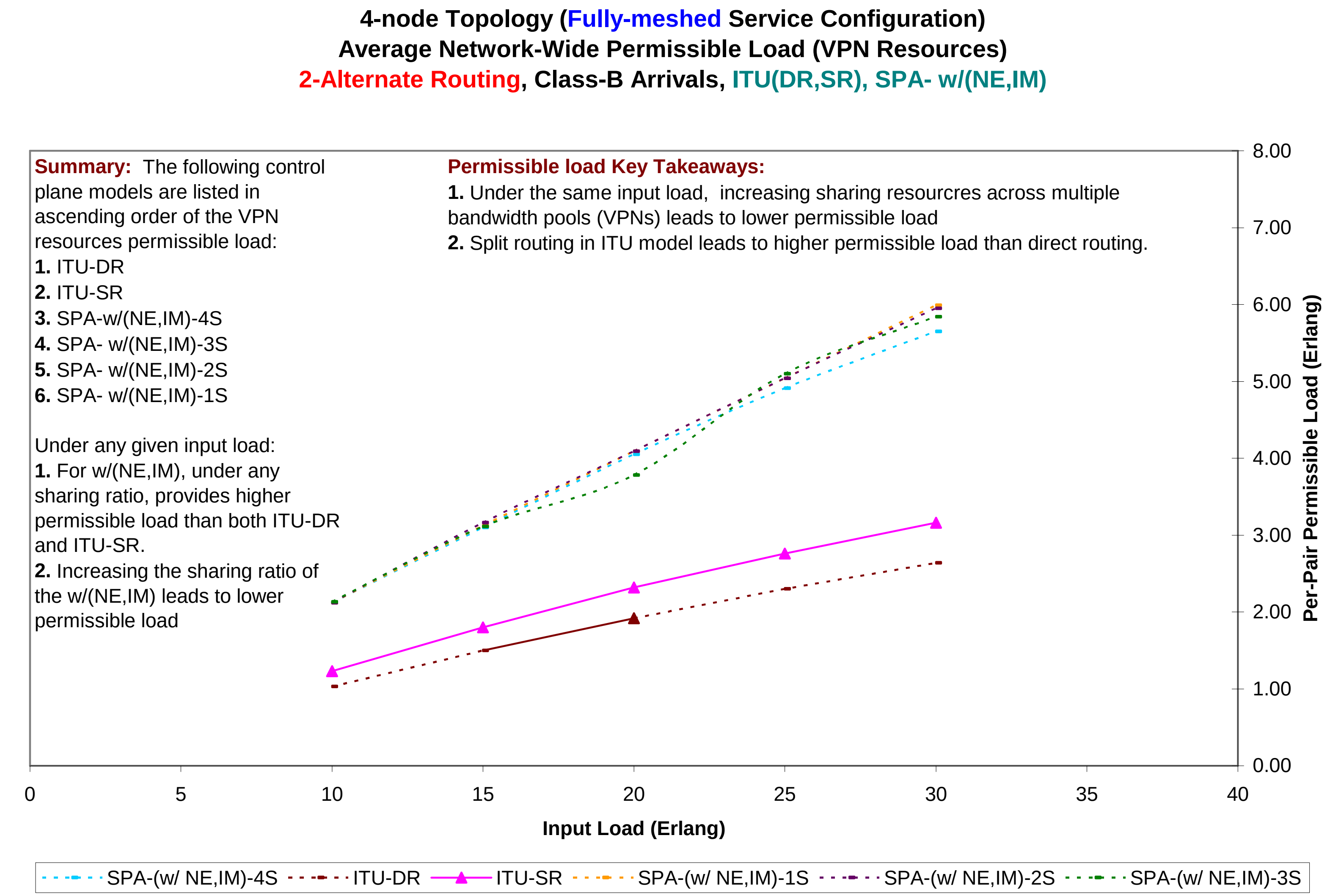

4-node Topology (Fully-meshed Service Configuration)
Average Network-Wide Permissible Load (VPN Resources)
2-Alternate Routing, Class-B Arrivals, ITU(DR,SR), SPA- w/(NE,IM)

Summary: The following control plane models are listed in ascending order of the VPN resources permissible load:

1. ITU-DR
2. ITU-SR
3. SPA-w/(NE,IM)-4S
4. SPA- w/(NE,IM)-3S
5. SPA- w/(NE,IM)-2S
6. SPA- w/(NE,IM)-1S

Under any given input load:
1. For w/(NE,IM), under any sharing ratio, provides higher permissible load than both ITU-DR and ITU-SR.
2. Increasing the sharing ratio of the w/(NE,IM) leads to lower permissible load

Permissible load Key Takeaways:
1. Under the same input load, increasing sharing resourcres across multiple bandwidth pools (VPNs) leads to lower permissible load
2. Split routing in ITU model leads to higher permissible load than direct routing.

Figure 19-31: Average Network-Wide Permissible Load (VPN Resources)-4 Node – 2 Alternate Route--ITU(DR,SR),SPA-w/(NE,IM)

19.2.4 Physical resources

This section provides detailed performance analysis of the network-wide permissible load on the physical resource level for the 4-node topology. The configured VPN service evaluated is the Fully-meshed Shared Granular (FSF) with the following service profile layer parameters:

a. Service flow connectivity: configured as “fully-meshed”.

b. Service demand granularity: configured as “granular” with 1 STS-1 granularity level.

c. Load partitioning flexibility: configured as “enabled”.

One input class was evaluated with the following parameters: $k = 2$, $b_k^A = 2$ STS-1, $\mu_k = 1$unit time, $\lambda_{rk} = 4$ calls/unit time. Range of input load for 4-node topology is 10 to 30 Erlangs. The five traffic management schemes of the SPA control plane model are evaluated as provided in Table 9-1.

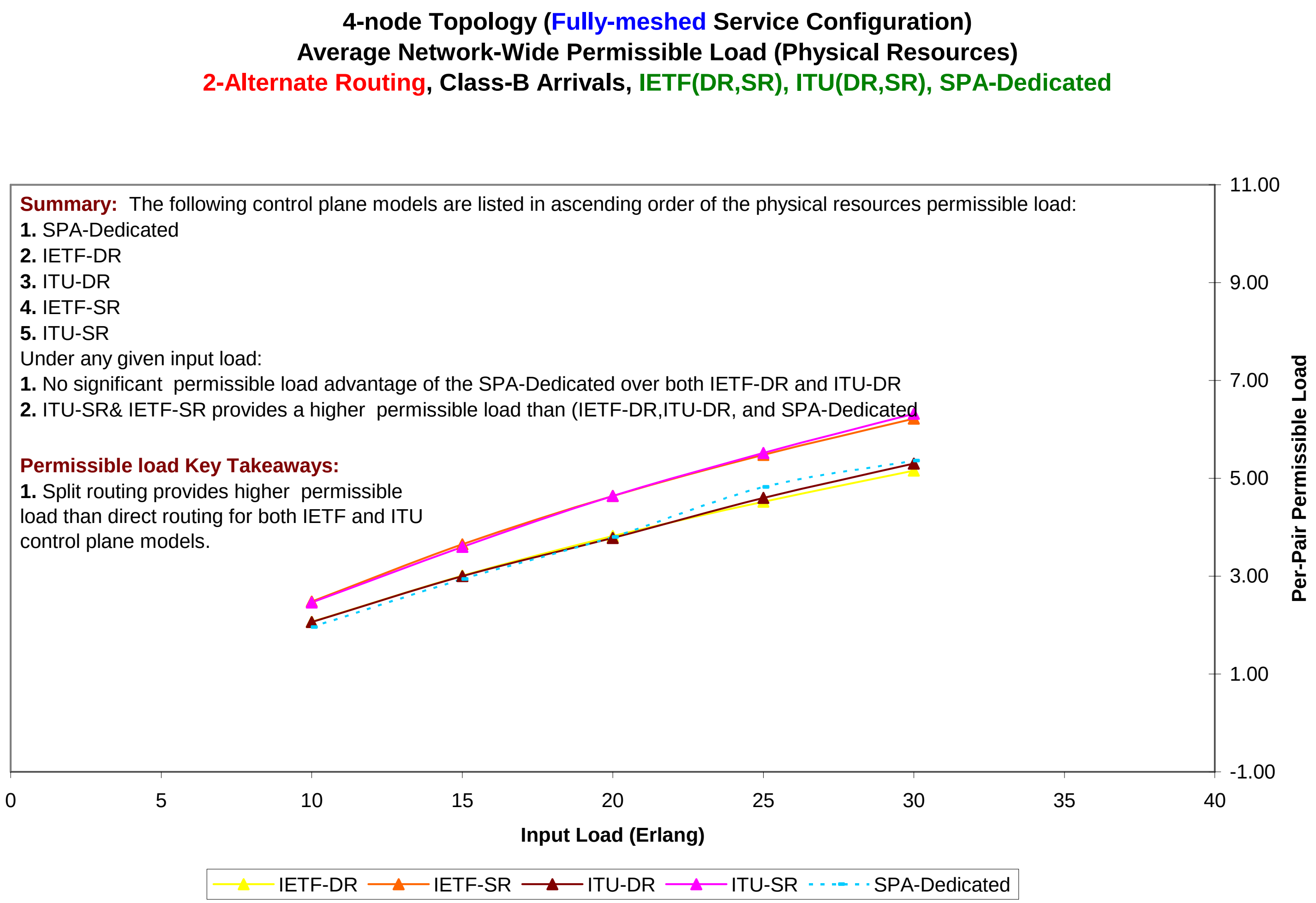

4-node Topology (Fully-meshed Service Configuration)
Average Network-Wide Permissible Load (Physical Resources)
2-Alternate Routing, Class-B Arrivals, IETF(DR,SR), ITU(DR,SR), SPA-Dedicated

Summary: The following control plane models are listed in ascending order of the physical resources permissible load:

1. SPA-Dedicated
2. IETF-DR
3. ITU-DR
4. IETF-SR
5. ITU-SR

Under any given input load:

1. No significant permissible load advantage of the SPA-Dedicated over both IETF-DR and ITU-DR
2. ITU-SR& IETF-SR provides a higher permissible load than (IETF-DR,ITU-DR, and SPA-Dedicated

Permissible load Key Takeaways:

1. Split routing provides higher permissible load than direct routing for both IETF and ITU control plane models.

Figure 19-32: Average Network-Wide Permissible Load (Physical Resources)-4 Node – IETF(DR,SR), ITU(DR,SR), SPA-Dedicated

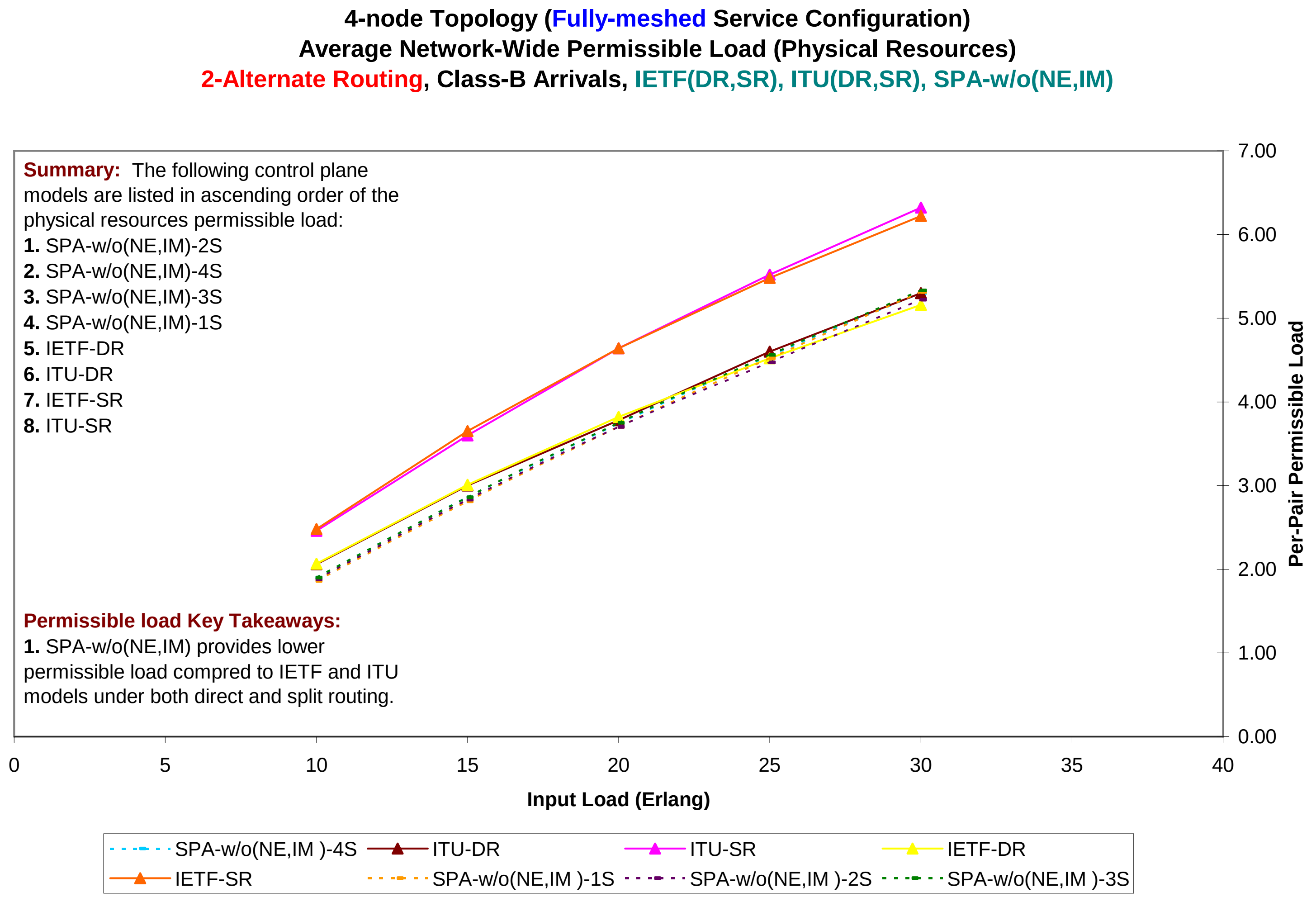

Summary: The following control plane models are listed in ascending order of the physical resources permissible load:

1. SPA-w/o(NE,IM)-2S
2. SPA-w/o(NE,IM)-4S
3. SPA-w/o(NE,IM)-3S
4. SPA-w/o(NE,IM)-1S
5. IETF-DR
6. ITU-DR
7. IETF-SR
8. ITU-SR

Permissible load Key Takeaways:

1. SPA-w/o(NE,IM) provides lower permissible load compred to IETF and ITU models under both direct and split routing.

Figure 19-33: Average Network-Wide Permissible Load (Physical Resources)-4 Node – IETF(DR,SR), ITU(DR,SR), SPA-w/o(NE,IM)

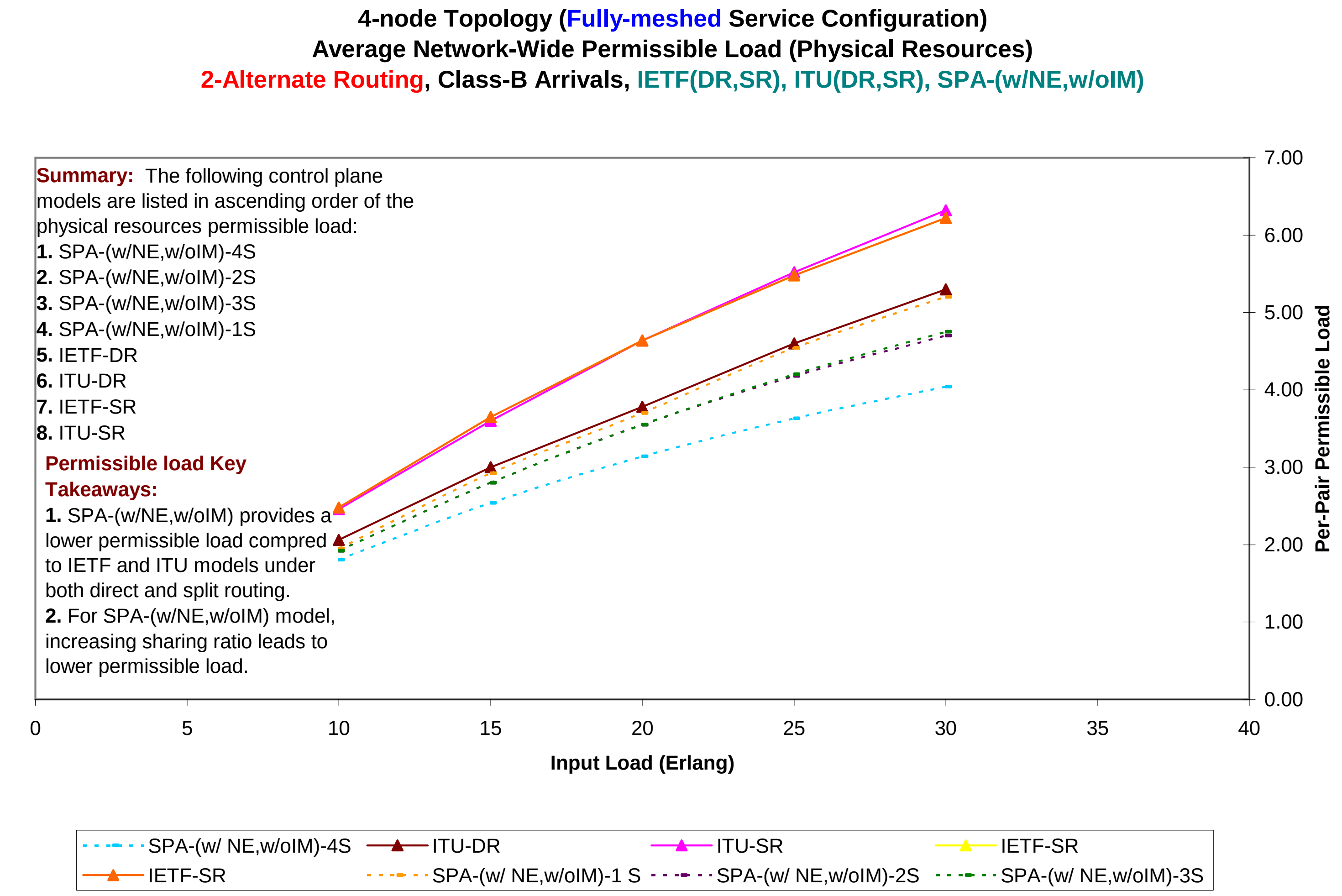

Summary: The following control plane models are listed in ascending order of the physical resources permissible load:

1. SPA-(w/NE,w/oIM)-4S
2. SPA-(w/NE,w/oIM)-2S
3. SPA-(w/NE,w/oIM)-3S
4. SPA-(w/NE,w/oIM)-1S
5. IETF-DR
6. ITU-DR
7. IETF-SR
8. ITU-SR

Permissible load Key Takeaways:

1. SPA-(w/NE,w/oIM) provides a lower permissible load compred to IETF and ITU models under both direct and split routing.

2. For SPA-(w/NE,w/oIM) model, increasing sharing ratio leads to lower permissible load.

Figure 19-34: Average Network-Wide Permissible Load (Physical Resources)-4 Node – IETF (DR, SR), ITU(DR,SR), SPA-(w/NE,w/oIM)

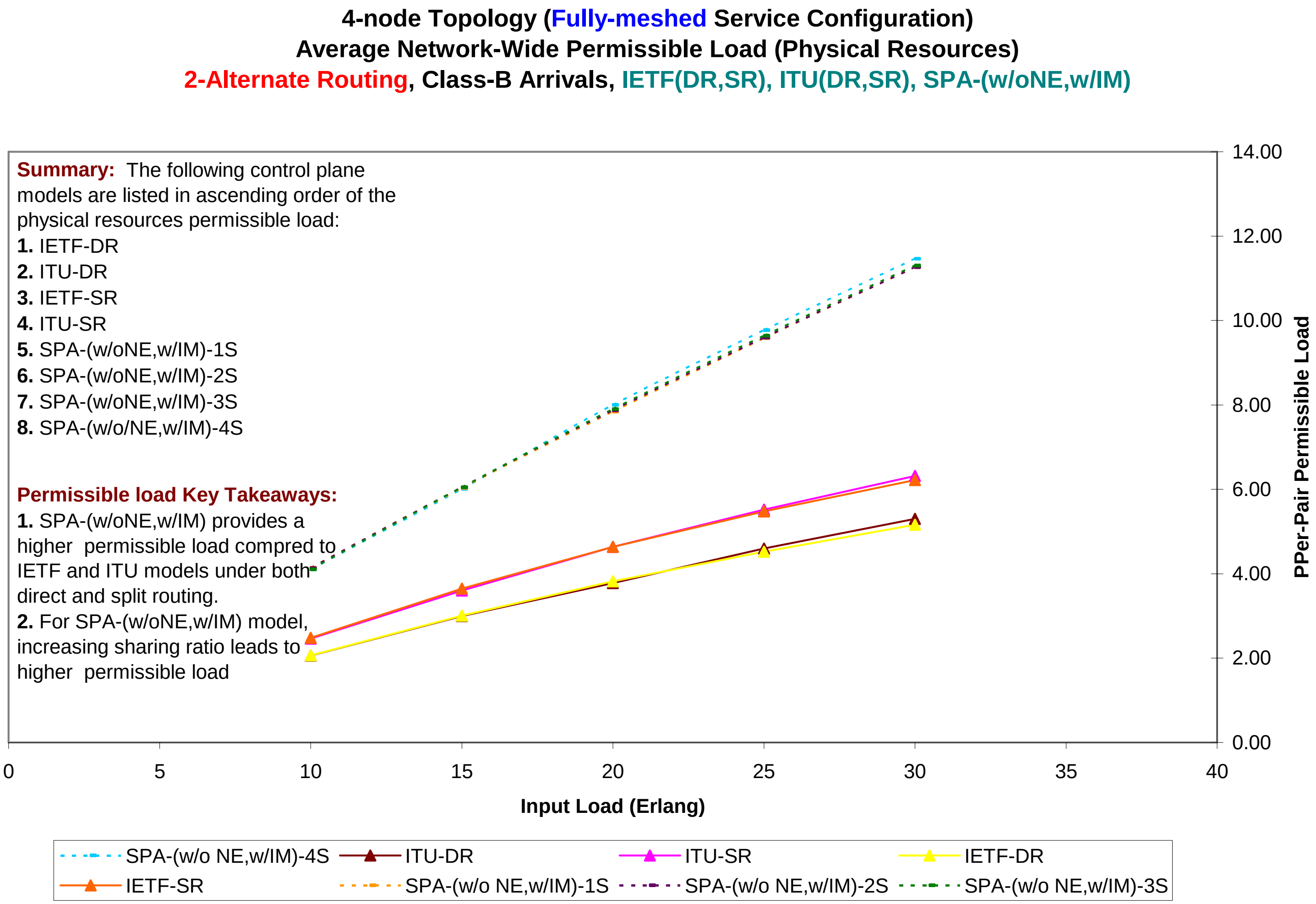

4-node Topology (Fully-meshed Service Configuration)
Average Network-Wide Permissible Load (Physical Resources)
2-Alternate Routing, Class-B Arrivals, IETF(DR,SR), ITU(DR,SR), SPA-(w/oNE,w/IM)

Summary: The following control plane models are listed in ascending order of the physical resources permissible load:

1. IETF-DR
2. ITU-DR
3. IETF-SR
4. ITU-SR
5. SPA-(w/oNE,w/IM)-1S
6. SPA-(w/oNE,w/IM)-2S
7. SPA-(w/oNE,w/IM)-3S
8. SPA-(w/o/NE,w/IM)-4S

Permissible load Key Takeaways:

1. SPA-(w/oNE,w/IM) provides a higher permissible load compred to IETF and ITU models under both direct and split routing.
2. For SPA-(w/oNE,w/IM) model, increasing sharing ratio leads to higher permissible load

Figure 19-35: Average Network-Wide Permissible Load (Physical Resources)-4 Node – IETF(DR,SR), ITU(DR,SR), SPA-(w/oNE,w/IM)

4-node Topology (Fully-meshed Service Configuration)
Average Network-Wide Permissible Load (Physical Resources)
2-Alternate Routing, Class-B Arrivals, IETF(DR,SR), ITU(DR,SR), SPA-w/(NE,IM)

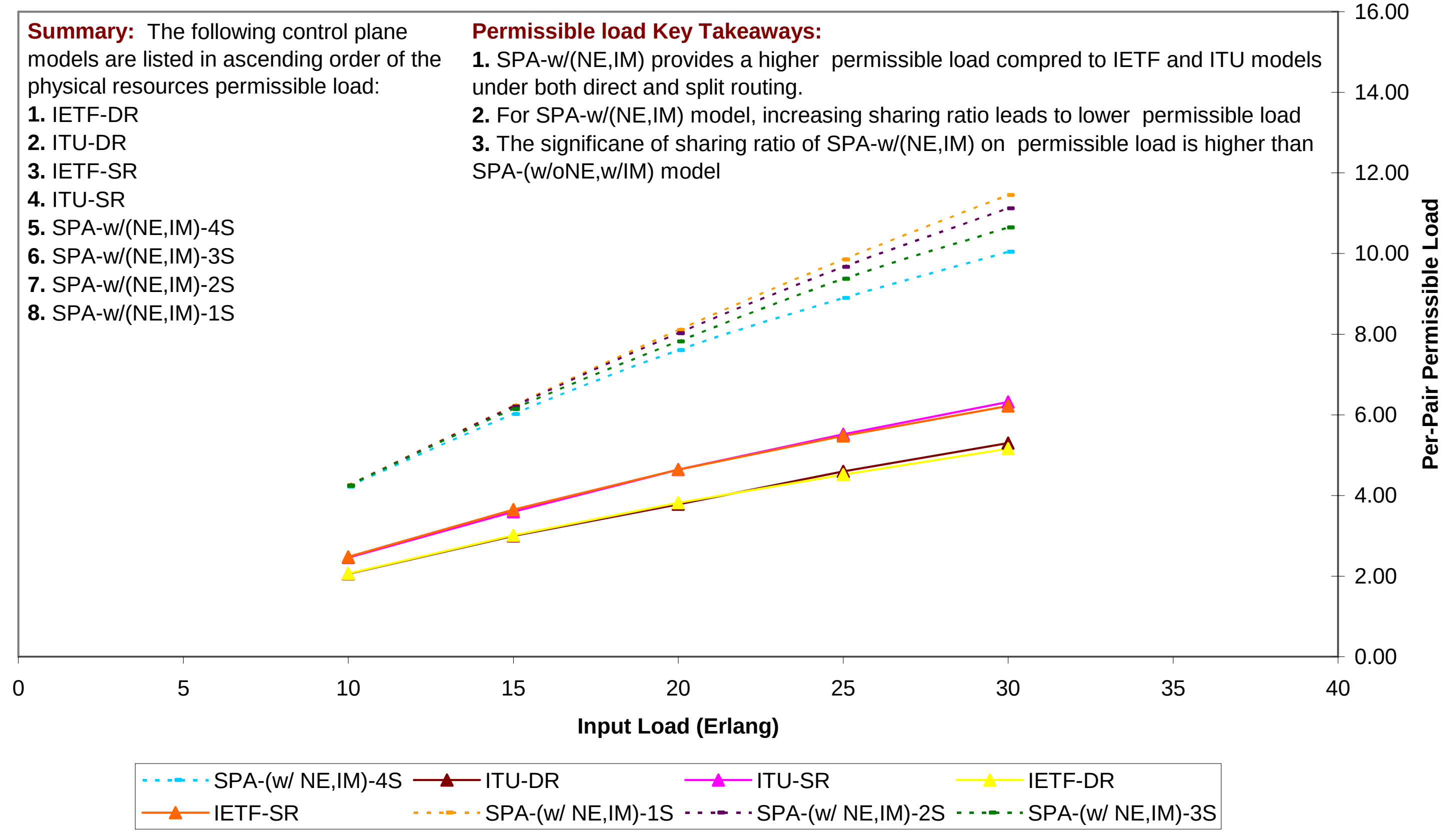

Summary: The following control plane models are listed in ascending order of the physical resources permissible load:

1. IETF-DR
2. ITU-DR
3. IETF-SR
4. ITU-SR
5. SPA-w/(NE,IM)-4S
6. SPA-w/(NE,IM)-3S
7. SPA-w/(NE,IM)-2S
8. SPA-w/(NE,IM)-1S

Permissible load Key Takeaways:
1. SPA-w/(NE,IM) provides a higher permissible load compred to IETF and ITU models under both direct and split routing.
2. For SPA-w/(NE,IM) model, increasing sharing ratio leads to lower permissible load
3. The significane of sharing ratio of SPA-w/(NE,IM) on permissible load is higher than SPA-(w/oNE,w/IM) model

Figure 19-36: Average Network-Wide Permissible Load (Physical Resources)-4 Node – IETF(DR,SR), ITU(DR,SR), SPA-w/(NE,IM)

19.3 Utilization

This section provides detailed performance analysis of the network-wide utilization on the physical resource level for the 4-node topology. The configured VPN service evaluated is the Fully-meshed Shared Granular (FSF) with the following service profile layer parameters:

a. Service flow connectivity: configured as “fully-meshed”.

b. Service demand granularity: configured as “granular” with 1 STS-1 granularity level.

c. Load partitioning flexibility: configured as “enabled”.

One input class was evaluated with the following parameters: $k = 2$, $b_k^A = 2$ STS-1, $\mu_k = 1$ unit time, $\lambda_{rk} = 4$ calls/unit time. Range of input load for 4-node topology is 10 to 30 Erlangs. The five traffic management schemes of the SPA control plane model are evaluated as provided in Table 9-1.

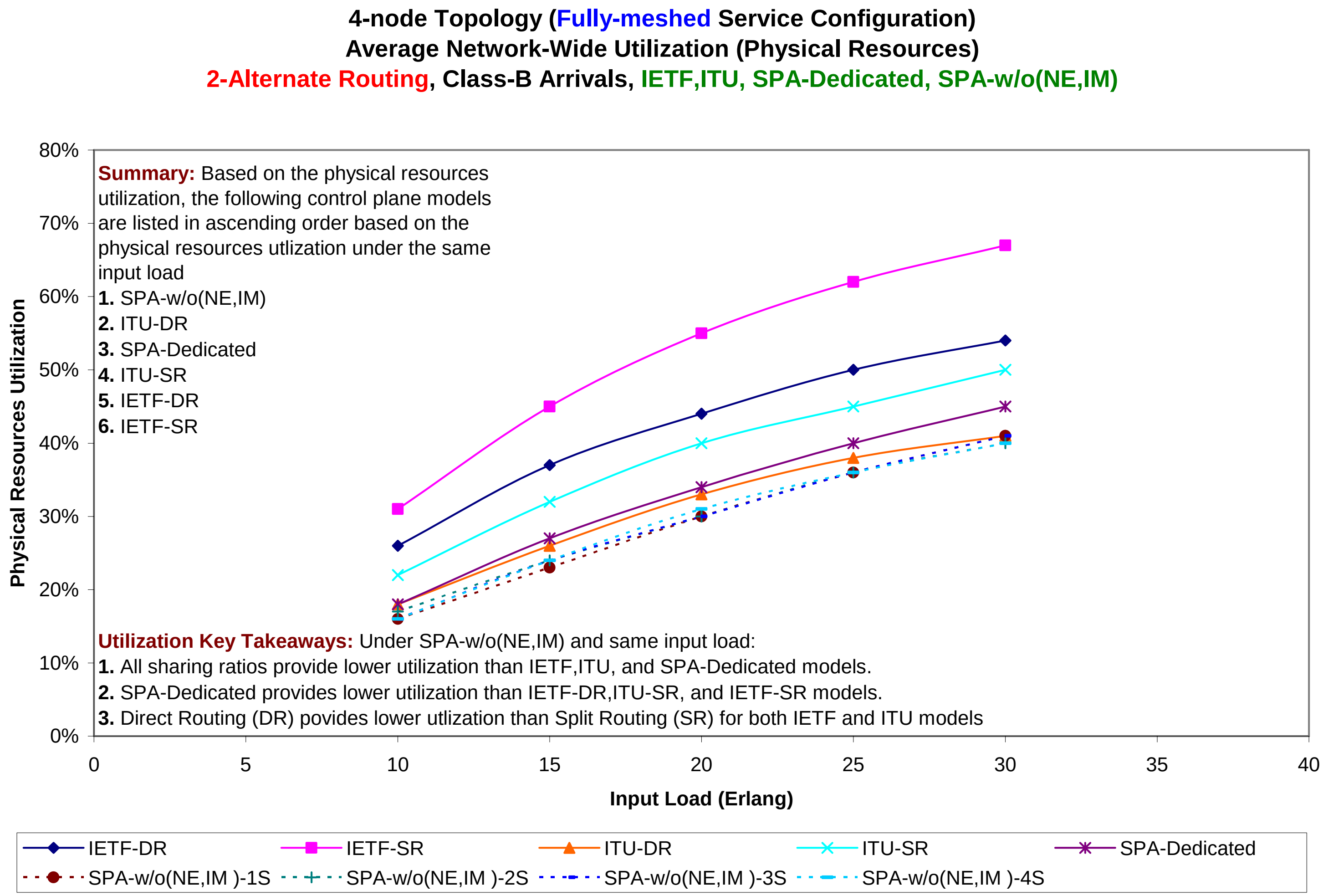

4-node Topology (Fully-meshed Service Configuration)
Average Network-Wide Utilization (Physical Resources)
2-Alternate Routing, Class-B Arrivals, IETF,ITU, SPA-Dedicated, SPA-w/o(NE,IM)

Summary: Based on the physical resources utilization, the following control plane models are listed in ascending order based on the physical resources utlization under the same input load

1. SPA-w/o(NE,IM)
2. ITU-DR
3. SPA-Dedicated
4. ITU-SR
5. IETF-DR
6. IETF-SR

Utilization Key Takeaways: Under SPA-w/o(NE,IM) and same input load:
1. All sharing ratios provide lower utilization than IETF,ITU, and SPA-Dedicated models.
2. SPA-Dedicated provides lower utilization than IETF-DR,ITU-SR, and IETF-SR models.
3. Direct Routing (DR) povides lower utlization than Split Routing (SR) for both IETF and ITU models

Figure 19-37: Average Network-Wide Utilization (Physical Resources)-4 Node – IETF,ITU, SPA-Dedicated, SPA-w/o(NE,IM)

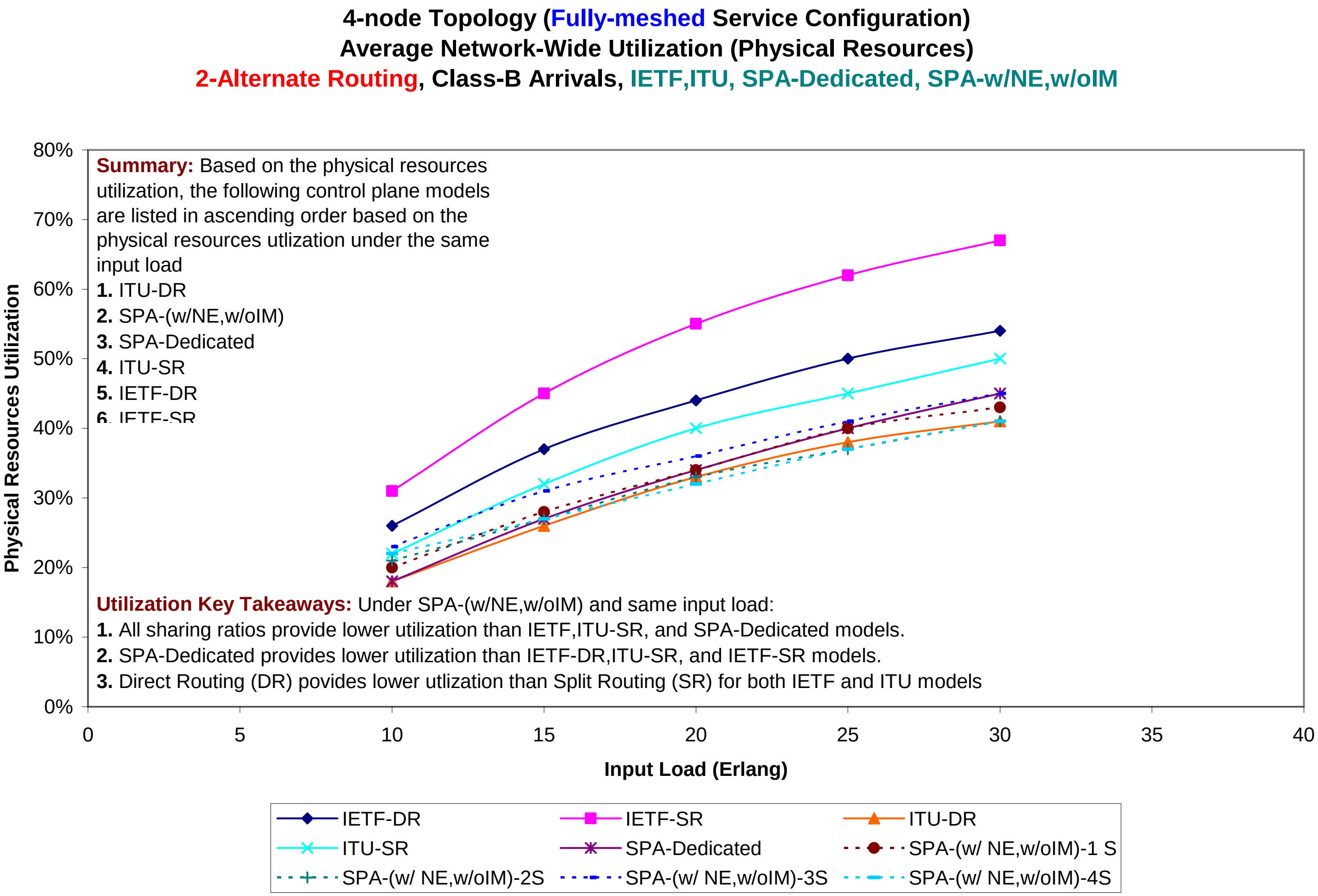

4-node Topology (Fully-meshed Service Configuration)
Average Network-Wide Utilization (Physical Resources)
2-Alternate Routing, Class-B Arrivals, IETF,ITU, SPA-Dedicated, SPA-w/NE,w/oIM

Summary: Based on the physical resources utilization, the following control plane models are listed in ascending order based on the physical resources utlization under the same input load

1. ITU-DR
2. SPA-(w/NE,w/oIM)
3. SPA-Dedicated
4. ITU-SR
5. IETF-DR
6. IETF-SR

Utilization Key Takeaways: Under SPA-(w/NE,w/oIM) and same input load:
1. All sharing ratios provide lower utilization than IETF,ITU-SR, and SPA-Dedicated models.
2. SPA-Dedicated provides lower utilization than IETF-DR,ITU-SR, and IETF-SR models.
3. Direct Routing (DR) povides lower utlization than Split Routing (SR) for both IETF and ITU models

Figure 19-38: Average Network-Wide Utilization (Physical Resources)-4 Node – IETF,ITU, SPA-Dedicated, SPA-w/NE,w/oIM

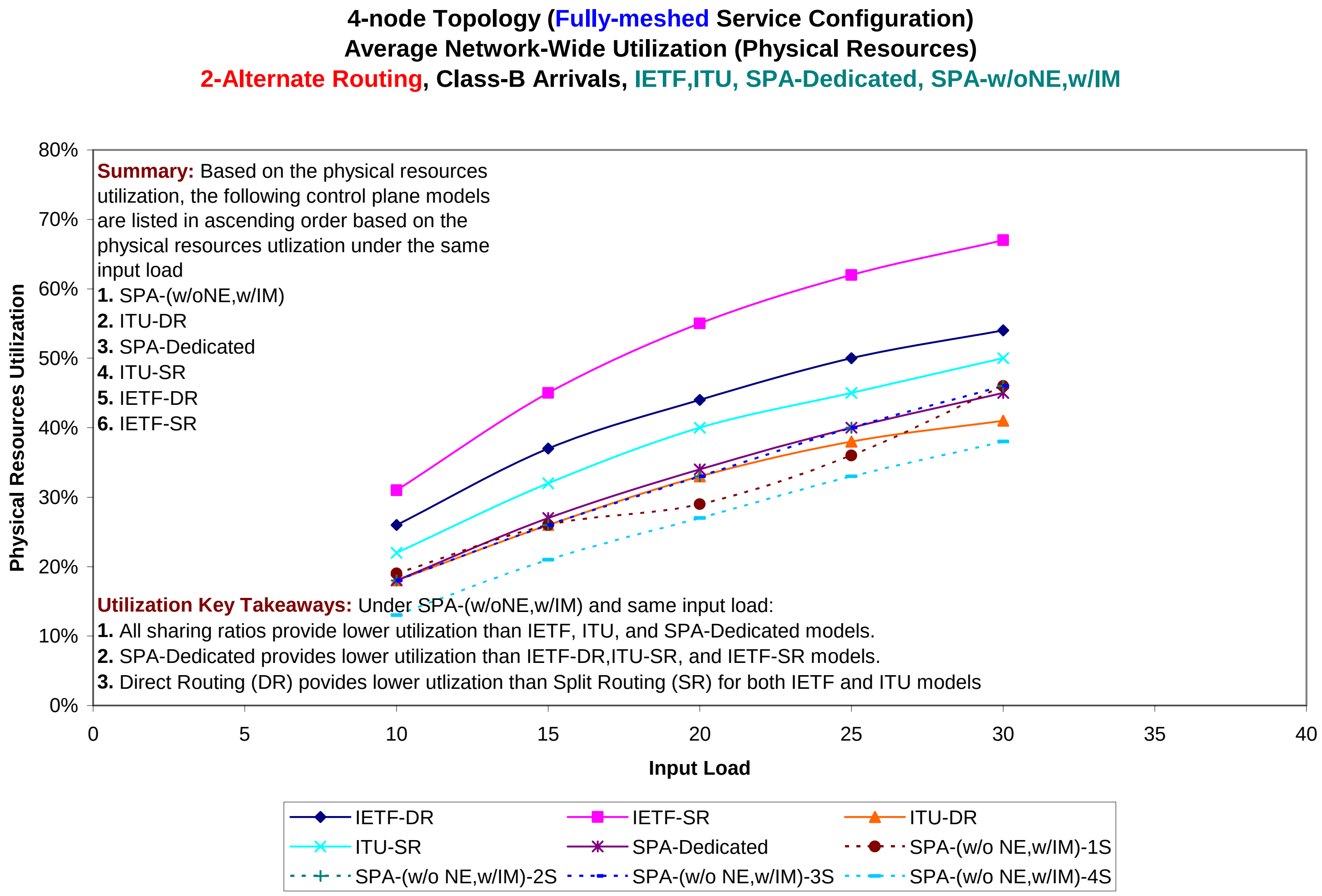
4-node Topology (Fully-meshed Service Configuration)
Average Network-Wide Utilization (Physical Resources)
2-Alternate Routing, Class-B Arrivals, IETF,ITU, SPA-Dedicated, SPA-w/oNE,w/IM

Summary: Based on the physical resources utilization, the following control plane models are listed in ascending order based on the physical resources utlization under the same input load

1. SPA-(w/oNE,w/IM)
2. ITU-DR
3. SPA-Dedicated
4. ITU-SR
5. IETF-DR
6. IETF-SR

Utilization Key Takeaways: Under SPA-(w/oNE,w/IM) and same input load:
1. All sharing ratios provide lower utilization than IETF, ITU, and SPA-Dedicated models.
2. SPA-Dedicated provides lower utilization than IETF-DR,ITU-SR, and IETF-SR models.
3. Direct Routing (DR) povides lower utlization than Split Routing (SR) for both IETF and ITU models

Figure 19-39: Average Network-Wide Utilization (Physical Resources)-4 Node – IETF,ITU, SPA-Dedicated, SPA-w/oNE,w/IM

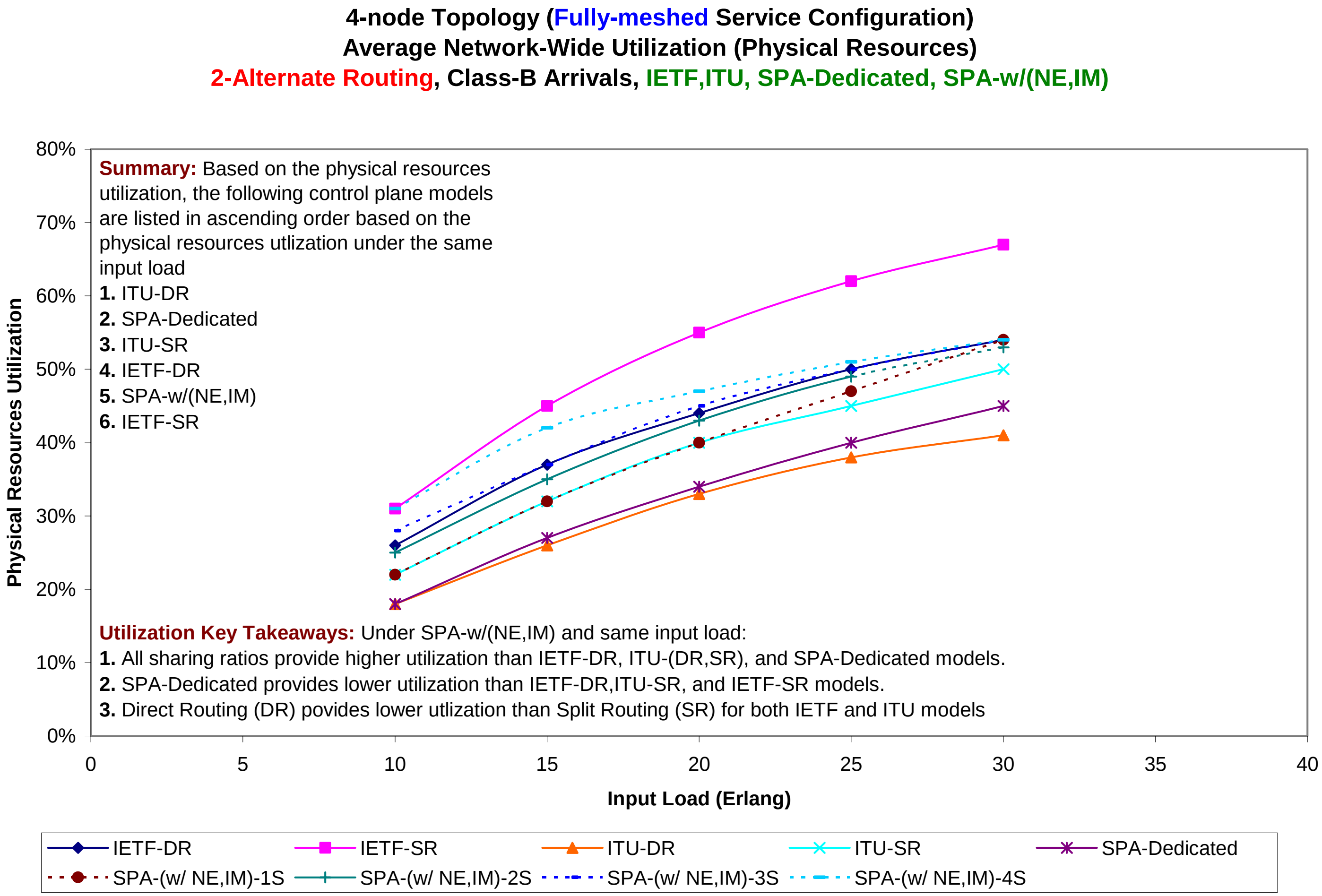

4-node Topology (Fully-meshed Service Configuration)
Average Network-Wide Utilization (Physical Resources)
2-Alternate Routing, Class-B Arrivals, IETF,ITU, SPA-Dedicated, SPA-w/(NE,IM)

Summary: Based on the physical resources utilization, the following control plane models are listed in ascending order based on the physical resources utlization under the same input load

1. ITU-DR
2. SPA-Dedicated
3. ITU-SR
4. IETF-DR
5. SPA-w/(NE,IM)
6. IETF-SR

Utilization Key Takeaways: Under SPA-w/(NE,IM) and same input load:

1. All sharing ratios provide higher utilization than IETF-DR, ITU-(DR,SR), and SPA-Dedicated models.
2. SPA-Dedicated provides lower utilization than IETF-DR,ITU-SR, and IETF-SR models.
3. Direct Routing (DR) povides lower utlization than Split Routing (SR) for both IETF and ITU models

Figure 19-40: Average Network-Wide Blocking Probability (Physical Resources)-4 Node-2 Alternate Route- IETF,ITU, SPA-Dedicated, SPA-w/(NE,IM)

20 Appendix-D: Detailed Modeling Results- 7-Node Topology with 2-Alternate Routing

20.1 Blocking probability

20.1.1 Dedicated resources

This section provides detailed performance analysis of the network-wide blocking probability on the dedicated network resources partition for the 7-node topology with two-alternate routing. The configured VPN service evaluated is the Fully-meshed Shared Granular (FSF) with the following service profile layer parameters:

a. Service flow connectivity: configured as “fully-meshed”.

b. Service demand granularity: configured as “granular” with 1 STS-1 granularity level.

c. Load partitioning flexibility: configured as “enabled”.

One input class was evaluated with the following parameters: $k = 2$, $b_k^A = 2$ STS-1, $\mu_k = 1$unit time, $\lambda_{rk} = 4$ calls/unit time. Range of input load for 4-node topology is 30 to 70 Erlangs. The five traffic management schemes of the SPA control plane model are evaluated as provided in Table 9-1. Four sharing levels are considered as follows:

a. STS-1 sharing: C_j^{vD}=11 STS-1, C_j^S=2 STS-1

b. STS-2 sharing: C_j^{vD}=10 STS-1, C_j^S=4 STS-1

c. STS-3 sharing: C_j^{vD}=9 STS-1, C_j^S=6 STS-1

d. STS-4 sharing: C_j^{vD}=8 STS-1, C_j^S=8 STS-1

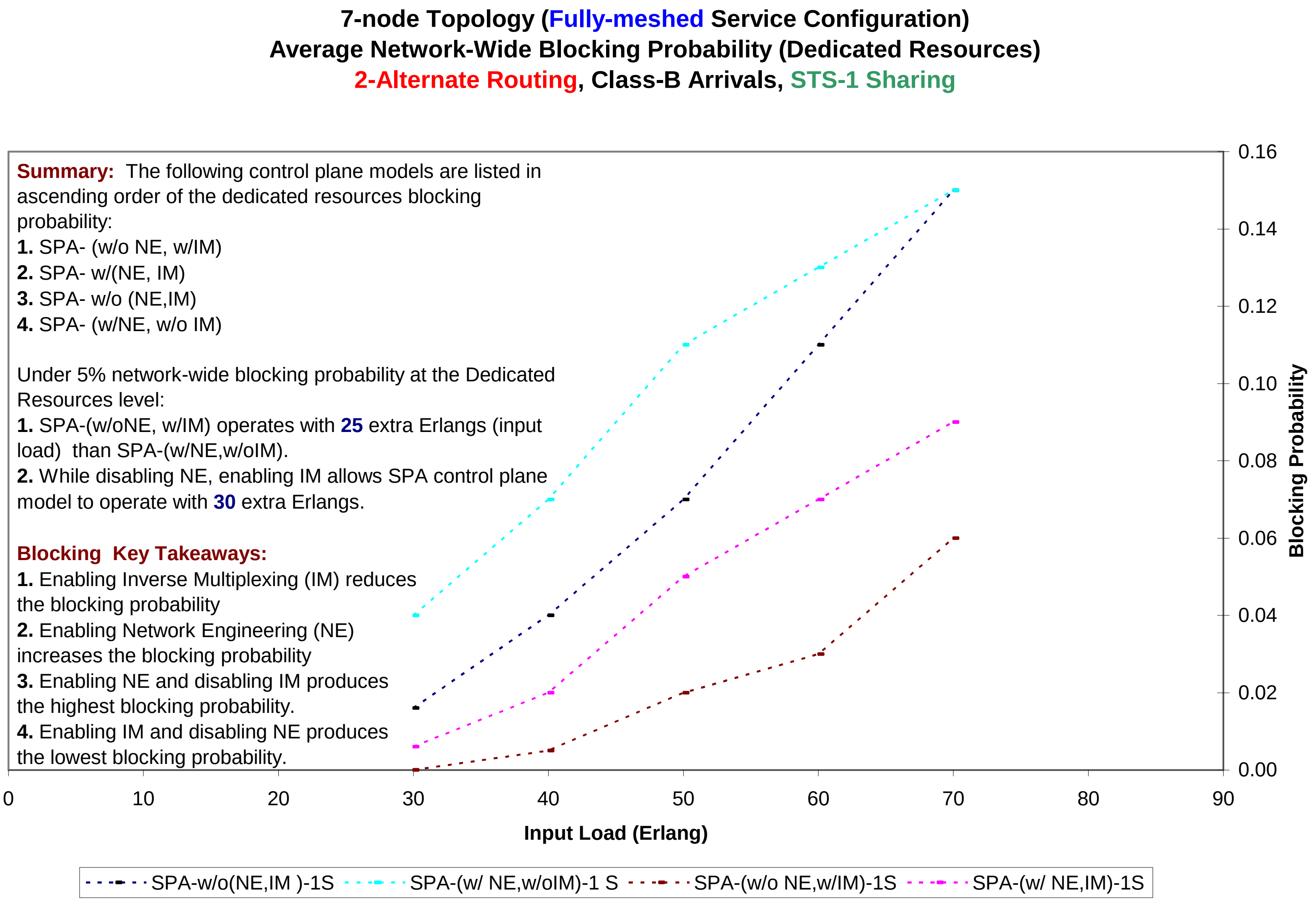
7-node Topology (Fully-meshed Service Configuration)
Average Network-Wide Blocking Probability (Dedicated Resources)
2-Alternate Routing, Class-B Arrivals, STS-1 Sharing

Summary: The following control plane models are listed in ascending order of the dedicated resources blocking probability:

1. SPA- (w/o NE, w/IM)
2. SPA- w/(NE, IM)
3. SPA- w/o (NE,IM)
4. SPA- (w/NE, w/o IM)

Under 5% network-wide blocking probability at the Dedicated Resources level:

1. SPA-(w/oNE, w/IM) operates with **25** extra Erlangs (input load) than SPA-(w/NE,w/oIM).
2. While disabling NE, enabling IM allows SPA control plane model to operate with **30** extra Erlangs.

Blocking Key Takeaways:

1. Enabling Inverse Multiplexing (IM) reduces the blocking probability
2. Enabling Network Engineering (NE) increases the blocking probability
3. Enabling NE and disabling IM produces the highest blocking probability.
4. Enabling IM and disabling NE produces the lowest blocking probability.

Figure 20-1: Average Network-Wide Blocking Probability (Dedicated Resources)-7 Node – 2 Alternate Route-STS-1 Sharing

7-node Topology (Fully-meshed Service Configuration)
Average Network-Wide Blocking Probability (Dedicated Resources)
2-Alternate Routing, Class-B Arrivals, STS-2 Sharing

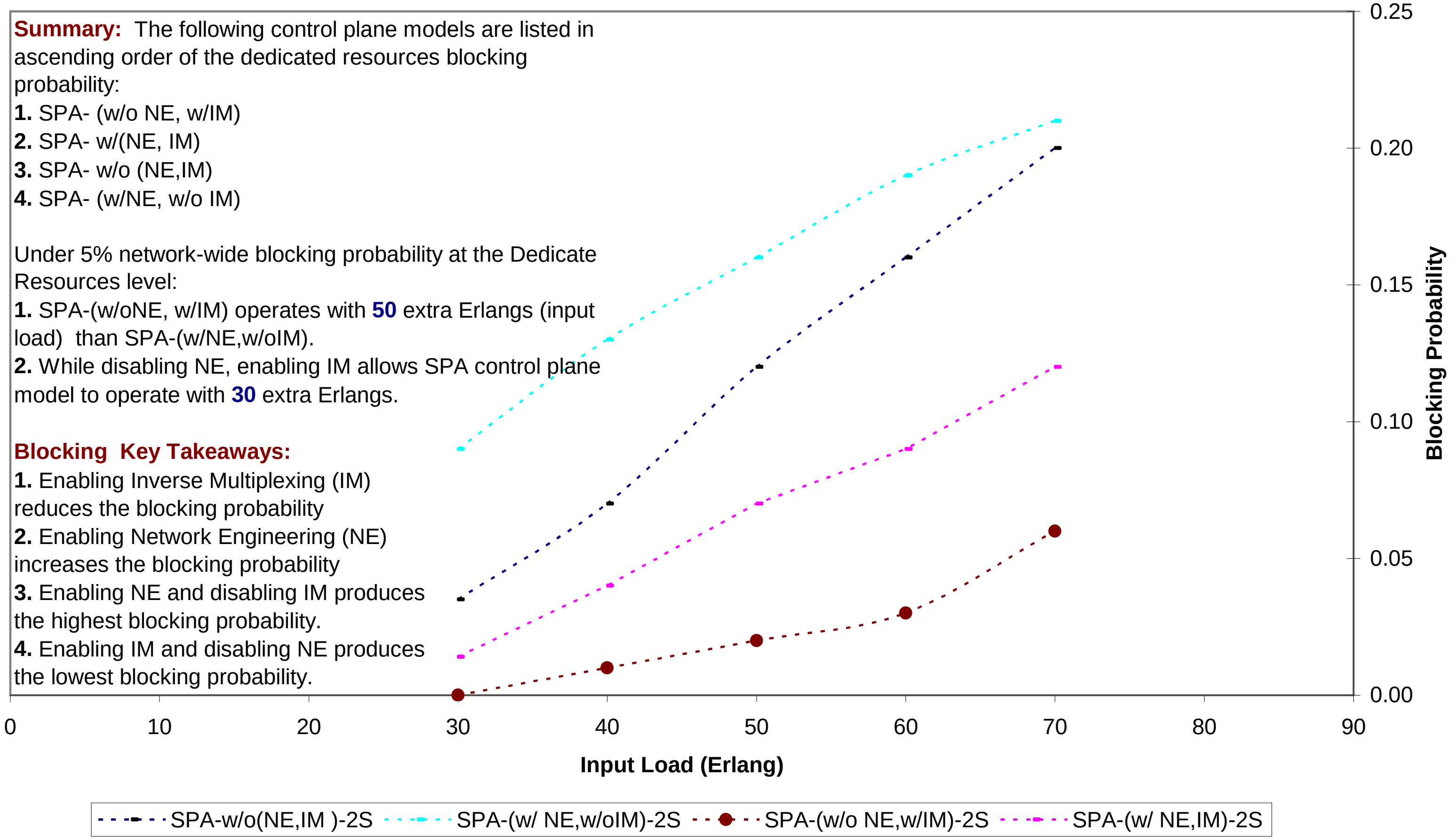

Summary: The following control plane models are listed in ascending order of the dedicated resources blocking probability:

1. SPA- (w/o NE, w/IM)
2. SPA- w/(NE, IM)
3. SPA- w/o (NE,IM)
4. SPA- (w/NE, w/o IM)

Under 5% network-wide blocking probability at the Dedicate Resources level:
1. SPA-(w/oNE, w/IM) operates with **50** extra Erlangs (input load) than SPA-(w/NE,w/oIM).
2. While disabling NE, enabling IM allows SPA control plane model to operate with **30** extra Erlangs.

Blocking Key Takeaways:
1. Enabling Inverse Multiplexing (IM) reduces the blocking probability
2. Enabling Network Engineering (NE) increases the blocking probability
3. Enabling NE and disabling IM produces the highest blocking probability.
4. Enabling IM and disabling NE produces the lowest blocking probability.

Figure 20-2: Average Network-Wide Blocking Probability (Dedicated Resources)-7 Node – 2 Alternate Route-STS-2 Sharing

7-node Topology (Fully-meshed Service Configuration)
Average Network-Wide Blocking Probability (Dedicated Resources)
2-Alternate Routing, Class-B Arrivals, STS-3 Sharing

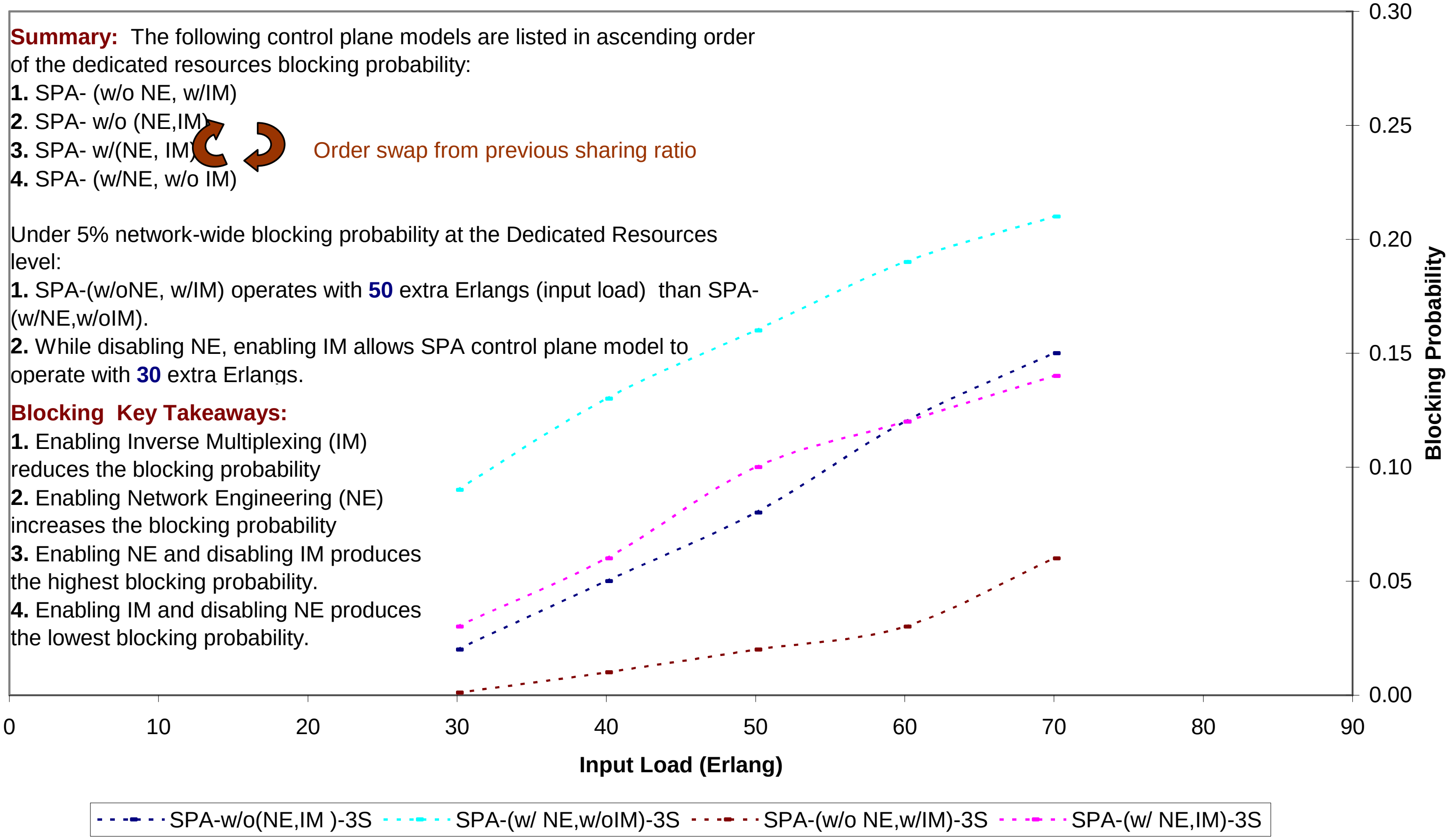

Summary: The following control plane models are listed in ascending order of the dedicated resources blocking probability:

1. SPA- (w/o NE, w/IM)
2. SPA- w/o (NE,IM)
3. SPA- w/(NE, IM)
4. SPA- (w/NE, w/o IM)

Order swap from previous sharing ratio

Under 5% network-wide blocking probability at the Dedicated Resources level:
1. SPA-(w/oNE, w/IM) operates with **50** extra Erlangs (input load) than SPA-(w/NE,w/oIM).
2. While disabling NE, enabling IM allows SPA control plane model to operate with **30** extra Erlangs.

Blocking Key Takeaways:
1. Enabling Inverse Multiplexing (IM) reduces the blocking probability
2. Enabling Network Engineering (NE) increases the blocking probability
3. Enabling NE and disabling IM produces the highest blocking probability.
4. Enabling IM and disabling NE produces the lowest blocking probability.

Figure 20-3: Average Network-Wide Blocking Probability (Dedicated Resources)-7 Node – 2 Alternate Route-STS-3 Sharing

7-node Topology (Fully-meshed Service Configuration)
Average Network-Wide Blocking Probability (Dedicated Resources)
2-Alternate Routing, Class-B Arrivals, STS-4 Sharing

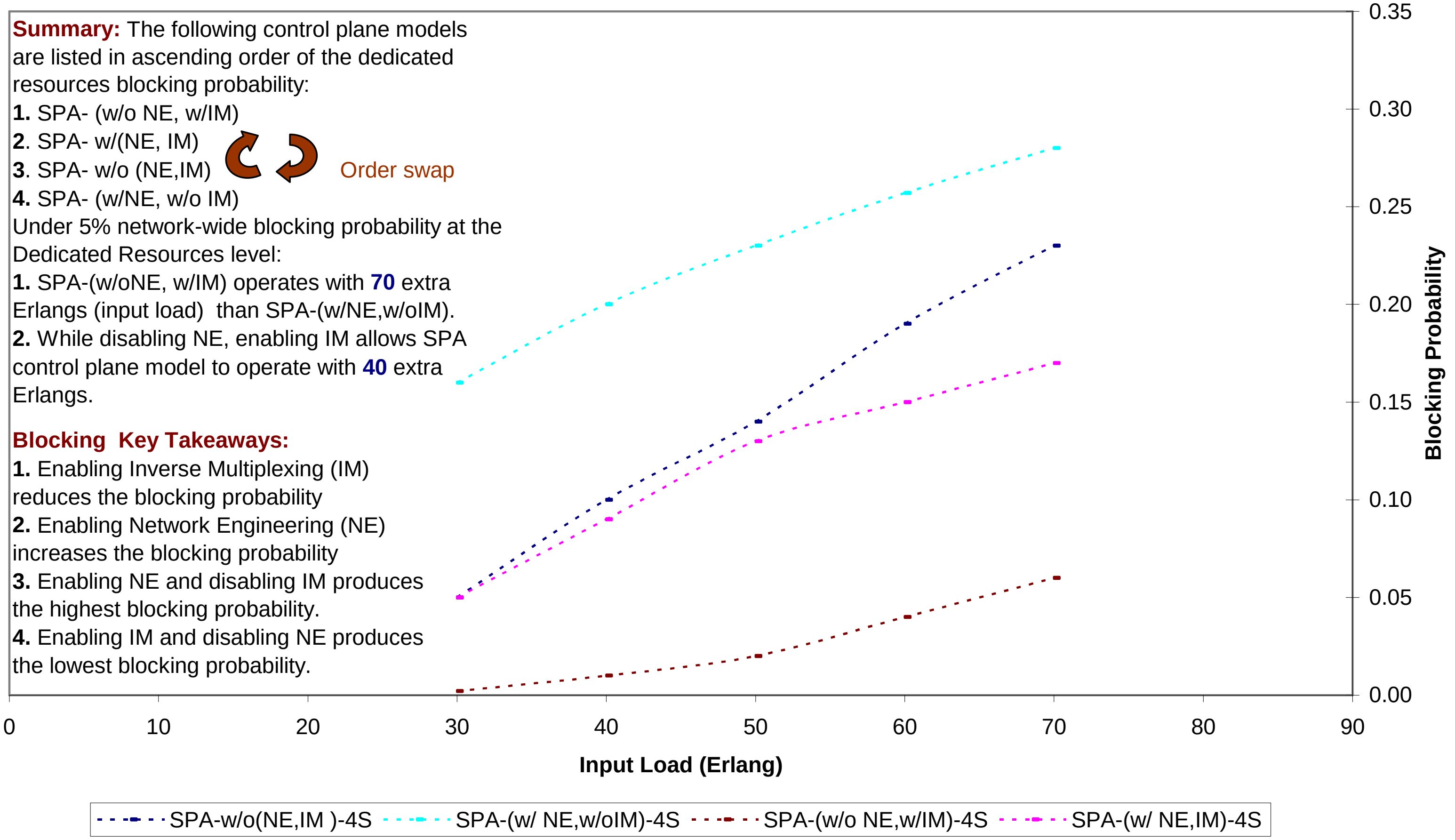

Summary: The following control plane models are listed in ascending order of the dedicated resources blocking probability:

1. SPA- (w/o NE, w/IM)
2. SPA- w/(NE, IM)
3. SPA- w/o (NE,IM)
4. SPA- (w/NE, w/o IM)

Order swap

Under 5% network-wide blocking probability at the Dedicated Resources level:

1. SPA-(w/oNE, w/IM) operates with **70** extra Erlangs (input load) than SPA-(w/NE,w/oIM).
2. While disabling NE, enabling IM allows SPA control plane model to operate with **40** extra Erlangs.

Blocking Key Takeaways:

1. Enabling Inverse Multiplexing (IM) reduces the blocking probability
2. Enabling Network Engineering (NE) increases the blocking probability
3. Enabling NE and disabling IM produces the highest blocking probability.
4. Enabling IM and disabling NE produces the lowest blocking probability.

Figure 20-4: Average Network-Wide Blocking Probability (Dedicated Resources)-7 Node – 2 Alternate Route-STS-4 Sharing

20.1.2 Shared resources

This section provides detailed performance analysis of the network-wide blocking probability on the shared network resources partition for the 7-node topology with two-alternate routing. The configured VPN service evaluated is the Fully-meshed Shared Granular (FSF) with the following service profile layer parameters:

a. Service flow connectivity: configured as “fully-meshed”.

b. Service demand granularity: configured as “granular” with 1 STS-1 granularity level.

c. Load partitioning flexibility: configured as “enabled”.

One input class was evaluated with the following parameters: $k = 2$, $b_k^A = 2$ STS-1, $\mu_k = 1$unit time, $\lambda_{rk} = 4$ calls/unit time. Range of input load for 4-node topology is 30 to 70 Erlangs. The five traffic management schemes of the SPA control plane model are evaluated as provided in Table 9-1. Four sharing levels are considered as follows:

a. STS-1 sharing: C_j^{vD} =11 STS-1, C_j^S =2 STS-1

b. STS-2 sharing: C_j^{vD} =10 STS-1, C_j^S =4 STS-1

c. STS-3 sharing: C_j^{vD} =9 STS-1, C_j^S =6 STS-1

d. STS-4 sharing: C_j^{vD} =8 STS-1, C_j^S =8 STS-1

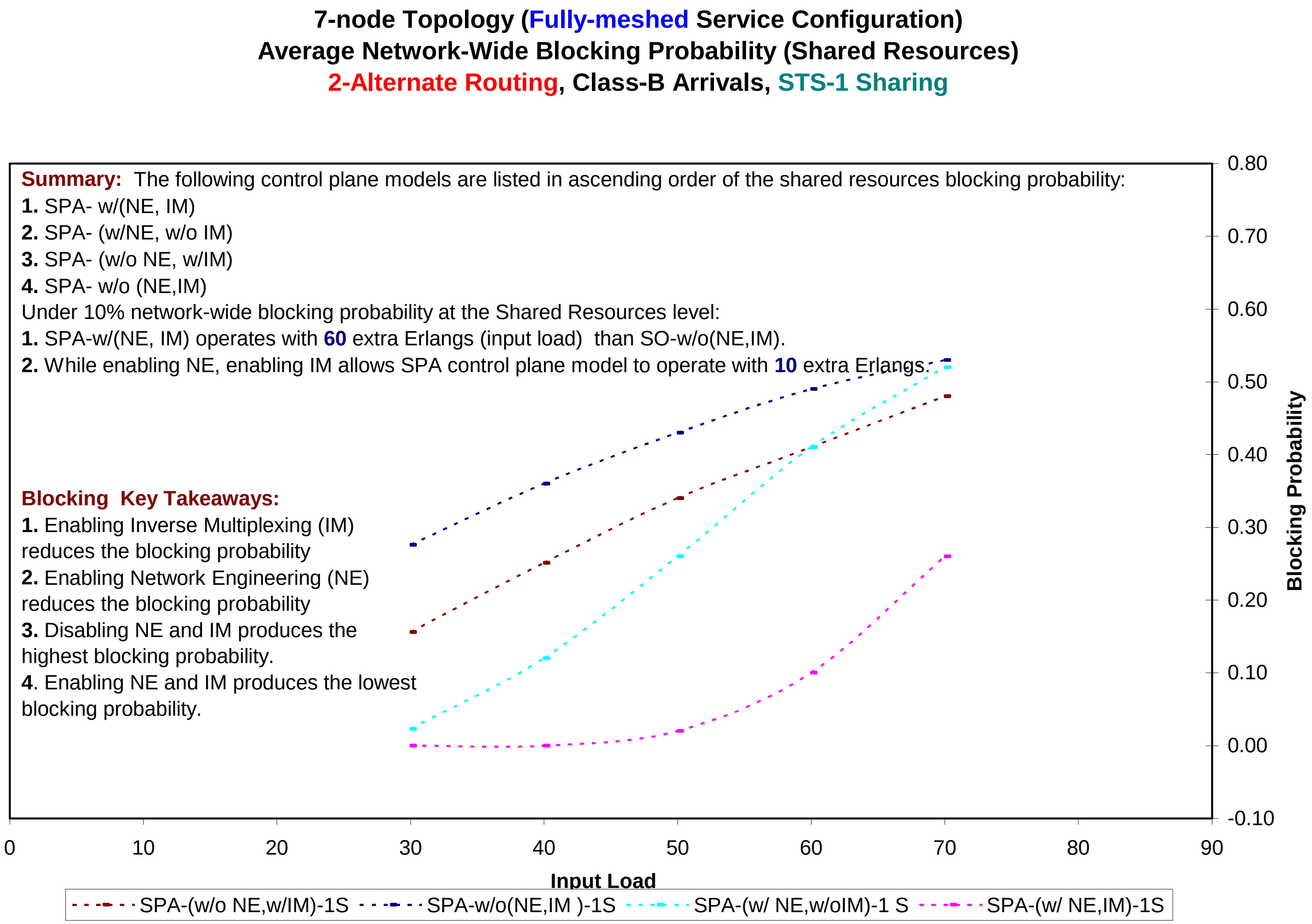

7-node Topology (Fully-meshed Service Configuration)
Average Network-Wide Blocking Probability (Shared Resources)
2-Alternate Routing, Class-B Arrivals, STS-1 Sharing

Summary: The following control plane models are listed in ascending order of the shared resources blocking probability:

1. SPA- w/(NE, IM)
2. SPA- (w/NE, w/o IM)
3. SPA- (w/o NE, w/IM)
4. SPA- w/o (NE,IM)

Under 10% network-wide blocking probability at the Shared Resources level:

1. SPA-w/(NE, IM) operates with **60** extra Erlangs (input load) than SO-w/o(NE,IM).
2. While enabling NE, enabling IM allows SPA control plane model to operate with **10** extra Erlangs.

Blocking Key Takeaways:

1. Enabling Inverse Multiplexing (IM) reduces the blocking probability
2. Enabling Network Engineering (NE) reduces the blocking probability
3. Disabling NE and IM produces the highest blocking probability.
4. Enabling NE and IM produces the lowest blocking probability.

Figure 20-5: Average Network-Wide Blocking Probability (Shared Resources)-7 Node – 2 Alternate Route-STS-1 Sharing

7-node Topology (Fully-meshed Service Configuration)
Average Network-Wide Blocking Probability (Shared Resources)
2-Alternate Routing, Class-B Arrivals, STS-2 Sharing

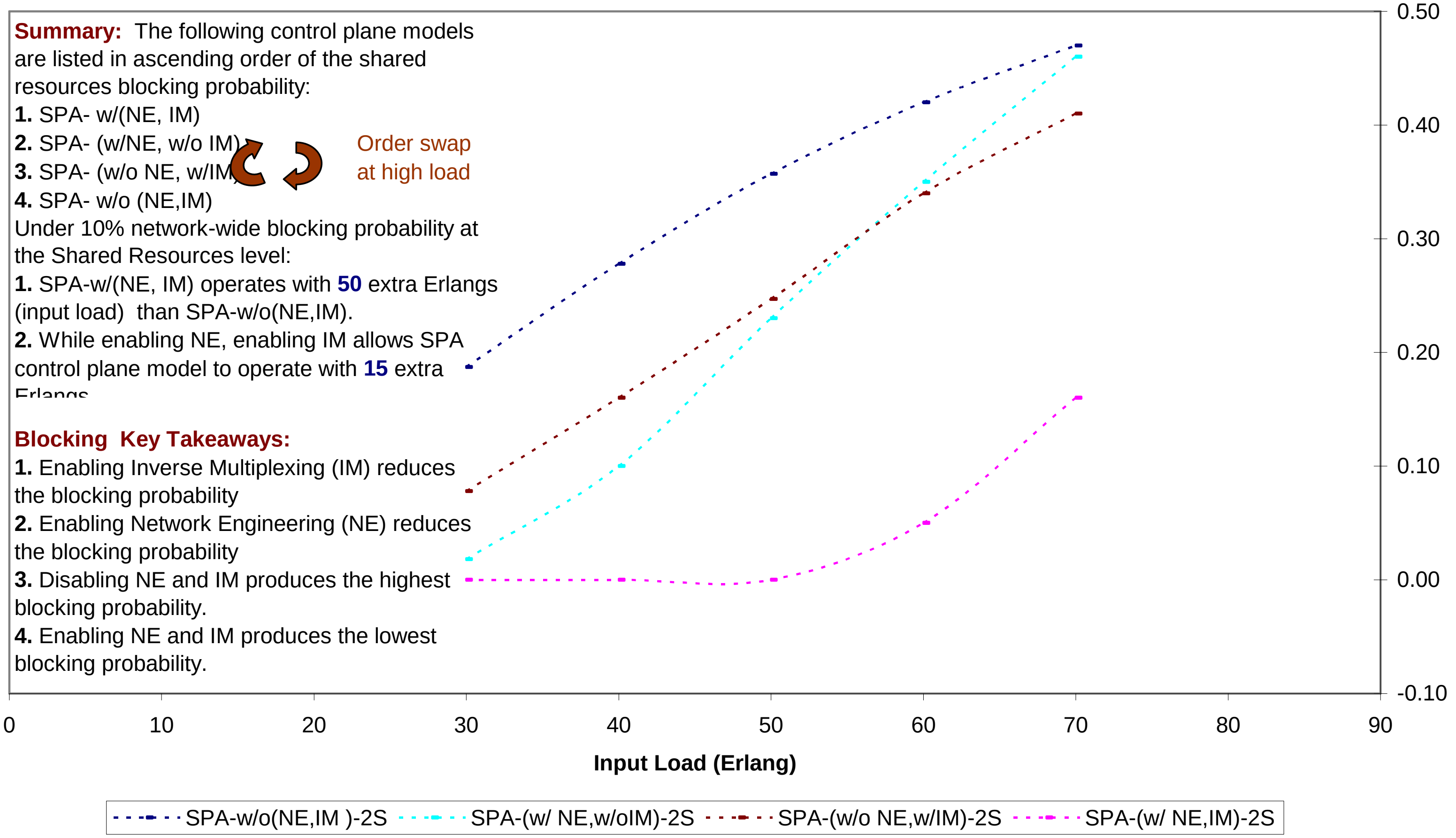

Summary: The following control plane models are listed in ascending order of the shared resources blocking probability:

1. SPA- w/(NE, IM)
2. SPA- (w/NE, w/o IM)
3. SPA- (w/o NE, w/IM)
4. SPA- w/o (NE,IM)

Order swap at high load

Under 10% network-wide blocking probability at the Shared Resources level:

1. SPA-w/(NE, IM) operates with **50** extra Erlangs (input load) than SPA-w/o(NE,IM).
2. While enabling NE, enabling IM allows SPA control plane model to operate with **15** extra Erlangs

Blocking Key Takeaways:

1. Enabling Inverse Multiplexing (IM) reduces the blocking probability
2. Enabling Network Engineering (NE) reduces the blocking probability
3. Disabling NE and IM produces the highest blocking probability.
4. Enabling NE and IM produces the lowest blocking probability.

Figure 20-6: Average Network-Wide Blocking Probability (Shared Resources)-7 Node – 2 Alternate Route-STS-2 Sharing

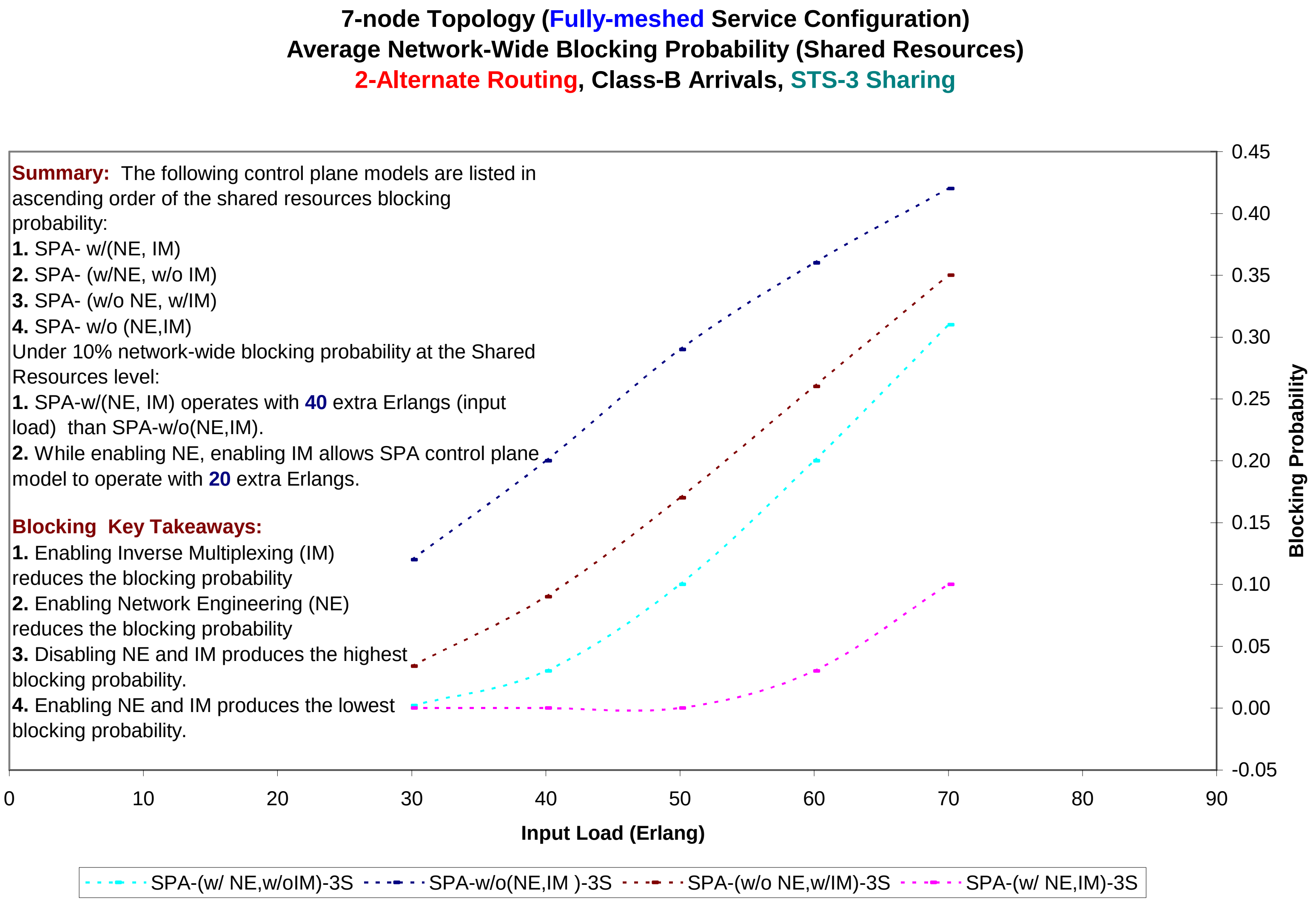

7-node Topology (Fully-meshed Service Configuration)
Average Network-Wide Blocking Probability (Shared Resources)
2-Alternate Routing, Class-B Arrivals, STS-3 Sharing

Summary: The following control plane models are listed in ascending order of the shared resources blocking probability:

1. SPA- w/(NE, IM)
2. SPA- (w/NE, w/o IM)
3. SPA- (w/o NE, w/IM)
4. SPA- w/o (NE,IM)

Under 10% network-wide blocking probability at the Shared Resources level:

1. SPA-w/(NE, IM) operates with **40** extra Erlangs (input load) than SPA-w/o(NE,IM).
2. While enabling NE, enabling IM allows SPA control plane model to operate with **20** extra Erlangs.

Blocking Key Takeaways:

1. Enabling Inverse Multiplexing (IM) reduces the blocking probability
2. Enabling Network Engineering (NE) reduces the blocking probability
3. Disabling NE and IM produces the highest blocking probability.
4. Enabling NE and IM produces the lowest blocking probability.

Figure 20-7: Average Network-Wide Blocking Probability (Shared Resources)-7 Node – 2 Alternate Route-STS-3 Sharing

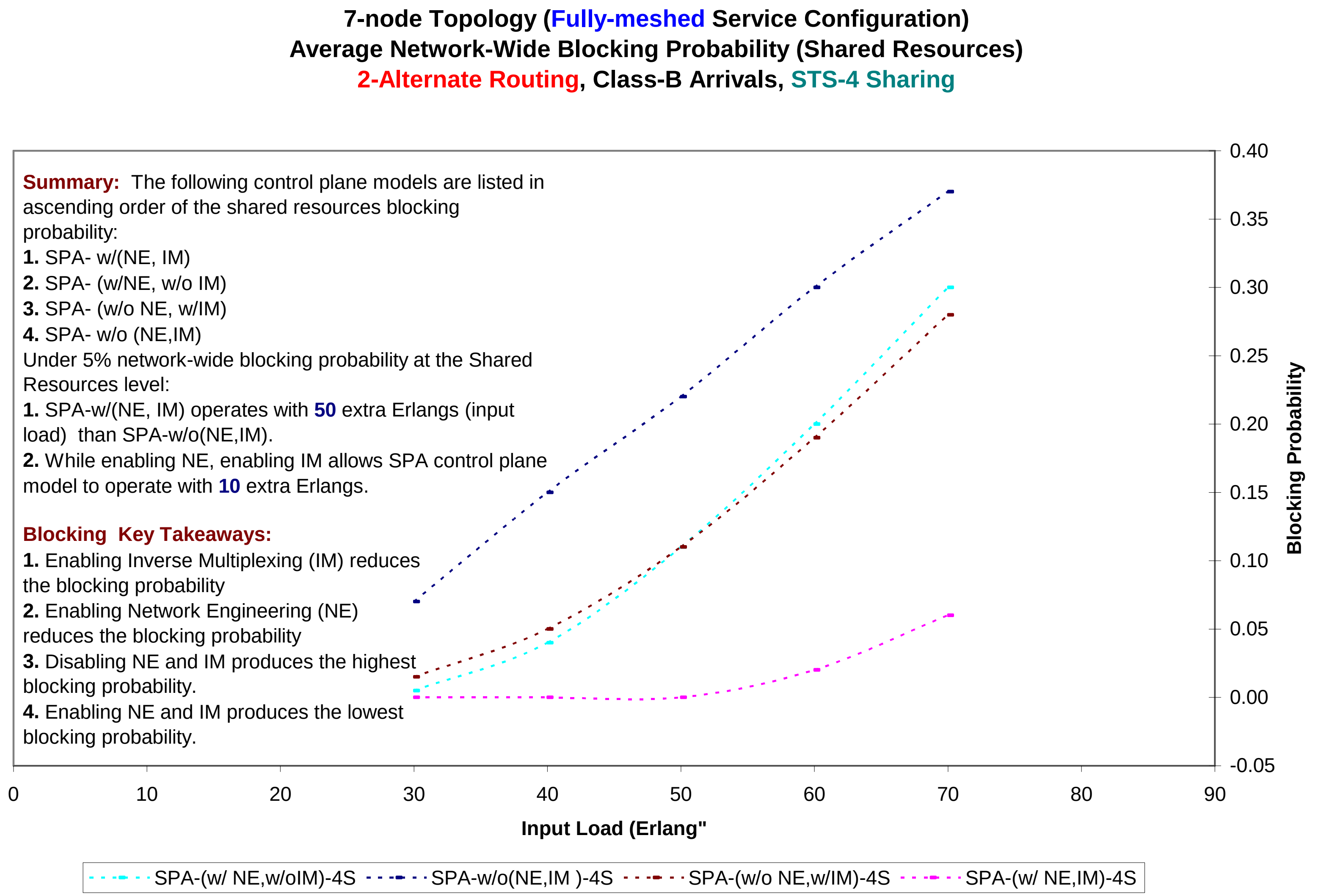

7-node Topology (Fully-meshed Service Configuration)
Average Network-Wide Blocking Probability (Shared Resources)
2-Alternate Routing, Class-B Arrivals, STS-4 Sharing

Summary: The following control plane models are listed in ascending order of the shared resources blocking probability:

1. SPA- w/(NE, IM)
2. SPA- (w/NE, w/o IM)
3. SPA- (w/o NE, w/IM)
4. SPA- w/o (NE,IM)

Under 5% network-wide blocking probability at the Shared Resources level:

1. SPA-w/(NE, IM) operates with **50** extra Erlangs (input load) than SPA-w/o(NE,IM).
2. While enabling NE, enabling IM allows SPA control plane model to operate with **10** extra Erlangs.

Blocking Key Takeaways:

1. Enabling Inverse Multiplexing (IM) reduces the blocking probability
2. Enabling Network Engineering (NE) reduces the blocking probability
3. Disabling NE and IM produces the highest blocking probability.
4. Enabling NE and IM produces the lowest blocking probability.

Figure 20-8: Average Network-Wide Blocking Probability (Shared Resources)-7 Node – 2 Alternate Route-STS-4 Sharing

20.1.3 VPN resources

This section provides detailed performance analysis of the network-wide blocking probability on the VPN network resources partition for the 7-node topology with two-alternate routing. The configured VPN service evaluated is the Fully-meshed Shared Granular (FSF) with the following service profile layer parameters:

a. Service flow connectivity: configured as “fully-meshed”.

b. Service demand granularity: configured as “granular” with 1 STS-1 granularity level.

c. Load partitioning flexibility: configured as “enabled”.

One input class was evaluated with the following parameters: $k = 2$, $b_k^A = 2$ STS-1, $\mu_k = 1$unit time, $\lambda_{rk} = 4$ calls/unit time. Range of input load for 4-node topology is 30 to 70 Erlangs. The five traffic management schemes of the SPA control plane model are evaluated as provided in Table 9-1. Four sharing levels are considered as follows:

a. STS-1 sharing: C_j^{vD} =11 STS-1, C_j^S =2 STS-1

b. STS-2 sharing: C_j^{vD} =10 STS-1, C_j^S =4 STS-1

c. STS-3 sharing: C_j^{vD} =9 STS-1, C_j^S =6 STS-1

d. STS-4 sharing: C_j^{vD} =8 STS-1, C_j^S =8 STS-1

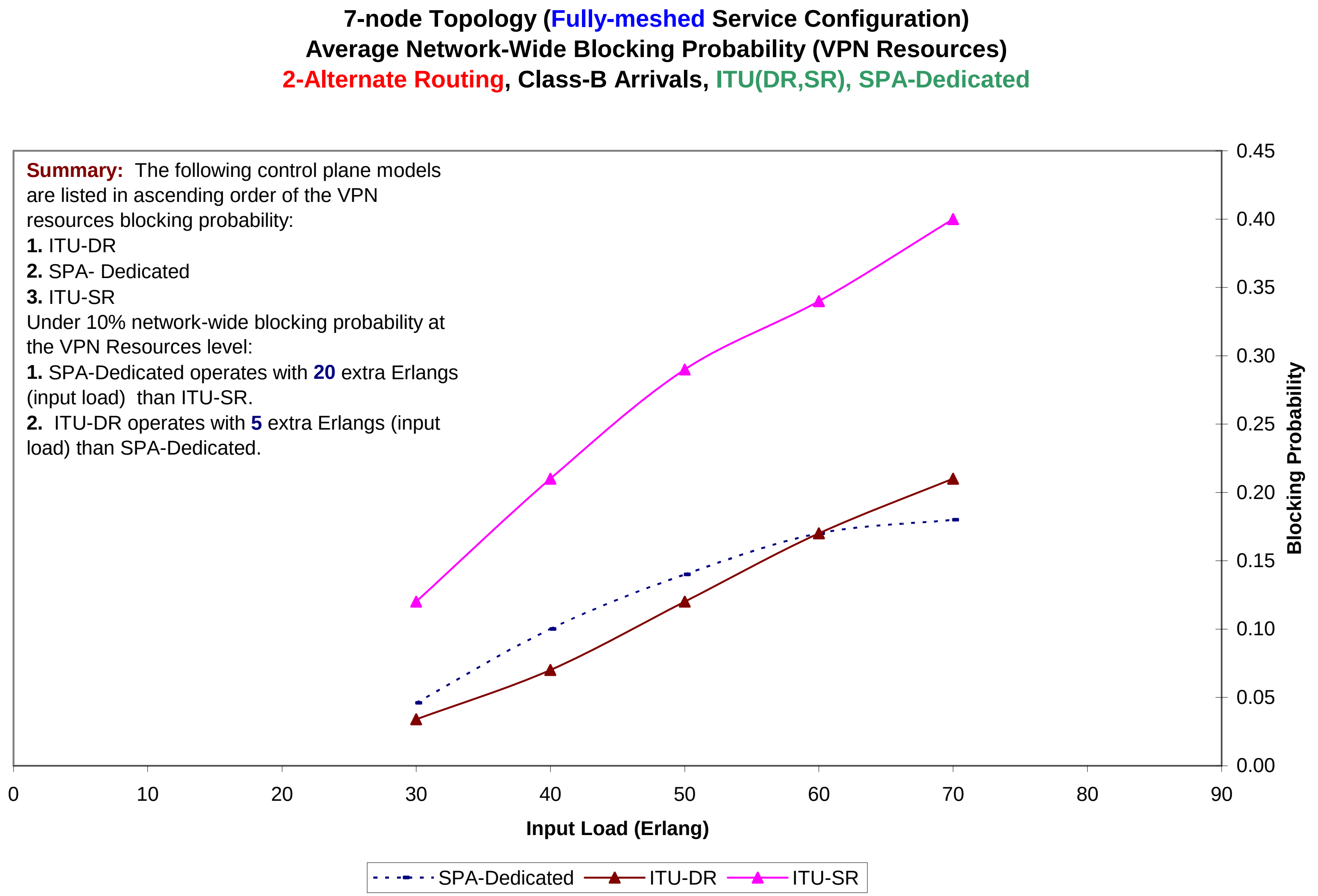

7-node Topology (Fully-meshed Service Configuration)
Average Network-Wide Blocking Probability (VPN Resources)
2-Alternate Routing, Class-B Arrivals, ITU(DR,SR), SPA-Dedicated

Summary: The following control plane models are listed in ascending order of the VPN resources blocking probability:

1. ITU-DR

2. SPA- Dedicated

3. ITU-SR

Under 10% network-wide blocking probability at the VPN Resources level:

1. SPA-Dedicated operates with **20** extra Erlangs (input load) than ITU-SR.

2. ITU-DR operates with **5** extra Erlangs (input load) than SPA-Dedicated.

Figure 20-9: Average Network-Wide Blocking Probability (VPN Resources)-7 Node – 2 Alternate Route-ITU(DR,SR), SPA-Dedicated

7-node Topology (Fully-meshed Service Configuration)
Average Network-Wide Blocking Probability (VPN Resources)
2-Alternate Routing, Class-B Arrivals, ITU(DR,SR), SPA- w/o(NE,IM)

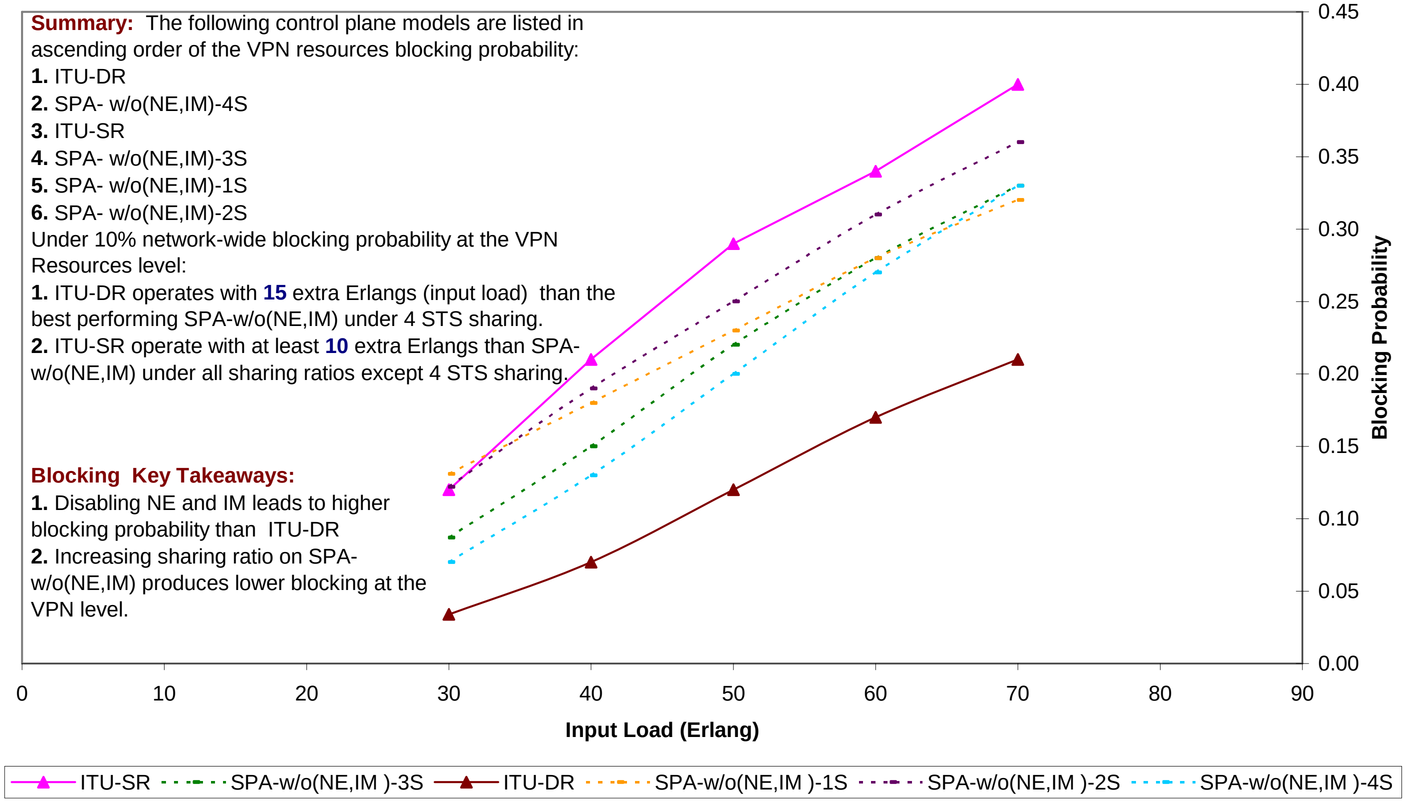

Summary: The following control plane models are listed in ascending order of the VPN resources blocking probability:

1. ITU-DR
2. SPA- w/o(NE,IM)-4S
3. ITU-SR
4. SPA- w/o(NE,IM)-3S
5. SPA- w/o(NE,IM)-1S
6. SPA- w/o(NE,IM)-2S

Under 10% network-wide blocking probability at the VPN Resources level:

1. ITU-DR operates with **15** extra Erlangs (input load) than the best performing SPA-w/o(NE,IM) under 4 STS sharing.
2. ITU-SR operate with at least **10** extra Erlangs than SPA-w/o(NE,IM) under all sharing ratios except 4 STS sharing.

Blocking Key Takeaways:

1. Disabling NE and IM leads to higher blocking probability than ITU-DR
2. Increasing sharing ratio on SPA-w/o(NE,IM) produces lower blocking at the VPN level.

Figure 20-10: Average Network-Wide Blocking Probability (VPN Resources)-7 Node – 2 Alternate Route-ITU(DR,SR), SPA-w/o(NE,IM)

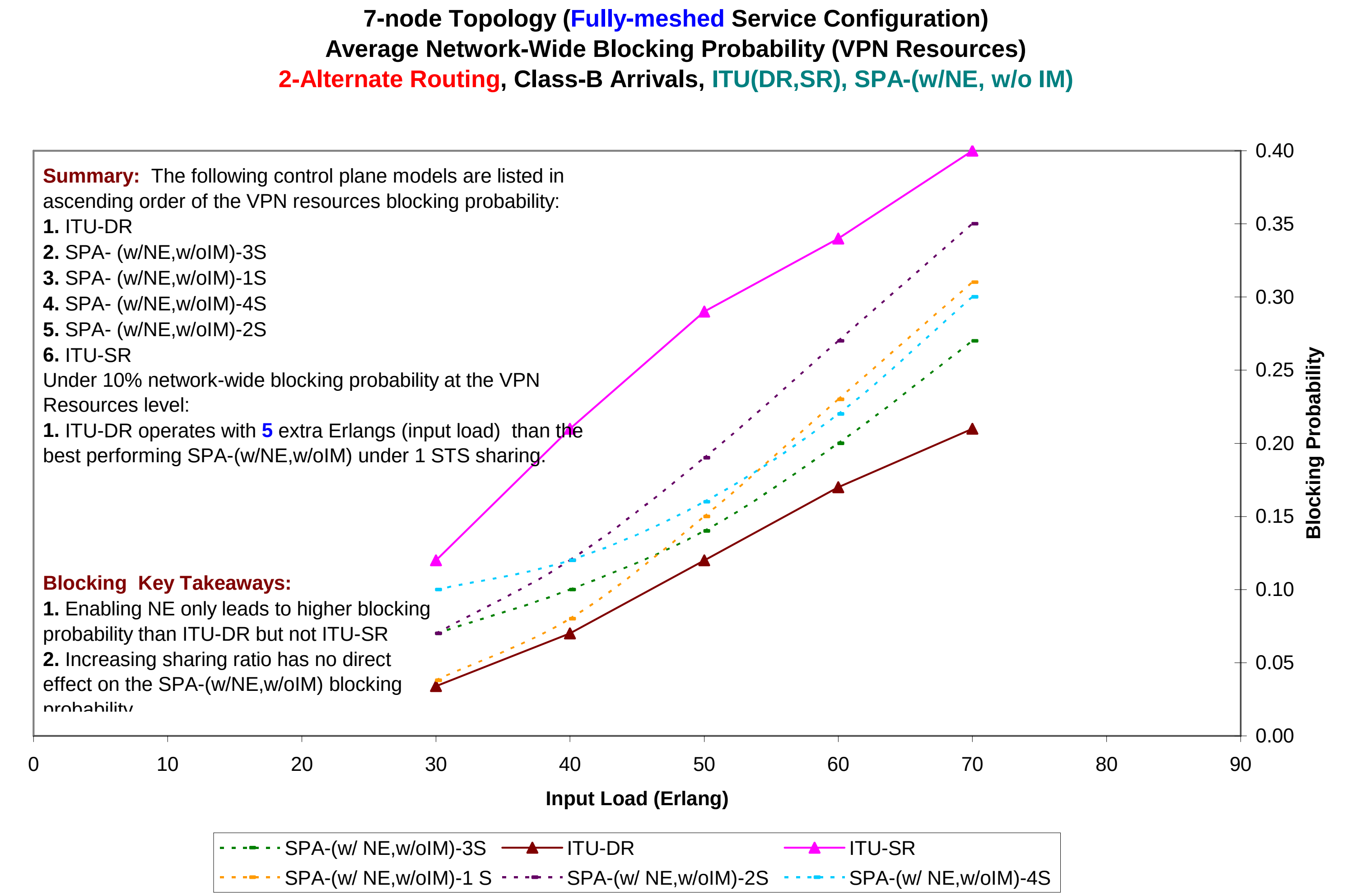

7-node Topology (Fully-meshed Service Configuration)
Average Network-Wide Blocking Probability (VPN Resources)
2-Alternate Routing, Class-B Arrivals, ITU(DR,SR), SPA-(w/NE, w/o IM)

Summary: The following control plane models are listed in ascending order of the VPN resources blocking probability:

1. ITU-DR
2. SPA- (w/NE,w/oIM)-3S
3. SPA- (w/NE,w/oIM)-1S
4. SPA- (w/NE,w/oIM)-4S
5. SPA- (w/NE,w/oIM)-2S
6. ITU-SR

Under 10% network-wide blocking probability at the VPN Resources level:
1. ITU-DR operates with **5** extra Erlangs (input load) than the best performing SPA-(w/NE,w/oIM) under 1 STS sharing.

Blocking Key Takeaways:
1. Enabling NE only leads to higher blocking probability than ITU-DR but not ITU-SR
2. Increasing sharing ratio has no direct effect on the SPA-(w/NE,w/oIM) blocking probability

Figure 20-11: Average Network-Wide Blocking Probability (VPN Resources)-7 Node – 2 Alternate Route-ITU(DR,SR), SPA-w/NE,w/oIM

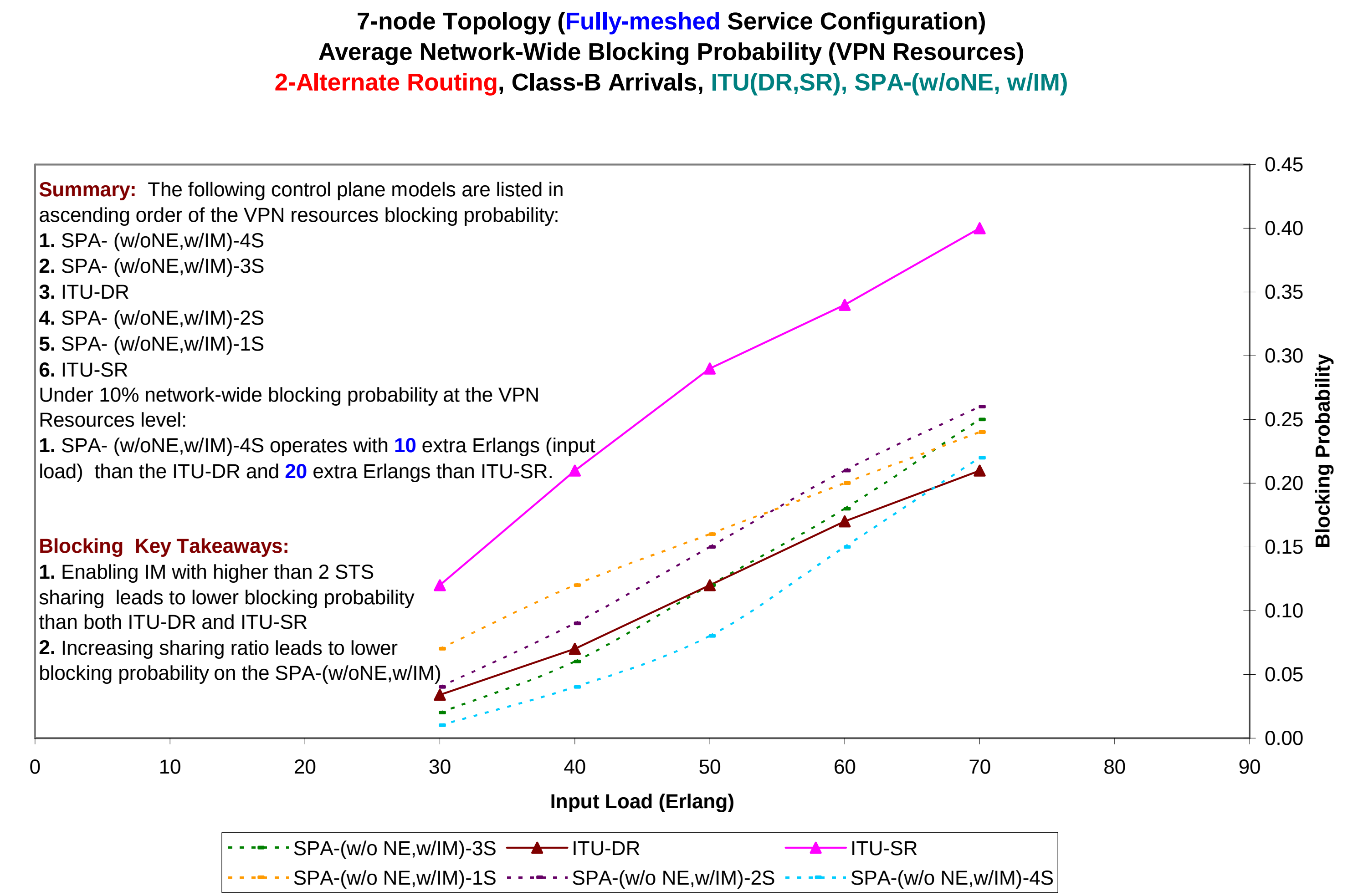
7-node Topology (Fully-meshed Service Configuration)
Average Network-Wide Blocking Probability (VPN Resources)
2-Alternate Routing, Class-B Arrivals, ITU(DR,SR), SPA-(w/oNE, w/IM)

Summary: The following control plane models are listed in ascending order of the VPN resources blocking probability:

1. SPA- (w/oNE,w/IM)-4S
2. SPA- (w/oNE,w/IM)-3S
3. ITU-DR
4. SPA- (w/oNE,w/IM)-2S
5. SPA- (w/oNE,w/IM)-1S
6. ITU-SR

Under 10% network-wide blocking probability at the VPN Resources level:

1. SPA- (w/oNE,w/IM)-4S operates with **10** extra Erlangs (input load) than the ITU-DR and **20** extra Erlangs than ITU-SR.

Blocking Key Takeaways:

1. Enabling IM with higher than 2 STS sharing leads to lower blocking probability than both ITU-DR and ITU-SR

2. Increasing sharing ratio leads to lower blocking probability on the SPA-(w/oNE,w/IM)

Figure 20-12: Average Network-Wide Blocking Probability (VPN Resources)-7 Node – 2 Alternate Route-ITU(DR,SR), SPA-w/oNE,w/IM

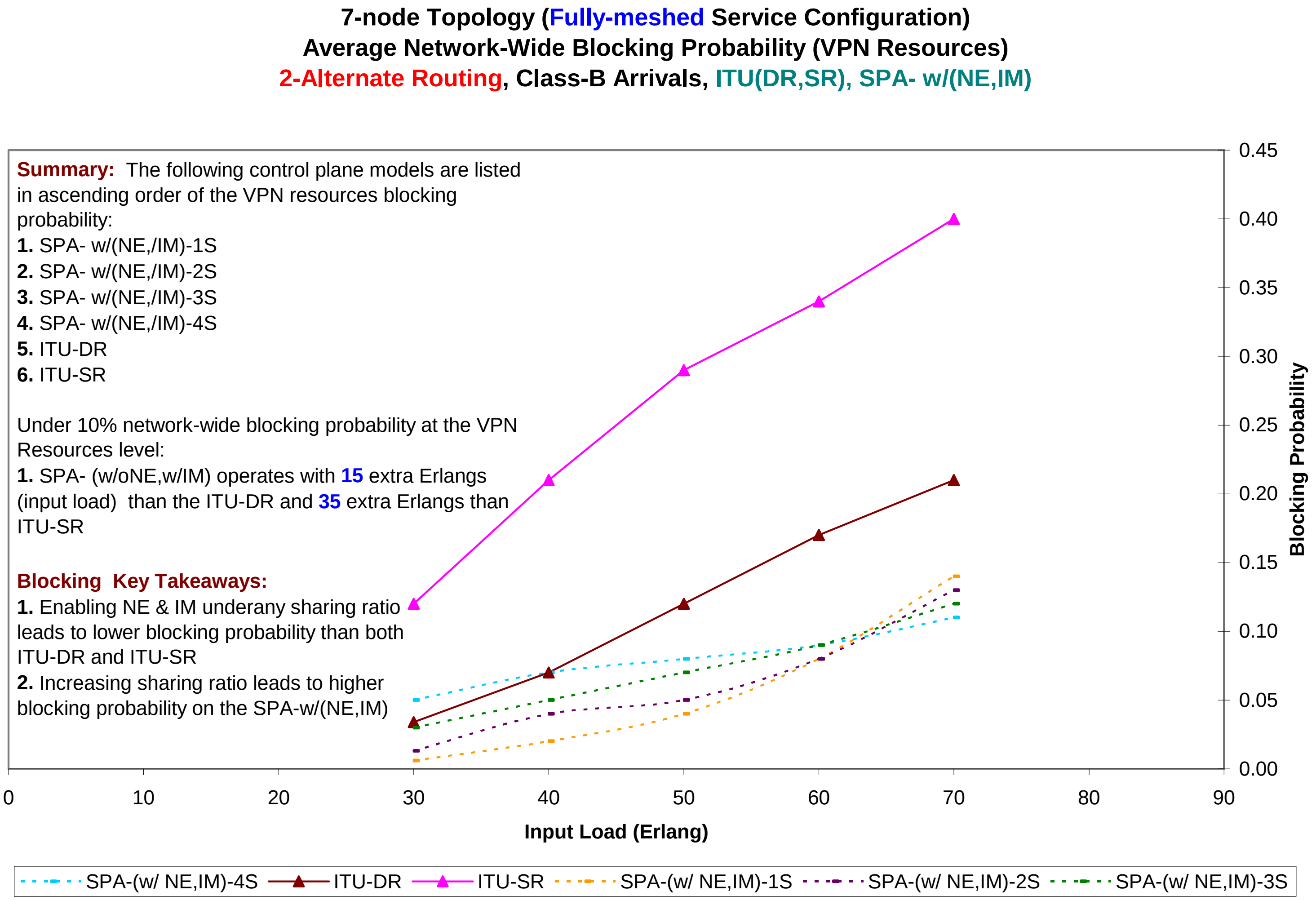

Summary: The following control plane models are listed in ascending order of the VPN resources blocking probability:

1. SPA- w/(NE,/IM)-1S
2. SPA- w/(NE,/IM)-2S
3. SPA- w/(NE,/IM)-3S
4. SPA- w/(NE,/IM)-4S
5. ITU-DR
6. ITU-SR

Under 10% network-wide blocking probability at the VPN Resources level:
1. SPA- (w/oNE,w/IM) operates with **15** extra Erlangs (input load) than the ITU-DR and **35** extra Erlangs than ITU-SR

Blocking Key Takeaways:
1. Enabling NE & IM underany sharing ratio leads to lower blocking probability than both ITU-DR and ITU-SR
2. Increasing sharing ratio leads to higher blocking probability on the SPA-w/(NE,IM)

Figure 20-13: Average Network-Wide Blocking Probability (VPN Resources)-7 Node – 2 Alternate Route-ITU(DR,SR), SPA-w/(NE,IM)

20.2 Permissible load

20.2.1 Dedicated resources

This section provides detailed performance analysis of the network-wide permissible load on the dedicated network resources partition for the 7-node topology with two-alternate routing. The configured VPN service evaluated is the Fully-meshed Shared Granular (FSF) with the following service profile layer parameters:

a. Service flow connectivity: configured as “fully-meshed”.

b. Service demand granularity: configured as “granular” with 1 STS-1 granularity level.

c. Load partitioning flexibility: configured as “enabled”.

One input class was evaluated with the following parameters: $k = 2$, $b_k^A = 2$ STS-1, $\mu_k = 1$unit time, $\lambda_{rk} = 4$ calls/unit time. Range of input load for 4-node topology is 30 to 70 Erlangs. The five traffic management schemes of the SPA control plane model are evaluated as provided in Table 9-1. Four sharing levels are considered as follows:

a. STS-1 sharing: C_j^{vD}=11 STS-1, C_j^S=2 STS-1

b. STS-2 sharing: C_j^{vD}=10 STS-1, C_j^S=4 STS-1

c. STS-3 sharing: C_j^{vD}=9 STS-1, C_j^S=6 STS-1

d. STS-4 sharing: C_j^{vD}=8 STS-1, C_j^S=8 STS-1

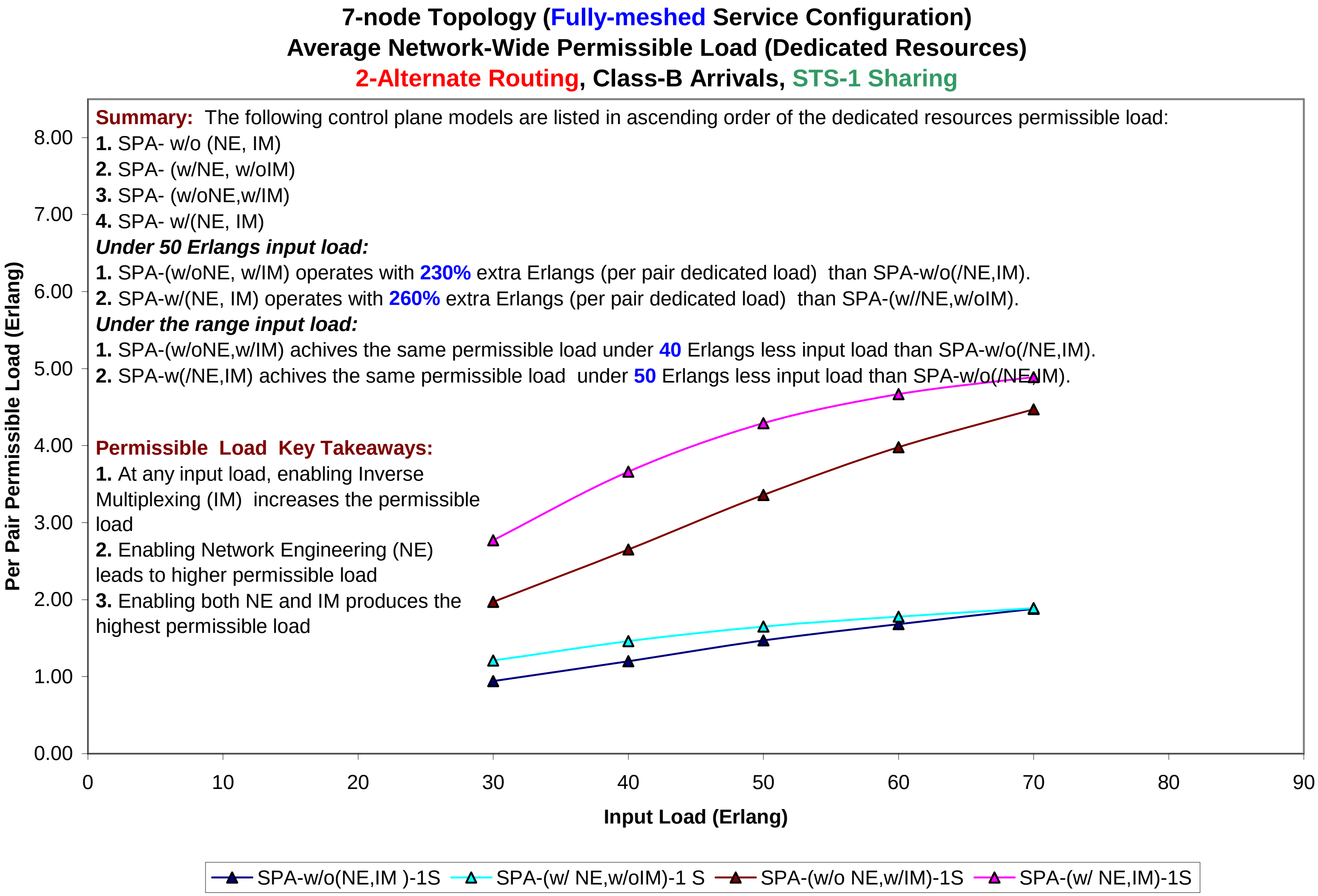

7-node Topology (Fully-meshed Service Configuration)
Average Network-Wide Permissible Load (Dedicated Resources)
2-Alternate Routing, Class-B Arrivals, STS-1 Sharing

Summary: The following control plane models are listed in ascending order of the dedicated resources permissible load:

1. SPA- w/o (NE, IM)
2. SPA- (w/NE, w/oIM)
3. SPA- (w/oNE,w/IM)
4. SPA- w/(NE, IM)

Under 50 Erlangs input load:

1. SPA-(w/oNE, w/IM) operates with **230%** extra Erlangs (per pair dedicated load) than SPA-w/o(/NE,IM).
2. SPA-w/(NE, IM) operates with **260%** extra Erlangs (per pair dedicated load) than SPA-(w//NE,w/oIM).

Under the range input load:

1. SPA-(w/oNE,w/IM) achives the same permissible load under **40** Erlangs less input load than SPA-w/o(/NE,IM).
2. SPA-w(/NE,IM) achives the same permissible load under **50** Erlangs less input load than SPA-w/o(/NE,IM).

Permissible Load Key Takeaways:

1. At any input load, enabling Inverse Multiplexing (IM) increases the permissible load
2. Enabling Network Engineering (NE) leads to higher permissible load
3. Enabling both NE and IM produces the highest permissible load

Figure 20-14: Average Network-Wide Permissible Load (Dedicated Resources)-7 Node – 2 Alternate Route-STS-1 Sharing

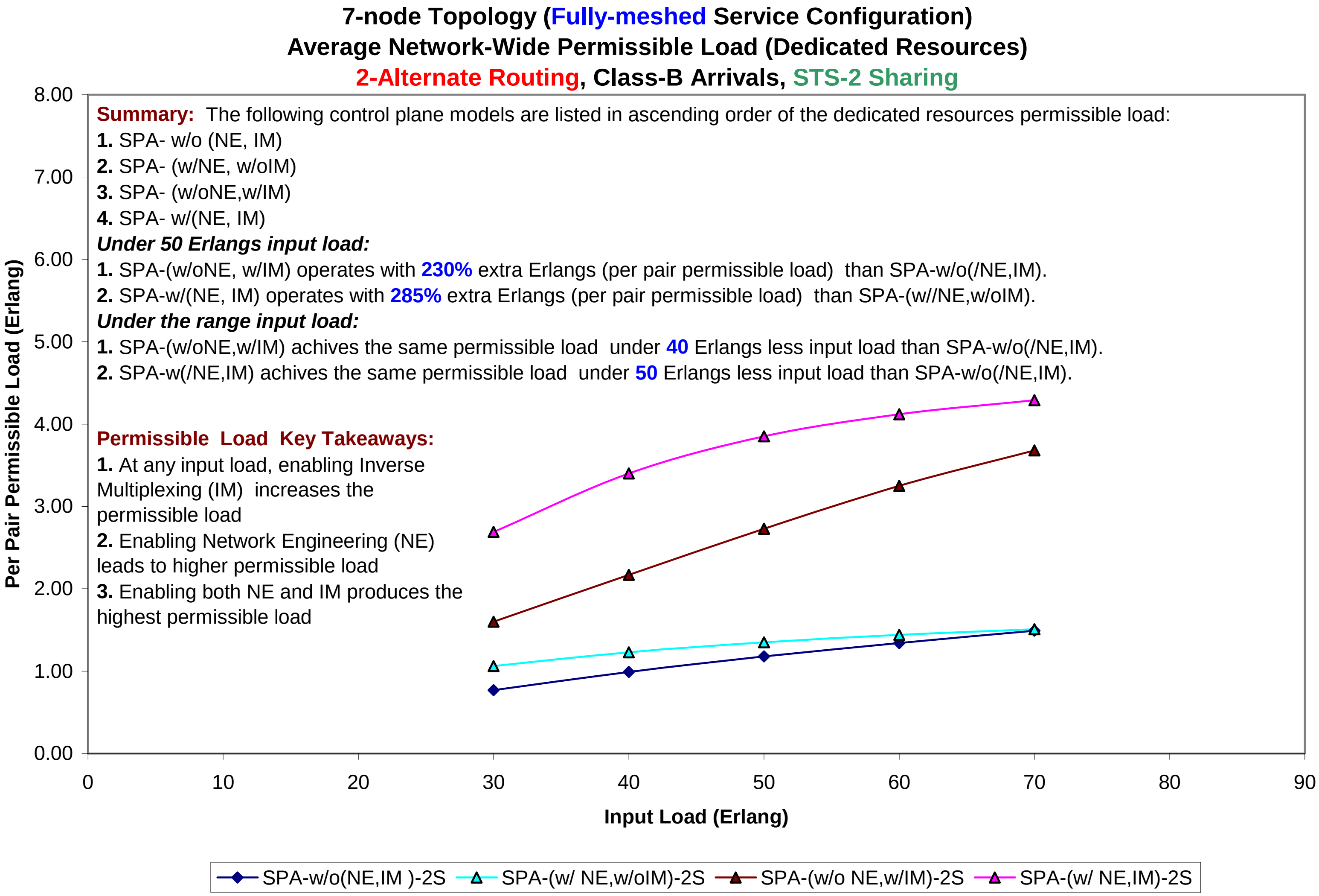

Summary: The following control plane models are listed in ascending order of the dedicated resources permissible load:

1. SPA- w/o (NE, IM)
2. SPA- (w/NE, w/oIM)
3. SPA- (w/oNE,w/IM)
4. SPA- w/(NE, IM)

Under 50 Erlangs input load:

1. SPA-(w/oNE, w/IM) operates with **230%** extra Erlangs (per pair permissible load) than SPA-w/o(/NE,IM).
2. SPA-w/(NE, IM) operates with **285%** extra Erlangs (per pair permissible load) than SPA-(w//NE,w/oIM).

Under the range input load:

1. SPA-(w/oNE,w/IM) achives the same permissible load under **40** Erlangs less input load than SPA-w/o(/NE,IM).
2. SPA-w(/NE,IM) achives the same permissible load under **50** Erlangs less input load than SPA-w/o(/NE,IM).

Permissible Load Key Takeaways:

1. At any input load, enabling Inverse Multiplexing (IM) increases the permissible load
2. Enabling Network Engineering (NE) leads to higher permissible load
3. Enabling both NE and IM produces the highest permissible load

Figure 20-15: Average Network-Wide Permissible Load (Dedicated Resources)-7 Node – 2 Alternate Route-STS-2 Sharing

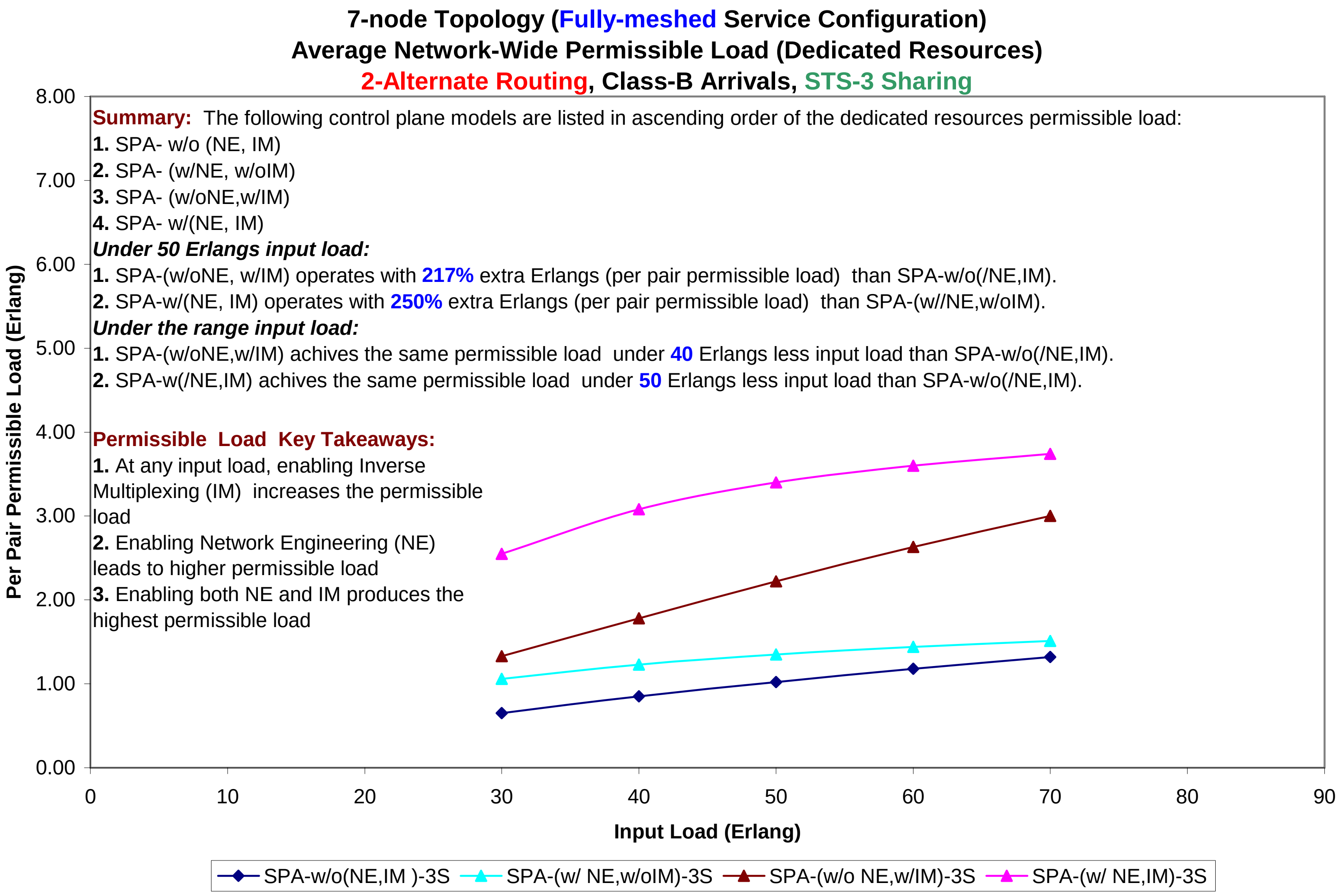

Summary: The following control plane models are listed in ascending order of the dedicated resources permissible load:

1. SPA- w/o (NE, IM)

2. SPA- (w/NE, w/oIM)

3. SPA- (w/oNE,w/IM)

4. SPA- w/(NE, IM)

Under 50 Erlangs input load:

1. SPA-(w/oNE, w/IM) operates with **217%** extra Erlangs (per pair permissible load) than SPA-w/o(/NE,IM).

2. SPA-w/(NE, IM) operates with **250%** extra Erlangs (per pair permissible load) than SPA-(w//NE,w/oIM).

Under the range input load:

1. SPA-(w/oNE,w/IM) achives the same permissible load under **40** Erlangs less input load than SPA-w/o(/NE,IM).

2. SPA-w(/NE,IM) achives the same permissible load under **50** Erlangs less input load than SPA-w/o(/NE,IM).

Permissible Load Key Takeaways:

1. At any input load, enabling Inverse Multiplexing (IM) increases the permissible load

2. Enabling Network Engineering (NE) leads to higher permissible load

3. Enabling both NE and IM produces the highest permissible load

Figure 20-16: Average Network-Wide Permissible Load (Dedicated Resources)-7 Node – 2 Alternate Route-STS-3 Sharing

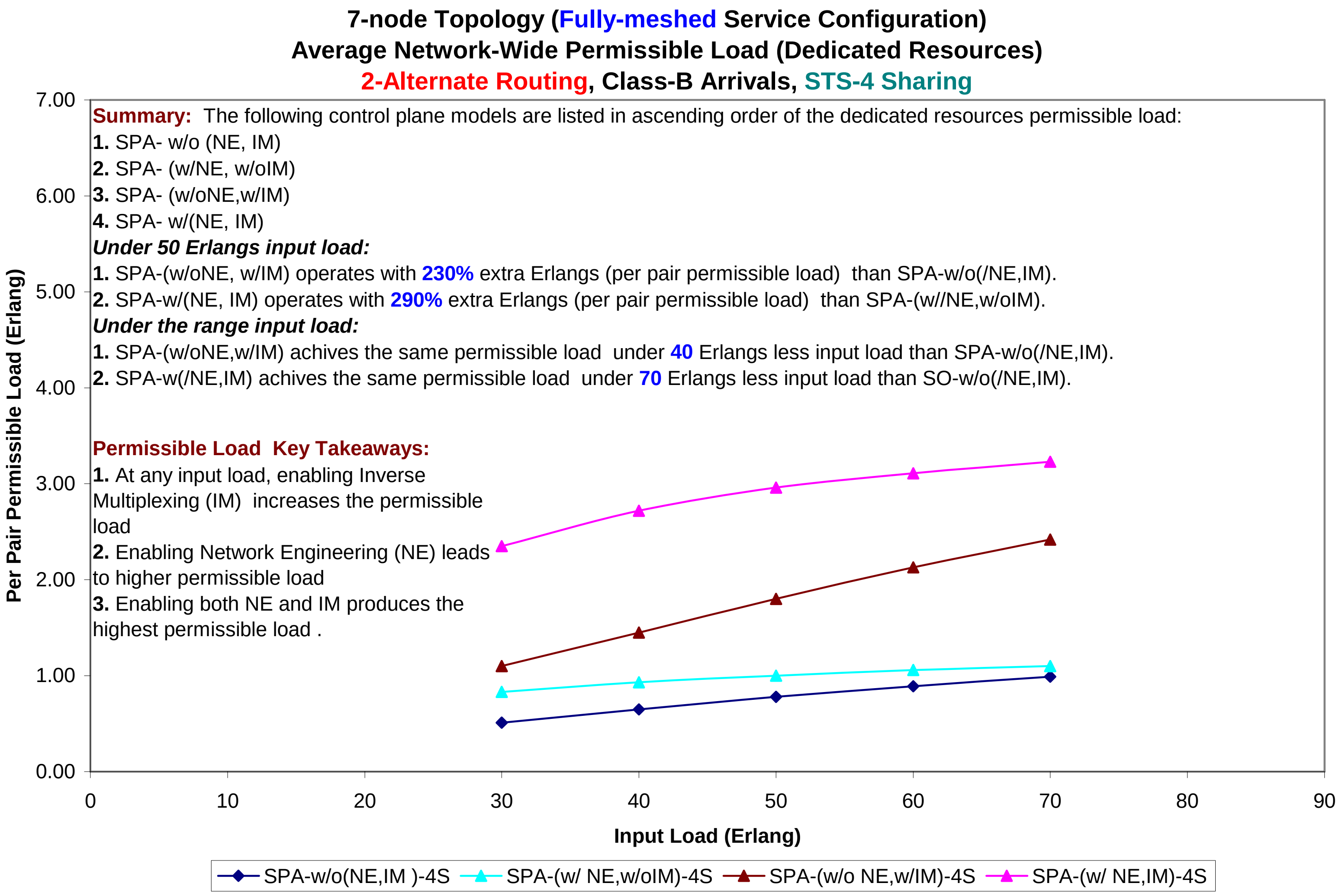

7-node Topology (Fully-meshed Service Configuration)
Average Network-Wide Permissible Load (Dedicated Resources)
2-Alternate Routing, Class-B Arrivals, STS-4 Sharing

Summary: The following control plane models are listed in ascending order of the dedicated resources permissible load:
1. SPA- w/o (NE, IM)
2. SPA- (w/NE, w/oIM)
3. SPA- (w/oNE,w/IM)
4. SPA- w/(NE, IM)

Under 50 Erlangs input load:
1. SPA-(w/oNE, w/IM) operates with **230%** extra Erlangs (per pair permissible load) than SPA-w/o(/NE,IM).
2. SPA-w/(NE, IM) operates with **290%** extra Erlangs (per pair permissible load) than SPA-(w//NE,w/oIM).

Under the range input load:
1. SPA-(w/oNE,w/IM) achives the same permissible load under **40** Erlangs less input load than SPA-w/o(/NE,IM).
2. SPA-w(/NE,IM) achives the same permissible load under **70** Erlangs less input load than SO-w/o(/NE,IM).

Permissible Load Key Takeaways:
1. At any input load, enabling Inverse Multiplexing (IM) increases the permissible load
2. Enabling Network Engineering (NE) leads to higher permissible load
3. Enabling both NE and IM produces the highest permissible load .

Figure 20-17: Average Network-Wide Permissible Load (Dedicated Resources)-7 Node – 2 Alternate Route-STS-4 Sharing

20.2.2 Shared resources

This section provides detailed performance analysis of the network-wide permissible load on the shared network resources partition for the 7-node topology with two-alternate routing. The configured VPN service evaluated is the Fully-meshed Shared Granular (FSF) with the following service profile layer parameters:

a. Service flow connectivity: configured as “fully-meshed”.

b. Service demand granularity: configured as “granular” with 1 STS-1 granularity level.

c. Load partitioning flexibility: configured as “enabled”.

One input class was evaluated with the following parameters: $k = 2$, $b_k^A = 2$ STS-1, $\mu_k = 1$unit time, $\lambda_{rk} = 4$ calls/unit time. Range of input load for 4-node topology is 30 to 70 Erlangs. The five traffic management schemes of the SPA control plane model are evaluated as provided in Table 9-1. Four sharing levels are considered as follows:

a. STS-1 sharing: C_j^{vD} =11 STS-1, C_j^S =2 STS-1

b. STS-2 sharing: C_j^{vD} =10 STS-1, C_j^S =4 STS-1

c. STS-3 sharing: C_j^{vD} =9 STS-1, C_j^S =6 STS-1

d. STS-4 sharing: C_j^{vD} =8 STS-1, C_j^S =8 STS-1

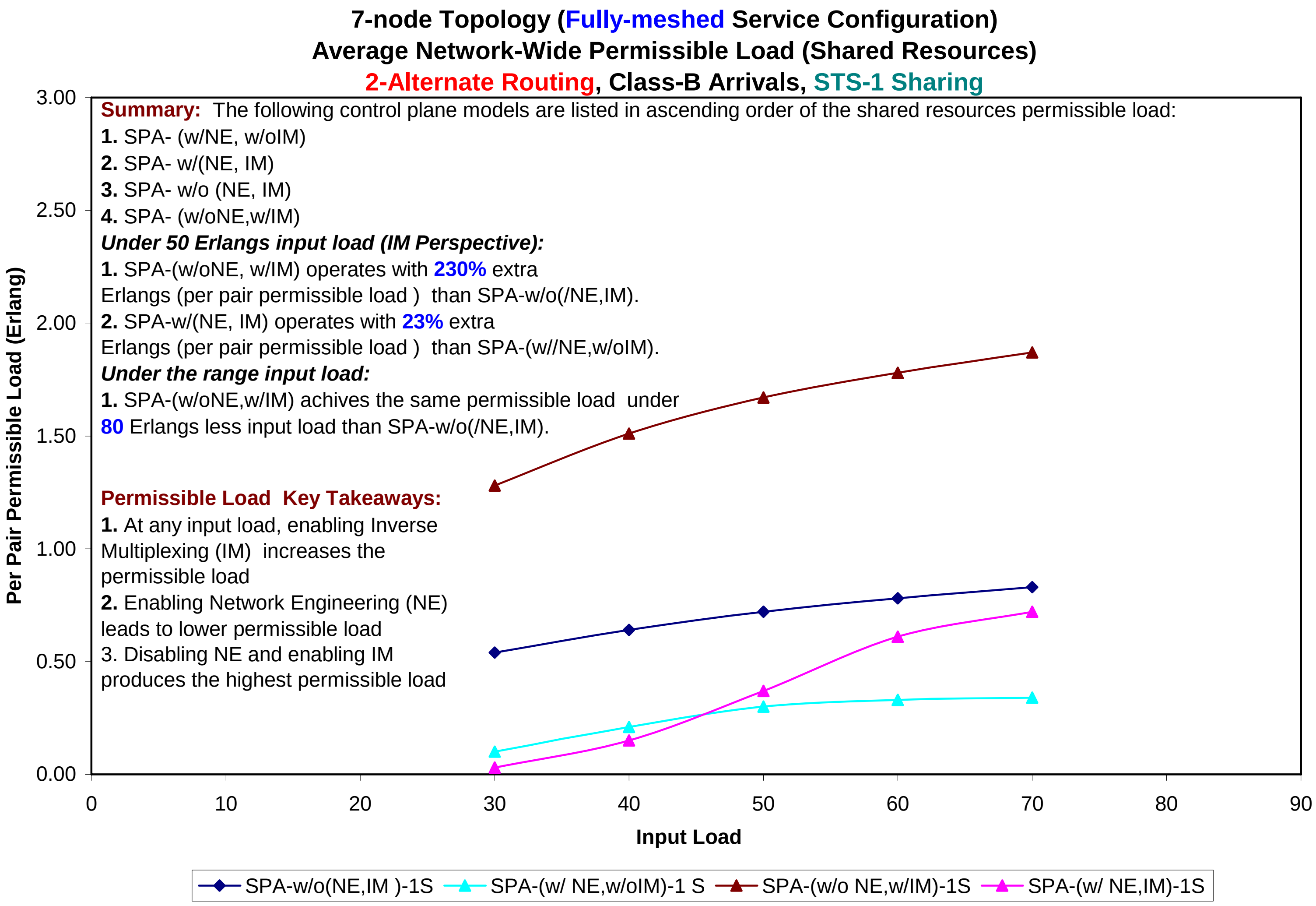

7-node Topology (Fully-meshed Service Configuration)
Average Network-Wide Permissible Load (Shared Resources)
2-Alternate Routing, Class-B Arrivals, STS-1 Sharing

Summary: The following control plane models are listed in ascending order of the shared resources permissible load:

1. SPA- (w/NE, w/oIM)
2. SPA- w/(NE, IM)
3. SPA- w/o (NE, IM)
4. SPA- (w/oNE,w/IM)

Under 50 Erlangs input load (IM Perspective):

1. SPA-(w/oNE, w/IM) operates with **230%** extra Erlangs (per pair permissible load) than SPA-w/o(/NE,IM).

2. SPA-w/(NE, IM) operates with **23%** extra Erlangs (per pair permissible load) than SPA-(w//NE,w/oIM).

Under the range input load:

1. SPA-(w/oNE,w/IM) achives the same permissible load under **80** Erlangs less input load than SPA-w/o(/NE,IM).

Permissible Load Key Takeaways:

1. At any input load, enabling Inverse Multiplexing (IM) increases the permissible load

2. Enabling Network Engineering (NE) leads to lower permissible load

3. Disabling NE and enabling IM produces the highest permissible load

Figure 20-18: Average Network-Wide Permissible Load (Shared Resources)-7 Node – 2 Alternate Route-STS-1 Sharing

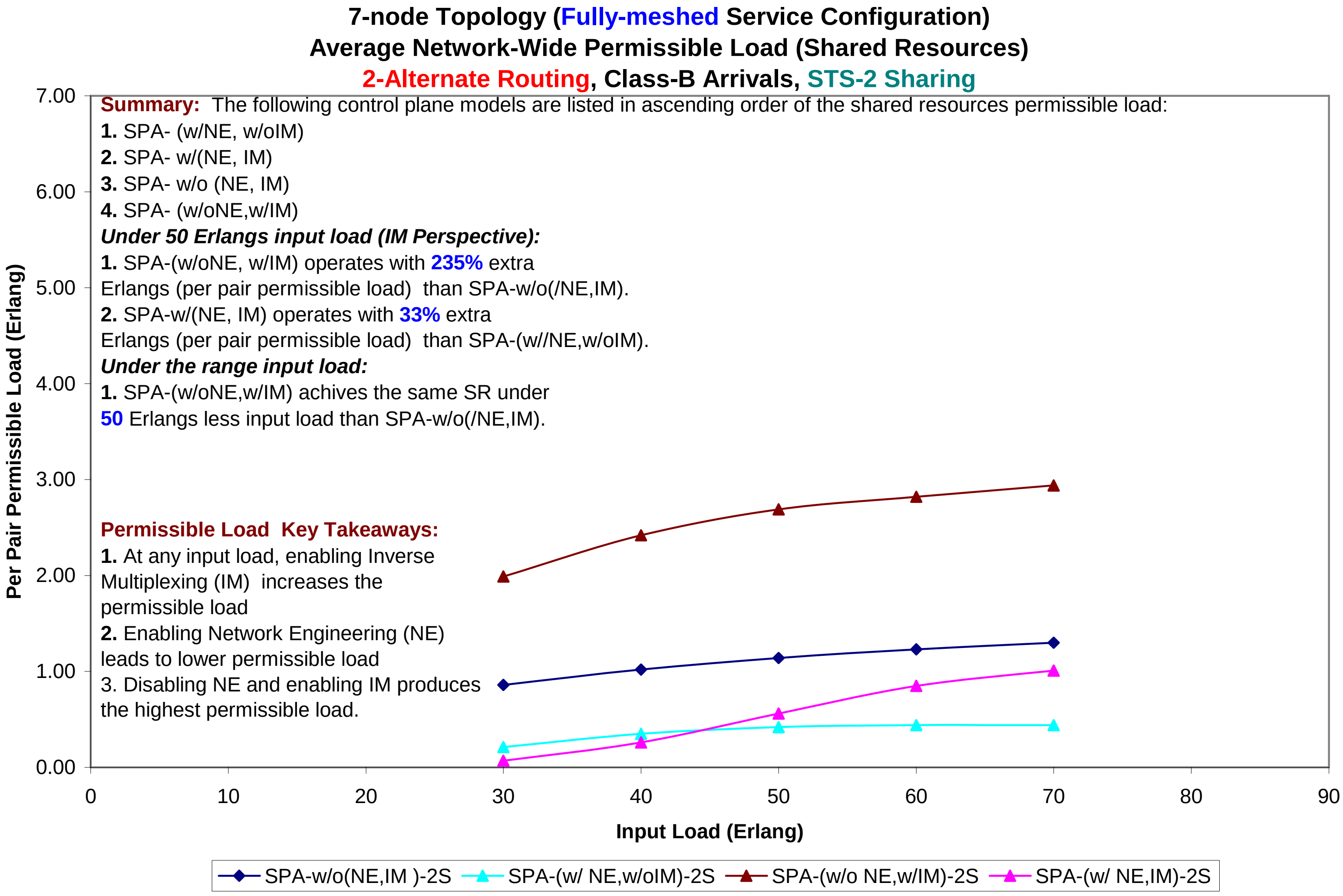

Summary: The following control plane models are listed in ascending order of the shared resources permissible load:

1. SPA- (w/NE, w/oIM)

2. SPA- w/(NE, IM)

3. SPA- w/o (NE, IM)

4. SPA- (w/oNE,w/IM)

Under 50 Erlangs input load (IM Perspective):

1. SPA-(w/oNE, w/IM) operates with **235%** extra Erlangs (per pair permissible load) than SPA-w/o(/NE,IM).

2. SPA-w/(NE, IM) operates with **33%** extra Erlangs (per pair permissible load) than SPA-(w//NE,w/oIM).

Under the range input load:

1. SPA-(w/oNE,w/IM) achives the same SR under **50** Erlangs less input load than SPA-w/o(/NE,IM).

Permissible Load Key Takeaways:

1. At any input load, enabling Inverse Multiplexing (IM) increases the permissible load

2. Enabling Network Engineering (NE) leads to lower permissible load

3. Disabling NE and enabling IM produces the highest permissible load.

Figure 20-19: Average Network-Wide Permissible Load (Shared Resources)-7 Node – 2 Alternate Route-STS-2 Sharing

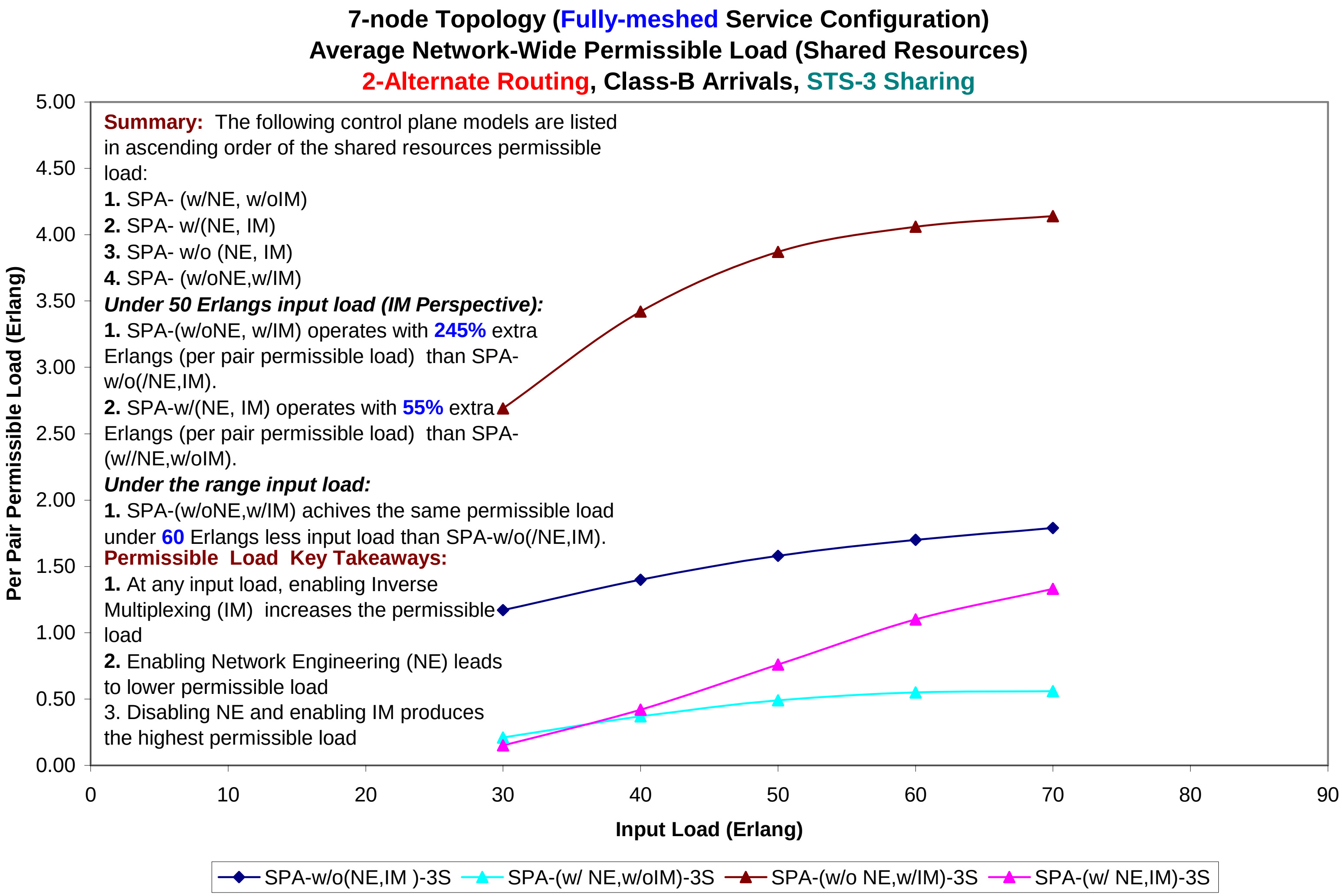

Figure 20-20: Average Network-Wide Permissible Load (Shared Resources)-7 Node – 2 Alternate Route-STS-3 Sharing

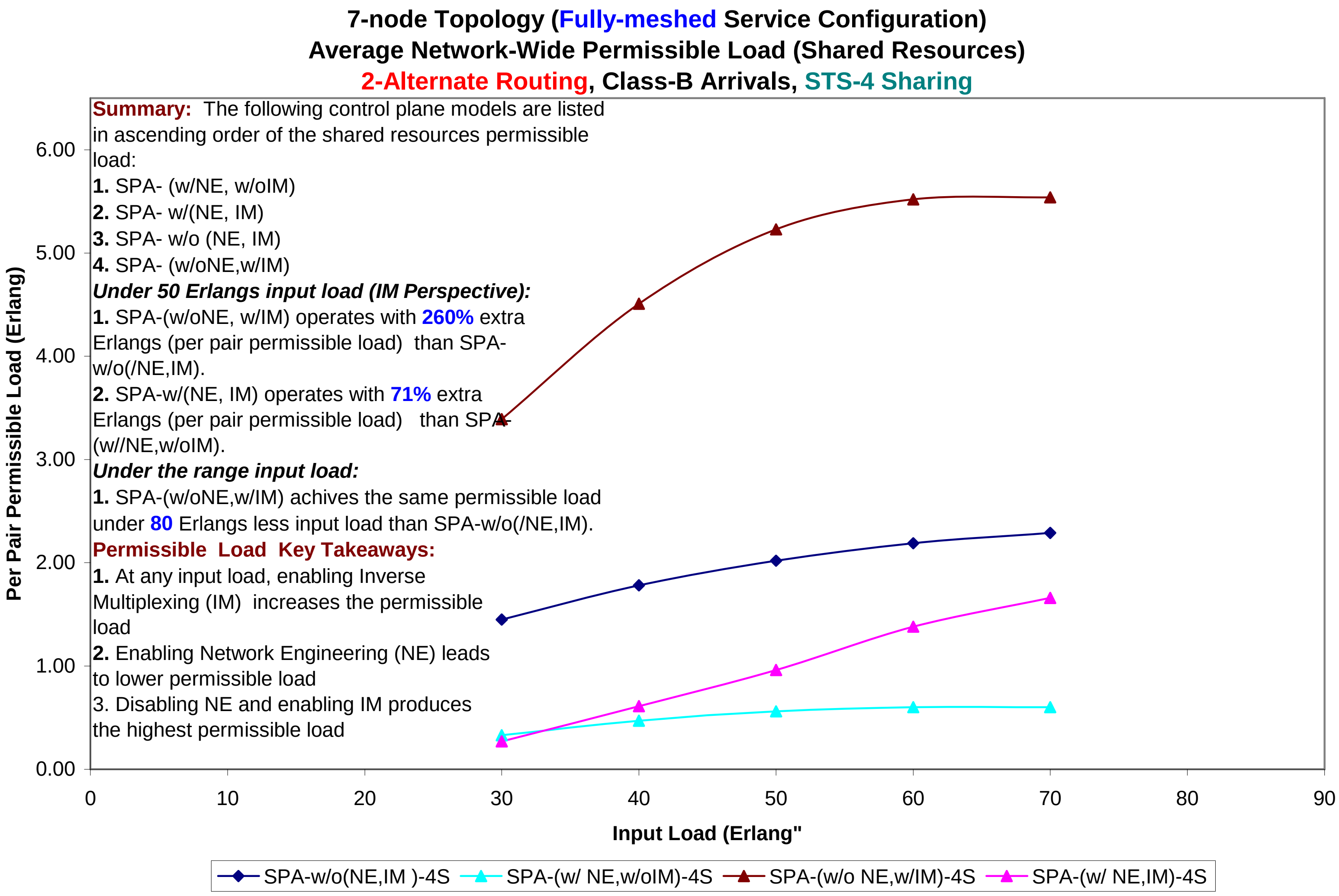

7-node Topology (Fully-meshed Service Configuration)
Average Network-Wide Permissible Load (Shared Resources)
2-Alternate Routing, Class-B Arrivals, STS-4 Sharing

Summary: The following control plane models are listed in ascending order of the shared resources permissible load:

1. SPA- (w/NE, w/oIM)
2. SPA- w/(NE, IM)
3. SPA- w/o (NE, IM)
4. SPA- (w/oNE,w/IM)

Under 50 Erlangs input load (IM Perspective):

1. SPA-(w/oNE, w/IM) operates with **260%** extra Erlangs (per pair permissible load) than SPA-w/o(/NE,IM).
2. SPA-w/(NE, IM) operates with **71%** extra Erlangs (per pair permissible load) than SPA-(w//NE,w/oIM).

Under the range input load:

1. SPA-(w/oNE,w/IM) achives the same permissible load under **80** Erlangs less input load than SPA-w/o(/NE,IM).

Permissible Load Key Takeaways:

1. At any input load, enabling Inverse Multiplexing (IM) increases the permissible load
2. Enabling Network Engineering (NE) leads to lower permissible load
3. Disabling NE and enabling IM produces the highest permissible load

Figure 20-21: Average Network-Wide Permissible Load (Shared Resources)-7 Node – 2 Alternate Route-STS-4 Sharing

20.2.3 VPN resources

This section provides detailed performance analysis of the network-wide permissible load on the VPN network resources partition for the 7-node topology with two-alternate routing. The configured VPN service evaluated is the Fully-meshed Shared Granular (FSF) with the following service profile layer parameters:

a. Service flow connectivity: configured as “fully-meshed”.

b. Service demand granularity: configured as “granular” with 1 STS-1 granularity level.

c. Load partitioning flexibility: configured as “enabled”.

One input class was evaluated with the following parameters: $k = 2$, $b_k^A = 2$ STS-1, $\mu_k = 1$unit time, $\lambda_{rk} = 4$ calls/unit time. Range of input load for 4-node topology is 30 to 70 Erlangs. The five traffic management schemes of the SPA control plane model are evaluated as provided in Table 9-1. Four sharing levels are considered as follows:

a. STS-1 sharing: C_j^{vD} =11 STS-1, C_j^S =2 STS-1

b. STS-2 sharing: C_j^{vD} =10 STS-1, C_j^S =4 STS-1

c. STS-3 sharing: C_j^{vD} =9 STS-1, C_j^S =6 STS-1

d. STS-4 sharing: C_j^{vD} =8 STS-1, C_j^S =8 STS-1

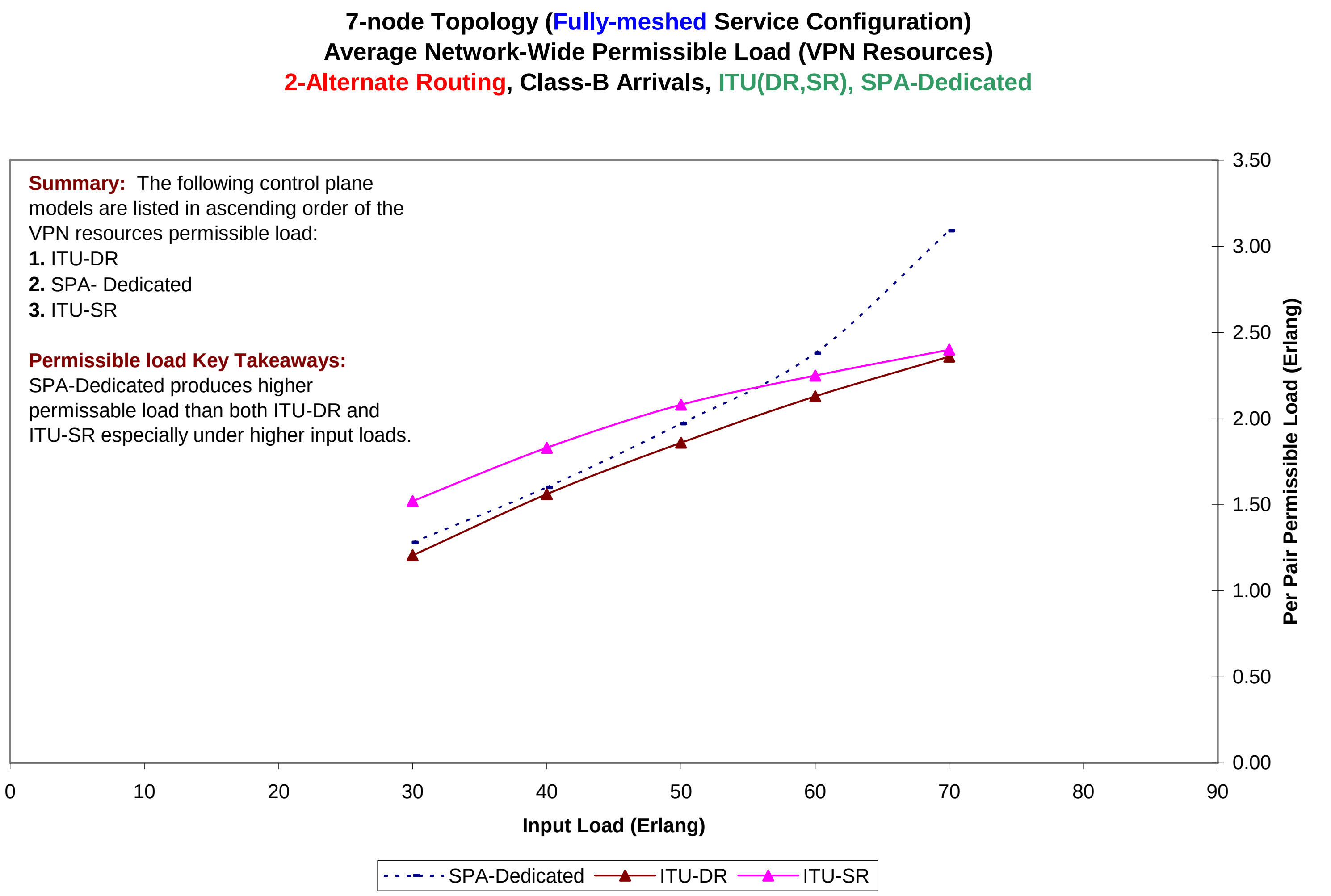

7-node Topology (Fully-meshed Service Configuration)
Average Network-Wide Permissible Load (VPN Resources)
2-Alternate Routing, Class-B Arrivals, ITU(DR,SR), SPA-Dedicated

Summary: The following control plane models are listed in ascending order of the VPN resources permissible load:
1. ITU-DR
2. SPA- Dedicated
3. ITU-SR

Permissible load Key Takeaways:
SPA-Dedicated produces higher permissable load than both ITU-DR and ITU-SR especially under higher input loads.

Figure 20-22: Average Network-Wide Permissible Load (VPN Resources)-7 Node – 2 Alternate Route-ITU(DR,SR), SPA-Dedicated

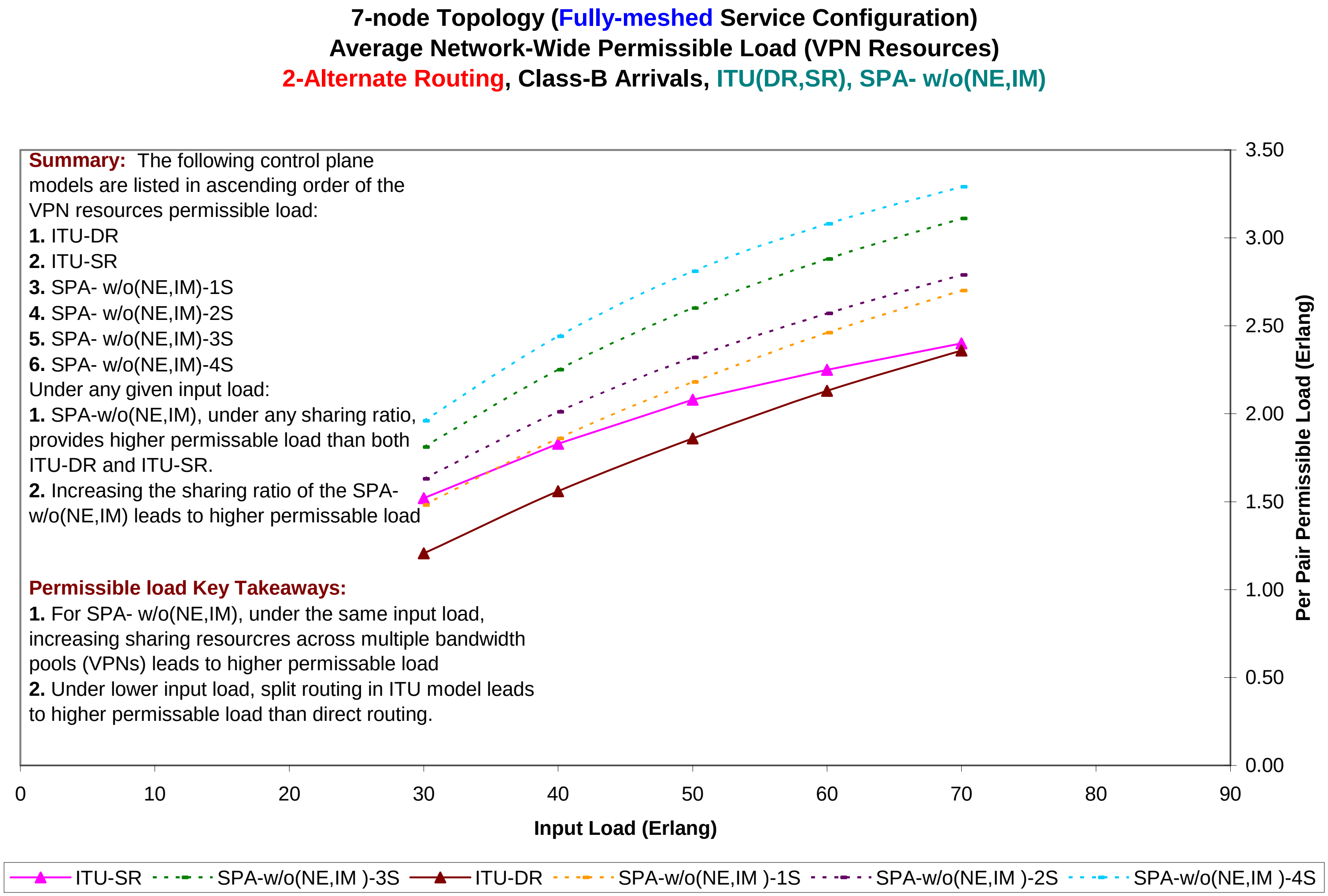

7-node Topology (Fully-meshed Service Configuration)
Average Network-Wide Permissible Load (VPN Resources)
2-Alternate Routing, Class-B Arrivals, ITU(DR,SR), SPA- w/o(NE,IM)

Summary: The following control plane models are listed in ascending order of the VPN resources permissible load:
1. ITU-DR
2. ITU-SR
3. SPA- w/o(NE,IM)-1S
4. SPA- w/o(NE,IM)-2S
5. SPA- w/o(NE,IM)-3S
6. SPA- w/o(NE,IM)-4S
Under any given input load:
1. SPA-w/o(NE,IM), under any sharing ratio, provides higher permissable load than both ITU-DR and ITU-SR.
2. Increasing the sharing ratio of the SPA-w/o(NE,IM) leads to higher permissable load

Permissible load Key Takeaways:
1. For SPA- w/o(NE,IM), under the same input load, increasing sharing resourcres across multiple bandwidth pools (VPNs) leads to higher permissable load
2. Under lower input load, split routing in ITU model leads to higher permissable load than direct routing.

Figure 20-23: Average Network-Wide Permissible Load (VPN Resources)-7 Node – 2 Alternate Route-ITU(DR,SR), SPA-w/o(NE,IM)

7-node Topology (Fully-meshed Service Configuration)
Average Network-Wide Permissible Load (VPN Resources)
2-Alternate Routing, Class-B Arrivals, ITU(DR,SR), SPA-(w/NE, w/o IM)

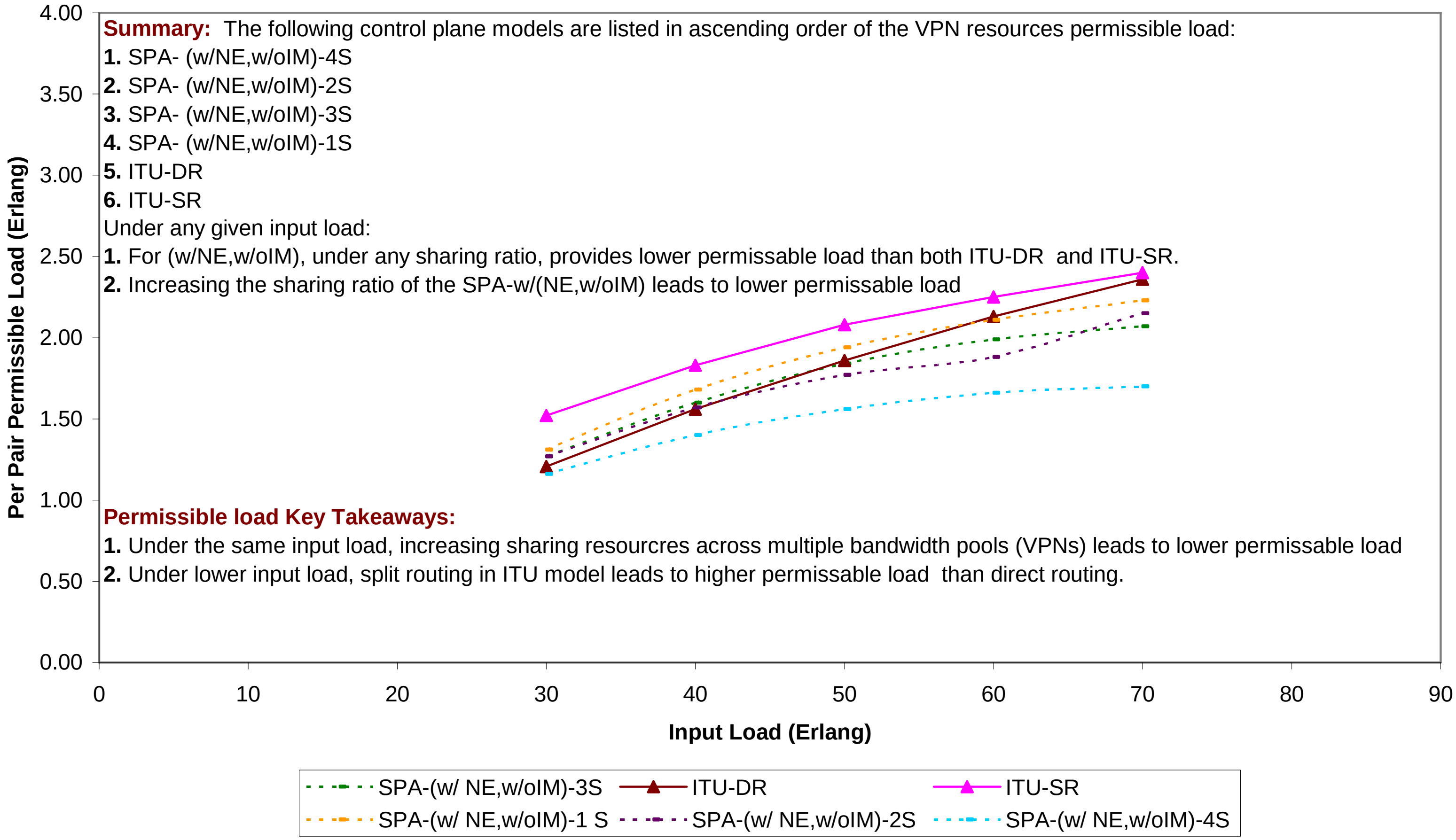

Summary: The following control plane models are listed in ascending order of the VPN resources permissible load:

1. SPA- (w/NE,w/oIM)-4S
2. SPA- (w/NE,w/oIM)-2S
3. SPA- (w/NE,w/oIM)-3S
4. SPA- (w/NE,w/oIM)-1S
5. ITU-DR
6. ITU-SR

Under any given input load:

1. For (w/NE,w/oIM), under any sharing ratio, provides lower permissable load than both ITU-DR and ITU-SR.
2. Increasing the sharing ratio of the SPA-w/(NE,w/oIM) leads to lower permissable load

Permissible load Key Takeaways:

1. Under the same input load, increasing sharing resourcres across multiple bandwidth pools (VPNs) leads to lower permissable load
2. Under lower input load, split routing in ITU model leads to higher permissable load than direct routing.

Figure 20-24: Average Network-Wide Permissible Load (VPN Resources)-7 Node – 2 Alternate Route-ITU(DR,SR), SPA-w/NE,w/oIM

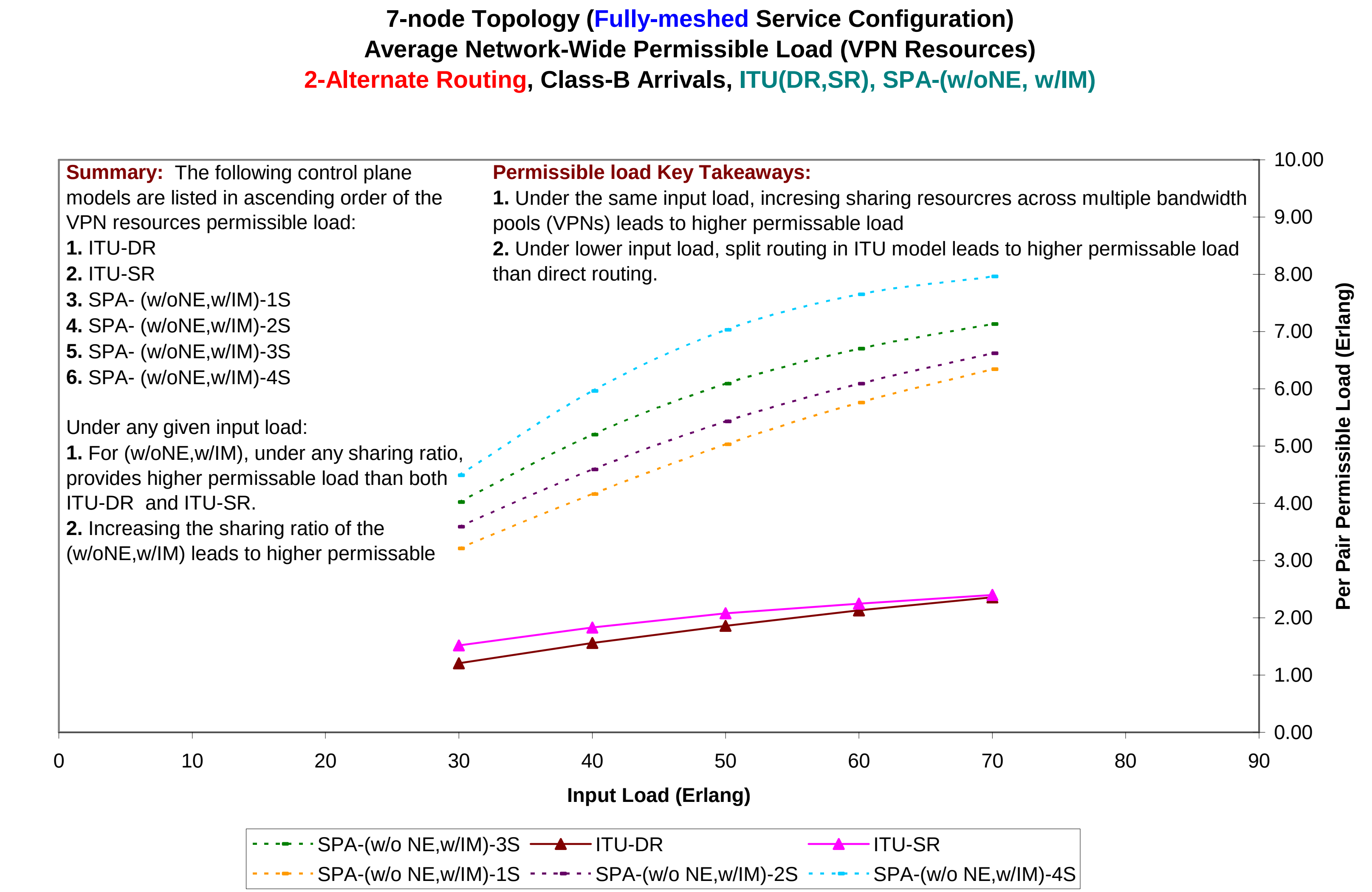

7-node Topology (Fully-meshed Service Configuration)
Average Network-Wide Permissible Load (VPN Resources)
2-Alternate Routing, Class-B Arrivals, ITU(DR,SR), SPA-(w/oNE, w/IM)

Summary: The following control plane models are listed in ascending order of the VPN resources permissible load:

1. ITU-DR
2. ITU-SR
3. SPA- (w/oNE,w/IM)-1S
4. SPA- (w/oNE,w/IM)-2S
5. SPA- (w/oNE,w/IM)-3S
6. SPA- (w/oNE,w/IM)-4S

Under any given input load:
1. For (w/oNE,w/IM), under any sharing ratio, provides higher permissable load than both ITU-DR and ITU-SR.
2. Increasing the sharing ratio of the (w/oNE,w/IM) leads to higher permissable

Permissible load Key Takeaways:
1. Under the same input load, incresing sharing resourcres across multiple bandwidth pools (VPNs) leads to higher permissable load
2. Under lower input load, split routing in ITU model leads to higher permissable load than direct routing.

Figure 20-25: Average Network-Wide Permissible Load (VPN Resources)-7 Node – 2 Alternate Route-ITU(DR,SR), SPA-w/oNE,w/IM

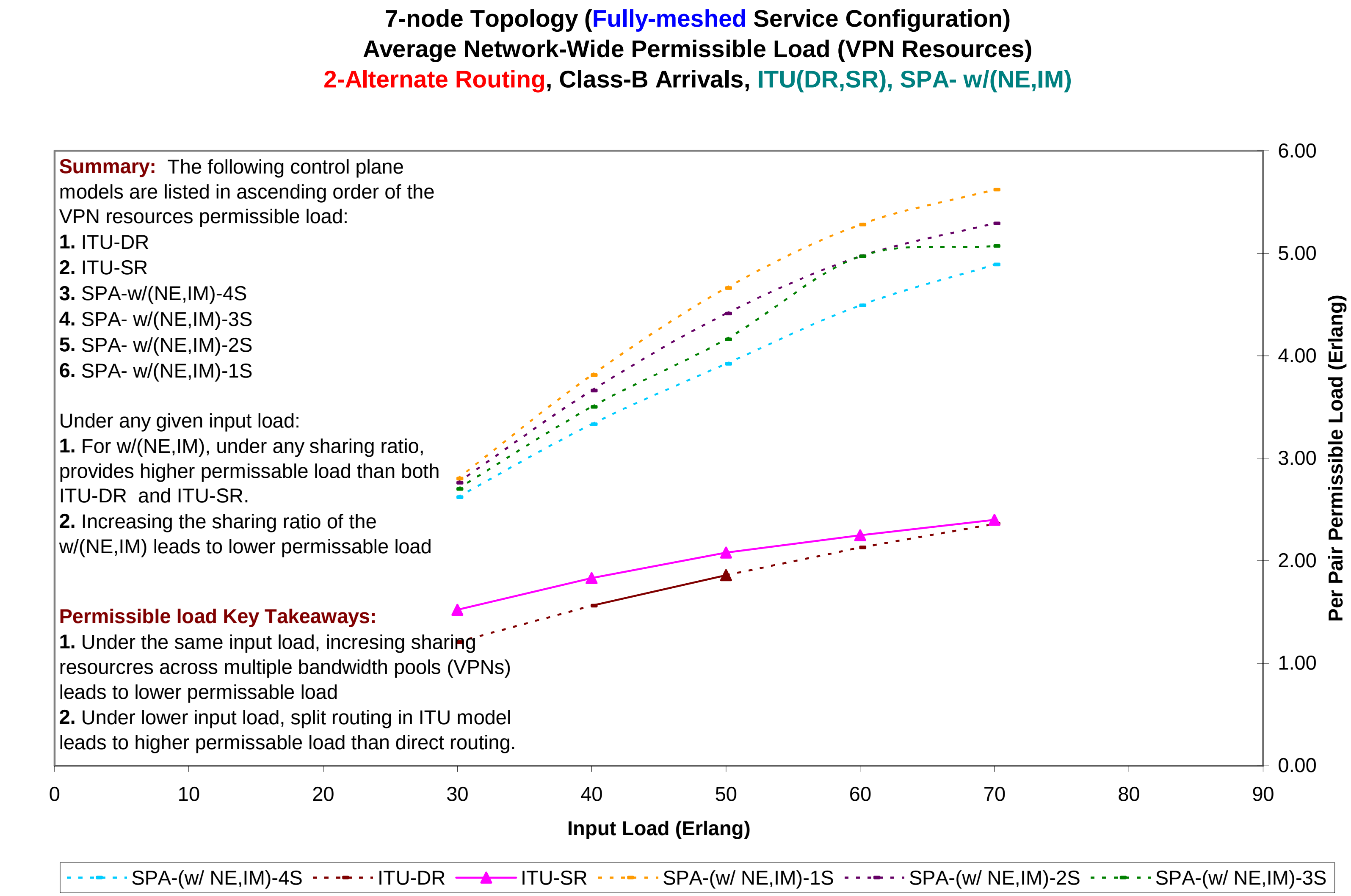

7-node Topology (Fully-meshed Service Configuration)
Average Network-Wide Permissible Load (VPN Resources)
2-Alternate Routing, Class-B Arrivals, ITU(DR,SR), SPA- w/(NE,IM)

Summary: The following control plane models are listed in ascending order of the VPN resources permissible load:

1. ITU-DR
2. ITU-SR
3. SPA-w/(NE,IM)-4S
4. SPA- w/(NE,IM)-3S
5. SPA- w/(NE,IM)-2S
6. SPA- w/(NE,IM)-1S

Under any given input load:
1. For w/(NE,IM), under any sharing ratio, provides higher permissable load than both ITU-DR and ITU-SR.
2. Increasing the sharing ratio of the w/(NE,IM) leads to lower permissable load

Permissible load Key Takeaways:
1. Under the same input load, incresing sharing resourcres across multiple bandwidth pools (VPNs) leads to lower permissable load
2. Under lower input load, split routing in ITU model leads to higher permissable load than direct routing.

Figure 20-26: Average Network-Wide Permissible Load (VPN Resources)-7 Node – 2 Alternate Route-ITU(DR,SR), SPA-w/(NE,IM)

21 Appendix-E: Detailed Modeling Results- 7-Node Topology with 3-Alternate Routing

21.1 Blocking probability

21.1.1 Dedicated resources

This section provides detailed performance analysis of the network-wide blocking probability on the dedicated network resources partition for the 7-node topology with three-alternate routing. The configured VPN service evaluated is the Fully-meshed Shared Granular (FSF) with the following service profile layer parameters:

a. Service flow connectivity: configured as "fully-meshed".

b. Service demand granularity: configured as "granular" with 1 STS-1 granularity level.

c. Load partitioning flexibility: configured as "enabled".

One input class was evaluated with the following parameters: $k = 2$, $b_k^A = 2$ STS-1, $\mu_k = 1$unit time, $\lambda_{rk} = 4$ calls/unit time. Range of input load for 4-node topology is 30 to 70 Erlangs. The five traffic management schemes of the SPA control plane model are evaluated as provided in Table 9-1. Four sharing levels are considered as follows:

a. STS-1 sharing: C_j^{vD}=11 STS-1, C_j^S=2 STS-1

b. STS-2 sharing: C_j^{vD}=10 STS-1, C_j^S=4 STS-1

c. STS-3 sharing: C_j^{vD}=9 STS-1, C_j^S=6 STS-1

d. STS-4 sharing: C_j^{vD}=8 STS-1, C_j^S=8 STS-1

7-node Topology (Fully-meshed Service Configuration)
Average Network-Wide Blocking Probability (Dedicated Resources)
3-Alternate Routing, Class-B Arrivals, STS-1 Sharing

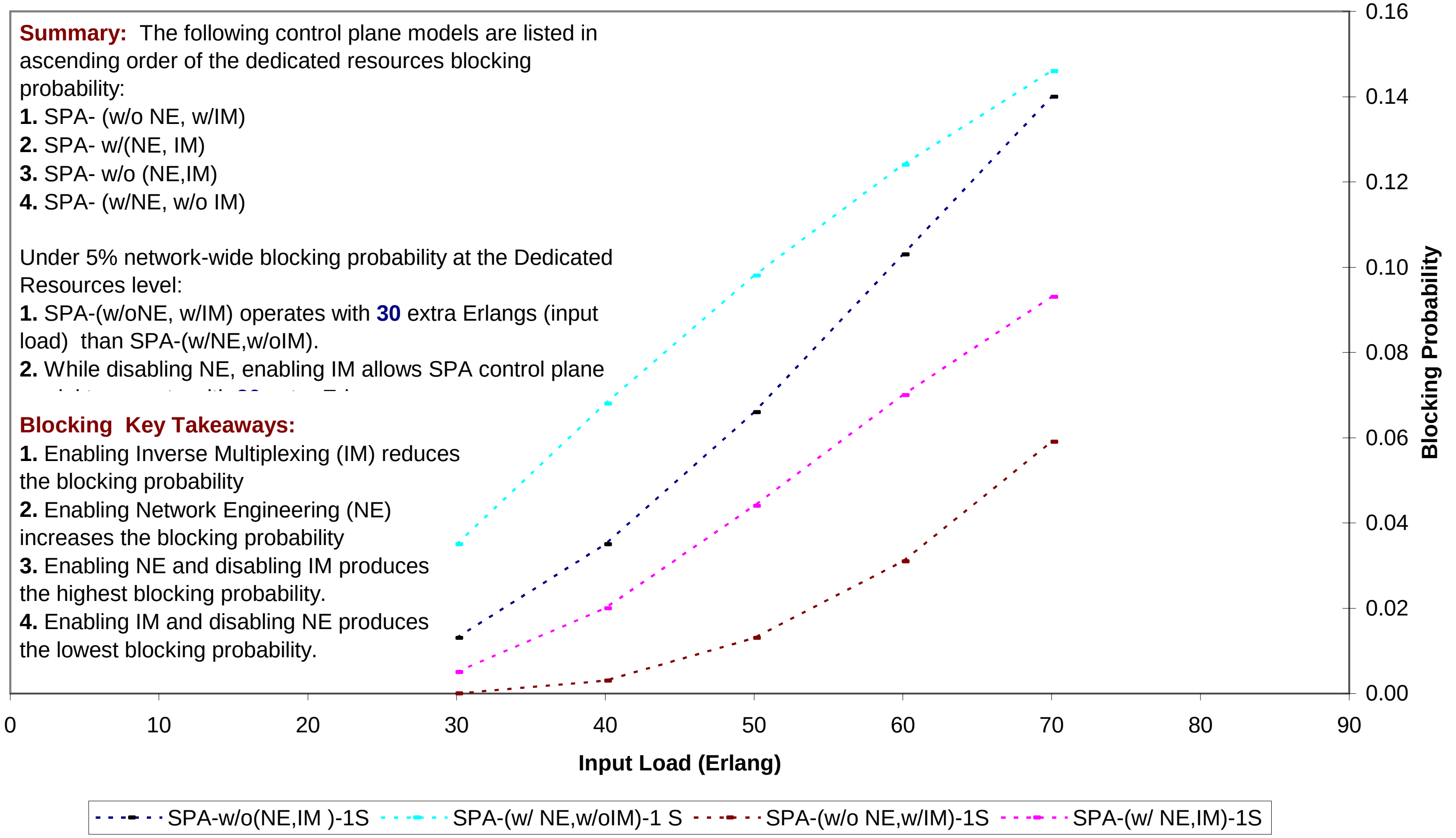

Summary: The following control plane models are listed in ascending order of the dedicated resources blocking probability:
1. SPA- (w/o NE, w/IM)
2. SPA- w/(NE, IM)
3. SPA- w/o (NE,IM)
4. SPA- (w/NE, w/o IM)

Under 5% network-wide blocking probability at the Dedicated Resources level:
1. SPA-(w/oNE, w/IM) operates with **30** extra Erlangs (input load) than SPA-(w/NE,w/oIM).
2. While disabling NE, enabling IM allows SPA control plane

Blocking Key Takeaways:
1. Enabling Inverse Multiplexing (IM) reduces the blocking probability
2. Enabling Network Engineering (NE) increases the blocking probability
3. Enabling NE and disabling IM produces the highest blocking probability.
4. Enabling IM and disabling NE produces the lowest blocking probability.

Figure 21-1: Average Network-Wide Blocking Probability (Dedicated Resources)-7 Node – 3 Alternate Route-STS-1 Sharing

7-node Topology (Fully-meshed Service Configuration)
Average Network-Wide Blocking Probability (Dedicated Resources)
3-Alternate Routing, Class-B Arrivals, STS-2 Sharing

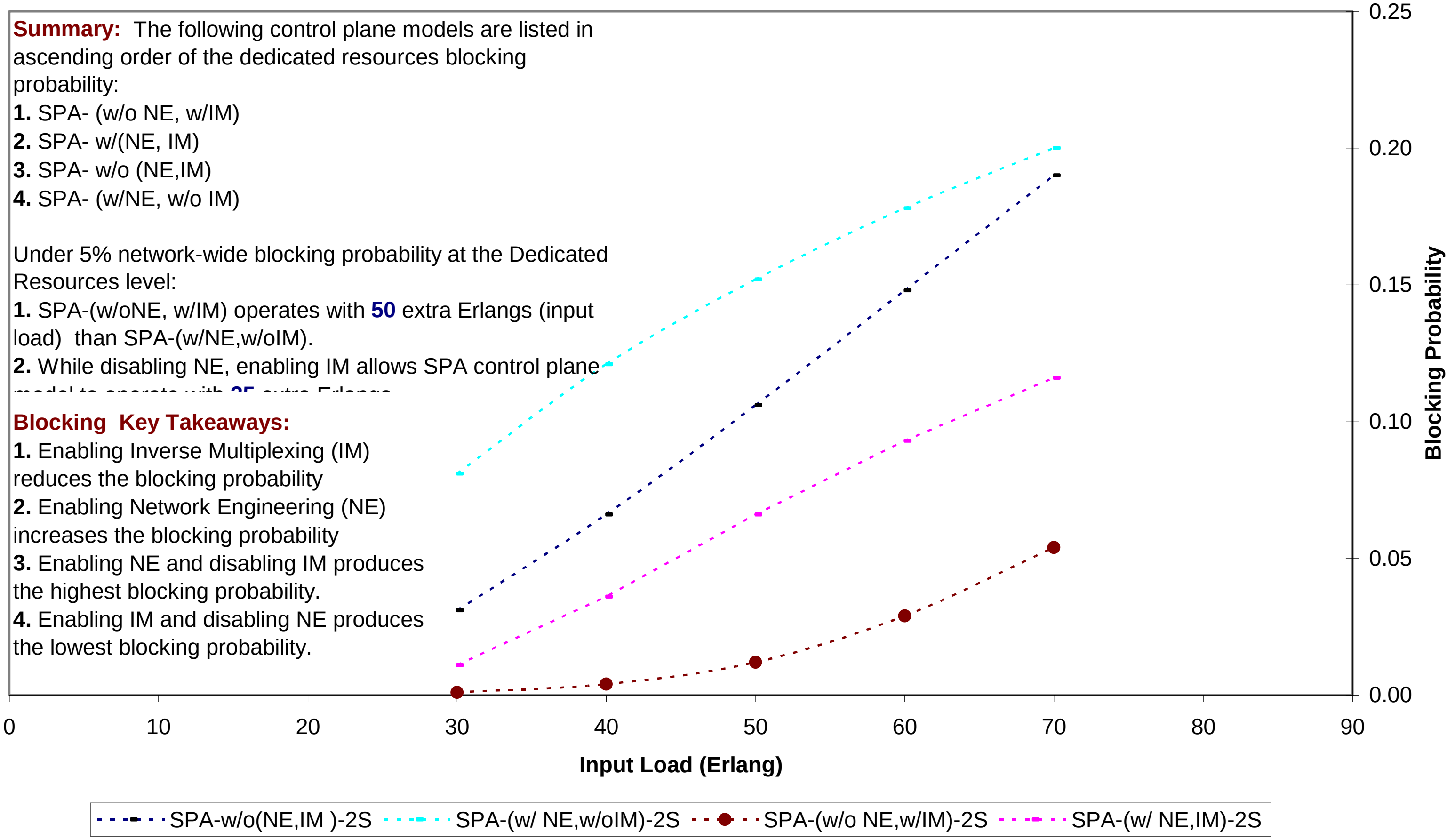

Summary: The following control plane models are listed in ascending order of the dedicated resources blocking probability:

1. SPA- (w/o NE, w/IM)
2. SPA- w/(NE, IM)
3. SPA- w/o (NE,IM)
4. SPA- (w/NE, w/o IM)

Under 5% network-wide blocking probability at the Dedicated Resources level:

1. SPA-(w/oNE, w/IM) operates with **50** extra Erlangs (input load) than SPA-(w/NE,w/oIM).
2. While disabling NE, enabling IM allows SPA control plane model to operate with **25** extra Erlangs

Blocking Key Takeaways:

1. Enabling Inverse Multiplexing (IM) reduces the blocking probability
2. Enabling Network Engineering (NE) increases the blocking probability
3. Enabling NE and disabling IM produces the highest blocking probability.
4. Enabling IM and disabling NE produces the lowest blocking probability.

Figure 21-2: Average Network-Wide Blocking Probability (Dedicated Resources)-7 Node – 3 Alternate Route-STS-2 Sharing

7-node Topology (Fully-meshed Service Configuration)
Average Network-Wide Blocking Probability (Dedicated Resources)
3-Alternate Routing, Class-B Arrivals, STS-3 Sharing

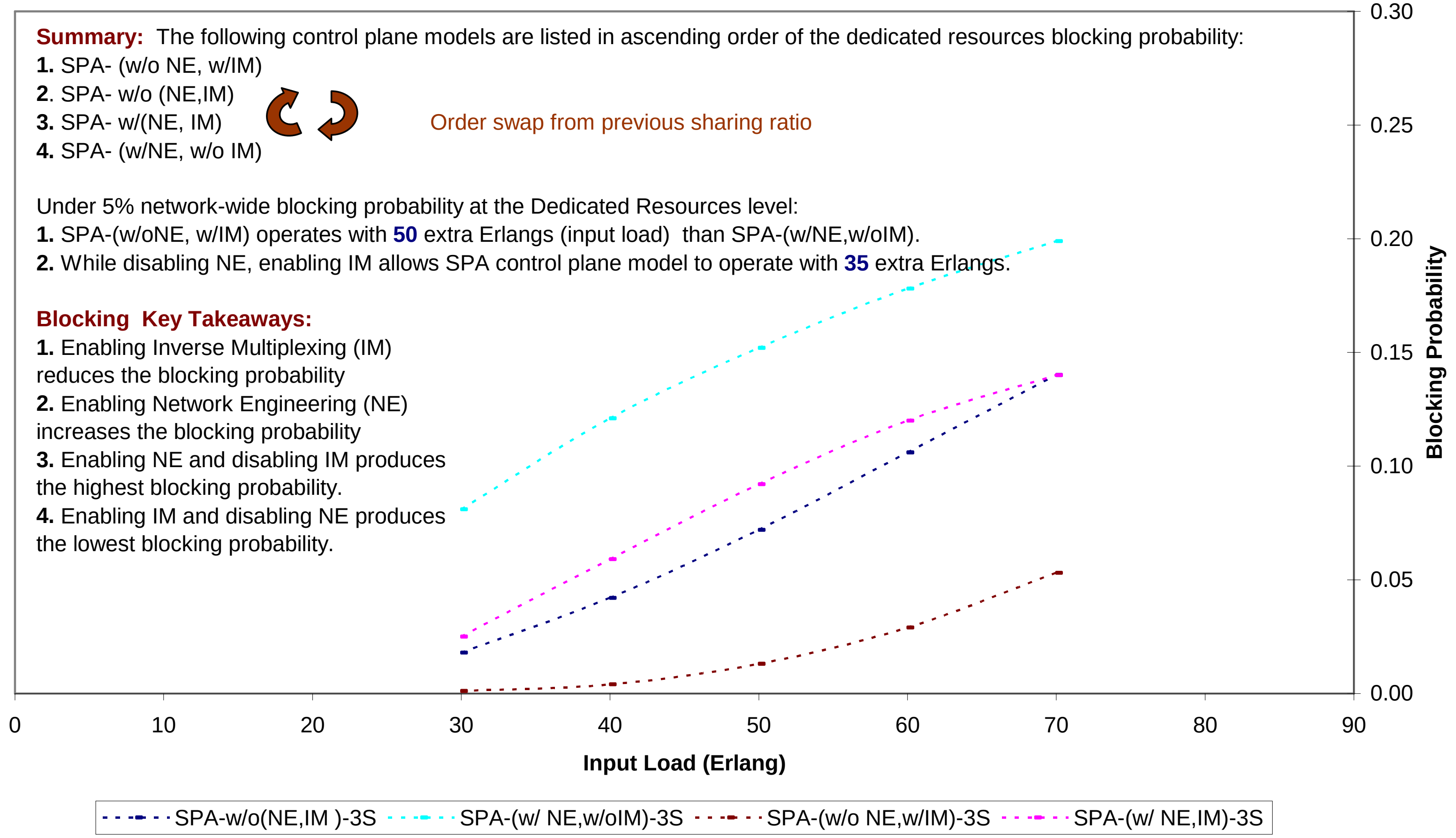

Summary: The following control plane models are listed in ascending order of the dedicated resources blocking probability:

1. SPA- (w/o NE, w/IM)
2. SPA- w/o (NE,IM)
3. SPA- w/(NE, IM)
4. SPA- (w/NE, w/o IM)

Order swap from previous sharing ratio

Under 5% network-wide blocking probability at the Dedicated Resources level:
1. SPA-(w/oNE, w/IM) operates with **50** extra Erlangs (input load) than SPA-(w/NE,w/oIM).
2. While disabling NE, enabling IM allows SPA control plane model to operate with **35** extra Erlangs.

Blocking Key Takeaways:
1. Enabling Inverse Multiplexing (IM) reduces the blocking probability
2. Enabling Network Engineering (NE) increases the blocking probability
3. Enabling NE and disabling IM produces the highest blocking probability.
4. Enabling IM and disabling NE produces the lowest blocking probability.

Figure 21-3: Average Network-Wide Blocking Probability (Dedicated Resources)-7 Node – 3 Alternate Route-STS-3 Sharing

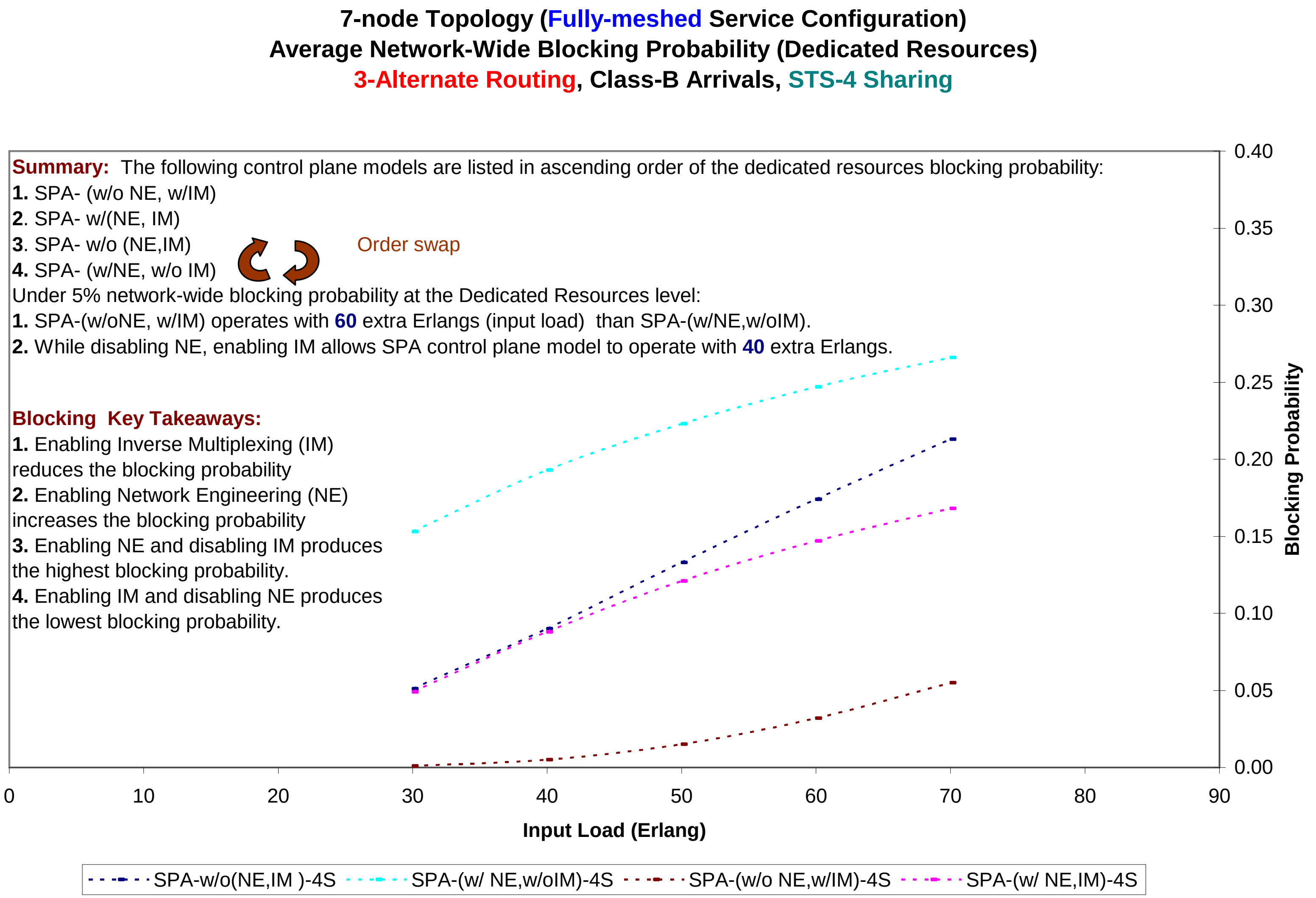

7-node Topology (Fully-meshed Service Configuration)
Average Network-Wide Blocking Probability (Dedicated Resources)
3-Alternate Routing, Class-B Arrivals, STS-4 Sharing

Summary: The following control plane models are listed in ascending order of the dedicated resources blocking probability:

1. SPA- (w/o NE, w/IM)
2. SPA- w/(NE, IM)
3. SPA- w/o (NE,IM)
4. SPA- (w/NE, w/o IM)

Order swap

Under 5% network-wide blocking probability at the Dedicated Resources level:
1. SPA-(w/oNE, w/IM) operates with **60** extra Erlangs (input load) than SPA-(w/NE,w/oIM).
2. While disabling NE, enabling IM allows SPA control plane model to operate with **40** extra Erlangs.

Blocking Key Takeaways:
1. Enabling Inverse Multiplexing (IM) reduces the blocking probability
2. Enabling Network Engineering (NE) increases the blocking probability
3. Enabling NE and disabling IM produces the highest blocking probability.
4. Enabling IM and disabling NE produces the lowest blocking probability.

Figure 21-4: Average Network-Wide Blocking Probability (Dedicated Resources)-7 Node – 3 Alternate Route-STS-4 Sharing

21.1.2 Shared resources

This section provides detailed performance analysis of the network-wide blocking probability on the shared network resources partition for the 7-node topology with three-alternate routing. The configured VPN service evaluated is the Fully-meshed Shared Granular (FSF) with the following service profile layer parameters:

a. Service flow connectivity: configured as “fully-meshed”.

b. Service demand granularity: configured as “granular” with 1 STS-1 granularity level.

c. Load partitioning flexibility: configured as “enabled”.

One input class was evaluated with the following parameters: $k=2$, $b_k^A=2$ STS-1, $\mu_k=1$unit time, $\lambda_{rk}=4$ calls/unit time. Range of input load for 4-node topology is 30 to 70 Erlangs. The five traffic management schemes of the SPA control plane model are evaluated as provided in Table 9-1. Four sharing levels are considered as follows:

a. STS-1 sharing: C_j^{vD}=11 STS-1, C_j^S=2 STS-1

b. STS-2 sharing: C_j^{vD}=10 STS-1, C_j^S=4 STS-1

c. STS-3 sharing: C_j^{vD}=9 STS-1, C_j^S=6 STS-1

d. STS-4 sharing: C_j^{vD}=8 STS-1, C_j^S=8 STS-1

7-node Topology (Fully-meshed Service Configuration)
Average Network-Wide Blocking Probability (Shared Resources)
3-Alternate Routing, Class-B Arrivals, STS-1 Sharing

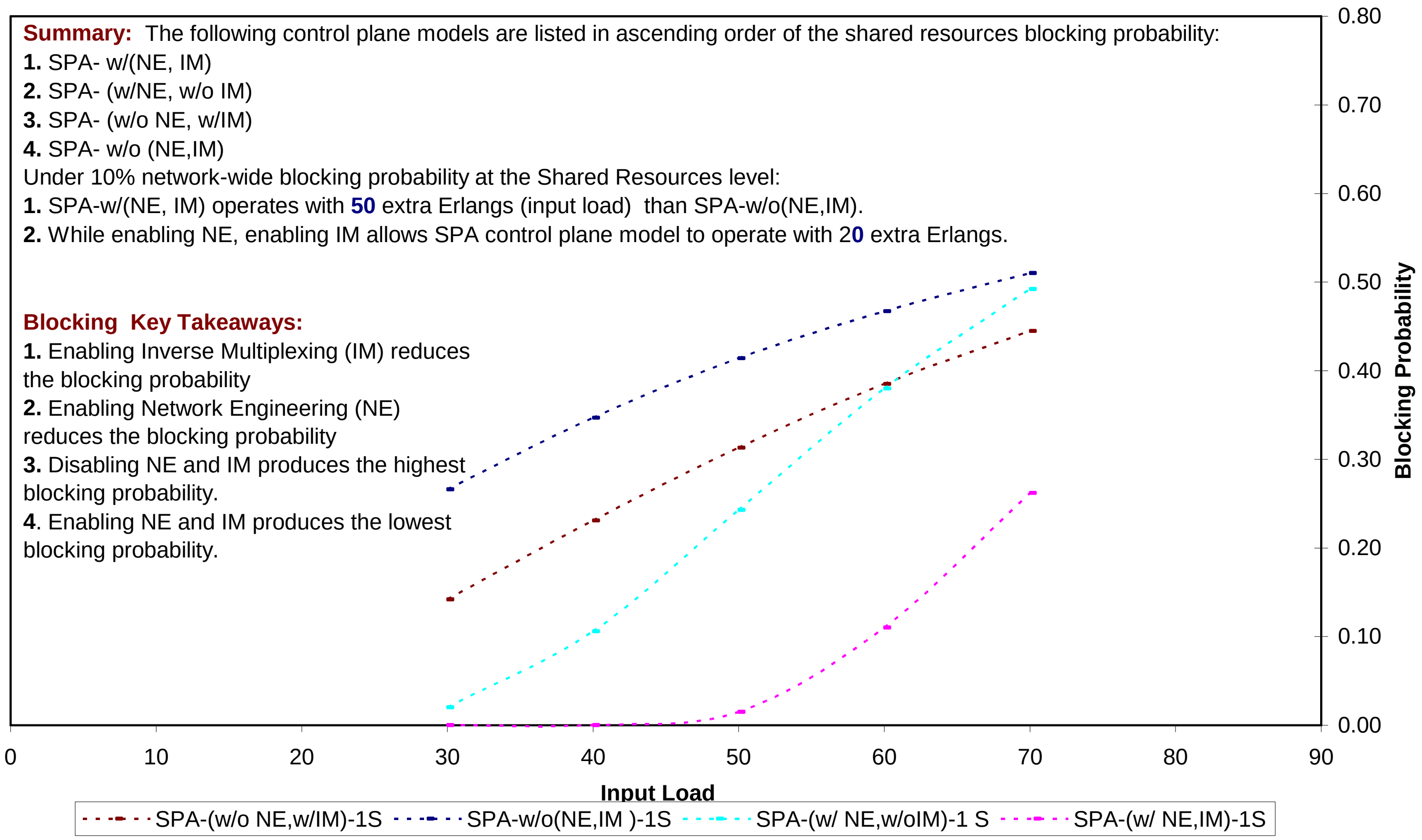

Summary: The following control plane models are listed in ascending order of the shared resources blocking probability:

1. SPA- w/(NE, IM)
2. SPA- (w/NE, w/o IM)
3. SPA- (w/o NE, w/IM)
4. SPA- w/o (NE,IM)

Under 10% network-wide blocking probability at the Shared Resources level:

1. SPA-w/(NE, IM) operates with **50** extra Erlangs (input load) than SPA-w/o(NE,IM).
2. While enabling NE, enabling IM allows SPA control plane model to operate with 2**0** extra Erlangs.

Blocking Key Takeaways:

1. Enabling Inverse Multiplexing (IM) reduces the blocking probability
2. Enabling Network Engineering (NE) reduces the blocking probability
3. Disabling NE and IM produces the highest blocking probability.
4. Enabling NE and IM produces the lowest blocking probability.

Figure 21-5: Average Network-Wide Blocking Probability (Shared Resources)-7 Node – 3 Alternate Route-STS-1 Sharing

7-node Topology (Fully-meshed Service Configuration)
Average Network-Wide Blocking Probability (Shared Resources)
3-Alternate Routing, Class-B Arrivals, STS-2 Sharing

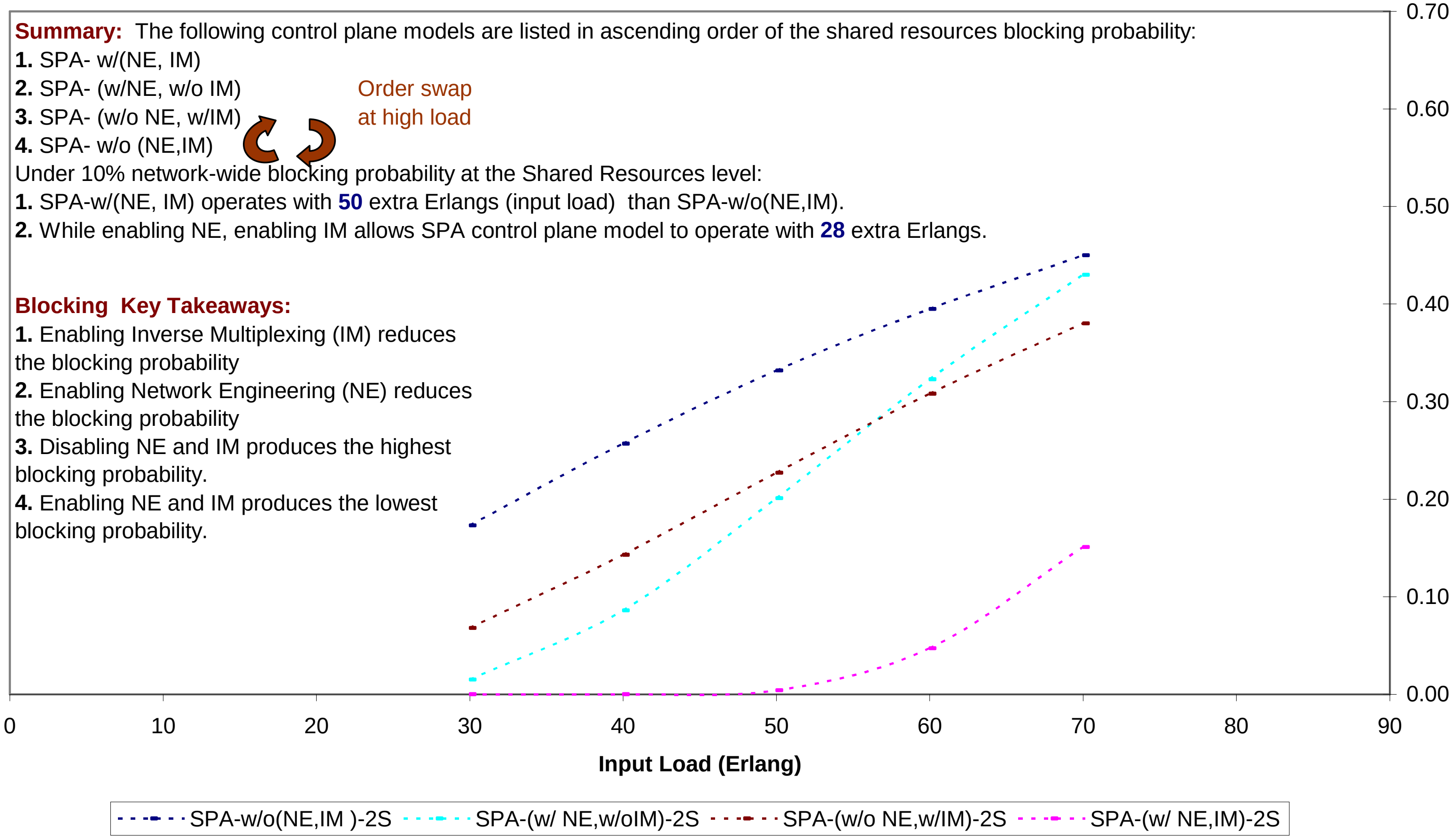

Summary: The following control plane models are listed in ascending order of the shared resources blocking probability:
1. SPA- w/(NE, IM)
2. SPA- (w/NE, w/o IM)
3. SPA- (w/o NE, w/IM)
4. SPA- w/o (NE,IM)

Order swap
at high load

Under 10% network-wide blocking probability at the Shared Resources level:
1. SPA-w/(NE, IM) operates with **50** extra Erlangs (input load) than SPA-w/o(NE,IM).
2. While enabling NE, enabling IM allows SPA control plane model to operate with **28** extra Erlangs.

Blocking Key Takeaways:
1. Enabling Inverse Multiplexing (IM) reduces the blocking probability
2. Enabling Network Engineering (NE) reduces the blocking probability
3. Disabling NE and IM produces the highest blocking probability.
4. Enabling NE and IM produces the lowest blocking probability.

Figure 21-6: Average Network-Wide Blocking Probability (Shared Resources)-7 Node – 3 Alternate Route-STS-2 Sharing

7-node Topology (Fully-meshed Service Configuration)
Average Network-Wide Blocking Probability (Shared Resources)
3-Alternate Routing, Class-B Arrivals, STS-3 Sharing

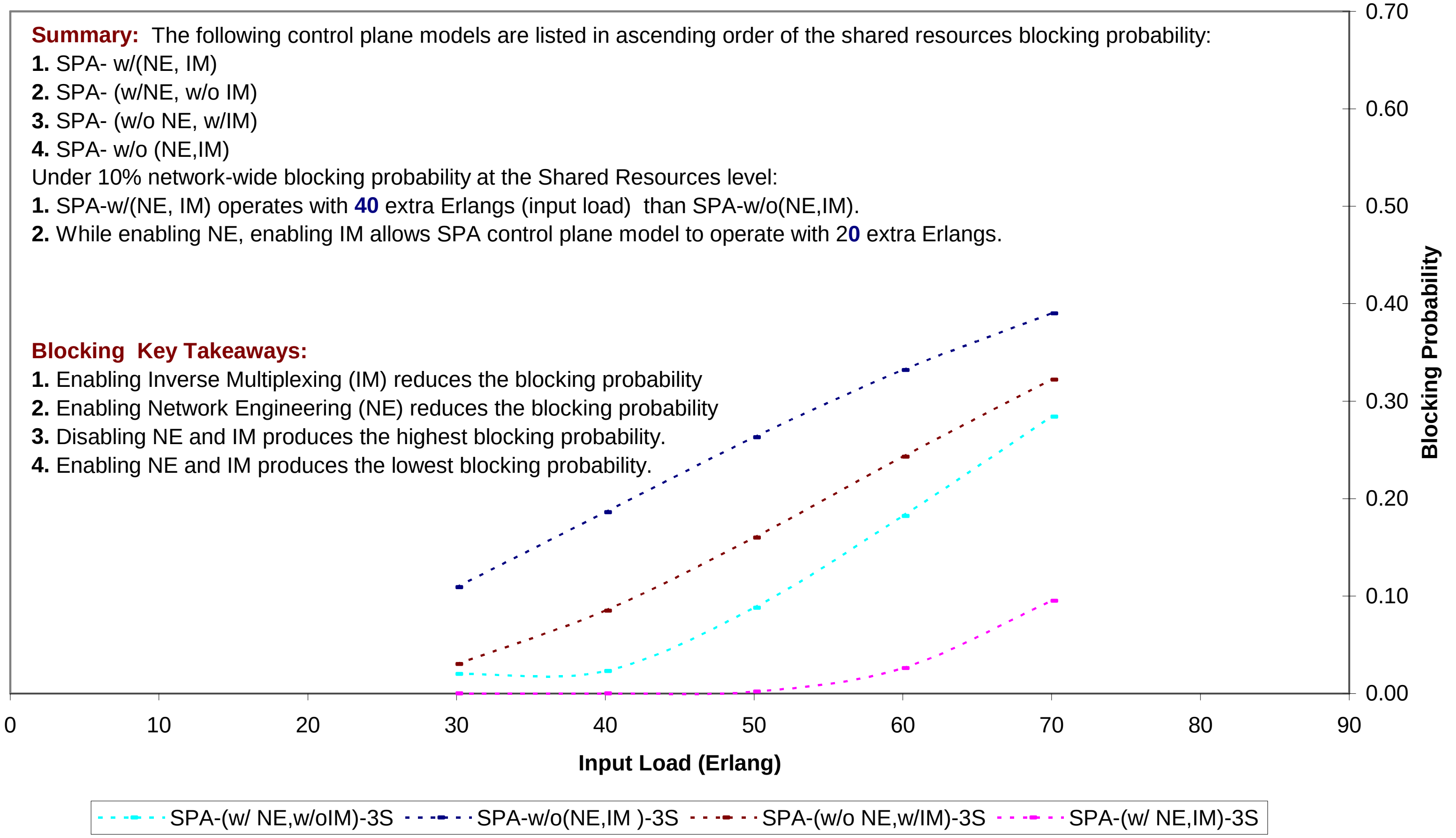

Summary: The following control plane models are listed in ascending order of the shared resources blocking probability:

1. SPA- w/(NE, IM)
2. SPA- (w/NE, w/o IM)
3. SPA- (w/o NE, w/IM)
4. SPA- w/o (NE,IM)

Under 10% network-wide blocking probability at the Shared Resources level:

1. SPA-w/(NE, IM) operates with **40** extra Erlangs (input load) than SPA-w/o(NE,IM).
2. While enabling NE, enabling IM allows SPA control plane model to operate with 2**0** extra Erlangs.

Blocking Key Takeaways:

1. Enabling Inverse Multiplexing (IM) reduces the blocking probability
2. Enabling Network Engineering (NE) reduces the blocking probability
3. Disabling NE and IM produces the highest blocking probability.
4. Enabling NE and IM produces the lowest blocking probability.

Figure 21-7: Average Network-Wide Blocking Probability (Shared Resources)-7 Node – 3 Alternate Route-STS-3 Sharing

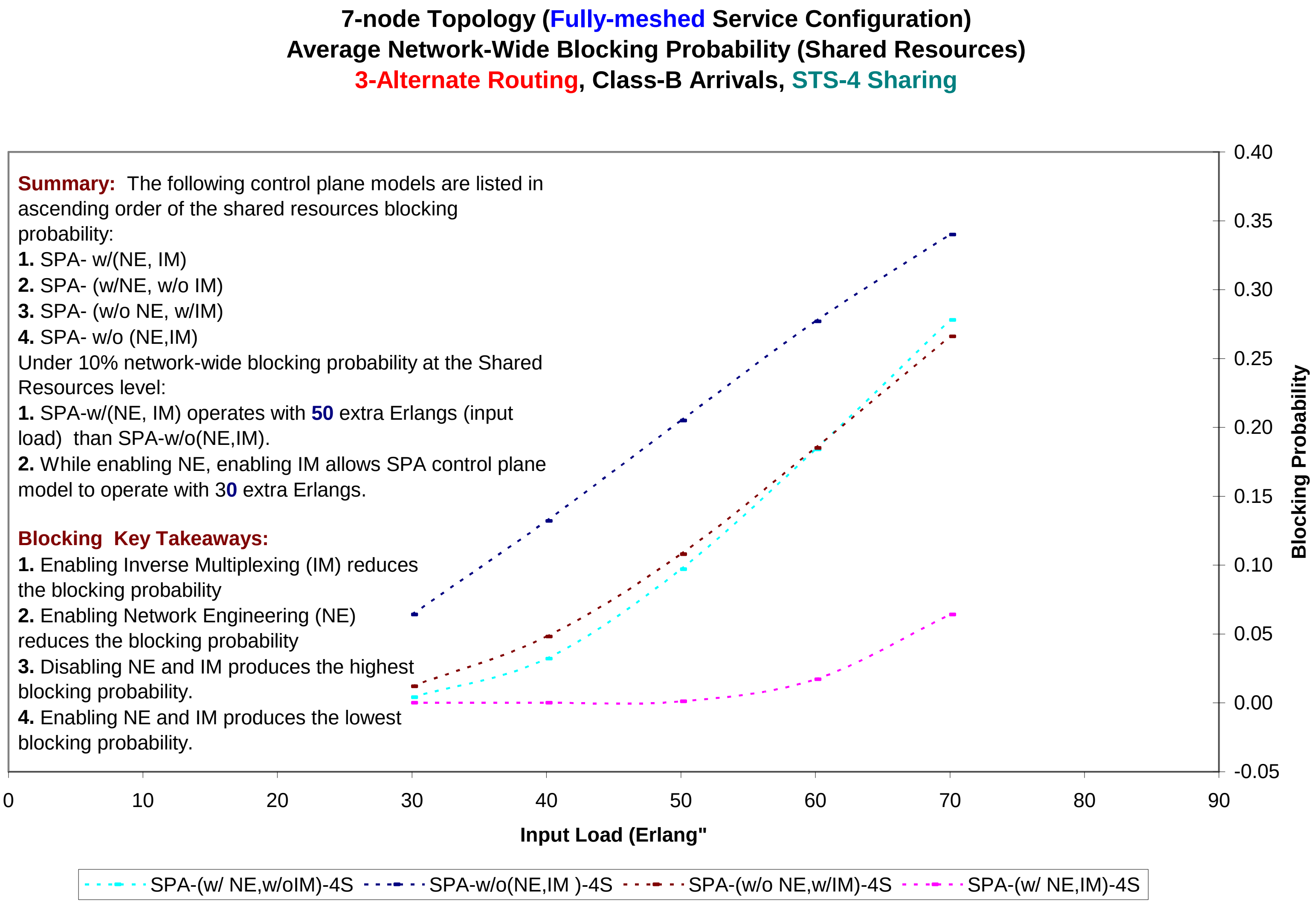

7-node Topology (Fully-meshed Service Configuration)
Average Network-Wide Blocking Probability (Shared Resources)
3-Alternate Routing, Class-B Arrivals, STS-4 Sharing

Summary: The following control plane models are listed in ascending order of the shared resources blocking probability:

1. SPA- w/(NE, IM)
2. SPA- (w/NE, w/o IM)
3. SPA- (w/o NE, w/IM)
4. SPA- w/o (NE,IM)

Under 10% network-wide blocking probability at the Shared Resources level:

1. SPA-w/(NE, IM) operates with **50** extra Erlangs (input load) than SPA-w/o(NE,IM).
2. While enabling NE, enabling IM allows SPA control plane model to operate with 3**0** extra Erlangs.

Blocking Key Takeaways:

1. Enabling Inverse Multiplexing (IM) reduces the blocking probability
2. Enabling Network Engineering (NE) reduces the blocking probability
3. Disabling NE and IM produces the highest blocking probability.
4. Enabling NE and IM produces the lowest blocking probability.

Figure 21-8: Average Network-Wide Blocking Probability (Shared Resources)-7 Node – 3 Alternate Route-STS-4 Sharing

21.1.3 VPN resources

This section provides detailed performance analysis of the network-wide blocking probability on the VPN network resources partition for the 7-node topology with three-alternate routing. The configured VPN service evaluated is the Fully-meshed Shared Granular (FSF) with the following service profile layer parameters:

a. Service flow connectivity: configured as "fully-meshed".

b. Service demand granularity: configured as "granular" with 1 STS-1 granularity level.

c. Load partitioning flexibility: configured as "enabled".

One input class was evaluated with the following parameters: $k = 2$, $b_k^A = 2$ STS-1, $\mu_k = 1$unit time, $\lambda_{rk} = 4$ calls/unit time. Range of input load for 4-node topology is 30 to 70 Erlangs. The five traffic management schemes of the SPA control plane model are evaluated as provided in Table 9-1. Four sharing levels are considered as follows:

a. STS-1 sharing: C_j^{vD}=11 STS-1, C_j^S=2 STS-1

b. STS-2 sharing: C_j^{vD}=10 STS-1, C_j^S=4 STS-1

c. STS-3 sharing: C_j^{vD}=9 STS-1, C_j^S=6 STS-1

d. STS-4 sharing: C_j^{vD}=8 STS-1, C_j^S=8 STS-1

7-node Topology (Fully-meshed Service Configuration)
Average Network-Wide Blocking Probability (VPN Resources)
3-Alternate Routing, Class-B Arrivals, ITU(DR,SR), SPA-Dedicated

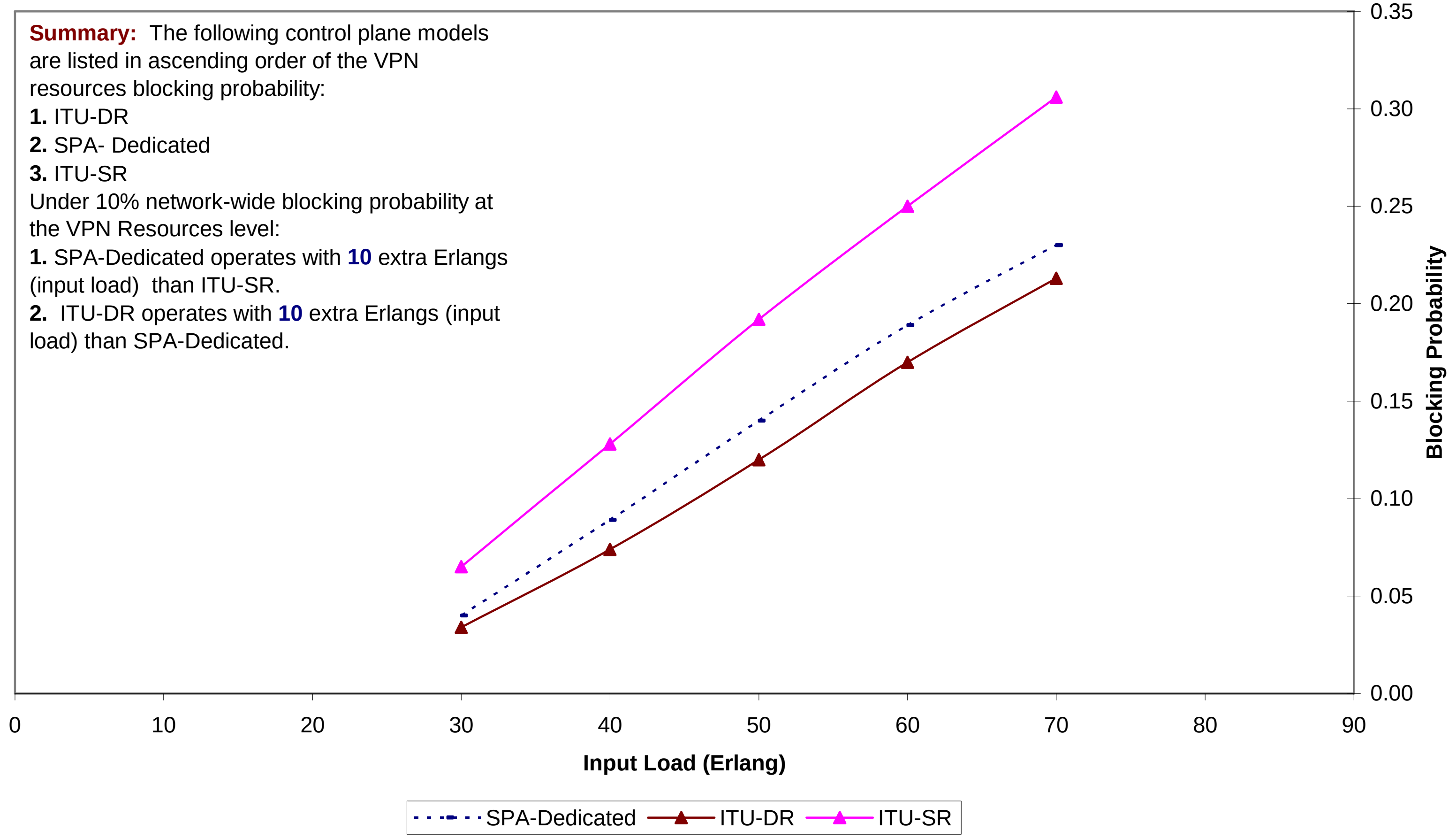

Summary: The following control plane models are listed in ascending order of the VPN resources blocking probability:

1. ITU-DR
2. SPA- Dedicated
3. ITU-SR

Under 10% network-wide blocking probability at the VPN Resources level:

1. SPA-Dedicated operates with **10** extra Erlangs (input load) than ITU-SR.
2. ITU-DR operates with **10** extra Erlangs (input load) than SPA-Dedicated.

Figure 21-9: Average Network-Wide Blocking Probability (VPN Resources)-7 Node – 3 Alternate Route-ITU(DR,SR), SPA-Dedicated

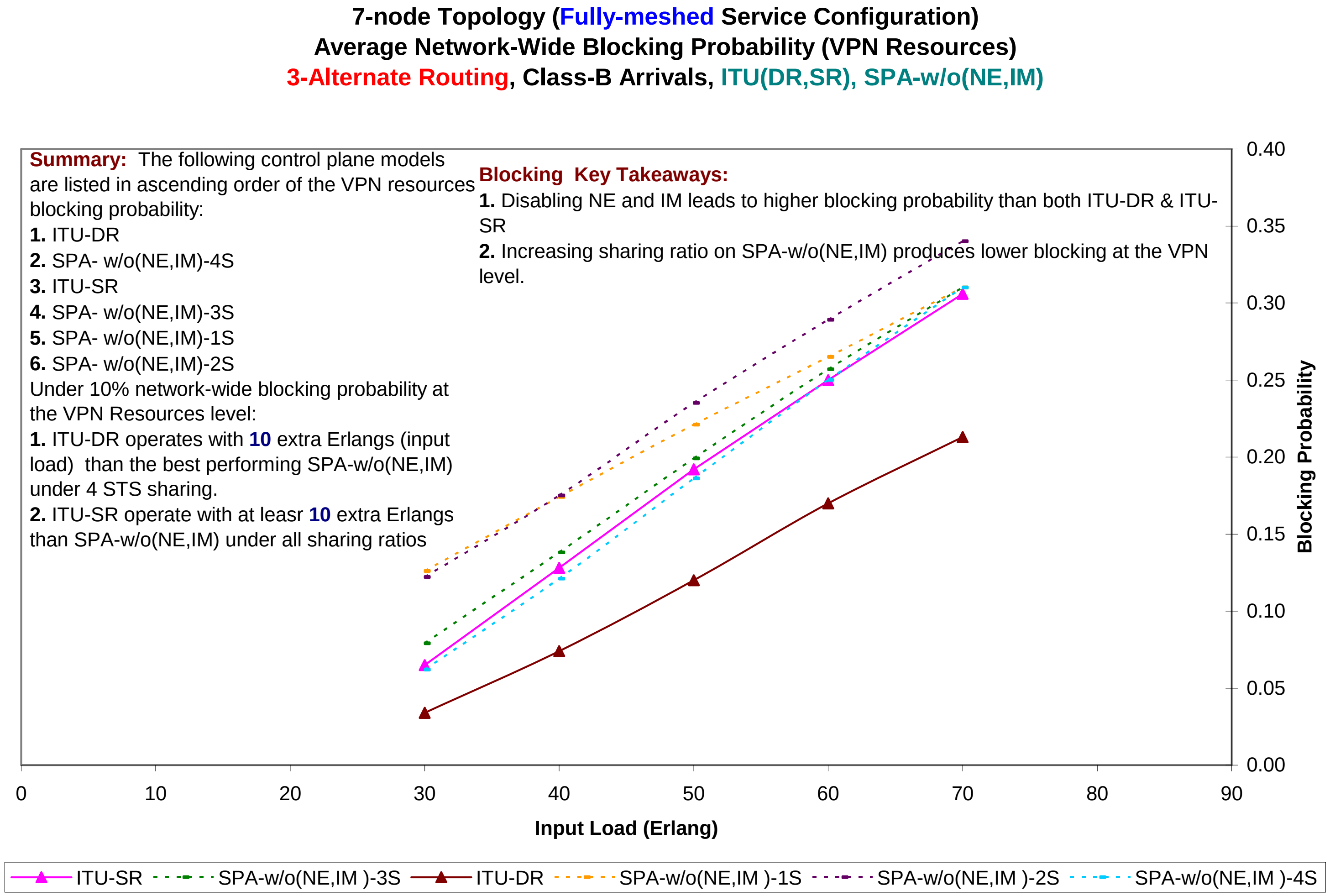

7-node Topology (Fully-meshed Service Configuration)
Average Network-Wide Blocking Probability (VPN Resources)
3-Alternate Routing, Class-B Arrivals, ITU(DR,SR), SPA-w/o(NE,IM)

Summary: The following control plane models are listed in ascending order of the VPN resources blocking probability:

1. ITU-DR
2. SPA- w/o(NE,IM)-4S
3. ITU-SR
4. SPA- w/o(NE,IM)-3S
5. SPA- w/o(NE,IM)-1S
6. SPA- w/o(NE,IM)-2S

Under 10% network-wide blocking probability at the VPN Resources level:

1. ITU-DR operates with **10** extra Erlangs (input load) than the best performing SPA-w/o(NE,IM) under 4 STS sharing.
2. ITU-SR operate with at leasr **10** extra Erlangs than SPA-w/o(NE,IM) under all sharing ratios

Blocking Key Takeaways:

1. Disabling NE and IM leads to higher blocking probability than both ITU-DR & ITU-SR
2. Increasing sharing ratio on SPA-w/o(NE,IM) produces lower blocking at the VPN level.

Figure 21-10: Average Network-Wide Blocking Probability (VPN Resources)-7 Node – 3 Alternate Route-ITU(DR,SR), SPA-w/o(NE,IM)

7-node Topology (Fully-meshed Service Configuration)
Average Network-Wide Blocking Probability (VPN Resources)
3-Alternate Routing, Class-B Arrivals, ITU(DR,SR), SPA- (w/NE, w/o IM)

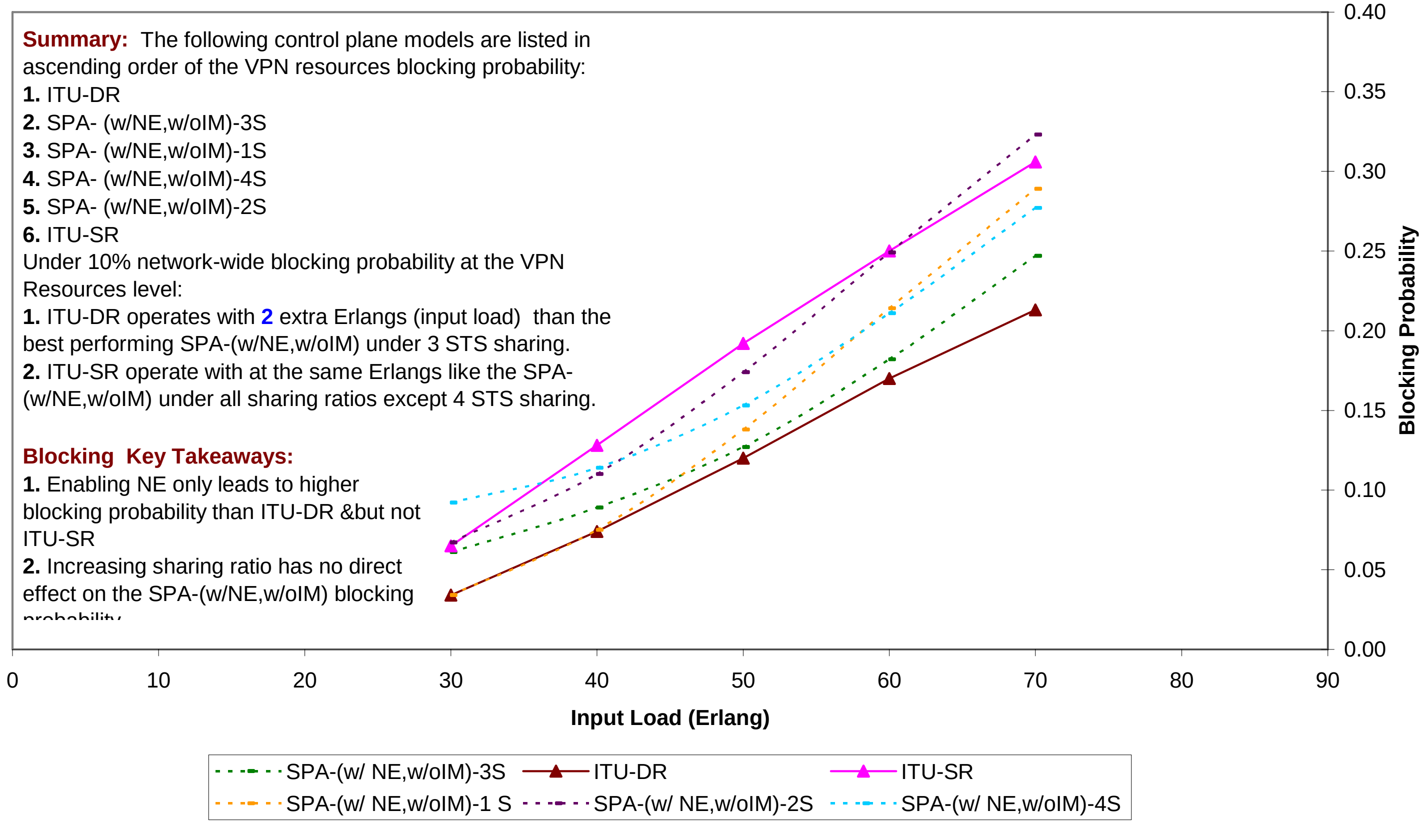

Summary: The following control plane models are listed in ascending order of the VPN resources blocking probability:

1. ITU-DR
2. SPA- (w/NE,w/oIM)-3S
3. SPA- (w/NE,w/oIM)-1S
4. SPA- (w/NE,w/oIM)-4S
5. SPA- (w/NE,w/oIM)-2S
6. ITU-SR

Under 10% network-wide blocking probability at the VPN Resources level:

1. ITU-DR operates with **2** extra Erlangs (input load) than the best performing SPA-(w/NE,w/oIM) under 3 STS sharing.
2. ITU-SR operate with at the same Erlangs like the SPA-(w/NE,w/oIM) under all sharing ratios except 4 STS sharing.

Blocking Key Takeaways:

1. Enabling NE only leads to higher blocking probability than ITU-DR &but not ITU-SR
2. Increasing sharing ratio has no direct effect on the SPA-(w/NE,w/oIM) blocking probability

Figure 21-11: Average Network-Wide Blocking Probability (VPN Resources)-7 Node – 3 Alternate Route-ITU(DR,SR), SPA-w/NE,w/oIM

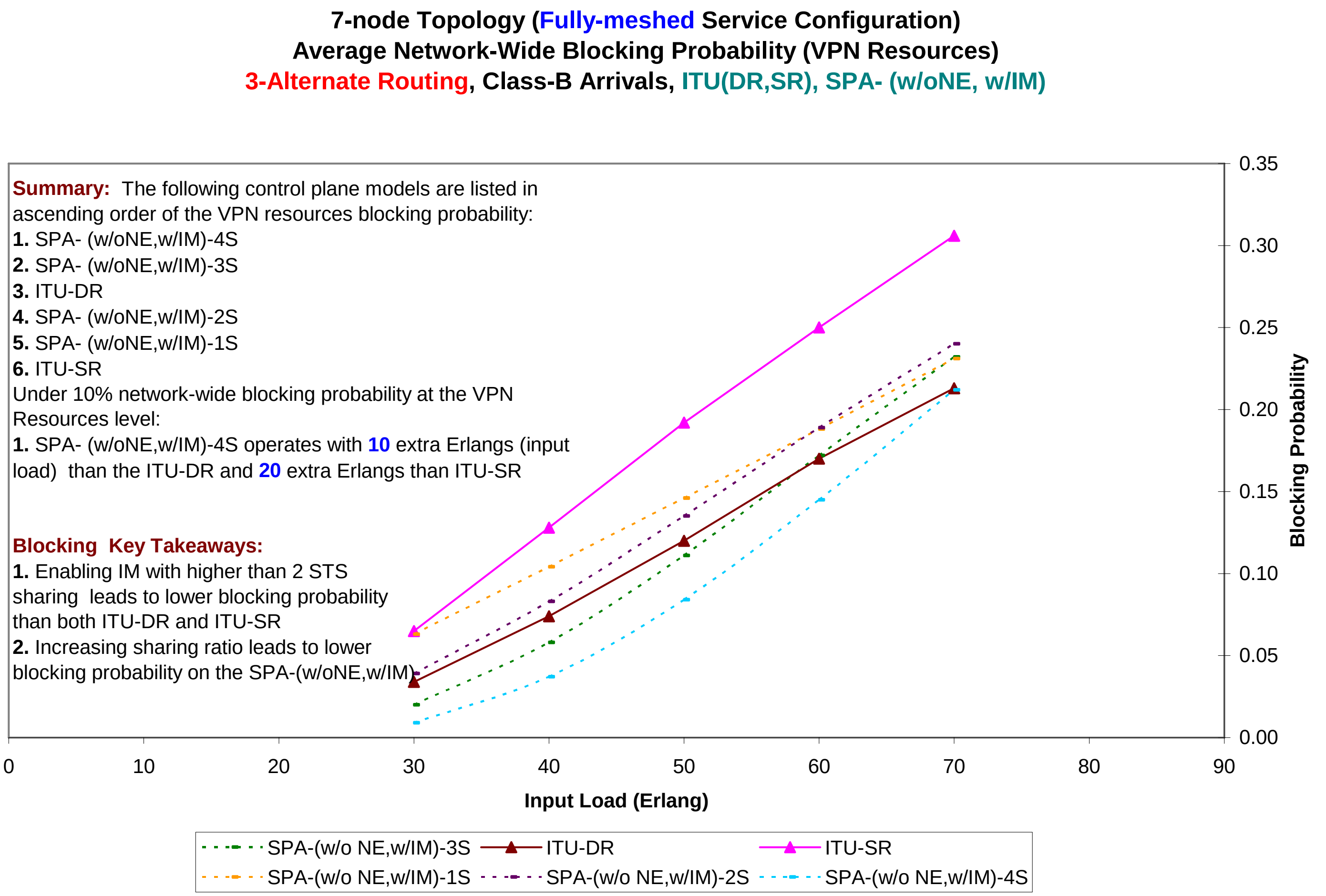

7-node Topology (Fully-meshed Service Configuration)
Average Network-Wide Blocking Probability (VPN Resources)
3-Alternate Routing, Class-B Arrivals, ITU(DR,SR), SPA- (w/oNE, w/IM)

Summary: The following control plane models are listed in ascending order of the VPN resources blocking probability:

1. SPA- (w/oNE,w/IM)-4S
2. SPA- (w/oNE,w/IM)-3S
3. ITU-DR
4. SPA- (w/oNE,w/IM)-2S
5. SPA- (w/oNE,w/IM)-1S
6. ITU-SR

Under 10% network-wide blocking probability at the VPN Resources level:

1. SPA- (w/oNE,w/IM)-4S operates with **10** extra Erlangs (input load) than the ITU-DR and **20** extra Erlangs than ITU-SR

Blocking Key Takeaways:

1. Enabling IM with higher than 2 STS sharing leads to lower blocking probability than both ITU-DR and ITU-SR

2. Increasing sharing ratio leads to lower blocking probability on the SPA-(w/oNE,w/IM)

Figure 21-12: Average Network-Wide Blocking Probability (VPN Resources)-7 Node – 3 Alternate Route-ITU(DR,SR), SPA-w/oNE,w/IM

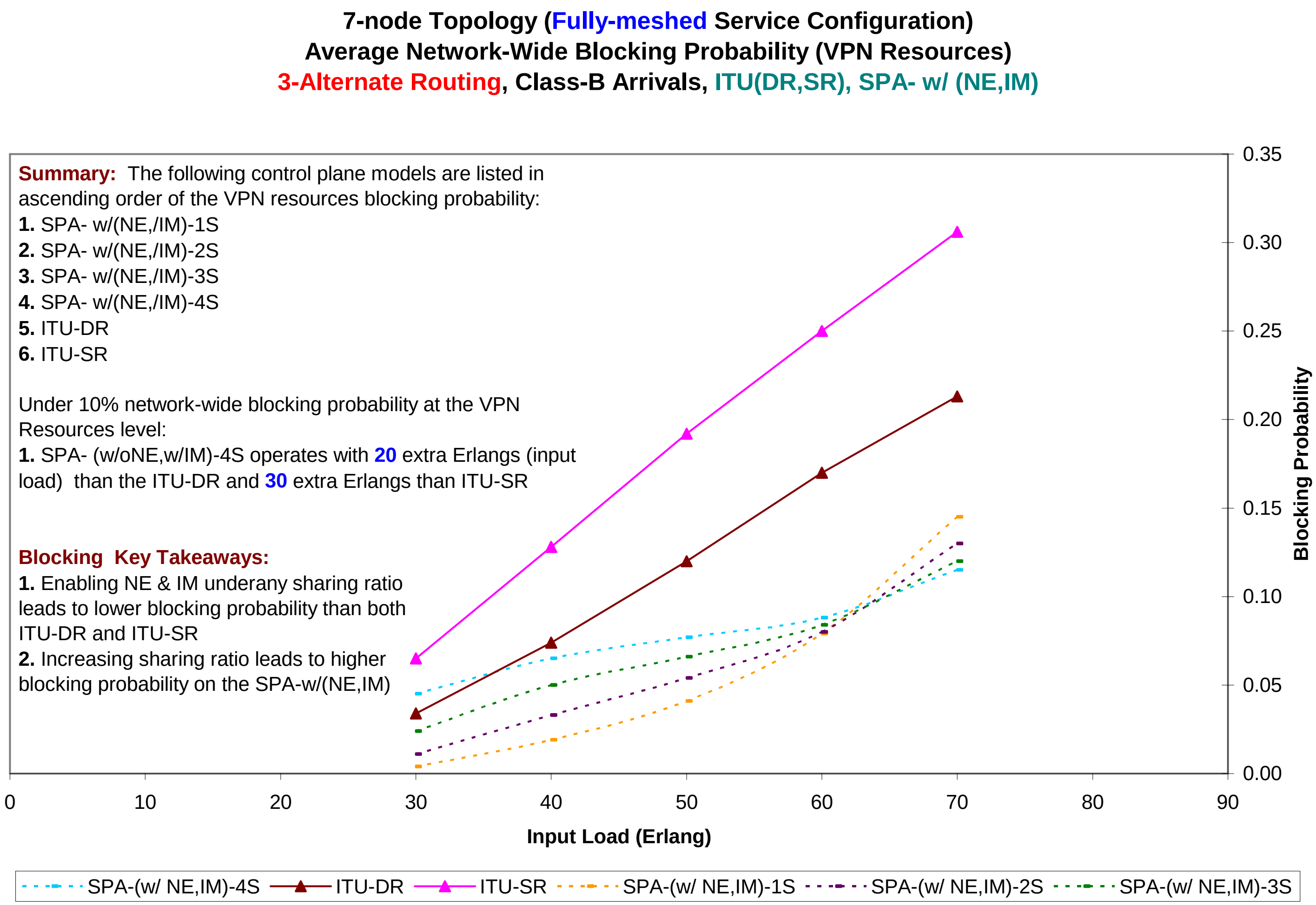

7-node Topology (Fully-meshed Service Configuration)
Average Network-Wide Blocking Probability (VPN Resources)
3-Alternate Routing, Class-B Arrivals, ITU(DR,SR), SPA- w/ (NE,IM)

Summary: The following control plane models are listed in ascending order of the VPN resources blocking probability:
1. SPA- w/(NE,/IM)-1S
2. SPA- w/(NE,/IM)-2S
3. SPA- w/(NE,/IM)-3S
4. SPA- w/(NE,/IM)-4S
5. ITU-DR
6. ITU-SR

Under 10% network-wide blocking probability at the VPN Resources level:
1. SPA- (w/oNE,w/IM)-4S operates with **20** extra Erlangs (input load) than the ITU-DR and **30** extra Erlangs than ITU-SR

Blocking Key Takeaways:
1. Enabling NE & IM underany sharing ratio leads to lower blocking probability than both ITU-DR and ITU-SR
2. Increasing sharing ratio leads to higher blocking probability on the SPA-w/(NE,IM)

Figure 21-13: Average Network-Wide Blocking Probability (VPN Resources)-7 Node – 3 Alternate Route-ITU(DR,SR), SPA-w/(NE,IM)

21.2 Permissible load

21.2.1 Dedicated resources

This section provides detailed performance analysis of the network-wide permissible load on the dedicated network resources partition for the 7-node topology with three-alternate routing. The configured VPN service evaluated is the Fully-meshed Shared Granular (FSF) with the following service profile layer parameters:

a. Service flow connectivity: configured as “fully-meshed”.

b. Service demand granularity: configured as “granular” with 1 STS-1 granularity level.

c. Load partitioning flexibility: configured as “enabled”.

One input class was evaluated with the following parameters: $k = 2$, $b_k^A = 2$ STS-1, $\mu_k = 1$unit time, $\lambda_{rk} = 4$ calls/unit time. Range of input load for 4-node topology is 30 to 70 Erlangs. The five traffic management schemes of the SPA control plane model are evaluated as provided in Table 9-1. Four sharing levels are considered as follows:

a. STS-1 sharing: C_j^{vD} =11 STS-1, C_j^S =2 STS-1

b. STS-2 sharing: C_j^{vD} =10 STS-1, C_j^S =4 STS-1

c. STS-3 sharing: C_j^{vD} =9 STS-1, C_j^S =6 STS-1

d. STS-4 sharing: C_j^{vD} =8 STS-1, C_j^S =8 STS-1

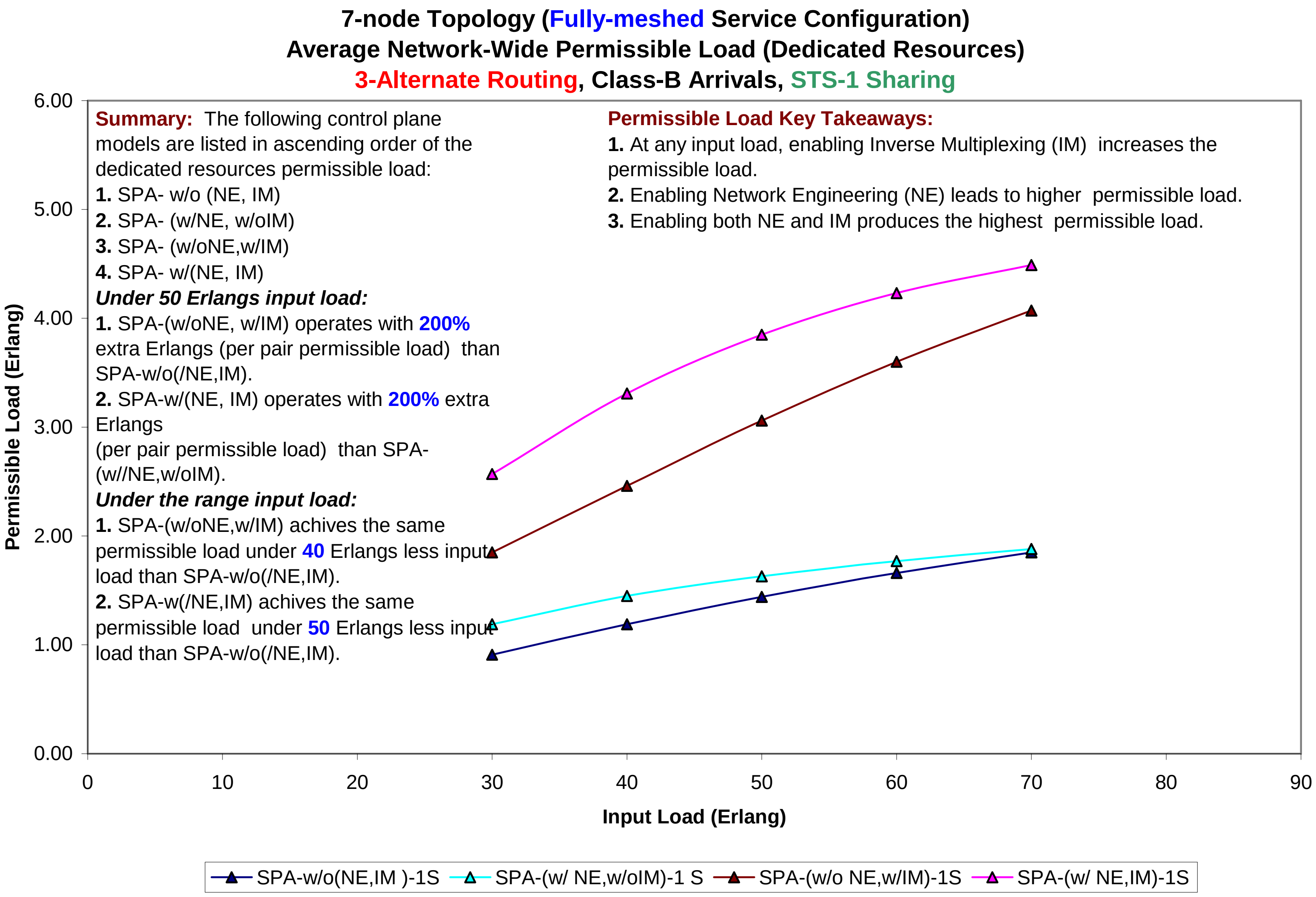

7-node Topology (Fully-meshed Service Configuration)
Average Network-Wide Permissible Load (Dedicated Resources)
3-Alternate Routing, Class-B Arrivals, STS-1 Sharing

Summary: The following control plane models are listed in ascending order of the dedicated resources permissible load:

1. SPA- w/o (NE, IM)
2. SPA- (w/NE, w/oIM)
3. SPA- (w/oNE,w/IM)
4. SPA- w/(NE, IM)

Under 50 Erlangs input load:

1. SPA-(w/oNE, w/IM) operates with **200%** extra Erlangs (per pair permissible load) than SPA-w/o(/NE,IM).

2. SPA-w/(NE, IM) operates with **200%** extra Erlangs
(per pair permissible load) than SPA-(w//NE,w/oIM).

Under the range input load:

1. SPA-(w/oNE,w/IM) achives the same permissible load under **40** Erlangs less input load than SPA-w/o(/NE,IM).

2. SPA-w(/NE,IM) achives the same permissible load under **50** Erlangs less input load than SPA-w/o(/NE,IM).

Permissible Load Key Takeaways:

1. At any input load, enabling Inverse Multiplexing (IM) increases the permissible load.

2. Enabling Network Engineering (NE) leads to higher permissible load.

3. Enabling both NE and IM produces the highest permissible load.

Figure 21-14: Average Network-Wide Permissible Load (Dedicated Resources)-7 Node – 3 Alternate Route-STS-1 Sharing

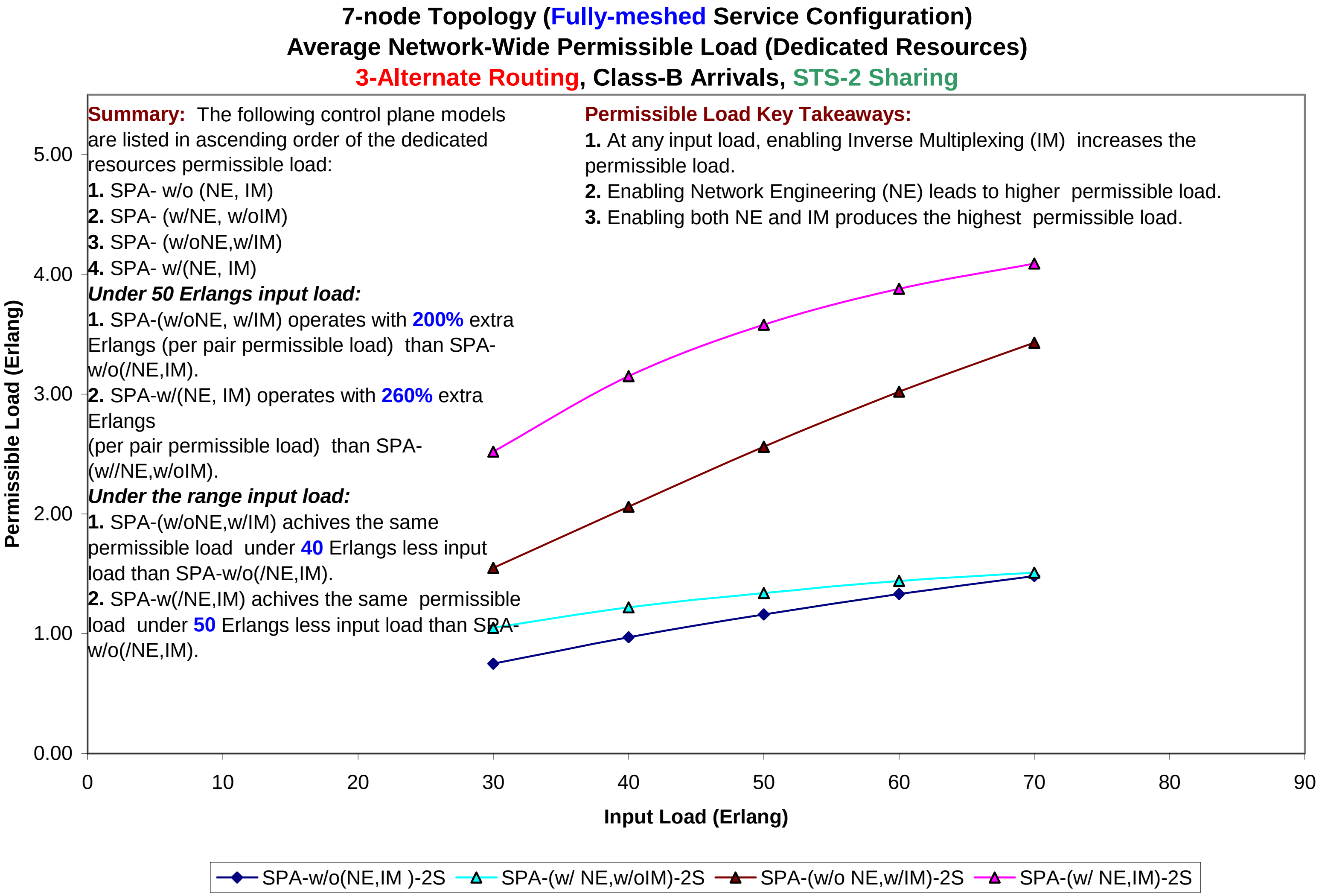

Figure 21-15: Average Network-Wide Permissible Load (Dedicated Resources)-7 Node – 3 Alternate Route-STS-2 Sharing

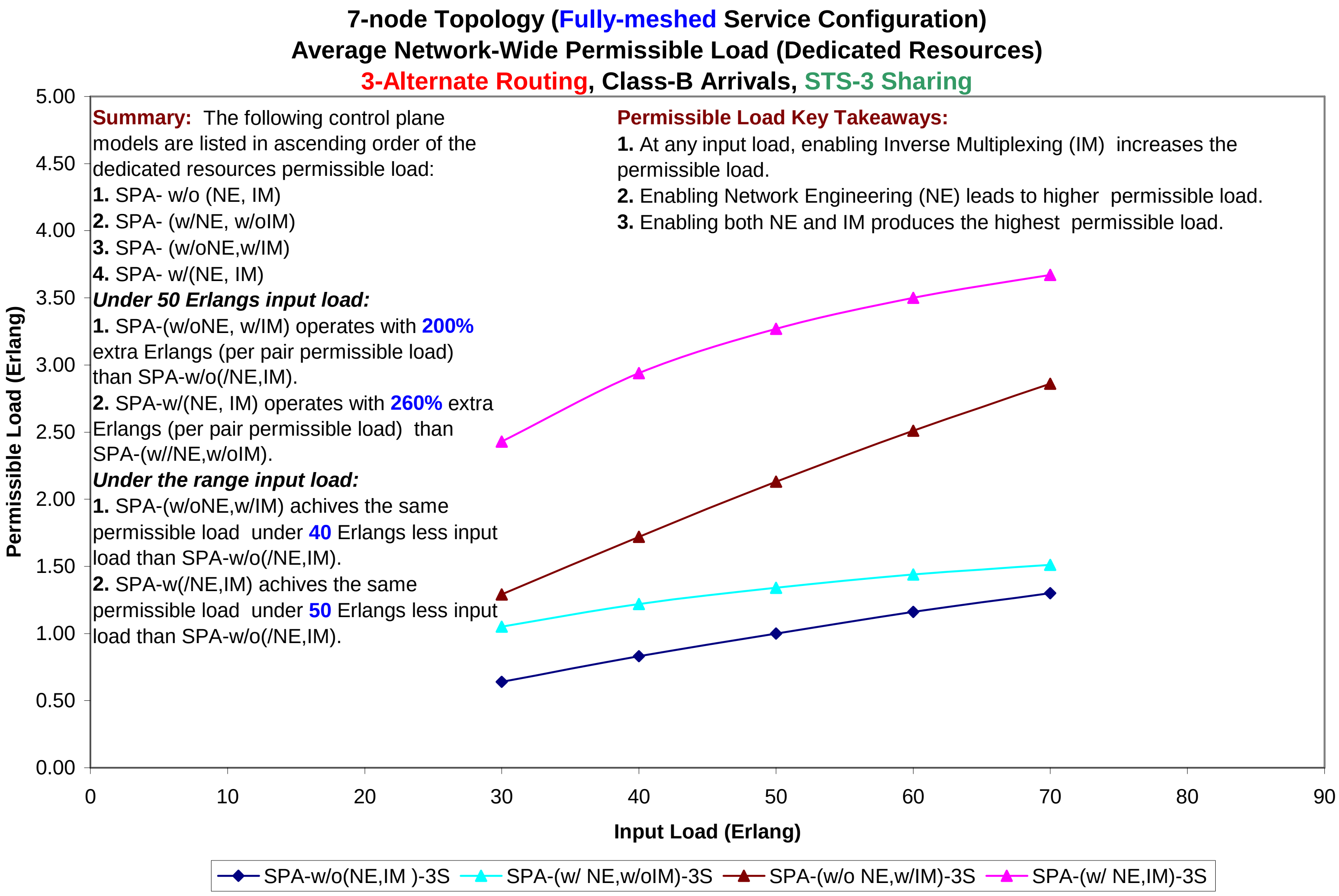

7-node Topology (Fully-meshed Service Configuration)
Average Network-Wide Permissible Load (Dedicated Resources)
3-Alternate Routing, Class-B Arrivals, STS-3 Sharing

Summary: The following control plane models are listed in ascending order of the dedicated resources permissible load:

1. SPA- w/o (NE, IM)
2. SPA- (w/NE, w/oIM)
3. SPA- (w/oNE,w/IM)
4. SPA- w/(NE, IM)

Under 50 Erlangs input load:

1. SPA-(w/oNE, w/IM) operates with **200%** extra Erlangs (per pair permissible load) than SPA-w/o(/NE,IM).

2. SPA-w/(NE, IM) operates with **260%** extra Erlangs (per pair permissible load) than SPA-(w//NE,w/oIM).

Under the range input load:

1. SPA-(w/oNE,w/IM) achives the same permissible load under **40** Erlangs less input load than SPA-w/o(/NE,IM).

2. SPA-w(/NE,IM) achives the same permissible load under **50** Erlangs less input load than SPA-w/o(/NE,IM).

Permissible Load Key Takeaways:

1. At any input load, enabling Inverse Multiplexing (IM) increases the permissible load.

2. Enabling Network Engineering (NE) leads to higher permissible load.

3. Enabling both NE and IM produces the highest permissible load.

Figure 21-16: Average Network-Wide Permissible Load (Dedicated Resources)-7 Node – 3 Alternate Route-STS-3 Sharing

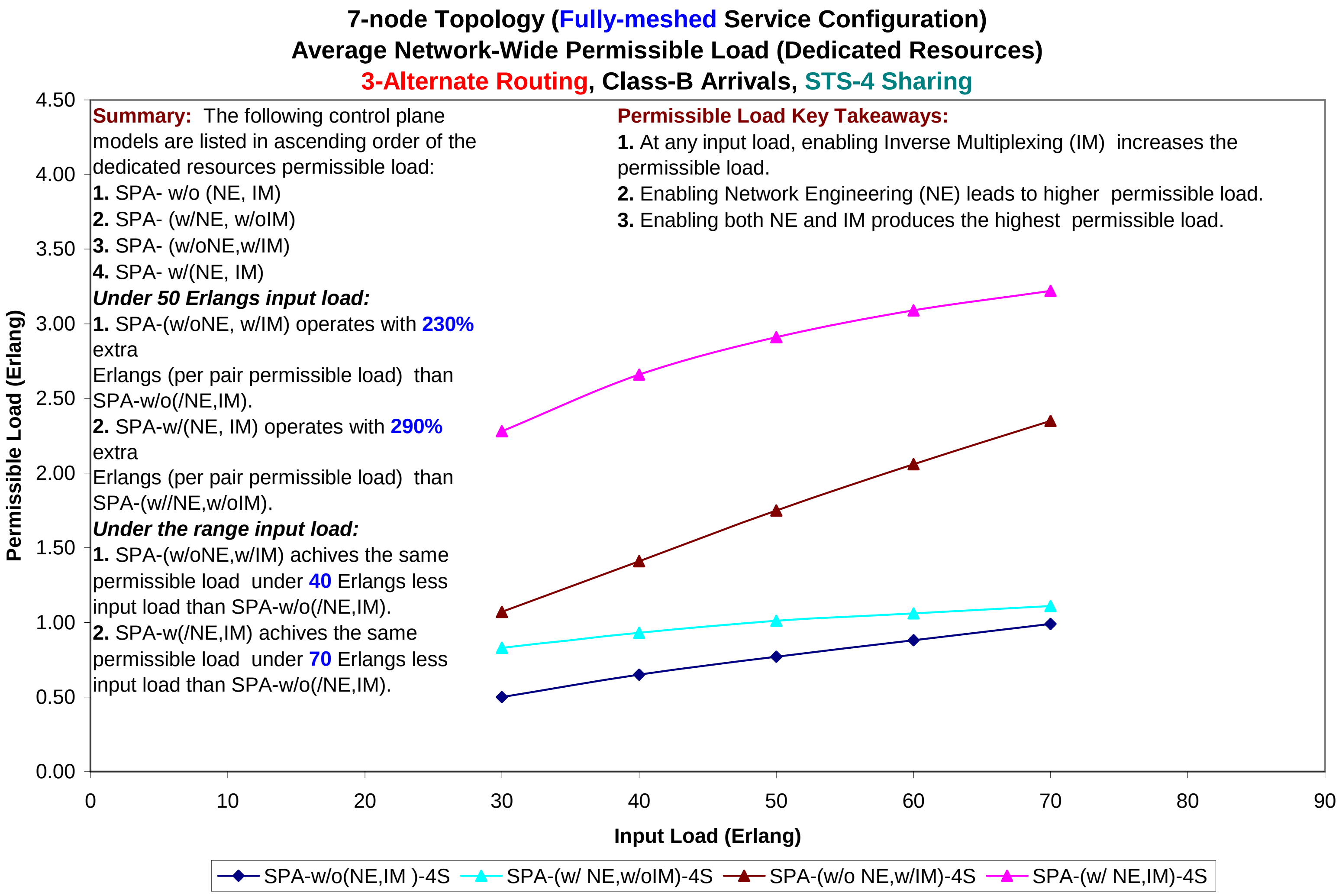

Summary: The following control plane models are listed in ascending order of the dedicated resources permissible load:

1. SPA- w/o (NE, IM)
2. SPA- (w/NE, w/oIM)
3. SPA- (w/oNE,w/IM)
4. SPA- w/(NE, IM)

Under 50 Erlangs input load:

1. SPA-(w/oNE, w/IM) operates with **230%** extra
Erlangs (per pair permissible load) than SPA-w/o(/NE,IM).
2. SPA-w/(NE, IM) operates with **290%** extra
Erlangs (per pair permissible load) than SPA-(w//NE,w/oIM).

Under the range input load:

1. SPA-(w/oNE,w/IM) achives the same permissible load under **40** Erlangs less input load than SPA-w/o(/NE,IM).
2. SPA-w(/NE,IM) achives the same permissible load under **70** Erlangs less input load than SPA-w/o(/NE,IM).

Permissible Load Key Takeaways:

1. At any input load, enabling Inverse Multiplexing (IM) increases the permissible load.
2. Enabling Network Engineering (NE) leads to higher permissible load.
3. Enabling both NE and IM produces the highest permissible load.

Figure 21-17: Average Network-Wide Permissible Load (Dedicated Resources)-7 Node – 3 Alternate Route-STS-4 Sharing

21.2.2 Shared resources

This section provides detailed performance analysis of the network-wide permissible load on the shared network resources partition for the 7-node topology with three-alternate routing. The configured VPN service evaluated is the Fully-meshed Shared Granular (FSF) with the following service profile layer parameters:

a. Service flow connectivity: configured as “fully-meshed”.

b. Service demand granularity: configured as “granular” with 1 STS-1 granularity level.

c. Load partitioning flexibility: configured as “enabled”.

One input class was evaluated with the following parameters: $k = 2$, $b_k^A = 2$ STS-1, $\mu_k = 1$unit time, $\lambda_{rk} = 4$ calls/unit time. Range of input load for 4-node topology is 30 to 70 Erlangs. The five traffic management schemes of the SPA control plane model are evaluated as provided in Table 9-1. Four sharing levels are considered as follows:

a. STS-1 sharing: C_j^{vD} =11 STS-1, C_j^S =2 STS-1

b. STS-2 sharing: C_j^{vD} =10 STS-1, C_j^S =4 STS-1

c. STS-3 sharing: C_j^{vD} =9 STS-1, C_j^S =6 STS-1

d. STS-4 sharing: C_j^{vD} =8 STS-1, C_j^S =8 STS-1

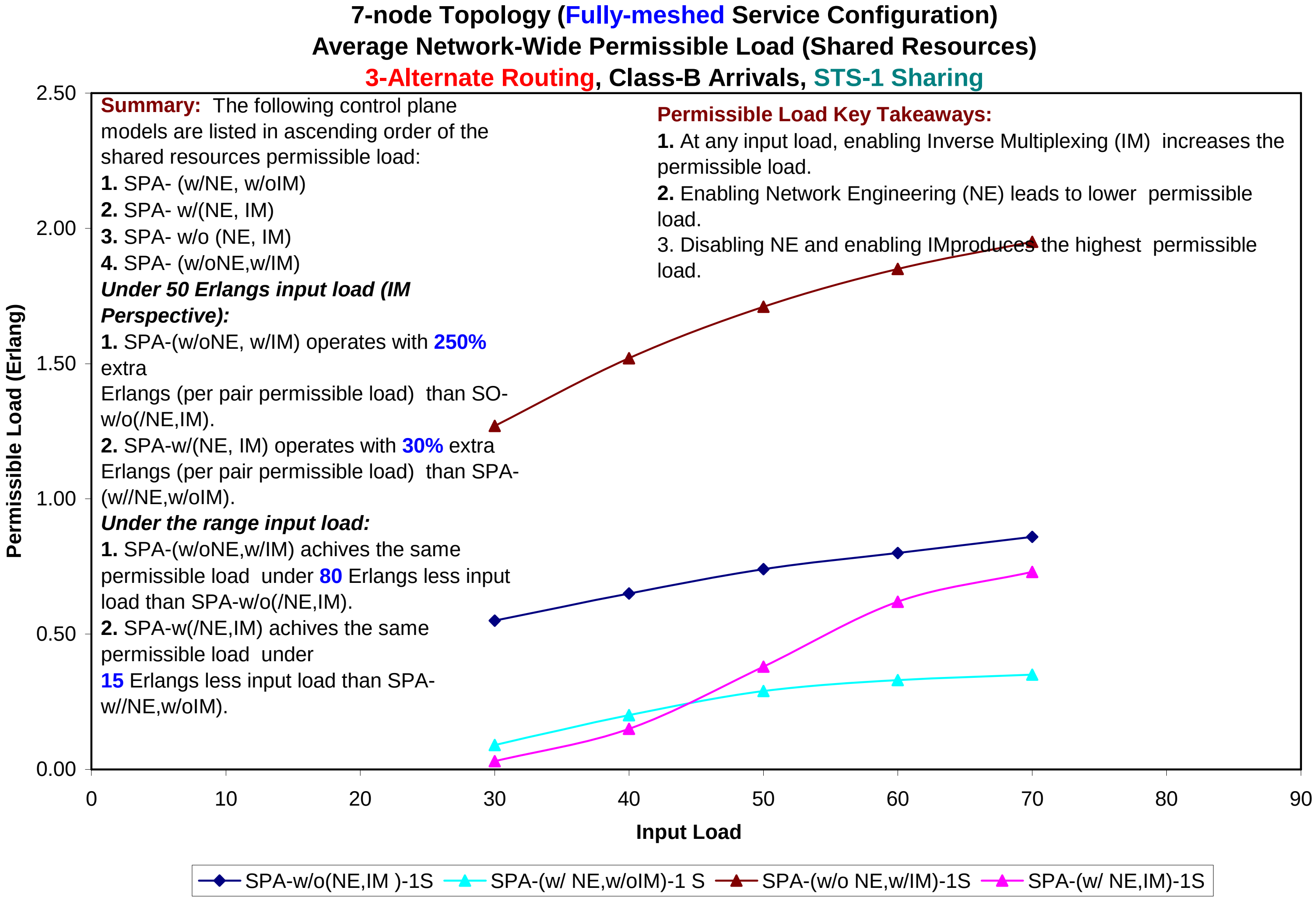

7-node Topology (Fully-meshed Service Configuration)
Average Network-Wide Permissible Load (Shared Resources)
3-Alternate Routing, Class-B Arrivals, STS-1 Sharing

Summary: The following control plane models are listed in ascending order of the shared resources permissible load:

1. SPA- (w/NE, w/oIM)
2. SPA- w/(NE, IM)
3. SPA- w/o (NE, IM)
4. SPA- (w/oNE,w/IM)

Under 50 Erlangs input load (IM Perspective):

1. SPA-(w/oNE, w/IM) operates with **250%** extra
Erlangs (per pair permissible load) than SO-w/o(/NE,IM).

2. SPA-w/(NE, IM) operates with **30%** extra Erlangs (per pair permissible load) than SPA-(w//NE,w/oIM).

Under the range input load:

1. SPA-(w/oNE,w/IM) achives the same permissible load under **80** Erlangs less input load than SPA-w/o(/NE,IM).

2. SPA-w(/NE,IM) achives the same permissible load under
15 Erlangs less input load than SPA-w//NE,w/oIM).

Permissible Load Key Takeaways:

1. At any input load, enabling Inverse Multiplexing (IM) increases the permissible load.

2. Enabling Network Engineering (NE) leads to lower permissible load.

3. Disabling NE and enabling IMproduces the highest permissible load.

Figure 21-18: Average Network-Wide Permissible Load (Shared Resources)-7 Node – 3 Alternate Route-STS-1 Sharing

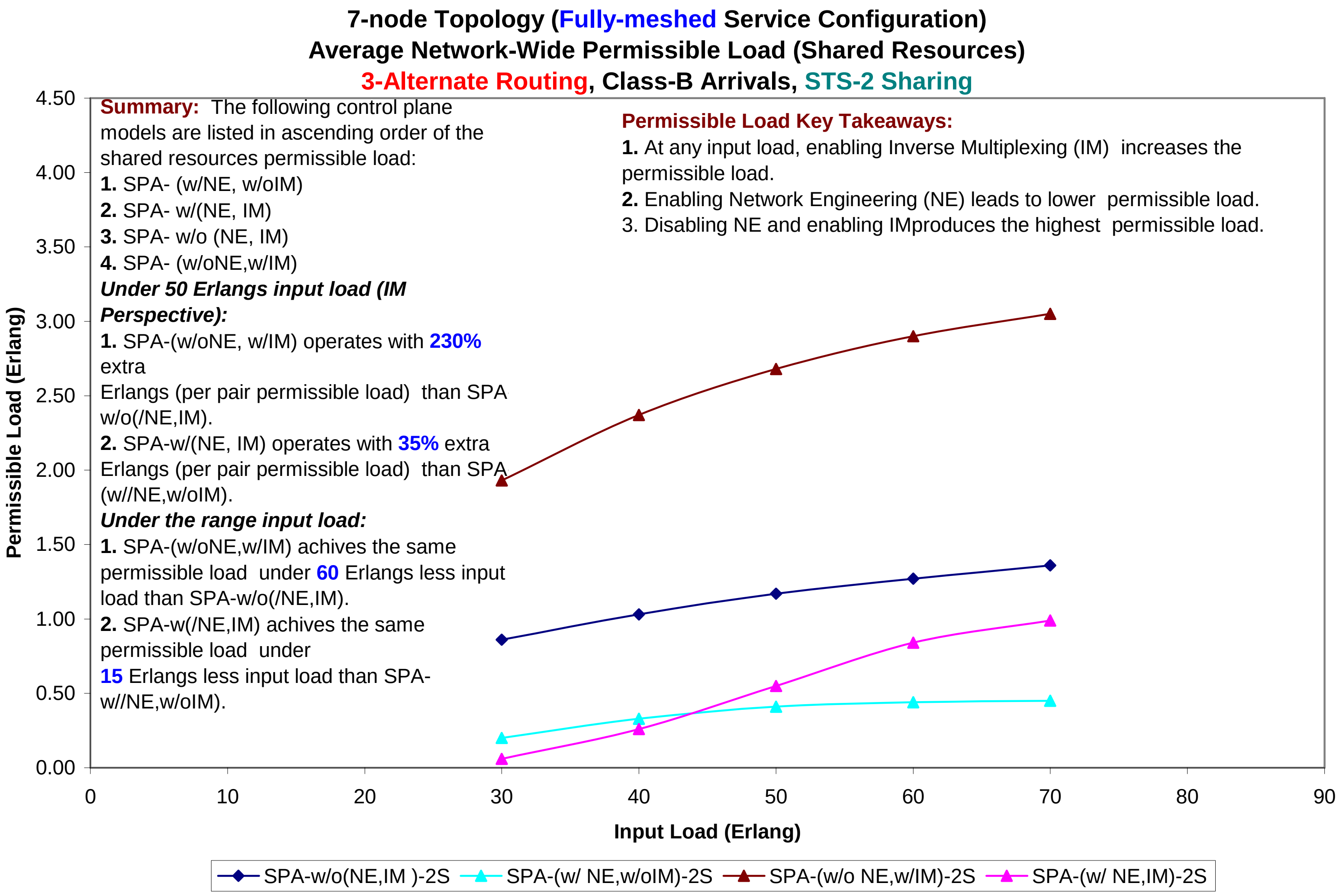
7-node Topology (Fully-meshed Service Configuration)
Average Network-Wide Permissible Load (Shared Resources)
3-Alternate Routing, Class-B Arrivals, STS-2 Sharing

Summary: The following control plane models are listed in ascending order of the shared resources permissible load:

1. SPA- (w/NE, w/oIM)
2. SPA- w/(NE, IM)
3. SPA- w/o (NE, IM)
4. SPA- (w/oNE,w/IM)

Under 50 Erlangs input load (IM Perspective):

1. SPA-(w/oNE, w/IM) operates with **230%** extra
Erlangs (per pair permissible load) than SPA w/o(/NE,IM).
2. SPA-w/(NE, IM) operates with **35%** extra Erlangs (per pair permissible load) than SPA (w//NE,w/oIM).

Under the range input load:

1. SPA-(w/oNE,w/IM) achives the same permissible load under **60** Erlangs less input load than SPA-w/o(/NE,IM).
2. SPA-w(/NE,IM) achives the same permissible load under
15 Erlangs less input load than SPA-w//NE,w/oIM).

Permissible Load Key Takeaways:

1. At any input load, enabling Inverse Multiplexing (IM) increases the permissible load.
2. Enabling Network Engineering (NE) leads to lower permissible load.
3. Disabling NE and enabling IMproduces the highest permissible load.

Figure 21-19: Average Network-Wide Permissible Load (Shared Resources)-7 Node – 3 Alternate Route-STS-2 Sharing

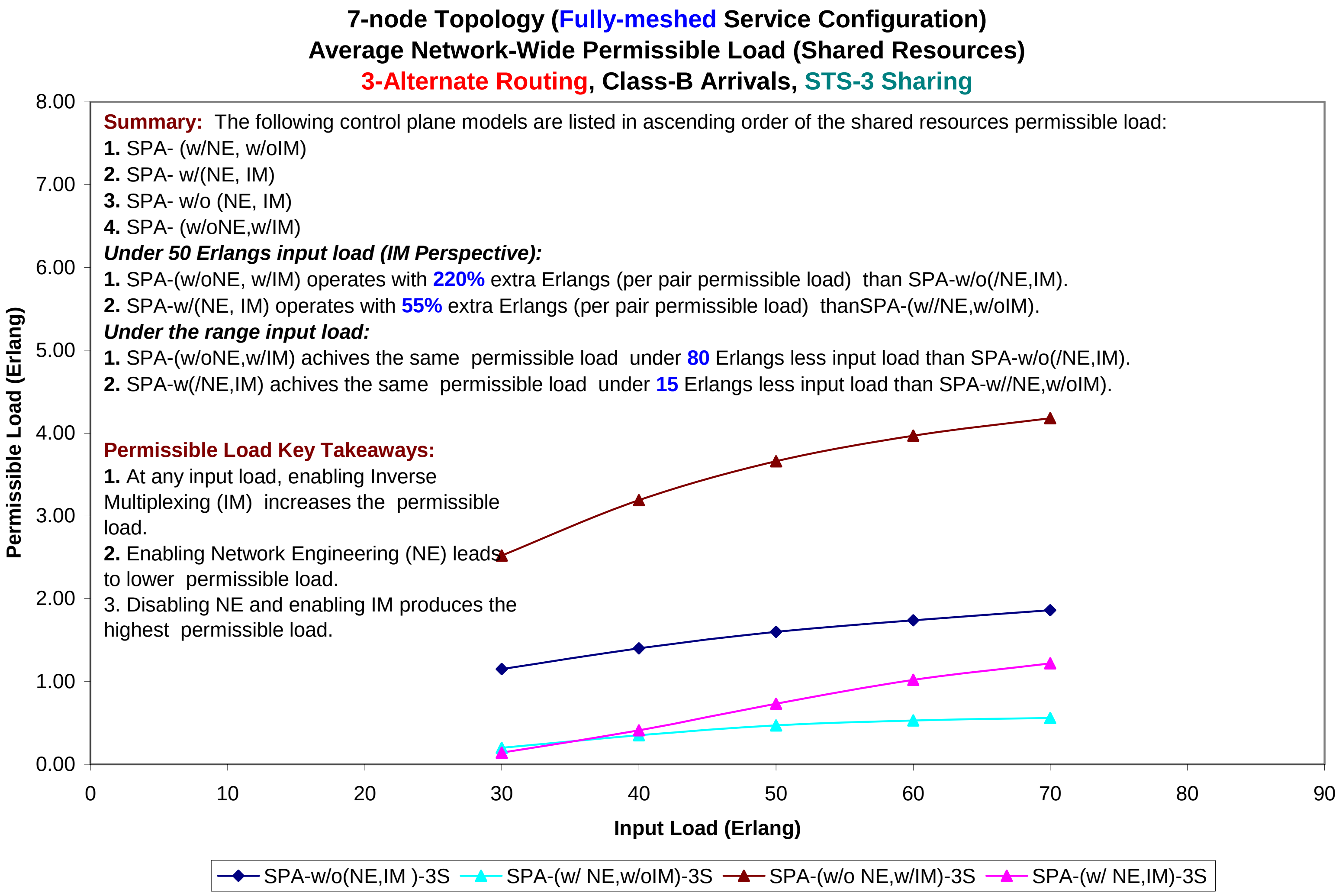

Summary: The following control plane models are listed in ascending order of the shared resources permissible load:

1. SPA- (w/NE, w/oIM)
2. SPA- w/(NE, IM)
3. SPA- w/o (NE, IM)
4. SPA- (w/oNE,w/IM)

Under 50 Erlangs input load (IM Perspective):

1. SPA-(w/oNE, w/IM) operates with **220%** extra Erlangs (per pair permissible load) than SPA-w/o(/NE,IM).
2. SPA-w/(NE, IM) operates with **55%** extra Erlangs (per pair permissible load) thanSPA-(w//NE,w/oIM).

Under the range input load:

1. SPA-(w/oNE,w/IM) achives the same permissible load under **80** Erlangs less input load than SPA-w/o(/NE,IM).
2. SPA-w(/NE,IM) achives the same permissible load under **15** Erlangs less input load than SPA-w//NE,w/oIM).

Permissible Load Key Takeaways:

1. At any input load, enabling Inverse Multiplexing (IM) increases the permissible load.
2. Enabling Network Engineering (NE) leads to lower permissible load.
3. Disabling NE and enabling IM produces the highest permissible load.

Figure 21-20: Average Network-Wide Permissible Load (Shared Resources)-7 Node – 3 Alternate Route-STS-3 Sharing

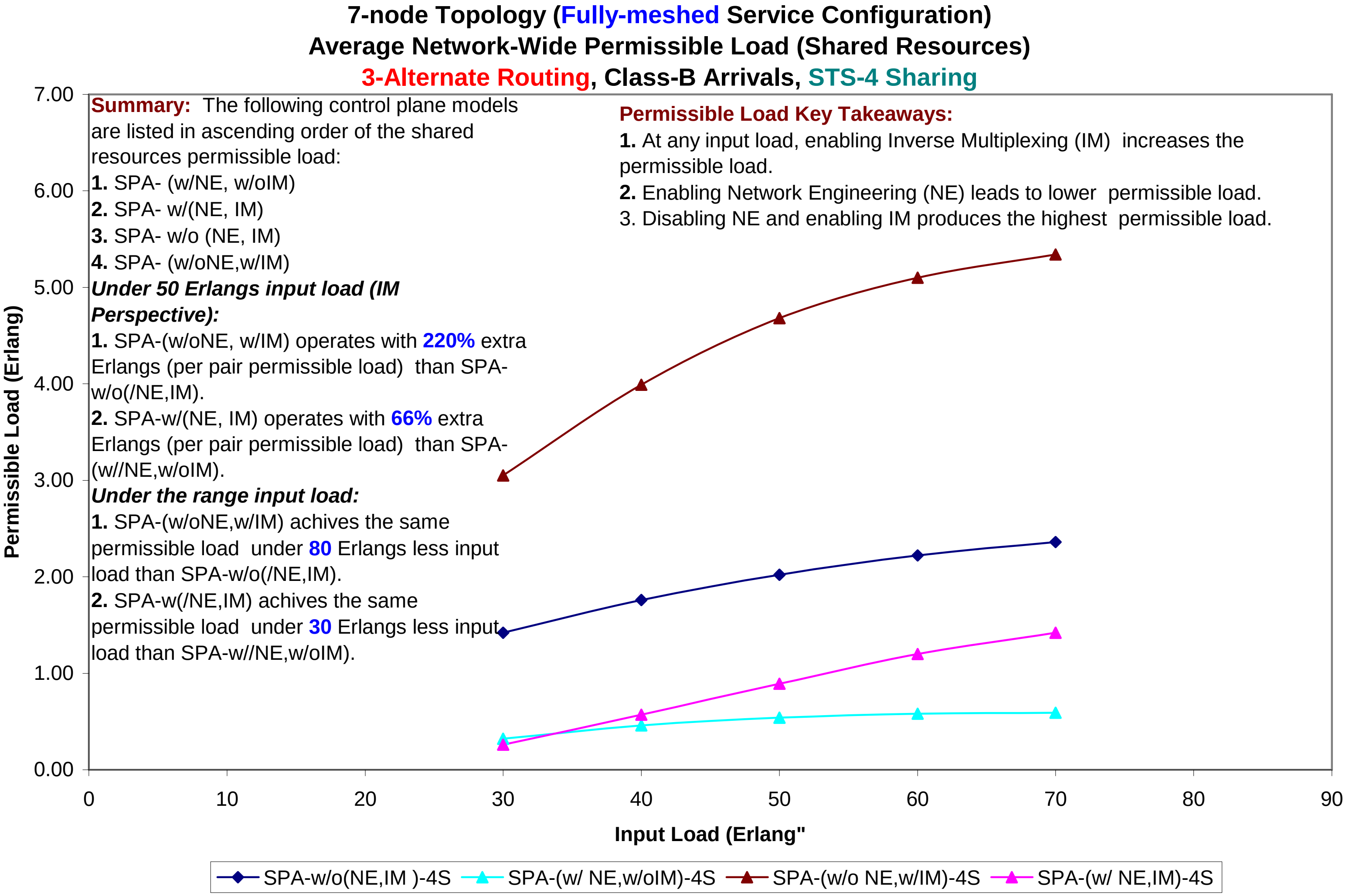

Figure 21-21: Average Network-Wide Permissible Load (Shared Resources)-7 Node – 3 Alternate Route-STS-4 Sharing

21.2.3 VPN resources

This section provides detailed performance analysis of the network-wide permissible load on the VPN network resources partition for the 7-node topology with three-alternate routing. The configured VPN service evaluated is the Fully-meshed Shared Granular (FSF) with the following service profile layer parameters:

a. Service flow connectivity: configured as "fully-meshed".

b. Service demand granularity: configured as "granular" with 1 STS-1 granularity level.

c. Load partitioning flexibility: configured as "enabled".

One input class was evaluated with the following parameters: $k = 2$, $b_k^A = 2$ STS-1, $\mu_k = 1$unit time, $\lambda_{rk} = 4$ calls/unit time. Range of input load for 4-node topology is 30 to 70 Erlangs. The five traffic management schemes of the SPA control plane model are evaluated as provided in Table 9-1. Four sharing levels are considered as follows:

a. STS-1 sharing: C_j^{vD} =11 STS-1, C_j^S =2 STS-1

b. STS-2 sharing: C_j^{vD} =10 STS-1, C_j^S =4 STS-1

c. STS-3 sharing: C_j^{vD} =9 STS-1, C_j^S =6 STS-1

d. STS-4 sharing: C_j^{vD} =8 STS-1, C_j^S =8 STS-1

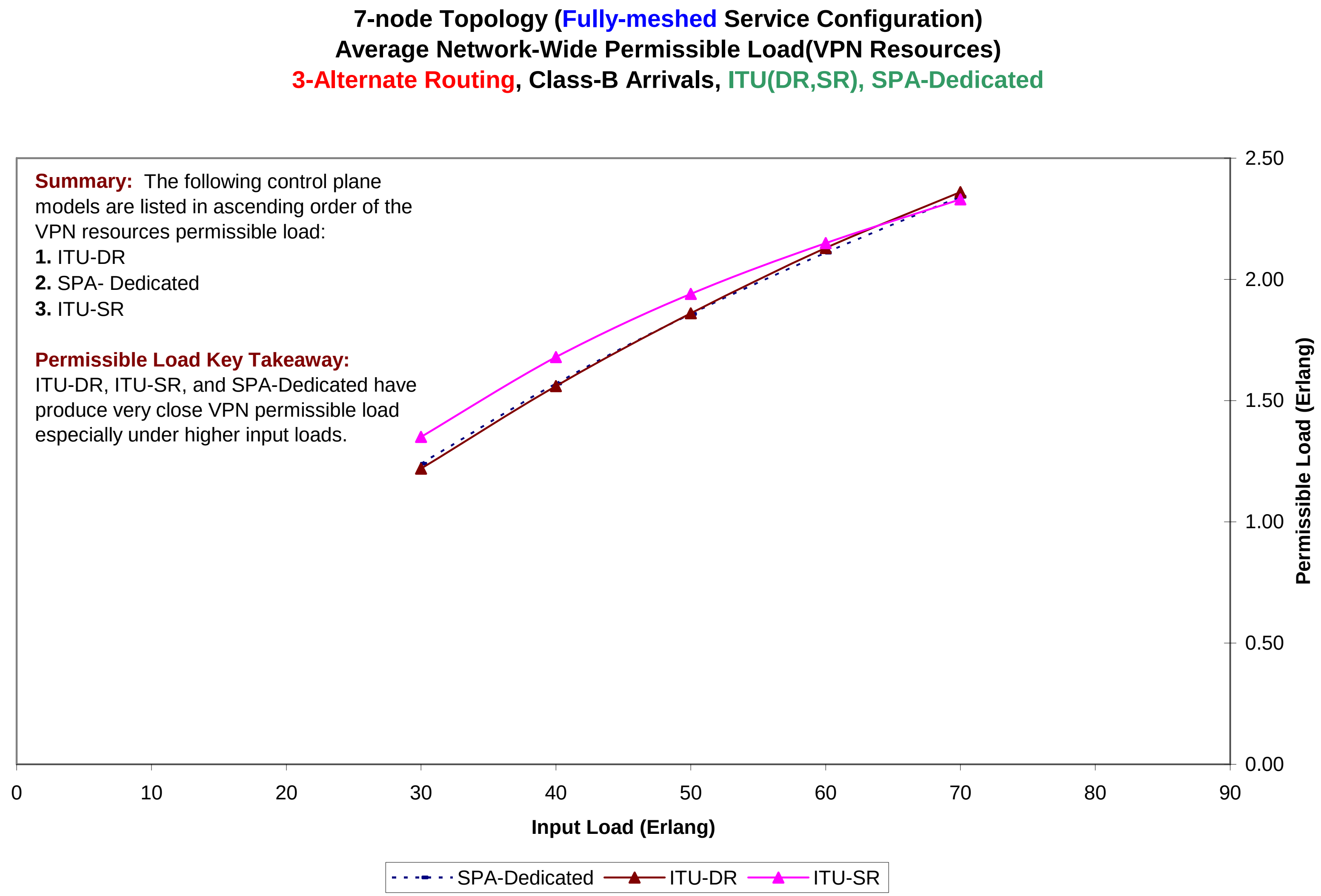

Summary: The following control plane models are listed in ascending order of the VPN resources permissible load:

1. ITU-DR

2. SPA- Dedicated

3. ITU-SR

Permissible Load Key Takeaway:
ITU-DR, ITU-SR, and SPA-Dedicated have produce very close VPN permissible load especially under higher input loads.

Figure 21-22: Average Network-Wide Permissible Load (VPN Resources)-7 Node – 3 Alternate Route-ITU(DR,SR), SPA-Dedicated

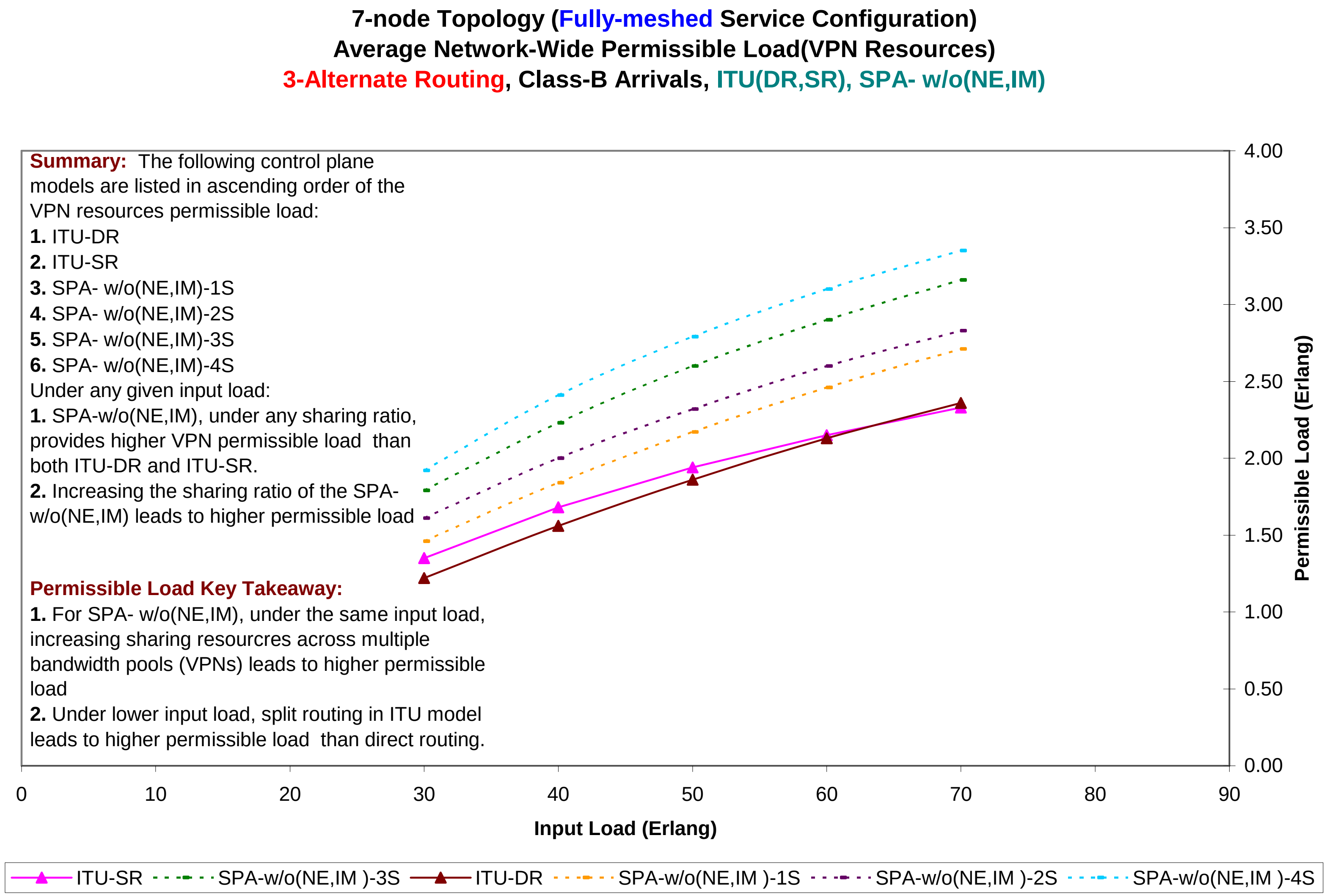

7-node Topology (Fully-meshed Service Configuration)
Average Network-Wide Permissible Load(VPN Resources)
3-Alternate Routing, Class-B Arrivals, ITU(DR,SR), SPA- w/o(NE,IM)

Summary: The following control plane models are listed in ascending order of the VPN resources permissible load:

1. ITU-DR
2. ITU-SR
3. SPA- w/o(NE,IM)-1S
4. SPA- w/o(NE,IM)-2S
5. SPA- w/o(NE,IM)-3S
6. SPA- w/o(NE,IM)-4S

Under any given input load:

1. SPA-w/o(NE,IM), under any sharing ratio, provides higher VPN permissible load than both ITU-DR and ITU-SR.

2. Increasing the sharing ratio of the SPA-w/o(NE,IM) leads to higher permissible load

Permissible Load Key Takeaway:

1. For SPA- w/o(NE,IM), under the same input load, increasing sharing resourcres across multiple bandwidth pools (VPNs) leads to higher permissible load

2. Under lower input load, split routing in ITU model leads to higher permissible load than direct routing.

Figure 21-23: Average Network-Wide Permissible Load (VPN Resources)-7 Node – 3 Alternate Route-ITU(DR,SR), SPA-w/o(NE,IM)

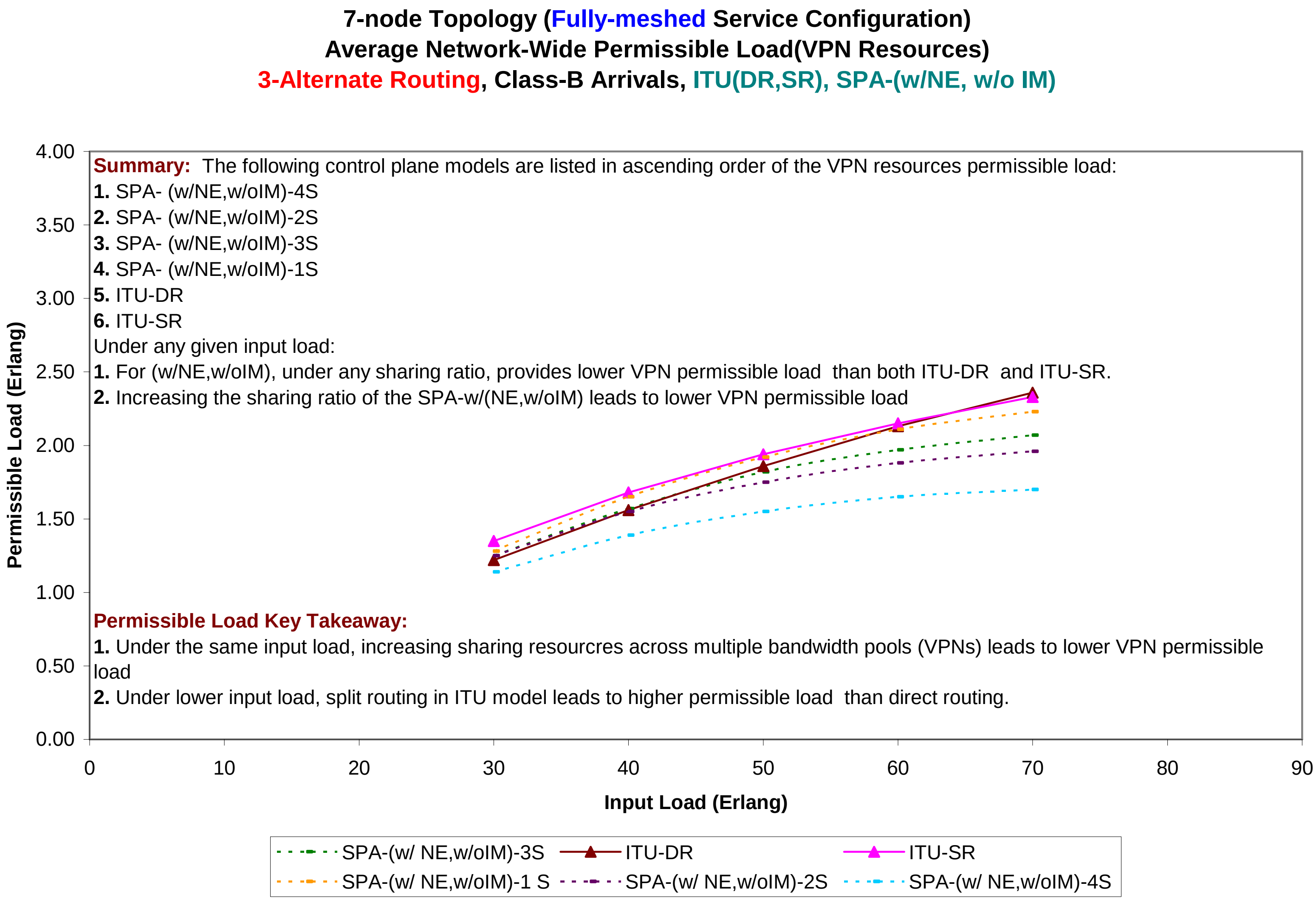

7-node Topology (Fully-meshed Service Configuration)
Average Network-Wide Permissible Load(VPN Resources)
3-Alternate Routing, Class-B Arrivals, ITU(DR,SR), SPA-(w/NE, w/o IM)

Summary: The following control plane models are listed in ascending order of the VPN resources permissible load:

1. SPA- (w/NE,w/oIM)-4S
2. SPA- (w/NE,w/oIM)-2S
3. SPA- (w/NE,w/oIM)-3S
4. SPA- (w/NE,w/oIM)-1S
5. ITU-DR
6. ITU-SR

Under any given input load:
1. For (w/NE,w/oIM), under any sharing ratio, provides lower VPN permissible load than both ITU-DR and ITU-SR.
2. Increasing the sharing ratio of the SPA-w/(NE,w/oIM) leads to lower VPN permissible load

Permissible Load Key Takeaway:
1. Under the same input load, increasing sharing resourcres across multiple bandwidth pools (VPNs) leads to lower VPN permissible load
2. Under lower input load, split routing in ITU model leads to higher permissible load than direct routing.

Figure 21-24: Average Network-Wide Permissible Load (VPN Resources)-7 Node – 3 Alternate Route-ITU(DR,SR), SPA-w/NE,w/oIM

7-node Topology (Fully-meshed Service Configuration)
Average Network-Wide Permissible Load(VPN Resources)
3-Alternate Routing, Class-B Arrivals, ITU(DR,SR), SPA-(w/oNE, w/IM)

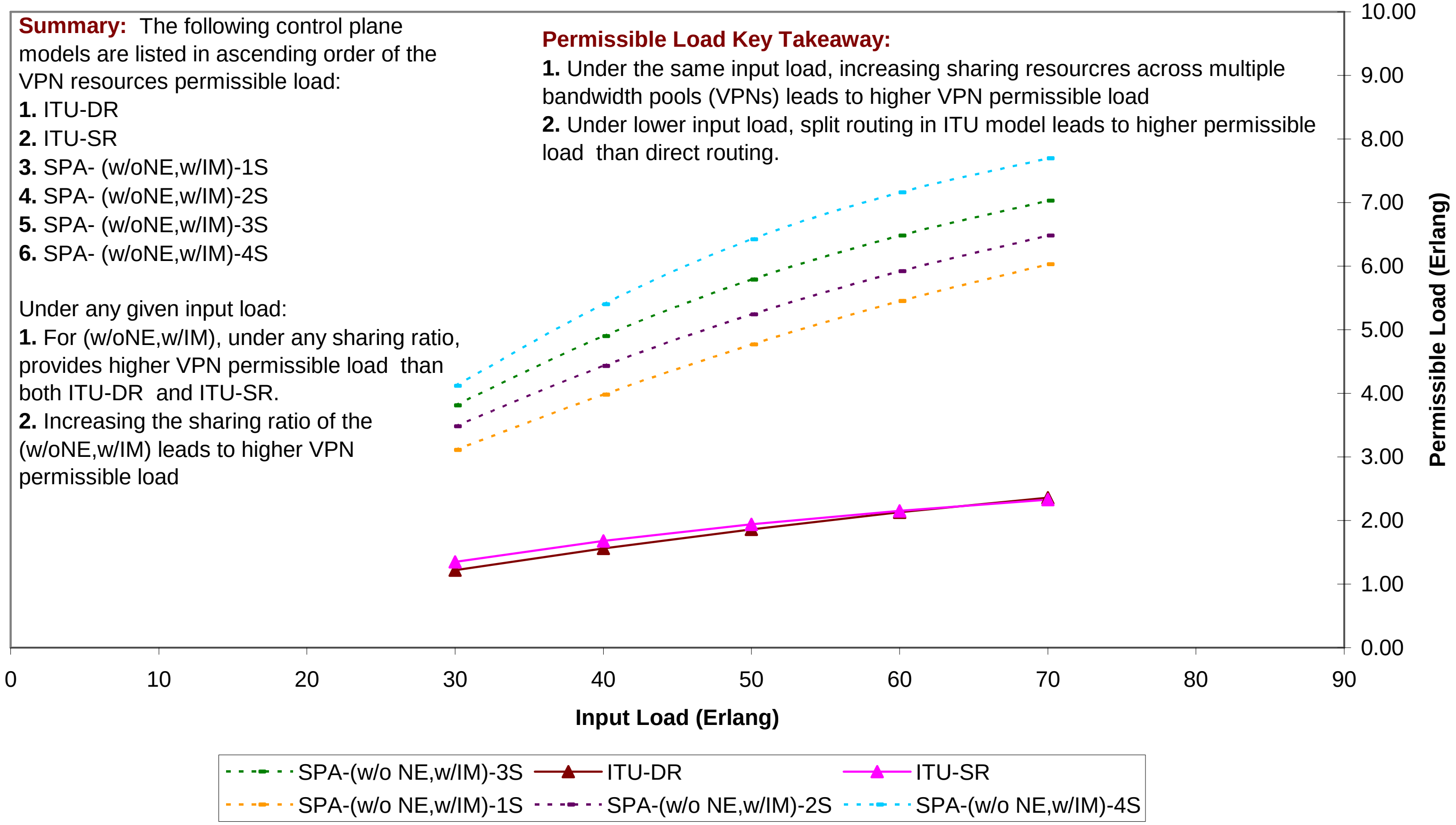

Summary: The following control plane models are listed in ascending order of the VPN resources permissible load:

1. ITU-DR
2. ITU-SR
3. SPA- (w/oNE,w/IM)-1S
4. SPA- (w/oNE,w/IM)-2S
5. SPA- (w/oNE,w/IM)-3S
6. SPA- (w/oNE,w/IM)-4S

Under any given input load:
1. For (w/oNE,w/IM), under any sharing ratio, provides higher VPN permissible load than both ITU-DR and ITU-SR.
2. Increasing the sharing ratio of the (w/oNE,w/IM) leads to higher VPN permissible load

Permissible Load Key Takeaway:
1. Under the same input load, increasing sharing resourcres across multiple bandwidth pools (VPNs) leads to higher VPN permissible load
2. Under lower input load, split routing in ITU model leads to higher permissible load than direct routing.

Figure 21-25: Average Network-Wide Permissible Load (VPN Resources)-7 Node – 3 Alternate Route-ITU(DR,SR), SPA-w/oNE,w/IM

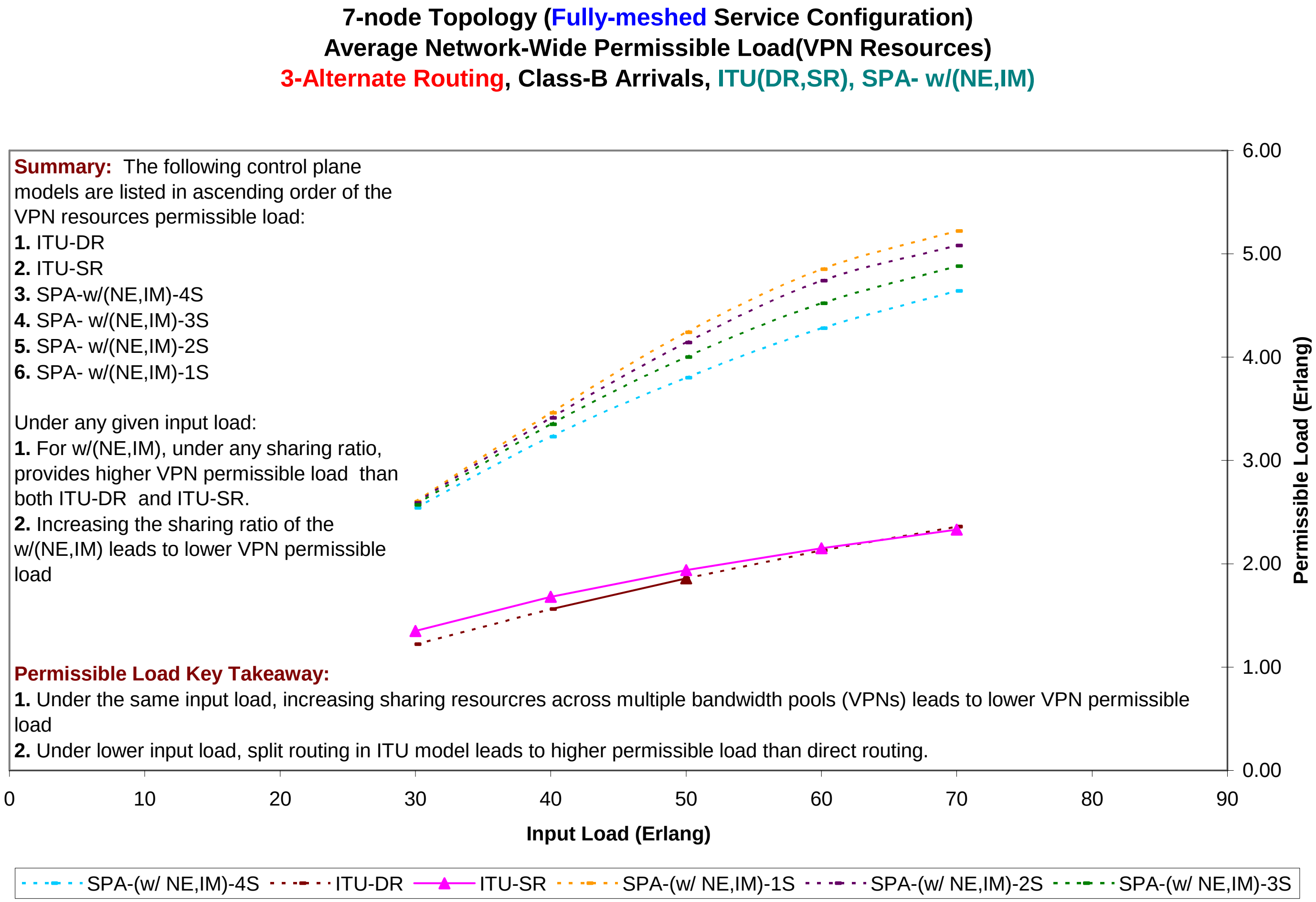

7-node Topology (Fully-meshed Service Configuration)
Average Network-Wide Permissible Load(VPN Resources)
3-Alternate Routing, Class-B Arrivals, ITU(DR,SR), SPA- w/(NE,IM)

Summary: The following control plane models are listed in ascending order of the VPN resources permissible load:

1. ITU-DR
2. ITU-SR
3. SPA-w/(NE,IM)-4S
4. SPA- w/(NE,IM)-3S
5. SPA- w/(NE,IM)-2S
6. SPA- w/(NE,IM)-1S

Under any given input load:
1. For w/(NE,IM), under any sharing ratio, provides higher VPN permissible load than both ITU-DR and ITU-SR.
2. Increasing the sharing ratio of the w/(NE,IM) leads to lower VPN permissible load

Permissible Load Key Takeaway:
1. Under the same input load, increasing sharing resourcres across multiple bandwidth pools (VPNs) leads to lower VPN permissible load
2. Under lower input load, split routing in ITU model leads to higher permissible load than direct routing.

Figure 21-26: Average Network-Wide Blocking Permissible Load (VPN Resources)-7 Node – 3 Alternate Route-ITU(DR,SR), SPA-w/(NE,IM)